UNIVERSITÉ DE GENÈVE
Section de mathématiques

FACULTÉ DES SCIENCES
Professeur Rinat Kashaev

Teichmüller TQFT Calculations for Infinite Families of Knots

THÈSE

Présentée à la Faculté des Sciences de l'Université de Genève
pour obtenir le grade de Docteur ès Sciences, mention Mathématiques

par

Eiichi PIGUET
de
Genève (GE)

Thèse XXXX

GENÈVE
Atelier d'impression ReproMail
2021

アイデアの秘訣は執念である。

湯川秀樹

Abstract

This thesis contains three parts with new results. The first one deals with calculations of partition functions of the Teichmüller Topological Quantum Field Theory (TQFT) for twist knots, and the second one for a family of fibered knots in lens spaces. The last part is devoted to the study of characters in quantum Teichmüller theory.

The Teichmüller TQFT was constructed in 2011 by Andersen and Kashaev. It is an invariant of triangulated knot complements and also a knot invariant which is an infinite-dimensional version of the Kashaev invariant. It has an associated volume conjecture, which gives a link between the two invariants above and furthermore says that the volume of the knot appears as a certain asymptotic coefficient.

In this thesis, we will at first build a new infinite family of ideal triangulations and H-triangulations for the family of hyperbolic twist knots. These triangulations give a new upper bound for the Matveev complexity of twist knot complements. We prove that the above ideal triangulations are geometric using the technique of Futer–Guéritaud, namely the study of the volume functional on the polyhedron of angle structures. We then use these triangulations to compute explicitly the partition function of the Teichmüller TQFT and prove the associated volume conjecture for all hyperbolic twist knots, using the saddle point method.

In a second step, we present similar calculations and results as for the twist knots, but this time for an infinite family of hyperbolic fibered knots in the lens spaces $L(n, 1)$ with $n \geqslant 1$. For the ideal triangulation, we use the monodromy triangulation of Floyd and Hatcher, which is geometric. For H-triangulations, we introduce a method called *T-surgery* which allows to construct H-triangulations from special ideal triangulations.

Quantum Teichmüller theory made it possible to construct unitary projective representations of mapping class groups of punctured surfaces on infinite-dimensional Hilbert spaces. It is expected that the trace of the associated quantum operators gives rise to invariants of mapping tori. The trace of a unitary operator is not always defined. However, we will see that one can give an interpretation of this trace, in the case of a pseudo-Anosov monodromy on the once-punctured torus, using the Teichmüller TQFT with some ideal triangulation of the mapping torus provided with an "almost" complete structure.

Résumé

Cette thèse comporte trois parties avec de nouveaux résultats. La première porte sur des calculs de fonctions de partition de la théorie topologique des champs quantiques (TQFT) de Teichmüller pour les nœuds twist, puis la deuxième pour une famille de nœuds fibrés dans des espaces lenticulaires. La dernière partie est consacrée à l'étude des caractères dans la théorie de Teichmüller quantique.

La TQFT de Teichmüller a été construite en 2011 par Andersen et Kashaev. Il s'agit d'un invariant de complémentaires de nœuds triangulés et aussi d'un invariant de nœuds qui est une analogie en dimension infinie de l'invariant de Kashaev. Elle a une conjecture du volume associée, qui donne un lien entre les deux invariants ci-dessus et qui dit en outre que le volume du nœud apparaît comme un certain coefficient asymptotique.

Dans cette thèse, nous allons tout d'abord construire une nouvelle famille infinie de triangulations idéales et de H-triangulations pour la famille des nœuds twist hyperboliques. Ces triangulations donnent une nouvelle borne supérieure pour la complexité de Matveev des complémentaires des nœuds twist. Nous prouvons que les triangulations idéales ci-dessus sont géométriques en utilisant la technique de Futer–Guéritaud, à savoir l'étude de la fonctionnelle volume sur le polyèdre des structures d'angles. Nous utilisons ensuite ces triangulations pour calculer explicitement la fonction de partition de la TQFT de Teichmüller et prouver la conjecture du volume associée pour tous les nœuds twist hyperboliques à l'aide de la méthode du point col.

Dans un deuxième temps, nous présentons des calculs et résultats similaires que pour les nœuds twist, mais cette fois pour une famille infinie de nœuds fibrés hyperboliques dans les espaces lenticulaires $L(n, 1)$ avec $n \geqslant 1$. Pour la triangulation idéale, nous utilisons la triangulation monodromique de Floyd et Hatcher qui est géométrique. En ce qui concerne les H-triangulations, nous introduisons une méthode appelée *T-chirurgie* qui permet de construire des H-triangulations à partir des triangulations idéales particulières.

La théorie de Teichmüller quantique a permis de construire des représentations projectives unitaires du groupe de difféotopies des surfaces épointées dans des espaces de Hilbert de dimension infinie. Il est espéré que la trace des opérateurs quantiques associés donne lieu à des invariants de tores d'applications. La trace d'un opérateur unitaire n'est pas toujours définie. Cependant, nous verrons qu'il est possible de donner une interprétation de cette trace, dans le cas d'une monodromie pseudo-Anosov du tore épointé, à travers la TQFT de Teichmüller avec une certaine triangulation idéale du tore d'application munie d'une structure "presque" complète.

概要

本論文には3つの新しい要素がある。最初にツイスト結び目のタイヒミュラー位相的量子場の理論（TQFT）の分配関数の計算、次にレンズ空間の中に存在する、あるファイバー結び目の無限例での計算、最後は量子タイヒミュラー理論においての指標の研究である。

タイヒミュラーTQFTは2011年にアンデルセン（Andersen）とカシャエフ（Kashaev）によって構成された。これは四面体分割された結び目補空間の不変量であり、カシャエフ不変量の無限次元版の結び目不変量でもある。 独自の体積予想を持ち、まず上記2つの不変量の間に具体的な関係性があるとされ、そして結び目の体積がある漸近係数として現れることが予想されている。

本論文では、まず、双曲ツイスト結び目に対して、新しい理想四面体分割とH-四面体分割の無限例を構成する。これらの四面体分割は、ツイスト結び目補空間のマトヴェーエフ複雑性の新しい上限を与える。 フュター・ゲリトー（Futer–Guéritaud）の手法、すなわち、角度構造の多面体上の体積関数の研究を用いて、上記の理想四面体分割が幾何学的であることを証明する。 そして、これらの四面体分割を用いて、タイヒミュラーTQFTの分配関数を明示的に計算し、すべての双曲ツイスト結び目について、鞍点法を用いて、関連する体積予想を証明する。

次いでツイスト結び目の場合と同様の計算と結果を提示するが、今回は、$n \geqslant 1$の時のレンズ空間$L(n,1)$での双曲ファイバー結び目の無限例に対しての計算である。理想四面体分割には、すでに幾何学的だと知られている、フロイド（Floyd）とハッチャー（Hatcher）によるモノドロミー四面体分割を使用する。H-四面体分割については、T-手術という特別な理想四面体分割からH-四面体分割を作り出す手法を導入する。

量子タイヒミュラー理論により、無限次元ヒルベルト空間上の穴あき曲面の写像類群の射影表現を構成することが可能になった。この理論の量子作用素のトレースが写像トーラス不変量であることが期待されている。本来、ユニタリ作用素のトレースは定義されていない。しかし、穴あきトーラス上の擬アノソフモノドロミーの場合、タイヒミュラーTQFTを“ほぼ完全”な構造を持つ写像トーラスの、ある理想四面体分割で計算することにより、このトレースを解釈することができるようになることを示す。

Remerciements

Cette thèse de doctorat était pour moi une grande aventure remplie d'enthousiasme et d'excitation, mais aussi parfois de moments difficiles. Notamment, l'année 2020 a, sans doute, été une année très spéciale pour tout le monde. Quasiment tout est passé à distance, et cela nous a permis de se rendre compte de l'importance de la solidarité. A cet égard, tous les obstacles rencontrés durant cette thèse n'auraient pas pu être surmontés sans le soutien de diverses personnes. Directement ou indirectement, elles ont toutes contribué à une partie de cette thèse. Par conséquent, ces pages de remerciements leur sont dédiées.

Je voudrais tout d'abord exprimer ma plus grande reconnaissance à Rinat Kashaev, mon directeur de thèse, sans qui l'aboutissement de cette thèse n'aurait pas été possible. Je le remercie pour sa disponibilité, sa patience, ses explications, ses conseils et pour m'avoir fait découvrir le monde de la recherche mathématique. Exigent, mais il m'a toujours considéré comme un chercheur plutôt que comme un étudiant. Outre sa capacité calculatoire exceptionnelle, j'admire aussi sa gentillesse et sa grande modestie, des qualités humaines précieuses dans notre nouvelle section que je surnomme le "Kremlin helvétique". Je me souviendrai comme il était impressionné d'avoir vu une maid quand je lui ai fait visiter le quartier d'Akihabara après la conférence à Waseda en 2016. J'ai aussi aimé les nombreuses discussions non-mathématiques (politique, Russie, sport, etc.) qu'on a eues dans son bureau. Enfin, merci aussi de m'avoir ordonné de m'inscrire à la course de l'Escalade, qui est devenue depuis un événement annuel essentiel pour moi.

Je voudrais ensuite remercier Fathi Ben Aribi (ancien post-doctorant de Rinat) et François Guéritaud, avec qui j'ai fait une grande partie de cette thèse et qui ont été mes modèles pour la rigueur mathématique. Mes remerciements vont également à Stavros Garoufalidis, Anders Karlsson et Alexis Virelizier pour avoir accepté de faire partie des membres du jury.

Je tiens aussi à remercier nos secrétaires qui étaient vraiment à l'écoute des assistants : Annick, Nathalie et en particulier Joselle, qui s'est occupée de tout mon dossier assez compliqué, qui m'a donné beaucoup de stylos et qui m'a fait beaucoup rigoler. Je voudrais aussi remercier nos bibliothécaires pour tous les bouquins que j'ai empruntés : Valérie, Manuela, Elodie et surtout notre ancienne collègue Anne-Sophie, qui m'a fait sauter les amendes et qui s'était battue pour me retrouver une référence perdue... Un merci aussi aux autres et anciens membres du groupe de topologie : Vân, David, Paul, Léo, Xavier, Virginie, Alan, et en particulier Loulou pour sa fameuse cafetière qui chante, toutes les discussions et les pannacottas.

Je suis très heureux d'avoir pu partager mon bureau (aux Acacias) avec Pratik et Ibrahim, avec qui on a beaucoup rigolé et qui ont toujours bien accueilli le grand nombre d'étudiants qui sont venus me voir (sauf celui qui venait, sans taper la porte, pour faire du shadow-boxing et dénigrer tout le monde...). Pratik inclinait toujours son écran pour que personne ne remarque qu'il regarde des matchs de cricket. Ibrahim pensait que je travaillais pour Mercedes-Benz avec tous mes tétraèdres que je dessinais.

J'apprécie aussi les moments que j'ai passés avec mes autres collègues et anciens collègues de la section : Jhih-Huang qui ne peut pas vivre sans betteraves et selon qui c'est la classe s'il y a le mot "quantique" dans le titre de la thèse ; Marco avec qui il ne faut surtout pas faire de blagues sur des jacobiens et qui est aussi allergique à la question "c'est bien défini ?" ; Tommaso pour qui j'étais cobaye pour ses techniques de karaté et aussi camarade (avec Pratik) pour les meilleures séances bodypump du monde ; Fayçal qui avait trop peur de venir au z-bar parce qu'il y avait trop de filles, mais qui n'a aucun problème de rencontrer des filles inconnues sur Bumble ; Pascaline qui fait toujours des corrections magnifiques que j'ai pu la remplacer en probabilités sur un sujet que je n'avais jamais étudié ; Parisa qui réagissait à chaque fois que je mettais du Christian Dior ; Caterina qui avait la gentillesse de venir nous chercher tous les jours à midi pour aller manger à Uni Mail ; Aitor le grand maître pokémon qui n'oublie surtout pas sa pomme pour venir au z-bar ; Renaud un des rares mathématiciens suffisamment fort mentalement pour servir son pays avec l'armée ; Giulio le womanizer qui était venu de Lille pendant un semestre pour draguer les Genevoises ; Thibaut qui aurait reçu une bonne claque s'il avait posé sa question préférée à Grothendieck ; Guillaume et Nicolas qui ont le talent inné de sourire 24h/24, même quand le café est trop amer ; Ding qui nous apportait du nougat après chaque voyage en Chine et qui restait à la section jusqu'à minuit ; Justine qui est souvent un peu timide, mais dont je suis persuadé qu'en réalité elle adore discuter ; Conor avec qui j'ai parfois eu des difficultés à communiquer à cause de son accent canadien, mais infiniment mieux que Yongxiang, mon tout premier collègue de bureau ; Raphaël qui apparaît toujours pendant les pauses-café quand Marco parle trop fort ; Yaroslav le coach de notre fameuse équipe de foot *les Lièvres* ; Johannes que j'ai plus croisé au fitness qu'à la section ; Giancarlo le bodybuilder de notre section ; Ausra qui n'aime apparemment pas trop les chaussures ; Adrien qui est généralement gentil, mais qui peut se transformer en un monstre très agressif quand il est "fatigué" ; Grégoire mon dernier collègue de bureau qui a tout fait pour nous apporter du confort pour nos derniers mois de thèse.

J'ai eu la chance de faire connaissance avec Sakie (咲衣) qui était venue à Genève en février 2017. Je voudrais la remercier particulièrement de m'avoir invité à Kyoto la même année, qui a été une expérience extraordinaire. J'adresse aussi mes remerciements à la famille Hongler pour toutes les chaleureuses invitations et les meilleurs gossips du monde.

Finalement, je n'oublierai pas les étudiants qui m'ont eu comme assistant pour leurs cours. J'ai toujours passé un bon moment à travailler avec eux, j'ai beaucoup appris d'eux, et j'espère aussi avoir pu les aider un petit peu. Les moments passés au z-bar auraient clairement été moins drôles sans eux. Je leur souhaite à tous beaucoup de succès pour l'avenir et j'espère qu'on se reverra !

最後に、普段は素直に口では伝えられないのですが、これまで自分の思う道を進むことに対し、温かく見守り続けてくれた両親に心から感謝したいと思います。彼らの支援がなければ到底ここまで来ることはできませんでした。本当にありがとう。

Contents

Introduction

Quantum topology began in 1984 with the discovery of the Jones polynomial [Jon85], using operator algebras. Shortly after, infinitely many new knot invariants, organized into a family called quantum invariants, were discovered from applications of different fields. For instance, using representations of quantum groups [Dri85, Jim85, Jim86] with solutions of the Yang–Baxter equation [Bax72, Bax16, Yan67] in statistical mechanics, or using solutions of the Knizhnik–Zamolodchikov equation [KZ84], related to quantum field theory. In the end of 1980s, Witten studied quantum Chern–Simons theory on a 3-manifold M with non-abelian, compact gauge group G, and showed that in the case where M is the 3-sphere and $G = SU(2)$, one can retrieve the Jones polynomial [Wit89]. The process that he used, called path integral, is still mathematically not completely well-defined at the time of writing this thesis. Nice explanations about quantum invariants are done in [Mur00, Oht99, Oht02, Oht15].

Topological Quantum Field Theories (or $TQFT$ for short), which are basically functors from a certain category of cobordisms to the category of vector spaces, were axiomatized by Atiyah [Ati88], Segal [Seg88] and Witten [Wit88]. First examples were constructed by Reshetikhin and Turaev [RT90, RT91, Tur10] using Kirby calculus, and by Turaev and Viro [TV92] using triangulations and quantum $6j$-symbols. The common algebraic tool in both constructions is finite dimensional representation theory of the quantum group $U_q(\mathfrak{sl}_2)$, where q is a root of unity. A purely topological approach using skein theory was proposed later by Blanchet, Habegger, Masbaum and Vogel [BHMV92, BHMV95].

The *volume conjecture* of Kashaev and Murakami–Murakami is probably one of the most studied conjecture in quantum topology currently [Kas97, Mur11, MM01, MY18]. It states that the colored Jones polynomials of a given hyperbolic knot evaluated at a certain root of unity grow asymptotically with an exponential rate, which is the hyperbolic volume of this knot. As such, it hints at a deep connection between quantum topology and hyperbolic geometry. This volume conjecture can be a possible answer to the problem suggested by Atiyah [Ati10], that is to relate quantum invariants to Perelman–Thurston theory [Per02, Per03a, Per03b, Thu82]. In the last twenty years, several variants of the volume conjecture have been proposed for other quantum invariants. For instance, the Baseilhac–Benedetti generalization in terms of quantum hyperbolic invariants [BB04], or the Chen–Yang volume conjecture for the Turaev–Viro invariants for hyperbolic 3-manifolds [CY18]. Some of these conjectures have been proven for several infinite families of examples, such as the fundamental shadow links [Cos07], the Whitehead chains [vdV08] and integral

Dehn fillings on the figure-eight knot complement [Oht18]. See [Mur11, MY18] for more examples. In general, solving a volume conjecture requires to find connections between quantum topology and hyperbolic geometry hidden in the invariant, and to overcome technical difficulties, which are often analytic in nature.

The Teichmüller TQFT volume conjecture

In [AK14c], Andersen and Kashaev constructed the *Teichmüller TQFT*, a generalized TQFT, in the sense that operators of the theory act on infinite-dimensional vector spaces. The partition function of the Teichmüller TQFT yields a quantum invariant $\mathcal{Z}_\hbar(X,\alpha) \in \mathbb{C}$ (indexed by a quantum parameter $\hbar > 0$) of a triangulated 3-manifold X endowed with a family of dihedral angles α, which are invariant under angled Pachner moves. Making use of *Faddeev's quantum dilogarithm* [Fad94, Fad95, FK94], which finds its origins in quantum integrable systems [BMS07, BMS08, FKV01, Tes07], this infinite-dimensional TQFT is constructed with state integrals on tempered distributions from the given triangulation with angles. Although the Teichmüller TQFT is still in progress, a generalized new formulation has already been proposed [AK13, AK18], and it is still not clear at the time of writing this thesis which formulation one should favor in order to best reduce the technical constraints in computations. Moreover, Andersen and Kashaev recently proved that these two formulations coincide on homology spheres and a counterexample was found in $\mathbb{R}P^3$. Nevertheless, two points remain clear regardless of the formulation chosen. First of all, the Teichmüller TQFT is a promising direction for obtaining a mathematical model of complex Chern–Simons theory with gauge group $SL_2(\mathbb{C})$ [AK14c, AK18, Mik18]. Secondly, the Teichmüller TQFT should also satisfy a *volume conjecture*, stated as follows without details (the details are explained in Section 3.4):

Conjecture 1 (Part (3) of Conjecture 3.68)**.** *Let M be a closed oriented 3-manifold and $K \subset M$ a knot whose complement is hyperbolic. Then the partition function of the Teichmüller TQFT associated to (M,K) follows an exponential decrease in the semi-classical limit $\hbar \to 0^+$, whose rate is the hyperbolic volume* $\mathrm{Vol}(M \setminus K)$.

In Chapter 4, we solve the Teichmüller TQFT volume conjecture for the infinite family of hyperbolic twist knots in S^3 (see Figure 1). Until now, this conjecture was only proven for the first two knots of this family [AK14c] and numerically checked for the next nine [AN17, BAPN19].

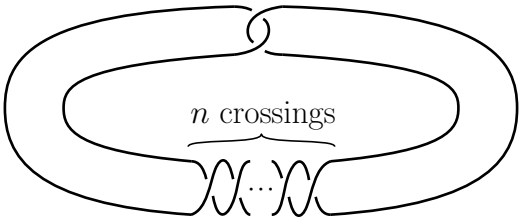

Figure 1: The twist knot K_n.

In Chapter 5, the same conjecture is proven for a family of hyperbolic fibered knots, such that each of these knots lives in the lens spaces $L(n,1)$ for $n \geqslant 1$. To the author's knowledge, the twist knots are the first infinite family of hyperbolic knots in S^3 for which a volume conjecture is proven. Similarly, there has never yet been a proof of a volume

conjecture for a family of knots in an infinite number of different lens spaces. We hope that the techniques and results of Chapters 4 and 5 can provide valuable insights and new developments for further studies of this volume conjecture. Notably, it could be interesting to apply the calculations of Chapters 4 and 5 to prove other conjectures.

Calculations for twist knots

We now precise the objects and the results of Chapter 4. All the results in this chapter are presented in [BAGPN20]. Before all, we should clarify that the results are separated in two parts. Sections 4.2 to 4.6 focus on hyperbolic twist knots with an *odd* number of crossings, while the *even* twist knots are treated in Section 4.7. The reason of this separation is because the constructions and proofs are slightly different whether the crossing number is odd or even.

The first part of this chapter (Sections 4.2 and 4.7.1) deals with topological constructions of triangulations for the twists knots.
In the 1970s, Thurston showed that hyperbolic geometry was deeply related to low-dimensional topology and he later conjectured that "almost every" irreducible atoroidal 3-manifolds admit a complete hyperbolic metric [Thu82]. This conjecture was proven in 2003 by Perelman using Ricci flow with surgery [Per02, Per03a, Per03b]. Moreover, this hyperbolic metric is unique up to isometry by the Mostow–Prasad rigidity theorem [Mos73, Pra73], and thus an important consequence is that hyperbolic geometry can provide topological invariants, such as the hyperbolic volume. Several knot invariants, such as the hyperbolic volume of a knot complement, can be computed from an *ideal triangulation* of a knot complement. Since a knot complement admits infinitely many different ideal triangulations, it seems natural, for simplicity, to work with triangulations with as few tetrahedra as possible.

The twist knots K_n of Figure 1 is the simplest infinite family of hyperbolic knots in S^3 (for $n \geqslant 2$). In order to study the Teichmüller TQFT for the family of twist knots, we constructed particularly convenient ideal triangulations of their complement. As an intermediate step, we constructed *H-triangulations* of pairs (S^3, K_n), which are triangulations of S^3, where the knot K_n is represented by an edge. More precisely, we state these results as follows.

Theorem 2 (Theorem 4.2)**.** *For every $n \geqslant 2$, there exist an ideal triangulation X_n of the twist knot complement $S^3 \setminus K_n$ with $\lfloor \frac{n+4}{2} \rfloor$ tetrahedra and an H-triangulation Y_n of the pair (S^3, K_n) with $\lfloor \frac{n+6}{2} \rfloor$ tetrahedra. Moreover, the edges of all these triangulations admit orientations for which no triangle is a cycle.*

The condition on edge orientations implies that every tetrahedron comes with a complete strict order on its vertices. Such a condition is needed to define the Teichmüller TQFT. Note that in [BB04], this property is called a *branching* on the triangulation, and it is one of the various similarities between the Teichmüller TQFT and the Baseilhac–Benedetti quantum hyperbolic invariants.

The proof of Theorem 2 is treated separately for the case n odd and even. Nevertheless, the technique that we use for the both cases is similar. We use a method introduced by Thurston [Thu78] and later improved by Menasco [Men83] and Kashaev–Luo–Vartanov

[KLV16]. We start from a diagram of the knot K_n and we obtain a combinatorial description of S^3 as a polyhedron glued to itself, where K_n is represented by one particular edge. We then apply a combinatorial trick to reduce the number of edges in the polyhedron, and finally we triangulate it. This yields an H-triangulation Y_n of (S^3, K_n), which then gives the ideal triangulation X_n of $S^3 \setminus K_n$ by collapsing the tetrahedron containing the edge K_n.

The numbers $\lfloor \frac{n+4}{2} \rfloor$ in Theorem 2 give new upper bounds for the Matveev complexities of the manifolds $S^3 \setminus K_n$. Moreover, experimental tests on the software `SnapPy` lead us to conjecture that these numbers are actually equal to the Matveev complexities for this family (see Conjecture 4.4).

In the second part of this chapter (Sections 4.3 and 4.7.2), we prove that these new ideal triangulations are *geometric*, which means that their tetrahedra can be endowed with positive dihedral angles corresponding to the complete hyperbolic structure on the underlying hyperbolic 3-manifold.

In [Thu78], Thurston introduced a method to study geometricity of a given ideal triangulation, which consists in solving a system of *gluing equations* in complex parameters associated to the tetrahedra. If this system admits a solution, then this solution is unique and corresponds to the complete hyperbolic metric on the triangulated manifold. However, this system of equations is difficult to solve in practice. In the 1990s, Casson and Rivin proposed a technique to prove geometricity without solving the gluing equations (see [FG11] for a survey). The idea is to focus on the argument part of the gluing equations, which is a linear system, and use properties of the volume functional. Futer and Guéritaud applied such a method for particular triangulations of once-punctured torus bundles over the circle and two-bridge link complements [Gué06]. Using a similar method, we prove that the ideal triangulations X_n of Theorem 2 are geometric.

Theorem 3 (Theorems 4.8 and 4.41)**.** *For every $n \geqslant 2$, X_n is geometric.*

To prove Theorem 3, we use techniques of Futer and Guéritaud (see [FG11, Gué06]). We first prove that the space of angle structures on X_n is non-empty (Lemma 4.9 for the odd case), and then that the volume functional cannot attain its maximum on the boundary of this space (Lemma 4.11 for the odd case). Then Theorem 3 follows from a result of Casson and Rivin (see Theorem 2.52).

In the third part of this chapter (Sections 4.4, 4.5 and 4.7.3), we compute the partition functions of the Teichmüller TQFT for the triangulations X_n and Y_n and we prove that they satisfy the first two points of Conjecture 3.68. Without going into details, we can summarize these properties as:

Theorem 4 (Theorems 4.13, 4.45, 4.20 and 4.47)**.** *For every $n \geqslant 2$ and every $\hbar > 0$, the partition function $\mathcal{Z}_\hbar(X_n, \alpha)$ of the ideal triangulation X_n (resp. $\mathcal{Z}_\hbar(Y_n, \alpha)$ of the H-triangulation Y_n) is computed explicitly for every angle structure α of X_n (resp. of Y_n). Moreover:*

- *the value $|\mathcal{Z}_\hbar(X_n, \alpha)|$ depends only on three entities: two linear combinations of angles $\mu_{X_n}(\alpha)$ and $\lambda_{X_n}(\alpha)$ (related to the meridian and longitude of the knot K_n),*

and a function $(x \mapsto J_{X_n}(\hbar, x))$*, defined on some open subset of* $\mathbb{C}$*, and independent of the angle structure* α*,*

- *the value* $|J_{X_n}(\hbar, 0)|$ *can be retrieved in a certain residue of the partition function* $\mathcal{Z}_\hbar(Y_n, \alpha)$ *of the H-triangulation* Y_n*.*

The function $(\hbar \mapsto J_{X_n}(\hbar, 0))$ should be seen as an analogue of the Kashaev invariant $\langle\cdot\rangle_N$ [Kas94, Kas95a, Kas95b, Kas97], or of the colored Jones polynomial evaluated at a certain root of unity $J_N(\cdot, e^{2i\pi/N})$ [MM01], where $\hbar$ behaves as the inverse of the color N. It is still not clear that $(\hbar \mapsto J_{X_n}(\hbar, 0))$ always yields a proper knot invariant independent of the triangulation. However, Theorem 4 states that we can reach this function in at least two ways, as suggested in Conjecture 3.68, and is also of interest for studying the AJ-conjecture for the Teichmüller TQFT [AM17].

To prove Theorem 4, we compute the aforementioned partition functions, using a computation technique introduced by Kashaev, which consists in separating the partition function into the *kinematical kernel* and the *dynamical content* (see Section 3.4.2). We then show a connection between the partition function and the argument part of gluing equations for the same triangulation, which allows us to prove that the partition function depends only on the angle structure α via the weight of α on each edge (that is equal to 2π) and via two angular holonomies $\mu_{X_n}(\alpha)$ and $\lambda_{X_n}(\alpha)$ related to the meridian and longitude of the twist knot K_n. Finally, we establish some uniform bounds on the quantum dilogarithm in order to apply the dominated convergence theorem in the computation of the residue of $\mathcal{Z}_\hbar(Y_n, \alpha)$.

In the fourth and final part of this chapter (Sections 4.6 and 4.7.4), we prove that the function $(\hbar \mapsto J_{X_n}(\hbar, 0))$ of Theorem 4 exponentially decreases in the semi-classical limit $\hbar \to 0^+$, with decrease rate the hyperbolic volume. More precisely, we have:

Theorem 5 (Theorems 4.22 and 4.48)**.** *For every* $n \geqslant 2$*, we have the following limit:*

$$\lim_{\hbar \to 0^+} 2\pi\hbar \log |J_{X_n}(\hbar, 0)| = -\mathrm{Vol}(S^3 \setminus K_n).$$

To prove Theorem 5, we apply the *saddle point method* on certain approximation S, called *potential function*, of $J_{X_n}(\hbar, 0)$, which is expressed with classical dilogarithms, and we then bound the remaining error terms with respect to $\hbar$. More precisely, the saddle point method is a common designation of various results which state that an integral $\int_\gamma \exp(\lambda S(z))\, dz$ behaves mostly as $\exp(\lambda \max_\gamma(\Re(S)))$ when $\lambda \to \infty$. In our case, we used a version due to Fedoryuk [Fed77, Fed89] (see Theorem 1.77). For a general survey, see [Won01]. In order to apply this method, we must check technical conditions such as the fact that the maximum of $\Re(S)$ on γ is unique and a simple critical point. Fortunately, all these conditions are consequences of Theorem 3. Indeed, the equations $\nabla S = 0$ correspond exactly to the complex gluing equations, and their unique solution, which is the complete hyperbolic structure, provides the expected saddle point. Geometricity was the main ingredient we needed, in order to go from a finite number of numerical checks of the Teichmüller TQFT volume conjecture [BAPN19] to an exact proof for an infinite family. Another important consequence of Theorem 3 is that we did not need to compute the exact value of the complete hyperbolic structure or of the hyperbolic volume, although such computations would be feasible in the manner of [CMY09] with our triangulations X_n.

The previously mentioned error bounds follow from the fact that $J_{X_n}(\hbar, 0)$ does not depend exactly on the potential function S made of classical dilogarithms, but on a quantum deformation $S'_\hbar$ using quantum dilogarithms. An additional difficulty comes from the fact that we must bound the error uniformly on a *non-compact* contour when $\hbar \to 0^+$. It would seem that this difficulty never appeared in studies of volume conjectures for other quantum invariants, since asymptotics of these invariants (such as the colored Jones polynomials) involve integrals on *compact* contours. Moreover, the parity trick in Lemma 4.33 and its application in the bound for the whole non-compact contour (Lemma 4.34) are our main additional points from the previous techniques of [AH06].

Calculations for knots in lens spaces

Let us now explain the results and the techniques used in Chapter 5. Consider the Whitehead link given in Figure 2. If we do an $(n, 1)$-surgery on the red component, then the remaining blue component becomes a knot $\mathcal{K}_n$ in the lens space $L(n, 1)$.

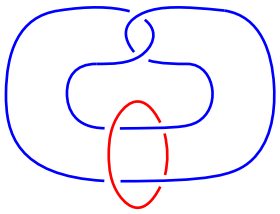

Figure 2: The Whitehead link.

In this chapter, we prove the Teichmüller TQFT volume conjecture for the knot $\mathcal{K}_n$ in $L(n, 1)$ for all $n \geqslant 1$. We thus start by looking for ideal triangulations of their complements, but since $\mathcal{K}_n$ lives in $L(n, 1)$ for all $n \geqslant 1$, the method of finding a triangulation used in Chapter 4 no longer works. Fortunately, all these knot complements are contained in the family of once-punctured torus bundles over the circle with pseudo-Anosov monodromy [HMW92], and Floyd and Hatcher [FH82] found a smart construction of ideal triangulations in this special case, called *monodromy triangulations*. Moreover, later studies showed that these monodromy triangulations are geometric [Aki99, Gué06, Lac03]. The idea of this construction is simple. Since pseudo-Anosov elements of the mapping class group of the punctured torus are elements in $SL_2(\mathbb{Z})$ with absolute value of trace strictly bigger than 2 (Theorem 1.13), we can write these elements as a product of matrices, which either represents a *right flip* or a *left flip* in $\mathbb{R}^2$ (Theorem 1.16). In their turn, each of these flips can be realized by laying exactly a tetrahedron, and finally we "close everything" to obtain the monodromy triangulation.
Although we found ideal triangulations of these knot complements, the previous construction does not provide H-triangulations of pairs $(L(n, 1), \mathcal{K}_n)$ for all $n \geqslant 1$.

The first part of this chapter (Section 5.1) proposes a simple method, called *T-surgery*, to construct H-triangulation of a pair (M, K) from a *split* ideal triangulation. Roughly speaking, an ideal triangulation is split if it contains a face with two same edges pointing in the same direction or coming out from the same direction. Furthermore, we also ask that in the cusp triangulation of the boundary torus, the boundary edge between the two aforementioned edges must be a *cylindrical curve*, namely a curve such that if we remove it, then the boundary torus becomes a cylinder. We then prove the following result, that we state here only for knots:

Proposition 6 (Proposition 5.7)**.** *Let X be a split ideal triangulation of a 3-manifold with torus boundary and with m tetrahedra. If we denote the ideal vertex by $*$, then there exists an H-triangulation of a pair (M, K) with $m + 1$ tetrahedra, such that $M \setminus K$ is homeomorphic to $X \setminus \{*\}$.*

The idea of the proof of Proposition 6, which is exactly the process of the T-surgery, is to cut along the cylindrical curve and modify the toroidal boundary into a spherical boundary only by adding one tetrahedron in the ideal triangulation. We end this first part with application of Proposition 6 to construct some H-triangulations of hyperbolic knots in $\mathbb{R}P^3$. Using carefully various results and tools [CMM13, GM18, Gai18, OS05] we manage to represent these knots with Drobotukhina's disk diagrams [Dro91, Dro94].

In the second part of this chapter (Section 5.2), we start by computing the partition functions of the Teichmüller TQFT for the monodromy triangulations X_n and we prove, as in Chapter 4, that they satisfy the first point of Conjecture 3.68.

Theorem 7 (Theorem 5.22)**.** *For every $n \geqslant 1$ and every $\hbar > 0$, the partition function $\mathcal{Z}_\hbar(X_n, \alpha)$ of the monodromy triangulation X_n is computed explicitly for every angle structure α of X_n. Moreover, the value $|\mathcal{Z}_\hbar(X_n, \alpha)|$ depends only on two linear combinations of angles $\mu_{X_n}(\alpha)$ and $\lambda_{X_n}(\alpha)$, and a function $(x \mapsto J_{X_n}(\hbar, x))$, defined on some open subset of $\mathbb{C}$, and independent of the angle structure α.*

We then apply Proposition 6 to monodromy triangulations X_n, which are all split. We obtain H-triangulations Y_n of pairs (M_n, K_n), such that $M_n \setminus K_n$ is homeomorphic to $L(n, 1) \setminus \mathcal{K}_n$ for all $n \geqslant 1$. Moreover, we found explicitly the manifold M_n and the knot K_n.

Proposition 8 (Proposition 5.39)**.** *For all $n \geqslant 1$, we have $M_n = L(n, 1)$ and K_n is ambient isotopic (up to mirror imaging) to $\mathcal{K}_n$.*

The proof of Proposition 8 is purely algebraic. Since, for any $n \geqslant 1$, we know that M_n is a closed oriented 3-manifold, we computed its fundamental group from the triangulation Y_n and we concluded that M_n is a lens space of form $L(n, k)$ with $1 \leqslant k \leqslant n - 1$. As an intermediate step, we also showed that K_n is trivial in the fundamental group. To prove actually that $k = 1$, we computed the Reidemeister torsion of Y_n and we showed that the value coincide with the one of $L(n, 1)$. Finally, to prove that K_n is ambient isotopic (up to mirror imaging) to $\mathcal{K}_n$, we use the same method as for finding the disk diagrams of knots constructed in the first part of this chapter.

We then calculate the partition functions of the Teichmüller TQFT for the H-triangulations Y_n, and we obtain the expected result (second point of Conjecture 3.68).

Theorem 9 (Theorem 5.42)**.** *For every $n \geqslant 1$ and every $\hbar > 0$, the partition function $\mathcal{Z}_\hbar(Y_n, \alpha)$ of the H-triangulation Y_n is computed explicitly for every angle structure α of Y_n. Moreover, the value $|J_{X_n}(\hbar, 0)|$ can be retrieved in a certain residue of the partition function $\mathcal{Z}_\hbar(Y_n, \alpha)$, where the function $(x \mapsto J_{X_n}(\hbar, x))$ is given in Theorem 7.*

To finish this second part, we prove that the function $(\hbar \mapsto J_{X_n}(\hbar, 0))$ of Theorem 7 exponentially decreases when $\hbar \to 0^+$, where the decrease rate is given by the hyperbolic

volume. Note that we exactly use the same techniques as those presented in Chapter 4, readjusted for this case.

Theorem 10 (Theorem 5.58)**.** *For every $n \geqslant 1$, we have the following limit:*

$$\lim_{\hbar \to 0^+} 2\pi\hbar \log |J_{X_n}(\hbar, 0)| = -\mathrm{Vol}(L(n,1) \setminus \mathcal{K}_n).$$

Finally, in the last part of this chapter (Section 5.3) we present calculations of partition functions for some examples in the Section 5.1. The last point of Conjecture 3.68 is checked numerically.

Characters in quantum Teichmüller theory

We finally come to Chapter 6, where we enter into the details of quantum Teichmüller theory, which has been developed by Kashaev [Kas98] and also independently by Chekhov and Fock [CF99]. In this thesis, we will follow the approach given by Kashaev. The main motivation of this theory was to understand more deeply quantum Chern–Simons theory with non-compact gauge group, such as $PSL_2(\mathbb{R})$ or $PSL_2(\mathbb{C})$, which are of significant importance in hyperbolic geometry. Moreover, quantum Teichmüller theory produces projective unitary representations of mapping class groups of punctured surfaces on infinite-dimensional Hilbert spaces. All these representations are denoted F_{b}, where b is a positive quantum parameter. Main ingredients to construct such representations are the *groupoid of decorated ideal triangulations* (also called *Ptolemy groupoid* [Pen87]) of punctured surfaces and the related notion of *basic algebraic system* (*BAS*), naturally arising from a presentation of the latter groupoid in terms of decorated ideal triangulations. Any BAS allows to construct a representation of the mapping class group in a canonical way. To construct unitary representations of mapping class groups on infinite-dimensional Hilbert spaces, we start by taking a particular BAS coming from Teichmüller theory. Then the idea is to "quantize" this BAS using Faddeev's quantum dilogarithm with the help of functional analysis. This will produce a new BAS in the category of Hilbert spaces. All the details are explained from Section 3.1 to 3.3. Note that as we deal with unitary representations on infinite-dimensional Hilbert spaces, all the eigenvalues of operators live on the unit circle. Therefore, the operators are not trace class.

In the first part of this chapter (Section 6.1), we start by defining a notion which could be used to generalize the trace of operators to a larger family of operators on $L^2(\mathbb{R}^n)$, originally proposed in [Kas17a]. The idea is to realize that any operator A on $L^2(\mathbb{R}^n)$ can be written in a unique way as an integral (in the sense of distributions) of some tempered distribution $f_A(\cdot,\cdot)$ with exponentials of position and momentum operators in quantum mechanics. Then we say that A is *extended trace class* if f_A is a continuous function in a neighborhood of $(0,0) \in \mathbb{R}^n \times \mathbb{R}^n$ and we define the *extended trace* of A by $\mathrm{Tr}_E(A) := f_A(0,0)$.

The second part of this chapter (Section 6.2) is devoted to give the construction of the *quantum monodromy triangulations* X_φ (where $\varphi : \Sigma_{1,1} \to \Sigma_{1,1}$ denotes a pseudo-Anosov monodromy) which generalize the Floyd–Hatcher monodromy triangulations that we used in Chapter 5. The reason that we introduce such a new construction is that the monodromy triangulation admits cycles in the case where the trace of the monodromy is negative, and thus one cannot compute the Teichmüller TQFT partition function. The idea of

the construction comes directly from the objects of quantum Teichmüller theory and we separate the case where the trace of the monodromy is positive and negative. We start by writing the matrices that represent the right/left flips in the monodromy triangulation with the generators of the Ptolemy groupoid of the once-punctured torus. We then realize each of these generators as an overlay of a 3-cell, that can either be a tetrahedron or a *cone over a bigon*. Note that these cones constitute the new part compared to the classical monodromy triangulations. Moreover, even thought monodromy triangulations are geometric, quantum monodromy triangulations are not, because the above cones create "flat tetrahedra" and so one cannot endow X_φ with a strict angle structure. Nevertheless, we will see that one can provide X_φ with a *quasi-complete structure*, which is roughly a structure such that if we eliminate all the cones on X_φ by applying 2-0 Pachner moves, then the new structure on the yielded triangulation (denoted $\check{X}_\varphi$) becomes the complete hyperbolic structure. We can now state the main result of this chapter as follows:

Theorem 11 (Theorem 6.18)**.** *Let $\varphi : \Sigma_{1,1} \to \Sigma_{1,1}$ be a pseudo-Anosov monodromy. There exists a quasi-complete structure α on X_φ, such that if $F_{\mathsf{b}}(\varphi)$ is extended trace class, then*

$$|\mathrm{Tr}_E(F_{\mathsf{b}}(\varphi))| = |\mathcal{Z}_\hbar(X_\varphi, \alpha)|.$$

Moreover, $\check{X}_\varphi$ is the monodromy triangulation.

We finish the chapter by giving the proof of Theorem 11.

Organization of this thesis

This thesis is separated into three parts. In the first two chapters, we recall some basic notions on various domains required for the lecture of this thesis. Chapters 3 to 6 are the main parts of this thesis, which are devoted to explain quantum Teichmüller theory/Teichmüller TQFT, and we present all the new results. In the last chapter, we propose some problems that may be interesting to study in a future work. More precisely, this thesis is divided as follows:

- Chapter 1: Overview on basics of surfaces and mapping tori. Presentation of important results in quantum theory, functional analysis and asymptotic analysis.
- Chapter 2: Explanation of different types of triangulations which appear in this thesis and several tools to deal with hyperbolic 3-manifolds.
- Chapter 3: Introduction to quantum Teichmüller theory and definition of the Teichmüller TQFT, the main object of this thesis.
- Chapter 4: Results on triangulations for twist knots and Matveev complexity. Calculations of the partition function and proof of the volume conjecture for all the hyperbolic twist knots.
- Chapter 5: Calculations of the partition function and proof of the volume conjecture for a family of hyperbolic fibered knots in infinitely many different lens spaces.
- Chapter 6: Result on characters of unitary representations of mapping class group for the once-punctured torus arising from quantum Teichmüller theory.
- Chapter 7: Suggestion of several open problems for future research.

❧ Chapter 1 ❧

Background: Surfaces and quantum theory

In this first chapter, we recall some basic notions about surfaces, quantum theory and functional analysis that will be used in this thesis. At the very end of this chapter, we will explain the saddle point method, which is a bit a separate topic.

1.1 Surfaces and mapping tori

In this thesis, when we say "surface", we will mean a connected, oriented 2-manifold. We recall some basic results about surfaces and mapping tori. Our main reference for this section is [FM12].

1.1.1 Teichmüller space

A *hyperbolic n-manifold* is an n-manifold equipped with a complete Riemannian metric of constant curvature -1 (for equivalent definitions, see [BP92, Rat06]). Denote by $\Sigma_{g,s}$ the surface of genus g and s punctures (removed points). It is well-known that $\Sigma_{g,s}$ is hyperbolic if and only if $\chi(\Sigma_{g,s}) = 2 - 2g - s < 0$ [FM12, Theorem 1.2]. One of the surprising properties of hyperbolic surfaces is the following result.

Proposition 1.1 ([FM12, Proposition 1.3])**.** *Let S be a hyperbolic surface. Then any non-trivial homotopy class of closed curves has a unique geodesic representative.*

Definition 1.2. A *marked hyperbolic surface of type* (g, s) is a pair (S, f), where S is a hyperbolic surface and $f : \Sigma_{g,s} \to S$ is a homeomorphism.

Definition 1.3. The *Teichmüller space* is defined by

$$\mathcal{T}(\Sigma_{g,s}) := \{(S, f) \mid (S, f) \text{ is a marked hyperbolic surface of type } (g, s)\} / \sim,$$

where $(X_1, f_1) \sim (X_2, f_2)$ if and only if $f_1 \circ f_2^{-1} : X_2 \to X_1$ is isotopic to an isometry.

Informally, one can see the Teichmüller space as the space of all the hyperbolic structures on a given hyperbolic surface. For more deep discussions, see [Abi80, Hub06].

Remarks 1.4.

(a) The Teichmüller space can also be interpreted as a space of surface group representations (see [FM12] or [Pen12]), and it can be endowed with a canonical symplectic form, called *Weil–Petersson symplectic form* (see [Do13] for a discussion).

(b) For a hyperbolic surface $\Sigma = \Sigma_{g,s}$, denote by $\mathcal{C}_\Sigma$ the set of isotopy classes of simple closed curves on Σ. If $\alpha \in \mathcal{C}_\Sigma$ and $x = (M, f)$ is a marked hyperbolic surface of type (g, s), then $f_*\alpha$ contains a unique closed geodesic α_x on M by Proposition 1.1. Then the map $\psi : \mathcal{T}(\Sigma) \to \mathbb{R}^{\mathcal{C}_\Sigma}$ defined by $\psi(x) := (l_\alpha(x))_{\alpha\in\mathcal{C}_\Sigma}$, where $l_\alpha(x)$ is the length of α_x, is an embedding. Consequently, the Teichmüller space $\mathcal{T}(\Sigma)$ can be equipped with the induced topology of the product space $\mathbb{R}^{\mathcal{C}_\Sigma}$ and one obtains the next result (see for example [Pen12]).

Theorem 1.5. *Assume that $\Sigma_{g,s}$ is hyperbolic. Then, $\mathcal{T}(\Sigma_{g,s})$ is homeomorphic to $\mathbb{R}^{6g-6+2s}$.*

The following notion will be used in Chapter 3, but we define it here since it is related to surfaces. Moreover, the existence of such structures are assured for punctured hyperbolic surfaces [Mar16, Proposition 7.4.2].

Definition 1.6. Let $\Sigma = \Sigma_{g,s}$ be a hyperbolic surface such that $s > 0$ and denote the set of punctures by $\{P_1, \dots, P_s\}$. An *ideal triangulation* of Σ is a CW-decomposition of $\Sigma_{g,0}$ with $\{P_1, \dots, P_s\}$ as vertices set (called *ideal vertices*) and all 2-cells are triangles (called *ideal triangles*).

Examples 1.7. Some ideal triangulations of $\Sigma_{0,3}, \Sigma_{0,4}, \Sigma_{1,1}$ are given in Figure 1.1.

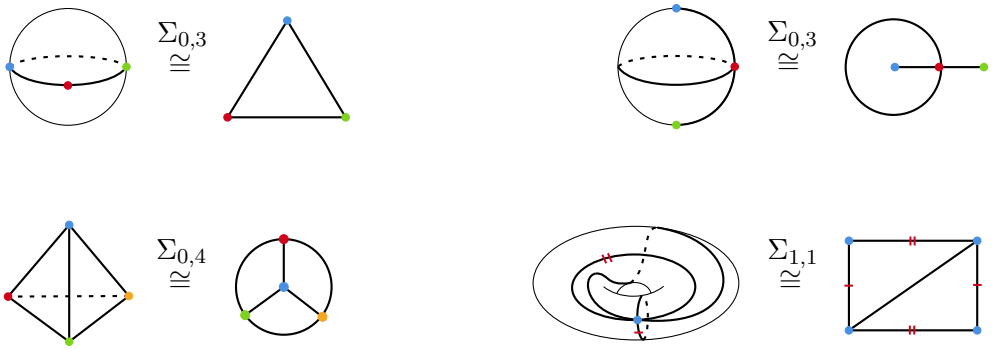

Figure 1.1: Examples of ideal triangulations of surfaces.

1.1.2 Mapping class group of a surface

Mapping class groups have been extensively studied in the literature. For more details about this subject, see [FM12].

Definition 1.8. The *mapping class group* of $\Sigma_{g,s}$ is the group

$$\mathrm{MCG}(\Sigma_{g,s}) := \mathrm{Homeo}^+(\Sigma_{g,s})/\mathrm{Homeo}_0(\Sigma_{g,s}),$$

where $\mathrm{Homeo}^+(\Sigma_{g,s})$ is the group of all orientation-preserving homeomorphisms of $\Sigma_{g,s}$ and $\mathrm{Homeo}_0(\Sigma_{g,s})$ the subgroup of all the elements in $\mathrm{Homeo}^+(\Sigma_{g,s})$ that are isotopic to the identity.

Example 1.9. It is well-known that in the case of the 2-sphere (which is $\Sigma_{0,0}$), there are only two self-homeomorphisms up to isotopy: the identity and a reflection. Since reflections change orientations, $\mathrm{MCG}(S^2)$ is trivial.

Remarks 1.10.

(a) Equivalently, one can also define $\mathrm{MCG}(\Sigma_{g,s})$ in a similar way but using diffeomorphisms. This comes from the fact that every homeomorphism of $\Sigma_{g,s}$ is isotopic to a diffeomorphism [FM12, Theorem 1.13].

(b) There is a natural action of the mapping class group on the Teichmüller space given in the following way. For $[\phi] \in \mathrm{MCG}(\Sigma_{g,s})$ and $[(X, f)] \in \mathcal{T}(\Sigma_{g,s})$, we define

$$[\phi] \cdot [(X, f)] := [(X, f \circ \phi^{-1})].$$

This operation is clearly well-defined and the quotient space is an orbifold of dimension $6g - 6 + 2s$ [Do13, Proposition 5], called the *moduli space*.

The elements of $\mathrm{MCG}(\Sigma_{g,s})$ are classified into three types according to Nielsen–Thurston classification [Thu88].

Theorem 1.11 (Nielsen–Thurston classification)**.** *Each element of* $\mathrm{MCG}(\Sigma_{g,s})$ *has a representative that is either periodic, reducible, or pseudo-Anosov. Furthermore, pseudo-Anosov elements are neither periodic nor reducible.*

These three mapping classes are characterized as follows. Let $f : \Sigma_{g,s} \to \Sigma_{g,s}$ be a homeomorphism. Then f is:

- *periodic* if f has finite order;
- *reducible* if there is a nonempty set $\{c_1, \ldots, c_n\}$ of isotopy classes of pairwise non-intersecting essential simple closed curves in $\Sigma_{g,s}$ such that

$$\{f(c_1), \ldots, f(c_n)\} = \{c_1, \ldots, c_n\};$$

- *pseudo-Anosov* if there is a pair of transverse measured foliations $(\mathcal{F}^u, \mu_u)$ and $(\mathcal{F}^s, \mu_s)$ on $\Sigma_{g,s}$, a number $\lambda > 1$, and a representative homeomorphism ϕ of f such that

$$\phi \cdot (\mathcal{F}^u, \mu_u) = (\mathcal{F}^u, \lambda\mu_u) \qquad \text{and} \qquad \phi \cdot (\mathcal{F}^s, \mu_s) = (\mathcal{F}^s, \lambda^{-1}\mu_s).$$

In general, the mapping class group of a surface is not easy to compute. However, in the case of the torus and once-punctured torus, we get a familiar group of matrices (see for example [FM12]).

Proposition 1.12. *We have* $\mathrm{MCG}(\Sigma_{1,s}) \cong SL_2(\mathbb{Z})$ *for* $s = 0, 1$.

In the case of the torus (see [FM12, Theorem 13.1]) and once-punctured torus (see [Gué06]), the above classification (Theorem 1.11) can be done, using Proposition 1.12, in terms of trace and becomes much simpler.

Theorem 1.13. *Let Σ be $\Sigma_{1,0}$ or $\Sigma_{1,1}$, and $A \in \mathrm{MCG}(\Sigma) \cong SL_2(\mathbb{Z})$. Then,*

1. *A is periodic $\iff$ $|\mathrm{Tr}(A)| \in \{0, 1\}$;*
2. *A is reducible $\iff$ $|\mathrm{Tr}(A)| = 2$;*
3. *A is pseudo-Anosov $\iff$ $|\mathrm{Tr}(A)| > 2$.*

Remark 1.14. It is known that $SL_2(\mathbb{Z})$ can be generated by

$$\begin{bmatrix} 1 & -1 \\ 0 & 1 \end{bmatrix} \qquad \text{and} \qquad \begin{bmatrix} 1 & 0 \\ 1 & 1 \end{bmatrix},$$

which represent Dehn twists in the torus. This remark is in fact a particular case of the next general result.

Theorem 1.15 (Dehn–Lickorish [Deh38, Lic64, Lic66])**.** *For $g, s \geqslant 0$, the mapping class group $\mathrm{MCG}(\Sigma_{g,s})$ is generated by Dehn twists.*

Finally let us give a fundamental result (see for example [Bon09]) that we will use later.

Theorem 1.16. *Let $A \in SL_2(\mathbb{Z})$ with $|\mathrm{Tr}(A)| > 2$. Then there exist $n \in \mathbb{N}_{>0}$ and positive integers $a_1, \ldots, a_n, b_1, \ldots, b_n$ such that A is conjugate to the product*

$$\pm R^{a_1} L^{b_1} \cdots R^{a_n} L^{b_n},$$

where

$$R = \begin{bmatrix} 1 & 1 \\ 0 & 1 \end{bmatrix} \qquad \text{and} \qquad L = \begin{bmatrix} 1 & 0 \\ 1 & 1 \end{bmatrix}. \tag{1.17}$$

1.1.3 Mapping torus of a surface

Definition 1.18. Let Σ be a surface and $\varphi : \Sigma \to \Sigma$ a homeomorphism. The *mapping torus of φ* is

$$M_\varphi := (\Sigma \times [0, 1])/(x, 0) \sim (\varphi(x), 1).$$

The homeomorphism φ is called the *monodromy* of M_φ.

Thurston used the classification of Theorem 1.11 to describe the geometry of mapping tori when the surface Σ is hyperbolic.

Theorem 1.19 (Thurston [Thu98])**.** *Let $\varphi : \Sigma \to \Sigma$ be a homeomorphism of a hyperbolic surface. Then,*

1. *φ is periodic $\iff$ M_φ admits a complete $(\mathbb{H}^2 \times \mathbb{R})$-structure;*
2. *φ is reducible $\iff$ M_φ contains an incompressible (i.e. π_1-injective) torus;*
3. *φ is pseudo-Anosov $\iff$ M_φ admits a complete hyperbolic structure.*

Remarks 1.20.

(a) One can check that surface bundles over S^1 are exactly mapping tori.

(b) Two mapping tori M_{φ_1} and M_{φ_2} are homeomorphic if φ_1 and φ_2 are isotopic, and thus one can take $\varphi \in \mathrm{MCG}(\Sigma)$ with a slight abuse of notation in Definition 1.18.

(c) Agol recently proved [Ago13] the famous *virtual Haken conjecture*, which says that any closed hyperbolic 3-manifold has a finite-sheeted cover that is a surface bundle over S^1.

To finish this section, we complete the Remark 1.20 (b) and give a topological classification of mapping tori according to elements of mapping class group (see [CJR82]).

Theorem 1.21. *Let $\varphi, \psi : \Sigma \to \Sigma$ be two homeomorphisms. Then,*

$$M_\varphi \text{ is isomorphic (as } \Sigma\text{-bundles over } S^1) \text{ to } M_\psi \iff \varphi \text{ is conjugate to } \psi \text{ in } \mathrm{MCG}(\Sigma).$$

Moreover, if $\Sigma = \Sigma_{1,1}$, then

$$M_\varphi \text{ is homeomorphic to } M_\psi \iff \varphi \text{ is conjugate to } \psi^{\pm 1} \text{ in } \mathrm{MCG}(\Sigma).$$

1.2 Elements of quantum theory

We now recall some basic tools and results of quantum theory and functional analysis. The main references of this section is [SS07] for the analysis part, and [Hal13, Kas14] for the quantum theory part. For additional informations about quantum theory, see also [FY09, Tak08]. At the end of the section we will explain the saddle point method, which is independent from the previous parts.

1.2.1 Schwartz space and tempered distributions

Recall that a Hilbert space $\mathcal{H}$ is a real or complex inner product space that is also a Banach space with respect to the norm induced by the inner product that we denote $\langle \cdot | \cdot \rangle$. Furthermore, we will assume in this thesis that all Hilbert spaces are separable and thus admit countable orthonormal bases. A central theorem in functional analysis is the following result [Hal13, Theorem A.52].

Theorem 1.22 (Fréchet–Riesz representation theorem)**.** *Let $\mathcal{H}$ be a Hilbert space and $\mathcal{H}'$ its topological dual space. Let $\varphi \in \mathcal{H}'$. Then there exists a unique $f \in \mathcal{H}$ such that for any $x \in \mathcal{H}$, we have $\varphi(x) = \langle f | x \rangle$.*

Our main Hilbert space for this thesis will be the $\mathbb{C}$-vector space $L^2(\mathbb{R}^n)$ with the usual inner product

$$\langle f | g \rangle := \int_{\mathbb{R}^n} \overline{f(\mathbf{x})} g(\mathbf{x}) \, d\mathbf{x}.$$

An important dense subspace of $L^2(\mathbb{R}^n)$ is the following definition.

Definition 1.23. The *Schwartz space* (or the *space of rapidly decreasing functions on $\mathbb{R}^n$*) is the function space

$$\mathcal{S}(\mathbb{R}^n) := \{ f \in \mathcal{C}^\infty(\mathbb{R}^n, \mathbb{C}) \mid \|f\|_{\alpha,\beta} < \infty \quad \forall \alpha, \beta \in \mathbb{N}^n \},$$

where α and β are multi-indices and

$$\|f\|_{\alpha,\beta} := \sup_{\mathbf{x}\in\mathbb{R}^n} |\mathbf{x}^\alpha D^\beta f(\mathbf{x})|$$

which is a family of semi-norms. The topology on $\mathcal{S}(\mathbb{R}^n)$ is the topology induced by these semi-norms, i.e. the sequential topology such that $(f_k) \subset \mathcal{S}(\mathbb{R}^n)$ converges to $f \in \mathcal{S}(\mathbb{R}^n)$ if and only if $\|f_k - f\|_{\alpha,\beta} \to 0$ for all $\alpha, \beta \in \mathbb{N}^n$.

Remark 1.24. Note that $\mathcal{S}(\mathbb{R}^n)$ is a metric space even if the topology is defined using semi-norms.

The Schwartz space admits very nice properties, that we will not give the details here, but the curious reader can see [SS07]. However we will nevertheless outline some basic properties which will be essential for the rest of the thesis. For proofs, see [SS07].

Proposition 1.25. *The Schwartz space is a non-unital commutative $\mathbb{C}$-algebra contained in $L^1(\mathbb{R}^n) \cap L^2(\mathbb{R}^n)$.*

We denote the Fourier transform by $\mathsf{F} : L^1(\mathbb{R}^n) \to \mathbb{C}^{\mathbb{R}^n}$ defined by

$$(\mathsf{F}f)(\mathbf{x}) := \int_{\mathbb{R}^n} f(\mathbf{y}) e^{2\pi i \mathbf{x}\cdot\mathbf{y}}\, d\mathbf{y}.$$

The next result on Schwartz spaces tells that it is invariant by Fourier transform. In fact, it is well-known that it is even a bijective mapping on $\mathcal{S}(\mathbb{R}^n)$ (see [SS07, Corollary 1.10]).

Theorem 1.26. *If $f \in \mathcal{S}(\mathbb{R}^n)$, then $\mathsf{F}f \in \mathcal{S}(\mathbb{R}^n)$.*

Definition 1.27. A *tempered distribution* on $\mathbb{R}^n$ is an element in the topological dual space of $\mathcal{S}(\mathbb{R}^n)$. The space of tempered distributions on $\mathbb{R}^n$ is denoted $\mathcal{S}'(\mathbb{R}^n)$.

If we want to consider a topology on $\mathcal{S}'(\mathbb{R}^n)$, we usually put the *weak topology*, that is the weakest topology with respect to which the linear map $e_\varphi : \mathcal{S}'(\mathbb{R}^n) \to \mathbb{C}$ defined by

$$e_\varphi(D) := D(\varphi)$$

is continuous for all $\varphi \in \mathcal{S}(\mathbb{R}^n)$.

There are several merits to work with tempered distributions. For example, there is a natural injection from $L^2(\mathbb{R}^n)$ to $\mathcal{S}'(\mathbb{R}^n)$ (Remark 1.28), the derivative (Definition 1.31) and the Fourier transform (Definition 1.39) can be generalized to tempered distributions.

Remarks 1.28.

(a) Let $i : \mathcal{S}(\mathbb{R}^n) \to L^2(\mathbb{R}^n)$ be the inclusion map and $i' : (L^2(\mathbb{R}^n))' \to \mathcal{S}'(\mathbb{R}^n)$ its dual map. Since $(L^2(\mathbb{R}^n))'$ is isomorphic to $L^2(\mathbb{R}^n)$ by Theorem 1.22, we get a map from $L^2(\mathbb{R}^n)$ to $\mathcal{S}'(\mathbb{R}^n)$. More concretely, if $\varphi \in L^2(\mathbb{R}^n)$, the corresponding tempered distribution is denoted $\langle\varphi, \cdot\rangle$ and defined by

$$\langle\varphi, f\rangle := \int_{\mathbb{R}^n} \varphi(\mathbf{x}) f(\mathbf{x})\, d\mathbf{x} \quad \forall f \in \mathcal{S}(\mathbb{R}^n).$$

Therefore, $L^2(\mathbb{R}^n)$ can be seen as a subspace of $\mathcal{S}'(\mathbb{R}^n)$. Moreover, the image of $\mathcal{S}(\mathbb{R}^n)$ by this injection in $\mathcal{S}'(\mathbb{R}^n)$ is dense with the weak topology.

(b) If we denote $\mathcal{L}(\mathcal{S}(\mathbb{R}^n), \mathcal{S}'(\mathbb{R}^m))$ the space of continuous linear maps from $\mathcal{S}(\mathbb{R}^n)$ to $\mathcal{S}'(\mathbb{R}^m)$, we have an isomorphism

$$\widetilde{\cdot} : \mathcal{L}(\mathcal{S}(\mathbb{R}^n), \mathcal{S}'(\mathbb{R}^m)) \to \mathcal{S}'(\mathbb{R}^{n+m})$$

defined by the formula

$$\widetilde{\varphi}(f \otimes g) := \varphi(f)(g)$$

for all $\varphi \in \mathcal{L}(\mathcal{S}(\mathbb{R}^n), \mathcal{S}'(\mathbb{R}^m))$, $f \in \mathcal{S}(\mathbb{R}^n)$ and $g \in \mathcal{S}(\mathbb{R}^m)$.

Notation 1.29. Let $\theta \in \mathcal{S}'(\mathbb{R}^n)$. Then Remark 1.28 (a) incites us to use the following formal notations

$$\theta(f) = \langle \theta, f \rangle = \int_{\mathbb{R}^n} \theta(\mathbf{x}) f(\mathbf{x})\, d\mathbf{x}$$

for all $f \in \mathcal{S}(\mathbb{R}^n)$.

Example 1.30. An important example is the *Dirac delta function* (or *Dirac distribution*) $\delta : \mathcal{S}(\mathbb{R}) \to \mathbb{C}$ (also denoted $\delta(x)$ or δ_x according to Notation 1.29) defined by

$$\delta(f) := f(0) \quad \forall f \in \mathcal{S}(\mathbb{R}).$$

We can easily check that δ is continuous. Indeed, if $(f_k) \subset \mathcal{S}(\mathbb{R})$ is a sequence of functions which converges to the zero function, then we have $|\delta(f_k)| = |f_k(0)| \leqslant \|f_k\|_{0,0}$, and thus $\delta(f_k)$ converges to 0. Note that for simplicity we only considered the case $n = 1$, but the definition of Dirac delta function and the arguments on the Dirac delta function in subsequent sections have multi-dimensional analogues (see for example [GRS12] or [Kan98] for details).

Let us try to guess the definition of the derivative of a tempered distribution in a natural way for the case $n = 1$. If $f, g \in \mathcal{S}(\mathbb{R})$, then an integration by parts gives

$$\langle f', g \rangle = \int_{\mathbb{R}} f'(x) g(x)\, dx = [f(x)g(x)]_{-\infty}^{+\infty} - \int_{\mathbb{R}} f(x) g'(x)\, dx = -\langle f, g' \rangle.$$

Since any Schwartz class function can be seen as a tempered distribution, this leads to the following definition.

Definition 1.31. Let $T \in \mathcal{S}'(\mathbb{R})$. We define the *derivative of* T, denoted T', by the formula

$$\left\langle T', f \right\rangle := - \left\langle T, f' \right\rangle$$

for all $f \in \mathcal{S}(\mathbb{R})$.

Remark 1.32. Note that $T' \in \mathcal{S}'(\mathbb{R})$ since if $f \in \mathcal{S}(\mathbb{R})$, then $f' \in \mathcal{S}(\mathbb{R})$. Moreover, Definition 1.31 can be generalized for multi-dimensional cases.

Example 1.33. Let $\theta \in \mathcal{S}'(\mathbb{R})$ defined by $\langle \theta, f \rangle = \int_0^{+\infty} f(x)\, dx$ for $f \in \mathcal{S}(\mathbb{R})$. Let us compute θ'. By definition, for $f \in \mathcal{S}(\mathbb{R})$, we have

$$\langle \theta', f \rangle = -\langle \theta, f' \rangle = -\int_0^{+\infty} f'(x)\, dx = f(0) = \langle \delta, f \rangle,$$

thus $\theta' = \delta$. Let us now compute the derivative of δ. For $f \in \mathcal{S}(\mathbb{R})$, we get

$$\langle \delta', f \rangle = -\langle \delta, f' \rangle = -f'(0).$$

As for the Dirac delta function, the derivative δ' will also be denoted by $\delta'(x)$ or δ'_x.

1.2.2 Unbounded operators

We now give several definitions which generalize bounded operators between Hilbert spaces.

Definition 1.34. An *unbounded operator* (or simply *operator*) between two Hilbert spaces $\mathcal{H}_1$ and $\mathcal{H}_2$, denoted $A : \mathcal{H}_1 \to \mathcal{H}_2$, is a linear map $A : D(A) \to \mathcal{H}_2$ where $D(A) \subset \mathcal{H}_1$ is a dense vector subspace called *domain* of A. An operator $A : \mathcal{H}_1 \to \mathcal{H}_2$ is *bounded* if $D(A) = \mathcal{H}_1$ and A is a continuous map. The space of bounded operators from $\mathcal{H}_1$ to $\mathcal{H}_2$ is denoted $\mathcal{B}(\mathcal{H}_1, \mathcal{H}_2)$ and simply $\mathcal{B}(\mathcal{H}_1)$ if $\mathcal{H}_1 = \mathcal{H}_2$.

Remark 1.35. We should be careful with the terminology in Definition 1.34. Indeed, "unbounded" does not mean "not bounded", but "not necessarily bounded" since nothing prevents us from having $D(A) = \mathcal{H}_1$ and having A bounded.

Let us now give definitions of different types of operators.

Definitions 1.36.

(a) The *adjoint* of an operator $A : \mathcal{H}_1 \to \mathcal{H}_2$ is an operator $A^* : \mathcal{H}_2 \to \mathcal{H}_1$, where a vector $f \in \mathcal{H}_1$ belongs in $D(A^*)$ if and only if the linear functional $\eta_{f,A} : D(A) \to \mathbb{C}$ defined by
$$\eta_{f,A}(g) := \langle f | Ag \rangle \quad \forall g \in D(A)$$
is continuous and
$$\langle A^* f | g \rangle = \langle f | Ag \rangle \tag{1.37}$$
for all $g \in D(A)$.

(b) An operator $A : \mathcal{H} \to \mathcal{H}$ is *self-adjoint* if $D(A) = D(A^*)$ and $Af = A^* f$ for all $f \in D(A)$.

(c) An operator $U : \mathcal{H} \to \mathcal{H}$ is *unitary* if it is bounded and $U^{-1} = U^*$. The space of unitary operators on $\mathcal{H}$ is denoted by $\mathcal{U}(\mathcal{H})$.

(d) An operator $A : \mathcal{H} \to \mathcal{H}$ is *non-negative* if $\langle f | Af \rangle \geqslant 0$ for all $f \in D(A)$.

Remark 1.38. Note that (1.37) makes sense because the vector $A^* f$ exists and is unique by Theorem 1.22.

Note that Theorem 1.26 implies that the Fourier transform defines an operator on $L^2(\mathbb{R}^n)$, and this operator is unitary. Moreover, using Notation 1.29, we have $\langle \mathsf{F} f, g \rangle = \langle f, \mathsf{F} g \rangle$ for any $f, g \in \mathcal{S}(\mathbb{R}^n)$, and this motivates the following definition.

Definition 1.39. Let $T \in \mathcal{S}'(\mathbb{R}^n)$. We define the *Fourier transform of* T, denoted $\mathsf{F}T$, by the formula
$$\langle \mathsf{F}T, f \rangle := \langle T, \mathsf{F} f \rangle$$
for all $f \in \mathcal{S}(\mathbb{R}^n)$.

Remark 1.40. If $(f_k) \subset \mathcal{S}(\mathbb{R}^n)$, then it is known that $f_k \to f$ in $\mathcal{S}(\mathbb{R}^n)$ if and only if $\mathsf{F} f_k \to \mathsf{F} f$ in $\mathcal{S}(\mathbb{R}^n)$ (see for example [GW99]), which allows to conclude that $\mathsf{F}T \in \mathcal{S}'(\mathbb{R}^n)$. Moreover, one can define in a similar way the inverse Fourier transform.

Example 1.41. Let us compute the Fourier transform of Dirac delta function. Let $f \in \mathcal{S}(\mathbb{R})$. Then for $f \in \mathcal{S}(\mathbb{R})$ we have

$$\langle \mathsf{F}\delta, f\rangle = \langle \delta, \mathsf{F}f\rangle = (\mathsf{F}f)(0) = \int_{\mathbb{R}} f(x)\,dx = \langle 1, f\rangle,$$

thus $\mathsf{F}\delta = 1$. Applying inverse Fourier transform, one obtains that $\delta = \mathsf{F}^{-1}1$ and thus Dirac delta function can be written as

$$\delta(x) = \int_{\mathbb{R}} e^{-2\pi i x y}\,dy. \tag{1.42}$$

Formula (1.42) is also mathematically consistent in the following sense. If $f \in \mathcal{S}(\mathbb{R})$, then

$$\int_{\mathbb{R}} \delta(x) f(x)\,dx = \int_{\mathbb{R}} \left(\int_{\mathbb{R}} e^{-2\pi i x y}\,dy \right) f(x)\,dx = f(0),$$

where the second equality follows from applying the Fourier transform F twice and using the fact that $(\mathsf{F}^{-2}f)(x) = (\mathsf{F}^2 f)(x) = f(-x)$ for $f \in \mathcal{S}(\mathbb{R})$ and $x \in \mathbb{R}$.

A simple change of variables gives rise the following formula. For any $f \in \mathcal{S}(\mathbb{R})$ and $a \in \mathbb{R}$, we have

$$\int_{\mathbb{R}} \delta(x-a) f(x)\,dx = f(a). \tag{1.43}$$

Similarly, a formal change of variables (according to Notation 1.29) gives the following rule

$$\int_{\mathbb{R}} \delta'(x-a) f(x)\,dx = -f'(a).$$

In fact, formula (1.43) is a special instance of the following result.

Proposition 1.44. *Let $\varphi : \mathbb{R} \to \mathbb{R}$ be a smooth function such that $\varphi'(a) \neq 0$ for any $a \in \varphi^{-1}(0)$. Then we have*

$$\delta(\varphi(x)) = \sum_{a \in \varphi^{-1}(0)} \frac{\delta(x-a)}{|\varphi'(a)|}.$$

Corollary 1.45. *We have*

$$\delta(ax) = \frac{\delta(x)}{|a|} \tag{1.46}$$

for all $a \in \mathbb{R}^*$.

The following result says that many operators can be defined from tempered distributions, and will be very important for us.

Theorem 1.47 (Schwartz kernel theorem)**.** *Let $A : L^2(\mathbb{R}^n) \to L^2(\mathbb{R}^m)$ be an operator with $D(A) \subset \mathcal{S}(\mathbb{R}^n)$. Then there exists a tempered distribution $K_A \in \mathcal{S}'(\mathbb{R}^m \times \mathbb{R}^n)$, called* integral kernel*, such that*

$$(Af)(\mathbf{x}) = \int_{\mathbb{R}^n} K_A(\mathbf{x}, \mathbf{y}) f(\mathbf{y})\,d\mathbf{y}.$$

Examples 1.48.

(a) The identity operator $\mathrm{id}_{L^2(\mathbb{R})} : L^2(\mathbb{R}) \to L^2(\mathbb{R})$ satisfies the hypothesis of Theorem 1.47, and the integral kernel is given by $K_{\mathrm{id}_{L^2(\mathbb{R})}}(x, y) = \delta(x - y)$.

(b) The Fourier transform $\mathsf{F} : L^2(\mathbb{R}) \to L^2(\mathbb{R})$ satisfies also the hypothesis of Theorem 1.47, and the integral kernel is given by $K_{\mathsf{F}}(x, y) = e^{2\pi i x y}$.

Let us give two important formulas to finish this section. We will use these formulas in Chapter 3. If A is an operator on a Hilbert space $\mathcal{H}$, we define the *exponential* of A, denoted e^A or $\exp(A)$, by the power series

$$e^A := \sum_{k=0}^{\infty} \frac{A^k}{k!}.$$

If B is also an operator on $\mathcal{H}$, then we have

$$e^A B e^{-A} = B + [A, B] + \frac{1}{2!}[A, [A, B]] + \frac{1}{3!}[A, [A, [A, B]]] + \cdots \tag{1.49}$$

and

$$e^A e^B = \exp\left(\sum_{n=1}^{\infty} \frac{(-1)^{n-1}}{n} \sum_{\substack{r_k + s_k > 0 \\ k=1,\ldots,n}} \frac{[A^{r_1} B^{s_1} \cdots A^{r_n} B^{s_n}]}{\left(\sum_{j=1}^{n} (r_j + s_j)\right) \prod_{i=1}^{n} r_i! s_i!} \right), \tag{1.50}$$

where

$$[A^{r_1} B^{s_1} \cdots A^{r_n} B^{s_n}] := [\underbrace{A, [A, \cdots [A}_{r_1}, [\underbrace{B, [B, \cdots [B}_{s_1}, \cdots [\underbrace{A, [A, \cdots [A}_{r_n}, [\underbrace{B, [B, \cdots B}_{s_n}]] \cdots]].$$

Formula (1.50) is called the *Baker–Campbell–Hausdorff formula* (also called *Dynkin's formula*). For more details, see [Hal15]. The first few terms inside the parentheses of formula (1.50) are given by

$$A + B + \frac{1}{2}[A, B] + \frac{1}{12}\left([A, [A, B]] + [B, [B, A]]\right) - \frac{1}{24}[B, [A, [A, B]]] + \cdots .$$

1.2.3 Heisenberg's position and momentum operators

In this section, we will consider two central unbounded self-adjoint operators that arise in quantum mechanics. The following definitions are well-defined ([Hal13, Corollary 9.31 and Proposition 9.32]).

Definition 1.51. For $k \in \{1, \ldots, n\}$, the *k-th position operator* $\mathsf{q}_k : L^2(\mathbb{R}^n) \to L^2(\mathbb{R}^n)$ is defined by

$$(\mathsf{q}_k f)(\mathbf{x}) := x_k f(\mathbf{x}) \qquad \forall f \in D(\mathsf{q}_k),$$

where $D(\mathsf{q}_k) := \{\varphi \in L^2(\mathbb{R}^n) \mid x_k \varphi(\mathbf{x}) \in L^2(\mathbb{R}^n)\}$.

Definition 1.52. For $k \in \{1, \ldots, n\}$, the *k-th momentum operator* $\mathsf{p}_k : L^2(\mathbb{R}^n) \to L^2(\mathbb{R}^n)$ is defined by

$$(\mathsf{p}_k f)(\mathbf{x}) := \frac{1}{2\pi i} \frac{\partial f}{\partial x_k}(\mathbf{x}) \qquad \forall f \in D(\mathsf{p}_k),$$

where $D(\mathsf{p}_k) := \{\varphi \in L^2(\mathbb{R}^n) \mid \varphi' \in L^2(\mathbb{R}^n)\}$.

Remarks 1.53.

(a) For $n = 1$, we will simply write q and p instead of q_1 and p_1 respectively. These operators satisfy the commutation relation

$$[\mathsf{p}_k, \mathsf{q}_l] = \frac{\delta_{k,l}}{2\pi i}$$

for $k, l = 1, \ldots, n$.

(b) The derivative in Definition 1.52 is computed in distribution sense and the integral kernels of the both operators are given by

$$K_{\mathsf{q}_k}(\mathbf{x}, \mathbf{y}) = x_k \prod_{j=1}^{n} \delta(x_j - y_j) \qquad \text{and} \qquad K_{\mathsf{p}_k}(\mathbf{x}, \mathbf{y}) = \frac{\delta'(x_k - y_k)}{2\pi i} \prod_{j \neq k} \delta(x_j - y_j)$$

for $k = 1, \ldots, n$.

(c) Note that Definition 1.52 is not the classical one involving the quantum parameter $\hbar > 0$. The reason of this choice is that one obtains the formulas

$$\mathsf{F}\mathsf{q}\mathsf{F}^{-1} = \mathsf{p} \qquad \text{and} \qquad \mathsf{F}\mathsf{p}\mathsf{F}^{-1} = -\mathsf{q}. \tag{1.54}$$

The key property of these two operators is the next result. For a proof, see for example [Hal13, pp. 185–186].

Theorem 1.55. *The position and momentum operators are self-adjoints on the domains given in Definitions 1.51 and 1.52 respectively.*

1.2.4 Dirac's bra-ket notation

In quantum mechanics, the *bra-ket notation*, which has been introduced by Dirac [Dir39], is very often used to describe quantum states and can also be used to denote abstract vectors and linear functionals. The idea is to see the bracket $\langle \cdot | \cdot \rangle$ of the inner product as one *bra* $\langle \cdot |$ and one *ket* $| \cdot \rangle$. More precisely, an element $f \in L^2(\mathbb{R}^n)$ is written as a ket $|f\rangle$ and we denote the bra $\langle f|$ for the linear functional which sends $|g\rangle$ to $\langle f|g\rangle$. We defined the rule that if a bra is followed by a ket, then we fuse them into an inner product.

Let $f, g \in L^2(\mathbb{R}^n)$. Using the above notations and rules, the expression $|f\rangle\langle g|$ denotes the operator on $L^2(\mathbb{R}^n)$ given by

$$(|f\rangle\langle g|)(\chi) = |f\rangle\langle g|\chi\rangle = \langle g|\chi\rangle|f\rangle.$$

Moreover, if A is an operator on $L^2(\mathbb{R}^n)$, then we set

$$\langle f|A|g\rangle := \langle f|Ag\rangle.$$

Using these notations, and taking any orthonormal basis $\{e_i\} \subset L^2(\mathbb{R}^n)$, we compute

$$\left(\sum_i |e_i\rangle\langle e_i| \right) (|e_j\rangle) = \sum_i \langle e_i|e_j\rangle |e_i\rangle = \sum_i \delta_{i,j} |e_i\rangle = |e_j\rangle,$$

which implies that

$$\mathrm{id}_{L^2(\mathbb{R}^n)} = \sum_i |e_i\rangle\langle e_i| \tag{1.56}$$

and this identity is called *decomposition of unit*.

Let us introduce two other formal notations. We denote

$$\langle \mathbf{x}|f\rangle := f(\mathbf{x}), \qquad \langle f|\mathbf{x}\rangle := \overline{\langle \mathbf{x}|f\rangle} = \overline{f(\mathbf{x})}.$$

Then we obtain that

$$\langle f|g\rangle = \int_{\mathbb{R}^n} \overline{f(\mathbf{x})} g(\mathbf{x})\, d\mathbf{x} = \int_{\mathbb{R}^n} \langle f|\mathbf{x}\rangle\langle \mathbf{x}|g\rangle\, d\mathbf{x},$$

and this equality makes us want to introduce, in the same philosophy as formula (1.56), the following convenient notation

$$\mathrm{id}_{L^2(\mathbb{R}^n)} = \int_{\mathbb{R}^n} |\mathbf{x}\rangle\langle \mathbf{x}|\, d\mathbf{x}. \tag{1.57}$$

Thus, one gets

$$(Af)(\mathbf{x}) = \langle \mathbf{x}|Af\rangle = \langle \mathbf{x}|A|f\rangle = \int_{\mathbb{R}^n} \langle \mathbf{x}|A|\mathbf{y}\rangle\langle \mathbf{y}|f\rangle\, d\mathbf{y}.$$

If we assume that $D(A) \subset \mathcal{S}(\mathbb{R}^n)$, then Theorem 1.47 forces us the following notation

$$\langle \mathbf{x}|A|\mathbf{y}\rangle = K_A(\mathbf{x}, \mathbf{y}).$$

Note that if we take $n = 1$ and $A = \mathrm{id}_{L^2(\mathbb{R})}$, then we have

$$\langle x|y\rangle = \langle x|\mathrm{id}_{L^2(\mathbb{R})}|y\rangle = \delta(x - y),$$

which can be seen as a continuous version of Kronecker delta.

Remark 1.58. Since $\langle y|\mathsf{q}|x\rangle = x\langle y|x\rangle$, the expression $|x\rangle$ can be seen as an "eigenvector" for the position operator with eigenvalue x, but is not a true eigenvector as the Dirac delta function is not an element of $L^2(\mathbb{R})$.

1.2.5 Trace of operators

Unlike matrices where everything is well-defined, the notion of trace is not defined for all operators, but only for a restricted family of operators. For more details about this topic, see [RS12]. For all this section, we denote $\mathcal{H}$ an arbitrary Hilbert space.

We start by defining the trace for bounded non-negative self-adjoint operators.

Proposition 1.59. *Let $A \in \mathcal{B}(\mathcal{H})$ be a non-negative and self-adjoint operator. Then for any two orthonormal bases $\{e_i\}$ and $\{f_i\}$ for $\mathcal{H}$, we have*

$$\sum_i \langle e_i|Ae_i\rangle = \sum_i \langle f_i|Af_i\rangle$$

and this quantity is called the trace *of A and is denoted by* $\mathrm{Tr}(A)$.

Remarks 1.60.

(a) Since A is non-negative, the trace of A is always well-defined, but may have the value $+\infty$.

(b) If $A \in \mathcal{B}(\mathcal{H})$, then A^*A is necessarily self-adjoint and non-negative, and thus the square root of A^*A can be defined with functional calculus. We obtain the next definition.

Definition 1.61. An element $A \in \mathcal{B}(\mathcal{H})$ is *trace class* if the trace of the non-negative self-adjoint operator $\sqrt{A^*A}$ is finite. The family of trace class operators on $\mathcal{H}$ is denoted $\mathcal{T}_1(\mathcal{H})$.

Proposition 1.62. *We have the following properties.*

1. *If $A \in \mathcal{T}_1(\mathcal{H})$, then for any orthonormal basis $\{e_i\}$ of $\mathcal{H}$, the sum $\sum_i \langle e_i | Ae_i \rangle$ is absolutely convergent, and thus $\mathrm{Tr}(A)$ is well-defined.*

2. *The family $\mathcal{T}_1(\mathcal{H})$ is a $\mathbb{C}$-vector space and $\mathrm{Tr} : \mathcal{T}_1(\mathcal{H}) \to \mathbb{C}$ is $\mathbb{C}$-linear.*

3. *If $A \in \mathcal{T}_1(\mathcal{H})$, then $A^* \in \mathcal{T}_1(\mathcal{H})$ and we have*

$$\mathrm{Tr}(A^*) = \overline{\mathrm{Tr}(A)}.$$

4. *If $A \in \mathcal{T}_1(\mathcal{H})$ and $B \in \mathcal{B}(\mathcal{H})$, then $AB \in \mathcal{T}_1(\mathcal{H})$ and $BA \in \mathcal{T}_1(\mathcal{H})$, and we have*

$$\mathrm{Tr}(AB) = \mathrm{Tr}(BA).$$

In the case where $\mathcal{H} = L^2(\mathbb{R}^n)$, according to Theorem 1.47, one can compute the trace more easily using the integral kernel.

Theorem 1.63 (Brislawn [Bri91])**.** *Assume that $A \in \mathcal{T}_1(L^2(\mathbb{R}^n))$ with integral kernel $K_A \in L^2(\mathbb{R}^n \times \mathbb{R}^n)$. If K_A is continuous almost everywhere on the diagonal, then we have*

$$\mathrm{Tr}(A) = \int_{\mathbb{R}^n} K_A(\mathbf{x}, \mathbf{x})\, d\mathbf{x}. \tag{1.64}$$

Formula (1.64) was first found by Duflo [Duf72] in the case where the integral kernel is a continuous function on $X \times X$, where X is a σ-compact and locally compact space with Radon measure. We can give a heuristic (but non-rigorous) explanation of this formula.

Let $\{e_i\} \subset L^2(\mathbb{R}^n)$ be any orthonormal basis. Then we have that

$$\mathrm{Tr}(A) = \sum_i \langle e_i | Ae_i \rangle = \sum_i \int_{\mathbb{R}^n} \overline{e_i(\mathbf{x})} (Ae_i)(\mathbf{x})\, d\mathbf{x} = \sum_i \int_{\mathbb{R}^{2n}} \overline{e_i(\mathbf{x})} K_A(\mathbf{x}, \mathbf{y}) e_i(\mathbf{y})\, d\mathbf{x} d\mathbf{y}.$$

If $f \in L^2(\mathbb{R}^n)$, then using formula (1.56), one gets

$$f(\mathbf{x}) = \langle \mathbf{x} | f \rangle = \sum_i \langle \mathbf{x} | e_i \rangle \langle e_i | f \rangle = \sum_i e_i(\mathbf{x}) \int_{\mathbb{R}^n} \overline{e_i(\mathbf{y})} f(\mathbf{y})\, d\mathbf{y},$$

then fixing $\mathbf{x}$ and taking $f(\mathbf{y}) = K_A(\mathbf{y}, \mathbf{x})$, we get

$$K_A(\mathbf{x}, \mathbf{x}) = \sum_i e_i(\mathbf{x}) \int_{\mathbb{R}^n} \overline{e_i(\mathbf{y})} K_A(\mathbf{y}, \mathbf{x})\, d\mathbf{y}.$$

Therefore,

$$\begin{aligned}\int_{\mathbb{R}^n} K_A(\mathbf{x}, \mathbf{x})\, d\mathbf{x} &= \int_{\mathbb{R}^n} d\mathbf{x} \sum_i e_i(\mathbf{x}) \int_{\mathbb{R}^n} d\mathbf{y}\, \overline{e_i(\mathbf{y})} K_A(\mathbf{y}, \mathbf{x}) \\ &= \sum_i \int_{\mathbb{R}^{2n}} e_i(\mathbf{y}) \overline{e_i(\mathbf{x})} K_A(\mathbf{x}, \mathbf{y})\, d\mathbf{x} d\mathbf{y} \\ &= \mathrm{Tr}(A).\end{aligned}$$

1.2.6 Gaussian integral with purely imaginary argument

For $a > 0$, the Gaussian integral

$$\int_{-\infty}^{+\infty} e^{-ax^2}\, dx = \sqrt{\frac{\pi}{a}} \tag{1.65}$$

is a well-known result. By analytic continuation, we can in fact see that this identity is also valid for the complex values of a with $\Re(a) > 0$ since the real part guarantees the absolute convergence of the integral. We would now like to find a formula when a is purely imaginary. Such integrals appear often in quantum field theory. Formally, if we replace a by $-ia$ in formula (1.65) and if we interpret $\sqrt{i} = e^{\frac{i\pi}{4}}$, then one gets

$$\int_{-\infty}^{+\infty} e^{iax^2}\, dx = \sqrt{\frac{i\pi}{a}} = e^{\frac{i\pi}{4}} \sqrt{\frac{\pi}{a}}.$$

However, this is not a proof, but simply an idea of the formula. If we want to prove it rigorously, we should consider the following contour integral

$$\oint_C e^{iaz^2}\, dz$$

where $a > 0$ and C is a closed contour defined in Figure 1.2.

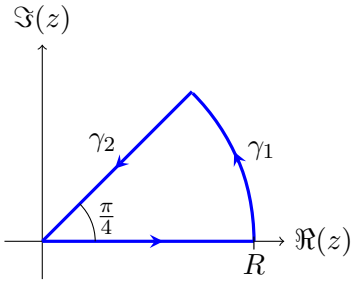

Figure 1.2: The contour C.

Since there are no singularities inside and on the contour C, we can apply Cauchy's theorem to conclude that

$$0 = \oint_C e^{iaz^2}\, dz = \int_0^R e^{iax^2}\, dx + \int_{\gamma_1} e^{iaz^2}\, dz + \int_{\gamma_2} e^{iaz^2}\, dz, \tag{1.66}$$

where $z = x + iy$, γ_1 is the arc portion of the contour, and γ_2 is the diagonal portion of the contour. Along γ_2, the integral is

$$\int_{\gamma_2} e^{iaz^2}\,dz = e^{\frac{i\pi}{4}} \int_R^0 e^{ia(re^{\frac{i\pi}{4}})^2}\,dr = e^{\frac{i\pi}{4}} \int_R^0 e^{-ar^2}\,dr. \tag{1.67}$$

Along γ_1, we have

$$\int_{\gamma_1} e^{iaz^2}\,dz = \int_0^{\frac{\pi}{4}} e^{iaR^2(\cos 2\theta + i\sin 2\theta)} iRe^{i\theta}\,d\theta.$$

Applying triangle inequality and a change of variables, we get

$$\left|\int_{\gamma_1} e^{iaz^2}\,dz\right| \leqslant R\int_0^{\frac{\pi}{4}} e^{-aR^2\sin 2\theta}\,d\theta = \frac{R}{2}\int_0^{\frac{\pi}{2}} e^{-aR^2\sin\alpha}\,d\alpha. \tag{1.68}$$

Recall the Jordan's inequality, which says that

$$\frac{2\alpha}{\pi} \leqslant \sin\alpha \leqslant \alpha, \qquad \text{for } 0 \leqslant \alpha \leqslant \tfrac{\pi}{2}.$$

Then applying Jordan's inequality to (1.68), we obtain that

$$\left|\int_{\gamma_1} e^{iaz^2}\,dz\right| \leqslant \frac{R}{2}\int_0^{\frac{\pi}{2}} e^{\frac{-2aR^2\alpha}{\pi}}\,d\alpha = \frac{\pi}{4aR}(1 - e^{-aR^2}).$$

Making $R \to +\infty$ and using the fact that $a > 0$, yields

$$\lim_{R\to+\infty}\int_{\gamma_1} e^{iaz^2}\,dz = 0,$$

and thus using (1.66), (1.67) and (1.65), we end up with

$$\int_0^{+\infty} e^{iax^2}\,dx = -\lim_{R\to+\infty}\int_{\gamma_2} e^{iaz^2}\,dz = e^{\frac{i\pi}{4}}\int_0^{+\infty} e^{-ar^2}\,dr = e^{\frac{i\pi}{4}}\sqrt{\frac{\pi}{4a}}. \tag{1.69}$$

Taking the complex conjugate of (1.69), we obtain

$$\int_0^{+\infty} e^{-iax^2}\,dx = e^{-\frac{i\pi}{4}}\sqrt{\frac{\pi}{4a}}, \qquad \text{for } a > 0. \tag{1.70}$$

Therefore, using the fact that the integrand is an even function, equations (1.69) and (1.70) can be combined into one formula by

$$\int_{-\infty}^{+\infty} e^{iax^2}\,dx = e^{\frac{i\pi\,\mathrm{sgn}(a)}{4}}\sqrt{\frac{\pi}{|a|}}, \qquad \text{for } a \in \mathbb{R}^*. \tag{1.71}$$

To finish this section, let us calculate the value of the following Fourier transform

$$\int_{-\infty}^{+\infty} e^{iax^2}e^{-ikx}\,dx$$

for $a \in \mathbb{R}^*$ and $k \in \mathbb{R}$. As in the real case, by completing the square and doing a change of variables, one gets

$$\int_{-\infty}^{+\infty} e^{iax^2}e^{-ikx}\,dx = e^{-\frac{ik^2}{4a}}\int_{-\infty}^{+\infty} e^{ia(x-\frac{k}{2a})^2}\,dx = e^{-\frac{ik^2}{4a}}\int_{-\infty}^{+\infty} e^{ia(x')^2}\,dx',$$

and thus using (1.71), we get

$$\int_{-\infty}^{+\infty} e^{iax^2} e^{-ikx}\, dx = e^{-\frac{ik^2}{4a}} e^{\frac{i\pi \mathrm{sgn}(a)}{4}} \sqrt{\frac{\pi}{|a|}}. \tag{1.72}$$

Finally, we can apply formula (1.72) to compute $\langle x|e^{a\pi i\mathsf{p}^2}|y\rangle$ for any $a \in \mathbb{R}^*$. Using the fact that

$$\langle x|e^{a\pi i\mathsf{q}^2}|y\rangle = e^{a\pi i x^2}\delta(x-y) \tag{1.73}$$

and (1.54), one obtains

$$\begin{aligned}
\langle x|e^{a\pi i\mathsf{p}^2}|y\rangle &= \langle x|\mathsf{F}e^{a\pi i\mathsf{q}^2}\mathsf{F}^{-1}|y\rangle \\
&= \int_{\mathbb{R}^2} \langle x|\mathsf{F}|s\rangle\langle s|e^{a\pi i\mathsf{q}^2}|t\rangle\langle t|\mathsf{F}^{-1}|y\rangle\, dsdt \\
&= \int_{\mathbb{R}} e^{a\pi i s^2} e^{2\pi i s(x-y)}\, ds \\
&= \frac{e^{\frac{\pi i \mathrm{sgn}(a)}{4}}}{\sqrt{|a|}} e^{-\frac{\pi i(x-y)^2}{a}}.
\end{aligned} \tag{1.74}$$

1.2.7 Saddle point method

This last part of this chapter is somewhat different and independent of the previous sections. The main references are [Fed89, Won01].

Let $n \geqslant 1$ be an integer. A complex-valued function $(z_1, \ldots, z_n) \mapsto S(z_1, \ldots, z_n)$ defined on an open subset of $\mathbb{C}^n$ is called *analytic* (or *holomorphic*) if it is analytic in every variable [Kra01] (as a function of one complex variable). Moreover:

- Its *holomorphic gradient* ∇S is the function valued in $\mathbb{C}^n$ whose coordinates are $\frac{\partial S}{\partial z_j}$.
- Its *holomorphic hessian* $\mathrm{Hess}(S)$ is the $n \times n$ matrix with coefficients $\frac{\partial^2 S}{\partial z_j \partial z_k}$.

Remark 1.75. In both of these cases, the *holomorphic* denomination comes from the absence of partial derivatives of the form $\frac{\partial}{\partial \overline{z_j}}$.

The *saddle point method* is a general name for studying asymptotics of integrals of the form $\int f e^{\lambda S}$ when $\lambda \to +\infty$. The main contribution is expected to be the value of the integrand at a saddle point of S maximizing $\Re S$. For a general overview of such methods, see [Won01, Chapter 2].

Before going in detail in the saddle point method, let us recall the notion of asymptotic expansion.

Definition 1.76. Let $f : \Omega \to \mathbb{C}$ be a function where $\Omega \subset \mathbb{C}$ is unbounded. A complex power series $\sum_{n=0}^{\infty} a_n z^{-n}$ (either convergent or divergent) is called an *asymptotic expansion* of f if, for every fixed integer $N \geqslant 0$, one has

$$f(z) = \sum_{n=0}^{N} a_n z^{-n} + \mathcal{O}(z^{-(N+1)})$$

when $z \to \infty$. In this case, one denotes

$$f(z) \underset{z\to\infty}{\cong} \sum_{n=0}^{\infty} a_n z^{-n}.$$

For various properties of asymptotic expansions, see [Won01].

The following result is due to Fedoryuk. The statement can be found in [Fed89, Section 2.4.5], and for details and proofs see [Fed77, Chapter 5] (in Russian). To the author's knowledge, this is the only version of the saddle point method in the literature when f and S are analytic functions in several complex variables.

Theorem 1.77 (Fedoryuk [Fed89])**.** *Let $m \geqslant 1$ be an integer, and γ^m an m-dimensional smooth compact real sub-manifold of $\mathbb{C}^m$ with connected boundary. Let us denote $\mathbf{z} = (z_1, \ldots, z_m) \in \mathbb{C}^m$ and $d\mathbf{z} = dz_1 \cdots dz_m$. Let $\mathbf{z} \mapsto f(\mathbf{z})$ and $\mathbf{z} \mapsto S(\mathbf{z})$ be two complex-valued functions analytic on a domain D such that $\gamma^m \subset D \subset \mathbb{C}^m$. We consider the integral*

$$F(\lambda) = \int_{\gamma^m} f(\mathbf{z}) \exp(\lambda S(\mathbf{z}))\, d\mathbf{z},$$

with parameter $\lambda \in \mathbb{R}$.

Assume that $\max_{\mathbf{z}\in\gamma^m} \Re S(\mathbf{z})$ is attained only at a point $\mathbf{z^0}$, which is an interior point of γ^m and a simple saddle point of S (i.e. $\nabla S(\mathbf{z^0}) = 0$ and $\det \mathrm{Hess}(S)(\mathbf{z^0}) \neq 0$).

Then as $\lambda \to +\infty$, there is the asymptotic expansion

$$F(\lambda) \underset{\lambda\to\infty}{\cong} \left(\frac{2\pi}{\lambda}\right)^{m/2} \frac{\exp\left(\lambda S(\mathbf{z^0})\right)}{\sqrt{\det \mathrm{Hess}(S)(\mathbf{z^0})}} \left[f(\mathbf{z^0}) + \sum_{k=1}^{\infty} c_k \lambda^{-k} \right],$$

where the c_k are complex numbers and the choice of branch for the root $\sqrt{\det \mathrm{Hess}(S)(\mathbf{z^0})}$ depends on the orientation of the contour γ^m.

In particular, $\lim_{\lambda\to+\infty} \frac{1}{\lambda} \log |F(\lambda)| = \Re S(\mathbf{z^0})$.

❧ Chapter 2 ❧

Triangulations and hyperbolic 3-manifolds

In this chapter, we at first give all the definitions of different types of triangulations, which will be fundamental for the rest of this thesis. Secondly, we explain some tools that will allow to study hyperbolic 3-manifolds more deeply.

2.1 Triangulations

We start by defining the notion of triangulation, then we will focus on different types of triangulations. First examples will appear from Section 2.1.2.

2.1.1 Triangulations and ideal triangulations

Let $\widetilde{\Delta}$ be a finite union of pairwise disjoint euclidean 3-simplices. Every k-simplex is contained in a unique 3-simplex. Let Φ be the set of *orientation-reversing* affine isomorphisms pairing the 2-simplices in $\widetilde{\Delta}$ such that $\varphi \in \Phi$ if and only if $\varphi^{-1} \in \Phi$, and every 2-simplex is the domain of a unique element of Φ. The quotient space $X = \widetilde{\Delta}/\Phi$ becomes a *closed pseudo-3-manifold* (see [ST80]) and we denote by $p : \widetilde{\Delta} \to X$ the quotient map. The reason of the "pseudo" is that X may fail to be a manifold only at a quotient vertex, whose regular neighbourhood might not be a 3-ball (but for instance a cone over a torus for exteriors of links). The triple $\mathcal{T} = (\widetilde{\Delta}, \Phi, p)$ is a *triangulation* of X, but for simplicity we will often say that X is given with the structure of a triangulation.

Remark 2.1. We took the elements of Φ to be orientation-reversing and we will only use these types of triangulations in this thesis. However, note that in general we do not require this condition and one obtains a more general definition of a triangulation.

Notations 2.2. For $k \in \{0, 1, 2, 3\}$, we will denote

$\widetilde{X}^k := \{k\text{-simplices in } \widetilde{\Delta}\}$

$X^k := \{p(\sigma) \mid \sigma \subset \widetilde{\Delta} \text{ is a } k\text{-simplex}\} = \{\text{equivalence classes of } k\text{-simplices in } \widetilde{\Delta}\}$.

An element of X^k is called a *vertex* for $k = 0$, an *edge* for $k = 1$, a *face* for $k = 2$ and a *tetrahedron* for $k = 3$. For $k \in \{0, 1, 2, 3\}$, we denote the restriction of the quotient map p by $\phi_k : \widetilde{X}^k \to X^k$ and we will, by a slight abuse, identify the sets $\widetilde{X}^3$ and X^3.

A tetrahedron with faces A, B, C, D is usually drawn as in Figure 2.1 (a), but we will represent it as in Figure 2.1 (b) in this thesis. The face outside the circle represents the back face and the center of the circle is the opposite vertex pointing towards the reader.

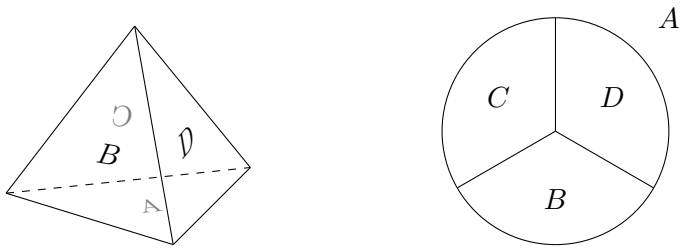

(a) Classical representation. (b) Circular representation.

Figure 2.1: Different representations of a tetrahedron with faces A, B, C, D.

In the case where X is a closed 3-manifold, all the triangulations are related by two types of moves that we explain in the following theorem (for details see [RST18]).

Theorem 2.3 (Alexander–Moise–Newman–Pachner)**.** *Any two triangulations of a closed* 3*-manifold are connected under 2-3, 3-2 moves (Figure 2.2 (a)) and 1-4, 4-1 moves (Figure 2.2 (b)).*

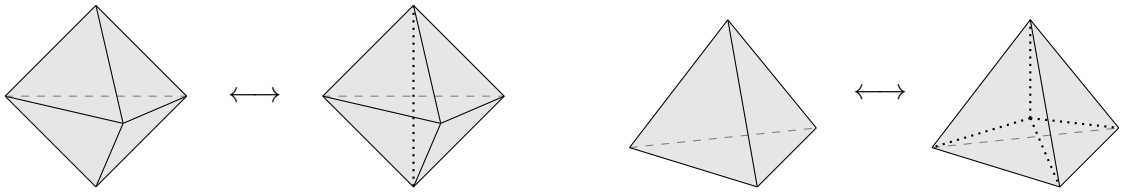

(a) 2-3, 3-2 moves. (b) 1-4, 4-1 moves.

Figure 2.2: The Pachner moves.

There is another type of move called *0-2 move* represented in Figure 2.3, which consists in bloating a pair of faces to two cones, which in turn are decomposed into two distinct tetrahedra. Note that it is not always possible to apply a 2-0 move. Denote by g and h the two edges on the cones that we flatten together (see Figure 2.3). These edges must be distinct and the faces on each cone that we flatten together must be distinct. Finally, even if two diagonal faces may be identified, we do not allow all four faces to be identified in pairs. For more details, see [Bur13].

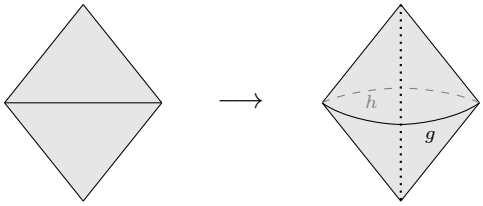

Figure 2.3: 0-2 move.

Consider now the space $M := X \setminus X^0$. Then M is a non-compact (or *cusped*) 3-manifold and we say that X is an *ideal triangulation* of M. An element of X^0 is called an *ideal vertex* of M and we keep the same terminology for the elements of X^k with $k = 1, 2, 3$.

Theorem 2.3 can in fact be improved in the case of ideal triangulations. Originally, the result was given for spines (which are dual objects of tetrahedra) [Mat07b, Pie88], but its equivalent version for ideal triangulations is the following theorem (see also [Ame05]).

Theorem 2.4 (Matveev–Piergallini)**.** *Any two ideal triangulations of a cusped* 3*-manifold are connected under 2-3, 3-2 moves.*

Remark 2.5. A key result of Moise [Moi52] implies that any closed (resp. cusped) 3-manifold admits triangulations (resp. ideal triangulations). Banagl and Friedman found a similar result and gave a version of Theorem 2.3 for more general pseudo-3-manifolds [BF04]. They use this to extend the Turaev–Viro invariants [TV92] to these pseudo-3-manifolds.

2.1.2 Ordered triangulations and graphical representation

An *ordered triangulation* (or simply *triangulation* if the situation makes it clear) is a special type of a triangulation. In this case, we choose an *order* on the four vertices of each tetrahedron T, and we call them $0_T, 1_T, 2_T, 3_T$ (or simply $0, 1, 2, 3$ if the context makes it obvious). If we rotate T such that 0 is at the center and 1 at the top, then there are two possible places for vertices 2 and 3. We call T a *positive* (resp. *negative*) tetrahedron if they are as in the left (resp. right) side of Figure 2.4. We denote $\varepsilon(T) \in \{\pm 1\}$ the corresponding *sign* of T. We *orient the edges* of T accordingly to the order on vertices. Thus there is only one way of gluing two triangular faces together while respecting the order of the vertices.

Notation 2.6. Let X be an ordered triangulation. We encode X into a graph, where a tetrahedron T is represented by a "comb"

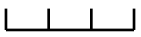

with four vertical segments numbered $0, 1, 2, 3$, from left to right. For $i = 0, 1, 2, 3$, we define $\partial_i : X^3 \to X^2$ the map such that $\partial_i(T)$ is the equivalence class of the face of T opposed to its vertex i. We join the segment i of T to the segment j of T' if $\partial_i(T) = \partial_j(T')$, and we sometimes add a $+$ or $-$ next to each tetrahedron according to its sign.

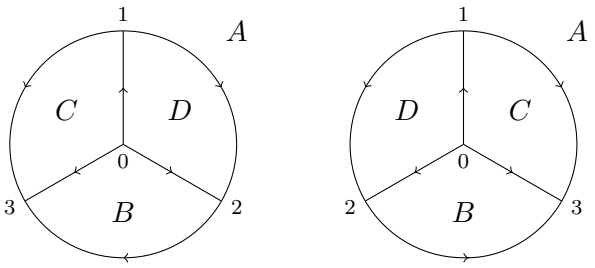

Figure 2.4: A positive (left) and negative (right) tetrahedron. In both cases, we have $\partial_0(T) = A, \partial_1(T) = B, \partial_2(T) = C$ and $\partial_3(T) = D$.

Example 2.7. Figure 2.5 displays the two possible ways of representing an ideal triangulation X of the complement of the figure-eight knot $S^3 \setminus 4_1$ with one positive and one negative tetrahedron. Here we have $X^3 = \{T_1, T_2\}$, $X^2 = \{A, B, C, D\}$, $X^1 = \{\uparrow, \Uparrow\}$ and X^0 is a singleton. We will see two different methods to find this ideal triangulation. The first one using the fact that the knot 4_1 is fibered (Section 2.1.6), and the second one directly from the knot diagram (Section 2.1.7.1).

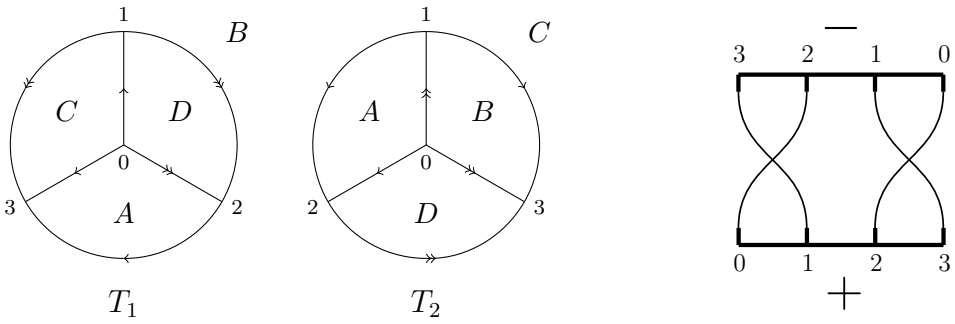

Figure 2.5: Two representations of an ideal triangulation of $S^3 \setminus 4_1$.

2.1.3 Truncated triangulations

Let $X = \widetilde{\Delta}/\Phi$ be a triangulation. One can construct a cell decomposition of a 3-manifold with boundary by removing an open neighbourhood of each vertex of X. Such a process is equivalent to truncate each 3-simplex of $\widetilde{\Delta}$ and we denote the result by $\widetilde{\Delta}_\lrcorner$. The new 3-cells (truncated tetrahedra) are bounded with *triangular* and *hexagonal* cells. In their turn, triangular cells are bounded by *short* 1-cells and hexagonal cells by short and *long* 1-cells (which come from 1-cells of $\widetilde{\Delta}$). See Figure 2.6 for a description. The resulting triangulation is called *truncated triangulation* of X and is denoted $\Theta(X) = \widetilde{\Delta}_\lrcorner/\Phi$. This induces a triangulation on the boundary of $\Theta(X)$, called *boundary triangulation* or sometimes *cusp triangulation* if the boundary is a torus (as for ideal triangulations of knot complements). Note that each triangle of the boundary triangulation comes from an element of $\widetilde{X}^0$. Finally, if $v \in X^0$, then the boundary component of $\Theta(X)$ which comes from v is called the *link* of v, and is denoted $\mathrm{Lk}(v)$.

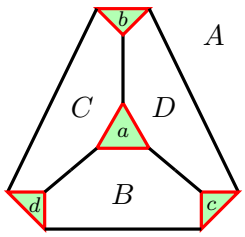

Figure 2.6: A truncated tetrahedron. Triangular cells in green (a, b, c, d), hexagonal cells in white (A, B, C, D), short 1-cells in red and long 1-cells are in black.

Notations 2.8. For a triangulation X, we introduce the following notations:

$$\widetilde{\mathfrak{h}}_X := \{\text{hexagonal cells in } \widetilde{\Delta}_\lrcorner\}, \qquad \widetilde{\mathfrak{s}}_X := \{\text{short 1-cells in } \widetilde{\Delta}_\lrcorner\}$$

and

$$\mathfrak{h}_X := \{p(\sigma) \mid \sigma \subset \widetilde{\Delta}_\lrcorner \text{ is a hexagonal cell}\}, \qquad \mathfrak{s}_X := \{p(\sigma) \mid \sigma \subset \widetilde{\Delta}_\lrcorner \text{ is a short 1-cell}\}.$$

Remark 2.9. Note that Θ can be seen as a bijection from the collection of triangulations into the collection of truncated triangulations. If X is an ideal triangulation of a link complement, then the underlying space of $\Theta(X)$ is a 3-manifold with boundary tori. According to this, we will say with a small abuse, "ideal triangulations of 3-manifolds with boundary tori" in Section 2.2. Moreover, Θ can obviously be descent to a bijection $\Theta : X^2 \to \mathfrak{h}_X$ and this will be used in Chapter 5.

2.1.4 H-triangulations

We start by giving a graph theoretical definition. Main references about H-triangulations are [Kas16, KLV16]. To the author's knowledge, the original formulation comes from [Kas94, Kas95a]. See also [BB04].

Definition 2.10. Let G be a graph. A subgraph $H \subset G$ is a *vertex-disjoint simple cycle cover* if H is a disjoint union of cycles which contains all the vertices of G exactly once.

Looking the 1-skeleton of a triangulation as a graph, we give the following definition.

Definition 2.11. Let M be a closed oriented 3-manifold and $L \subset M$ a link. An *H-triangulation* of (M, L) is an ordered triangulation Y of M such that the 1-skeleton of Y contains a vertex-disjoint simple cycle cover which is ambient isotopic to L. If Y admits only one vertex, then Y is an *one-vertex H-triangulation* of (M, L).

Example 2.12. Figure 2.7 gives two representations of an one-vertex H-triangulation of $(S^3, 3_1)$, where the blue bold edge represents the trefoil knot. Surprisingly, this triangulation is built with only one tetrahedron. We will see how to find this H-triangulation in Section 2.1.7.2.

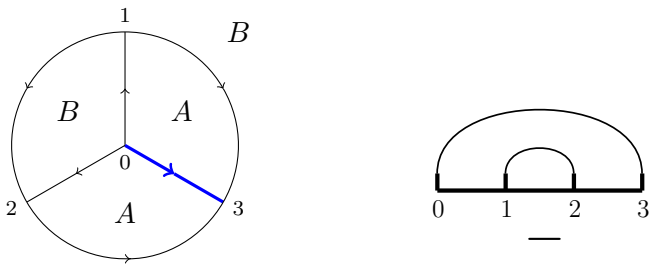

Figure 2.7: Two representations of an one-vertex H-triangulation of $(S^3, 3_1)$.

2.1.5 Shaped triangulations and gauge transformations

We now add extra structures on triangulations. We will come back to this topic in Section 2.2.

Definition 2.13. Let X be a triangulation with tetrahedra $T_1, \dots, T_n$. We assign a real number α_j, called *angle* (or *dihedral angle*), to each pair of opposite 1-simplices of each tetrahedron. The angles associated to T_i are denoted $\alpha_{3i-2}, \alpha_{3i-1}, \alpha_{3i}$, and we impose that for each tetrahedron T_i, we have $\alpha_{3i-2}+\alpha_{3i-1}+\alpha_{3i} = \pi$. A vector $\alpha = (\alpha_1, \dots, \alpha_{3n}) \in \mathbb{R}^{3n}$ satisfying such conditions is called a *generalized shape structure* on X. Moreover, we say that α is

- a *shape structure* on X if $\alpha_j \in (0, \pi)$ for all j;
- an *extended shape structure* on X if $\alpha_j \in [0, \pi]$ for all j.

A triangulation with a shape structure is called a *shaped triangulation*.

Notations 2.14. A triangulation X endowed with a shape structure α will be denoted by (X, α). Moreover, we use the following notations:

$$\begin{aligned} \mathcal{GS}_X &:= \text{ set of generalized shape strutures on } X, \\ \mathcal{S}_X &:= \text{ set of shape strutures on } X, \\ \overline{\mathcal{S}_X} &:= \text{ set of extended shape strutures on } X. \end{aligned}$$

Remark 2.15. A generalized shape structure on a triangulation X can also be seen as a map $\alpha : \widetilde{X}^1 \to \mathbb{R}$, where $\alpha(e)$ is the angle on e.

Definition 2.16. Let X be a triangulation with generalized shape structure α. We denote $\omega_{X,\alpha} : X^1 \to \mathbb{R}$ the associated *weight function*, which sends an edge $e \in X^1$ surrounded by angles $\alpha_{j_1}, \ldots, \alpha_{j_m}$ to their sum $\sum \alpha_{j_k}$. An edge $e \in X^1$ is *balanced* if $\omega_{X,\alpha}(e) = 2\pi$. A triangulation with a generalized shape structure is *balanced* if all the edges are balanced.

Notation 2.17. If X is an ordered triangulation and $\alpha \in \mathcal{GS}_X$, then we define three associated maps $\alpha_i : X^3 \to \mathbb{R}$ (for $i = 1, 2, 3$) which send a tetrahedron T to the angle on the $\overrightarrow{0i}$ edge of T. In the case where $X^3 = \{T_1, \ldots, T_n\}$, we will write $a_k := \alpha_1(T_k), b_k := \alpha_2(T_k)$ and $c_k := \alpha_3(T_k)$ for $k = 1, \ldots, n$.

Let X be a triangulation. Define an equivalence relation on $\widetilde{X}^1$ by

$$e_1 \sim e_2 \iff e_1 = e_2 \quad \text{or} \quad e_1 \text{ and } e_2 \text{ are opposite}$$

for any $e_1, e_2 \in \widetilde{X}^1$. Denote the quotient space $\widetilde{X}^1_p := \widetilde{X}^1/\sim$ and the quotient map $p_1 : \widetilde{X}^1 \to \widetilde{X}^1_p$. For each 0-simplex of each tetrahedron of X, we can put a cyclic clockwise order on the three 1-simplices meeting at the 0-simplex. This induces a cyclic order on $\widetilde{X}^1_p$. Let us define a skew-symmetric function (also called *Neumann–Zagier Poisson bracket*)

$$\{\cdot, \cdot\} : \widetilde{X}^1_p \times \widetilde{X}^1_p \to \{-1, 0, 1\}, \tag{2.18}$$

by $\{x, y\} = 0$ if the underlying tetrahedra are distinct and $\{x, y\} = +1$ if the underlying tetrahedra coincide and a representative of y is cyclically preceded by a representative of x.

Definition 2.19. Let X be a triangulation and $\alpha, \beta \in \mathcal{GS}_X$. We say that α and β are *gauge equivalent* if there exists a function $g : X^1 \to \mathbb{R}$ such that

$$\beta(a) = \alpha(a) + \sum_{b \in \widetilde{X}^1} \{p_1(a), p_1(b)\} g(\phi_1(b))$$

for any $a \in \widetilde{X}^1$. For any $e \in X^1$, the function $h_e : \mathcal{GS}_X \times \mathbb{R} \to \mathcal{GS}_X$ defined by

$$h_e(\alpha, \lambda)(a) := \alpha(a) + \sum_{\substack{b \in \widetilde{X}^1 \\ \phi_1(b) = e}} \{p_1(a), p_1(b)\} \lambda$$

for all $a \in \widetilde{X}^1$ is called a *gauge transformation*.

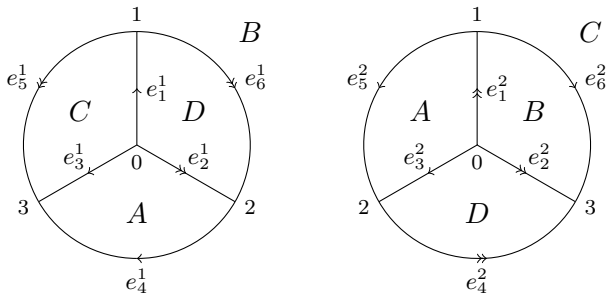

Figure 2.8: Ideal triangulation of $S^3 \setminus 4_1$ with elements of $\widetilde{X}^1$.

Example 2.20. Since the notion of gauge equivalence of Definition 2.19 is not very common in the literature and is often only used by experts, we give a detailed example with the ideal triangulation X of the figure-eight knot complement in Example 2.7. Let us denote the elements of $\widetilde{X}^1$ by $e_1^1, \dots, e_6^1, e_1^2, \dots, e_6^2$ (see Figure 2.8).

By definition of (2.18), we easily see that $\{p_1(e_k^i), p_1(e_l^j)\} = \delta_{i,j}\eta(k,l)$ for all $i,j \in \{1,2\}$ and $k,l \in \{1,\dots,6\}$, where

$$\eta(k,l) = \begin{cases} 0 & \text{if } k \equiv l \pmod 3, \\ 1 & \text{if } k \equiv l-1 \pmod 3, \\ -1 & \text{if } k \equiv l+1 \pmod 3. \end{cases}$$

Let α and β be two generalized shape structures on X. Then α and β are gauge equivalent if there is a function $g : X^1 \to \mathbb{R}$ such that

$$\beta(e_k^i) = \alpha(e_k^i) + \sum_{j=1}^{2}\sum_{l=1}^{6} \delta_{i,j}\eta(k,l)g(\phi_1(e_l^j)) \tag{2.21}$$

for all $i = 1,2$ and $k = 1,\dots,6$. Equation (2.21) can be written more explicitly if we define $g : X^1 \to \mathbb{R}$ by $g(\uparrow) = \lambda_1$ and $g(\Uparrow) = \lambda_2$. In this case, (2.21) becomes

$$\beta(e_a^1) = \alpha(e_a^1) - \lambda_1 + \lambda_2, \qquad \beta(e_b^1) = \alpha(e_b^1) - \lambda_1 + \lambda_2, \qquad \beta(e_c^1) = \alpha(e_c^1) + 2\lambda_1 - 2\lambda_2$$

and

$$\beta(e_a^2) = \alpha(e_a^2) - \lambda_1 + \lambda_2, \qquad \beta(e_b^2) = \alpha(e_b^2) + 2\lambda_1 - 2\lambda_2, \qquad \beta(e_c^2) = \alpha(e_c^2) - \lambda_1 + \lambda_2,$$

where $a \in \{1,4\}, b \in \{2,5\}$ and $c \in \{3,6\}$. Consequently, if we denote a generalized shape structure on X by $\alpha = (a_1, b_1, c_1, a_2, b_2, c_2)$ (see Notation 2.17), then the only linearly independent gauge transformation $h : \mathcal{GS}_X \times \mathbb{R} \to \mathcal{GS}_X$ is given by

$$h(\alpha, \varepsilon) = (a_1 - \varepsilon, b_1 - \varepsilon, c_1 + 2\varepsilon, a_2 - \varepsilon, b_2 - \varepsilon, c_2 + 2\varepsilon). \tag{2.22}$$

The weights on each edge are given by

$$\omega_{X,\alpha}(\uparrow) = 2a_1 + c_1 + 2b_2 + c_2 \qquad \text{and} \qquad \omega_{X,\alpha}(\Uparrow) = 2b_1 + c_1 + 2a_2 + c_2,$$

and we see that they are unchanged by (2.22). In fact, this is a special instance of the fact that gauge transformations do not affect the weights.

2.1.6 Monodromy triangulations

We will now see a special type of ideal triangulation for once-punctured torus bundles over the circle with pseudo-Anosov monodromy. In this case, there exists a natural way to construct an ideal triangulation from the fiber and the monodromy [FH82]. The idea is to connect the torus to its image (by the monodromy) with a composition of *flips* (or *Whitehead moves*), which consist in removing one of the edges in the triangulation and to replace it by the other diagonal one, by piling up flat tetrahedra (Figure 2.9). Nice explanations about this topic are done in [FKP10, Lac03]. We present the one from [Lac03] now.

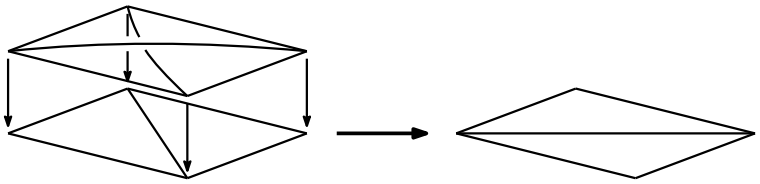

Figure 2.9: A flip by adding a tetrahedron.

Floyd and Hatcher [FH82] gave a beautiful method to construct an ideal triangulation of an once-punctured torus bundle over the circle using Farey tessellation and its dual tree, illustrated in Figure 2.10. The ideal vertices of this tessellation live in $\mathbb{Q} \cup \{\infty\}$, represented in the circle at infinity. For each ideal vertex, there is a corresponding curve in Σ with this slope, where Σ denotes the punctured torus (see Figure 2.10). Therefore, the ideal vertices of an ideal triangle correspond to three disjoint non-parallel curves in Σ, and thus to an ideal triangulation of Σ. If we translate in terms of the dual tree, this means that one has a correspondence between vertices of the tree (bullets in Figure 2.10) and ideal triangulations of Σ. Moreover, two vertices of the tree are joined by an edge (dashed in Figure 2.10) if and only if their corresponding ideal triangulations are related by a flip.

The monodromy of an once-punctured torus bundle induces a homeomorphism of the tree, and it is known that any homeomorphism of a simplicial tree fixes either a point or leaves invariant a unique subgraph isomorphic to $\mathbb{R}$, that we call the *axis*. In the first case, the monodromy is periodic and thus the bundle is not hyperbolic (Theorem 1.19). In the second case, the monodromy becomes pseudo-Anosov and thus the bundle is hyperbolic. Take in this latter case, any vertex in this axis. Since there is a unique path in the tree from this vertex to its image under the monodromy, this determines a sequence of flips. This induces a natural ideal triangulation of the bundle in the following way. We start by the once-punctured torus with its initial ideal triangulation. We then apply the flips corresponding to each edge of the path by adding a flat tetrahedron, as shown in Figure 2.9. Once arrived at the end of the sequence, we glue the top and the bottom ideal triangulation using the monodromy. The result is called the *monodromy triangulation* (or *Floyd–Hatcher triangulation*) of the once-punctured torus bundle over the circle.

Remarks 2.23.

(a) Recall that by Theorem 1.16, any element $A \in SL_2(\mathbb{Z})$ with $|\mathrm{Tr}(A)| > 2$ is conjugate to the product

$$\pm R^{a_1} L^{b_1} \cdots R^{a_n} L^{b_n} \tag{2.24}$$

for some $n \in \mathbb{N}_{>0}$ and $a_1, \ldots, a_n, b_1, \ldots, b_n \in \mathbb{N}_{>0}$.

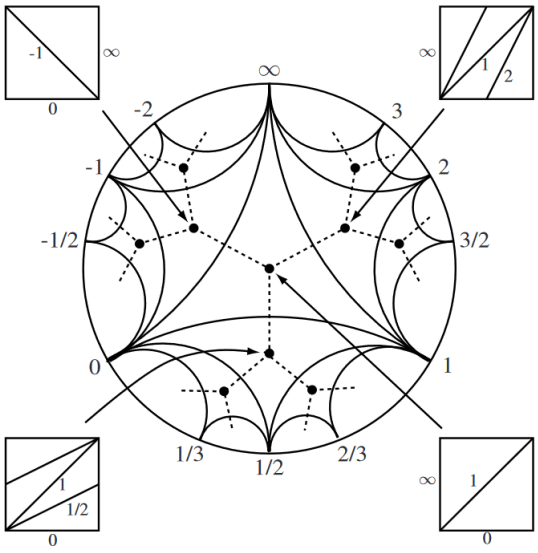

Figure 2.10: Farey tessellation and its dual tree (picture from [Lac03]).

Each letter in this decomposition represents a flip. These informations can be used to find the monodromy triangulation. More precisely, the R represent *right flips* and the L represent *left flips*, and we identify the top of the last tetrahedron to the bottom of the first tetrahedron using the monodromy. We illustrate this in Example 2.25. Note that if $\mathrm{Tr}(A)$ is negative (or equivalently: if there is a minus sign in the decomposition (2.24)), then the monodromy triangulation admits cycles (see Example 2.26). Nonetheless, we will see in Chapter 6 new ideal triangulations of once-punctured torus bundles over the circle without cycles.

(b) Agol [Ago11] generalized this construction for any punctured surface bundles with pseudo-Anosov monodromy using periodic splitting sequences of train tracks.

Example 2.25. We recall that the figure-eight knot is a fibered knot (see for example [BZH13]). Its complement can be described as an once-punctured torus bundle over the circle with monodromy conjugate to the product RL, where R and L are given in (1.17). Let us start by the ideal triangulation of the punctured torus on the top left side of Figure 2.11 (in red and green). As the first letter is an R, we start by doing a right flip. For that, we first bring the red triangle to the right side, which does not affect the initial triangulation. Then we apply our first flip by adding the tetrahedron T_1 in Figure 2.11. The second letter is an L, thus we bring up the blue triangle and we apply our second flip by adding the tetrahedron T_2 in Figure 2.11. We finally identify the first triangulation and the last triangulation in Figure 2.11 respecting the colors. All this process induces identifications on the two tetrahedra T_1 and T_2. For simplicity of reading, we only denote the identified edges in Figure 2.11, since the identifications on faces can be deduced automatically from the informations on the edges. We thus succeeded to find an ideal triangulation of $S^3 \setminus 4_1$ and we immediately see that this ideal triangulation is exactly the same as the one of Figure 2.5. We will see in Section 2.1.7.1 another method to find this ideal triangulation directly from the diagram of the knot.

Example 2.26. If we had taken $-RL$ instead of RL in Example 2.25, we would have obtained exactly the same picture as Figure 2.11 with the only difference that the colors

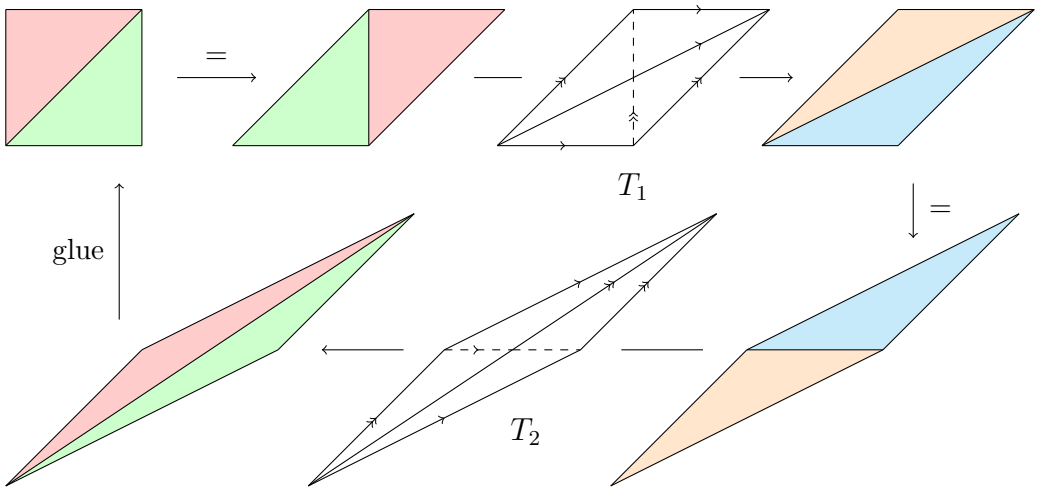

Figure 2.11: Process of finding monodromy triangulation of $S^3 \setminus 4_1$.

of the last triangulation (the bottom left one) are exchanged. This difference leads different identifications than those shown in Figure 2.5 and the resulting ideal triangulation is given in Figure 2.12. Note that this ideal triangulation contains cycles (thus not ordered). The underlying cusped 3-manifold is called the *figure-eight knot sister*.

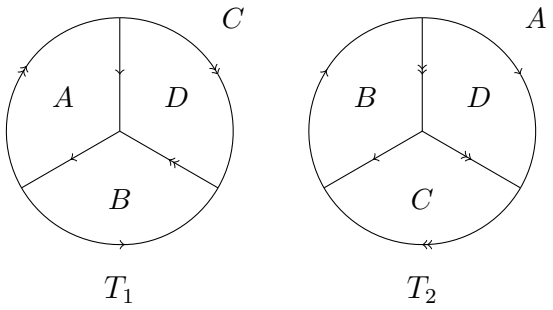

Figure 2.12: Monodromy triangulation of figure-eight knot sister.

2.1.7 Examples of constructions

In this last part on triangulations, we present a method to construct an H-triangulation of a pair (S^3, K) and an ideal triangulation of $S^3 \setminus K$ starting from a knot diagram of K with the example of the figure-eight knot and the trefoil knot. We will see another detailed example with the twist knots in Chapter 4. The method dates back to Thurston [Thu78] and refined by Menasco [Men83] and Kashaev–Luo–Vartanov [KLV16]. See also [BP92, Pur20].

2.1.7.1 The figure-eight knot

We start, as in Figure 2.13, by choosing a middle point for each arc of the diagram, except for one arc we choose two (the top one on the figure), and we draw quadrilaterals around the crossings with the chosen points as vertices (in dashed lines and filled in gray in Figure 2.13).

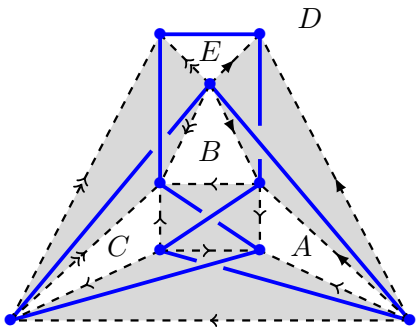

Figure 2.13: Building an H-triangulation from a diagram of 4_1.

We consider the equivalence relation on the dotted edges generated by "being part of the same quadrilateral", and we choose a way of drawing each class. Moreover, we orient the arrow such that the directions are alternating when one goes around any quadrilateral. In Figure 2.13 there are three such edges. One simple arrow, one double arrow and one full arrow.

In Figure 2.13, we see that around each crossing of the diagram, there are six edges (two in blue from the knot, four dotted with arrows) and that delimit an embedded tetrahedron. We now collapse all these tetrahedra into one segment, so that the blue edges (parts of the knot) are collapsed to a point of the segment and all the four dotted edges fuse into one edge (see Figure 2.14). The homeomorphism type does not change if we collapse every tetrahedron in such a way.

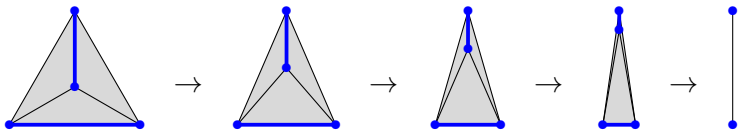

Figure 2.14: An isotopy which collapses a tetrahedron to a segment.

After collapsing, the ambient space (which is still S^3) is decomposed into one 0-cell, four edges (simple arrow, double arrow, full arrow and blue edge coming from the knot), five polygonal 2-cells (denoted A, B, C, D, E) and two polygonal 3-balls B_+ and B_-, respectively from below and upper the figure. The boundaries of B_+ and B_- are described in Figure 2.15. Note that the boundary of B_+ is obtained from Figure 2.13 by collapsing the upper strands of the knot, and B_+ is implicitly residing behind Figure 2.15 (a). Similarly, B_- resides above Figure 2.15 (b).

We can now give a new description of S^3 gluing B_+ and B_- along the 2-cell D. The two 3-cells fuse into one, and its boundary is now as in Figure 2.16 (a). Note that in Figure 2.16 (a) the red dashed faces lie on the back of the figure, and the only 3-cell lives inside the polyhedron. Finally, we can rotate this polyhedron and obtain the cellular decomposition of S^3 in Figure 2.16 (b).

Orienting the edge representing the knot from right to left in Figure 2.16 and by tearing off the obvious tetrahedra, we get the triangulation of Figure 2.17.

We are now ready to obtain an ideal triangulation of $S^3 \setminus 4_1$. From the H-triangulation

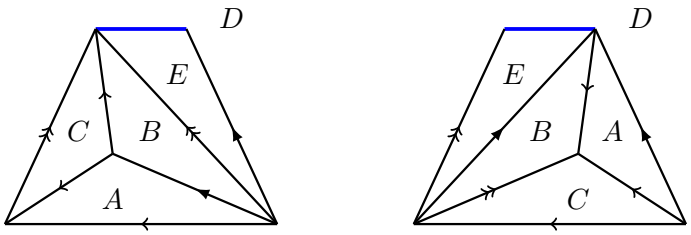

(a) Boundary of B_+ (B_+ behind the figure).

(b) Boundary of B_- (B_- above the figure).

Figure 2.15: Boundaries of B_+ and B_-.

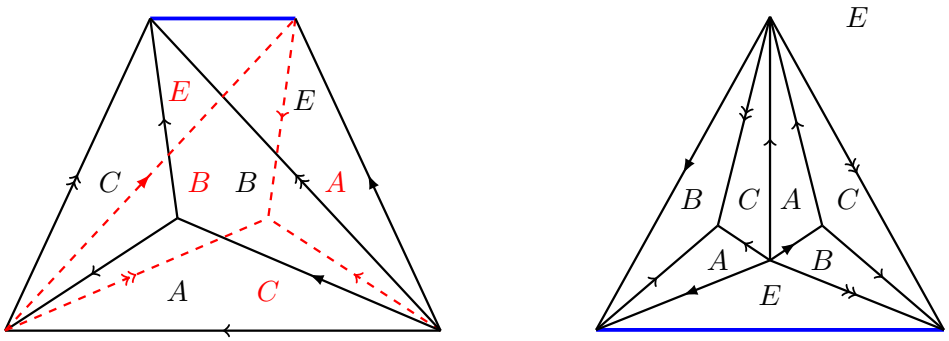

(a) (b)

Figure 2.16: A cellular decomposition of $(S^3, 4_1)$ as a polyhedron glued to itself.

of $(S^3, 4_1)$ of Figure 2.17, we collapse the whole tetrahedron T_0 into a triangle. This transforms the blue edge (which corresponds to the knot) into a point, collapses the two faces E and the faces D and F are identified together, and the double arrow and the full arrow will be identified. We finally obtain the ideal triangulation of $S^3 \setminus 4_1$ of Figure 2.5. Note that we could also have found the ideal triangulation of Figure 2.5 by applying the same process to find the H-triangulation of $(S^3, 4_1)$, but starting this time by already collapsing the knot to a point. We will illustrate this with the example of the trefoil knot (Section 2.1.7.2).

Finally, note that the figure-eight knot is a *hyperbolic knot* (i.e. its complement is a hyperbolic 3-manifold) and we will see this and compute the volume of its complement in Example 2.47, using the ideal triangulation of Figure 2.5.

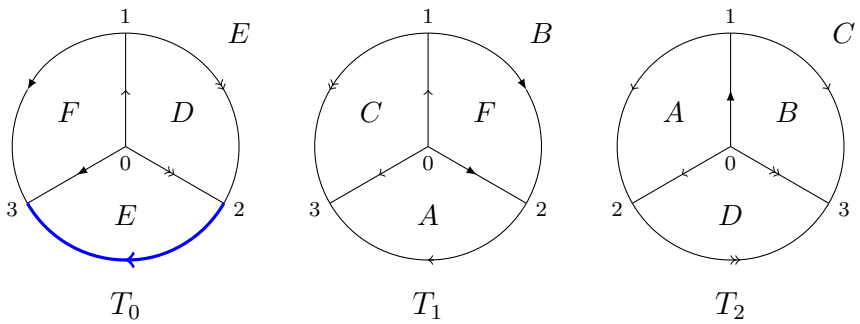

Figure 2.17: An one-vertex H-triangulation of $(S^3, 4_1)$.

2.1.7.2 The trefoil knot

Again, starting from the knot diagram (Figure 2.18), we apply the same method that we used in Section 2.1.7.1.

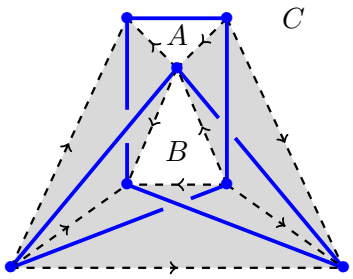

Figure 2.18: Building an H-triangulation from a diagram of 3_1.

After collapsing the shaded tetrahedra, we obtain two 3-balls B_+ and B_-, for which their boundaries are represented in Figure 2.19.

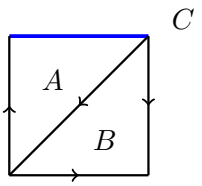

(a) Boundary of B_+ (B_+ behind the figure).

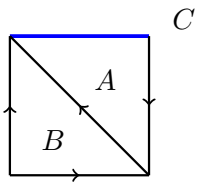

(b) Boundary of B_- (B_- above the figure).

Figure 2.19: Boundaries of B_+ and B_-.

We orient the edge representing the knot from right to left in Figure 2.18 and glue B_+ and B_- along the 1-cell C. We get the triangulation of Figure 2.7.

We can also find an ideal triangulation of $S^3 \setminus 3_1$, but the situation is not as easy as the case of the figure-eight knot in Section 2.1.7.1 since we cannot simply collapse the knot and delete the tetrahedron containing the knot. To find such an ideal triangulation, it will be convenient to start by the diagram of Figure 2.20. This time, we do not keep the knot as an edge, but we collapse it into a point. Thus the homeomorphism type is changed.

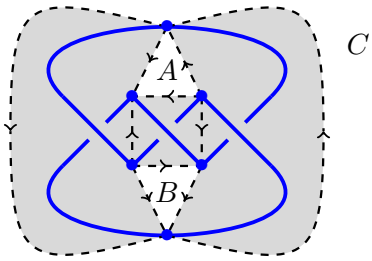

Figure 2.20: Building an ideal triangulation from a diagram of 3_1.

Nonetheless, the space is again decomposed into two balls B_+ and B_- for which their boundaries and the gluing on the 2-cell C are represented in Figure 2.21.

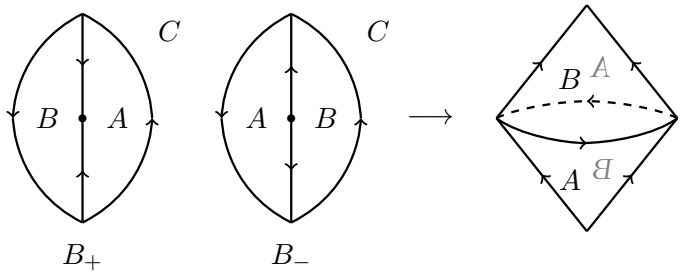

Figure 2.21: Boundaries of B_+ (B_+ behind the figure) and B_- (B_- above the figure) and their gluing on C.

Finally, applying a 0-2 Pachner move (without creating cycle) to the 3-cell of Figure 2.21, we immediately get the triangulation of Figure 2.22.

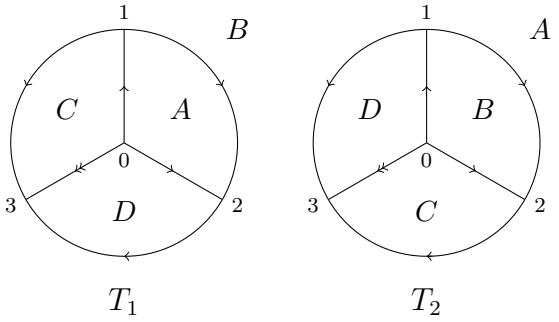

Figure 2.22: An ideal triangulation of $S^3 \setminus 3_1$.

2.2 Hyperbolic 3-manifolds

Thurston showed in [Thu82] that "almost every" 3-manifold M, whether closed or bounded, admits a complete hyperbolic structure, which is unique up to isometry if the boundary of M consists of tori [Mos73, Pra73]. Furthermore, he introduced a method to find this unique metric in [Thu78]. For this purpose, he considers the decomposition of the interior of M into ideal tetrahedra and associate to each ideal tetrahedron a shape, described by a complex number. Using these shapes, he wrote down a system of equations, called *gluing equations*, whose solution corresponds to the unique complete hyperbolic metric on the interior of M. Very nice explanations about this topic are done in [FG11].

2.2.1 Gluing equations

We use the approach given in [FG11, FG13]. Let M be a compact connected orientable 3-manifold whose boundary ∂M is a non-empty union of tori.

The notion of ideal tetrahedron in $\mathbb{H}^3$ will be important, since it will be the isometric model of each tetrahedron in the ideal triangulation of M.

Definition 2.27. An *ideal tetrahedron in* $\mathbb{H}^3$, denoted T, is the convex hull in $\mathbb{H}^3$ of four distinct points in $\partial\overline{\mathbb{H}}^3$. The four points in $\partial\overline{\mathbb{H}}^3$ are called *ideal vertices* of T, and are not contained in T. The ideal tetrahedron T is called *degenerate* if it lies in a plane, and *non-degenerate* otherwise.

Recall that any isometry of $\mathbb{H}^3$ acts 3-transitively. In other words, the isometry is completely determined by its action on three points in $\partial\overline{\mathbb{H}}^3$ and according to this we can assume that three ideal vertices of any ideal tetrahedron $T \subset \mathbb{H}^3$ are 0, 1 and ∞. Therefore, a non-degenerate ideal tetrahedron $T \subset \mathbb{H}^3$ is determined (up to isometry) by a complex number $z \in \mathbb{C}$ with $\Im(z) > 0$ and we say that z is a *complex shape* (or *shape parameter*) of T.

If $T \subset \mathbb{H}^3$ is a non-degenerate ideal tetrahedron with ideal vertices $0, 1, \infty$ and z, then by applying an orientation-preserving isometry to T which sends three ideal vertices again to $0, 1$ and ∞, we can easily check that the last vertex of T is sent to one of the following values:

$$z, \qquad z' := \frac{1}{1-z}, \qquad z'' := \frac{z-1}{z}.$$

This shows that a complex shape of T can be given either by z, z' or z''. Moreover, if e denotes the edge connecting 0 and ∞ in the ideal tetrahedron with ideal vertices $0, 1, \infty$ and z, then we say that z is the *shape parameter of* e. One easily checks that opposite edges have same shape parameter and that

$$zz'z'' = -1, \qquad 1 - z' + zz' = 0. \tag{2.28}$$

Conversely, if we have $z, z', z'' \in \mathbb{C}$ with strictly positive imaginary parts which satisfy equations (2.28), then there exists (up to orientation preserving isometry) a unique ideal tetrahedron $T \subset \mathbb{H}^3$ where the complex shapes are z, z' and z'' [Rat06, Theorem 10.5.2].

Geometrically, the arguments of z, z' and z'' represent the dihedral angles of T, which are angles on the euclidean triangle with vertices $0, 1$ and z. Moreover, if an ideal vertex of T is truncated by a horosphere, then the intersection between T and this horosphere will be an euclidean triangle and is called *boundary triangle* of T (see Figure 2.23, in gray). If the three dihedral angles meeting at an ideal vertex of T are denoted α, β, γ in clockwise order, then the corresponding shape parameter to α is given by (see Figure 2.23)

$$z(\alpha) = \frac{\sin\gamma}{\sin\beta} e^{i\alpha}. \tag{2.29}$$

Consequently, one can do a correspondence between the set of shape structures on an ideal triangulation X and the set of all the complex shapes on each tetrahedron of X.

Definition 2.30. Let S be a closed surface with a specified triangulation. A *segment* in S is an embedded arc in one triangle, which is disjoint from the vertices of S, and whose endpoints lie in distinct edges of S. A *normal curve* $\sigma \subset S$ is an immersed curve that is transverse to the edges of S, such that the intersection between σ and a triangle is a segment.

In this thesis, we will use the following definition of the complex logarithm:

$$\mathrm{Log}(z) := \log|z| + i\arg(z) \quad \text{ for } z \in \mathbb{C}^*,$$

where $\arg(z) \in (-\pi, \pi]$.

Let X be an ideal triangulation of M, and let S be one torus boundary component of ∂M. Then X induces a truncated triangulation (Remark 2.9), which in turn induces a

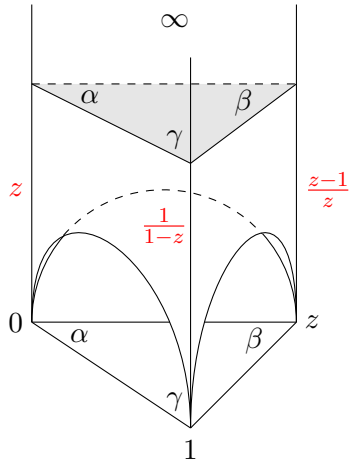

Figure 2.23: An ideal tetrahedron in $\mathbb{H}^3$.

boundary triangulation of S. We assign to each 1-simplex of each tetrahedron of X a shape parameter. Then every corner of each boundary triangle can be labeled with the corresponding shape parameter.

Definition 2.31. Let $\sigma \subset S$ be an oriented normal closed curve. Then every segment in a boundary triangle of S will cover a corner of the triangle labelled by a shape parameter (see Figure 2.24). If $z_1, \ldots, z_k$ are the shape parameters corresponding to σ, then we define the *complex holonomy* (or simply *holonomy*) of σ by

$$H^{\mathbb{C}}(\sigma) := \sum_{i=1}^{k} \epsilon_i \mathrm{Log}(z_i), \tag{2.32}$$

where $\epsilon_i = -1$ for corners of triangles which are on the right of σ, and $\epsilon_i = +1$ for corners on the left.

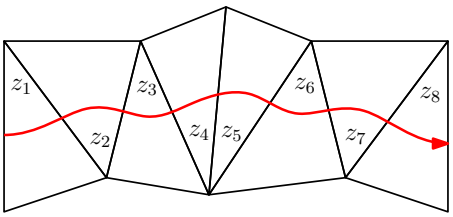

Figure 2.24: A normal curve passing through boundary triangles in the torus boundary.

If $\alpha \in \mathcal{GS}_X$, the *angular holonomy* $H^{\mathbb{R}}(\sigma)$ of σ is similarly defined, replacing the term $\mathrm{Log}(z_i)$ in (2.32) by the angle lying on i-th corner.

Definition 2.33. Let X be an ideal triangulation and $\alpha \in \mathcal{S}_X$. The *complex weight function* $\omega^{\mathbb{C}}_{X,\alpha} : X^1 \to \mathbb{C}$ sends an edge $e \in X^1$ to the sum of logarithms of each shape parameter associated (by formula (2.29)) to each angle surrounding e.

Thurston introduced in [Thu78] a family of equations called *gluing equations* for an ideal triangulation X of M, which is again divided in two families called *hyperbolicity equations*

and *completeness equations*. As the name suggests, a non-degenerate solution for the hyperbolicity equations is equivalent to obtain a hyperbolic metric on M (but not necessarily complete), and if this solution satisfies the completeness equations, the latter metric will be complete [FG11, Proposition 2.5]. More precisely, we have the following definition.

Definition 2.34. Let X be an ideal triangulation of M and α be a shape structure on X. The *hyperbolicity equations* associated to X consist in asking that the holonomies of each normal closed curve in ∂M surrounding a vertex of the induced boundary triangulation are all equal to $2\pi i$. In other words, we have that

$$\omega^{\mathbb{C}}_{X,\alpha}(e) = 2\pi i \quad \forall e \in X^1.$$

The *completeness equations* require that the holonomies of all normal closed curves generating $H_1(\partial M, \mathbb{Z})$ vanish.

Finally, if X admits a non-degenerate solution to its gluing equations, we say that X is *geometric*.

Remarks 2.35.

(a) If X is a geometric ideal triangulation, then the solution to gluing equations is unique by Mostow–Prasad rigidity theorem [Mos73, Pra73] (Theorem 2.46).

(b) The works of Akiyoshi [Aki99] and Lackenby [Lac03] showed that for any pseudo-Anosov mapping of the once-punctured torus, its associated monodromy triangulation is geometric. Guéritaud [Gué06] obtained the same conclusion using a direct argument. See also [FTW18, HIS16, Wor20].

(c) Assume that a shape structure α on X satisfies the hyperbolicity equations. For any toroidal boundary component S of M, if one calls l, m two curves generating $H_1(S, \mathbb{Z})$, then the following are equivalent formulations of the completeness equations for S:

- $H^{\mathbb{C}}(m) = 0$,
- $H^{\mathbb{C}}(l) = 0$,
- $H^{\mathbb{R}}(m) = 0$ and $H^{\mathbb{R}}(l) = 0$.

This can be compared with the equivalent definitions for a quadrilateral $ABCD$ to be a parallelogram: either you ask that AB and CD are parallel of same length, or the same for AD and BC, or equivalently that AB and CD are parallel and AD and BC are too.

We saw that one can describe the shape of a tetrahedron T of an ideal triangulation either using angles on T (coming from shape structures) or using shape parameters (z, z', z''). In the case of ordered ideal triangulations, these shapes can also be described by the complex number

$$y := \varepsilon(T)(\mathrm{Log}(z) - i\pi) \in \mathbb{R} - i\varepsilon(T)(0, \pi).$$

Note by a, b, c the angles on edges $\overrightarrow{01}, \overrightarrow{02}, \overrightarrow{03}$ respectively. The various equations relating $(a, b, c), (z, z', z'')$ and y for both possible signs of T are given as follows:

$$\begin{aligned}
\underline{\text{Positive tetrahedron:}}\quad & y + i\pi = \mathrm{Log}(z) = \log\left(\frac{\sin(c)}{\sin(b)}\right) + ia. \\
& -\mathrm{Log}(1 + e^{y}) = \mathrm{Log}(z') = \log\left(\frac{\sin(b)}{\sin(a)}\right) + ic. \\
& \mathrm{Log}(1 + e^{-y}) = \mathrm{Log}(z'') = \log\left(\frac{\sin(a)}{\sin(c)}\right) + ib. \\
& y = \log\left(\frac{\sin(c)}{\sin(b)}\right) - i(\pi - a) \in \mathbb{R} - i(\pi - a). \\
& z = -e^{y} \in \mathbb{R} + i\mathbb{R}_{>0}.
\end{aligned}$$

$$\begin{aligned}
\underline{\text{Negative tetrahedron:}}\quad & -y + i\pi = \mathrm{Log}(z) = \log\left(\frac{\sin(b)}{\sin(c)}\right) + ia. \\
& -\mathrm{Log}(1 + e^{-y}) = \mathrm{Log}(z') = \log\left(\frac{\sin(c)}{\sin(a)}\right) + ib. \\
& \mathrm{Log}(1 + e^{y}) = \mathrm{Log}(z'') = \log\left(\frac{\sin(a)}{\sin(b)}\right) + ic. \\
& y = \log\left(\frac{\sin(c)}{\sin(b)}\right) + i(\pi - a) \in \mathbb{R} + i(\pi - a). \\
& z = -e^{-y} \in \mathbb{R} + i\mathbb{R}_{>0}.
\end{aligned}$$

For clarity, let us define the diffeomorphism

$$\psi_T \colon \mathbb{R} + i\mathbb{R}_{>0} \to \mathbb{R} - i\varepsilon(T)(0, \pi),\ z \mapsto \varepsilon(T)(\mathrm{Log}(z) - i\pi),$$

and its inverse

$$\psi_T^{-1} \colon \mathbb{R} - i\varepsilon(T)(0, \pi) \to \mathbb{R} + i\mathbb{R}_{>0},\ y \mapsto -\exp\left(\varepsilon(T)y\right).$$

2.2.2 Angle structures

In general, solving Thurston's gluing equations is a difficult problem because of their non-linearity. Even proving the existence of a non-degenerate solution remains hard. Later, Casson and Rivin (see [FG11, Riv94]) developed a powerful method to solve this problem. This consists in separating the system of gluing equations into *linear part* and *non-linear part*. We will now explain how it goes on for the linear part.

We take the same M as in Section 2.2.1.

Definition 2.36. Let X be an ideal triangulation with tetrahedra $T_1, \ldots, T_n$ and $\alpha = (\alpha_1, \ldots, \alpha_{3n}) \in \mathcal{GS}_X$ a balanced generalized shape structure on X. Then α is called a *generalized angle structure* on X. Moreover, we say that α is

- an *angle structure* on X if α is a shape structure;
- an *extended angle structure* on X if α is an extended shape structure;

- a *taut angle structure* on X if $\alpha_j \in \{0, \pi\}$ for all j.

Notations 2.37. One uses the following notations:

$$\begin{aligned} \mathcal{GA}_X &:= \text{ set of generalized angle strutures on } X, \\ \mathcal{A}_X &:= \text{ set of angle strutures on } X, \\ \overline{\mathcal{A}_X} &:= \text{ set of extended angle strutures on } X, \\ \mathcal{TA}_X &:= \text{ set of taut angle strutures on } X. \end{aligned}$$

For an ideal triangulation, admitting an angle structure is a necessary condition to find non-degenerate solutions for gluing equations, but not sufficient. Nonetheless, Casson proved the following important result [FG11, Theorem 1.1].

Theorem 2.38 (Casson)**.** *Let M be an orientable 3-manifold with boundary consisting of tori, and let X be an ideal triangulation of M. If $\mathcal{A}_X \neq \varnothing$, then M admits a complete hyperbolic metric.*

In general, for a given 3-manifold M, there is no guarantee that M admits an ideal triangulation with angle structures or taut angles structures. Nevertheless, under some conditions it becomes possible.

Remarks 2.39.

(a) If M is a hyperbolic cusped 3-manifold with torus or Klein bottle boundary components such that $H_1(M, \mathbb{Z}/2\mathbb{Z}) \to H_1(M, \partial M, \mathbb{Z}/2\mathbb{Z})$ is the zero map, then M admits an ideal triangulation with an angle structure [HRS12, Theorem 1.1]. In particular, a hyperbolic link complement in S^3 admits an ideal triangulation with angle structures [HRS12, Corollary 1.2].

(b) If M is an orientable irreducible an-annular 3-manifold such that ∂M is a non-empty collection of incompressible tori, then M has an ideal triangulation with a taut angle structure [Lac00, Theorem 1].

(c) For any ideal triangulation X, the set $\mathcal{GA}_X$ is non-empty [LT08, Theorem 1].

2.2.3 Hyperbolic volume

Let us see how to compute the volume of a hyperbolic 3-manifold with boundary tori. To achieve this, we start by calculating the volume of an ideal tetrahedron in $\mathbb{H}^3$, which uses the *Lobachevsky function* $\Lambda : \mathbb{R} \to \mathbb{R}$ defined by

$$\Lambda(\theta) := -\int_0^\theta \log|2\sin t|\, dt.$$

This odd function is continuous and π-periodic on $\mathbb{R}$ [Rat06, Theorem 10.4.3]. The key property of the Lobachevsky function is the following result. For proof and further properties, see for example [Mil82] or [Rat06].

Theorem 2.40. *If T is an ideal tetrahedron in $\mathbb{H}^3$ with dihedral angles α, β, γ, its volume is given by*

$$\mathrm{Vol}(T) = \Lambda(\alpha) + \Lambda(\beta) + \Lambda(\gamma).$$

One can also compute the volume of an ideal tetrahedron in $\mathbb{H}^3$ directly from complex shapes. We use the *dilogarithm*, that is a special function defined by the power series

$$\mathrm{Li}_2(z) := \sum_{n=1}^{\infty} \frac{z^n}{n^2} \qquad \text{for } |z| < 1,$$

with analytic continuation

$$\mathrm{Li}_2(z) = -\int_0^z \frac{\log(1-s)}{s}\, ds \qquad \text{for } z \in \mathbb{C} \setminus [1, \infty).$$

We will use the following properties of the dilogarithm function, referring for example to [AH06, Appendix A] for the proofs and for further properties, see [Kir95] or [Zag06].

Proposition 2.41 (Some properties of Li_2)**.**

(1) (inversion relation) For all $z \in \mathbb{C} \setminus [1, \infty)$,

$$\mathrm{Li}_2(z) + \mathrm{Li}_2\left(\frac{1}{z}\right) = -\frac{1}{2}\log^2(-z) - \frac{\pi^2}{6}.$$

(2) (integral form) For all $y \in \mathbb{R} + i(-\pi, \pi)$,

$$-\frac{i}{2\pi}\mathrm{Li}_2(-e^y) = \int_{v \in \mathbb{R}+i0} \frac{\exp\left(-i\frac{yv}{\pi}\right)}{4v^2 \sinh(v)}\, dv.$$

We define the *Bloch–Wigner function* by

$$D(z) := \Im(\mathrm{Li}_2(z)) + \arg(1-z)\log|z| \qquad \text{for } z \in \mathbb{C} \setminus [1, \infty),$$

Surprisingly, this function is real-analytic on $\mathbb{C}\setminus\{0,1\}$ and plays a central role in hyperbolic geometry and even in algebraic K-theory [Zag06]. The following result will be important for us (for a proof, see [NZ85]).

Theorem 2.42. *Let T be an ideal tetrahedron in $\mathbb{H}^3$ with complex shape z. Then, its volume is given by*

$$\mathrm{Vol}(T) = D(z) = D\left(\frac{1}{1-z}\right) = D\left(\frac{z-1}{z}\right).$$

Example 2.43. The volume of the regular ideal tetrahedron in $\mathbb{H}^3$ is $3\Lambda(\frac{\pi}{3}) = 1.01494...$. Moreover, the regular ideal tetrahedron has the maximal volume among all the ideal tetrahedra in $\mathbb{H}^3$ [Rat06, Theorem 10.4.11].

Let M be a hyperbolic 3-manifold with boundary tori. Assume that X is a geometric ideal triangulation of M with tetrahedra $T_1, \ldots, T_n$. Then the volume of M can be computed taking the sum of the volumes of each tetrahedron (with complex shapes corresponding to the complete structure):

$$\mathrm{Vol}(M) = \sum_{i=1}^{n} \mathrm{Vol}(T_i). \tag{2.44}$$

Let us give some important results about hyperbolic volume.

Remarks 2.45.

(a) The volume of a hyperbolic knot is defined as the volume of its complement, and it is known that there are only finitely many hyperbolic knots for any given volume [Wie81].

(b) Two mutant knots have the same volume [Rub87].

(c) The hyperbolic volume can also be computed for closed hyperbolic 3-manifolds using hyperbolic Dehn surgery [Thu78] (see also [NZ85]), but it is not known whether all hyperbolic 3-manifolds of finite volume can be constructed in this way [PP99]. However, in practice, this is how computational softwares (such as `SnapPy` or `Regina`) store informations about hyperbolic 3-manifolds [CHW99].

(d) Jørgensen and Thurston proved that the set of real numbers that are hyperbolic volumes of 3-manifolds is well-ordered, with order type ω^ω (see [NZ85]).

A crucial property is that Mostow–Prasad rigidity theorem [Mos73, Pra73], that we restate now, implies that the volume of a hyperbolic 3-manifold becomes a topological invariant.

Theorem 2.46 (Mostow–Prasad rigidity theorem)**.** *Suppose that M and N are complete finite-volume hyperbolic 3-manifolds. If there exists an isomorphism between $\pi_1(M)$ and $\pi_1(N)$, then it is induced by a unique isometry from M to N.*

Example 2.47. Let us show that $S^3 \setminus 4_1$ is a hyperbolic (complete) 3-manifold using the ideal triangulation X of Figure 2.5, and let us calculate its hyperbolic volume. Consider the truncation of X given in Figure 2.25. We denote the shape parameters in blue and the identifications of short 1-cells in red.

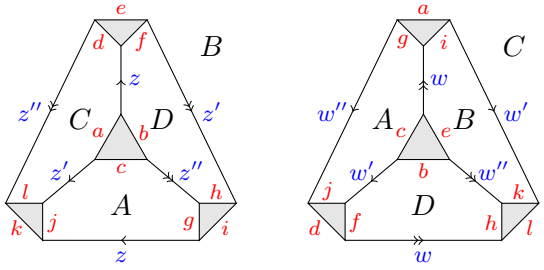

Figure 2.25: Truncated triangulation of the ideal triangulation of Figure 2.5.

Let $\alpha \in \mathcal{S}_X$ be the shape structure corresponding to the shape parameters. The hyperbolicity equations are

$$\omega^{\mathbb{C}}_{X,\alpha}(\uparrow) = \omega^{\mathbb{C}}_{X,\alpha}(\Uparrow) = 2\pi i,$$

which is simply equivalent to say

$$z^2 \left(\frac{1}{1-z}\right)\left(\frac{1}{1-w}\right)^2 \left(\frac{w-1}{w}\right) = 1. \tag{2.48}$$

To find the completeness equation, we take the curve m_X on the cusp triangulation of Figure 2.26.

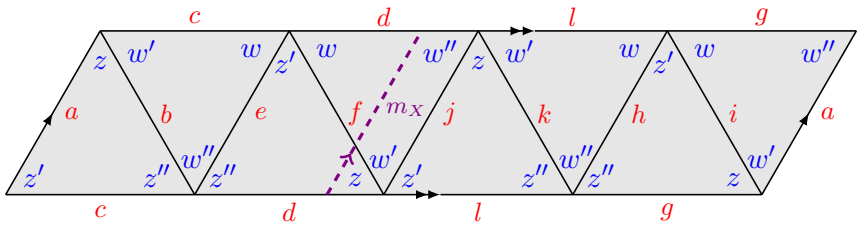

Figure 2.26: Triangulation of the boundary torus for the truncation of X, with shape parameters (blue), identifications of short 1-cells (red) and the curve m_X (violet, dashed).

Then we see that the completeness equation coming from m_X is equivalent to say $z = w$. Substituting w by z in equation (2.48), we easily find that the unique solution (z^0, w^0) for the gluing equations with $\Im(z^0) > 0$, $\Im(w^0) > 0$ is given by $z^0 = w^0 = e^{\frac{i\pi}{3}}$, and thus the two tetrahedra are regular. Using Theorem 2.40 and (2.44), we obtain that the volume of $S^3 \setminus 4_1$ is $6\Lambda(\frac{\pi}{3}) = 2.02988...$. In a similar way, using the ideal triangulation of Figure 2.12, one can show that the figure-eight knot sister has also the same volume. Nevertheless, these two 3-manifolds are not homeomorphic.

Even though the volume is an efficient hyperbolic knot invariant, it requires, a priori, to know the solution of gluing equations. Let us get back to Casson–Rivin program. We are now going to explain how they solve the non-linear part of gluing equations.

Definition 2.49. Let X be an ideal triangulation with n tetrahedra. The *volume functional* is a function $\mathcal{V} : \overline{\mathcal{A}_X} \to \mathbb{R}$ which attribute to an element $\alpha = (\alpha_1, \dots, \alpha_{3n}) \in \overline{\mathcal{A}_X}$ the real number

$$\mathcal{V}(\alpha) := \sum_{i=1}^{3n} \Lambda(\alpha_i). \tag{2.50}$$

Remark 2.51. By [Gué06, Propositions 6.1 and 6.6] and [FG11, Lemma 5.3] the volume functional $\mathcal{V}$ is strictly concave on $\mathcal{A}_X$ and concave on $\overline{\mathcal{A}_X}$.

Casson and Rivin proved that the maximum of the volume functional is related to the complete hyperbolic structure that we restate now [FG11, Theorem 1.2].

Theorem 2.52 (Casson–Rivin)**.** *Let M be an orientable 3-manifold with boundary consisting of tori, and let X be an ideal triangulation of M. Then an angle structure $\alpha \in \mathcal{A}_X$ corresponds to a complete hyperbolic metric on the interior of M if and only if α is a critical point of the functional $\mathcal{V} : \overline{\mathcal{A}_X} \to \mathbb{R}$.*

Using Theorem 2.52, solving the non-linear part of gluing equations is translated into a problem of finding maximal points, which can be accomplished in practice by gradient-flow algorithm. The program `SnapPy` uses this method to compute the volume of cusped hyperbolic 3-manifolds.

2.2.4 Veering triangulations

Originally, this notion has been introduced by Agol in [Ago11]. Later, another equivalent definition was given in [HRST11]. We will state the second definition in this thesis.

A *taut tetrahedron* is an oriented tetrahedron with two opposite edges with dihedral angle π and the other four edges with angle 0. A *veering tetrahedron* is a taut tetrahedron such that the edges with angle 0 are colored either in red or in blue, as in Figure 2.27.

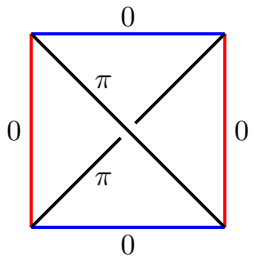

Figure 2.27: A veering tetrahedron.

Definition 2.53. Let X be an ideal triangulation. A *veering structure* on X is an element $\alpha \in \mathcal{TA}_X$ with a choice of assignment of a color (red or blue) to every edge of X such that each tetrahedron is veering. An ideal triangulation with a veering structure is a *veering triangulation*.

Example 2.54. The ideal triangulation of $S^3 \setminus 4_1$ given in Figure 2.5 is veering. The unique (up to color exchanging) veering structure is described in Figure 2.28.

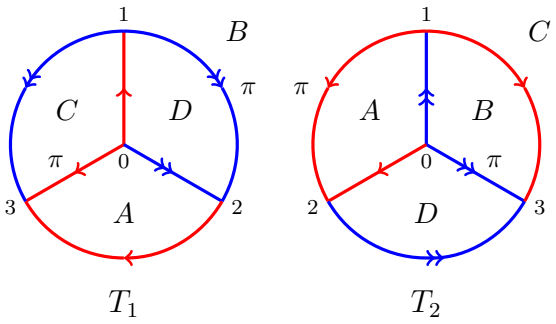

Figure 2.28: A veering triangulation of $S^3 \setminus 4_1$.

One main property of veering triangulations is the next result, which was initially proved in [HRST11, Theorem 1.5] using duality in linear programming. Later, a constructive proof was found [FG13, Theorem 1.3] using *leading-trailing deformations*.

Theorem 2.55. *If X is a veering triangulation, then $\mathcal{A}_X \neq \varnothing$.*

Combining Theorems 2.38 and 2.55, we immediately obtain the following result.

Corollary 2.56. *An orientable cusped 3-manifold which has a veering triangulation admits a complete hyperbolic metric.*

Let us come back to monodromy triangulations. We first state Agol's result, then we give some relevant remarks.

Theorem 2.57 (Agol [Ago11])**.** *Monodromy triangulations are veering.*

Remarks 2.58.

(a) Theorem 2.57 has in fact been proven for a more general family of ideal triangulations which come from Agol's construction (Remark 2.23 (b))

(b) We recall that monodromy triangulations are geometric (Remark 2.35 (b)), but there are veering triangulations that are not geometric [HIS16].

The last result of this chapter is an implicit consequence of several results in [FG11, FG13]. We will use this result in Chapter 6.

Theorem 2.59. *Let X be a geometric veering triangulation, where we denote the complete angle structure by α^0 and the veering structure by τ. Then α^0 and τ are gauge equivalent.*

The main steps of the proof are as follows.

- Realize that gauge transformations are in fact special instances of leading-trailing deformations [FG11, Definition 4.1].
- Using [FG11, Proposition 3.2] and [FG13, Lemma 6.6] remark that two elements in $\mathcal{GA}_X$ are gauge equivalent if and only if they have the same angular holonomy.
- The angular holonomy of the complete angle structure and any veering structure is always zero [FG13, Lemma 6.5].

❧ Chapter 3 ❧

Quantum Teichmüller theory

In the first three sections of this chapter, we give a quick survey about quantum Teichmüller theory developed by Kashaev [Kas98]. The last section of this chapter is devoted to explain the recently created Teichmüller TQFT by Andersen and Kashaev [AK14c], which is the principal object of this thesis. Main references are [Kas17a, Kas17b, Kas98] for Sections 3.1 to 3.3, and [AK14c, Kas16, Kas17a] for the Section 3.4.

3.1 Groupoid of decorated ideal triangulations and BAS

From now, unless otherwise specified, Σ denotes the surface of genus g with s punctures, such that $s > 0$ and $2g - 2 + s > 0$. Under these conditions, the surface Σ becomes hyperbolic and thus admits ideal triangulations.

Definition 3.1. A *decorated ideal triangulation* of Σ is an ideal triangulation of Σ where all the triangles are ordered, and in each triangle a distinguished corner is specified. The set of all decorated ideal triangulation (up to isotopy) of Σ is denoted Δ_Σ.

Example 3.2. An example of a decorated ideal triangulation of $\Sigma_{0,4}$ is illustrated in Figure 3.1.

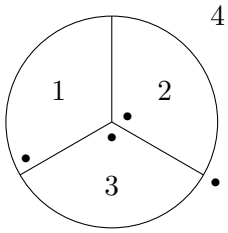

Figure 3.1: A decorated ideal triangulation of $\Sigma_{0,4}$.

Proposition 3.3. *Let G be a group freely acting on a set X. Then, one can define a connected groupoid $\mathcal{G}_{G,X}$ as follows:*

(1) $\mathrm{Ob}\,\mathcal{G}_{G,X} := X/G$*;*

(2) $\mathrm{Mor}\,\mathcal{G}_{G,X} := (X \times X)/G$ *(with respect to diagonal action);*

(3) Let us denote $[x] = Gx$ *and* $[x, y] = G(x, y)$ *for any* $x, y \in X$*. Then* $[x, y], [u, v] \in \operatorname{Mor} \mathcal{G}_{G,X}$ *are composable if and only if* $[y] = [u]$*. In this case, there exists a unique* $g \in G$ *such that* $y = gu$*, and we have*

$$[x, y][u, v] = [x, y][gu, gv] = [x, y][y, gv] := [x, gv],$$

where we used convention for the composition as the one adopted for the fundamental groupoid of topological spaces.

Remarks 3.4.

(a) Note that $\mathrm{id}_{[x]} = [x, x]$ and $[x, y]^{-1} = [y, x]$ for all $x, y \in X$.

(b) We see that $\mathcal{G}_{G,X}$ is a connected groupoid, and thus $\operatorname{Mor}([x], [x])$ is isomorphic to G for any $x \in X$.

Terminology 3.5. If we consider the special case $G = \mathrm{MCG}(\Sigma)$ and $X = \Delta_\Sigma$, then $\mathcal{G}_{\mathrm{MCG}(\Sigma),\Delta_\Sigma}$ is called the *groupoid of decorated ideal triangulations* (or the *Ptolemy groupoid*) of Σ.

The next result has been assumed and used in the literature during many years, but a complete proof has never been published until recently that Kim comes up with a proof [Kim16, Proposition 4.1].

Theorem 3.6 (Kim [Kim16])**.** *The set* $\operatorname{Mor} \mathcal{G}_{\mathrm{MCG}(\Sigma),\Delta_\Sigma}$ *admits the following presentation.*

Generators

1. $(i, j) :=$ 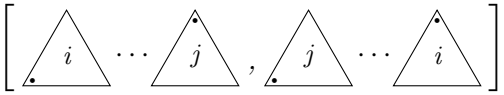

;
2. $\rho_i :=$ 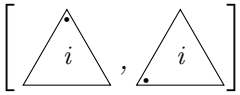

;
3. $\omega_{i,j} :=$ 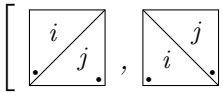

.

Relations

1. $(i, j) = (i, j)^{-1}$;
2. $(i, j)(j, k)(i, j) = (j, k)(i, j)(j, k)$;
3. $\rho_i \rho_i = \rho_i^{-1}$;
4. $\omega_{i,j}\omega_{j,k} = \omega_{j,k}\omega_{i,k}\omega_{i,j}$;
5. $\rho_i \rho_j \omega_{j,i} \rho_i^{-1} \omega_{i,j} = (i, j)$;
6. *trivial relations:* $\rho_i \rho_j = \rho_j \rho_i$, $\rho_i \omega_{j,k} = \omega_{j,k} \rho_i$ *(if* $i \neq j \neq k$*),* $\rho_i(i, j) = (i, j)\rho_j$*, etc.*

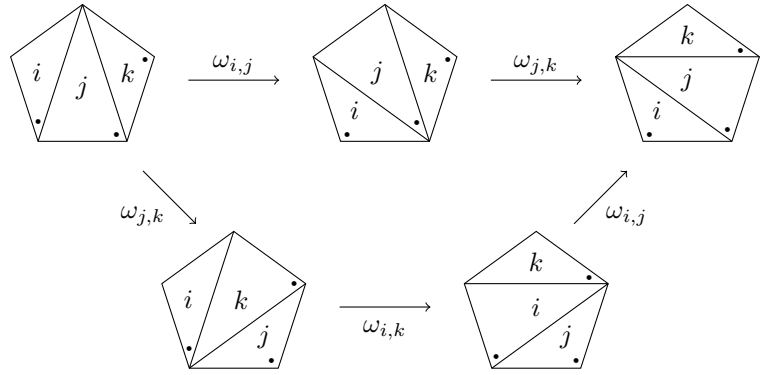

Figure 3.2: Graphical representation of relation 4.

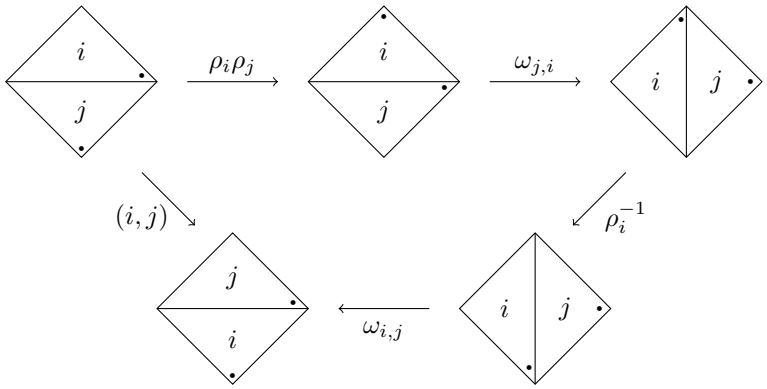

Figure 3.3: Graphical representation of relation 5.

Remark 3.7. All the relations in Theorem 3.6 are easily verified by pictures (see Figures 3.2 and 3.3 for relations 4 and 5 respectively). What is less obvious is that the above generators and relations provide a full presentation of the groupoid $\mathcal{G}_{\mathrm{MCG}(\Sigma),\Delta_\Sigma}$. Note also that Kim gave in [Kim16] an extra "consistency" relation given by

$$\rho_i\omega_{i,j}\rho_j = \rho_j\omega_{j,i}\rho_i. \tag{3.8}$$

However, relation (3.8) is in fact a consequence of relations 3 and 5 as follows. At first, we remark that

$$(i,j) = \rho_i(i,j)\rho_j^{-1} = \rho_i^{-1}\rho_j\omega_{j,i}\rho_i^{-1}\omega_{i,j}\rho_j^{-1}. \tag{3.9}$$

Then we have that

$$\begin{aligned}\omega_{i,j} &= \rho_i\omega_{j,i}^{-1}\rho_j^{-1}\rho_i^{-1}\rho_i\rho_j\omega_{j,i}\rho_i^{-1}\omega_{i,j}\\ &= \rho_i\omega_{j,i}^{-1}\rho_j^{-1}\rho_i^{-1}(i,j)\\ &= (i,j)\rho_j\omega_{i,j}^{-1}\rho_i^{-1}\rho_j^{-1}\\ &= \rho_i^{-1}\rho_j\omega_{j,i}\rho_i\rho_j^{-1},\end{aligned}$$

where we used relation (3.9) in the last equality.

The main idea of the proof of Theorem 3.6 is to construct a CW-complex (called *Kashaev complex*) having $\mathrm{Ob}\,\mathcal{G}_{\mathrm{MCG}(\Sigma),\Delta_\Sigma}$ as vertices, generators as edges and relations as 2-cells, and finally to show that this complex is connected and simply connected.

Definition 3.10. Let $\mathcal{C} = (\mathcal{C}, \otimes, \{P_{X,Y}\}_{X,Y \in \mathrm{Ob}\,\mathcal{C}})$ be a symmetric monoidal category. A *basic algebraic system* (BAS) in $\mathcal{C}$ is a triple (V, R, W), where $V \in \mathrm{Ob}\,\mathcal{C}$, $R \in \mathrm{End}(V)$ and $W \in \mathrm{End}(V \otimes V)$ such that

1. $R^3 = \mathrm{id}_V$;
2. $W_{1,2}W_{2,3} = W_{2,3}W_{1,3}W_{1,2}$ in $\mathrm{End}(V^{\otimes 3})$, where
   $W_{1,2} := W \otimes \mathrm{id}_V, \quad W_{2,3} := \mathrm{id}_V \otimes W, \quad W_{1,3} := P_{2,3}W_{1,2}P_{2,3}^{-1}, \quad P_{2,3} := \mathrm{id}_V \otimes P_{V,V}$;
3. $R_1R_2W_{2,1}R_1^{-1}W_{1,2} = P_{1,2}$ in $\mathrm{End}(V^{\otimes 2})$, where
   $R_1 := R \otimes \mathrm{id}_V, \quad R_2 := \mathrm{id}_V \otimes R, \quad W_{1,2} := W, \quad W_{2,1} := P_{1,2}WP_{1,2}^{-1}, \quad P_{1,2} := P_{V,V}$.

Using Theorem 3.6 and Definition 3.10, we immediately obtain the following result.

Theorem 3.11. *Let (V, R, W) be a BAS in a symmetric monoidal category $\mathcal{C}$. Then there exists a canonical functor $F : \mathcal{G}_{\mathrm{MCG}(\Sigma),\Delta_\Sigma} \to \mathcal{C}$ which sends all the objects to $V^{\otimes 2(2g-2+s)}$ and $(i,j) \mapsto P_{i,j}$, $\rho_i \mapsto R_i$, $\omega_{i,j} \mapsto W_{i,j}$.*

Remark 3.12. Note that the quantity $2(2g-2+s)$ in Theorem 3.11 is exactly the number of ideal triangles in any ideal triangulation of Σ.

Example 3.13. Let us take the once-punctured torus $\Sigma = \Sigma_{1,1}$ naturally identified with $\mathbb{R}^2/\mathbb{Z}^2$. Recall (Proposition 1.12) that $\mathrm{MCG}(\Sigma_{1,1}) \cong SL_2(\mathbb{Z})$, and we know that $SL_2(\mathbb{Z})$ is generated by

$$T = \begin{bmatrix} 1 & 1 \\ 0 & 1 \end{bmatrix} \qquad \text{and} \qquad S = \begin{bmatrix} 0 & 1 \\ -1 & 0 \end{bmatrix}.$$

We take $\tau \in \Delta_\Sigma$ as follows

$\tau =$ 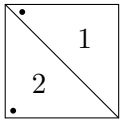

The action of T on τ gives

$T(\tau) =$ 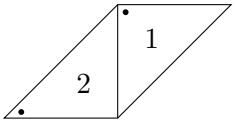

$=$ 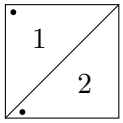

thus we see that $[\tau, T(\tau)] = \omega_{1,2}$. Similarly, the action of S on τ gives

$S(\tau) =$ 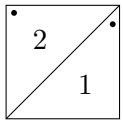

On the other hand, we have

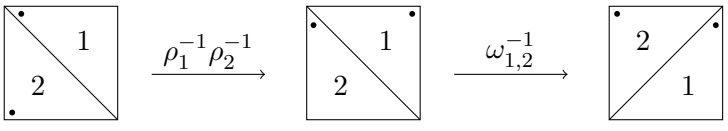

thus $[\tau, S(\tau)] = \rho_1^{-1}\rho_2^{-1}\omega_{1,2}^{-1}$. Then, if (V, R, W) is a BAS in some category, we get a representation $F : SL_2(\mathbb{Z}) \to \mathrm{Aut}(V^{\otimes 2})$ by

$$F(T) = W_{1,2} \qquad \text{and} \qquad F(S) = R_1^{-1}R_2^{-1}W_{1,2}^{-1}.$$

3.2 BAS from Teichmüller theory

In this section, we at first give an example of a BAS coming from Teichmüller theory and we explain the idea of how to get this BAS.

3.2.1 Example of BAS

We give an example of a BAS in the category **Set** of sets with the monoidal structure given by cartesian product, and the symmetry by transpositions of the components. We take $V = \mathbb{R}^2_{>0}$, we denote $\mathbf{x} := (x_1, x_2), \mathbf{y} := (y_1, y_2)$ and we define $R : V \to V$ and $W : V^2 \to V^2$ by

$$R(x_1, x_2) := \left(\frac{1}{x_2}, \frac{x_1}{x_2}\right) \qquad \text{and} \qquad W(\mathbf{x}, \mathbf{y}) := (\mathbf{x} \cdot \mathbf{y}, \mathbf{x} * \mathbf{y}),$$

where

$$\mathbf{x} \cdot \mathbf{y} := (x_1y_1, x_1y_2 + x_2) \qquad \text{and} \qquad \mathbf{x} * \mathbf{y} := \left(\frac{x_2y_1}{x_1y_2 + x_2}, \frac{y_2}{x_1y_2 + x_2}\right). \tag{3.14}$$

3.2.2 Decorated Teichmüller space

Definition 3.15. The *decorated Teichmüller space* of the surface $\Sigma = \Sigma_{g,s}$ is defined by

$$\widetilde{\mathcal{T}}(\Sigma) := \left\{ (m, h_1, \ldots, h_s) \;\middle|\; \begin{array}{l} m \in \mathcal{T}(\Sigma) \text{ and } h_i \text{ is an } m\text{-horocycle} \\ \text{around the puncture } P_i \text{ for } i = 1, \ldots, s \end{array} \right\}$$

Remark 3.16. There is a natural projection $\phi : \widetilde{\mathcal{T}}(\Sigma) \to \mathcal{T}(\Sigma)$ which simply forgets the horocycles. This provides $\widetilde{\mathcal{T}}(\Sigma)$ with a structure of trivial $\mathbb{R}^s_{>0}$-bundle over $\mathcal{T}(\Sigma)$ [Pen12].

Definition 3.17. An *ideal arc* of Σ is a non-trivial isotopy class of a simple path running between two punctures (possibly coinciding). See Figure 3.4.

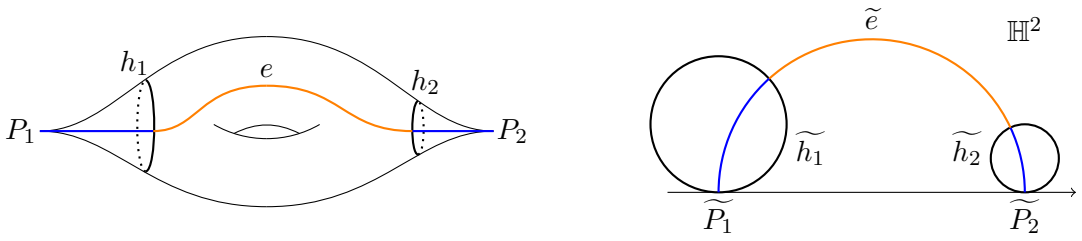

Figure 3.4: An ideal arc e on the surface $\Sigma_{1,2}$ (left) and a lift $\widetilde{e}$ in $\mathbb{H}^2$ of the unique geodesic representative of e (right).

Definition 3.18. Let $e \subset \Sigma$ be an ideal arc. The *λ-length* associated to e is the function $\lambda_e : \widetilde{\mathcal{T}}(\Sigma) \to \mathbb{R}_{>0}$ defined by $\lambda_e(\widetilde{m}) := e^{\frac{\delta}{2}}$, where δ is the signed hyperbolic length of the segment of $\widetilde{e}$ between the horocycles (see Figure 3.4 (right), where the segment is drawn in orange). More concretely, if the two horocycles do not intersect, we are in the situation of Figure 3.4 (right) and otherwise the length δ is counted with a minus sign (see Figure 3.5).

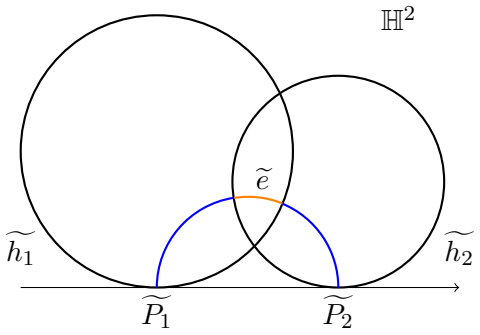

Figure 3.5: The case where δ is negative.

If τ is an ideal triangulation of a hyperbolic surface, we denote by τ_i the set of all the i-dimensional cells in τ. The following result is a gathering of Penner's most important results about decorated Teichmüller spaces.

Theorem 3.19 (Penner [Pen87, Pen12])**.** *Let τ be an ideal triangulation of Σ.*

1. *The map $\lambda_\tau : \widetilde{\mathcal{T}}(\Sigma) \to \mathbb{R}_{>0}^{\tau_1}$ defined by $\lambda_\tau(\widetilde{m})(e) := \lambda_e(\widetilde{m})$ is a homeomorphism.*

2. *If τ' and τ'' are two ideal triangulations of Σ related by one diagonal flip*

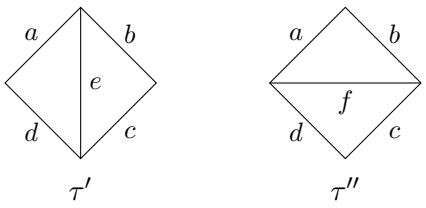

   then we have $\lambda_e\lambda_f = \lambda_a\lambda_c + \lambda_b\lambda_d$ (Ptolemy relation).

3. *If $\omega_{WP} \in \Omega^2(\mathcal{T}(\Sigma))$ is the Weil–Petersson symplectic form, then*

$$(\phi \circ \lambda_\tau^{-1})^* \omega_{WP} = \sum_{t \in \tau_2} \left(\frac{d\lambda_a \wedge d\lambda_b}{\lambda_a \lambda_b} + \frac{d\lambda_b \wedge d\lambda_b}{\lambda_b \lambda_c} + \frac{d\lambda_c \wedge d\lambda_a}{\lambda_c \lambda_a} \right),$$

   where a, b, c are the sides of the triangle t in the clockwise order with respect to the orientation of the surface.

4. *For $\widetilde{m}, \widetilde{m}' \in \widetilde{\mathcal{T}}(\Sigma)$, we have $\phi(\widetilde{m}) = \phi(\widetilde{m}')$ if and only if there exists $\alpha \in \mathbb{R}_{>0}^{\tau_0}$ such that $\lambda_e(\widetilde{m}') = \alpha(P_i)\alpha(P_j)\lambda_e(\widetilde{m})$ for any ideal arc e running between the punctures P_i and P_j.*

3.2.3 Ratio coordinates

If $\dot{\tau} \in \Delta_\Sigma$ is a decorated ideal triangulation of Σ, the underlying non-decorated ideal triangulation is denoted by τ. We also denote $\mathbb{R}_{>0}^{2\dot{\tau}_2} := (\mathbb{R}_{>0}^2)^{\dot{\tau}_2}$. To each decorated ideal triangulation, we associate two maps:

$$r_{\dot{\tau}} : \mathbb{R}_{>0}^{\tau_1} \to \mathbb{R}_{>0}^{2\dot{\tau}_2},$$

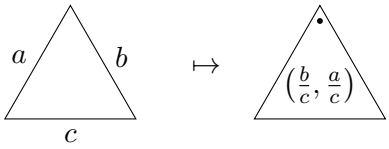

and $s_{\dot{\tau}} : \mathbb{R}_{>0}^{2\dot{\tau}_2} \to H^1(\Sigma, \mathbb{R}_{>0})$ by associating to any oriented normal curve $\gamma \subset \Sigma$ the quantity $s_{\dot{\tau}}(\mathbf{x})(\gamma) := \prod_{t \in \dot{\tau}_2} \langle \mathbf{x}(t), \gamma \rangle$, where

$$\langle \mathbf{x}(t), \gamma \rangle := \begin{cases} x_1(t) & \text{if } t = t_1, \\ x_2(t) & \text{if } t = t_2, \\ x_1(t)/x_2(t) & \text{if } t = t_3, \\ 1 & \text{otherwise,} \end{cases}$$

with $\mathbf{x}(t) = (x_1(t), x_2(t))$ and the three possible configurations for normal arcs are:

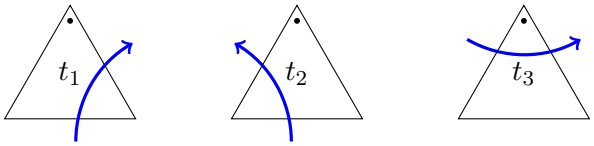

Theorem 3.20 (Kashaev [Kas98])**.**

1. *The following sequence of group homomorphisms is exact:*

$$1 \longrightarrow \mathbb{R}_{>0} \xrightarrow{\Delta} \mathbb{R}_{>0}^{\tau_1} \xrightarrow{r_{\dot{\tau}}} \mathbb{R}_{>0}^{2\dot{\tau}_2} \xrightarrow{s_{\dot{\tau}}} H^1(\Sigma, \mathbb{R}_{>0}) \longrightarrow 1,$$

   where Δ is defined by $\Delta(\lambda)(e) = \lambda$ for any $e \in \tau_1$ and $\lambda \in \mathbb{R}_{>0}$.

2. *$(\phi \circ \lambda_\tau^{-1})^* \omega_{WP} = r_{\dot{\tau}}^* \omega_{\dot{\tau}}$, where $\omega_{\dot{\tau}} := \sum_{t \in \dot{\tau}_2} \frac{dt_2 \wedge dt_1}{t_2 t_1}$, where we interpret a triangle $t \in \dot{\tau}_2$ as a pair of coordinate functions on $\mathbb{R}_{>0}^{2\dot{\tau}_2}$.*

3. *For any $\dot{\tau}, \dot{\tau}' \in \Delta_\Sigma$, there exists a unique homeomorphism $f_{\dot{\tau},\dot{\tau}'} : \mathbb{R}_{>0}^{2\dot{\tau}_2} \to \mathbb{R}_{>0}^{2\dot{\tau}'_2}$ such that the diagram*

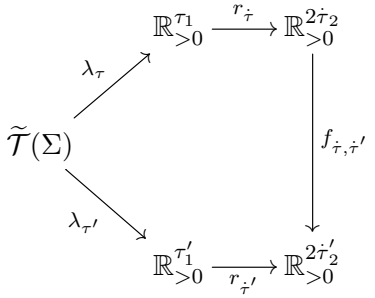

   commutes and $f_{\dot{\tau},\dot{\tau}'}^* \omega_{\dot{\tau}} = \omega_{\dot{\tau}'}$. In particular, if $\dot{\tau}$ and $\dot{\tau}'$ are related by

a) a change of the distinguished corner in one triangle

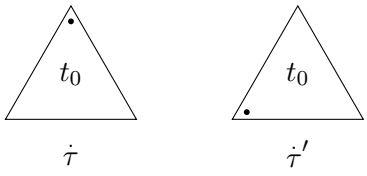

then

$$f_{\dot{\tau},\dot{\tau}'}(\mathbf{x})(t) = \begin{cases} \left(\frac{x_2(t)}{x_1(t)}, \frac{1}{x_1(t)}\right) & \text{if } t = t_0, \\ \mathbf{x}(t) & \text{otherwise,} \end{cases}$$

b) a diagonal flip

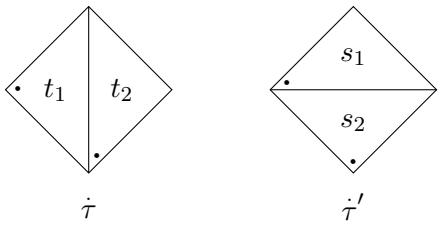

then

$$f_{\dot{\tau},\dot{\tau}'}(\mathbf{x})(s) = \begin{cases} \mathbf{x}(t_1) \cdot \mathbf{x}(t_2) & \text{if } s = s_1, \\ \mathbf{x}(t_1) * \mathbf{x}(t_2) & \text{if } s = s_2, \\ \mathbf{x}(s) & \text{otherwise,} \end{cases}$$

where the dot and star operations are defined in (3.14).

Consequently, using λ-lengths and their ratio coordinates in the decorated Teichmüller space, we managed to construct the BAS given in Section 3.2.1. From now on, we will focus only on this BAS and we will "quantize" it in the next section in order to get a BAS in the category **Hilb** of Hilbert spaces.

3.3 Quantization of the BAS from Teichmüller theory

The BAS (V, R, W) coming from Teichmüller theory given in Section 3.2.1 admits a crucial property for quantization, that is its compatibility with the symplectic form on V defined by $\omega_V := \frac{dx_2 \wedge dx_1}{x_2 x_1}$. More precisely, this fact is given by the following result.

Theorem 3.21 (Kashaev [Kas17a])**.** *The maps R and W are symplectomorphisms, i.e. $R^*\omega_V = \omega_V$ and $W^*\omega_{V^2} = \omega_{V^2}$, where $\omega_{V^2} := \mathrm{pr}_1^*\,\omega_V + \mathrm{pr}_2^*\,\omega_V$ and $\mathrm{pr}_i : V^2 \to V$ are the canonical projections for $i = 1, 2$.*

Our goal is to quantize this BAS using the general principle of (canonical) quantization that we recall now.

3.3.1 Two steps of quantization

Let (M, ω) be a symplectic space and G a subgroup of symplectomorphisms of M. The *Poisson bracket* $\{\cdot,\cdot\}_{PB}$ associated to (M, ω) is defined by the formula

$$\{f, g\}_{PB} := X_f[g] \qquad f, g \in C^\infty(M),$$

where X_f is the vector field on M defined by $\iota_{X_f}\omega = df$. The *quantization* of (M, ω, G) consists of two main steps.

Step 1: Choose an 1-parameter family of associative algebras $\{A_t\}_{t\in\mathbb{R}_{\geqslant 0}}$ and group homomorphisms $(\cdot)_t : G \to \mathrm{Aut}(A_t)$ such that

1. For any $t > 0$, there exists an isomorphism of vector spaces (over $\mathbb{C}$) $\hat{\cdot} : A_0 \to A_t$, where $A_0 \subset C^\infty(M, \mathbb{C})$.
2. $\lim_{t\to 0} \frac{\hat{x}\hat{y}-\hat{y}\hat{x}}{it} = \{x, y\}_{PB} \in A_0 \quad \forall x, y \in A_0$.
3. $\lim_{t\to 0}(g^{-1})_t = g^*|_{A_0} \quad \forall g \in G$.

Step 2: For any $t > 0$, one realizes A_t in a Hilbert space $\mathcal{H}$ in such a way that

1. For any real function $f \in A_0$, the operator $\hat{f}$ is symmetric (eventually self-adjoint).
2. For any $g \in G$, there exists a unitary operator $\hat{g} : \mathcal{H} \to \mathcal{H}$ such that $\hat{g}\hat{x}\hat{g}^{-1} = (g)_t(\hat{x})$ for any $x \in A_0$.

3.3.2 Quantization of (V, ω_V, R)

Let us work in logarithmic coordinates $X_i := \log(x_i)$. In this case, the space V is equivalent with $\mathbb{R}^2$ with the canonical symplectic form $\omega_V = dX_2 \wedge dX_1$.

Step 1: We associate to V an algebra V_t given by the presentation

$$V_t := \mathbb{C}\langle \hat{x}_1, \hat{x}_2 \mid \hat{x}_1\hat{x}_2 = e^{it}\hat{x}_2\hat{x}_1 \rangle. \tag{3.22}$$

Note that Definition (3.22) is natural, because in logarithmic coordinates we get

$$V_t = \mathbb{C}\langle \hat{X}_1, \hat{X}_2 \mid \hat{X}_1\hat{X}_2 - \hat{X}_2\hat{X}_1 = it \rangle.$$

Indeed, if we take $\hat{x}_i = e^{\hat{X}_i}$, then by formula (1.50) we get

$$\hat{x}_1\hat{x}_2 = e^{\hat{X}_1+\hat{X}_2+\frac{it}{2}} \qquad \text{and} \qquad \hat{x}_2\hat{x}_1 = e^{\hat{X}_1+\hat{X}_2-\frac{it}{2}},$$

and thus $\hat{x}_1\hat{x}_2 = e^{it}\hat{x}_2\hat{x}_1$.

Since $R^*(X_1, X_2) = (-X_2, X_1 - X_2)$, this leads us to define

$$(R^{-1})_t(\hat{X}_1, \hat{X}_2) := (-\hat{X}_2, \hat{X}_1 - \hat{X}_2),$$

and using again formula (1.50) one gets

$$(R^{-1})_t(\hat{x}_1, \hat{x}_2) = (\hat{x}_2^{-1}, e^{-\frac{it}{2}}\hat{x}_2^{-1}\hat{x}_1).$$

Therefore, we get

$$(R)_t(\hat{x}_1, \hat{x}_2) = (e^{\frac{it}{2}}\hat{x}_1^{-1}\hat{x}_2, \hat{x}_1^{-1}).$$

Step 2: We choose the Hilbert space $\mathcal{H}_V = L^2(\mathbb{R})$ and we realize the algebra V_t in $\mathcal{H}_V$ through the operators

$$\hat{x}_1 = e^{2\pi \mathsf{bq}} \qquad \text{and} \qquad \hat{x}_2 = e^{2\pi \mathsf{bp}},$$

where we take the parameter b as the positive solution of the equation $t = 2\pi\mathsf{b}^2$. The system of equations that we have to solve is as follows:

$$\mathsf{R}\hat{x}_i\mathsf{R}^{-1} = (R)_t(\hat{x}_i), \quad i = 1, 2 \quad \Longleftrightarrow \quad \begin{cases} \mathsf{R}\mathsf{q}\mathsf{R}^{-1} = \mathsf{p} - \mathsf{q}, \\ \mathsf{R}\mathsf{p}\mathsf{R}^{-1} = -\mathsf{q}, \end{cases} \tag{3.23}$$

which can also be written as

$$\mathsf{R}(\mathsf{p}, \mathsf{q})\mathsf{R}^{-1} = (\mathsf{p}, \mathsf{q}) \begin{pmatrix} 0 & 1 \\ -1 & -1 \end{pmatrix}.$$

Since the matrix on the right hand side belongs in $SL_2(\mathbb{R})$ (which coincide with the symplectic group $Sp(2, \mathbb{R})$), it means that the operator R is an element of the metaplectic group in $\mathcal{U}(L^2(\mathbb{R}))$ generated by the family of unitary operators $\{e^{it\mathsf{q}^2}\}_{t\in\mathbb{R}}$ and the Fourier transform operator $\mathsf{F} \in \mathcal{U}(L^2(\mathbb{R}))$ that can also be written as

$$e^{\frac{\pi i}{4}}\mathsf{F} = e^{\pi i\mathsf{q}^2}e^{\pi i\mathsf{p}^2}e^{\pi i\mathsf{q}^2} = e^{\pi i\mathsf{p}^2}e^{\pi i\mathsf{q}^2}e^{\pi i\mathsf{p}^2}. \tag{3.24}$$

After some work, we get the following result.

Theorem 3.25 (Kashaev [Kas17a])**.** *Any solution of the system (3.23) satisfying the normalization condition* $\mathsf{R}^3 = \mathrm{id}_{L^2(\mathbb{R})}$ *is of the form* $\mathsf{R} = \zeta e^{3\pi i\mathsf{q}^2}e^{\pi i(\mathsf{p}+\mathsf{q})^2}$*, where* $\zeta \in \mathbb{C}$ *is any root of the equation* $\zeta^3 = -1$*.*

3.3.3 Quantization of (V^2, ω_{V^2}, W)

Step 1: For $t > 0$, we define the algebra $(V^2)_t := V_t \otimes V_t$, where V_t is defined as in (3.22) and the automorphism $(W)_t \in \mathrm{Aut}((V^2)_t)$ by

$$\begin{aligned}
&(W^{-1})_t(\hat{x}_1 \otimes 1) := \hat{x}_1 \otimes \hat{x}_1, \\
&(W^{-1})_t(\hat{x}_2 \otimes 1) := \hat{x}_1 \otimes \hat{x}_2 + \hat{x}_2 \otimes 1, \\
&(W^{-1})_t(1 \otimes \hat{x}_1) := (\hat{x}_2 \otimes \hat{x}_1)(\hat{x}_1 \otimes \hat{x}_2 + \hat{x}_2 \otimes 1)^{-1}, \\
&(W^{-1})_t(1 \otimes \hat{x}_2) := (1 \otimes \hat{x}_2)(\hat{x}_1 \otimes \hat{x}_2 + \hat{x}_2 \otimes 1)^{-1}.
\end{aligned}$$

Remarks 3.26.

(a) There is no ordering problem here since the relevant operators are commuting. For example, $\hat{x}_2 \otimes \hat{x}_1$ commutes with $\hat{x}_1 \otimes \hat{x}_2$ and $\hat{x}_2 \otimes 1$ etc.

(b) For any $t > 0$, the triple $(V_t, (R)_t, (W)_t)$ is a BAS in the category $(\mathbf{Vect}, \hat{\otimes})$, where $\hat{\otimes}$ is the completed tensor product.

(c) In particular, the linear map $\Delta : V_t \to V_t \otimes V_t$ given by

$$\Delta(a) := (W^{-1})_t(a \otimes 1) \quad \forall a \in V_t$$

gives rise to a Hopf algebra structure on V_t coinciding with the Borel subalgebra of $\mathcal{U}_q(\mathfrak{sl}_2)$ with $q = e^{it}$.

Step 2: We choose $\mathcal{H}_{V^2} = L^2(\mathbb{R}^2)$ and we realize $(V^2)_t$ in $\mathcal{H}_{V^2}$ by

$$\hat{x}_1 \otimes 1 = e^{2\pi \mathsf{b} \mathsf{q}_1}, \qquad \hat{x}_2 \otimes 1 = e^{2\pi \mathsf{b} \mathsf{p}_1}, \qquad 1 \otimes \hat{x}_1 = e^{2\pi \mathsf{b} \mathsf{q}_2}, \qquad 1 \otimes \hat{x}_2 = e^{2\pi \mathsf{b} \mathsf{p}_2},$$

where b is a positive solution of the equation $t = 2\pi \mathsf{b}^2$.

We want to find $\mathsf{W} \in \mathcal{U}(L^2(\mathbb{R}^2))$ satisfying the equations

$$\mathsf{W}^{-1} \hat{a} \mathsf{W} = (W^{-1})_t(\hat{a}) \qquad \forall \hat{a} \in (V^2)_t.$$

In fact, it suffices to consider only the equations corresponding to the four generators of the algebra

$$\hat{a} \in \{e^{2\pi \mathsf{b} \mathsf{q}_i}, e^{2\pi \mathsf{b} \mathsf{p}_i} \mid i = 1, 2\}.$$

Explicitly, we have

$$\begin{cases} \mathsf{W}^{-1} e^{2\pi \mathsf{b} \mathsf{q}_1} \mathsf{W} = e^{2\pi \mathsf{b}(\mathsf{q}_1 + \mathsf{q}_2)} \iff \mathsf{W}^{-1} \mathsf{q}_1 \mathsf{W} = \mathsf{q}_1 + \mathsf{q}_2, \\ \mathsf{W}^{-1} e^{2\pi \mathsf{b} \mathsf{p}_1} \mathsf{W} = e^{2\pi \mathsf{b}(\mathsf{q}_1 + \mathsf{p}_2)} + e^{2\pi \mathsf{b} \mathsf{p}_1}, \\ \mathsf{W}^{-1} e^{2\pi \mathsf{b} \mathsf{q}_2} \mathsf{W} = e^{2\pi \mathsf{b}(\mathsf{q}_2 + \mathsf{p}_1)} \mathsf{W}^{-1} e^{-2\pi \mathsf{b} \mathsf{p}_1} \mathsf{W} \iff \mathsf{W}^{-1}(\mathsf{q}_2 + \mathsf{p}_1)\mathsf{W} = \mathsf{q}_2 + \mathsf{p}_1, \\ \mathsf{W}^{-1} e^{2\pi \mathsf{b} \mathsf{p}_2} \mathsf{W} = e^{2\pi \mathsf{b} \mathsf{p}_2} \mathsf{W}^{-1} e^{-2\pi \mathsf{b} \mathsf{p}_1} \mathsf{W} \iff \mathsf{W}^{-1}(\mathsf{p}_1 + \mathsf{p}_2)\mathsf{W} = \mathsf{p}_2. \end{cases} \tag{3.27}$$

Theorem 3.28 (Kashaev [Kas17a])**.** *Any solution of the system (3.27) is of the form* $\mathsf{W} = \varphi(\mathsf{q}_1 - \mathsf{q}_2 + \mathsf{p}_2) e^{-2\pi i \mathsf{p}_1 \mathsf{q}_2}$*, where* $\varphi : \mathbb{R} \to \mathbb{C}^*$ *admits analytic continuation into the strip* $|\Im(z)| < \mathsf{b}$ *and satisfies the functional equation*

$$\varphi\left(x - \frac{i\mathsf{b}}{2}\right) = \left(1 + e^{2\pi \mathsf{b} x}\right) \varphi\left(x + \frac{i\mathsf{b}}{2}\right) \tag{3.29}$$

for all $x \in \mathbb{R}$*.*

Remark 3.30. Using formula (1.49), we can see that equation (3.29) is equivalent to the operator equation

$$\varphi(\mathsf{q})^{-1} e^{2\pi \mathsf{b} \mathsf{p}} \varphi(\mathsf{q}) = e^{2\pi \mathsf{b} \mathsf{p}} + e^{2\pi \mathsf{b}(\mathsf{p} + \mathsf{q})}.$$

In the RHS we have a non-negative self-adjoint operator and in the LHS we have a conjugation of another non-negative self-adjoint operator with well-known spectral decomposition. Therefore, finding a unitary $\varphi(\mathsf{q})$ is equivalent to solve the spectral problem for the RHS. This gives an alternative approach to construct $\varphi(\mathsf{q})$ using only functional analysis methods.

3.3.4 Solving the equation $\varphi\left(x - \frac{i\mathsf{b}}{2}\right) = \left(1 + e^{2\pi \mathsf{b} x}\right) \varphi\left(x + \frac{i\mathsf{b}}{2}\right)$

Let us consider the logarithmic equation

$$\operatorname{Log} \varphi\left(x - \frac{i\mathsf{b}}{2}\right) = \log\left(1 + e^{2\pi \mathsf{b} x}\right) + \operatorname{Log} \varphi\left(x + \frac{i\mathsf{b}}{2}\right), \tag{3.31}$$

and set $f(x) := \operatorname{Log} \varphi(x)$ for $x \in \mathbb{R}$. Then equation (3.31) becomes equivalent to

$$f\left(x - \frac{i\mathsf{b}}{2}\right) - f\left(x + \frac{i\mathsf{b}}{2}\right) = \log\left(1 + e^{2\pi \mathsf{b} x}\right). \tag{3.32}$$

We solve the functional equation (3.32) by Fourier transform. Define

$$I(z) := \int_{\mathbb{R}} \operatorname{Log}\left(1 + e^{2\pi \mathsf{b} z}\right) e^{2\pi i x z} \, dx. \tag{3.33}$$

Assume that $\Im(z) > 0$. Then the integral (3.33) converges absolutely when $x \to +\infty$. On the other hand, when $x \to -\infty$, the asymptotic behaviour of terms in (3.33) are given by

$$\log\left(1 + e^{2\pi \mathsf{b} x}\right) \sim e^{2\pi \mathsf{b} x} \qquad \text{and} \qquad \left|e^{2\pi i x z}\right| \sim e^{-2\pi \Im(z) x},$$

and thus the integral (3.33) converges absolutely when $x \to -\infty$ if and only if $\mathsf{b} > \Im(z)$. Consequently, for any $z \in \mathbb{C}$ with $0 < \Im(z) < \mathsf{b}$, the integral (3.33) converges absolutely. By integrating by parts, we calculate

$$\begin{aligned} I(z) &= \int_{\mathbb{R}} \log\left(1 + e^{2\pi \mathsf{b} x}\right) \frac{d\left(e^{2\pi i x z}\right)}{2\pi i z} \\ &= -\int_{\mathbb{R}} \frac{e^{2\pi i x z}}{2\pi i z}\, d\log\left(1 + e^{2\pi \mathsf{b} x}\right) \\ &= -\frac{\mathsf{b}}{iz} \int_{\mathbb{R}} \frac{e^{2\pi i x z}}{e^{-2\pi \mathsf{b} x} + 1}\, dx \\ &= \frac{i\mathsf{b}}{2z} \int_{\mathbb{R}} \frac{e^{2\pi i x z + \pi \mathsf{b} x}}{\cosh\left(\pi \mathsf{b} x\right)}\, dx \\ &= \frac{i}{2z} \int_{\mathbb{R}} \frac{e^{2\pi i x \left(\frac{z}{\mathsf{b}} - \frac{i}{2}\right)}}{\cosh\left(\pi x\right)}\, dx. \end{aligned}$$

Since the function $x \mapsto \frac{1}{\cosh(\pi x)}$ is invariant by Fourier transform, the value of the last integral becomes

$$\frac{i}{2z \cosh\left(\pi\left(\frac{z}{\mathsf{b}} - \frac{i}{2}\right)\right)}.$$

Moreover, since

$$0 < \Im(z) < \mathsf{b} \iff -\frac{\pi}{2} < \Im\left(\pi\left(\frac{z}{\mathsf{b}} - \frac{i}{2}\right)\right) < \frac{\pi}{2},$$

it confirms the absolute convergence of the integral. Finally, using trigonometric identities, the value of the integral becomes

$$I(z) = \frac{i}{2z \cos\left(\pi\left(\frac{iz}{\mathsf{b}} + \frac{1}{2}\right)\right)} = \frac{i}{2z \sin\left(\frac{\pi z}{i\mathsf{b}}\right)} = -\frac{1}{2z \sinh\left(\frac{\pi z}{\mathsf{b}}\right)}.$$

Therefore, for $0 < \Im(z) < \mathsf{b}$, equation (3.32) becomes equivalent to

$$\int_{\mathbb{R}} f\left(x - \frac{i\mathsf{b}}{2}\right) e^{2\pi i x z}\, dx - \int_{\mathbb{R}} f\left(x + \frac{i\mathsf{b}}{2}\right) e^{2\pi i x z}\, dx = -\frac{1}{2z \sinh\left(\frac{\pi z}{\mathsf{b}}\right)}.$$

The first integral gives

$$\begin{aligned} \int_{x \in \mathbb{R}} f\left(x - \frac{i\mathsf{b}}{2}\right) e^{2\pi i x z}\, dx &= \int_{w + \frac{i\mathsf{b}}{2} \in \mathbb{R}} f(w) e^{2\pi i (w + \frac{i\mathsf{b}}{2}) z}\, dw \\ &= \int_{\mathbb{R} - \frac{i\mathsf{b}}{2}} f(w) e^{2\pi i (w + \frac{i\mathsf{b}}{2}) z}\, dw \\ &= \int_{\mathbb{R}} f(x) e^{2\pi i (x + \frac{i\mathsf{b}}{2}) z}\, dw \\ &= \widetilde{f}(z) e^{-\pi \mathsf{b} z}, \end{aligned}$$

where we used analyticity of f in the strip $\{z \in \mathbb{C} \mid 0 \leqslant \Im(z) \leqslant \frac{\mathsf{b}}{2}\}$ for the third equality, and we denoted

$$\widetilde{f}(z) := \int_{\mathbb{R}} f(x) e^{2\pi i x z}\, dx.$$

Similarly, the second integral can be written by

$$\int_{x\in\mathbb{R}} f\left(x + \frac{i\mathsf{b}}{2}\right) e^{2\pi i x z}\, dx = \widetilde{f}(z) e^{\pi \mathsf{b} z}.$$

Thus, for $0 < \Im(z) < \mathsf{b}$, equation (3.32) is equivalent to

$$-2\widetilde{f}(z)\sinh(\pi\mathsf{b}z) = -\frac{1}{2z\sinh\left(\frac{\pi z}{\mathsf{b}}\right)},$$

which implies that

$$\widetilde{f}(z) = \frac{1}{4z\sinh(\pi\mathsf{b}z)\sinh\left(\frac{\pi z}{\mathsf{b}}\right)}.$$

Taking the inverse Fourier transform, we have immediately that

$$\operatorname{Log}\varphi(x) = f(x) = \int_{\mathbb{R}+i\varepsilon} \widetilde{f}(z) e^{-2\pi i x z}\, dz \qquad \text{for } 0 < \varepsilon < \mathsf{b},$$

and finally, we get

$$\Phi_{\mathsf{b}}(x) := \varphi(x) = \exp\left(\int_{\mathbb{R}+i\varepsilon} \frac{e^{-2ixz}}{4z\sinh(\mathsf{b}z)\sinh(\mathsf{b}^{-1}z)}\, dz\right). \tag{3.34}$$

The function given in (3.34) is called *Faddeev's quantum dilogarithm* [Fad94, Fad95, FK94], which depends only on $\hbar := \frac{1}{(\mathsf{b}+\mathsf{b}^{-1})^2}$ and is holomorphic inside the strip $\mathbb{R}+i\left(-\frac{1}{2\sqrt{\hbar}}, \frac{1}{2\sqrt{\hbar}}\right)$.

Remark 3.35. Surprisingly, we have a symmetry $\Phi_{\mathsf{b}} = \Phi_{\mathsf{b}^{-1}}$. This is a consequence of the modular duality of quantum Teichmüller theory and quantum Liouville theory [Tes01].

We now list several useful properties of Faddeev's quantum dilogarithm. We refer to [AK14c, Appendix A] for these properties.

Theorem 3.36 (Some properties of Φ_{b})**.**

(1) (inversion relation) For any $\mathsf{b} \in \mathbb{R}_{>0}$ and any $z \in \mathbb{R} + i\left(-\frac{1}{2\sqrt{\hbar}}, \frac{1}{2\sqrt{\hbar}}\right)$, we have

$$\Phi_{\mathsf{b}}(z)\Phi_{\mathsf{b}}(-z) = \Phi_{\mathsf{b}}(0)^2 e^{\pi i z^2} \qquad \text{and} \qquad \Phi_{\mathsf{b}}(0) = e^{\frac{\pi i}{24}\left(\mathsf{b}^2+\mathsf{b}^{-2}\right)}. \tag{3.37}$$

(2) (unitarity) For any $\mathsf{b} \in \mathbb{R}_{>0}$ and any $z \in \mathbb{R} + i\left(-\frac{1}{2\sqrt{\hbar}}, \frac{1}{2\sqrt{\hbar}}\right)$, we have

$$\overline{\Phi_{\mathsf{b}}(z)} = \frac{1}{\Phi_{\mathsf{b}}(\overline{z})}.$$

(3) (zeros and poles) For any $\mathsf{b} \in \mathbb{R}_{>0}$, the function Φ_{b} admits analytic continuation to $\mathbb{C}$ as a meromorphic function (via equation (3.29)) with poles (resp. zeros) at $\mathcal{P}_+$ (resp. $\mathcal{P}_-$), where

$$\mathcal{P}_{\pm} = \{\pm i\mathsf{b}\left(m + \tfrac{1}{2}\right) \pm i\mathsf{b}^{-1}\left(n + \tfrac{1}{2}\right) \mid m, n \in \mathbb{N}\}.$$

(4) (behaviour at infinity) For any $\mathsf{b} \in \mathbb{R}_{>0}$*, we have*

$$\Phi_{\mathsf{b}}(z) \underset{\Re(z)\to-\infty}{\sim} 1, \qquad \Phi_{\mathsf{b}}(z) \underset{\Re(z)\to+\infty}{\sim} \Phi_{\mathsf{b}}(0)^2 e^{\pi i z^2}.$$

In particular, for any $\mathsf{b} \in \mathbb{R}_{>0}$ *and any* $d \in \left(-\frac{1}{2\sqrt{\hbar}}, \frac{1}{2\sqrt{\hbar}}\right)$*, we have*

$$|\Phi_{\mathsf{b}}(x+id)| \underset{\mathbb{R}\ni x\to-\infty}{\sim} 1, \qquad |\Phi_{\mathsf{b}}(x+id)| \underset{\mathbb{R}\ni x\to+\infty}{\sim} e^{-2\pi x d}.$$

This function behaves nicely with Fourier transform and the formulas are given in the next result.

Theorem 3.38 (Fourier transform formulas)**.** *We have*

$$\int_{\mathbb{R}+i\varepsilon} \Phi_{\mathsf{b}}(u) e^{-2\pi i u z}\, du = \zeta_{\mathsf{b}} e^{-\pi i z^2} \Phi_{\mathsf{b}}\left(\frac{i}{2}\left(\mathsf{b}+\mathsf{b}^{-1}\right) - z\right), \tag{3.39}$$

where $0 < \Im(z) < \varepsilon < \frac{\mathsf{b}+\mathsf{b}^{-1}}{2} = \frac{1}{2\sqrt{\hbar}}$ *and* $\zeta_{\mathsf{b}} := e^{\frac{\pi i}{4} + \frac{\pi i}{12}(\mathsf{b}^2+\mathsf{b}^{-2})}$*. Moreover, the integral in (3.39) converges absolutely.*

One of the most important properties of Φ_{b} is the following result, which was suggested in [Fad95] and proved in [Wor00].

Theorem 3.40 (Quantum pentagon identity)**.** *For any* $\mathsf{b} \in \mathbb{R}_{>0}$*, we have*

$$\Phi_{\mathsf{b}}(\mathsf{p})\Phi_{\mathsf{b}}(\mathsf{q}) = \Phi_{\mathsf{b}}(\mathsf{q})\Phi_{\mathsf{b}}(\mathsf{p}+\mathsf{q})\Phi_{\mathsf{b}}(\mathsf{p}),$$

where p *and* q *are the normalized Heisenberg operators satisfying* $[\mathsf{p},\mathsf{q}] = \frac{1}{2\pi i}$*.*

Another important result about this function is its asymptotic behaviour when $\mathsf{b} \to 0$. See [AH06, Lemma 3] for an alternate proof.

Theorem 3.41 (Semi-classical limit)**.** *For any* $z \in \mathbb{R} + i(-\pi, \pi)$*, we have*

$$\Phi_{\mathsf{b}}\left(\frac{z}{2\pi\mathsf{b}}\right) = \exp\left(\frac{1}{2\pi i \mathsf{b}^2} \mathrm{Li}_2\left(-e^z\right)\right)\left(1 + \mathcal{O}(\mathsf{b}^2)\right)$$

when $\mathsf{b} \to 0$*.*

Finally, Theorem 3.40 allows to prove the following main result of this section.

Theorem 3.42 (Kashaev [Kas01])**.** *The triple* $(L^2(\mathbb{R}), \mathsf{R}, \mathsf{W})$ *is a projective BAS in the category* $(\mathbf{Hilb}, \hat{\otimes})$*, where* $\hat{\otimes}$ *denotes the completed tensor product.*

We finish this section with a remark on representations.

Remark 3.43. In Theorem 3.42, the word "projective" means (in this thesis) that it is defined up to a multiplication by a phase factor. As a consequence of Theorem 3.42, the BAS $(L^2(\mathbb{R}), \mathsf{R}, \mathsf{W})$ gives unitary projective representations F_{b} of the mapping class groups of punctured surfaces Σ with negative Euler characteristic. We will see in Chapter 6 that one can define an extended notion of the trace and in the case where $\Sigma = \Sigma_{1,1}$ and $\varphi \in \mathrm{MCG}(\Sigma)$ pseudo-Anosov, we will give a link between this extended trace of $F_{\mathsf{b}}(\varphi)$ and the partition function of the Teichmüller TQFT, that will be defined in the next section.

3.4 Teichmüller TQFT

The end of this chapter is devoted to explain the recent and main object of this thesis, called the *Teichmüller TQFT*, which has been constructed by Andersen and Kashaev [AK14c] using quantum Teichmüller theory and new developments are still going on. See also [AK13, AK14a, AK14b, AK15, AK18].

3.4.1 Angled tetrahedral weights

We start from an ordered triangulation and the idea is to associate the integral kernel of the operator W to a negative tetrahedron, and its conjugate to a positive tetrahedron. Taking the product over all the tetrahedra and integrating over the face variables, we get potentially a complex number. In this case, the operator identity

$$\mathsf{W}_{1,2}\mathsf{W}_{2,3} = \mathsf{W}_{2,3}\mathsf{W}_{1,3}\mathsf{W}_{1,2}$$

is interpreted as a 2-3 Pachner move. Unfortunately, there is no guarantee that the above integral is well-defined. In order to make it absolutely convergent, we add some extra informations on each tetrahedron which are angles on each edge and modify the operator W, as we will explain now.

Let (X, α) be a shaped ordered triangulation and $T \in X^3$. Denote by $a, b, c \in (0, \pi)$ the three angles on T, where we assign the angle a to the edge $\overrightarrow{01}$, b to the edge $\overrightarrow{02}$ and c to the edge $\overrightarrow{03}$. Define a new operator $\mathsf{W}(a, c)$ by

$$\mathsf{W}(a, c) := \varphi_{a,c}(\mathsf{q}_1 - \mathsf{q}_2 + \mathsf{p}_2)e^{-2\pi i \mathsf{p}_1 \mathsf{q}_2},$$

where

$$\varphi_{a,c}(x) := \Phi_{\mathsf{b}}\left(x + i\xi_{\mathsf{b}}(a + c)\right) e^{2\pi\xi_{\mathsf{b}} a x}$$

for all $x \in \mathbb{R}$ and $\xi_{\mathsf{b}} := \frac{\mathsf{b}+\mathsf{b}^{-1}}{2\pi} = \frac{1}{2\pi\sqrt{\hbar}}$. Consider the functions

$$\psi_{a,c}(x) := \overline{\varphi_{a,c}(x)} = \frac{e^{2\pi\xi_{\mathsf{b}} a x}}{\Phi_{\mathsf{b}}\left(x - i\xi_{\mathsf{b}}(a + c)\right)}$$

and

$$\widetilde{\psi}'_{a,c}(x) := e^{-\pi i x^2}\widetilde{\psi}_{a,c}(x), \qquad \widetilde{\psi}_{a,c}(x) := \int_{\mathbb{R}} \psi_{a,c}(y)e^{-2\pi i x y}\, dy. \tag{3.44}$$

Note that the conditions we imposed on a and c ensure that the Fourier transform is absolutely convergent. The Fourier transform formula for the Faddeev's quantum dilogarithm (Theorem 3.38) leads to the identity

$$\widetilde{\psi}'_{a,c}(x) = e^{-\frac{\pi i}{12}}\psi_{c,b}(x). \tag{3.45}$$

Moreover, with respect to complex conjugation, we also have

$$\overline{\psi_{a,c}(x)} = e^{-\frac{\pi i}{6}} e^{\pi i x^2}\psi_{c,a}(-x) = e^{-\frac{\pi i}{12}}\widetilde{\psi}_{b,c}(-x). \tag{3.46}$$

These can be combined and one obtains

$$\overline{\widetilde{\psi}'_{a,c}(x)} = e^{\frac{\pi i}{12}}\overline{\psi_{c,b}(x)} = e^{-\frac{\pi i}{12}} e^{\pi i x^2}\psi_{b,c}(-x). \tag{3.47}$$

Let us come back to the definition of the Teichmüller TQFT. We write by

$$\mathsf{T}(a,c) := e^{2\pi i \mathsf{p}_1 \mathsf{q}_2} \psi_{a,c}(\mathsf{q}_1 - \mathsf{q}_2 + \mathsf{p}_2)$$

the adjoint operator of $\mathsf{W}(a,c)$. To each face $\partial_i(T)$ we assign the formal real variable x_i and set $\mathbf{x} := (x_0, x_1, x_2, x_3)$. Then we associate to T the quantity $\mathcal{Z}_\hbar(T, \mathbf{x})$ following the rule of Figure 3.6.

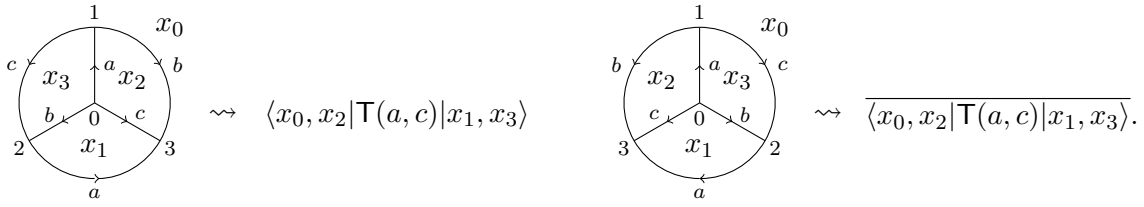

Figure 3.6: Corresponding integral kernel to each tetrahedron.

Notation 3.48. From now on, we will denote $\overset{\star}{=}$ if we have equality up to multiplication by a phase factor depending only on angles and the parameter b.

Remarks 3.49.

(a) One can show that the integral kernel of $\mathsf{T}(a,c)$ is given by (see [AK14c])

$$\begin{aligned}\langle x_0, x_2 | \mathsf{T}(a,c) | x_1, x_3 \rangle &= \delta(x_0 - x_1 + x_2) \widetilde{\psi}'_{a,c}(x_3 - x_2) e^{2\pi i x_0 (x_3 - x_2)} \\ &\overset{\star}{=} \frac{\delta(x_0 - x_1 + x_2) e^{(2\pi i x_0 + 2\pi \xi_{\mathsf{b}} c)(x_3 - x_2)}}{\Phi_{\mathsf{b}}\left(x_3 - x_2 - i\xi_{\mathsf{b}}(b+c)\right)},\end{aligned}$$

where we used the identity (3.45) for the second equality.

(b) The following angled pentagon identity (illustrated in Figure 3.7) is satisfied (see [AK14c])

$$\mathsf{T}_{1,2}(a_4, c_4)\mathsf{T}_{1,3}(a_2, c_2)\mathsf{T}_{2,3}(a_0, c_0) \overset{\star}{=} \mathsf{T}_{2,3}(a_1, c_1)\mathsf{T}_{1,2}(a_3, c_3), \tag{3.50}$$

where $a_0, \dots, a_4, c_0, \dots, c_4 \in (0, \pi)$ are such that

$$a_1 = a_0 + a_2, \quad a_3 = a_2 + a_4, \quad c_1 = c_0 + a_4, \quad c_3 = a_0 + c_4, \quad c_2 = c_1 + c_3. \tag{3.51}$$

Note that using relations (3.51), we obtain that the total angle around the edge $\overrightarrow{13}$ in the right polyhedron of Figure 3.7 is $b_0 + c_2 + b_4 = 2\pi$. Identity (3.50) is a direct analogue of the charged pentagon identity of [Kas94]. See also [GKT12].

(c) If we take the degenerate case $a = c = 0$ in the operator $\mathsf{T}(a,c)$, we retrieve the operator $\mathsf{T} := \mathsf{W}^{-1}$.

Theorem 3.52 (Andersen–Kashaev [AK14c])**.** *Let (X, α) be a shaped ordered triangulation and denote by $\mathbf{x} \in \mathbb{R}^{X^2}$ the vector of formal variables assigned to each face of X. If $H_2(X \setminus X^0, \mathbb{Z}) = 0$, then the quantity defined by*

$$\mathcal{Z}_\hbar(X, \alpha) := \int_{\mathbf{x} \in \mathbb{R}^{X^2}} \prod_{T \in X^3} \mathcal{Z}_\hbar(T, \mathbf{x}|_T)\, d\mathbf{x} \tag{3.53}$$

is a well-defined complex number. Moreover, if (X, α) and (X', α') are two shaped triangulations, then we have that $|\mathcal{Z}_\hbar(X, \alpha)| = |\mathcal{Z}_\hbar(X', \alpha')|$ if (X, α) and (X', α') satisfy one of the following conditions:

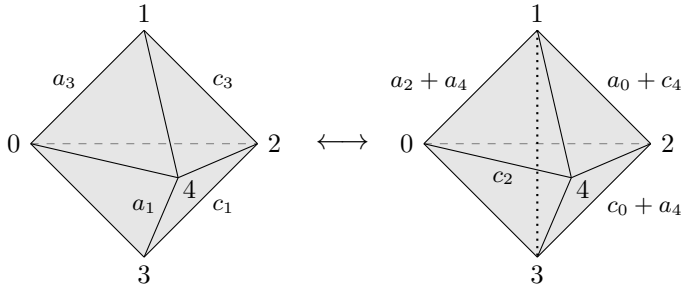

Figure 3.7: 2-3, 3-2 angled Pachner moves.

(1) X and X' differ by the orientation of an edge.

(2) (X, α) and (X', α') are related by 2-3, 3-2 angles Pachner moves.

(3) (X, α) and (X', α') are gauge equivalent.

The quantity (3.53) is called the Teichmüller TQFT partition function *of* (X, α).

Remarks 3.54.

(a) If X is a shaped ordered triangulation, then the partition function is a complex valued continuous function on the space $\mathcal{S}_X$ of shape structures. Furthermore, the partition function admits an analytic continuation to the space of shape structures with complex angles and with some possible singularities.

(b) The partition function cannot be computed for link complements in S^3 with at least two components, because if X is an ideal triangulation of such a link complement, then we have $H_2(X \setminus X^0, \mathbb{Z}) \neq 0$ (see Theorem 3.52). However, using the new formulation [AK13], the computation becomes possible. Moreover, for ideal triangulations, it is conjectured that the value of the partition function for the both formulations are related by the *Weil–Gelfand–Zak transform* [Gel50, Wei51, Zak67]. This has been checked for the first three hyperbolic twist knots in [AN17]. Finally, it was recently proven by Andersen and Kashaev that these two formulations coincide for H-triangulations on homology spheres and a counterexample was found for rational homology spheres.

(c) Considering ideal triangulations of complement of hyperbolic knots in closed 3-manifolds with angle structures, one obtains knot invariants in the sense of Theorem 3.52, which are direct analogues of Baseilhac–Benedetti invariants [BB04]. Moreover, we can also sometimes compute these invariants for non-hyperbolic knots whose complements do not admit angle structures (Theorem 2.38). In this case, we first compute the partition function for a not balanced shape structure, and then we try to take the limit to a balanced non-negative shape structure. If such a limit exists (possibly infinite), then this will be the value of the invariant.

(d) Another invariant is to consider one-vertex H-triangulations of pairs (M, K), where M is an oriented closed 3-manifold and $K \subset M$ a knot, with shape structures, where the weight on the knot tends to 0 and simultaneously the weights on all the other edges tend to 2π (assuming that such structure can be approached by shape

structures). This limit is divergent as a simple pole (after analytic continuation as said in point (a)), but the residue at this pole is a knot invariant (up to a phase factor). This is a direct analogue of the Kashaev invariant [Kas94, Kas95a], which is at the origin of the volume conjecture [Kas97].

(e) If we denote $X^\sharp$ the *mirror image* of the triangulation X (obtained by applying a reflection to each tetrahedron), then all tetrahedron signs are multiplied by -1. Therefore, it follows from the definition of the Teichmüller TQFT and Theorem 3.36 (2) that $\mathcal{Z}_\hbar(X^\sharp,\alpha) = \overline{\mathcal{Z}_\hbar(X,\alpha)}$, and thus $\left|\mathcal{Z}_\hbar(X^\sharp,\alpha)\right| = |\mathcal{Z}_\hbar(X,\alpha)|$. Consequently, the results from Chapter 4 to 6 will also stand for their mirror image knots.

(f) Another type of TQFT on shaped triangulations has been defined in [KLV16] by Kashaev, Luo and Vartanov. Similarly to Turaev–Viro theory, the state variables live on edges. Moreover, it is conjectured that for H-triangulations, the partition function of this TQFT is twice the absolute value squared of the partition function of Teichmüller TQFT. This is similar to the well-known relationship between the Turaev–Viro and the Witten–Reshetikhin–Turaev invariants of 3-manifolds.

3.4.2 Kinematical kernel and dynamical content

Kashaev recently discovered a remarkable method to make easier the computations of partition functions. The idea is to separate the partition function into "easy part" (kinematical kernel) and "hard part" (dynamical content). See [Kas16].

Given an ordered triangulation X with tetrahedra $T_1,\dots,T_n$, we identify X^3 to a set of formal real variables t_j, $j=1,\dots,n$ via the map $\mathtt{t}\colon T_j \mapsto t_j$. We also denote $\mathbf{t}=(t_1,\dots,t_n)$ a formal vector in $\mathbb{R}^{X^3}$. Define a map $p : X^3 \to \mathcal{S}'(\mathbb{R}^{X^2}\times\mathbb{R}^{X^3})$ by

$$p(T)(\mathbf{x},\mathbf{t}) := e^{2\pi i\varepsilon(T)x_0\mathtt{t}(T)}\delta(x_0(T)-x_1(T)+x_2(T))\delta(x_2(T)-x_3(T)+\mathtt{t}(T)),$$

where $\mathbf{x}\in\mathbb{R}^{X^2}$ is as in Theorem 3.52 and $x_i(T)$ denotes the formal real variable associated to the face $\partial_i(T)$ that is part of the vector $\mathbf{x}$.

Definition 3.55. Let X be an ordered triangulation such that $H_2(X\setminus X^0,\mathbb{Z})=0$. The *kinematical kernel* of X is the element $\mathcal{K}_X\in\mathcal{S}'(\mathbb{R}^{X^3})$ defined by

$$\mathcal{K}_X(\mathbf{t}) := \int_{\mathbf{x}\in\mathbb{R}^{X^2}} d\mathbf{x} \prod_{T\in X^3} p(T)(\mathbf{x},\mathbf{t}). \tag{3.56}$$

The fact that $\mathcal{K}_X\in\mathcal{S}'(\mathbb{R}^{X^3})$ is implicit from the proof of Theorem 3.52 (see [AK14c, Theorem 7]). However, in order to allow a better understanding, we now give some additional explanations on formula (3.56).

One should understand the integral of formula (3.56), similarly as in Example 1.41, as the following equality of tempered distributions:

$$\mathcal{K}_X(\mathbf{t}) = \int_{\mathbf{x}\in\mathbb{R}^{X^2}} d\mathbf{x} \int_{\mathbf{w}\in\mathbb{R}^{2n}} d\mathbf{w}\; e^{2i\pi\mathbf{t}^T R\mathbf{x}} e^{-2i\pi\mathbf{w}^T A\mathbf{x}} e^{-2i\pi\mathbf{w}^T B\mathbf{t}} \;\in\mathcal{S}'(\mathbb{R}^{X^3}), \tag{3.57}$$

where $\mathbf{w}=(w_1,w_1',\dots,w_n,w_n')$ is a vector of $2n$ new real variables, such that w_j,w_j' are associated to $\delta(x_0(T_j)-x_1(T_j)+x_2(T_j))$ and $\delta(x_2(T_j)-x_3(T_j)+\mathtt{t}(T_j))$, and where

R, A, B are matrices with integer coefficients depending on the values $x_k(T_j)$, i.e. on the combinatorics of the face gluings. More precisely, the rows (resp. columns) of R are indexed by the vector of tetrahedron variables $\mathbf{t}$ (resp. of face variables $\mathbf{x}$) and R has a coefficient $\varepsilon(T_j)$ at coordinate $(t_j, x_0(T_j))$ and zero everywhere else. The matrix B is indexed by $\mathbf{w}$ (rows) and $\mathbf{t}$ (columns) and has an 1 at the coordinate (w'_j, t_j). Finally, A is such that $A\mathbf{x} + B\mathbf{t}$ is a column vector indexed by $\mathbf{w}$ containing the values $x_0(T_j) - x_1(T_j) + x_2(T_j),\ x_2(T_j) - x_3(T_j) + t_j$ in order.

Lemma 3.58. *If the $2n \times 2n$ matrix A in formula (3.57) is invertible, then the kinematical kernel is simply a bounded function given by:*

$$\mathcal{K}_X(\mathbf{t}) = \frac{1}{|\det(A)|} e^{2i\pi \mathbf{t}^T(-RA^{-1}B)\mathbf{t}}.$$

Proof. The lemma follows from the same argument as in Example 1.41 (swapping integration symbols and applying the Fourier transform F twice), this time for the multi-dimensional function $f_{\mathbf{t}} := \left(\mathbf{x} \mapsto e^{2i\pi \mathbf{t}^T R \mathbf{x}}\right)$. More precisely:

$$\begin{aligned}
\mathcal{K}_X(\mathbf{t}) &= \int_{\mathbf{x}\in\mathbb{R}^{X^2}} d\mathbf{x} \int_{\mathbf{w}\in\mathbb{R}^{2n}} d\mathbf{w}\ e^{2i\pi \mathbf{t}^T R \mathbf{x}} e^{-2i\pi \mathbf{w}^T A \mathbf{x}} e^{-2i\pi \mathbf{w}^T B \mathbf{t}} \\
&= \int_{\mathbf{w}\in\mathbb{R}^{2n}} d\mathbf{w}\ e^{-2i\pi \mathbf{w}^T B \mathbf{t}} \int_{\mathbf{x}\in\mathbb{R}^{2n}} d\mathbf{x}\ f_{\mathbf{t}}(\mathbf{x}) e^{-2i\pi \mathbf{w}^T A \mathbf{x}} \\
&= \int_{\mathbf{w}\in\mathbb{R}^{2n}} d\mathbf{w}\ e^{-2i\pi \mathbf{w}^T B \mathbf{t}}\ \mathsf{F}^{-1}\left(f_{\mathbf{t}}\right)\left(A^T \mathbf{w}\right) \\
&= \frac{1}{|\det(A)|} \int_{\mathbf{v}\in\mathbb{R}^{2n}} d\mathbf{v}\ e^{-2i\pi \mathbf{v}^T A^{-1} B \mathbf{t}}\ \mathsf{F}^{-1}\left(f_{\mathbf{t}}\right)(\mathbf{v}) \\
&= \frac{1}{|\det(A)|} \mathsf{F}^{-1}\left(\mathsf{F}^{-1}\left(f_{\mathbf{t}}\right)\right)\left(A^{-1} B \mathbf{t}\right) \\
&= \frac{1}{|\det(A)|} f_{\mathbf{t}}(-A^{-1} B \mathbf{t}) \\
&= \frac{1}{|\det(A)|} e^{2i\pi \mathbf{t}^T(-RA^{-1}B)\mathbf{t}}.
\end{aligned}$$

□

The product of several Dirac delta functions might not be a tempered distribution in general. However the kinematical kernels in this thesis will always be, thanks to the assumption that $H_2(X \setminus X^0, \mathbb{Z}) = 0$. See [AK14c] for more details, via the theory of wave fronts. The key property to notice is the linear independence of the terms $x_0(T_j) - x_1(T_j) + x_2(T_j),\ x_2(T_j) - x_3(T_j) + t_j$.

Definition 3.59. Let X be an ordered triangulation. Its *dynamical content* associated to $\hbar > 0$ is the function $\mathcal{D}_{\hbar,X} : \mathcal{S}_X \to \mathcal{S}(\mathbb{R}^{X^3})$ defined for each $\alpha \in \mathcal{S}_X$ by

$$\mathcal{D}_{\hbar,X}(\mathbf{t}, \alpha) := \prod_{T\in X^3} \frac{\exp\left(\hbar^{-1/2} \alpha_3(T) \mathsf{t}(T)\right)}{\Phi_{\mathsf{b}}\left(\mathsf{t}(T) - \frac{i}{2\pi\sqrt{\hbar}} \varepsilon(T)(\alpha_2(T) + \alpha_3(T))\right)^{\varepsilon(T)}}.$$

The fact that $\mathcal{D}_{\hbar,X}(\cdot,\alpha) \in \mathcal{S}(\mathbb{R}^{X^3})$ is a consequence of the properties of Faddeev's quantum dilogarithm function and the positivity of the dihedral angles. For more details, see [AK14c]. More precisely, each term in the dynamical content has exponential decrease as described in the following lemma.

Lemma 3.60. *Let $\mathsf{b} \in \mathbb{R}_{>0}$ and $a, b, c \in (0, \pi)$ such that $a + b + c = \pi$. Then*

$$\left| \frac{e^{\frac{1}{\sqrt{\hbar}}cx}}{\Phi_{\mathsf{b}}\left(x - \frac{i}{2\pi\sqrt{\hbar}}(b+c)\right)} \right| \underset{\mathbb{R}\ni x\to\pm\infty}{\sim} \left| e^{\frac{1}{\sqrt{\hbar}}cx} \Phi_{\mathsf{b}}\left(x + \frac{i}{2\pi\sqrt{\hbar}}(b+c)\right) \right| \quad \begin{cases} \underset{\mathbb{R}\ni x\to-\infty}{\sim} e^{\frac{1}{\sqrt{\hbar}}cx}, \\ \underset{\mathbb{R}\ni x\to+\infty}{\sim} e^{-\frac{1}{\sqrt{\hbar}}bx}. \end{cases}$$

Proof. The lemma immediately follows from Theorem 3.36 (4). □

Lemma 3.60 illustrates why we need the three angles a, b, c to be in $(0, \pi)$: b and c must be positive in order to have exponential decrease in both directions, and a must be as well so that $b + c < \pi$ and $\Phi_{\mathsf{b}}\left(x \pm \frac{i}{2\pi\sqrt{\hbar}}(b+c)\right)$ is always defined.

We directly obtain the following result.

Theorem 3.61. *Let (X, α) be a shaped ordered triangulation such that $H_2(X \setminus X^0, \mathbb{Z}) = 0$. Then the partition function of (X, α) is given by*

$$\mathcal{Z}_\hbar(X, \alpha) = \int_{\mathbf{t}\in\mathbb{R}^{X^3}} d\mathbf{t}\, \mathcal{K}_X(\mathbf{t}) \mathcal{D}_{\hbar,X}(\mathbf{t}, \alpha).$$

3.4.3 Special TQFT rules with cones

The purpose of this section is to give a different interpretation of the partition function from the one using tetrahedral weights explained in Section 3.4.1, but with *cones over bigons*. These techniques can be helpful as we will see in Example 3.67 and especially in the Chapter 6. Let us consider the cones with orientation on edges given in Figure 3.8 and we call them cones of type A_+, A_-, B_+ and B_- respectively. To each of them we associate a tempered distribution defined as follows.

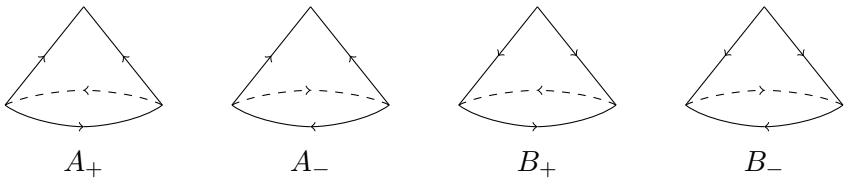

Figure 3.8: Different types of cones with orientation on edges.

We define tempered ket-distributions $|A_+\rangle, |B_+\rangle \in \mathcal{S}'(\mathbb{R}^2)$ by the formulas

$$\langle x, y|A_+\rangle := \delta(x+y)e^{\pi i x^2}, \qquad \langle x, y|B_+\rangle := e^{\pi i(x-y)^2}, \tag{3.62}$$

and two tempered bra-distributions $\langle A_-|, \langle B_-| \in \mathcal{S}'(\mathbb{R}^2)$ by

$$\langle A_-|x, y\rangle := \overline{\langle x, y|A_+\rangle}, \qquad \langle B_-|x, y\rangle := \overline{\langle x, y|B_+\rangle}. \tag{3.63}$$

Note that all the cones of Figure 3.8 are symmetric with respect to rotation by angle π around the vertical axis, and this symmetry corresponds to the fact that we can swap the roles of x and y in formulas (3.62) and (3.63). We now explain how these formulas can be used to compute the partition function. For that, we introduce some definitions.

Definition 3.64. Let X be a triangulation. A *bigon suspension* S of X is the gluing of two tetrahedra T_1 and T_2 arranged around a degree two edge as in Figure 3.9. In this case, the pair (T_1, T_2) is *friendly*. A bigon suspension is *well-oriented* if the two edges on the bigon are oppositely oriented. A triangulation is *well-oriented* if all the bigon suspensions are well-oriented.

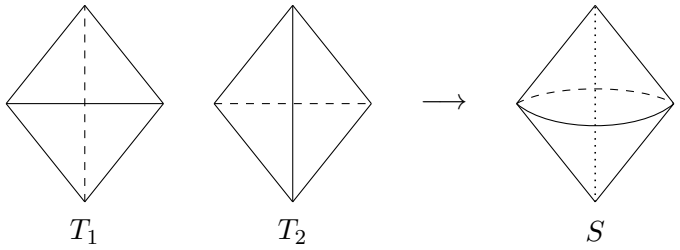

Figure 3.9: A friendly pair turned into a bigon suspension.

Definition 3.65. Let X be an ideal triangulation and $\alpha \in \mathcal{GA}_X$. We say that α is *sharpened* if the angles of each friendly pair are given as in Figure 3.10.

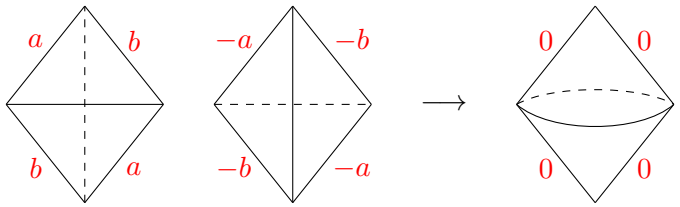

Figure 3.10: Angles on a friendly pair of a sharpened structure.

Remark 3.66. Assume that X is an ideal triangulation endowed with a sharpened structure $\alpha \in \mathcal{GA}_X$. If $\beta \in \mathcal{GA}_X$ is gauge equivalent to α, then β is also sharpened.

Let us come back to the partition function. If X is a well-oriented ideal triangulation provided with a sharpened structure $\alpha \in \mathcal{GA}_X$, then the partition function $\mathcal{Z}_\hbar(X, \alpha)$ can be computed (up to a phase factor) using formulas (3.62) and (3.63) on the bigon suspensions according to the types of cones.

Example 3.67. Let us compute the partition for the complement of the trefoil knot using the ideal triangulation X found in Section 2.1.7.2. Let $\alpha \in \mathcal{S}_X$ be a shape structure. If we denote by e_1 the simple arrow and by e_2 the double arrow, then the weights around these edges are given by

$$\omega_{X,\alpha}(e_1) = 4\pi - c_1 - c_2 =: 4\pi - w, \qquad \omega_{X,\alpha}(e_2) = c_1 + c_2 = w.$$

As the trefoil knot is not hyperbolic, the balanced case ($w = 2\pi$) is not accessible directly, but it can be approached taking the limit

$$(a_i, b_i, c_i) \to (0, 0, \pi) \quad \text{for } i \in \{1, 2\}.$$

Let us denote this generalized angle structure by $\beta \in \mathcal{GA}_X$. If we look at Figure 2.21, we see that X is a gluing of two cones of type A_+ and B_-. Moreover, from Figure 2.22, we also see that β is a sharpened structure on X. We associate the variable y for the face A and the variable x for the face B. Thus, using formulas (3.62) and (3.63), one gets

$$\lim_{w\to 2\pi} \mathcal{Z}_\hbar(X,\alpha) = \mathcal{Z}_\hbar(X,\beta) \overset{\star}{=} \int_{\mathbb{R}^2} \delta(x+y) e^{\pi i x^2} e^{-\pi i (x-y)^2}\, dxdy = \int_{\mathbb{R}} e^{-3\pi i x^2}\, dx \overset{\star}{=} \frac{1}{\sqrt{3}},$$

which is exactly the same value (up to a phase factor) as the one found in [AK14c].

3.4.4 The volume conjecture for Teichmüller TQFT

We now state a version of the *volume conjecture* for the Teichmüller TQFT, in a slightly different (and less powerful) way from Andersen–Kashaev in [AK14c, Conjecture 1]. Notably, we make the statements depend on specific chosen triangulations X and Y and thus we will not be interested in this thesis in how the following properties change under Pachner moves or depend on the triangulations. For some insights on these points, see [AK14c]. We also introduced a new combination of angles μ_X, which has an interesting topological origin in the case of the 3-sphere. The conjecture is separated in three parts, where the first two parts suggest a relationship between the two invariants (see Remarks 3.54 (c) and (d)) and the last part says that the hyperbolic volume of the knot complement appears as an asymptotic value.

Conjecture 3.68. *Let M be a connected closed oriented 3-manifold and $K \subset M$ be a hyperbolic knot. There exist an ideal triangulation X of $M \setminus K$ and an one-vertex H-triangulation Y of (M,K) such that K is represented by an edge $\overrightarrow{K}$ in a single tetrahedron Z of Y, and $\overrightarrow{K}$ has only one pre-image. Moreover, there exists a function $J_X \colon \mathbb{R}_{>0}\times\mathbb{C} \to \mathbb{C}$ such that the following properties hold:*

(1) There exist μ_X, λ_X linear combinations of dihedral angles in X such that for all angle structures $\alpha \in \mathcal{A}_X$ and all $\hbar > 0$, we have:

$$|\mathcal{Z}_\hbar(X,\alpha)| = \left| \int_{\mathbb{R}+i\frac{\mu_X(\alpha)}{2\pi\sqrt{\hbar}}} J_X(\hbar,x) e^{\frac{1}{2\sqrt{\hbar}} x \lambda_X(\alpha)} dx \right|.$$

Moreover, if $M = S^3$, then J_X can be chosen such that μ_X, λ_X are angular holonomies associated to a meridian and a preferred longitude of K.

(2) For every $\mathsf{b} > 0$, and for every $\tau \in \mathcal{S}_{Y\setminus Z} \times \overline{\mathcal{S}_Z}$ such that $\omega_{Y,\tau}$ vanishes on the edge $\overrightarrow{K}$ and is equal to 2π on every other edge, one has:

$$\lim_{\substack{\alpha \to \tau \\ \alpha \in \mathcal{S}_Y}} \left| \Phi_{\mathsf{b}} \left(\frac{\pi - \omega_{Y,\alpha}\left(\overrightarrow{K}\right)}{2\pi i \sqrt{\hbar}} \right) \mathcal{Z}_\hbar(Y,\alpha) \right| = |J_X(\hbar,0)|.$$

(3) In the semi-classical limit $\hbar \to 0^+$, we retrieve the hyperbolic volume of K as:

$$\lim_{\hbar\to 0^+} 2\pi\hbar \log|J_X(\hbar,0)| = -\mathrm{Vol}(M\setminus K).$$

So far, Conjecture 3.68 is proved for:

- the pairs $(S^3, 4_1)$, $(S^3, 5_2)$ by Andersen and Kashaev in [AK14c, Theorem 5],
- the pair $(S^3, 6_1)$ by Andersen and Nissen in [AN17, Theorem 5.1], but the part (3) is checked only numerically.

In the Chapter 4, we will generalize these results to an infinite family of knots, which are hyperbolic twist knots (in Theorems 4.2, 4.13, 4.20, 4.22, 4.45, 4.47 and 4.48). In Chapter 5, we prove Conjecture 3.68 for a family of hyperbolic fibered knots in infinitely many different lens spaces. We finish this chapter by giving several remarks concerning Conjecture 3.68.

Remarks 3.69.

(a) In Conjecture 3.68 (1), one may notice that J_X, μ_X and λ_X are not unique, since one can, for example, replace $(J_X(\hbar, x), x, \mu_X, \lambda_X)$ by

- either $(J_X(\hbar, x)e^{-\frac{1}{2\sqrt{\hbar}}Cx}, x, \mu_X, \lambda_X + C)$ for any constant $C \in \mathbb{R}$,
- or $(DJ_X(\hbar, Dx'), x', \mu_X/D, D\lambda_X)$ for any constant $D \in \mathbb{R}^*$ (via the change of variable $x' = x/D$).

Note however that in both cases, the expected limit $\lim_{\hbar\to 0^+} 2\pi\hbar \log|J_X(\hbar, 0)|$ does not change. When $M = S^3$, a promising way to reduce ambiguity in the definition of J_X is to impose that $\mu_X(\alpha)$ and $\lambda_X(\alpha)$ are uniquely determined as the angular holonomies of a meridian and a preferred longitude of the knot K. In proving Conjecture 3.68 (1) for the twist knots in Theorems 4.13 and 4.45, we find such properties for μ_X and λ_X.

(b) The function $(\hbar \mapsto J_X(\hbar, 0))$ should play the role of the Kashaev invariant in the comparison with the Kashaev–Murakami–Murakami volume conjecture [Kas97, MM01]. Notably, the statement of Conjecture 3.68 (2) has a similar form as the definition of the Kashaev invariant in [Kas94, Kas95a] (see Remark 3.54 (d)) and Conjecture 3.68 (3) resembles the original volume conjecture stated in [Kas97], where $\hbar$ corresponds to the inverse of the color N.

(c) The final form of the Teichmüller TQFT volume conjecture is not yet set in stone, notably because of the unoptimal definitions of the function $(\hbar \mapsto J_X(\hbar, 0))$ (in Conjecture 3.68 (1) and (2)) and the uncertain invariance of the variables and statements under (ordered) Pachner moves. Nevertheless, we hope Conjecture 3.68 as stated here and its resolution can help us understand better how to solve these difficulties in the future.

❧ Chapter 4 ❧

Calculations for twist knots

In this chapter, we treat at first the odd twist knots. We start by finding an H-triangulation for each twist knot and also ideal triangulations of their complement. This leads to new upper bounds for the Matveev complexity. Then we prove that these ideal triangulations are geometric and we compute the partition function for the ideal triangulations and H-triangulations. This will prove the parts (1) and (2) of Conjecture 3.68. Finally, we prove the part (3) of Conjecture 3.68 for all the odd twist knots. All these results are also available for even twist knots and are done in the last section of this chapter. All the work in this chapter is presented in [BAGPN20].

4.1 Definitions and notations

We start by giving the definition of a general twist knot and some notations and conventions which will be used later.

4.1.1 Twist knots

We denote by K_n the unoriented twist knot with n half-twists and $n+2$ crossings, according to Figure 4.1.

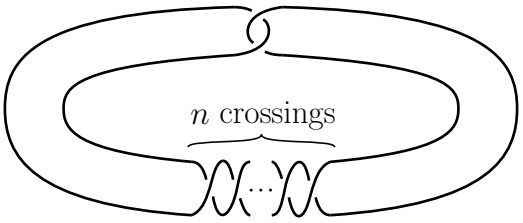

Figure 4.1: The twist knot K_n.

For clarity, we list the names of the 13 first twist knots in the table of Figure 4.2, along with their hyperbolic volume and the coefficient of the Dehn filling one must apply on the Whitehead link (Figure 4.3) to obtain the considered knot. This last one is useful for studying K_n for large n on the software `SnapPy` without having to draw a huge knot diagram by hand.

n	K_n	Dehn surgery coefficient from the Whitehead link	Hyperbolic volume
0	0_1	$(1, 0)$	not hyperbolic
1	3_1	$(1, -1)$	not hyperbolic
2	4_1	$(1, 1)$	2.02988321...
3	5_2	$(1, -2)$	2.82812208...
4	6_1	$(1, 2)$	3.16396322...
5	7_2	$(1, -3)$	3.33174423...
6	8_1	$(1, 3)$	3.42720524...
7	9_2	$(1, -4)$	3.48666014...
8	10_1	$(1, 4)$	3.52619599...
9	11_{a247}	$(1, -5)$	3.55381991...
10	12_{a803}	$(1, 5)$	3.57388254...
11	13_{a3143}	$(1, -6)$	3.58891391...
12	14_{a12741}	$(1, 6)$	3.60046726...

Figure 4.2: The first twist knots.

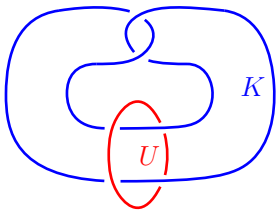

Figure 4.3: The Whitehead link.

The twist knots form, in a sense, the simplest infinite family of hyperbolic knots (for $n \geqslant 2$). This is why our initial motivation was to study the volume conjecture for the Teichmüller TQFT for this particular family (see [BAPN19]).

Remark 4.1. The twist knots K_{2n-1} and K_{2n} are obtained by Dehn filling on one component of the Whitehead link with respective coefficients $(1, -n)$ and $(1, n)$. Note that U and K play symmetric roles in Figure 4.3. As a consequence of the Jørgensen–Thurston theorem (Remark 2.45 (d)) the hyperbolic volume of K_n tends to 3.66386... (the volume of the Whitehead link) as $n \to +\infty$.

4.1.2 Notations and conventions

Let $p \in \mathbb{N}$. In the various following sections, we will use the following recurring conventions:

- A roman letter in **bold** will denote a vector of $p+2$ variables (often integration variables), which are the aforementioned letter indexed by $1, \dots, p, U, W$. For example, $\mathbf{y} = (y_1, \dots, y_p, y_U, y_W)$.
- A roman letter in **bold** and with a tilde $\widetilde{\ }$ will have $p + 3$ variables indexed by $1, \dots, p, U, V, W$. For example, $\widetilde{\mathbf{y}}' = (y'_1, \dots, y'_p, y'_U, y'_V, y'_W)$.
- Matrices and other vectors of size $p+3$ will also wear a tilde but will not necessarily be in bold, for example $\widetilde{C}(\alpha) = (c_1, \dots, c_p, c_U, c_V, c_W)$.

- A roman letter in **bold** and with a hat $\widehat{\ }$ will have $p+4$ variables indexed by $1,\dots,p,U,V,W,Z$. For example, $\widehat{\mathbf{t}} = (t_1,\dots,t_p,t_U,t_V,t_W,t_Z)$.

For $j \in \{1,\dots,p,U,V,W,Z\}$, we will also use the conventions that:

- the symbols e_j, f_j are faces of a triangulation (for $j \in \{1,\dots,p\}$),
- the symbol $\overrightarrow{e_j}$ is an edge of a triangulation (for $j \in \{1,\dots,p\}$),
- the integration variable t_j lives in $\mathbb{R}$,
- the symbols a_j, b_j, c_j are angles in $(0,\pi)$ (sometimes $[0,\pi]$) with sum π,
- the integration variable y'_j lives in $\mathbb{R} \pm \frac{i(\pi-a_j)}{2\pi\sqrt{h}}$,
- the integration variable y_j lives in $\mathbb{R} \pm i(\pi - a_j)$,
- the symbols x_j, d_j are the real and imaginary part of y_j,
- the symbol z_j lives in $\mathbb{R} + i\mathbb{R}_{>0}$,

and are (each time) naturally associated to the tetrahedron T_j. Moreover, we will simply note U,V,W,Z for the tetrahedra T_U,T_V,T_W,T_Z.

4.2 New triangulations for the twist knots

We describe the construction of new triangulations for the twist knots, starting from a knot diagram and using the method described in Section 2.1.7. For the odd twist knots the details are in this section, and for the even twist knots they are in Section 4.7.

4.2.1 Statement of results

Theorem 4.2. *For every $n \geqslant 3$ odd (respectively for every $n \geqslant 2$ even), the triangulations X_n and Y_n represented in Figure 4.4 (respectively in Figure 4.5) are an ideal triangulation of $S^3 \setminus K_n$ and an H-triangulation of (S^3, K_n) respectively.*

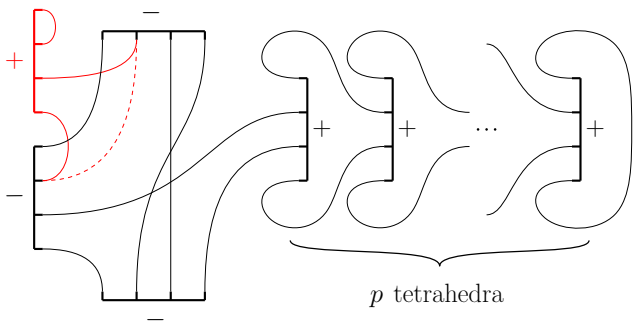

Figure 4.4: An H-triangulation Y_n of (S^3, K_n) (full red part) and an ideal triangulation X_n of $S^3 \setminus K_n$ (dotted red part), for odd $n \geqslant 3$, with $p = \frac{n-3}{2}$.

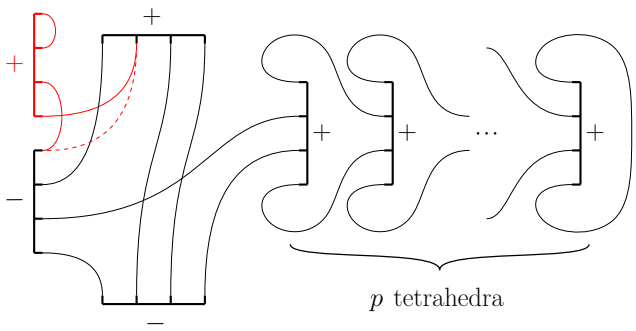

Figure 4.5: An H-triangulation Y_n of (S^3, K_n) (full red part) and an ideal triangulation X_n of $S^3 \setminus K_n$ (dotted red part), for even $n \geqslant 2$, with $p = \frac{n-2}{2}$.

Figures 4.4 and 4.5 display an H-triangulation Y_n of (S^3, K_n), and the corresponding ideal triangulation X_n of $S^3 \setminus K_n$ is obtained by replacing the upper left red tetrahedron (partially glued to itself) by the dotted line (note that we omitted the numbers $0, 1, 2, 3$ of the vertices for simplicity). Theorem 4.2 is proven by applying a method due to Thurston (later refined by Menasco and Kashaev–Luo–Vartanov), explained in Section 2.1.7, to construct a polyhedral decomposition of S^3 where the knot K_n is one of the edges, starting from a diagram of K_n. Along the way, we apply a combinatorial trick to reduce the number of edges and we finish by choosing a convenient triangulation of the polyhedron. Once we have the H-triangulation of (S^3, K_n), we can collapse both the edge representing the knot K_n and its underlying tetrahedron to obtain an ideal triangulation of $S^3 \setminus K_n$. This is detailed in Section 4.2.3 (for odd n) and in Section 4.7.1 (for even n).

4.2.2 Consequences on Matveev complexity

An immediate consequence of Theorem 4.2 is a new upper bound for the Matveev complexity of a general twist knot complement. Recall that the Matveev complexity $\mathfrak{c}(S^3 \setminus K)$ of a knot complement is equal to the minimal number of tetrahedra in an ideal triangulation of this knot complement $S^3 \setminus K$ (see [Mat07a] for this definition and the original wider definition using simple spines).

Corollary 4.3. *Let $n \geqslant 2$. Then the Matveev complexity $\mathfrak{c}\left(S^3 \setminus K_n\right)$ of the n-th twist knot complement satisfies:*

$$\mathfrak{c}\left(S^3 \setminus K_n\right) \leqslant \left\lfloor \frac{n+4}{2} \right\rfloor.$$

Corollary 4.3 follows immediately from Theorem 4.2 and is of double interest.

Firstly, this new upper bound, which is roughly half the crossing number of the knot, is stricly better than the upper bounds existing currently in the literature (to the author's knowledge). Indeed, the usual upper bound for $\mathfrak{c}\left(S^3 \setminus K_n\right)$ is roughly 4 times the crossing number (see for example [Mat07a, Proposition 2.1.11]). A better upper bound for two-bridge knots is given in [IN16, Theorem 1.1], and is equal to n for the n-th twist knot K_n.

Secondly, experiments on the software `SnapPy` lead us to conjecture that the bound of Corollary 4.3 is actually an exact value for $n \geqslant 3$. Indeed, up to $n = 12$, when we

generated an ideal triangulation for $S^3 \setminus K_n$ on `SnapPy`, it always had at least $\left\lfloor \frac{n+4}{2} \right\rfloor$ tetrahedra. Of course, this is only experimental evidence, and proving that $\left\lfloor \frac{n+4}{2} \right\rfloor$ is an actual lower bound seems like a tall order. Notably, lower bounds for $\mathfrak{c}\left(S^3 \setminus K_n\right)$ have not yet been found, to the author's knowledge.

Nevertheless, we propose the following conjecture:

Conjecture 4.4. *Let $n \geqslant 3$. Then the Matveev complexity $\mathfrak{c}\left(S^3 \setminus K_n\right)$ of the n-th twist knot complement satisfies:*

$$\mathfrak{c}\left(S^3 \setminus K_n\right) = \left\lfloor \frac{n+4}{2} \right\rfloor.$$

In the rest of this section, we present one last lead that gives credence to Conjecture 4.4, via the notion of complexity of *pairs*.

As defined in [PP09], the Matveev complexity $\mathfrak{c}\left(S^3, K_n\right)$ of the knot K_n in S^3 is the minimal number of tetrahedra in a triangulation of S^3 where K_n is the union of some quotient edges. Since H-triangulations (as defined in this article) are such triangulations, we deduce from Theorem 4.2 the following corollary:

Corollary 4.5. *Let $n \geqslant 2$. Then the Matveev complexity $\mathfrak{c}\left(S^3, K_n\right)$ of the n-th twist knot in S^3 satisfies:*

$$\mathfrak{c}\left(S^3, K_n\right) \leqslant \left\lfloor \frac{n+6}{2} \right\rfloor.$$

The upper bound of $\left\lfloor \frac{n+6}{2} \right\rfloor$ for the knots K_n in Corollary 4.5 is better than the upper bound of $4n + 10$ in [PP09, Propostion 5.1], which can be a motivation to see how the results of this section can be expanded to other families of knots in S^3. For these same knots K_n, the best lower bound to date seems to be in $\log_5(n)$, see [PP09, Theorem 5.4]. Still, we offer the following conjecture:

Conjecture 4.6. *Let $n \geqslant 3$. Then the Matveev complexity $\mathfrak{c}\left(S^3, K_n\right)$ of the n-th twist knot in S^3 satisfies:*

$$\mathfrak{c}\left(S^3, K_n\right) = \left\lfloor \frac{n+6}{2} \right\rfloor.$$

If true, Conjecture 4.6 would be all the more astonishing that the H-triangulation Y_n of cardinality $\left\lfloor \frac{n+6}{2} \right\rfloor$ would be minimal although it has the double restriction that the knot K_n lies in only one edge of the triangulation of S^3 and that Y_n admits a vertex ordering.

Conjectures 4.4 and 4.6 are equivalent if and only if the following question admits a positive answer:

Question 4.7. Let $n \geqslant 2$. Do the respective Matveev complexities of the n-th twist knot complement and of the n-th twist knot in S^3 differ by 1, i.e. do we always have

$$\mathfrak{c}\left(S^3, K_n\right) = \mathfrak{c}\left(S^3 \setminus K_n\right) + 1 \quad ?$$

Question 4.7 looks far from easy to solve, though. On one hand, it is not clear that the minimal triangulation for the pair (S^3, K_n) can always yield an ideal triangulation for

$S^3 \setminus K_n$ by collapsing exactly one tetrahedron (which is the case for X_n and Y_n as we will see in the following section). On the other hand, it is not clear that one can always construct an H-triangulation of (S^3, K_n) from an ideal triangulation of $S^3 \setminus K_n$ by adding only one tetrahedron.

The previously mentioned lower bound of the form $\log_5(n)$ for $\mathfrak{c}\left(S^3, K_n\right)$ comes from the general property that

$$\frac{1}{2}\mathfrak{c}\left(M_n\right) \leqslant \mathfrak{c}\left(S^3, K_n\right)$$

where M_n is the double branched cover of (S^3, K_n) [PP09, Proposition 5.2]. Here M_n happens to be the lens space $L(2n+1, n)$ (see for example [BZH13, Section 12]), whose Matveev complexity is not yet known but conjectured to be $n-1$ through a general conjecture on the complexity of lens spaces [Mat07a, p. 77].

Hence, if the lens space complexity conjecture holds, then we would have from Corollary 4.5 the double bound

$$\left\lceil \frac{n-1}{2} \right\rceil \leqslant \mathfrak{c}\left(S^3, K_n\right) \leqslant \left\lfloor \frac{n+6}{2} \right\rfloor,$$

which would imply that $\mathfrak{c}\left(S^3, K_n\right)$ can only take four possible values. All this makes Conjecture 4.6 sound more plausible, and Conjecture 4.4 as well by extension.

4.2.3 Construction for odd twist knots

We first consider a general twist knot K_n for $n \geqslant 3$ with n odd. We will construct an H-triangulation of (S^3, K_n) and an ideal triangulation of $S^3 \setminus K_n$ starting from a knot diagram of K_n. We apply the method explained in Section 2.1.7.

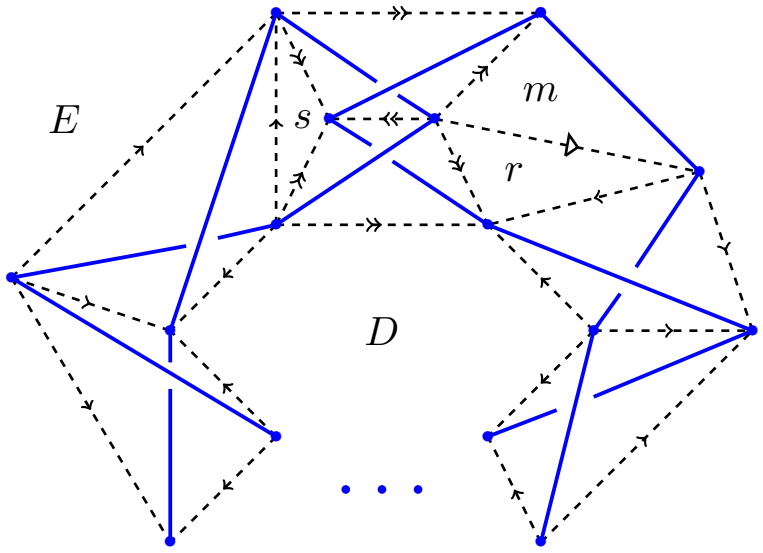

Figure 4.6: Building an H-triangulation from a diagram of K_n.

The first step is to choose a middle point for each arc of the diagram, except for one arc where we choose two (the upper right one on the figure), and we draw quadrilaterals around the crossings with the chosen points as vertices (in dashed lines in Figure 4.6).

We consider again the equivalence relation on dotted edges as in Section 2.1.7 and we choose a way of drawing each class. In Figure 4.6 there are two such edges, one with a

simple arrow and one with a double arrow. We orient the arrows such that the directions keep alternating when one goes around any quadrilateral.

There remains one quadrilateral with three dotted edges and one edge from the knot K_n. We cut this one into two triangles m and r, introducing a third arrow type, the "white triangle" one (see Figure 4.6).

Here m, r, s, D, E are the polygonal 2-cells that decompose the equatorial plane around the knot. Note that m, r, s are triangles, D is an $(n+1)$-gon and E is an $(n+2)$-gon.

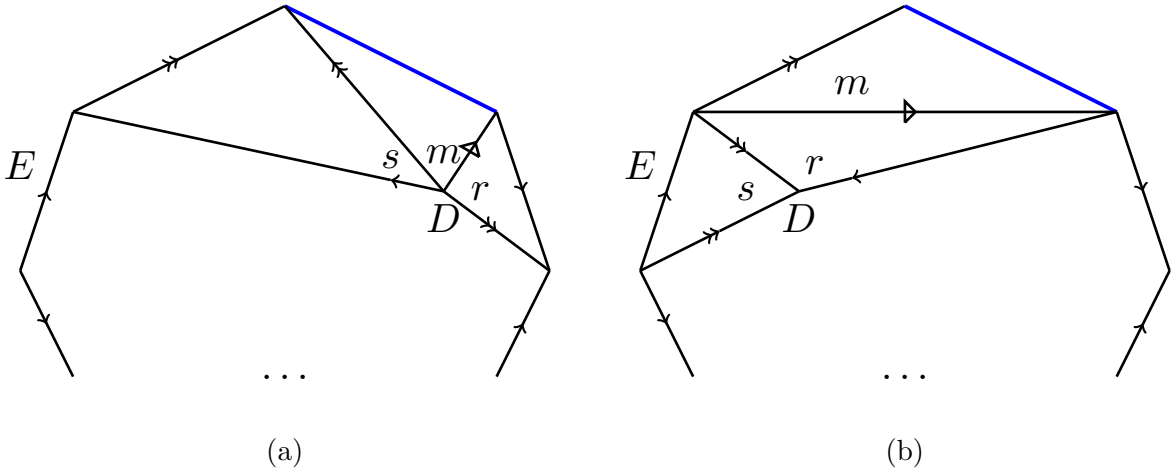

(a) (b)

Figure 4.7: Boundaries of B_+ and B_-.

In Figure 4.6 we can see that around each crossing of the diagram, there are six edges (two in blue from the knot, four dotted with arrows) that delimit an embedded tetrahedron. We will now collapse each of these tetrahedra into one segment, so that each of the two "knot edges" are collapsed to an extremal point of the segment and all four dotted edges fuse into a single one, with natural orientation. The homeomorphism type of (S^3, K_n) does not change if we collapse every tetrahedron in such a way, and that is what we do next.

After such a collapse, the ambient space (that we will call again S^3) decomposes as one 0-cell (the collapsed point), four edges (simple arrow, double arrow, arrow with a triangle and blue edge coming from K_n), five polygonal 2-cells still denoted m, r, s, D, E, and two 3-balls B_+ and B_-, respectively from upper and below the figure. The boundaries of B_+ and B_- are given in Figure 4.7. Note that the boundary of B_+ is obtained from Figure 4.6 by collapsing the upper strands of K_n, and B_+ is implicitly residing above Figure 4.7 (a). Similarly, B_- resides behind Figure 4.7 (b). Note that the boundary of D, read clockwise, is the sequence of $n+1$ arrows $\twoheadrightarrow, \leftarrow, \rightarrow, \ldots, \leftarrow$ with the simple arrows alternating directions.

We can now give a new description of S^3 by gluing the balls B_+ and B_- along the face E. The two 3-cells fuse into one, and its boundary is now as in Figure 4.8 (a). Indeed, since B_- is behind Figure 4.7 (b) and B_+ in front of Figure 4.7 (a), we can picture the gluing along E in the following way, from front to back:

- the faces D, m, r, s of B_-,
- the 3-cell B_-,

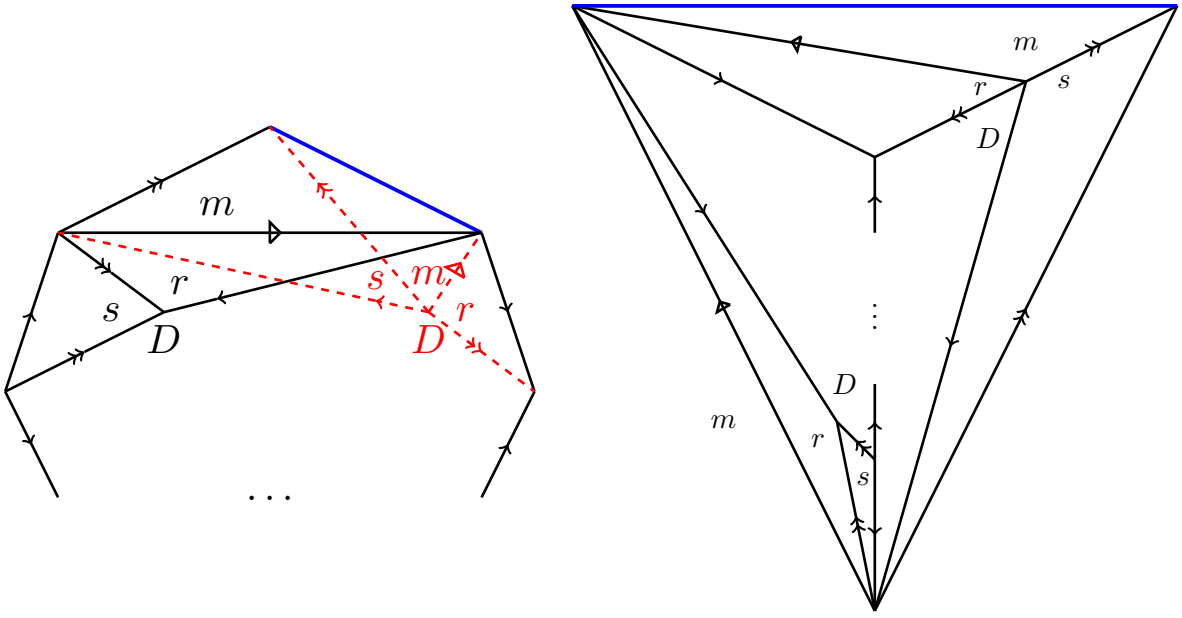

(a) (b)

Figure 4.8: A cellular decomposition of (S^3, K_n) as a polyhedron glued to itself.

- the face E of B_-,
- the face E of B_+,
- the 3-cell B_+,
- the faces D, m, r, s of B_+.

Note that in Figure 4.8 (a) the red dashed faces lie on the back of the figure, and the only 3-cell now lives inside the polyhedron. Finally we can rotate this polyhedron and obtain the cellular decomposition of S^3 in Figure 4.8 (b), where one face m is in the back and the seven other faces lie in front.

We will now use the *bigon trick* to find another polyhedral description of (S^3, K_n) with many fewer edges. The bigon trick is described in Figure 4.9 (a) to (f). We start at (a), with the two faces F having several edges in common, and a triangle u adjacent to F (note that there is a second face u adjacent to the other F somewhere else). Then we go to (b) by cutting F along a new edge (with double full arrow) into F' and a triangle v. The CW-complex described in (b) is the same as the one in (c), where the right part is a 3-ball whose boundary is cut into the triangles u and v and the bigon w. The picture in (d) is simply the one from (c) with the ball rotated so that v lies in the back instead of w. Then we obtain (e) by gluing the two parts of (d) along the face v, and finally (f) by fusing F' and w into a new face F''. As a result, we replaced two simple arrows by one longer different (full) arrow and we slided the face u up.

Let us now go back to our cellular decomposition of (S^3, K_n). We start from Figure 4.8 (b) and cut D into new faces u and D' as in Figure 4.10 (a). Then we apply the bigon trick p times, where $p := \frac{n-3}{2}$, to slide the cell u on the left D', and finally we cut the face

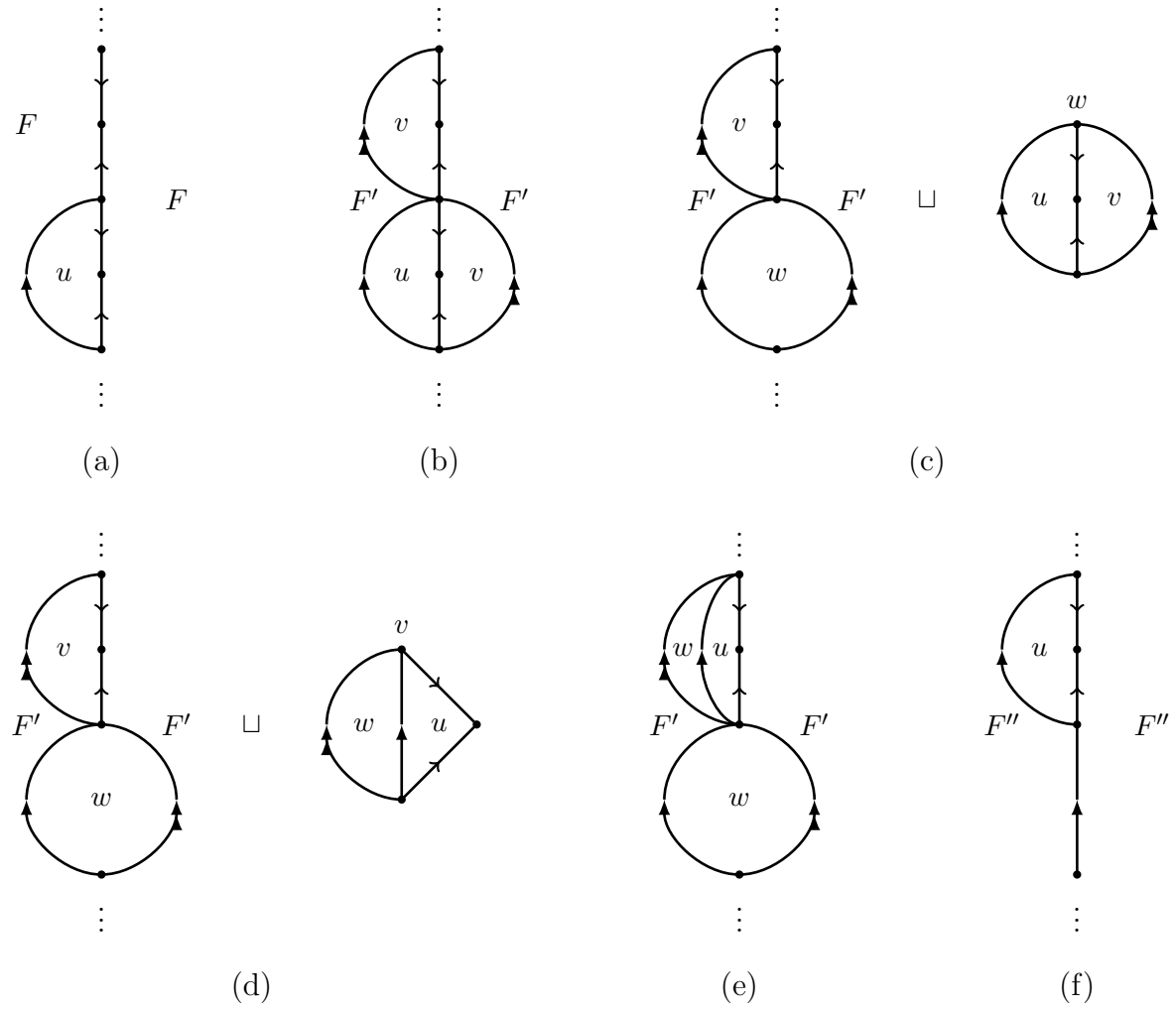

Figure 4.9: The bigon trick.

obtained from D' a final time into a $(p+2)$-gon G and a triangle v by adding a double full arrow. See Figure 4.10 (b).

Note that if $n = 3$, i.e. $p = 0$, we do not use the bigon trick, and simply denote D' by v. In this case, G is empty and the double full arrow should be identified with the simple full arrow.

Then, if $p \geqslant 1$, we triangulate the two faces G as in Figure 4.11: we add $p-1$ new edges drawn with simple arrows and circled k for $k = 1, \ldots, p-1$ (and drawn in different colors in Figure 4.11 but not in the following pictures), and G is cut into p triangles $e_1, \ldots, e_p$. This still makes sense if $p = 1$, in this case we have $G = e_p = e_1$ and no new edges.

Now, by combining Figures 4.10 (b) and 4.11, we obtain a decomposition of S^3 as a polyhedron with only triangular faces glued to one another, and K_n still represents the blue edge after identifications. In order to harmonize the notations with the small cases $(p = 0, 1)$, we do the following arrow replacements:

- full black simple arrow by simple arrow with circled 0,

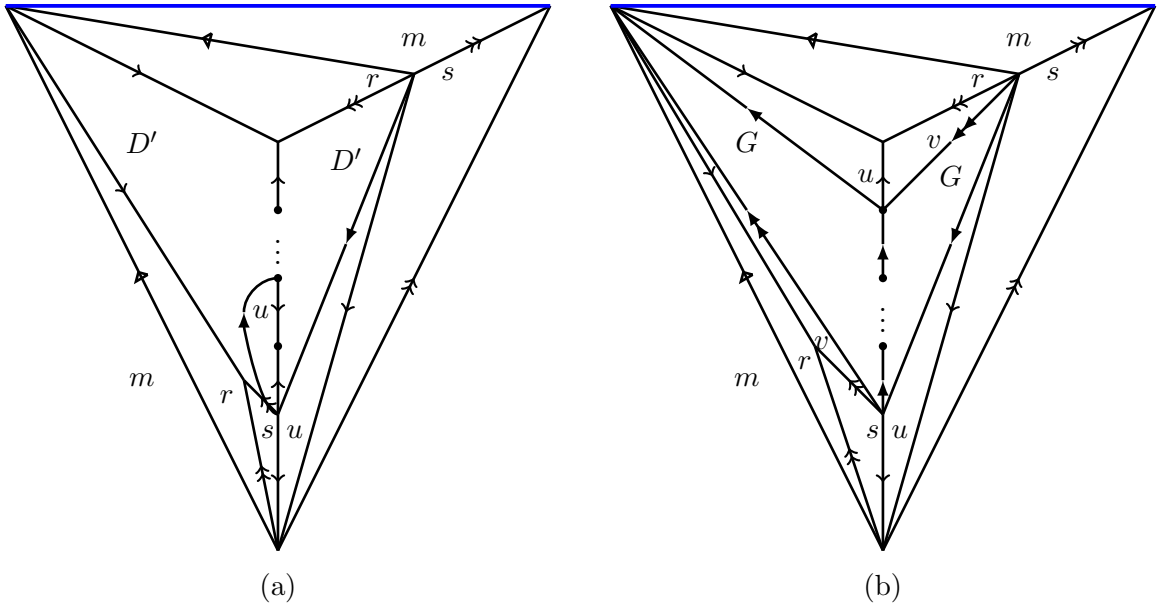

Figure 4.10: A cellular decomposition of (S^3, K_n) before and after the bigon trick.

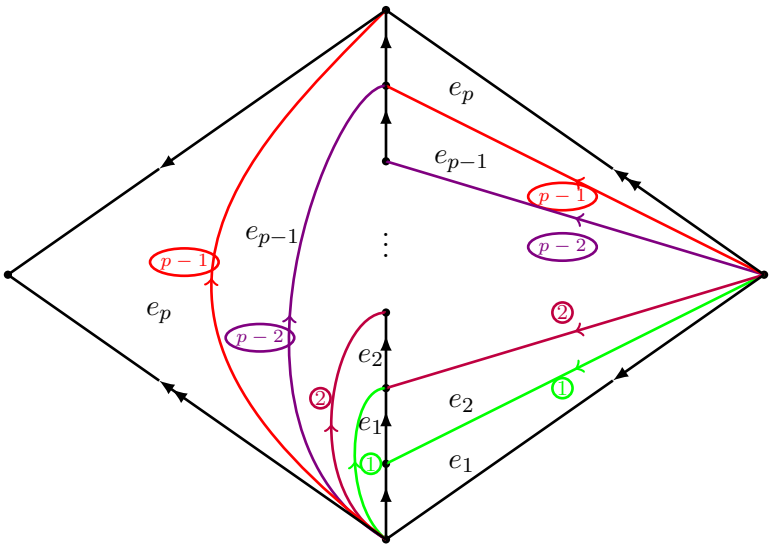

Figure 4.11: Decomposing the two faces G in a tower of tetrahedra.

- full black double arrow by simple arrow with circled p,
- white triangle simple arrow by simple arrow with circled $p+1$.

Moreover, we cut the previous polyehdron of Figures 4.10 (b) and 4.11 into $p+4$ tetrahedra, introducing new triangular faces e_{p+1} (behind r, u, v), g (behind r, s, v), s' (completing m, m, s), f_p (completing g, s', u) and $f_1, \ldots, f_{p-1}$ at each of the $p-1$ "floors" of the tower of Figure 4.11 (from front to back of the figure). We add the convention $f_0 = e_1$ to account for the case $p = 0$. We also choose an orientation for the blue edge and thus a sign for the tetrahedron that contains it (this choice will not have any influence on the ideal triangulation, though).

Finally, we obtain the H-triangulation for (S^3, K_n) described in Figure 4.12, for any $p \geqslant 0$ (recalling the convention $f_0 = e_1$ if need be).

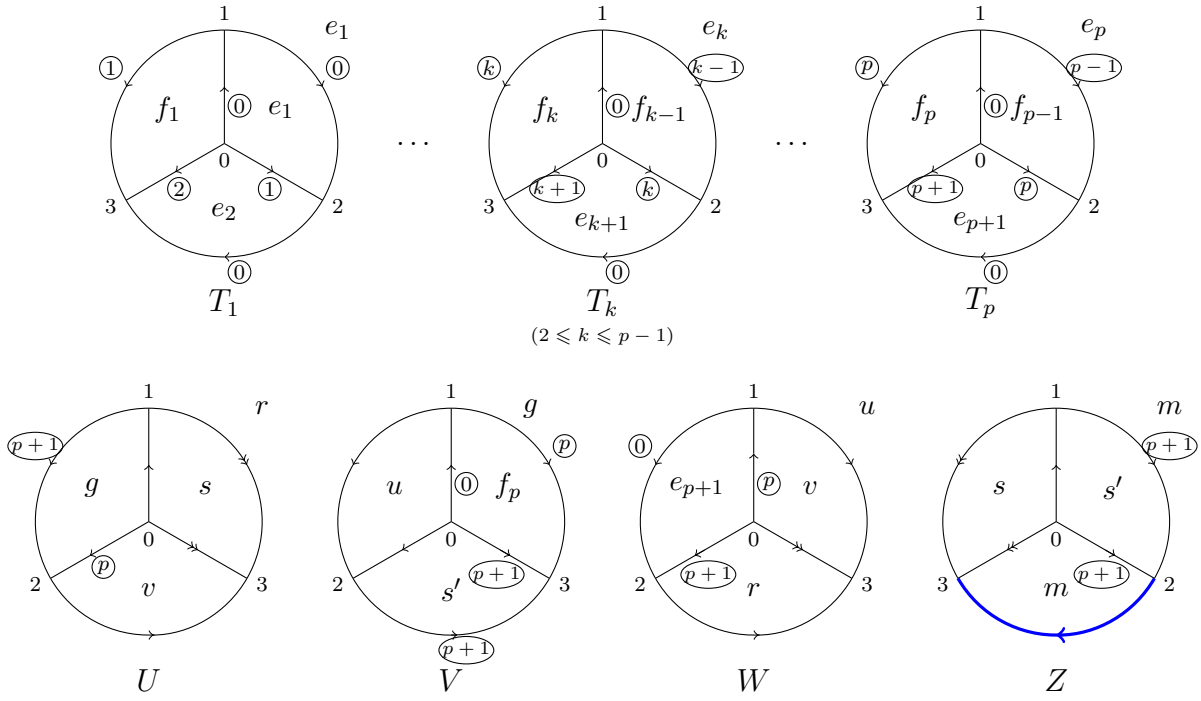

Figure 4.12: The H-triangulation Y_n for (S^3, K_n), n odd, $n \geqslant 3$, with $p = \frac{n-3}{2}$.

In the H-triangulation of Figure 4.12 there are

- 1 common vertex,
- $p + 5 = \frac{n+7}{2}$ edges (simple arrow $\overrightarrow{e_s}$, double arrow $\overrightarrow{e_d}$, blue simple arrow $\overrightarrow{K_n}$, and the simple arrows $\overrightarrow{e_0}, \ldots, \overrightarrow{e_{p+1}}$ indexed by $0, \ldots p+1$ in circles),
- $2p + 8 = n + 5$ faces $(e_1, \ldots, e_{p+1}, f_1, \ldots, f_p, g, m, r, s, s', u, v)$,
- $p + 4 = \frac{n+5}{2}$ tetrahedra $(T_1, \ldots, T_p, U, V, W, Z)$.

We are now ready to obtain an ideal triangulation of $S^3 \setminus K_n$. From the H-triangulation of (S^3, K_n) of Figure 4.12, let us collapse the whole tetrahedron Z into a triangle: this transforms the blue edge (corresponding to K_n) into a point, collapses the two faces m, and identifies the faces s and s' in a new face also called s, and the double arrow edge to the arrow with circled $p + 1$.

Hence we obtain an ideal triangulation of the knot complement $S^3 \setminus K_n$, described in Figure 4.13.

In Figure 4.13 there are

- 1 common vertex,
- $p + 3 = \frac{n+3}{2}$ edges (simple arrow $\overrightarrow{e_s}$ and the simple arrows $\overrightarrow{e_0}, \ldots, \overrightarrow{e_{p+1}}$ indexed by $0, \ldots p+1$ in circles),

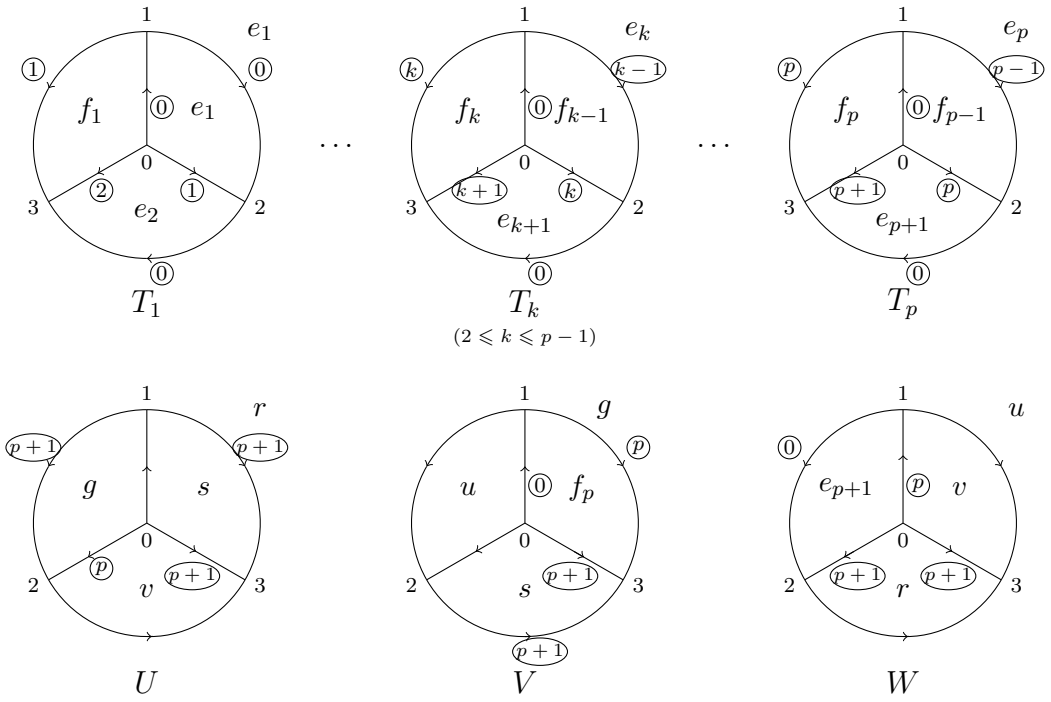

Figure 4.13: The ideal triangulation X_n for $S^3 \setminus K_n$, n odd, $n \geqslant 3$, with $p = \frac{n-3}{2}$.

- $2p + 6 = n + 3$ faces $(e_1, \ldots, e_{p+1}, f_1, \ldots, f_p, g, r, s, u, v)$,
- $p + 3 = \frac{n+3}{2}$ tetrahedra $(T_1, \ldots, T_p, U, V, W)$.

We can now conclude with the proof of Theorem 4.2.

Proof of Theorem 4.2. The triangulations of Figures 4.12 and 4.13 correspond to the common "comb representation" of Figure 4.4.

Similarly, the triangulations of Figures 4.21 and 4.22 (constructed in Section 4.7.1) correspond to the common "comb representation" of Figure 4.5. □

4.3 Angle structures and geometricity (odd case)

In this section, n will be an odd integer greater than or equal to 3.

4.3.1 Geometricity of the ideal triangulations

Here we will compute the balanced angle relations for the ideal triangulations X_n and their spaces of angle structures $\mathcal{A}_{X_n}$. We will then prove that the X_n are *geometric*.

Theorem 4.8. *For every odd $n \geqslant 3$, the ideal triangulation X_n of the n-th twist knot complement $S^3 \setminus K_n$ is geometric.*

To prove Theorem 4.8, we follow the method of Futer–Guéritaud [FG11]: we first prove that the space of angle structures $\mathcal{A}_{X_n}$ is non-empty (Lemma 4.9). Then we prove by

contradiction that the volume functional cannot attain its maximum on the boundary $\overline{\mathcal{A}_{X_n}} \setminus \mathcal{A}_{X_n}$ (Lemma 4.11).

For the remainder of this section, n will be a fixed odd integer, $n \geqslant 7$. Recall that $p = \frac{n-3}{2}$. The cases $n = 3, 5$ (i.e. $p = 0, 1$) are similar and simpler than the general following $n \geqslant 7$ case, and will be discussed at the end of this section (Remark 4.12).

Recall that we denoted $\overrightarrow{e_0}, \dots, \overrightarrow{e_{p+1}}, \overrightarrow{e_s} \in X_n^1$ the $p+3$ edges in X_n respectively represented in Figure 4.13 by arrows with circled 0, ..., circled $p+1$ and simple arrow.

For $\alpha = (a_1, b_1, c_1, \dots, a_p, b_p, c_p, a_U, b_U, c_U, a_V, b_V, c_V, a_W, b_W, c_W) \in \mathcal{S}_{X_n}$ a shape structure on X_n, we compute the weights of each edge:

- $\omega_s(\alpha) := \omega_{X_n,\alpha}(\overrightarrow{e_s}) = 2a_U + b_V + c_V + a_W + b_W$
- $\omega_0(\alpha) := \omega_{X_n,\alpha}(\overrightarrow{e_0}) = 2a_1 + c_1 + 2a_2 + \cdots + 2a_p + a_V + c_W$
- $\omega_1(\alpha) := \omega_{X_n,\alpha}(\overrightarrow{e_1}) = 2b_1 + c_2$
- $\omega_k(\alpha) := \omega_{X_n,\alpha}(\overrightarrow{e_k}) = c_{k-1} + 2b_k + c_{k+1}$ (for $2 \leqslant k \leqslant p-1$)
- $\omega_p(\alpha) := \omega_{X_n,\alpha}(\overrightarrow{e_p}) = c_{p-1} + 2b_p + b_U + b_V + a_W$
- $\omega_{p+1}(\alpha) := \omega_{X_n,\alpha}(\overrightarrow{e_{p+1}}) = c_p + b_U + 2c_U + a_V + c_V + b_W + c_W$.

The space of angle structures $\mathcal{A}_{X_n}$ is made of shape structures $\alpha \in \mathcal{S}_{X_n}$ satisfying $\omega_j(\alpha) = 2\pi$ for all $j \in \{s, 0, \dots, p+1\}$. The sum of all these equations says that all the angles add up to $(p+3)\pi$, which is true in any shape structure, therefore we can drop $\omega_0(\alpha)$ as redundant. Using the properties of shape structures, $\mathcal{A}_{X_n}$ is thus defined by the $p+2$ following equations on α:

- $E_s(\alpha)$: $2a_U = a_V + c_W$
- $E_1(\alpha)$: $2b_1 + c_2 = 2\pi$
- $E_k(\alpha)$: $c_{k-1} + 2b_k + c_{k+1} = 2\pi$ (for $2 \leqslant k \leqslant p-1$)
- $E_p(\alpha)$: $c_{p-1} + 2b_p + (b_U + b_V + a_W) = 2\pi$
- $E_{p+1}(\alpha)$: $3c_p + (a_U + a_V + c_W) + 3(c_U + c_V + b_W) = 3\pi$.

The last line was obtained as $3B_{p+1} + 2B_s - 3F_U - 2F_V - 2F_W$, where F_j is the relationship $a_j + b_j + c_j = \pi$ and B_j is the relationship $\omega_j(\alpha) = 2\pi$. In other words,

$$\mathcal{A}_{X_n} = \{\alpha \in \mathcal{S}_{X_n} \mid \forall j \in \{s, 1, \dots, p+1\},\ E_j(\alpha)\}.$$

Lemma 4.9. *The set $\mathcal{A}_{X_n}$ is non-empty.*

Proof. For small $\epsilon > 0$, define:

$$\begin{pmatrix} a_j \\ b_j \\ c_j \end{pmatrix} := \begin{pmatrix} \epsilon \\ \pi - \epsilon(j^2+1) \\ \epsilon j^2 \end{pmatrix} \text{ for } 1 \leqslant j \leqslant p-1, \quad \begin{pmatrix} a_p \\ b_p \\ c_p \end{pmatrix} := \begin{pmatrix} \pi/2 - \epsilon(p^2+2p-1)/2 \\ \pi/2 - \epsilon(p^2-2p+1)/2 \\ \epsilon p^2 \end{pmatrix},$$

$$\begin{pmatrix} a_U \\ b_U \\ c_U \end{pmatrix} = \begin{pmatrix} a_V \\ b_V \\ c_V \end{pmatrix} = \begin{pmatrix} c_W \\ a_W \\ b_W \end{pmatrix} := \begin{pmatrix} \pi/2 + \epsilon p^2/2 \\ \pi/3 \\ \pi/6 - \epsilon p^2/2 \end{pmatrix}.$$

By direct computation, we can check that this α is a shape structure (the angles are in $(0,\pi)$ if ϵ is small enough), and that the equations $E_j(\alpha)$ are satisfied for $j \in \{s, 1, \dots, p+1\}$. □

We will say that a tetrahedron T of a triangulation X endowed with an extended shape structure $\alpha \in \overline{\mathcal{S}_X}$ is *flat for* α if one of the three angles of T is zero, and *taut for* α if two angles are zero and the third is π. In both cases, T has a volume equal to zero.

Lemma 4.10. *Suppose $\alpha \in \overline{\mathcal{A}_{X_n}} \setminus \mathcal{A}_{X_n}$ is such that the volume functional on $\overline{\mathcal{A}_{X_n}}$ is maximal at α. If an angle of α equals 0, then the other two angles for the same tetrahedron are 0 and π. In other words, if a tetrahedron is flat for α, then it is taut for α.*

Proof. We refer to [Gué06, Proposition 7.1] for the proof. □

Next, we claim that among the volume maximizers, there is one such that $(a_U, b_U, c_U) = (a_V, b_V, c_V) = (c_W, a_W, b_W)$. The involution $(a_V, b_V, c_V) \leftrightarrow (c_W, a_W, b_W)$ preserves all equations $E_j(\alpha)$, so by concavity of the volume function, there is a maximizer such that $(a_V, b_V, c_V) = (c_W, a_W, b_W)$. By $E_s(\alpha)$ this implies $a_U = a_V = c_W$. The order-3 substitution of variables

$$(a_U, b_U, c_U) \to (a_V, b_V, c_V) \to (c_W, a_W, b_W) \to (a_U, b_U, c_U)$$

then clearly leaves E_p and E_{p+1} unchanged, so by concavity we may average out and find a maximizer such that U, V, W have the same angles, as desired.

These identifications make $E_s(\alpha)$ redundant. Moreover, dropping the angles of V and W as variables, we may now rewrite the system of constraints as

- $E_1 :\ 2b_1 + c_2 = 2\pi$
- $E_k :\ c_{k-1} + 2b_k + c_{k+1} = 2\pi \quad (\text{for } 2 \leqslant k \leqslant p-1)$
- $E'_p :\ c_{p-1} + 2b_p + 3b_U = 2\pi$
- $E'_{p+1} :\ c_p + a_U + 3c_U = \pi \quad (\text{not } 2\pi!).$

Lemma 4.11. *Suppose that the volume functional on $\overline{\mathcal{A}_{X_n}}$ is maximal at α. Then α cannot be on the boundary $\overline{\mathcal{A}_{X_n}} \setminus \mathcal{A}_{X_n}$, and is necessarily in the interior $\mathcal{A}_{X_n}$.*

Proof. First, the tetrahedron T_p is not flat, i.e. not taut. Indeed, on one hand $c_p = \pi$ would by E'_{p+1} entail $a_U = c_U = 0$, hence $b_U = \pi$, incompatible with E'_p. On the other hand, suppose $c_p = 0$, then the non-negative sequence $(0, c_1, \dots, c_p)$ is convex, because E_k can be rewritten $c_{k-1} - 2c_k + c_{k+1} = 2a_k \geqslant 0$ (agreeing that "c_0" stands for 0). Hence $c_1 = \cdots = c_p = 0$, and $b_p \in \{0, \pi\}$ by Lemma 4.10. If $b_p = 0$ then (E'_p, E'_{p+1}) yield $(a_U, b_U, c_U) = (0, 2\pi/3, \pi/3)$. If $b_p = \pi$ they yield $(a_U, b_U, c_U) = (\pi, 0, 0)$. In either case, all tetrahedra are flat so the volume vanishes and cannot be maximal: this contradiction shows $c_p > 0$.

Next, we show that U is not flat. We cannot have $c_U = \pi$ or $b_U = \pi$, by E'_{p+1} and E'_p. But $a_U = \pi$ is also impossible, since by E'_{p+1} it would imply $c_p = 0$, ruled out above.

We can see by induction that $b_1, \dots, b_{p-1} > 0$: the initialization is given by E_1, written as $b_1 = \pi - c_2/2 \geqslant \pi/2$. For the induction step, suppose $b_{k-1} > 0$ for some $1 < k \leqslant p-1$: then $c_{k-1} < \pi$, hence E_k implies $b_k > 0$.

Finally, $b_1, \dots, b_{p-1} < \pi$: we show this by *descending* induction. Initialization: by E_{p-1}, we have $b_{p-1} \leqslant \pi - c_p/2 < \pi$ since T_p is not flat. For the induction step, suppose $b_{k+1} < \pi$ for some $1 \leqslant k < p-1$: then $0 < b_{k+1} < \pi$ by the previous induction, hence $c_{k+1} > 0$ by Lemma 4.10, hence E_k implies $b_k < \pi$. □

Remark 4.12 (Cases $p = 0, 1$)**.** The above discussion is valid for $p \geqslant 2$. If $p = 1$, we have only the weights ω_s, ω_{p+1} and ω_p, the latter taking the form $2b_p + b_U + b_V + a_W$ (i.e. the variable "c_{p-1}" disappears from equation E'_p). The argument is otherwise unchanged — the inductions in the proof of Lemma 4.11 being empty.

If $p = 0$, we find only one equation E'_{p+1} : $a_U + 3c_U = \pi$ (i.e. the variable "c_p" disappears). The volume maximizer (a_U, b_U, c_U) on the segment from $(\pi, 0, 0)$ to $(0, 2\pi/3, \pi/3)$ yields the complete hyperbolic metric.

Proof of Theorem 4.8. In the case $n \geqslant 7$, we have proven in Lemma 4.9 that $\mathcal{A}_{X_n}$ is non-empty, thus the volume functional $\mathcal{V} \colon \overline{\mathcal{A}_{X_n}} \to \mathbb{R}$ admits a maximum at a certain point $\alpha \in \overline{\mathcal{A}_{X_n}}$ as a continuous function on a non-empty compact set. We proved in Lemma 4.11 that $\alpha \notin \overline{\mathcal{A}_{X_n}} \setminus \mathcal{A}_{X_n}$, therefore $\alpha \in \mathcal{A}_{X_n}$. It follows from Theorem 2.52 that X_n is geometric.

For the cases $n = 3$ and $n = 5$, we follow the same reasoning, replacing Lemma 4.11 with Remark 4.12. □

4.3.2 The cusp triangulation

Consider the truncation of the ideal triangulation X_n of Figure 4.13 by removing a small neighborhood of the unique ideal vertex. Then we obtain a truncated triangulation of the knot exterior $S^3 \setminus \nu(K_n)$ (where $\nu(K)$ is an open tubular neighborhood of K), which in turn induces a triangulation on the boundary torus $\partial\nu(K_n)$. See Figure 4.14 for the full description of the triangulation of this torus.

The triangles are called (in blue) by the names of the corresponding truncated vertices (written k_j for the k-th vertex in the j-th tetrahedron), the edges are called (in black) by the names of the truncated faces they are part of, and the angles a, b, c at each corner

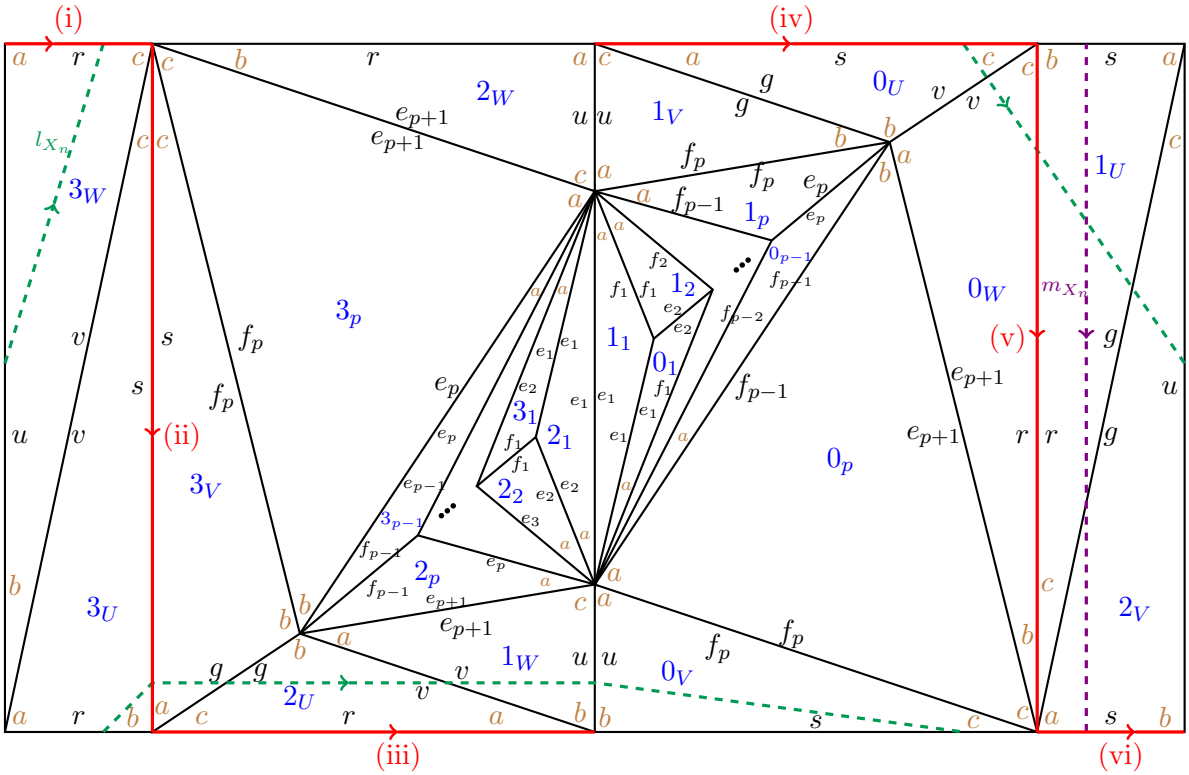

Figure 4.14: Triangulation of the boundary torus for the truncation of X_n, n odd, with angles (brown), meridian curve m_{X_n} (violet, dashed), longitude curve l_{X_n} (green, dashed) and preferred longitude curve (i)$\cup\cdots\cup$(vi) (red).

of a triangle (in brown) obviously come from the corresponding truncated edges in X_n. Note that we did not put the indices on a, b, c for readability, but it goes without saying that angles a, b, c in the triangle k_j are actually the coordinates a_j, b_j, c_j. Moreover, for some small faces, we only indicated the brown a angle for readability. The b and c follow clockwise (since all the concerned tetrahedra have positive sign).

We drew three particular curves in Figure 4.14: m_{X_n} in violet and dashed, l_{X_n} in green and dashed, and finally the concatenation (i) $\cup\cdots\cup$ (vi) in red. These curves can be seen as generators of the first homology group of the torus. We call m_{X_n} a *meridian curve* since it actually comes from the projection to $\partial\nu(K_n)$ of a meridian curve in $S^3 \setminus K_n$, the one circling the knot and going through faces s and E on the upper left of Figure 4.6, to be exact (we encourage the motivated reader to check this fact by following the curve on the several pictures from Figure 4.6 to 4.13). Similarly, l_{X_n} and (i) $\cup\cdots\cup$ (vi) are two distinct *longitude curves*, and (i) $\cup\cdots\cup$ (vi) corresponds to a *preferred longitude* of the knot K_n, i.e. a longitude with zero linking number with the knot.

This last fact can be checked in Figure 4.15: on the bottom of the figure, the sub-curves (i) to (vi) are drawn on a truncated tetrahedron U. On the top of the figure, the corresponding full longitude curve (in red) is drawn in the exterior of the knot (in blue) before the collapsing of the knot into one point (compare with Figure 4.6). We check that in each square on the left of the figure, the sum of the signs of crossings between blue and red strands is zero (the signs are marked in green circled + and −), and thus the red longitude

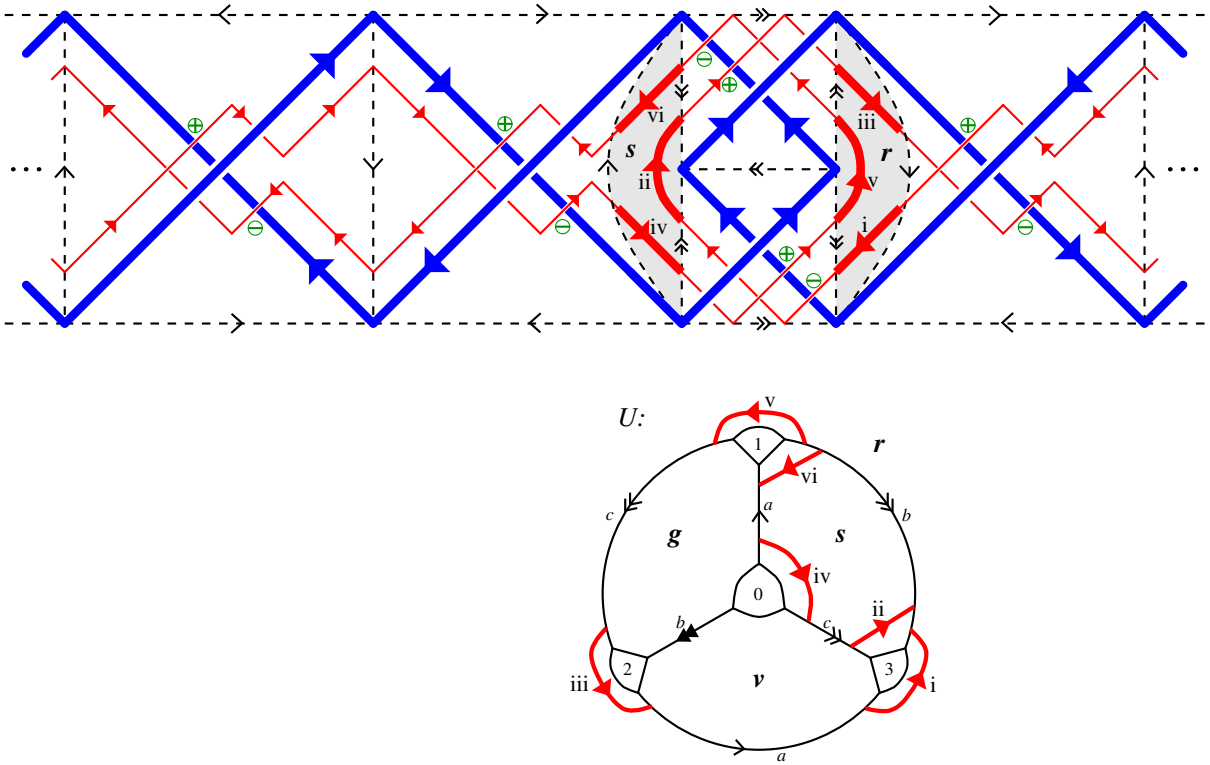

Figure 4.15: A preferred longitude (i)$\cup\cdots\cup$(vi) (in red) for the odd twist knot K_n, seen in $S^3 \setminus K_n$ (top) and on the truncated tetrahedron U (bottom).

curve has zero linking number with the knot, i.e. is a preferred longitude.

To the curves m_{X_n} and l_{X_n} are associated combinations of angles (the angular holonomies)

$$m_{X_n}(\alpha) := H^{\mathbb{R}}(m_{X_n}) = a_U - a_V \quad \text{and} \quad l_{X_n}(\alpha) := H^{\mathbb{R}}(l_{X_n}) = 2(c_V - b_W),$$

following the convention (already explained in Section 2.2.1) that when the curve crosses a triangle, the lone angle among the three is counted positively if it lies on the left of the curve, and negatively if it lies on the right. Remark that this convention cannot rigorously be applied to the red curve (i) $\cup\cdots\cup$ (vi) in Figure 4.14, since it lies on edges and vertices. Nevertheless, one can see in Figure 4.14 that in the homology group of the boundary torus, we have the relation

$$\text{(i)} \cup \cdots \cup \text{(vi)} = l_{X_n} + 2m_{X_n}.$$

4.3.3 The gluing equations

Here seems to be an appropriate place to list the hyperbolicity and completeness equations for X_n, which will be useful in Section 4.6.

For a complex shape structure $\widetilde{\mathbf{z}} = (z_1, \ldots, z_p, z_U, z_V, z_W) \in (\mathbb{R} + i\mathbb{R}_{>0})^{p+3}$, its complex weight functions are:

- $\omega_s^{\mathbb{C}}(\widetilde{\mathbf{z}}) := \omega_{X_n,\alpha}^{\mathbb{C}}(\overrightarrow{e_s}) = 2\mathrm{Log}(z_U) + \mathrm{Log}(z'_V) + \mathrm{Log}(z''_V) + \mathrm{Log}(z_W) + \mathrm{Log}(z'_W)$
- $\omega_0^{\mathbb{C}}(\widetilde{\mathbf{z}}) := \omega_{X_n,\alpha}^{\mathbb{C}}(\overrightarrow{e_0}) = 2\mathrm{Log}(z_1) + \mathrm{Log}(z'_1) + 2\mathrm{Log}(z_2) + \cdots + 2\mathrm{Log}(z_p) + \mathrm{Log}(z_V) + \mathrm{Log}(z''_W)$

- $\omega_1^{\mathbb{C}}(\widetilde{\mathbf{z}}) := \omega_{X_n,\alpha}^{\mathbb{C}}(\overrightarrow{e_1}) = 2\mathrm{Log}(z_1'') + \mathrm{Log}(z_2')$
- $\omega_k^{\mathbb{C}}(\widetilde{\mathbf{z}}) := \omega_{X_n,\alpha}^{\mathbb{C}}(\overrightarrow{e_k}) = \mathrm{Log}(z_{k-1}') + 2\mathrm{Log}(z_k'') + \mathrm{Log}(z_{k+1}')$ (for $2 \leqslant k \leqslant p-1$)
- $\omega_p^{\mathbb{C}}(\widetilde{\mathbf{z}}) := \omega_{X_n,\alpha}^{\mathbb{C}}(\overrightarrow{e_p}) = \mathrm{Log}(z_{p-1}') + 2\mathrm{Log}(z_p'') + \mathrm{Log}(z_U') + \mathrm{Log}(z_V') + \mathrm{Log}(z_W)$
- $\omega_{p+1}^{\mathbb{C}}(\widetilde{\mathbf{z}}) := \omega_{X_n,\alpha}^{\mathbb{C}}(\overrightarrow{e_{p+1}}) = \mathrm{Log}(z_p') + \mathrm{Log}(z_U') + 2\mathrm{Log}(z_U'') + \mathrm{Log}(z_V) + \mathrm{Log}(z_V'') + \mathrm{Log}(z_W') + \mathrm{Log}(z_W'')$.

It follows from Theorem 4.8 that there exists exactly one complex angle structure $\widetilde{\mathbf{z^0}} = (z_1^0, \ldots, z_p^0, z_U^0, z_V^0, z_W^0) \in (\mathbb{R} + i\mathbb{R}_{>0})^{p+3}$ corresponding to the complete hyperbolic metric. This $\widetilde{\mathbf{z^0}}$ is the only $\widetilde{\mathbf{z}} \in (\mathbb{R} + i\mathbb{R}_{>0})^{p+3}$ satisfying

$$\omega_s^{\mathbb{C}}(\widetilde{\mathbf{z}}) = \omega_0^{\mathbb{C}}(\widetilde{\mathbf{z}}) = \ldots = \omega_{p+1}^{\mathbb{C}}(\widetilde{\mathbf{z}}) = 2i\pi$$

as well as the completeness equation

$$\mathrm{Log}(z_U) - \mathrm{Log}(z_V) = 0$$

coming from the meridian curve m_{X_n}.

These conditions are equivalent to the following system $\mathcal{E}_{X_n}^{co}(\widetilde{\mathbf{z}})$ of equations on $\widetilde{\mathbf{z}}$:

- $\mathcal{E}_{X_n,0}(\widetilde{\mathbf{z}})$: $\mathrm{Log}(z_1') + 2\mathrm{Log}(z_1) + \cdots + 2\mathrm{Log}(z_p) + 2\mathrm{Log}(z_U) = 2i\pi$
- $\mathcal{E}_{X_n,1}(\widetilde{\mathbf{z}})$: $2\mathrm{Log}(z_1'') + \mathrm{Log}(z_2') = 2i\pi$
- $\mathcal{E}_{X_n,k}(\widetilde{\mathbf{z}})$: $\mathrm{Log}(z_{k-1}') + 2\mathrm{Log}(z_k'') + \mathrm{Log}(z_{k+1}') = 2i\pi$ (for $2 \leqslant k \leqslant p-1$)
- $\mathcal{E}_{X_n,p+1}^{co}(\widetilde{\mathbf{z}})$: $\mathrm{Log}(z_p') + 2\mathrm{Log}(z_U'') - \mathrm{Log}(z_W) = 0$
- $\mathcal{E}_{X_n,s}^{co}(\widetilde{\mathbf{z}})$: $\mathrm{Log}(z_W'') - \mathrm{Log}(z_U) = 0$
- $z_V = z_U$.

Indeed, notice that the equation $\omega_p^{\mathbb{C}}(\widetilde{\mathbf{z}}) = 2i\pi$ was redundant with the other complex balancing equation. Remark furthermore that the variable z_V only appears in the equation $z_V = z_U$, which is why we will allow a slight abuse of notation to use the equations

$$\mathcal{E}_{X_n,0}(\mathbf{z}), \ldots, \mathcal{E}_{X_n,p-1}(\mathbf{z}), \mathcal{E}_{X_n,p+1}^{co}(\mathbf{z}), \mathcal{E}_{X_n,s}^{co}(\mathbf{z})$$

also for a variable $\mathbf{z} = (z_1, \ldots, z_p, z_U, z_W) \in (\mathbb{R} + i\mathbb{R}_{>0})^{p+2}$ without the coordinate z_V (see Lemma 4.25).

4.4 Partition function for the ideal triangulations (odd case)

In this section, n will be an odd integer greater than or equal to 3, and $p := \frac{n-3}{2}$. We will compute the partition functions of the Teichmüller TQFT for the ideal triangulations X_n of the twist knot complements $S^3 \setminus K_n$ constructed in Section 4.2 and we will prove that they can be expressed in a simple way using an one-variable function independent of the angle structure, as well as only two linear combinations of angles, which are two independant angular holonomies in the cusp link triangulation.

This results in a slightly different version of the first statement in the Andersen–Kashaev volume conjecture of [AK14c, Conjecture 1 (1)]. Note that our partition functions are computed only for the specific ideal triangulations X_n. In order to generalize Theorem 4.13 to any ideal triangulation of a twist knot complement, one would need further properties of invariance under change of triangulation (more general than the ones discussed in [AK14c]). A version for the even case is proved in Section 4.7.3 (see Theorem 4.45).

Theorem 4.13. *Let $n \geqslant 3$ be an odd integer and $p = \frac{n-3}{2}$. Consider the ideal triangulation X_n of $S^3 \setminus K_n$ described in Figure 4.13. Then for all angle structures $\alpha = (a_1, \dots, c_W) \in \mathcal{A}_{X_n}$ and all $\hbar > 0$, we have:*

$$\mathcal{Z}_\hbar(X_n, \alpha) \overset{\star}{=} \int_{\mathbb{R}+i\frac{\mu_{X_n}(\alpha)}{2\pi\sqrt{\hbar}}} J_{X_n}(\hbar, x) e^{\frac{1}{2\sqrt{\hbar}} x \lambda_{X_n}(\alpha)} dx,$$

with

- *the degree one angle polynomial $\mu_{X_n} \colon \alpha \mapsto a_U - a_V$,*
- *the degree one angle polynomial $\lambda_{X_n} \colon \alpha \mapsto 2(a_U - a_V + c_V - b_W)$,*
- *the map $(\hbar, x) \mapsto$*

$$J_{X_n}(\hbar, x) := \int_{\mathcal{Y}'} d\mathbf{y}' \, e^{2i\pi(\mathbf{y}'^T Q_n \mathbf{y}' + x(x - y'_U - y'_W))} e^{\frac{1}{\sqrt{\hbar}}(\mathbf{y}'^T \mathcal{W}_n - \pi x)} \frac{\Phi_{\mathsf{b}}(y'_U)\, \Phi_{\mathsf{b}}(y'_U + x)\, \Phi_{\mathsf{b}}(y'_W)}{\Phi_{\mathsf{b}}(y'_1) \cdots \Phi_{\mathsf{b}}(y'_p)},$$

where $\mathcal{Y}' := \prod_{k=1}^{p} \left(\mathbb{R} - \frac{i}{2\pi\sqrt{\hbar}}(\pi - a_k)\right) \times \prod_{l=U,W} \left(\mathbb{R} + \frac{i}{2\pi\sqrt{\hbar}}(\pi - a_l)\right)$,

$$\mathbf{y}' := \begin{bmatrix} y'_1 \\ \vdots \\ y'_p \\ y'_U \\ y'_W \end{bmatrix}, \quad \mathcal{W}_n := \begin{bmatrix} -2p\pi \\ \vdots \\ -2\pi\left(kp - \frac{k(k-1)}{2}\right) \\ \vdots \\ -p(p+1)\pi \\ (p^2+p+1)\pi \\ \pi \end{bmatrix} \quad \text{and} \quad Q_n := \begin{bmatrix} 1 & 1 & \cdots & 1 & -1 & 0 \\ 1 & 2 & \cdots & 2 & -2 & 0 \\ \vdots & \vdots & \ddots & \vdots & \vdots & \vdots \\ 1 & 2 & \cdots & p & -p & 0 \\ -1 & -2 & \cdots & -p & p & \frac{1}{2} \\ 0 & 0 & \cdots & 0 & \frac{1}{2} & 0 \end{bmatrix}.$$

The reader may notice that indices corresponding to V are missing in the integration variables. This comes from the change of variables $x = y'_V - y'_U$, which makes x replace the variable y'_V. Simply speaking, we chose to make V disappear rather than U, because V appeared a lot less than U in the defining gluing equations (see end of Section 4.3).

Remark 4.14. Note that, if you fix $\hbar > 0$ and $x \in \mathbb{R}+i\left(-\frac{1}{2\sqrt{\hbar}}, \frac{1}{2\sqrt{\hbar}}\right)$, the integration contour $\mathcal{Y}'$ in the definition of $J_{X_n}(\hbar, x)$ depends a priori on the angle structure α. However, since the integrand in $J_{X_n}(\hbar, x)$ is a holomorphic function of the variables in $\mathbf{y}'$ on a neighborhood of $\mathcal{Y}'$ in $\mathbb{C}^{p+2}$, it follows from the Bochner–Martinelli formula (that generalizes the Cauchy theorem, see [Kra01]) and the fast decay properties of this integrand at infinity that $\mathcal{Y}'$ could be replaced with a different contour. In this sense, $J_{X_n}(\hbar, x)$ is independent of the angle structure α. Nevertheless, picking the particular contour $\mathcal{Y}' = \mathcal{Y}'(\hbar, \alpha)$ with the complete structure $\alpha = \alpha^0$ will help us prove the volume conjecture in Section 4.6.

Remark 4.15. The quantities $\mu_{X_n}(\alpha)$ and $\lambda_{X_n}(\alpha)$ in Theorem 4.13 satisfy the following relations with the angular holonomies corresponding to the meridian and longitude curves $m_{X_n}(\alpha), l_{X_n}(\alpha)$ from Section 4.3.2:

$$\mu_{X_n}(\alpha) = m_{X_n}(\alpha) \quad \text{and} \quad \lambda_{X_n}(\alpha) = l_{X_n}(\alpha) + 2m_{X_n}(\alpha).$$

Hence, $\lambda_{X_n}(\alpha)$ is the angular holonomy of a curve on $\partial\nu(K_n)$ that is equal in homology to the curve (i) $\cup\cdots\cup$ (vi) (of Figures 4.14 and 4.15), thus $\lambda_{X_n}(\alpha)$ comes from a preferred longitude of the knot, as expected in Conjecture 3.68 (1). Similarly, $\mu_{X_n}(\alpha)$ is associated to a meridian of the knot.

We will need two lemmas to prove Theorem 4.13.

Lemma 4.16. *Let $n \geqslant 3$ be an odd integer and $p = \frac{n-3}{2}$. For the ideal triangulation X_n of $S^3 \setminus K_n$ described in Figure 4.13, the kinematical kernel is $\mathcal{K}_{X_n}\left(\widetilde{\mathbf{t}}\right) = \exp\left(2i\pi\widetilde{\mathbf{t}}^T\widetilde{Q}_n\widetilde{\mathbf{t}}\right)$, where $\widetilde{\mathbf{t}} := (t_1, \ldots, t_p, t_U, t_V, t_W)^T \in \mathbb{R}^{X_n^3}$ and $\widetilde{Q}_n$ is the following symmetric matrix with half-integer coefficients:*

$$\widetilde{Q}_n = \begin{array}{c|ccccc|ccc} & t_1 & t_2 & \cdots & t_{p-1} & t_p & t_U & t_V & t_W \\ \hline t_1 & 1 & 1 & \cdots & 1 & 1 & -1 & 0 & 0 \\ t_2 & 1 & 2 & \cdots & 2 & 2 & -2 & 0 & 0 \\ \vdots & \vdots & \vdots & \ddots & \vdots & \vdots & \vdots & \vdots & \vdots \\ t_{p-1} & 1 & 2 & \cdots & p-1 & p-1 & -(p-1) & 0 & 0 \\ t_p & 1 & 2 & \cdots & p-1 & p & -p & 0 & 0 \\ \hline t_U & -1 & -2 & \cdots & -(p-1) & -p & p+2 & -3/2 & 1 \\ t_V & 0 & 0 & \cdots & 0 & 0 & -3/2 & 1 & -1/2 \\ t_W & 0 & 0 & \cdots & 0 & 0 & 1 & -1/2 & 0 \end{array}.$$

Proof. Let $n \geqslant 3$ be an odd integer and $p = \frac{n-3}{2}$. We will denote

$$\widetilde{\mathbf{t}} := (\mathtt{t}(T_1), \ldots, \mathtt{t}(W))^T = (t_1, \ldots, t_p, t_U, t_V, t_W)^T \in \mathbb{R}^{X_n^3}$$

a vector whose coordinates are associated to the tetrahedra (t_j for T_j). The generic vector in $\mathbb{R}^{X_n^2}$ corresponding to the face variables will be denoted

$$\mathbf{x} := (e_1, \ldots, e_p, e_{p+1}, f_1, \ldots, f_p, v, r, s, g, u)^T \in \mathbb{R}^{X_n^2}.$$

By definition, the kinematical kernel is:

$$\mathcal{K}_{X_n}\left(\widetilde{\mathbf{t}}\right) = \int_{\mathbf{x}\in\mathbb{R}^{X_n^2}} d\mathbf{x} \prod_{T\in X_n^3} e^{2i\pi\varepsilon(T)x_0(T)\mathtt{t}(T)}\delta(x_0(T)-x_1(T)+x_2(T))\delta(x_2(T)-x_3(T)+\mathtt{t}(T)).$$

Following Lemma 3.58, we compute from Figure 4.13 that:

$$\mathcal{K}_{X_n}\left(\widetilde{\mathbf{t}}\right) = \int_{\mathbf{x}\in\mathbb{R}^{X_n^2}} d\mathbf{x} \int_{\mathbf{w}\in\mathbb{R}^{2(p+3)}} d\mathbf{w}\, e^{2i\pi\widetilde{\mathbf{t}}^T R\mathbf{x}} e^{-2i\pi\mathbf{w}^T A\mathbf{x}} e^{-2i\pi\mathbf{w}^T B\widetilde{\mathbf{t}}},$$

where $\mathbf{w} := (w_1, \ldots, w_W, w'_1, \ldots, w'_W)^T \in \mathbb{R}^{2(p+3)}$ and the matrices R, A, B are given by:

$$R := \begin{array}{c} \\ t_1 \\ \vdots \\ t_p \\ \hline t_U \\ t_V \\ t_W \end{array} \left[\begin{array}{ccccc|ccc|ccccc} e_1 & \ldots & e_p & e_{p+1} & & f_1 & \ldots & f_p & v & r & s & g & u \\ \hline 1 & & & 0 & & & & & & & & & \\ & \ddots & & & & 0 & & & & & 0 & & \\ 0 & & 1 & & & & & & & & & & \\ \hline & & & & & & & & 0 & -1 & 0 & 0 & 0 \\ & 0 & & & & 0 & & & 0 & 0 & 0 & -1 & 0 \\ & & & & & & & & 0 & 0 & 0 & 0 & -1 \end{array}\right],$$

$$A := \begin{array}{c} \\ w_1 \\ \vdots \\ \vdots \\ w_p \\ \hline w_U \\ w_V \\ w_W \\ \hline w'_1 \\ \vdots \\ \vdots \\ w'_p \\ \hline w'_U \\ w'_V \\ w'_W \end{array} \left[\begin{array}{ccccc|ccccc|ccccc} e_1 & e_2 & \ldots & e_p & e_{p+1} & f_1 & f_2 & \ldots & f_p & v & r & s & g & u \\ \hline 1 & -1 & & & & 1 & & & & & & & & \\ & \ddots & \ddots & & 0 & & \ddots & & 0 & & & & & \\ & 0 & \ddots & \ddots & & & 0 & \ddots & & & & 0 & & \\ & & & 1 & -1 & & & & 1 & & & & & \\ \hline & & & & & & & & 0 & -1 & 1 & 1 & 0 & 0 \\ & & 0 & & & & & & 1 & 0 & 0 & -1 & 1 & 0 \\ & & & & & & & & 0 & 1 & -1 & 0 & 0 & 1 \\ \hline -1 & & & & & 1 & & & & & & & & \\ & & & & & -1 & \ddots & & 0 & & & & & \\ & & & & & & \ddots & \ddots & & & & 0 & & \\ & & & & & 0 & & -1 & 1 & & & & & \\ \hline & & & & & & & & 0 & 0 & 0 & 1 & -1 & 0 \\ & & & & & & & & 1 & 0 & 0 & 0 & 0 & -1 \\ & & & & -1 & & & & 0 & 1 & 0 & 0 & 0 & 0 \end{array}\right],$$

$$B := \begin{array}{c} \\ w_1 \\ \vdots \\ w_p \\ \hline w_U \\ w_V \\ w_W \\ \hline w'_1 \\ \vdots \\ w'_p \\ \hline w'_U \\ w'_V \\ w'_W \end{array} \left[\begin{array}{ccc|ccc} t_1 & \ldots & t_p & t_U & t_V & t_W \\ \hline & & & & & \\ & & & & & \\ & & & & & \\ & & 0 & & & \\ & & & & & \\ & & & & & \\ \hline 1 & & & & & \\ & \ddots & & & 0 & \\ & & & \ddots & & \\ & & & & & \\ 0 & & & & \ddots & \\ & & & & & 1 \end{array}\right].$$

Careful computation yields that $\det(A) = 1$ and that the inverse A^{-1} is equal to

$$\begin{array}{c|ccccc|ccc|ccccc|ccc}
 & w_1 & w_2 & \dots & w_{p-1} & w_p & w_U & w_V & w_W & w'_1 & w'_2 & \dots & w'_{p-1} & w'_p & w'_U & w'_V & w'_W \\
\hline
e_1 & 0 & & \cdots & & 0 & 0 & 1 & 0 & -1 & -1 & & \cdots & -1 & 1 & 0 & 0 \\
e_2 & -1 & 0 & & & & 0 & 2 & 0 & -1 & -2 & & \cdots & -2 & 2 & 0 & 0 \\
\vdots & -1 & -1 & \ddots & & \vdots & & & & & & \ddots & & \vdots & & & \\
 & \vdots & & \ddots & 0 & 0 & \vdots & \vdots & \vdots & \vdots & \vdots & & 1-p & 1-p & \vdots & \vdots & \vdots \\
e_p & & & & -1 & 0 & & & & & & & 1-p & -p & & & \\
e_{p+1} & -1 & & \cdots & & -1 & 0 & p+1 & 0 & -1 & -2 & \cdots & 1-p & -p & p+1 & 0 & 0 \\
\hline
f_1 & & & & & & 0 & 1 & 0 & 0 & -1 & & \cdots & -1 & 1 & 0 & 0 \\
f_2 & & & & & & & 1 & & 0 & 0 & \ddots & & \vdots & 1 & & \\
\vdots & & & 0 & & & \vdots & \vdots & \vdots & \vdots & & \ddots & -1 & -1 & \vdots & \vdots & \vdots \\
f_{p-1} & & & & & & & & & 0 & & & 0 & -1 & & & \\
f_p & & & & & & 0 & 1 & 0 & 0 & & \cdots & & 0 & 1 & 0 & 0 \\
\hline
v & -1 & & \cdots & & -1 & 0 & p+1 & 0 & -1 & -2 & & \cdots & -p & p+1 & 0 & 1 \\
r & -1 & & \cdots & & -1 & 0 & p+2 & -1 & -1 & -2 & & \cdots & -p & p+2 & -1 & 1 \\
s & & & & & & 1 & -1 & 1 & & & & & & -1 & 1 & 0 \\
g & & & 0 & & & 1 & -1 & 1 & & & 0 & & & -2 & 1 & 0 \\
u & & & & & & 0 & 1 & 0 & & & & & & 1 & -1 & 0
\end{array}.$$

Hence, following Lemma 3.58, we have

$$\mathcal{K}_{X_n}\left(\widetilde{\mathbf{t}}\right) = \frac{1}{|\det(A)|} e^{2i\pi\widetilde{\mathbf{t}}^T(-RA^{-1}B)\widetilde{\mathbf{t}}} = e^{2i\pi\widetilde{\mathbf{t}}^T(-RA^{-1}B)\widetilde{\mathbf{t}}}.$$

The lemma finally follows from the identity $2\widetilde{Q}_n = (-RA^{-1}B) + (-RA^{-1}B)^T$, where $\widetilde{Q}_n$ is defined in the statement of the lemma. □

The following lemma relates the symmetric matrix $\widetilde{Q}_n$ to the gluing equations.

Lemma 4.17. *Let $n \geqslant 3$ be an odd integer and $p = \frac{n-3}{2}$. Let $\alpha = (a_1, b_1, c_1, \dots, a_W, b_W, c_W) \in \mathcal{S}_{X_n}$ denote a shape structure. If we denote $\widetilde{Q}_n$ the symmetric matrix from Lemma 4.16, $\widetilde{C}(\alpha) := (c_1, \dots, c_W)^T$, and $\widetilde{\Gamma}(\alpha) := (a_1 - \pi, \dots, a_p - \pi, \pi - a_U, \pi - a_V, \pi - a_W)^T$, then (indexing entries by $k \in \{1, \dots, p\}$ and U, V, W) we have the vector equality $2\widetilde{Q}_n\widetilde{\Gamma}(\alpha) + \widetilde{C}(\alpha) =$*

$$\begin{array}{c} k=1 \\ \vdots \\ k=p \end{array} \left(\begin{array}{c} \vdots \\ k(\omega_s(\alpha) - 2(p+2)\pi) + \sum_{j=1}^{k} j\omega_{k-j}(\alpha) \\ \vdots \\ \omega_{p+1}(\alpha) - \omega_s(\alpha) - \left(p(\omega_s(\alpha) - 2(p+2)\pi) + \sum_{j=1}^{p} j\omega_{p-j}(\alpha)\right) + 2\pi - \frac{1}{2}\lambda_{X_n}(\alpha) \\ \frac{1}{2}\lambda_{X_n}(\alpha) + \omega_s(\alpha) - 3\pi \\ 3\pi - \omega_s(\alpha) \end{array} \right),$$

where $\lambda_{X_n}(\alpha) := 2(a_U - a_V + c_V - b_W)$.

In particular, for $\alpha \in \mathcal{A}_{X_n}$ an angle structure, the vector of angles

$$2\widetilde{Q}_n\widetilde{\Gamma}(\alpha) + \widetilde{C}(\alpha) = \begin{matrix} k=1 \\ \vdots \\ k=p \\ \\ \\ \\ \end{matrix} \begin{pmatrix} \vdots \\ -2\pi\left(kp - \dfrac{k(k-1)}{2}\right) \\ \vdots \\ (p^2+p+2)\pi - \frac{1}{2}\lambda_{X_n}(\alpha) \\ \frac{1}{2}\lambda_{X_n}(\alpha) - \pi \\ \pi \end{pmatrix}$$

only depends on the linear combination $\lambda_{X_n}(\alpha)$.

Proof. The lemma follows from direct computations. □

We can now proceed with the proof of Theorem 4.13.

Proof of Theorem 4.13. Let $n \geqslant 3$ be an odd integer and $p := \frac{n-3}{2}$. We want to compute the partition function associated to X_n and prove that it is of the desired form. We know the form of the kinematical kernel from Lemma 4.16. Let us now compute the dynamical content. Let $\alpha = (a_1, b_1, c_1, \ldots, a_W, b_W, c_W) \in \mathcal{A}_{X_n}$, $\hbar > 0$ and $\widetilde{\mathbf{t}} := (t_1, \ldots, t_p, t_U, t_V, t_W)^T \in \mathbb{R}^{X_n^3}$.

By definition, the dynamical content $\mathcal{D}_{\hbar,X_n}\left(\widetilde{\mathbf{t}}, \alpha\right)$ is equal to:

$$e^{\frac{1}{\sqrt{\hbar}}\widetilde{C}(\alpha)^T\widetilde{\mathbf{t}}} \frac{\Phi_{\mathsf{b}}\left(t_U + \frac{i}{2\pi\sqrt{\hbar}}(\pi - a_U)\right)\Phi_{\mathsf{b}}\left(t_V + \frac{i}{2\pi\sqrt{\hbar}}(\pi - a_V)\right)\Phi_{\mathsf{b}}\left(t_W + \frac{i}{2\pi\sqrt{\hbar}}(\pi - a_W)\right)}{\Phi_{\mathsf{b}}\left(t_1 - \frac{i}{2\pi\sqrt{\hbar}}(\pi - a_1)\right)\cdots\Phi_{\mathsf{b}}\left(t_p - \frac{i}{2\pi\sqrt{\hbar}}(\pi - a_p)\right)},$$

where $\widetilde{C}(\alpha) := (c_1, \ldots, c_p, c_U, c_V, c_W)^T$ as in the statement of Lemma 4.17.

Now we can compute the partition function of the Teichmüller TQFT. By Theorem 3.61, we have:

$$\mathcal{Z}_\hbar(X_n, \alpha) = \int_{\widetilde{\mathbf{t}} \in \mathbb{R}^{X_n^3}} d\widetilde{\mathbf{t}}\, \mathcal{K}_{X_n}\left(\widetilde{\mathbf{t}}\right) \mathcal{D}_{\hbar,X_n}\left(\widetilde{\mathbf{t}}, \alpha\right).$$

We do the following change of variables:

- $y'_k = t_k - \frac{i}{2\pi\sqrt{\hbar}}(\pi - a_k)$ for $1 \leqslant k \leqslant p$,
- $y'_l = t_l + \frac{i}{2\pi\sqrt{\hbar}}(\pi - a_l)$ for $l \in \{U, V, W\}$,

and we denote $\widetilde{\mathbf{y}}' := \left(y'_1, \ldots, y'_p, y'_U, y'_V, y'_W\right)^T$. We also denote

$$\widetilde{\mathcal{Y}}'_{\hbar,\alpha} := \prod_{k=1}^{p}\left(\mathbb{R} - \frac{i}{2\pi\sqrt{\hbar}}(\pi - a_k)\right) \times \prod_{l=U,V,W}\left(\mathbb{R} + \frac{i}{2\pi\sqrt{\hbar}}(\pi - a_l)\right),$$

the subset of $\mathbb{C}^{p+3}$ on which the variables in $\widetilde{\mathbf{y}}'$ will reside. Finally we denote:

$$\widetilde{\Gamma}(\alpha) := \frac{2\pi\sqrt{\hbar}}{i}(\widetilde{\mathbf{y}}' - \widetilde{\mathbf{t}}) = (a_1 - \pi, \dots, a_p - \pi, \pi - a_U, \pi - a_V, \pi - a_W)^T.$$

as in the statement of Lemma 4.17. We can now compute:

$$\begin{aligned}
\mathcal{Z}_\hbar(X_n, \alpha) &= \int_{\widetilde{\mathbf{t}} \in \mathbb{R}^{X_n^3}} d\widetilde{\mathbf{t}}\, \mathcal{K}_{X_n}\left(\widetilde{\mathbf{t}}\right) \mathcal{D}_{\hbar, X_n}\left(\widetilde{\mathbf{t}}, \alpha\right) \\
&= \int_{\widetilde{\mathbf{y}}' \in \widetilde{\mathcal{Y}}'_{\hbar,\alpha}} d\widetilde{\mathbf{y}}'\, \mathcal{K}_{X_n}\left(\widetilde{\mathbf{y}}' - \frac{i}{2\pi\sqrt{\hbar}}\widetilde{\Gamma}(\alpha)\right) \mathcal{D}_{\hbar, X_n}\left(\widetilde{\mathbf{y}}' - \frac{i}{2\pi\sqrt{\hbar}}\widetilde{\Gamma}(\alpha), \alpha\right) \\
&= \int_{\widetilde{\mathbf{y}}' \in \widetilde{\mathcal{Y}}'_{\hbar,\alpha}} d\widetilde{\mathbf{y}}'\, e^{2i\pi\widetilde{\mathbf{y}}'^T\widetilde{Q}_n\widetilde{\mathbf{y}}' + \frac{2}{\sqrt{\hbar}}\widetilde{\Gamma}(\alpha)^T\widetilde{Q}_n\widetilde{\mathbf{y}}' - \frac{i}{2\pi\hbar}\widetilde{\Gamma}(\alpha)^T\widetilde{Q}_n\widetilde{\Gamma}(\alpha) + \frac{1}{\sqrt{\hbar}}\widetilde{C}(\alpha)^T\widetilde{\mathbf{y}}' - \frac{i}{2\pi\hbar}\widetilde{C}(\alpha)^T\widetilde{\Gamma}(\alpha)} \frac{\Phi_{\mathsf{b}}\left(y'_U\right)\Phi_{\mathsf{b}}\left(y'_V\right)\Phi_{\mathsf{b}}\left(y'_W\right)}{\Phi_{\mathsf{b}}\left(y'_1\right)\cdots\Phi_{\mathsf{b}}\left(y'_p\right)} \\
&\overset{\star}{=} \int_{\widetilde{\mathbf{y}}' \in \widetilde{\mathcal{Y}}'_{\hbar,\alpha}} d\widetilde{\mathbf{y}}'\, e^{2i\pi\widetilde{\mathbf{y}}'^T\widetilde{Q}_n\widetilde{\mathbf{y}}' + \frac{2}{\sqrt{\hbar}}\widetilde{\Gamma}(\alpha)^T\widetilde{Q}_n\widetilde{\mathbf{y}}' + \frac{1}{\sqrt{\hbar}}\widetilde{C}(\alpha)^T\widetilde{\mathbf{y}}'} \frac{\Phi_{\mathsf{b}}\left(y'_U\right)\Phi_{\mathsf{b}}\left(y'_V\right)\Phi_{\mathsf{b}}\left(y'_W\right)}{\Phi_{\mathsf{b}}\left(y'_1\right)\cdots\Phi_{\mathsf{b}}\left(y'_p\right)} \\
&= \int_{\widetilde{\mathbf{y}}' \in \widetilde{\mathcal{Y}}'_{\hbar,\alpha}} d\widetilde{\mathbf{y}}'\, e^{2i\pi\widetilde{\mathbf{y}}'^T\widetilde{Q}_n\widetilde{\mathbf{y}}' + \frac{1}{\sqrt{\hbar}}\widetilde{\mathcal{W}}(\alpha)^T\widetilde{\mathbf{y}}'} \frac{\Phi_{\mathsf{b}}\left(y'_U\right)\Phi_{\mathsf{b}}\left(y'_V\right)\Phi_{\mathsf{b}}\left(y'_W\right)}{\Phi_{\mathsf{b}}\left(y'_1\right)\cdots\Phi_{\mathsf{b}}\left(y'_p\right)},
\end{aligned}$$

where $\widetilde{\mathcal{W}}(\alpha) := 2\widetilde{Q}_n\widetilde{\Gamma}(\alpha) + \widetilde{C}(\alpha)$. Now, from Lemma 4.17, we have

$$\widetilde{\mathcal{W}}(\alpha) = \begin{pmatrix} -2p\pi \\ \vdots \\ -2\pi\left(kp - \dfrac{k(k-1)}{2}\right) \\ \vdots \\ -p(p+1)\pi \\ (p^2+p+2)\pi - \frac{1}{2}\lambda_{X_n}(\alpha) \\ \frac{1}{2}\lambda_{X_n}(\alpha) - \pi \\ \pi \end{pmatrix}.$$

We define a new variable $x := y'_V - y'_U$ living in the set

$$\mathcal{Y}'^0_{\hbar,\alpha} := \mathbb{R} + \frac{i}{2\pi\sqrt{\hbar}}(a_U - a_V),$$

and we also define $\mathbf{y}'$ (respectively $\mathcal{Y}'_{\hbar,\alpha}$) exactly like $\widetilde{\mathbf{y}}'$ (respectively $\widetilde{\mathcal{Y}}'_{\hbar,\alpha}$) but with the second-to-last coordinate (corresponding to the tetrahedron V) taken out. We finally define

$$\mathcal{W}_n = \begin{bmatrix} \mathcal{W}_{n,1} \\ \vdots \\ \mathcal{W}_{n,k} \\ \vdots \\ \mathcal{W}_{n,p} \\ \mathcal{W}_{n,U} \\ \mathcal{W}_{n,W} \end{bmatrix} := \begin{bmatrix} -2p\pi \\ \vdots \\ -2\pi\left(kp - \frac{k(k-1)}{2}\right) \\ \vdots \\ -p(p+1)\pi \\ (p^2+p+1)\pi \\ \pi \end{bmatrix} \qquad \text{and} \qquad Q_n := \begin{bmatrix} 1 & 1 & \cdots & 1 & -1 & 0 \\ 1 & 2 & \cdots & 2 & -2 & 0 \\ \vdots & \vdots & \ddots & \vdots & \vdots & \vdots \\ 1 & 2 & \cdots & p & -p & 0 \\ -1 & -2 & \cdots & -p & p & \frac{1}{2} \\ 0 & 0 & \cdots & 0 & \frac{1}{2} & 0 \end{bmatrix}. \tag{4.18}$$

Notice that Q_n is obtained from $\widetilde{Q}_n$ by the following operations:

- add the V-row to the U-row,
- add the V-column to the U-column,
- delete the V-row and the V-column,

and $\mathcal{W}_n$ is obtained from $\widetilde{\mathcal{W}}(\alpha)$ by the same operations on rows.

We can now use the substitution $y'_V = y'_U + x$ to compute:

$$\begin{aligned} 2i\pi\widetilde{\mathbf{y}}'^T\widetilde{Q}_n\widetilde{\mathbf{y}}' &= 2i\pi\left((\mathbf{y}'^T Q_n\mathbf{y}' - p{y'_U}^2 - y'_U y'_W) + (p+2){y'_U}^2 - 3y'_U y'_V + 2y'_U y'_W + {y'_V}^2 - y'_V y'_W\right) \\ &= 2i\pi\left(\mathbf{y}'^T Q_n\mathbf{y}' - xy'_U - xy'_W + x^2\right), \end{aligned}$$

and $\frac{1}{\sqrt{\hbar}}\widetilde{\mathcal{W}}(\alpha)^T\widetilde{\mathbf{y}}' = \frac{1}{\sqrt{\hbar}}\left(\mathcal{W}_n^T\mathbf{y}' + x(\frac{1}{2}\lambda_{X_n}(\alpha) - \pi)\right)$, thus

$$\begin{aligned} \mathcal{Z}_\hbar(X_n,\alpha) &\overset{\star}{=} \int_{\widetilde{\mathbf{y}}'\in\widetilde{\mathcal{Y}}'_{\hbar,\alpha}} d\widetilde{\mathbf{y}}'\, e^{2i\pi\widetilde{\mathbf{y}}'^T\widetilde{Q}_n\widetilde{\mathbf{y}}' + \frac{1}{\sqrt{\hbar}}\widetilde{\mathcal{W}}(\alpha)^T\widetilde{\mathbf{y}}'} \frac{\Phi_{\mathsf{b}}(y'_U)\,\Phi_{\mathsf{b}}(y'_V)\,\Phi_{\mathsf{b}}(y'_W)}{\Phi_{\mathsf{b}}(y'_1)\cdots\Phi_{\mathsf{b}}(y'_p)} \\ &\overset{\star}{=} \int dx d\mathbf{y}'\, e^{2i\pi\left(\mathbf{y}'^T Q_n\mathbf{y}' + x(x-y'_U-y'_W)\right) + \frac{1}{\sqrt{\hbar}}\left(\mathcal{W}_n^T\mathbf{y}' + x(\frac{1}{2}\lambda_{X_n}(\alpha)-\pi)\right)} \frac{\Phi_{\mathsf{b}}(y'_U)\,\Phi_{\mathsf{b}}(y'_U+x)\,\Phi_{\mathsf{b}}(y'_W)}{\Phi_{\mathsf{b}}(y'_1)\cdots\Phi_{\mathsf{b}}(y'_p)}, \end{aligned}$$

where the variables $(\mathbf{y}', x)$ in the last integral lie in $\mathcal{Y}'_{\hbar,\alpha}\times\mathcal{Y}'^0_{\hbar,\alpha}$.

Finally we obtain that

$$\mathcal{Z}_\hbar(X_n,\alpha) \overset{\star}{=} \int_{x\in\mathbb{R}+\frac{i}{2\pi\sqrt{\hbar}}\mu_{X_n}(\alpha)} J_{X_n}(\hbar,x) e^{\frac{1}{2\sqrt{\hbar}}x\lambda_{X_n}(\alpha)}\, dx,$$

where

$$J_{X_n}(\hbar,x) := \int_{\mathcal{Y}'} d\mathbf{y}'\, e^{2i\pi\left(\mathbf{y}'^T Q_n\mathbf{y}' + x(x-y'_U-y'_W)\right)} e^{\frac{1}{\sqrt{\hbar}}\left(\mathbf{y}'^T\mathcal{W}_n - \pi x\right)} \frac{\Phi_{\mathsf{b}}(y'_U)\,\Phi_{\mathsf{b}}(y'_U+x)\,\Phi_{\mathsf{b}}(y'_W)}{\Phi_{\mathsf{b}}(y'_1)\cdots\Phi_{\mathsf{b}}(y'_p)},$$

$\mathcal{Y}' := \mathcal{Y}'_{\hbar,\alpha}$, and $\mu_{X_n}(\alpha) := a_U - a_V$, which concludes the proof. □

We conclude this section with a slight rephrasing of Theorem 4.13, in the following Corollary 4.19. Although the expression in Theorem 4.13 was the closest to the statement of [AK14c, Conjecture 1 (1)], we find that the following reformulation has additional benefits: the integration multi-contour is now independent of $\hbar$ and the integrand is closer to the form $e^{\frac{1}{2\pi\hbar}S(\mathbf{y})}$ that we need in order to apply the saddle point method (see Theorem 1.77, where $\lambda\to\infty$ should be thought of as $2\pi\hbar\to 0^+$).

Corollary 4.19. *Let $n\geqslant 3$ be an odd integer and $p = \frac{n-3}{2}$. Consider the ideal triangulation X_n of $S^3\setminus K_n$ from Figure 4.13. Then for all angle structures $\alpha\in\mathcal{A}_{X_n}$ and all $\hbar>0$, we have:*

$$\mathcal{Z}_\hbar(X_n,\alpha) \overset{\star}{=} \int_{\mathbb{R}+i\mu_{X_n}(\alpha)} \mathfrak{J}_{X_n}(\hbar,\mathsf{x}) e^{\frac{1}{4\pi\hbar}\mathsf{x}\lambda_{X_n}(\alpha)}\, d\mathsf{x},$$

with the map

$$\mathfrak{J}_{X_n}\colon(\hbar,\mathsf{x})\mapsto\left(\frac{1}{2\pi\sqrt{\hbar}}\right)^{p+3}\int_{\mathcal{Y}_\alpha}d\mathbf{y}\,e^{\frac{i\mathbf{y}^TQ_n\mathbf{y}+i\mathsf{x}(\mathsf{x}-y_U-y_W)+\mathbf{y}^T\mathcal{W}_n-\pi\mathsf{x}}{2\pi\hbar}}\frac{\Phi_{\mathsf{b}}\left(\frac{y_U}{2\pi\sqrt{\hbar}}\right)\Phi_{\mathsf{b}}\left(\frac{y_U+\mathsf{x}}{2\pi\sqrt{\hbar}}\right)\Phi_{\mathsf{b}}\left(\frac{y_W}{2\pi\sqrt{\hbar}}\right)}{\Phi_{\mathsf{b}}\left(\frac{y_1}{2\pi\sqrt{\hbar}}\right)\cdots\Phi_{\mathsf{b}}\left(\frac{y_p}{2\pi\sqrt{\hbar}}\right)},$$

where $\mu_{X_n},\lambda_{X_n},\mathcal{W}_n,Q_n$ are the same as in Theorem 4.13, and

$$\mathcal{Y}_\alpha:=\prod_{k=1}^{p}(\mathbb{R}-i(\pi-a_k))\times\prod_{l=U,W}(\mathbb{R}+i(\pi-a_l))\,.$$

Proof. We start from the expressions in Theorem 4.13, and, with $\hbar>0$ fixed, we do the change of variables $y_j=(2\pi\sqrt{\hbar})y'_j$ for $j\in\{1,\dots,p,U,W\}$ and $\mathsf{x}=(2\pi\sqrt{\hbar})x$. □

4.5 Partition function for the H-triangulations (odd case)

Before stating Theorem 4.20, we compute the weights on each edge of the H-triangulation Y_n given in Figure 4.12 (for $n\geqslant 3$ odd).

Recall that we denoted $\overrightarrow{e_0},\dots,\overrightarrow{e_{p+1}},\overrightarrow{e_s},\overrightarrow{e_d},\overrightarrow{K_n}\in Y_n^1$ the $p+5$ edges in Y_n respectively represented in Figure 4.12 by arrows with circled 0, …, circled $p+1$, simple arrow, double arrow and blue simple arrow.

For $\alpha=(a_1,b_1,c_1,\dots,a_p,b_p,c_p,a_U,b_U,c_U,a_V,b_V,c_V,a_W,b_W,c_W,a_Z,b_Z,c_Z)\in\mathcal{S}_{Y_n}$ a shape structure on Y_n, the weights of each edge are given by:

- $\widehat{\omega}_s(\alpha):=\omega_{Y_n,\alpha}(\overrightarrow{e_s})=2a_U+b_V+c_V+a_W+b_W+a_Z$
- $\widehat{\omega}_d(\alpha):=\omega_{Y_n,\alpha}(\overrightarrow{e_d})=b_U+c_U+c_W+b_Z+c_Z$
- $\omega_0(\alpha):=\omega_{Y_n,\alpha}(\overrightarrow{e_0})=2a_1+c_1+2a_2+\dots+2a_p+a_V+c_W$
- $\omega_1(\alpha):=\omega_{Y_n,\alpha}(\overrightarrow{e_1})=2b_1+c_2$
- $\omega_k(\alpha):=\omega_{Y_n,\alpha}(\overrightarrow{e_k})=c_{k-1}+2b_k+c_{k+1}\quad(\text{for }2\leqslant k\leqslant p-1)$
- $\omega_p(\alpha):=\omega_{Y_n,\alpha}(\overrightarrow{e_p})=c_{p-1}+2b_p+b_U+b_V+a_W$
- $\widehat{\omega}_{p+1}(\alpha):=\omega_{Y_n,\alpha}(\overrightarrow{e_{p+1}})=c_p+c_U+a_V+c_V+b_W+b_Z+c_Z$
- $\widehat{\omega}_{\overrightarrow{K_n}}(\alpha):=\omega_{Y_n,\alpha}(\overrightarrow{K_n})=a_Z$.

Note that some of these weights have the same value as the ones for X_n listed in Section 4.3 (and are thus also denoted $\omega_j(\alpha)$), and some are specific to Y_n (and are written with a hat).

We can now compute the partition function of the Teichmüller TQFT for the H-triangulations Y_n, and prove the following theorem. We will denote $\mathcal{S}_{Y_n\setminus Z}$ the space of shape structures on every tetrahedron of Y_n except for Z.

Theorem 4.20. *Let $n \geqslant 3$ be an odd integer, $p = \frac{n-3}{2}$ and Y_n the one-vertex H-triangulation of the pair (S^3, K_n) from Figure 4.12. Then for every $\hbar > 0$ and for every $\tau \in \mathcal{S}_{Y_n \setminus Z} \times \overline{\mathcal{S}_Z}$ such that $\omega_{Y_n,\tau}$ vanishes on $\overrightarrow{K_n}$ and is equal to 2π on every other edge, one has*

$$\lim_{\substack{\alpha \to \tau \\ \alpha \in \mathcal{S}_{Y_n}}} \Phi_{\mathsf{b}} \left(\frac{\pi - \omega_{Y_n,\alpha}\left(\overrightarrow{K_n}\right)}{2\pi i \sqrt{\hbar}} \right) \mathcal{Z}_\hbar(Y_n, \alpha) \stackrel{\star}{=} J_{X_n}(\hbar, 0),$$

where J_{X_n} is defined in Theorem 4.13.

Before proving Theorem 4.20, let us mention a useful result: the fact that Φ_{b} is bounded on compact horizontal bands.

Lemma 4.21. *Let $\hbar > 0$ and $\delta \in (0, \pi/2)$. Then $M_{\delta,\hbar} := \max_{z \in \mathbb{R} + i[\delta, \pi - \delta]} |\Phi_{\mathsf{b}}(z)|$ is finite.*

Proof. Let $\hbar > 0$ and $\delta \in (0, \pi/2)$. By contradiction, let us assume that $M_{\delta,\hbar} = \infty$. Then there exists a sequence $(z_n)_{n \in \mathbb{N}} \in (\mathbb{R} + i[\delta, \pi - \delta])^{\mathbb{N}}$ such that $|\Phi_{\mathsf{b}}(z_n)| \underset{n \to \infty}{\to} \infty$.

If $(\Re(z_n))_{n \in \mathbb{N}}$ is bounded, then $(z_n)_{n \in \mathbb{N}}$ lives in a compact set, which contradicts the continuity of $|\Phi_{\mathsf{b}}|$.

If $(\Re(z_n))_{n \in \mathbb{N}}$ admits a subsequence going to $-\infty$ (resp. ∞), then the image of this subsequence by $|\Phi_{\mathsf{b}}|$ should still tend to ∞, which contradicts Theorem 3.36 (4). □

Proof of Theorem 4.20. Let $n \geqslant 3$ be an odd integer and $p = \frac{n-3}{2}$. The proof will consist in three steps: computing the partition function $\mathcal{Z}_\hbar(Y_n, \alpha)$, applying the dominated convergence theorem in $\alpha \to \tau$ and finally retrieving the value $J_{X_n}(\hbar, 0)$ in $\alpha = \tau$.

Step 1. Computing the partition function $\mathcal{Z}_\hbar(Y_n, \alpha)$.

Like in the proof of Theorem 4.13 we start by computing the kinematical kernel. We denote

$$\widehat{\mathbf{t}} := (t_1, \dots, t_{p-1}, t_p, t_U, t_V, t_W, t_Z) \in \mathbb{R}^{Y_n^3}$$

the vector whose coordinates are associated to the tetrahedra (t_j for T_j). The generic vector in $\mathbb{R}^{Y_n^2}$ which corresponds to the faces variables will be denoted

$$\widehat{\mathbf{x}} := (e_1, \dots, e_{p+1}, f_1, \dots, f_p, v, r, s, s', g, u, m) \in \mathbb{R}^{Y_n^2}.$$

By definition, the kinematical kernel is:

$$\mathcal{K}_{Y_n}\left(\widehat{\mathbf{t}}\right) = \int_{\widehat{\mathbf{x}} \in \mathbb{R}^{Y_n^2}} d\widehat{\mathbf{x}} \prod_{T \in Y_n^3} e^{2i\pi\varepsilon(T) x_0(T) \mathsf{t}(T)} \delta(x_0(T) - x_1(T) + x_2(T)) \delta(x_2(T) - x_3(T) + \mathsf{t}(T)).$$

Following Lemma 3.58, we compute from Figure 4.12 that:

$$\mathcal{K}_{Y_n}\left(\widehat{\mathbf{t}}\right) = \int_{\widehat{\mathbf{x}} \in \mathbb{R}^{Y_n^2}} d\widehat{\mathbf{x}} \int_{\widehat{\mathbf{w}} \in \mathbb{R}^{2(p+4)}} d\widehat{\mathbf{w}}\, e^{2i\pi \widehat{\mathbf{t}}^T \widehat{S} \widehat{\mathbf{x}}} e^{-2i\pi \widehat{\mathbf{w}}^T \widehat{H} \widehat{\mathbf{x}}} e^{-2i\pi \widehat{\mathbf{w}}^T \widehat{D} \widehat{\mathbf{t}}},$$

where the matrices $\widehat{S}, \widehat{H}, \widehat{D}$ are given by:

$$\widehat{S} := \begin{array}{c} \\ t_1 \\ \vdots \\ t_p \\ \hline t_U \\ t_V \\ t_W \\ t_Z \end{array} \begin{array}{c} \begin{array}{cccc|ccc|ccccccc} e_1 & \dots & e_p & e_{p+1} & f_1 & \dots & f_p & v & r & s & s' & g & u & m \end{array} \\ \left[\begin{array}{cccc|ccc|ccccccc} 1 & & & 0 & & & & & & & & & & \\ & \ddots & & & & 0 & & & & & 0 & & & \\ 0 & & 1 & & & & & & & & & & & \\ \hline & & 0 & & & & 0 & 0 & -1 & 0 & 0 & 0 & 0 & 0 \\ & & & & & & & 0 & 0 & 0 & 0 & -1 & 0 & 0 \\ & & & & & & & 0 & 0 & 0 & 0 & 0 & -1 & 0 \\ & & & & & & & 0 & 0 & 0 & 0 & 0 & 0 & 1 \end{array}\right] \end{array},$$

$$\widehat{H} := \begin{array}{c} \\ w_1 \\ \vdots \\ \vdots \\ w_p \\ \hline w_U \\ w_V \\ w_W \\ w_Z \\ \hline w'_1 \\ \vdots \\ \vdots \\ w'_p \\ \hline w'_U \\ w'_V \\ w'_W \\ w'_Z \end{array} \begin{array}{c} \begin{array}{ccccc|ccccc|ccccccc} e_1 & e_2 & \dots & e_p & e_{p+1} & f_1 & f_2 & \dots & f_p & v & r & s & s' & g & u & m \end{array} \\ \left[\begin{array}{ccccc|ccccc|ccccccc} 1 & -1 & & & & 1 & & & & & & & & & & \\ & \ddots & \ddots & & 0 & & \ddots & & 0 & & & & & & & \\ & 0 & \ddots & \ddots & & & 0 & & \ddots & & & & 0 & & & \\ & & & 1 & -1 & & & & 1 & & & & & & & \\ \hline & & & & & & & & & -1 & 1 & 1 & 0 & 0 & 0 & 0 \\ & & & & & & & & 1 & 0 & 0 & 0 & -1 & 1 & 0 & 0 \\ & & 0 & & & & & & & 1 & -1 & 0 & 0 & 0 & 1 & 0 \\ & & & & & & & & & 0 & 0 & 1 & 0 & 0 & 0 & 0 \\ \hline -1 & & & & & 1 & & & & & & & & & & \\ & & & & & -1 & \ddots & & 0 & & & & & & & \\ & & & & & & \ddots & \ddots & & & & & 0 & & & \\ & & & & & 0 & & -1 & 1 & & & & & & & \\ \hline & & & & & & & & & 0 & 0 & 1 & 0 & -1 & 0 & 0 \\ & & & & & & & & 1 & 0 & 0 & 0 & 0 & 0 & -1 & 0 \\ & & & & -1 & & & & & 1 & 0 & 0 & 0 & 0 & 0 & 0 \\ & & & & & & & & & 0 & 0 & 1 & -1 & 0 & 0 & 0 \end{array}\right] \end{array},$$

$$\widehat{D} := \begin{array}{c} \\ w_1 \\ \vdots \\ w_p \\ \hline w_U \\ w_V \\ w_W \\ w_Z \\ \hline w'_1 \\ \vdots \\ w'_p \\ \hline w'_U \\ w'_V \\ w'_W \\ w'_Z \end{array} \begin{array}{c} \begin{array}{ccc|cccc} t_1 & \dots & t_p & t_U & t_V & t_W & t_Z \end{array} \\ \left[\begin{array}{ccc|cccc} & & & & & & \\ & & & & & & \\ & & & & & & \\ \hline & & & 0 & & & \\ & & & & & & \\ & & & & & & \\ & & & & & & \\ \hline 1 & & & & & & \\ & \ddots & & & & 0 & \\ & & & & & & \\ \hline & & & \ddots & & & \\ & & & & & & \\ 0 & & & & & \ddots & \\ & & & & & & 1 \end{array}\right] \end{array}.$$

Let us define S the submatrix of $\widehat{S}$ without the m-column, H the submatrix of $\widehat{H}$ without the m-column and the w_V-row, R_V this very w_V-row of $\widehat{H}$, D the submatrix of $\widehat{D}$ without the w_V-row, $\mathbf{x}$ the subvector of $\widehat{\mathbf{x}}$ without the variable m and $\mathbf{w}$ the subvector of $\widehat{\mathbf{w}}$ without the variable w_V. Finally let us denote $f_{\widehat{\mathbf{t}},w_V}(\mathbf{x}) := e^{2i\pi(\widehat{\mathbf{t}}^T S - w_V R_V)\mathbf{x}}$. We remark that H is invertible (whereas $\widehat{H}$ was not) and $\det(H) = -1$. Hence, by using multi-dimensional Fourier transform and the integral definition of the Dirac delta function, we compute:

$$
\begin{aligned}
\mathcal{K}_{Y_n}\left(\widehat{\mathbf{t}}\right) &= \int_{\widehat{\mathbf{x}}\in\mathbb{R}^{Y_n^2}} d\widehat{\mathbf{x}} \int_{\widehat{\mathbf{w}}\in\mathbb{R}^{2(p+4)}} d\widehat{\mathbf{w}}\, e^{2i\pi\widehat{\mathbf{t}}^T\widehat{S}\widehat{\mathbf{x}}} e^{-2i\pi\widehat{\mathbf{w}}^T\widehat{H}\widehat{\mathbf{x}}} e^{-2i\pi\widehat{\mathbf{w}}^T\widehat{D}\widehat{\mathbf{t}}} \\
&= \int_{m\in\mathbb{R}} dm \int_{w_V\in\mathbb{R}} dw_V \int_{\mathbf{x}\in\mathbb{R}^{2p+7}} d\mathbf{x} \int_{\mathbf{w}\in\mathbb{R}^{2p+7}} d\mathbf{w}\, e^{2i\pi t_Z m} e^{-2i\pi w_V R_V\mathbf{x}} e^{2i\pi\widehat{\mathbf{t}}^T S\mathbf{x}} e^{-2i\pi\mathbf{w}^T H\mathbf{x}} e^{-2i\pi\mathbf{w}^T D\widehat{\mathbf{t}}} \\
&= \int_{m\in\mathbb{R}} dm\ e^{2i\pi t_Z m} \int_{w_V\in\mathbb{R}} dw_V \int_{\mathbf{w}\in\mathbb{R}^{2p+7}} d\mathbf{w}\, e^{-2i\pi\mathbf{w}^T D\widehat{\mathbf{t}}} \int_{\mathbf{x}\in\mathbb{R}^{2p+7}} d\mathbf{x}\, f_{\widehat{\mathbf{t}},w_V}(\mathbf{x}) e^{-2i\pi\mathbf{w}^T H\mathbf{x}} \\
&= \delta(-t_Z) \int_{w_V\in\mathbb{R}} dw_V \int_{\mathbf{w}\in\mathbb{R}^{2p+7}} d\mathbf{w}\, e^{-2i\pi\mathbf{w}^T D\widehat{\mathbf{t}}}\ \mathsf{F}^{-1}\left(f_{\widehat{\mathbf{t}},w_V}\right)(H^T\mathbf{w}) \\
&= \delta(-t_Z) \int_{w_V\in\mathbb{R}} dw_V\ \frac{1}{|\det(H)|} \mathsf{F}^{-1}\left(\mathsf{F}^{-1}\left(f_{\widehat{\mathbf{t}},w_V}\right)\right)\left(H^{-1}D\widehat{\mathbf{t}}\right) \\
&= \delta(-t_Z) \int_{w_V\in\mathbb{R}} dw_V\ f_{\widehat{\mathbf{t}},w_V}\left(-H^{-1}D\widehat{\mathbf{t}}\right) \\
&= \delta(-t_Z) \int_{w_V\in\mathbb{R}} dw_V\ e^{2i\pi\left(\widehat{\mathbf{t}}^T S - w_V R_V\right)\left(-H^{-1}D\widehat{\mathbf{t}}\right)} \\
&= \delta(-t_Z) e^{2i\pi\widehat{\mathbf{t}}^T(-SH^{-1}D)\widehat{\mathbf{t}}} \int_{w_V\in\mathbb{R}} dw_V\ e^{-2i\pi w_V\left(-R_V H^{-1}D\widehat{\mathbf{t}}\right)} \\
&= \delta(-t_Z) e^{2i\pi\widehat{\mathbf{t}}^T(-SH^{-1}D)\widehat{\mathbf{t}}} \delta\left(-R_V H^{-1}D\widehat{\mathbf{t}}\right).
\end{aligned}
$$

We can now compute $H^{-1} =$

	w_1	w_2	...	w_{p-1}	w_p	w_U	w_W	w_Z	w'_1	w'_2	...	w'_{p-1}	w'_p	w'_U	w'_V	w'_W	w'_Z
e_1	0		$\cdots$		0	1	1	-1	-1	-1		$\cdots$	-1	0	1	0	0
e_2	-1	0				2	2	-2	-1	-2		$\cdots$	-2	0	2	0	0
$\vdots$	-1	-1	$\ddots$		$\vdots$						$\ddots$		$\vdots$				
	$\vdots$		$\ddots$	0	0	$\vdots$	$\vdots$	$\vdots$	$\vdots$	$\vdots$		$1-p$	$1-p$	$\vdots$	$\vdots$	$\vdots$	$\vdots$
e_p				-1	0							$1-p$	$-p$				
e_{p+1}	-1		$\cdots$		-1	$p+1$	$p+1$	$-p-1$	-1	-2	$\cdots$	$1-p$	$-p$	0	$p+1$	0	0
f_1						1	1	-1	0	-1		$\cdots$	-1	0	1	0	0
f_2									0	0	$\ddots$		$\vdots$				
$\vdots$			0			$\vdots$	$\vdots$	$\vdots$	$\vdots$		$\ddots$	-1	-1	$\vdots$	$\vdots$	$\vdots$	$\vdots$
f_{p-1}									0			0	-1				
f_p						1	1	-1	0		$\cdots$		0	0	1	0	0
v	-1		$\cdots$		-1	$p+1$	$p+1$	$-p-1$	-1	-2		$\cdots$	$-p$	0	$p+1$	1	0
r	-1		$\cdots$		-1	$p+2$	$p+1$	$-p-2$	-1	-2		$\cdots$	$-p$	0	$p+1$	1	0
s						0	0	1						0	0	0	0
s'						0	0	1						0	0	0	-1
g			0			0	0	1			0			-1	0	0	0
u						1	1	-1						0	0	0	0

,

and thus compute that $-R_V H^{-1} D\widehat{\mathbf{t}} = t_U - t_V - t_Z$ and

$$-SH^{-1}D = \begin{array}{c} \\ t_1 \\ t_2 \\ \vdots \\ t_{p-1} \\ t_p \\ \hline t_U \\ t_V \\ t_W \\ t_Z \end{array} \left[\begin{array}{ccccc|cccc} t_1 & t_2 & \cdots & t_{p-1} & t_p & t_U & t_V & t_W & t_Z \\ \hline 1 & 1 & \cdots & 1 & 1 & 0 & -1 & 0 & 0 \\ 1 & 2 & \cdots & 2 & 2 & 0 & -2 & 0 & 0 \\ \vdots & \vdots & \ddots & \vdots & \vdots & \vdots & \vdots & \vdots & \vdots \\ 1 & 2 & \cdots & p-1 & p-1 & 0 & -(p-1) & 0 & 0 \\ 1 & 2 & \cdots & p-1 & p & 0 & -p & 0 & 0 \\ \hline -1 & -2 & \cdots & -(p-1) & -p & 0 & p+1 & 1 & 0 \\ 0 & 0 & \cdots & 0 & 0 & -1 & 0 & 0 & 0 \\ 0 & 0 & \cdots & 0 & 0 & 0 & 0 & 0 & 0 \\ 0 & 0 & \cdots & 0 & 0 & 0 & 0 & 0 & 0 \end{array}\right].$$

Since $\widehat{\mathbf{t}}^T(-SH^{-1}D)\widehat{\mathbf{t}} = \mathbf{t}^T Q_n \mathbf{t} + (t_V - t_U)(t_1 + \cdots + pt_p - pt_U)$, where $\mathbf{t} := (t_1, \ldots, t_p, t_U, t_W)$ and Q_n is defined in Theorem 4.13, we conclude that the kinematical kernel can be written as

$$\mathcal{K}_{Y_n}\left(\widehat{\mathbf{t}}\right) = e^{2i\pi\left(\mathbf{t}^T Q_n \mathbf{t} + (t_V - t_U)(t_1 + \cdots + pt_p - pt_U)\right)} \delta(t_Z)\delta(t_U - t_V - t_Z).$$

We now compute the dynamical content. We denote $\alpha = (a_1, b_1, c_1, \ldots, a_W, b_W, c_W, a_Z, b_Z, c_Z)$ a general vector in $\mathcal{S}_{Y_n}$. Let $\hbar > 0$. The dynamical content $\mathcal{D}_{\hbar, Y_n}\left(\widehat{\mathbf{t}}, \alpha\right)$ is equal to:

$$e^{\frac{1}{\sqrt{\hbar}}\widehat{C}(\alpha)^T\widehat{\mathbf{t}}} \frac{\Phi_{\mathsf{b}}\left(t_U + \frac{i}{2\pi\sqrt{\hbar}}(\pi - a_U)\right)\Phi_{\mathsf{b}}\left(t_V + \frac{i}{2\pi\sqrt{\hbar}}(\pi - a_V)\right)\Phi_{\mathsf{b}}\left(t_W + \frac{i}{2\pi\sqrt{\hbar}}(\pi - a_W)\right)}{\Phi_{\mathsf{b}}\left(t_1 - \frac{i}{2\pi\sqrt{\hbar}}(\pi - a_1)\right)\cdots\Phi_{\mathsf{b}}\left(t_p - \frac{i}{2\pi\sqrt{\hbar}}(\pi - a_p)\right)\Phi_{\mathsf{b}}\left(t_Z - \frac{i}{2\pi\sqrt{\hbar}}(\pi - a_Z)\right)},$$

where $\widehat{C}(\alpha) := (c_1, \ldots, c_p, c_U, c_V, c_W, c_Z)^T$.

Let us come back to the computation of the partition function of the Teichmüller TQFT. By Theorem 3.61, we have

$$\mathcal{Z}_\hbar(Y_n, \alpha) = \int_{\widehat{\mathbf{t}} \in \mathbb{R}^{Y_n^3}} d\widehat{\mathbf{t}}\, \mathcal{K}_{Y_n}\left(\widehat{\mathbf{t}}\right) \mathcal{D}_{\hbar, Y_n}\left(\widehat{\mathbf{t}}, \alpha\right).$$

We begin by integrating over the variables t_V and t_Z, which consists in removing the two Dirac delta functions $\delta(t_Z)$ and $\delta(t_U - t_V - t_Z)$ in the kinematical kernel and replacing t_Z by 0 and t_V by t_U in the other terms. Therefore, we have

$$\Phi_{\mathsf{b}}\left(\frac{\pi - a_Z}{2\pi i\sqrt{\hbar}}\right)\mathcal{Z}_\hbar(Y_n, \alpha) = \int_{\mathbf{t} \in \mathbb{R}^{p+2}} d\mathbf{t}\, e^{2i\pi \mathbf{t}^T Q_n \mathbf{t}} e^{\frac{1}{\sqrt{\hbar}}(c_1 t_1 + \cdots + c_p t_p + (c_U + c_V)t_U + c_W t_W)} \Pi(\mathbf{t}, \alpha, \hbar),$$

where $\mathbf{t} := (t_1, \ldots, t_p, t_U, t_W)$ and

$$\Pi(\mathbf{t}, \alpha, \hbar) := \frac{\Phi_{\mathsf{b}}\left(t_U + \frac{i}{2\pi\sqrt{\hbar}}(\pi - a_U)\right)\Phi_{\mathsf{b}}\left(t_U + \frac{i}{2\pi\sqrt{\hbar}}(\pi - a_V)\right)\Phi_{\mathsf{b}}\left(t_W + \frac{i}{2\pi\sqrt{\hbar}}(\pi - a_W)\right)}{\Phi_{\mathsf{b}}\left(t_1 - \frac{i}{2\pi\sqrt{\hbar}}(\pi - a_1)\right)\cdots\Phi_{\mathsf{b}}\left(t_p - \frac{i}{2\pi\sqrt{\hbar}}(\pi - a_p)\right)}.$$

Step 2. Applying the dominated convergence theorem for $\alpha \to \tau$.

For the rest of the proof, let

$$\tau := (a_1^\tau, b_1^\tau, c_1^\tau, \ldots, a_Z^\tau, b_Z^\tau, c_Z^\tau) \in \mathcal{S}_{Y_n \setminus Z} \times \overline{\mathcal{S}_Z}$$

be such that $\omega_j(\tau) = 2\pi$ for all $j \in \{0, 1, \dots, p-1, p\}$, $\widehat{\omega}_j(\tau) = 2\pi$ for all $j \in \{s, d, p+1\}$ and $\widehat{\omega}_{\overrightarrow{K_n}}(\tau) = a_Z^\tau = 0$.

Let $\delta > 0$ such that there exists a neighborhood $\mathfrak{U}$ of τ in $\mathcal{S}_{Y_n \setminus Z} \times \overline{\mathcal{S}_Z}$ such that for each $\alpha \in \mathfrak{U} \cap \mathcal{S}_{Y_n}$ the $3p+9$ first coordinates $a_1, \dots, c_W$ of α live in $(\delta, \pi - \delta)$.

Then for all $\alpha \in \mathfrak{U} \cap \mathcal{S}_{Y_n}$, for any $j \in \{1, \dots, p, U, V, W\}$, and for any $t \in \mathbb{R}$, we have

$$\left| e^{\frac{1}{\sqrt{\hbar}} c_j t} \Phi_{\mathsf{b}} \left(t \pm \frac{i}{2\pi\sqrt{\hbar}} (b_j + c_j) \right)^{\pm 1} \right| \leqslant M_{\delta,\hbar}\, e^{-\frac{1}{\sqrt{\hbar}} \delta |t|}.$$

Indeed, this is immediate for $t \leqslant 0$ by Lemma 4.21 and the fact that $c_j > \delta$. For $t \geqslant 0$, one has to use that $b_j > \delta$ but also Theorem 3.36 (1) and (2) to remark that :

$$\left| \Phi_{\mathsf{b}} \left(t + \frac{i}{2\pi\sqrt{\hbar}} (b_j + c_j) \right) \right| = \left| \Phi_{\mathsf{b}} \left(-t + \frac{i}{2\pi\sqrt{\hbar}} (b_j + c_j) \right) \right| \left| e^{i\pi \left(\frac{i}{2\pi\sqrt{\hbar}} (b_j + c_j) \right)^2} \right| \leqslant M_{\delta,\hbar} e^{-\frac{1}{\sqrt{\hbar}} (b_j + c_j) t}.$$

Consequently, we have a domination of the previous integrand uniformly over $\mathfrak{U} \cap \mathcal{S}_{Y_n}$, i.e.

$$\left| e^{2i\pi \mathbf{y}^T Q_n \mathbf{y}} e^{\frac{1}{\sqrt{\hbar}} (c_1 t_1 + \dots + c_p t_p + (c_U + c_V) t_U + c_W t_W)} \Pi(\mathbf{t}, \alpha, \hbar) \right| \leqslant (M_{\delta,\hbar})^{p+3}\, e^{-\frac{1}{\sqrt{\hbar}} \delta (|t_1| + \dots + |t_p| + 2|t_U| + |t_W|)}$$

for all $\alpha \in \mathfrak{U} \cap \mathcal{S}_{Y_n}$ and for all $\mathbf{t} \in \mathbb{R}^{p+2}$.

Since the right hand side of this inequality is integrable over $\mathbb{R}^{p+2}$, we can then apply the dominated convergence theorem to conclude that $\Phi_{\mathsf{b}} \left(\frac{\pi - a_Z}{2\pi i \sqrt{\hbar}} \right) \mathcal{Z}_\hbar(Y_n, \alpha)$ tends to

$$\int_{\mathbf{t} \in \mathbb{R}^{p+2}} d\mathbf{t}\, e^{2i\pi \mathbf{t}^T Q_n \mathbf{t}} e^{\frac{1}{\sqrt{\hbar}} (c_1^\tau t_1 + \dots + c_p^\tau t_p + (c_U^\tau + c_V^\tau) t_U + c_W^\tau t_W)} \Pi(\mathbf{t}, \tau, \hbar)$$

as $\alpha \in \mathcal{S}_{Y_n}, \alpha \to \tau$ (recall that c_j^τ denotes the c_j coordinate of τ).

Step 3. Retrieving the value $J_{X_n}(\hbar, 0)$ in $\alpha = \tau$.

Let us now prove that

$$\int_{\mathbf{t} \in \mathbb{R}^{p+2}} d\mathbf{t}\, e^{2i\pi \mathbf{t}^T Q_n \mathbf{t}} e^{\frac{1}{\sqrt{\hbar}} (c_1^\tau t_1 + \dots + c_p^\tau t_p + (c_U^\tau + c_V^\tau) t_U + c_W^\tau t_W)} \Pi(\mathbf{t}, \tau, \hbar) = J_{X_n}(\hbar, 0).$$

We first do the following change of variables:

- $y'_k = t_k - \frac{i}{2\pi\sqrt{\hbar}} (\pi - a_k^\tau)$ for $1 \leqslant k \leqslant p$,
- $y'_l = t_l + \frac{i}{2\pi\sqrt{\hbar}} (\pi - a_l^\tau)$ for $l \in \{U, W\}$,

and we denote $\mathbf{y}' := \left(y'_1, \dots, y'_p, y'_U, y'_W \right)^T$. Note that the term $\Phi_{\mathsf{b}} \left(t_U + \frac{i}{2\pi\sqrt{\hbar}} (\pi - a_V^\tau) \right)$ will become $\Phi_{\mathsf{b}} \left(y'_U + \frac{i}{2\pi\sqrt{\hbar}} (a_U^\tau - a_V^\tau) \right) = \Phi_{\mathsf{b}} \left(y'_U \right)$, since $a_U^\tau - a_V^\tau = (\widehat{\omega}_s(\tau) - 2\pi) + (\widehat{\omega}_d(\tau) - 2\pi) = 0$.

We also denote

$$\mathcal{Y}'_{\hbar,\tau} := \prod_{k=1}^{p}\left(\mathbb{R} - \frac{i}{2\pi\sqrt{\hbar}}(\pi - a_k^\tau)\right) \times \prod_{l=U,W}\left(\mathbb{R} + \frac{i}{2\pi\sqrt{\hbar}}(\pi - a_l^\tau)\right),$$

the subset of $\mathbb{C}^{p+2}$ on which the variables in $\mathbf{y}'$ reside.

By a similar computation as in the proof of Theorem 4.13, we obtain

$$\begin{aligned}&\int_{\mathbf{t}\in\mathbb{R}^{p+2}} d\mathbf{t}\, e^{2i\pi\mathbf{t}^T Q_n \mathbf{t}} e^{\frac{1}{\sqrt{\hbar}}(c_1^\tau t_1 + \cdots + c_p^\tau t_p + (c_U^\tau + c_V^\tau)t_U + c_W^\tau t_W)} \Pi(\mathbf{t},\tau,\hbar)\\ &\stackrel{\star}{=} \int_{\mathbf{y}'\in\mathcal{Y}'_{\hbar,\tau}} d\mathbf{y}' e^{2i\pi\mathbf{y}'^T Q_n \mathbf{y}' + \frac{1}{\sqrt{\hbar}}\mathcal{W}(\tau)^T\mathbf{y}'} \frac{\Phi_{\mathsf{b}}(y'_U)\,\Phi_{\mathsf{b}}(y'_U)\,\Phi_{\mathsf{b}}(y'_W)}{\Phi_{\mathsf{b}}(y'_1)\cdots\Phi_{\mathsf{b}}(y'_p)},\end{aligned}$$

where for any $\alpha \in \mathcal{S}_{Y_n\setminus Z}$, $\mathcal{W}(\alpha)$ is defined as

$$\mathcal{W}(\alpha) := 2Q_n\Gamma(\alpha) + C(\alpha) + (0,\ldots,0,c_V,0)^T,$$

with $\Gamma(\alpha) := (a_1 - \pi, \ldots, a_p - \pi, \pi - a_U, \pi - a_W)^T$ and $C(\alpha) := (c_1,\ldots,c_p,c_U,c_W)^T$. Hence, from the value of $J_{X_n}(\hbar,0)$, it remains only to prove that $\mathcal{W}(\tau) = \mathcal{W}_n$.

Let us denote $\Lambda : (u_1,\ldots,u_p,u_U,u_V,u_W) \mapsto (u_1,\ldots,u_p,u_U,u_W)$ the process of forgetting the second-to-last coordinate. Then obviously $C(\alpha) = \Lambda(\widetilde{C}(\alpha))$. Recall from Lemma 4.17 that $\widetilde{\mathcal{W}}(\alpha) = 2\widetilde{Q}_n\widetilde{\Gamma}(\alpha) + \widetilde{C}(\alpha)$ depends almost only on edge weights of the angles in X_n.

Thus, a direct calculation shows that for any $\alpha \in \mathcal{S}_{Y_n\setminus Z}$, we have

$$\mathcal{W}(\alpha) = \Lambda(\widetilde{\mathcal{W}}(\alpha)) + \begin{bmatrix} 0 \\ \vdots \\ 0 \\ c_V - 4(\pi - a_U) + 3(\pi - a_V) - (\pi - a_W) \\ a_U - a_V \end{bmatrix}.$$

Now, if we specify $\alpha = \tau$, then the weights $\omega_{X_n,j}(\alpha)$ appearing in $\Lambda(\widetilde{\mathcal{W}}(\alpha))$ will all be equal to 2π, since $\omega_s(\tau) = \widehat{\omega}_s(\tau) - \widehat{\omega}_{\overrightarrow{K_n}}(\tau) = 2\pi$ and

$$\omega_{p+1}(\tau) = \widehat{\omega}_d(\tau) + \widehat{\omega}_{p+1}(\tau) - 2\left(\pi - \widehat{\omega}_{\overrightarrow{K_n}}(\tau)\right) = 2\pi.$$

Hence

$$\mathcal{W}(\tau) = \mathcal{W}_n + \begin{bmatrix} 0 \\ \vdots \\ 0 \\ \pi - \frac{1}{2}\lambda_{X_n}(\tau) + c_V^\tau - 4(\pi - a_U^\tau) + 3(\pi - a_V^\tau) - (\pi - a_W^\tau) \\ a_U^\tau - a_V^\tau \end{bmatrix}.$$

Recall that $a_U^\tau - a_V^\tau = 0$, and remark finally that

$$\begin{aligned}&\pi - \frac{1}{2}\lambda_{X_n}(\tau) + c_V^\tau - 4(\pi - a_U^\tau) + 3(\pi - a_V^\tau) - (\pi - a_W^\tau)\\ &= 3a_U^\tau - 2a_V^\tau + a_W^\tau + b_W^\tau - \pi\\ &= 2(a_U^\tau - a_V^\tau) + (a_U^\tau - c_W^\tau)\\ &= -(\widehat{\omega}_d(\tau) - 2\pi) - \widehat{\omega}_{\overrightarrow{K_n}}(\tau) = 0.\end{aligned}$$

Hence $\mathcal{W}(\tau) = \mathcal{W}_n$ and the theorem is proven. □

4.6 Proving the volume conjecture (odd case)

We now arrive to a technical part of this thesis, that is to say the proof of the volume conjecture using detailed analytical methods. We advise the reader to be familiar with the proofs and notations of Section 4.4 before reading this section. Having read Section 4.5 is not as essential, but can nevertheless help understanding some arguments in the following first three subsections. The main result is as follows:

Theorem 4.22. *Let n be an odd integer greater or equal to 3. Let J_{X_n} and $\mathfrak{J}_{X_n}$ be the functions defined in Theorem 4.13 and Corollary 4.19. Then we have:*

$$\lim_{\hbar\to 0^+} 2\pi\hbar \log|J_{X_n}(\hbar, 0)| = \lim_{\hbar\to 0^+} 2\pi\hbar \log|\mathfrak{J}_{X_n}(\hbar, 0)| = -\mathrm{Vol}(S^3 \setminus K_n).$$

In other words, the Teichmüller TQFT volume conjecture of Andersen–Kashaev is proved for the infinite family of odd twist knots.

The proof of Theorem 4.22 will be split into several lemmas. The general idea is to translate the expressions in Theorem 4.22 into asymptotics of the form of Theorem 1.77, and check that the assumptions of Theorem 1.77 are satisfied one by one, i.e. that we are allowed to apply the saddle point method. Technical analytical lemmas are required for the asymptotics and error bounds, notably due to the fact that we work with *unbounded* integration contours.

More precisely, here is an overview of Section 4.6:

- Sections 4.6.1, 4.6.2 and 4.6.3: For the "classical" potential S, we check the prerequisites for the saddle point method, notably that $\Re(S)$ attains a maximum of $-\mathrm{Vol}(S^3 \setminus K_n)$ at the complete angle structure (from Lemma 4.23 to Lemma 4.29). This part refers to Thurston's gluing equations and the properties of the classical dilogarithm.

- Section 4.6.4: We apply the saddle point method to the classical potential S on a compact integration contour (Proposition 4.30) and we then deduce asymptotics when the contour is unbounded (Lemma 4.31 and Proposition 4.32). This part is where the analytical arguments start.

- Section 4.6.5: We compare the classical and quantum dilogarithms Li_2 and Φ_{b} in the asymptotic $\mathsf{b} \to 0^+$ (Lemmas 4.33, 4.34, 4.35) and deduce asymptotics for the quantum potential S_{b} (Proposition 4.36). This part, and Lemma 4.34 in particular, contains the heart of the proof, and needs several new analytical arguments to establish uniform bounds on an unbounded integration contour.

- Section 4.6.6: In order to get back to the functions J_{X_n} and $\mathfrak{J}_{X_n}$ of Theorem 4.22, we compare the two previous potentials with a second quantum potential S'_{b} related to J_{X_n} (Remark 4.37) and we deduce the corresponding asymptotics for S'_{b} (Lemma 4.38 and Proposition 4.39). This part uses similar analytical arguments as the previous one, and is needed because of the particular construction of the Teichmüller TQFT partition function and the subtle difference between $\frac{1}{\mathsf{b}^2}$ and $\frac{1}{\hbar}$.

- Section 4.6.7: We conclude with the (now short) proof of Theorem 4.22 and we offer comments on how our techniques could be re-used for further works.

Let us finish this introduction by establishing some notations. For the remainder of this section, n will be an odd integer greater or equal to 3 and $p := \frac{n-3}{2}$.

Let us now recall and define some notations:

- We denote the following product of open "horizontal bands" in $\mathbb{C}$, and

$$\mathcal{U} := \prod_{k=1}^{p} (\mathbb{R} + i(-\pi, 0)) \times \prod_{l=U,W} (\mathbb{R} + i(0, \pi)),$$

  an open subset of $\mathbb{C}^{p+2}$.

- For any angle structure $\alpha = (a_1, \dots, c_W) \in \mathcal{A}_{X_n}$, we denote

$$\mathcal{Y}_\alpha := \prod_{k=1}^{p} (\mathbb{R} - i(\pi - a_k)) \times \prod_{l=U,W} (\mathbb{R} + i(\pi - a_l)),$$

  an affine real plane of real dimension $p+2$ in $\mathbb{C}^{p+2}$, contained in the band $\mathcal{U}$.

- For the complete angle structure $\alpha^0 = (a_1^0, \dots, c_W^0) \in \mathcal{A}_{X_n}$ (which exists because of Theorem 4.8), we denote

$$\mathcal{Y}^0 := \mathcal{Y}_{\alpha^0}.$$

- We define the potential function $S \colon \mathcal{U} \to \mathbb{C}$, a holomorphic function on $p+2$ complex variables, by:

  $$S(\mathbf{y}) := i\mathbf{y}^T Q_n \mathbf{y} + \mathbf{y}^T \mathcal{W}_n + i\mathrm{Li}_2(-e^{y_1}) + \cdots + i\mathrm{Li}_2(-e^{y_p}) - 2i\mathrm{Li}_2(-e^{y_U}) - i\mathrm{Li}_2(-e^{y_W}),$$

  where Q_n and $\mathcal{W}_n$ are like in Theorem 4.13.

4.6.1 Properties of the potential function S on the open band $\mathcal{U}$

The following lemma will be very useful to prove the invertibility of the holomorphic hessian of the potential S.

Lemma 4.23. *Let $m \geqslant 1$ an integer, and $S_1, S_2 \in M_m(\mathbb{R})$ such that S_1 is symmetric positive definite and S_2 is symmetric. Then the complex symmetric matrix $S_1 + iS_2$ is invertible.*

Proof. Let us denote by $\langle \cdot | \cdot \rangle$ the usual inner product on $\mathbb{C}^m$. Let $\mathbf{v} \in \mathbb{C}^m$ such that $(S_1 + iS_2)\mathbf{v} = 0$. Let us prove that $\mathbf{v} = 0$.

Since S_1 and S_2 are real symmetric, we have $\langle \mathbf{v} | S_1 \mathbf{v} \rangle, \langle \mathbf{v} | S_2 \mathbf{v} \rangle \in \mathbb{R}$.

Now, since $(S_1 + iS_2)\mathbf{v} = 0$, then

$$0 = \langle \mathbf{v} | (S_1 + iS_2)\mathbf{v} \rangle = \langle \mathbf{v} | S_1 \mathbf{v} \rangle + i \langle \mathbf{v} | S_2 \mathbf{v} \rangle,$$

thus, by taking the real part, we get $0 = \langle \mathbf{v} | S_1 \mathbf{v} \rangle$, which implies $\mathbf{v} = 0$ since S_1 is positive definite. □

We can now prove that the holomorphic hessian is non-degenerate at each point.

Lemma 4.24. *For every $\mathbf{y} \in \mathcal{U}$, the holomorphic hessian of S is given by:*

$$\mathrm{Hess}(S)(\mathbf{y}) = \left(\frac{\partial^2 S}{\partial y_j \partial y_k}\right)_{j,k\in\{1,\dots,p,U,W\}}(\mathbf{y}) = 2iQ_n + i\begin{pmatrix} \frac{-1}{1+e^{-y_1}} & & 0 & 0 & 0 \\ & \ddots & & \vdots & \vdots \\ 0 & & \frac{-1}{1+e^{-y_p}} & 0 & 0 \\ 0 & \cdots & 0 & \frac{2}{1+e^{-y_U}} & 0 \\ 0 & \cdots & 0 & 0 & \frac{1}{1+e^{-y_W}} \end{pmatrix}.$$

Furthermore, $\mathrm{Hess}(S)(\mathbf{y})$ *has non-zero determinant for every* $\mathbf{y} \in \mathcal{U}$.

Proof. The first part follows from the double differentiation of S and the fact that

$$\frac{\partial \mathrm{Li}_2(-e^y)}{\partial y} = -\mathrm{Log}(1+e^y)$$

for $y \in \mathbb{R} \pm i(0,\pi)$ (note that $y \in \mathbb{R} \pm i(0,\pi)$ implies $-e^y \in \mathbb{C} \setminus \mathbb{R}$).

Let us prove the second part. Let $\mathbf{y} \in \mathcal{U}$. Then $\Im(\mathrm{Hess}(S)(\mathbf{y}))$ is a symmetric matrix (as the sum of Q_n and a diagonal matrix), and

$$\Re(\mathrm{Hess}(S)(\mathbf{y})) = \begin{pmatrix} -\Im\left(\frac{-1}{1+e^{-y_1}}\right) & & 0 & 0 & 0 \\ & \ddots & & \vdots & \vdots \\ 0 & & -\Im\left(\frac{-1}{1+e^{-y_p}}\right) & 0 & 0 \\ 0 & \cdots & 0 & -\Im\left(\frac{2}{1+e^{-y_U}}\right) & 0 \\ 0 & \cdots & 0 & 0 & -\Im\left(\frac{1}{1+e^{-y_W}}\right) \end{pmatrix}$$

is diagonal with negative coefficients (because $\Im(y_1), \dots, \Im(y_p) \in (-\pi, 0)$ and $\Im(y_U), \Im(y_W) \in (0,\pi)$). Hence it follows from Lemma 4.23 that $\mathrm{Hess}(S)(\mathbf{y})$ is invertible for every $\mathbf{y} \in \mathcal{U}$. □

The following lemma establishes an equivalence between critical points of the potential S and complex shape structures that solve the balancing and completeness equations.

Lemma 4.25. *Let us consider the diffeomorphism*

$$\psi := \left(\prod_{T\in\{T_1,\dots,T_p,U,W\}} \psi_T\right) : (\mathbb{R} + i\mathbb{R}_{>0})^{p+2} \to \mathcal{U},$$

where ψ_T was defined in Section 2.2.1. Then ψ induces a bijective mapping between $\{\mathbf{y} \in \mathcal{U} \mid \nabla S(\mathbf{y}) = 0\}$ *and*

$$\left\{\mathbf{z} = (z_1, \dots, z_p, z_U, z_W) \in (\mathbb{R} + i\mathbb{R}_{>0})^{p+2} \mid \mathcal{E}_{X_n,0}(\mathbf{z}) \wedge \dots \wedge \mathcal{E}_{X_n,p-1}(\mathbf{z}) \wedge \mathcal{E}^{co}_{X_n,p+1}(\mathbf{z}) \wedge \mathcal{E}^{co}_{X_n,s}(\mathbf{z})\right\},$$

where the equations $\mathcal{E}_{X_n,0}(\mathbf{z}), \dots, \mathcal{E}_{X_n,p-1}(\mathbf{z}), \mathcal{E}^{co}_{X_n,p+1}(\mathbf{z}), \mathcal{E}^{co}_{X_n,s}(\mathbf{z})$ were defined at the end of Section 4.3.

In particular, S admits only one critical point $\mathbf{y^0}$ on $\mathcal{U}$, corresponding to the complete hyperbolic structure $\mathbf{z^0}$ on the geometric ideal triangulation X_n (adding z^0_V equal to z^0_U).

Proof. First we compute, for every $\mathbf{y} \in \mathcal{U}$,

$$\nabla S(\mathbf{y}) = \begin{pmatrix} \partial_1 S(\mathbf{y}) \\ \vdots \\ \partial_p S(\mathbf{y}) \\ \partial_U S(\mathbf{y}) \\ \partial_W S(\mathbf{y}) \end{pmatrix} = 2iQ_n\mathbf{y} + \mathcal{W}_n + i \begin{pmatrix} -\mathrm{Log}(1+e^{y_1}) \\ \vdots \\ -\mathrm{Log}(1+e^{y_p}) \\ 2\mathrm{Log}(1+e^{y_U}) \\ \mathrm{Log}(1+e^{y_W}) \end{pmatrix}.$$

Then, we define a lower triangular matrix $A =$

	y_1	y_2	y_3	$\cdots$	y_p	y_U	y_W
y_1	1						
y_2	-2	1			0		
y_3	1	-2	1				
$\vdots$		$\ddots$	$\ddots$	$\ddots$			
y_p			1	-2	1	0	0
y_U					1	1	0
y_W		0			0	0	1

$\in GL_{p+2}(\mathbb{Z})$, and we compute

$$A \cdot \nabla S(\mathbf{y}) = \begin{pmatrix} 2i(y_1 + \cdots + y_p - y_U) - 2\pi p - i\mathrm{Log}(1+e^{y_1}) \\ -2iy_1 + 2\pi + 2i\mathrm{Log}(1+e^{y_1}) - i\mathrm{Log}(1+e^{y_2}) \\ 2\pi - i\mathrm{Log}(1+e^{y_1}) + 2i\mathrm{Log}(1+e^{y_2}) - 2iy_2 - i\mathrm{Log}(1+e^{y_3}) \\ \vdots \\ 2\pi - i\mathrm{Log}(1+e^{y_{k-1}}) + 2i\mathrm{Log}(1+e^{y_k}) - 2iy_k - i\mathrm{Log}(1+e^{y_{k+1}}) \\ \vdots \\ 2\pi - i\mathrm{Log}(1+e^{y_{p-2}}) + 2i\mathrm{Log}(1+e^{y_{p-1}}) - 2iy_{p-1} - i\mathrm{Log}(1+e^{y_p}) \\ \pi - i\mathrm{Log}(1+e^{y_p}) + 2i\mathrm{Log}(1+e^{y_U}) + iy_W \\ \pi + iy_U + i\mathrm{Log}(1+e^{y_W}) \end{pmatrix}.$$

For $1 \leqslant k \leqslant p$, by denoting $y_k := \psi_{T_k}(z_k)$, we have

$$\mathrm{Log}(z_k) = y_k + i\pi,\ \mathrm{Log}(z_k') = -\mathrm{Log}(1+e^{y_k}),\ \mathrm{Log}(z_k'') = \mathrm{Log}(1+e^{-y_k}),$$

and for $l = U, W$, by denoting $y_l := \psi_{T_l}(z_l)$, we have

$$\mathrm{Log}(z_l) = -y_l + i\pi,\ \mathrm{Log}(z_l') = -\mathrm{Log}(1+e^{-y_l}),\ \mathrm{Log}(z_l'') = \mathrm{Log}(1+e^{y_l}).$$

Hence we compute, for all $\mathbf{z} \in (\mathbb{R} + i\mathbb{R}_{>0})^{p+2}$,

$$A \cdot (\nabla S)(\psi(\mathbf{z})) = i \begin{pmatrix} \mathrm{Log}(z_1') + 2\mathrm{Log}(z_1) + \cdots + 2\mathrm{Log}(z_p) + 2\mathrm{Log}(z_U) - 2i\pi \\ 2\mathrm{Log}(z_1'') + \mathrm{Log}(z_2') - 2i\pi \\ \mathrm{Log}(z_1') + 2\mathrm{Log}(z_2'') + \mathrm{Log}(z_3') - 2i\pi \\ \vdots \\ \mathrm{Log}(z_{k-1}') + 2\mathrm{Log}(z_k'') + \mathrm{Log}(z_{k+1}') - 2i\pi \\ \vdots \\ \mathrm{Log}(z_{p-2}') + 2\mathrm{Log}(z_{p-1}'') + \mathrm{Log}(z_p') - 2i\pi \\ \mathrm{Log}(z_p') + 2\mathrm{Log}(z_U'') - \mathrm{Log}(z_W) \\ \mathrm{Log}(z_W'') - \mathrm{Log}(z_U) \end{pmatrix}.$$

This last vector is zero if and only if one has

$$\mathcal{E}_{X_n,0}(\mathbf{z}) \wedge \cdots \wedge \mathcal{E}_{X_n,p-1}(\mathbf{z}) \wedge \mathcal{E}^{co}_{X_n,p+1}(\mathbf{z}) \wedge \mathcal{E}^{co}_{X_n,s}(\mathbf{z}).$$

Since A is invertible, we thus have

$$\begin{array}{c} \mathbf{z} \in (\mathbb{R} + i\mathbb{R}_{>0})^{p+2} \quad \text{and} \quad \mathcal{E}_{X_n,0}(\mathbf{z}) \wedge \cdots \wedge \mathcal{E}_{X_n,p-1}(\mathbf{z}) \wedge \mathcal{E}^{co}_{X_n,p+1}(\mathbf{z}) \wedge \mathcal{E}^{co}_{X_n,s}(\mathbf{z}) \\ \Updownarrow \\ \psi(\mathbf{z}) \in \mathcal{U} \quad \text{and} \quad (\nabla S)(\psi(\mathbf{z})) = 0. \end{array}$$

□

Let us now consider the multi-contour

$$\mathcal{Y}^0 := \mathcal{Y}_{\alpha^0} = \prod_{k=1}^{p} \left(\mathbb{R} - i(\pi - a_k^0)\right) \times \prod_{l=U,W} \left(\mathbb{R} + i(\pi - a_l^0)\right),$$

where $\alpha^0 \in \mathcal{A}_{X_n}$ is the complete hyperbolic angle structure corresponding to the complete hyperbolic complex shape structure $\mathbf{z^0}$. Notice that $\mathbf{y^0} \in \mathcal{Y}^0 \subset \mathcal{U}$.

We will parametrize $\mathbf{y} \in \mathcal{Y}^0$ as

$$\mathbf{y} = \begin{pmatrix} y_1 \\ \vdots \\ y_W \end{pmatrix} = \begin{pmatrix} x_1 + id_1^0 \\ \vdots \\ x_W + id_W^0 \end{pmatrix} = \mathbf{x} + i\mathbf{d^0},$$

where $d_k^0 := -(\pi - a_k^0) < 0$ for $k = 1, \ldots, p$ and $d_l^0 := \pi - a_l^0 > 0$ for $l = U, W$. For the scrupulous readers, this means that $\mathbf{d^0}$ is a new notation for $\Gamma(\alpha^0)$, where $\Gamma(\alpha)$ was defined at the end of Section 4.5. Notice that $\mathcal{Y}^0 = \mathbb{R}^{p+2} + i\mathbf{d^0} \subset \mathbb{C}^{p+2}$ is an $\mathbb{R}$-affine subspace of $\mathbb{C}^{p+2}$.

4.6.2 Concavity of $\Re S$ on each contour $\mathcal{Y}_\alpha$

Now we focus on the behaviour of the real part $\Re S$ of the classical potential, on each horizontal contour $\mathcal{Y}_\alpha$.

Lemma 4.26. *For any $\alpha \in \mathcal{A}_{X_n}$, the function $\Re S \colon \mathcal{Y}_\alpha \to \mathbb{R}$ is strictly concave on $\mathcal{Y}_\alpha$.*

Proof. Let $\alpha \in \mathcal{A}_{X_n}$. Since $\Re S \colon \mathcal{Y}_\alpha \to \mathbb{R}$ is twice continuously differentiable (as a function on $p+2$ real variables), we only need to check that its (real) hessian matrix $(\Re S|_{\mathcal{Y}_\alpha})''$ is negative definite on every point $\mathbf{x} + i\mathbf{d} \in \mathcal{Y}_\alpha$.

Now, since this real hessian is equal to the real part of the holomorphic hessian of S, it follows from Lemma 4.24 that for all $\mathbf{x} \in \mathbb{R}^{p+2}$, this real hessian is:

$$\begin{aligned} &(\Re S|_{\mathcal{Y}_\alpha})''(\mathbf{x} + i\mathbf{d}) = \Re(\mathrm{Hess}(S)(\mathbf{x} + i\mathbf{d})) \\ &= \begin{pmatrix} -\Im\left(\frac{-1}{1+e^{-x_1 - id_1}}\right) & & 0 & 0 & 0 \\ & \ddots & & \vdots & \vdots \\ 0 & & -\Im\left(\frac{-1}{1+e^{-x_p - id_p}}\right) & 0 & 0 \\ 0 & \cdots & 0 & -\Im\left(\frac{2}{1+e^{-x_U - id_U}}\right) & 0 \\ 0 & \cdots & 0 & 0 & -\Im\left(\frac{1}{1+e^{-x_W - id_W}}\right) \end{pmatrix}, \end{aligned}$$

which is diagonal with negative coefficients, since $d_1, \dots, d_p \in (-\pi, 0)$ and $d_U, d_W \in (0, \pi)$.

In particular $(\Re S|_{\mathcal{Y}_\alpha})''$ is negative definite everywhere, thus $\Re S|_{\mathcal{Y}_\alpha}$ is strictly concave. □

4.6.3 Properties of $\Re S$ on the complete contour $\mathcal{Y}^0$

On the complete contour $\mathcal{Y}^0$, the function $\Re S$ is not only strictly concave but also admits a strict global maximum, at the complete structure $\mathbf{y^0}$.

Lemma 4.27. *The function $\Re S \colon \mathcal{Y}^0 \to \mathbb{R}$ admits a strict global maximum on $\mathbf{y^0} \in \mathcal{Y}^0$.*

Proof. Since the holomorphic gradient of $S \colon \mathcal{U} \to \mathbb{C}$ vanishes on $\mathbf{y^0}$ by Lemma 4.25, the (real) gradient of $\Re S|_{\mathcal{Y}^0}$ (which is the real part of the holomorphic gradient of S) then vanishes as well on $\mathbf{y^0}$, thus $\mathbf{y^0}$ is a critical point of $\Re S|_{\mathcal{Y}^0}$.

Besides, $\Re S|_{\mathcal{Y}^0}$ is strictly concave by Lemma 4.26, thus $\mathbf{y^0}$ is a global maximum of $\Re S|_{\mathcal{Y}^0}$. □

Before computing the value $\Re S(\mathbf{y^0})$, we establish a useful formula for the potential S:

Lemma 4.28. *The function $S \colon \mathcal{U} \to \mathbb{C}$ can be re-written*

$$S(\mathbf{y}) = i\mathrm{Li}_2\left(-e^{y_1}\right) + \dots + i\mathrm{Li}_2\left(-e^{y_p}\right) + 2i\mathrm{Li}_2\left(-e^{-y_U}\right) + i\mathrm{Li}_2\left(-e^{-y_W}\right) + i\mathbf{y}^T Q_n \mathbf{y} + iy_U^2 + i\frac{y_W^2}{2} + \mathbf{y}^T \mathcal{W}_n + i\frac{\pi^2}{2}.$$

Proof. We first recall the well-known formula for the dilogarithm (see Proposition 2.41 (1)):

$$\mathrm{Li}_2\left(\frac{1}{z}\right) = -\mathrm{Li}_2(z) - \frac{\pi^2}{6} - \frac{1}{2}\mathrm{Log}(-z)^2 \qquad \forall z \in \mathbb{C} \setminus [1, +\infty).$$

We then apply this formula for $z = -e^{y_l}$ for $l \in \{U, W\}$ to conclude the proof. □

We can now use this formula to prove that the hyperbolic volume appears at the complete structure $\mathbf{y^0}$, in the following lemma.

Lemma 4.29. *We have*

$$\Re(S)(\mathbf{y^0}) = -\mathrm{Vol}(S^3 \setminus K_n).$$

Proof. From Lemma 4.28, for all $\mathbf{y} \in \mathcal{U}$ we have

$$S(\mathbf{y}) = i\mathrm{Li}_2\left(-e^{y_1}\right) + \dots + i\mathrm{Li}_2\left(-e^{y_p}\right) + 2i\mathrm{Li}_2\left(-e^{-y_U}\right) + i\mathrm{Li}_2\left(-e^{-y_W}\right) + i\mathbf{y}^T Q_n \mathbf{y} + iy_U^2 + i\frac{y_W^2}{2} + \mathbf{y}^T \mathcal{W}_n + i\frac{\pi^2}{2},$$

thus

$$\Re(S)(\mathbf{y}) = -\Im\left(\mathrm{Li}_2\left(-e^{y_1}\right)\right) - \dots - \Im\left(\mathrm{Li}_2\left(-e^{y_p}\right)\right) - 2\Im\left(\mathrm{Li}_2\left(-e^{-y_U}\right)\right) - \Im\left(\mathrm{Li}_2\left(-e^{-y_W}\right)\right) - \Im\left(\mathbf{y}^T Q_n \mathbf{y} + y_U^2 + \frac{y_W^2}{2}\right) + \Re\left(\mathbf{y}^T \mathcal{W}_n\right).$$

Recall that for $z \in \mathbb{R} + i\mathbb{R}_{>0}$, the ideal hyperbolic tetrahedron of complex shape z has hyperbolic volume $D(z) = \Im(\mathrm{Li}_2(z)) + \arg(1-z)\log|z|$ (Theorem 2.42). Note that for $z = z_k = -e^{y_k}$ (with $1 \leqslant k \leqslant p$), we have $\arg(1-z)\log|z| = -c_k x_k$ and for $z = z_l = -e^{-y_l}$ (with $l \in \{U, W\}$), we have $\arg(1-z)\log|z| = b_l x_l$. Thus we have for $\mathbf{y} \in \mathcal{U}$:

$$\begin{aligned}\Re(S)(\mathbf{y}) = -D(z_1) - \cdots - D(z_p) - 2D(z_U) - D(z_W) - c_1 x_1 - \cdots - c_p x_p + 2b_U x_U + b_W x_W \\ - 2\mathbf{x}^T Q_n \mathbf{d} - 2d_U x_U - d_W x_W + \mathbf{x}^T \mathcal{W}_n.\end{aligned}$$

Recall that $\mathbf{z^0}$ is the complex shape structure corresponding to the complete hyperbolic structure on the ideal triangulation X_n where z_U^0 is the complex shape of both tetrahedra U and V (because of the completeness equation $z_U = z_V$). Thus

$$\begin{aligned}-\mathrm{Vol}(S^3 \setminus K_n) &= -D(z_1^0) - \cdots - D(z_p^0) - D(z_U^0) - D(z_V^0) - D(z_W^0) \\ &= -D(z_1^0) - \cdots - D(z_p^0) - 2D(z_U^0) - D(z_W^0).\end{aligned}$$

Hence we only need to prove that $(\mathbf{x^0})^T \mathcal{T} = 0$, where

$$\mathcal{T} := \begin{pmatrix} -c_1^0 \\ \vdots \\ -c_p^0 \\ 2b_U^0 \\ b_W^0 \end{pmatrix} + \mathcal{W}_n - 2Q_n\mathbf{d^0} + \begin{pmatrix} 0 \\ \vdots \\ 0 \\ -2d_U^0 \\ -d_W^0 \end{pmatrix}.$$

Since $d_l^0 = \pi - a_l^0 = b_l^0 + c_l^0$ for $l = U, W$, we have $\mathcal{T} = -\begin{pmatrix} c_1^0 \\ \vdots \\ c_p^0 \\ 2c_U^0 \\ c_W^0 \end{pmatrix} + \mathcal{W}_n - 2Q_n\mathbf{d^0}$.

It then follows from the definitions of $\mathcal{W}, \mathcal{W}_n, \widetilde{\Gamma}, \widetilde{C}, \mathbf{d^0}$ and their connections established in Sections 4.4 and 4.5 that $\mathcal{T} = 0$. More precisely, define for instance

$$\tau^0 := \alpha^0 \oplus (0, 0, \pi) \in \mathcal{S}_{Y_n \setminus Z} \times \overline{\mathcal{S}_Z},$$

which satisfies the assumptions on τ in Theorem 4.20 (as can be checked by computing the weights listed at the beginning of Section 4.5). Then recall from the end of the proof of Theorem 4.20 and the fact that $(a_U^0, b_U^0, c_U^0) = (a_V^0, b_V^0, c_V^0)$ that

$$\mathcal{W}_n = \mathcal{W}(\tau^0) := 2Q_n\Gamma(\tau^0) + C(\tau^0) + (0, \ldots, 0, c_V^{\tau^0}, 0)^T = 2Q_n\mathbf{d^0} + (c_1^0, \ldots, c_p^0, 2c_U^0, c_W^0)^T,$$

and thus $\mathcal{T} = 0$. The readers having skipped Section 4.5 can instead use the identity $\widetilde{\mathcal{W}}(\alpha) = 2\widetilde{Q}_n\widetilde{\Gamma}(\alpha) + \widetilde{C}(\alpha)$ at the end of Section 4.4 to arrive at the same conclusion. □

4.6.4 Asymptotics of integrals on $\mathcal{Y}^0$

For the remainder of the section, let $r_0 > 0$ and $\gamma := \{\mathbf{y} \in \mathcal{Y}^0 \mid \| \mathbf{y} - \mathbf{y^0} \| \leqslant r_0\}$ a $(p+2)$-dimensional ball inside $\mathcal{Y}^0$ containing $\mathbf{y^0}$. We start with asymptotics of an integral on this compact contour γ.

Proposition 4.30. *There exists a constant $\rho \in \mathbb{C}^*$ such that, as $\lambda \to \infty$,*

$$\int_\gamma d\mathbf{y}\, e^{\lambda S(\mathbf{y})} = \rho \lambda^{-\frac{p+2}{2}} \exp\left(\lambda S(\mathbf{y^0})\right) \left(1 + o_{\lambda\to\infty}(1)\right).$$

In particular,

$$\frac{1}{\lambda} \log \left| \int_\gamma d\mathbf{y}\, e^{\lambda S(\mathbf{y})} \right| \underset{\lambda\to\infty}{\longrightarrow} \Re S(\mathbf{y^0}) = -\mathrm{Vol}(S^3 \setminus K_n).$$

Proof. We apply the saddle point method as in Theorem 1.77, with $m = p+2$, $\gamma^m = \gamma$, $z = \mathbf{y}$, $z^0 = \mathbf{y^0}$, $D = \mathcal{U}$, $f = 1$ and S as defined in the beginning of Section 4.6. Let us check the technical requirements:

- $\mathbf{y^0}$ is an interior point of γ by construction.
- $\max_\gamma \Re S$ is attained only at $\mathbf{y^0}$ by Lemma 4.27.
- $\nabla S(\mathbf{y^0}) = 0$ by Lemma 4.25.
- $\det \mathrm{Hess}(S)(\mathbf{y^0}) \neq 0$ by Lemma 4.24.

Thus the first statement follows from Theorem 1.77, with $\rho := \dfrac{(2\pi)^{\frac{p+2}{2}}}{\sqrt{\det \mathrm{Hess}(S)(\mathbf{y^0})}} \in \mathbb{C}^*$.

The second statement then follows from immediate computation and Lemma 4.29. □

Now we compute an upper bound on the remainder term, i.e. the integral on $\mathcal{Y}^0 \setminus \gamma$ the whole unbounded contour minus the compact ball.

Lemma 4.31. *There exist constants $A, B > 0$ such that for all $\lambda > A$,*

$$\left| \int_{\mathcal{Y}^0 \setminus \gamma} d\mathbf{y}\, e^{\lambda S(\mathbf{y})} \right| \leqslant B e^{\lambda M},$$

where $M := \max_{\partial\gamma} \Re S$.

Proof. First we apply a change of variables to $(p+2)$-dimensional spherical coordinates

$$\mathbf{y} \in \mathcal{Y}^0 \setminus \gamma \Longleftrightarrow r\overrightarrow{e} \in (r_0, \infty) \times \mathbb{S}^{p+1},$$

which yields:

$$\int_{\mathcal{Y}^0 \setminus \gamma} d\mathbf{y}\, e^{\lambda S(\mathbf{y})} = \int_{\mathbb{S}^{p+1}} dvol_{\mathbb{S}^{p+1}} \int_{r_0}^\infty r^{p+1} e^{\lambda S(r\overrightarrow{e})}\, dr$$

for all $\lambda > 0$.

Consequently, we have for all $\lambda > 0$:

$$\left| \int_{\mathcal{Y}^0 \setminus \gamma} d\mathbf{y}\, e^{\lambda S(\mathbf{y})} \right| \leqslant \mathrm{vol}(\mathbb{S}^{p+1}) \sup_{\overrightarrow{e} \in \mathbb{S}^{p+1}} \int_{r_0}^\infty r^{p+1} e^{\lambda \Re(S)(r\overrightarrow{e})}\, dr.$$

Let us fix $\overrightarrow{e} \in \mathbb{S}^{p+1}$ and denote $f = f_{\overrightarrow{e}} := (r \mapsto \Re(S)(r\overrightarrow{e}))$ the restriction of $\Re(S)$ on the ray $(r_0, \infty)\overrightarrow{e}$. Let $\lambda > 0$. Let us find an upper bound on $\int_{r_0}^{\infty} r^{p+1} e^{\lambda f(r)}\, dr$.

Since $\Re(S)$ is strictly concave by Lemma 4.26 and f is its restriction on a convex set, f is strictly concave as well on $(r_0, +\infty)$ (and even on $[0, +\infty)$). Now let us consider the slope function $N\colon [r_0, +\infty) \to \mathbb{R}$ defined by $N(r) := \dfrac{f(r) - f(r_0)}{r - r_0}$ for $r > r_0$ and $N(r_0) := f'(r_0)$. The function N is C^1 and satisfies $N'(r) = \frac{f'(r) - N(r)}{r - r_0}$ for $r > r_0$. Now, since f is strictly concave, we have $f'(r) < N(r)$ for any $r \in (r_0, \infty)$, thus N is decreasing on this same interval. Hence

$$\int_{r_0}^{\infty} r^{p+1} e^{\lambda f(r)}\, dr = e^{\lambda f(r_0)} \int_{r_0}^{\infty} r^{p+1} e^{\lambda N(r)(r-r_0)}\, dr \leqslant e^{\lambda f(r_0)} \int_{r_0}^{\infty} r^{p+1} e^{\lambda N(r_0)(r-r_0)}\, dr.$$

Note that $N(r_0) = f'(r_0) < 0$ by Lemmas 4.26 and 4.27. Using integration by parts, we can prove by induction that

$$\int_{r_0}^{\infty} r^{p+1} e^{\lambda N(r_0)(r-r_0)}\, dr = \frac{1}{(\lambda N(r_0))^{p+2}} \sum_{k=0}^{p+1} (-1)^{p+1-k} \frac{(p+1)!}{k!} (\lambda N(r_0))^k r_0^k.$$

Moreover, $N(r_0) = f'(r_0) = (\nabla \Re(S))(r_0 \overrightarrow{e}) \cdot \overrightarrow{e}$, and since S is holomorphic, we conclude that $(\overrightarrow{e} \mapsto N(r_0) = f'_{\overrightarrow{e}}(r_0))$ is a continous map from $\mathbb{S}^{p+1}$ to $\mathbb{R}_{<0}$. Hence there exist $m_1, m_2 > 0$ such that $0 < m_1 \leqslant |N(r_0)| \leqslant m_2$ for all vectors $\overrightarrow{e} \in \mathbb{S}^{p+1}$.

We thus conclude that for all $\lambda > \frac{1}{m_1 r_0}$, we have the (somewhat unoptimal) upper bound:

$$\begin{aligned}
\int_{r_0}^{\infty} r^{p+1} e^{\lambda f(r)}\, dr &\leqslant e^{\lambda f(r_0)} \frac{1}{(\lambda N(r_0))^{p+2}} \sum_{k=0}^{p+1} (-1)^{p+1-k} \frac{(p+1)!}{k!} (\lambda N(r_0))^k r_0^k \\
&\leqslant e^{\lambda f(r_0)} \left| \frac{1}{(\lambda N(r_0))^{p+2}} \sum_{k=0}^{p+1} (-1)^{p+1-k} \frac{(p+1)!}{k!} (\lambda N(r_0))^k r_0^k \right| \\
&\leqslant e^{\lambda f(r_0)} \frac{1}{|\lambda N(r_0)|^{p+2}} \sum_{k=0}^{p+1} (p+1)!\ |\lambda N(r_0) r_0|^k \\
&\leqslant e^{\lambda f(r_0)} \frac{(p+2)!\ |\lambda N(r_0) r_0|^{p+2}}{|\lambda N(r_0)|^{p+2}} = (p+2)!\ r_0^{p+2} e^{\lambda f(r_0)}.
\end{aligned}$$

Now, since $\int_{r_0}^{\infty} r^{p+1} e^{\lambda f_{\overrightarrow{e}}(r)} dr \leqslant C e^{\lambda f_{\overrightarrow{e}}(r_0)}$ for all $\lambda > \frac{1}{m_1 r_0}$, for all $\overrightarrow{e} \in \mathbb{S}^{p+1}$ and with the constant $C > 0$ independent of λ and $\overrightarrow{e}$, we can finally conclude that:

$$\left| \int_{\mathcal{Y}^0 \setminus \gamma} d\mathbf{y}\, e^{\lambda S(\mathbf{y})} \right| \leqslant \mathrm{vol}(\mathbb{S}^{p+1}) \sup_{\overrightarrow{e} \in \mathbb{S}^{p+1}} \int_{r_0}^{\infty} r^{p+1} e^{\lambda \Re(S)(r\overrightarrow{e})}\, dr \leqslant C \mathrm{vol}(\mathbb{S}^{p+1}) e^{\lambda M}$$

for all $\lambda > \frac{1}{m_1 r_0}$, where $M := \max_{\partial\gamma} \Re S$. This concludes the proof, by putting $A := \frac{1}{m_1 r_0}$ and $B := C\mathrm{vol}(\mathbb{S}^{p+1})$. □

Finally we obtain the asymptotics for the integral on the whole contour $\mathcal{Y}^0$:

Proposition 4.32. *For the same constant $\rho \in \mathbb{C}^*$ as in Proposition 4.30, we have, as $\lambda \to \infty$,*

$$\int_{\mathcal{Y}^0} d\mathbf{y}\, e^{\lambda S(\mathbf{y})} = \rho \lambda^{-\frac{p+2}{2}} \exp\left(\lambda S(\mathbf{y^0})\right) \left(1 + o_{\lambda\to\infty}(1)\right).$$

In particular,

$$\frac{1}{\lambda} \log \left| \int_{\mathcal{Y}^0} d\mathbf{y}\, e^{\lambda S(\mathbf{y})} \right| \underset{\lambda\to\infty}{\longrightarrow} \Re S(\mathbf{y^0}) = -\mathrm{Vol}(S^3 \setminus K_n).$$

Proof. As for Proposition 4.30, the second statement imediately follows from the first one. Let us prove the first statement.

From Lemma 4.31, for all $\lambda > A$, we have $\left|\int_{\mathcal{Y}^0\setminus\gamma} d\mathbf{y}\, e^{\lambda S(\mathbf{y})}\right| \leqslant Be^{\lambda M}$. Then, since $M < \Re(S)(\mathbf{y^0})$ by Lemmas 4.26 and 4.27, we have

$$\int_{\mathcal{Y}^0\setminus\gamma} d\mathbf{y}\, e^{\lambda S(\mathbf{y})} = o_{\lambda\to\infty}\left(\lambda^{-\frac{p+2}{2}} \exp\left(\lambda S(\mathbf{y^0})\right)\right).$$

The first statement then follows from Proposition 4.30 and the equality

$$\int_{\mathcal{Y}^0} d\mathbf{y}\, e^{\lambda S(\mathbf{y})} = \int_{\gamma} d\mathbf{y}\, e^{\lambda S(\mathbf{y})} + \int_{\mathcal{Y}^0\setminus\gamma} d\mathbf{y}\, e^{\lambda S(\mathbf{y})}.$$

□

4.6.5 Extending the asymptotics to the quantum dilogarithm

Let us now introduce some new notations:

- We let R denote any positive number in $(0, \pi)$, for example $\pi/2$. Its exact value will not be relevant.
- We denote $I_R^+ := (R, \infty)$, $I_R^- := (-\infty, -R)$, Λ_R the closed upper half circle of radius R in the complex plane, and $\Omega_R := I_R^- \cup \Lambda_R \cup I_R^+$. Remark that we can replace the contour $\mathbb{R} + i0^+$ with Ω_R in the definition of Φ_{b}, by the Cauchy theorem.
- For $\delta > 0$, we define the product of closed "horizontal bands" in $\mathbb{C}$

  $$\mathcal{U}_\delta := \prod_{k=1}^{p} (\mathbb{R} + i[-\pi + \delta, -\delta]) \times \prod_{l=U,W} (\mathbb{R} + i[\delta, \pi - \delta])$$

  a closed subset of $\mathcal{U}$.
- For $\mathsf{b} > 0$, we define a new potential function $S_{\mathsf{b}} \colon \mathcal{U} \to \mathbb{C}$, a holomorphic function on $p + 2$ complex variables, by:

  $$S_{\mathsf{b}}(\mathbf{y}) := i\mathbf{y}^T Q_n \mathbf{y} + \mathbf{y}^T \mathcal{W}_n + 2\pi\mathsf{b}^2 \operatorname{Log}\left(\frac{\Phi_{\mathsf{b}}\left(\frac{y_U}{2\pi\mathsf{b}}\right)^2 \Phi_{\mathsf{b}}\left(\frac{y_W}{2\pi\mathsf{b}}\right)}{\Phi_{\mathsf{b}}\left(\frac{y_1}{2\pi\mathsf{b}}\right) \cdots \Phi_{\mathsf{b}}\left(\frac{y_p}{2\pi\mathsf{b}}\right)},\right)$$

  where Q_n and $\mathcal{W}_n$ are like in Theorem 4.13.

The following lemma establishes a "parity property" for the difference between classical and quantum dilogarithms on the horizontal band $\mathbb{R} + i(0, \pi)$.

Lemma 4.33. *For all* $\mathsf{b} \in (0,1)$ *and all* $y \in \mathbb{R} + i(0,\pi)$,

$$\Re\left(\mathrm{Log}\left(\Phi_{\mathsf{b}}\left(\frac{-\overline{y}}{2\pi\mathsf{b}}\right)\right) - \left(\frac{-i}{2\pi\mathsf{b}^2}\mathrm{Li}_2(-e^{-\overline{y}})\right)\right) = \Re\left(\mathrm{Log}\left(\Phi_{\mathsf{b}}\left(\frac{y}{2\pi\mathsf{b}}\right)\right) - \left(\frac{-i}{2\pi\mathsf{b}^2}\mathrm{Li}_2(-e^{y})\right)\right).$$

Proof. Let $\mathsf{b} \in (0,1)$ and $y \in \mathbb{R} + i(0,\pi)$.

From the fact that Li_2 is real-analytic and Proposition 2.41 (1) applied to $z = -e^y$, we have

$$\begin{aligned}\overline{\exp\left(\frac{-i}{2\pi\mathsf{b}^2}\mathrm{Li}_2(-e^{-\overline{y}})\right)} &= \exp\left(\frac{i}{2\pi\mathsf{b}^2}\mathrm{Li}_2(-e^{-y})\right)\\ &= \exp\left(\frac{i}{2\pi\mathsf{b}^2}\left(-\mathrm{Li}_2(-e^{y}) - \frac{\pi^2}{6} - \frac{y^2}{2}\right)\right)\\ &= \exp\left(\frac{-i}{2\pi\mathsf{b}^2}\mathrm{Li}_2(-e^{y})\right)\exp\left(\frac{-i\pi}{12\mathsf{b}^2}\right)\exp\left(\frac{-iy^2}{4\pi\mathsf{b}^2}\right).\end{aligned}$$

Moreover, from Theorem 3.36 (1) and (2), we have

$$\overline{\Phi_{\mathsf{b}}\left(\frac{-\overline{y}}{2\pi\mathsf{b}}\right)} = \frac{1}{\Phi_{\mathsf{b}}\left(\frac{-y}{2\pi\mathsf{b}}\right)} = \Phi_{\mathsf{b}}\left(\frac{y}{2\pi\mathsf{b}}\right)\exp\left(-i\frac{\pi}{12}(\mathsf{b}^2+\mathsf{b}^{-2})\right)\exp\left(i\pi\left(\frac{y}{2\pi\mathsf{b}}\right)^2\right).$$

Therefore

$$\overline{\mathrm{Log}\left(\Phi_{\mathsf{b}}\left(\frac{-\overline{y}}{2\pi\mathsf{b}}\right)\right) - \left(\frac{-i}{2\pi\mathsf{b}^2}\mathrm{Li}_2(-e^{-\overline{y}})\right)} = \mathrm{Log}\left(\Phi_{\mathsf{b}}\left(\frac{y}{2\pi\mathsf{b}}\right)\right) - \left(\frac{-i}{2\pi\mathsf{b}^2}\mathrm{Li}_2(-e^{y})\right) - \frac{i\pi}{12}\mathsf{b}^2,$$

and the statement follows. □

As a consequence, we can bound uniformly the difference between classical and quantum dilogarithms on compact horizontal bands above the horizontal axis.

Lemma 4.34. *For all* $\delta > 0$*, there exists a constant* $B_\delta > 0$ *such that for all* $\mathsf{b} \in (0,1)$ *and all* $y \in \mathbb{R} + i[\delta, \pi - \delta]$,

$$\left|\Re\left(\mathrm{Log}\left(\Phi_{\mathsf{b}}\left(\frac{y}{2\pi\mathsf{b}}\right)\right) - \left(\frac{-i}{2\pi\mathsf{b}^2}\mathrm{Li}_2(-e^{y})\right)\right)\right| \leqslant B_\delta\mathsf{b}^2.$$

Moreover, B_δ *is of the form* $B_\delta = C/\delta + C'$ *with* $C, C' > 0$.

The proof of Lemma 4.34 is quite lengthy, but contains relatively classical calculus arguments. The key points are the fact that $\Im(y)$ is uniformly upper bounded by a quantity *strictly smaller* than π, and that we can restrict ourselves to $y \in (-\infty, 0] + i[\delta, \pi - \delta]$ (thanks to Lemma 4.33) which implies that $\Re(y)$ is uniformly upper bounded by 0. The necessity of this last remark stems from the fact that the state variable y must be integrated on a contour with *unbounded real part* in the definition of the Teichmüller TQFT, whereas the contour is usually bounded when studying the volume conjecture for the colored Jones polynomials. Compare with [AH06, Lemma 3]. The parity trick of Lemma 4.33 and its application to an unbounded contour are the main technical novelties compared with the methods of [AH06].

Proof. Let $\delta > 0$. In the following proof, $y = x + id$ will denote a generic element in $(-\infty, 0] + i[\delta, \pi - \delta]$, with $x \in (-\infty, 0], d \in [\delta, \pi - \delta]$. We remark that we only need to prove the statement for $y \in (-\infty, 0] + i[\delta, \pi - \delta]$, thanks to Lemma 4.33.

We first compute, for any $\mathsf{b} \in (0,1)$ and $y \in \mathbb{R} + i[\delta, \pi - \delta]$:

$$\begin{aligned}\operatorname{Log}\,\Phi_{\mathsf{b}}\left(\frac{y}{2\pi\mathsf{b}}\right) &= \int_{w\in\Omega_{R\mathsf{b}}} \frac{\exp\left(-i\frac{yw}{\pi\mathsf{b}}\right) dw}{4w\sinh(\mathsf{b}w)\sinh(\mathsf{b}^{-1}w)} \\ &= \int_{v\in\Omega_R} \frac{\exp\left(-i\frac{yv}{\pi}\right) dv}{4v\sinh(\mathsf{b}^2 v)\sinh(v)} \\ &= \frac{1}{\mathsf{b}^2}\int_{v\in\Omega_R} \frac{\exp\left(-i\frac{yv}{\pi}\right)}{4v^2\sinh(v)} \frac{(v\mathsf{b}^2)}{\sinh(v\mathsf{b}^2)}\, dv,\end{aligned}$$

where the first equality comes from the definition of Φ_{b} (choosing the integration contour $\Omega_{R\mathsf{b}}$), the second one comes from the change of variables $v = \frac{w}{\mathsf{b}}$ and the last one is a simple re-writing.

Next, we remark that there exists a constant $\sigma_R > 0$ such that $|(\frac{v}{\sinh(v)})''| \leqslant \sigma_R$ for all $v \in \mathbb{R} \cup D_R$, where D_R is the upper half disk of radius R. Indeed, note first that sinh is non-zero everywhere on $\mathbb{R} \cup D_R$. Then a quick computation yields $\left(\frac{v}{\sinh(v)}\right)'' = \dfrac{v(1+\cosh(v)^2) - 2\sinh(v)\cosh(v)}{\sinh(v)^3}$, which is well-defined and continuous on $\mathbb{R} \cup D_R$, has a limit of $-1/3$ at $v = 0$ and has a zero limit in $v \in \mathbb{R}, v \to \pm\infty$. The boundedness on $\mathbb{R} \cup D_R$ follows.

Now, it follows from Taylor's theorem that for every $\mathsf{b} \in (0,1)$ and every $v \in \Omega_R$,

$$\frac{(v\mathsf{b}^2)}{\sinh(v\mathsf{b}^2)} = 1 + (v\mathsf{b}^2)^2\epsilon(v\mathsf{b}^2),$$

where $\epsilon(v\mathsf{b}^2) := \int_0^1 (1-t)\left(\frac{z}{\sinh(z)}\right)''(v\mathsf{b}^2 t)\, dt$. It then follows from the previous paragraph that $|\epsilon(v\mathsf{b}^2)| \leqslant \sigma_R$ for every $\mathsf{b} \in (0,1)$ and every $v \in \Omega_R$.

Recall from Proposition 2.41 (2) that for all $\mathsf{b} \in (0,1)$ and all $y \in \mathbb{R} + i[\delta, \pi - \delta]$,

$$\frac{1}{\mathsf{b}^2}\int_{v\in\Omega_R} \frac{\exp\left(-i\frac{yv}{\pi}\right)}{4v^2\sinh(v)}\, dv = \frac{-i}{2\pi\mathsf{b}^2}\operatorname{Li}_2(-e^y).$$

Therefore we can write for all $\mathsf{b} \in (0,1)$ and all $y \in \mathbb{R} + i[\delta, \pi - \delta]$:

$$\begin{aligned}\operatorname{Log}\left(\Phi_{\mathsf{b}}\left(\frac{y}{2\pi\mathsf{b}}\right)\right) - \left(\frac{-i}{2\pi\mathsf{b}^2}\operatorname{Li}_2(-e^y)\right) &= \frac{1}{\mathsf{b}^2}\int_{v\in\Omega_R} \frac{\exp\left(-i\frac{yv}{\pi}\right)}{4v^2\sinh(v)}\left(\frac{(v\mathsf{b}^2)}{\sinh(v\mathsf{b}^2)} - 1\right) dv \\ &= \frac{1}{\mathsf{b}^2}\int_{v\in\Omega_R} \frac{\exp\left(-i\frac{yv}{\pi}\right)}{4v^2\sinh(v)}(v\mathsf{b}^2)^2\epsilon(v\mathsf{b}^2)\, dv \\ &= \mathsf{b}^2\int_{v\in\Omega_R} \epsilon(v\mathsf{b}^2)\frac{\exp\left(-i\frac{yv}{\pi}\right)}{4\sinh(v)}\, dv.\end{aligned}$$

Now it suffices to prove that the quantity

$$\Re\left(\int_{v\in\Omega_R}\epsilon(v\mathsf{b}^2)\frac{\exp\left(-i\frac{yv}{\pi}\right)}{4\sinh(v)}\,dv\right)$$

is uniformly bounded on $y\in(-\infty,0]+i[\delta,\pi-\delta],\mathsf{b}\in(0,1)$. We will split this integral into three parts and prove that each part is uniformly bounded in this way.

Firstly, on the contour I_R^+, we have for all $\mathsf{b}\in(0,1)$ and all $y\in\mathbb{R}+i[\delta,\pi-\delta]$:

$$\begin{aligned}\left|\Re\left(\int_{v\in I_R^+}\epsilon(v\mathsf{b}^2)\frac{\exp\left(-i\frac{yv}{\pi}\right)}{4\sinh(v)}\,dv\right)\right| &\leqslant \left|\int_{v\in I_R^+}\epsilon(v\mathsf{b}^2)\frac{\exp\left(-i\frac{yv}{\pi}\right)}{4\sinh(v)}\,dv\right|\\ &\leqslant \int_R^\infty|\epsilon(v\mathsf{b}^2)|\frac{\left|\exp\left(-i\frac{yv}{\pi}\right)\right|}{4\sinh(v)}\,dv\\ &\leqslant \frac{\sigma_R}{4}\int_R^\infty\frac{\exp\left(\frac{\Im(y)v}{\pi}\right)}{\sinh(v)}\,dv\\ &\leqslant \frac{\sigma_R}{4}\int_R^\infty\frac{\exp\left(\frac{(\pi-\delta)v}{\pi}\right)}{\frac{1-e^{-2R}}{2}e^v}\,dv\\ &= \frac{\pi\sigma_R e^{-\frac{\delta R}{\pi}}}{2\delta(1-e^{-2R})},\end{aligned}$$

where in the last inequality we used the fact that $\frac{1-e^{-2R}}{2}e^v\leqslant\sinh(v)$ for all $v\geqslant R$.

Secondly, on the contour I_R^-, we have similarly for all $\mathsf{b}\in(0,1)$ and all $y\in\mathbb{R}+i[\delta,\pi-\delta]$:

$$\begin{aligned}\left|\Re\left(\int_{v\in I_R^-}\epsilon(v\mathsf{b}^2)\frac{\exp\left(-i\frac{yv}{\pi}\right)}{4\sinh(v)}\,dv\right)\right| &\leqslant \left|\int_{v\in I_R^-}\epsilon(v\mathsf{b}^2)\frac{\exp\left(-i\frac{yv}{\pi}\right)}{4\sinh(v)}\,dv\right|\\ &\leqslant \int_{-\infty}^{-R}|\epsilon(v\mathsf{b}^2)|\frac{\left|\exp\left(-i\frac{yv}{\pi}\right)\right|}{4|\sinh(v)|}\,dv\\ &= \int_R^\infty|\epsilon(-v\mathsf{b}^2)|\frac{\left|\exp\left(i\frac{yv}{\pi}\right)\right|}{4\sinh(v)}\,dv\\ &\leqslant \frac{\sigma_R}{4}\int_R^\infty\frac{\exp\left(\frac{-\Im(y)v}{\pi}\right)}{\sinh(v)}\,dv\\ &\leqslant \frac{\sigma_R}{4}\int_R^\infty\frac{1}{\frac{1-e^{-2R}}{2}e^v}\,dv\\ &= \frac{\sigma_R e^{-R}}{2(1-e^{-2R})}\\ &= \frac{\sigma_R}{4\sinh(R)}.\end{aligned}$$

Finally, to obtain the bound on the contour Λ_R, we will need the assumption that $y\in(-\infty,0]+i[\delta,\pi-\delta]$, since the upper bound will depend on $\Re(y)$. Moreover, we will use the fact that since $|\sinh|$ is a continuous non-zero function on the contour Λ_R, it is lower

bounded by a constant $s_R > 0$ on this countour. We then obtain, for all $\mathsf{b} \in (0,1)$ and all $y \in (-\infty, 0] + i[\delta, \pi - \delta]$:

$$\begin{aligned}
\left| \Re\left(\int_{v \in \Lambda_R} \epsilon(v\mathsf{b}^2) \frac{\exp\left(-i\frac{yv}{\pi}\right)}{4\sinh(v)}\, dv \right) \right| &\leqslant \left| \int_{v \in \Lambda_R} \epsilon(v\mathsf{b}^2) \frac{\exp\left(-i\frac{yv}{\pi}\right)}{4\sinh(v)}\, dv \right| \\
&\leqslant \int_{v \in \Lambda_R} |\epsilon(v\mathsf{b}^2)| \frac{\left|\exp\left(-i\frac{yv}{\pi}\right)\right|}{4|\sinh(v)|}\, dv \\
&\leqslant \frac{\sigma_R}{4s_R} \int_{v \in \Lambda_R} \exp\left(\Re\left(-i\frac{yv}{\pi}\right)\right) dv \\
&= \frac{\sigma_R}{4s_R} \int_{v \in \Lambda_R} \exp\left(\frac{\Re(y)\Im(v) + \Im(y)\Re(v)}{\pi}\right) dv \\
&\leqslant \frac{\sigma_R}{4s_R} (\pi R) \exp\left(\frac{0 + (\pi - \delta)R}{\pi}\right) \\
&\leqslant \frac{\sigma_R \pi R e^R}{4s_R},
\end{aligned}$$

where the fourth inequality is due to the fact that $\Re(y) \leqslant 0$, $\Im(v) \geqslant 0$, $0 < \Im(y) \leqslant \pi - \delta$ and $\Re(v) \leqslant R$.

The lemma follows, by taking for example the constant

$$B_\delta := \frac{\pi \sigma_R e^{-\frac{\delta R}{\pi}}}{2\delta(1 - e^{-2R})} + \frac{\sigma_R}{4\sinh(R)} + \frac{\sigma_R \pi R e^R}{4s_R}.$$

□

The following lemma is simply a variant of Lemma 4.34 for compact horizontal bands with negative imaginary part.

Lemma 4.35. *For all $\delta > 0$, there exists a constant $B_\delta > 0$ (the same as in Lemma 4.34) such that for all $\mathsf{b} \in (0,1)$ and all $y \in \mathbb{R} - i[\delta, \pi - \delta]$,*

$$\left| \Re\left(\mathrm{Log}\left(\Phi_{\mathsf{b}}\left(\frac{y}{2\pi\mathsf{b}} \right) \right) - \left(\frac{-i}{2\pi\mathsf{b}^2} \mathrm{Li}_2(-e^y) \right) \right) \right| \leqslant B_\delta \mathsf{b}^2.$$

Proof. The result follows immediately from the fact that $\mathrm{Li}_2(\bar{\cdot}) = \overline{\mathrm{Li}_2(\cdot)}$, Theorem 3.36 (2) and Lemma 4.34. □

The following Proposition 4.36 will not actually be used in the proof of Theorem 4.22, but fits naturally in the current discussion.

Proposition 4.36. *For some constant $\rho' \in \mathbb{C}^*$, we have, as $\mathsf{b} \to 0^+$,*

$$\begin{aligned}
\int_{\mathcal{Y}^0} d\mathbf{y}\, e^{\frac{1}{2\pi\mathsf{b}^2} S_{\mathsf{b}}(\mathbf{y})} &= \int_{\mathcal{Y}^0} d\mathbf{y}\, e^{\frac{i\mathbf{y}^T Q_n \mathbf{y} + \mathbf{y}^T \mathcal{W}_n}{2\pi\mathsf{b}^2}} \frac{\Phi_{\mathsf{b}}\left(\frac{y_U}{2\pi\mathsf{b}}\right)^2 \Phi_{\mathsf{b}}\left(\frac{y_W}{2\pi\mathsf{b}}\right)}{\Phi_{\mathsf{b}}\left(\frac{y_1}{2\pi\mathsf{b}}\right) \cdots \Phi_{\mathsf{b}}\left(\frac{y_p}{2\pi\mathsf{b}}\right)} \\
&= e^{\frac{1}{2\pi\mathsf{b}^2} S(\mathbf{y}^{\mathbf{0}})} \left(\rho' \mathsf{b}^{p+2} \left(1 + o_{\mathsf{b}\to 0^+}(1)\right) + \mathcal{O}_{\mathsf{b}\to 0^+}(1) \right).
\end{aligned}$$

In particular,

$$2\pi\mathsf{b}^2 \log \left| \int_{\mathcal{Y}^0} d\mathbf{y}\, e^{\frac{1}{2\pi\mathsf{b}^2} S_{\mathsf{b}}(\mathbf{y})} \right| \underset{\mathsf{b}\to 0^+}{\longrightarrow} \Re S(\mathbf{y}^{\mathbf{0}}) = -\mathrm{Vol}(S^3 \setminus K_n).$$

Proof. The second statement follows from the first one from the fact that the behaviour of

$$\left(\rho' \mathsf{b}^{p+2} \left(1 + o_{\mathsf{b}\to 0^+}(1)\right) + \mathcal{O}_{\mathsf{b}\to 0^+}(1)\right)$$

is polynomial in b as $\mathsf{b} \to 0^+$.

To prove the first statement, we will split the integral on $\mathcal{Y}^0$ into two parts, one on the compact contour γ from before and the other on the unbounded contour $\mathcal{Y}^0 \setminus \gamma$.

First we notice that there exists a $\delta > 0$ such that for all $\mathbf{y} = (y_1, \dots, y_p, y_U, y_W)$ in $\mathcal{Y}^0$, $\Im(y_1), \dots \Im(y_p) \in [-(\pi - \delta), -\delta]$ and $\Im(y_U), \Im(y_W) \in [\delta, \pi - \delta]$. From Lemmas 4.34 and 4.35, if we denote $(\eta_1, \dots, \eta_p, \eta_U, \eta_W) := (-1, \dots, -1, 2, 1)$, it then follows that:

$$\begin{aligned}
\left|\Re\left(\frac{1}{2\pi\mathsf{b}^2} S_{\mathsf{b}}(\mathbf{y}) - \frac{1}{2\pi\mathsf{b}^2} S(\mathbf{y})\right)\right| &= \left|\Re\left(\sum_{j=1}^{W} \eta_j \left(\mathrm{Log}\left(\Phi_{\mathsf{b}}\left(\frac{y_j}{2\pi\mathsf{b}}\right)\right) - \left(\frac{-i}{2\pi\mathsf{b}^2}\mathrm{Li}_2(-e^{y_j})\right)\right)\right)\right| \\
&\leqslant \sum_{j=1}^{W} |\eta_j| \left|\Re\left(\left(\mathrm{Log}\left(\Phi_{\mathsf{b}}\left(\frac{y_j}{2\pi\mathsf{b}}\right)\right) - \left(\frac{-i}{2\pi\mathsf{b}^2}\mathrm{Li}_2(-e^{y_j})\right)\right)\right)\right| \\
&\leqslant (p+3) B_\delta \mathsf{b}^2.
\end{aligned}$$

Let us now focus on the compact contour γ and prove that

$$\int_\gamma d\mathbf{y}\, e^{\frac{1}{2\pi\mathsf{b}^2} S_{\mathsf{b}}(\mathbf{y})} = e^{\frac{1}{2\pi\mathsf{b}^2} S(\mathbf{y^0})} \left(\rho' \mathsf{b}^{p+2} \left(1 + o_{\mathsf{b}\to 0^+}(1)\right) + \mathcal{O}_{\mathsf{b}\to 0^+}(1)\right).$$

From Proposition 4.30, by identifying $\lambda = \frac{1}{2\pi\mathsf{b}^2}$ and $\rho' = \rho(2\pi)^{\frac{p+2}{2}}$ it suffices to prove that

$$\int_\gamma d\mathbf{y}\, e^{\frac{1}{2\pi\mathsf{b}^2} S(\mathbf{y})} \left(e^{\frac{1}{2\pi\mathsf{b}^2}(S_{\mathsf{b}}(\mathbf{y}) - S(\mathbf{y}))} - 1\right) = e^{\frac{1}{2\pi\mathsf{b}^2} S(\mathbf{y^0})} \mathcal{O}_{\mathsf{b}\to 0^+}(1).$$

This last equality follows from the upper bound $(p+3)B_\delta \mathsf{b}^2$ of the previous paragraph, the compactness of γ, and Lemma 4.27.

Finally, let us prove that on the unbounded contour, we have

$$\int_{\mathcal{Y}^0 \setminus \gamma} d\mathbf{y}\, e^{\frac{1}{2\pi\mathsf{b}^2} S_{\mathsf{b}}(\mathbf{y})} = e^{\frac{1}{2\pi\mathsf{b}^2} S(\mathbf{y^0})} \mathcal{O}_{\mathsf{b}\to 0^+}(1).$$

Let A, B be the constants from Lemma 4.31. From the proof of Lemma 4.31, we have that for all $\mathsf{b} < (2\pi A)^{-1/2}$:

$$\int_{\mathcal{Y}^0 \setminus \gamma} d\mathbf{y}\, e^{\frac{1}{2\pi\mathsf{b}^2} \Re(S)(\mathbf{y})} \leqslant B e^{\frac{1}{2\pi\mathsf{b}^2} M}.$$

Moreover, for all $\mathsf{b} \in (0,1)$ and $\mathbf{y} \in \mathcal{Y}^0 \setminus \gamma$, we have $e^{\frac{1}{2\pi\mathsf{b}^2} \Re(S_{\mathsf{b}}(\mathbf{y}) - S(\mathbf{y}))} \leqslant e^{(p+3)B_\delta \mathsf{b}^2}$.
Let us denote $\upsilon := \frac{\Re(S)(\mathbf{y^0}) - M}{2}$. Thus, for all $b > 0$ smaller than both $(2\pi A)^{-1/2}$ and

$\left(\frac{\upsilon}{2\pi(p+3)B_\delta}\right)^{1/4}$, we have:

$$\begin{aligned}\left|\int_{\mathcal{Y}^0\setminus\gamma} d\mathbf{y}\, e^{\frac{1}{2\pi\mathsf{b}^2}S_\mathsf{b}(\mathbf{y})}\right| &= \left|\int_{\mathcal{Y}^0\setminus\gamma} d\mathbf{y}\, e^{\frac{1}{2\pi\mathsf{b}^2}S(\mathbf{y})} e^{\frac{1}{2\pi\mathsf{b}^2}(S_\mathsf{b}(\mathbf{y})-S(\mathbf{y}))}\right| \\ &\leqslant \int_{\mathcal{Y}^0\setminus\gamma} d\mathbf{y}\, e^{\frac{1}{2\pi\mathsf{b}^2}\Re(S)(\mathbf{y})} e^{\frac{1}{2\pi\mathsf{b}^2}\Re(S_\mathsf{b}(\mathbf{y})-S(\mathbf{y}))} \\ &\leqslant B e^{\frac{1}{2\pi\mathsf{b}^2}M} e^{(p+3)B_\delta\mathsf{b}^2} \\ &\leqslant B e^{\frac{1}{2\pi\mathsf{b}^2}(M+\upsilon)} \\ &= e^{\frac{1}{2\pi\mathsf{b}^2}S(\mathbf{y^0})}\mathcal{O}_{\mathsf{b}\to 0^+}(1),\end{aligned}$$

which concludes the proof. □

4.6.6 Going from b to $\hbar$

Recall that for every $\mathsf{b} > 0$, we associate a corresponding parameter $\hbar := \mathsf{b}^2(1+\mathsf{b}^2)^{-2} > 0$.

For $\mathsf{b} > 0$, we define a new potential function $S'_\mathsf{b} \colon \mathcal{U} \to \mathbb{C}$, a holomorphic function on $p+2$ complex variables, by:

$$S'_\mathsf{b}(\mathbf{y}) := i\mathbf{y}^T Q_n \mathbf{y} + \mathbf{y}^T \mathcal{W}_n + 2\pi\hbar \operatorname{Log}\left(\frac{\Phi_\mathsf{b}\left(\frac{y_U}{2\pi\sqrt{\hbar}}\right)^2 \Phi_\mathsf{b}\left(\frac{y_W}{2\pi\sqrt{\hbar}}\right)}{\Phi_\mathsf{b}\left(\frac{y_1}{2\pi\sqrt{\hbar}}\right)\cdots\Phi_\mathsf{b}\left(\frac{y_p}{2\pi\sqrt{\hbar}}\right)}\right),$$

where Q_n and $\mathcal{W}_n$ are like in Theorem 4.13.

Remark 4.37. Notice that

$$|\mathfrak{J}_{X_n}(\hbar,0)| = \left|\left(\frac{1}{2\pi\sqrt{\hbar}}\right)^{p+3}\int_{\mathcal{Y}^0} d\mathbf{y}\, e^{\frac{1}{2\pi\hbar}S'_\mathsf{b}(\mathbf{y})}\right|.$$

Indeed, this follows from taking $\tau = \tau^0$ in Theorem 4.20, where τ^0 is defined at the end of the proof of Lemma 4.29.

The following Lemma 4.38 will play a similar role as Lemmas 4.34 and 4.35, but its proof is fortunately shorter.

Lemma 4.38. *For all $\delta \in (0, \frac{\pi}{2})$, there exist constants $c_\delta, C_\delta > 0$ such that for all $\mathsf{b} \in (0, c_\delta)$ and all $y \in \mathbb{R} + i\left([-(\pi-\delta), -\delta] \cup [\delta, \pi-\delta]\right)$, we have:*

$$\left|\Re\left(\left(\frac{-i}{2\pi\mathsf{b}^2}\mathrm{Li}_2\left(-e^{y(1+\mathsf{b}^2)}\right)\right) - \left(\frac{-i}{2\pi\mathsf{b}^2}(1+\mathsf{b}^2)^2\mathrm{Li}_2(-e^y)\right)\right)\right| \leqslant C_\delta.$$

Proof. Let $\delta \in (0, \frac{\pi}{2})$. Let us define $c_\delta := \sqrt{\frac{\delta}{2(\pi-\delta)}}$, so that $(\pi-\delta)(1+c_\delta^2) = \pi - \delta/2$.

We consider the function

$$(x, d, u, \mathsf{b}) \mapsto \left|\operatorname{Log}\left(1 + e^{(x+id)(1+u\mathsf{b}^2)}\right)\right|,$$

which is continous and well-defined on $[-1,0]\times[\delta,\pi-\delta]\times[0,1]\times[0,c_\delta]$. Indeed, since

$$d(1+u\mathsf{b}^2)\leqslant(\pi-\delta)(1+c_\delta^2)=\pi-\delta/2<\pi,$$

the exponential will then never be -1. Let us denote $L_\delta>0$ the maximum of this function.

Let us define

$$\Delta(\mathsf{b},y):=\Im\left(\mathrm{Li}_2\left(-e^{y(1+\mathsf{b}^2)}\right)-(1+\mathsf{b}^2)^2\mathrm{Li}_2(-e^y)\right)$$

for all $\mathsf{b}\in(0,1)$ and all $y\in\mathbb{R}+i\left([-(\pi-\delta),-\delta]\cup[\delta,\pi-\delta]\right)$.

We first remark a parity property like in Lemma 4.33. Indeed, it similarly follows from Proposition 2.41 (1) that $\Delta(\mathsf{b},y)=-\Delta(\mathsf{b},-y)=-\Delta(\mathsf{b},\overline{y})=\Delta(\mathsf{b},-\overline{y})$ for all $\mathsf{b}\in(0,1)$ and all $y\in\mathbb{R}+i\left([-(\pi-\delta),-\delta]\cup[\delta,\pi-\delta]\right)$. Thus we can consider that $y\in\mathbb{R}_{\leqslant0}+i[\delta,\pi-\delta]$ in the remainder of the proof.

It then follows from a change of variables that for all $\mathsf{b}\in(0,1)$ and all $y\in\mathbb{R}_{\leqslant0}+i[\delta,\pi-\delta]$,

$$\begin{aligned}\Delta(\mathsf{b},y)&=\Im\left(-\left(\int_0^1\mathrm{Log}\left(1+e^{y(1+u\mathsf{b}^2)}\right)(-y\mathsf{b}^2)\,du\right)-(2\mathsf{b}^2+\mathsf{b}^4)\mathrm{Li}_2(-e^y)\right)\\&=-\mathsf{b}^2\Im\left(y\left(\int_0^1\mathrm{Log}\left(1+e^{y(1+u\mathsf{b}^2)}\right)du\right)+(2+\mathsf{b}^2)\mathrm{Li}_2(-e^y)\right).\end{aligned}$$

We will bound $\left|\dfrac{\Delta(\mathsf{b},y)}{-\mathsf{b}^2}\right|$ separately for $\Re(y)\in[-1,0]$ and then for $\Re(y)\in(-\infty,-1)$.

Firstly, we have for all $y\in[-1,0]+i[\delta,\pi-\delta]$ and all $\mathsf{b}\in(0,c_\delta)$:

$$\begin{aligned}\left|\frac{\Delta(\mathsf{b},y)}{-\mathsf{b}^2}\right|&\leqslant|y|\left(\int_0^1\left|\mathrm{Log}\left(1+e^{y(1+u\mathsf{b}^2)}\right)\right|du\right)+(2+\mathsf{b}^2)|\mathrm{Li}_2(-e^y)|\\&\leqslant\sqrt{1+(\pi-\delta)^2}L_\delta+3L'_\delta,\end{aligned}$$

where L'_δ is the maximum of $(x,d)\mapsto|\mathrm{Li}_2(-e^y)|$ on $(-\infty,0]\times[\delta,\pi-\delta]$.

Secondly, let $y=x+id\in(-\infty,-1]+i[\delta,\pi-\delta]$ and $\mathsf{b}\in(0,c_\delta)$. For all $u\in[0,1]$, we have $\left|e^{y(1+u\mathsf{b}^2)}\right|<1$, therefore (from the triangle inequality on the Taylor expansion):

$$\left|\mathrm{Log}\left(1+e^{y(1+u\mathsf{b}^2)}\right)\right|\leqslant-\log\left(1-\left|e^{y(1+u\mathsf{b}^2)}\right|\right)=\log\left(1+\frac{e^{x(1+u\mathsf{b}^2)}}{1-e^{x(1+u\mathsf{b}^2)}}\right)\leqslant\frac{e^{2x}}{1-e^{2x}},$$

hence

$$\begin{aligned}\left|\frac{\Delta(\mathsf{b},y)}{-\mathsf{b}^2}\right|&\leqslant|y|\left(\int_0^1\left|\mathrm{Log}\left(1+e^{y(1+u\mathsf{b}^2)}\right)\right|du\right)+(2+\mathsf{b}^2)|\mathrm{Li}_2(-e^y)|\\&\leqslant\sqrt{x^2+(\pi-\delta)^2}\frac{e^{2x}}{1-e^{2x}}+3L'_\delta\\&\leqslant E_\delta+3L'_\delta,\end{aligned}$$

where E_δ is the maximum of the function $(-\infty,-1]\ni x\mapsto\sqrt{x^2+(\pi-\delta)^2}\dfrac{e^{2x}}{1-e^{2x}}$.

We now conclude the proof by defining $C_\delta:=\frac{1}{2\pi}\max\{\sqrt{1+(\pi-\delta)^2}L_\delta+3L'_\delta,E_\delta+3L'_\delta\}$. □

We can now state and prove the final piece of the proof of Theorem 4.22.

Proposition 4.39. *For the constant $\rho' \in \mathbb{C}^*$ defined in Proposition 4.36, we have, as $\hbar \to 0^+$,*

$$\begin{aligned}\int_{\mathcal{Y}^0} d\mathbf{y}\, e^{\frac{1}{2\pi\hbar}S'_{\mathsf{b}}(\mathbf{y})} &= \int_{\mathcal{Y}^0} d\mathbf{y}\, e^{\frac{i\mathbf{y}^T Q_n \mathbf{y} + \mathbf{y}^T \mathcal{W}_n}{2\pi\hbar}} \frac{\Phi_{\mathsf{b}}\left(\frac{y_U}{2\pi\sqrt{\hbar}}\right)^2 \Phi_{\mathsf{b}}\left(\frac{y_W}{2\pi\sqrt{\hbar}}\right)}{\Phi_{\mathsf{b}}\left(\frac{y_1}{2\pi\sqrt{\hbar}}\right)\cdots\Phi_{\mathsf{b}}\left(\frac{y_p}{2\pi\sqrt{\hbar}}\right)} \\ &= e^{\frac{1}{2\pi\hbar}S(\mathbf{y^0})}\left(\rho'\hbar^{\frac{p+2}{2}}\left(1+o_{\hbar\to 0^+}(1)\right)+\mathcal{O}_{\hbar\to 0^+}(1)\right).\end{aligned}$$

In particular,

$$(2\pi\hbar)\log\left|\int_{\mathcal{Y}^0} d\mathbf{y}\, e^{\frac{1}{2\pi\hbar}S'_{\mathsf{b}}(\mathbf{y})}\right| \underset{\hbar\to 0^+}{\longrightarrow} \Re S(\mathbf{y^0}) = -\mathrm{Vol}(S^3\setminus K_n).$$

Proof. The proof will be similar to the one of Proposition 4.36 (notably, the second statement follows from the first one in the exact same way), but will need also Lemma 4.38 to bound an extra term. Let us prove the first statement.

Let $\delta > 0$ such that the absolute value of the imaginary parts of the coordinates of any $\mathbf{y} \in \mathcal{Y}^0$ lie in $[\delta, \pi-\delta]$. Let us again denote $(\eta_1,\dots,\eta_p,\eta_U,\eta_W) := (-1,\dots,-1,2,1)$. Then for all $\mathbf{y}\in\mathcal{Y}^0$ and all $\mathsf{b}\in(0,c_\delta)$, it follows from Lemmas 4.34, 4.35 and 4.38 that

$$\begin{aligned}\left|\Re\left(\frac{1}{2\pi\hbar}S'_{\mathsf{b}}(\mathbf{y})-\frac{1}{2\pi\hbar}S(\mathbf{y})\right)\right| &= \left|\Re\left(\sum_{j=1}^W \eta_j\left(\mathrm{Log}\left(\Phi_{\mathsf{b}}\left(\frac{y_j}{2\pi\sqrt{\hbar}}\right)\right)-\left(\frac{-i}{2\pi\hbar}\mathrm{Li}_2(-e^{y_j})\right)\right)\right)\right| \\ &\leqslant \sum_{j=1}^W|\eta_j|\left|\Re\left(\left(\mathrm{Log}\left(\Phi_{\mathsf{b}}\left(\frac{y_j(1+\mathsf{b}^2)}{2\pi\mathsf{b}}\right)\right)-\left(\frac{-i}{2\pi\mathsf{b}^2}\mathrm{Li}_2(-e^{y_j(1+\mathsf{b}^2)})\right)\right)\right)\right| \\ &\quad+\sum_{j=1}^W|\eta_j|\left|\Re\left(\left(\frac{-i}{2\pi\mathsf{b}^2}\mathrm{Li}_2(-e^{y_j(1+\mathsf{b}^2)})\right)-\left(\frac{-i}{2\pi\mathsf{b}^2}(1+\mathsf{b}^2)^2\mathrm{Li}_2(-e^{y_j})\right)\right)\right| \\ &\leqslant (p+3)\left(B_{\frac{\delta}{2}}\mathsf{b}^2+C_\delta\right)\leqslant(p+3)\left(B_{\frac{\delta}{2}}+C_\delta\right).\end{aligned}$$

The remainder of the proof is now the same as for Proposition 4.36, by identifying $\lambda=\frac{1}{2\pi\hbar}$ and taking $\hbar$ small enough so that the associated b satisfies

$$0<\mathsf{b}<\min\left\{c_\delta,(2\pi A)^{-1/2},\left(\frac{\upsilon}{2\pi(p+3)(B_{\delta/2}+C_\delta)}\right)^{1/2}\right\}.$$

□

4.6.7 Conclusion and comments

Proof of Theorem 4.22. The second equality follows from Remark 4.37 and Proposition 4.39, and the first equality follows from the identity

$$J_{X_n}(\hbar,x) = 2\pi\sqrt{\hbar}\,\mathfrak{J}_{X_n}(\hbar,(2\pi\sqrt{\hbar})x).$$

□

Some comments are in order.

- The various upper bounds we constructed were far from optimal, since we were mostly interested to prove that the *exponential decrease rate* yielded the hyperbolic volume. Anyone interested in computing a more detailed asymptotic expansion of $\mathfrak{J}_{X_n}(\hbar, 0)$ (looking for the *complex volume*, the *Reidemeister torsions* or potential deeper terms such as the n-loop invariants of [DG13]) would probably need to develop the estimations of Lemmas 4.31, 4.34 and 4.38 at higher order and with sharper precision, as well as carefully study the coefficients appearing in Theorem 1.77.
- In this theory, the integration variables y_j in $\mathfrak{J}_{X_n}(\hbar, 0)$ lie in an *unbounded* part of $\mathbb{C}$, contrary to what happens for Kashaev's invariant or the colored Jones polynomials. This is why uniform bounds such as the ones of Lemmas 4.31, 4.34 and 4.38 were new but absolutely necessary technical difficulties to overcome to obtain the desired asymptotics. Since these results do not depend of the knot, triangulation or potential function S (assuming it has the same general form as in here), we hope that they can be of use to further studies of asymptotics of quantum invariants such as the Teichmüller TQFT. These techniques will be used again in Chapter 5.

4.7 The case of even twist knots

When the twist knot K_n has an even number of crossings, we can prove the same results as for the odd twist knots, which are:

- the construction of convenient H-triangulations and ideal triangulations (Section 4.7.1),
- the geometricity of the ideal triangulations (Section 4.7.2),
- the computation of the partition functions of the Teichmüller TQFT (Section 4.7.3),
- the volume conjecture as a consequence of geometricity (Section 4.7.4).

We tried to provide details of only the parts of proofs that differ from the case of odd twist knots. As the reader will see, most of these differences lie in explicit values and not in general processes of proof. As such, we expect that the techniques developed in the previous sections and adapted in this one can be generalized to several other families of knots in 3-manifolds.

4.7.1 Construction of triangulations

In the rest of this section we consider a twist knot K_n with n even, $n \geqslant 4$ (the case $n = 2$ will be treated in Remark 4.40). We proceed as in Section 4.2, and build an H-triangulation of (S^3, K_n) from a diagram of K_n. The first step is described in Figure 4.16. Note that D is once again an $(n+1)$-gon, and E is an $(n+2)$-gon.

From Figure 4.16 we go to Figure 4.17 and Figure 4.18 exactly as in Section 4.2.

Then we add a new edge (with simple full arrow) and cut D into u and D' (see Figure 4.19 (a)), and then we apply the bigon trick p times, where $p := \frac{n-2}{2}$. We finally obtain the polyhedron in Figure 4.19 (b).

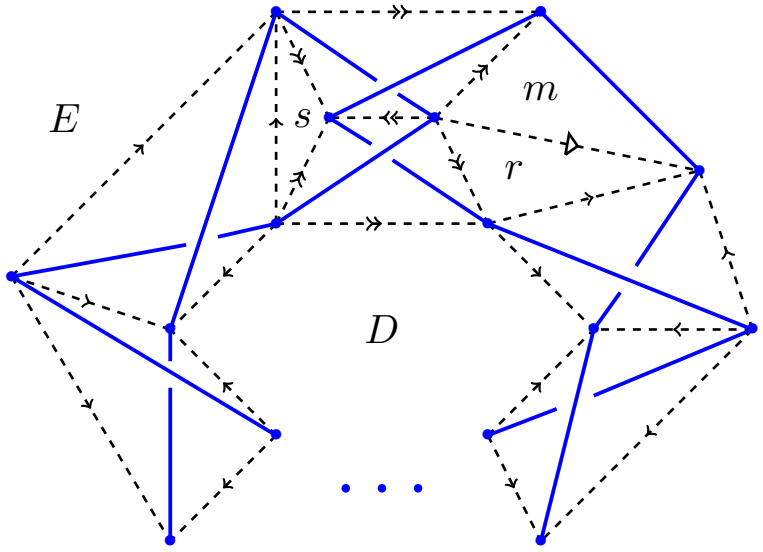

Figure 4.16: Building an H-triangulation from a diagram of K_n.

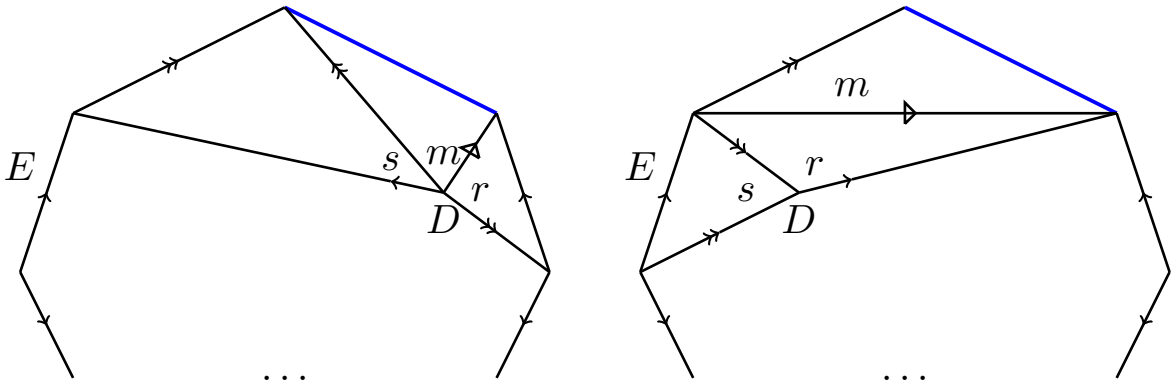

(a) (b)

Figure 4.17: Boundaries of B_+ and B_-.

We now chop off the quadrilateral made up of the two adjacent faces G (which are $(p+2)$-gons) and we add a new edge (double full arrow) and two new faces e_{p+1}, f_p. We triangulate the previous quadrilateral as in Figure 4.11 and we finally obtain a decomposition of S^3 in three polyhedra glued to one another, as described in Figure 4.20. Note that if $p = 1$, then $G = e_1 = e_p = f_0 = f_{p-1}$ and there is no tower.

We can then decompose the polyhedra in Figure 4.20 into ordered tetrahedra and obtain the H-triangulation of Figure 4.21. Along the way, in order to harmonize the notation with the small cases $(p = 0, 1)$, we did the following arrow replacements:

- full black simple arrow by simple arrow with circled 0,
- full black double arrow by simple arrow with circled $p + 1$,
- double arrow by simple arrow with circled p,
- full white arrow by double full white arrow.

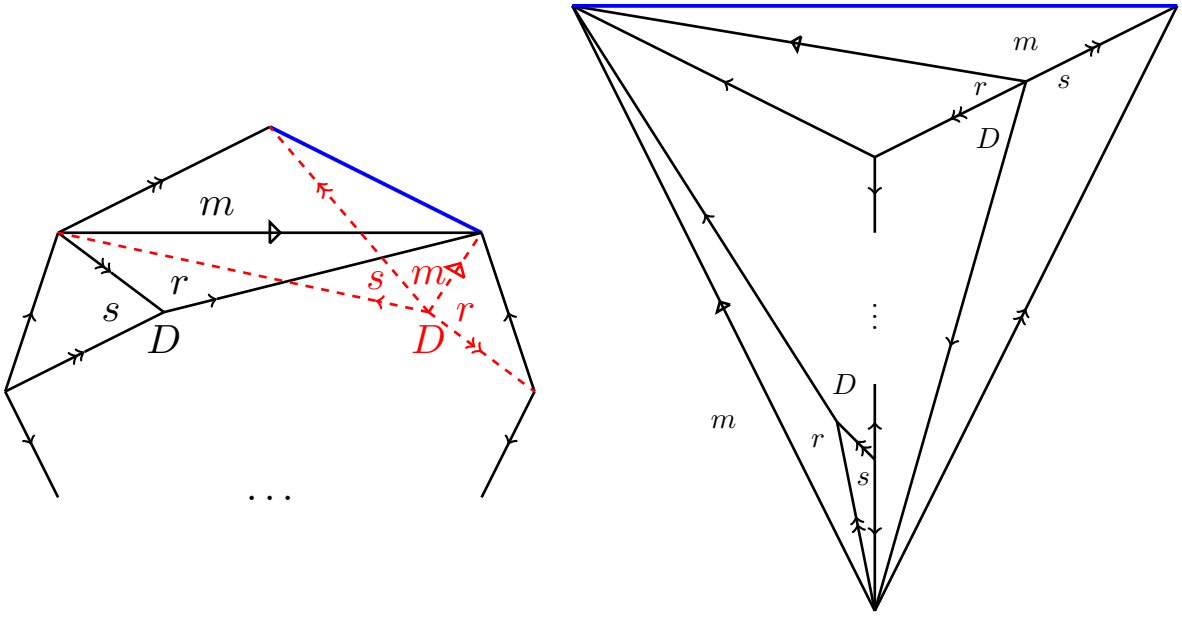

(a) (b)

Figure 4.18: A cellular decomposition of (S^3, K_n) as a polyhedron glued to itself.

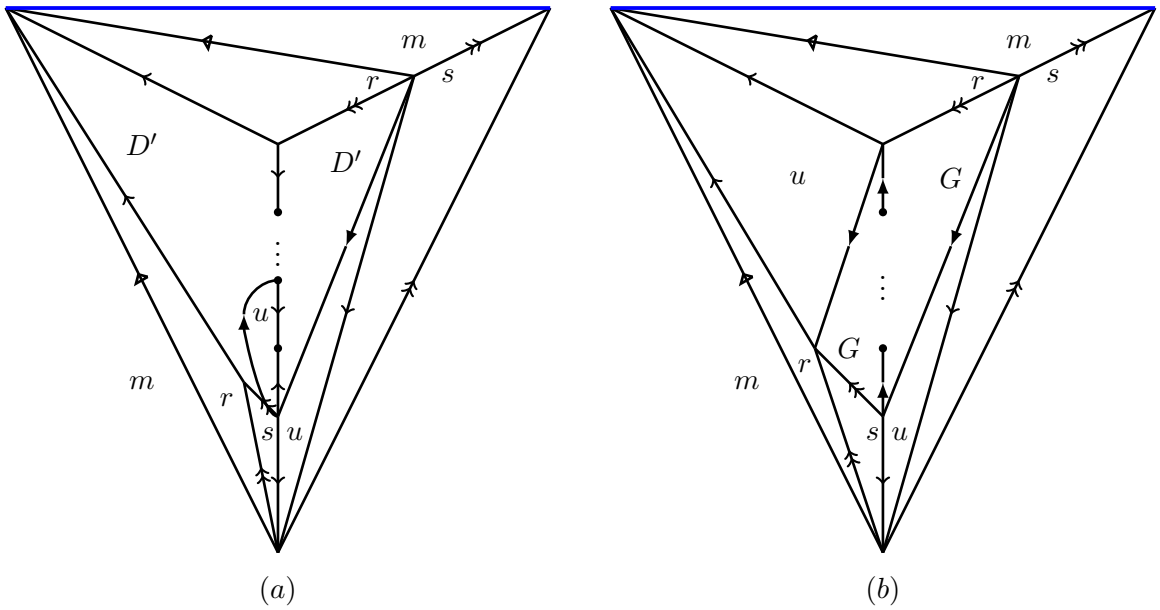

(a) (b)

Figure 4.19: A cellular decomposition of (S^3, K_n) before and after the bigon trick.

Moreover, we cut the previous polyehdron into $p+4$ tetrahedra, introducing new triangular faces v (behind e_{p+1}, r, u), g (behind f_p, s, u), s' (completing m, m, s), and $f_1, \ldots, f_{p-1}$ at each of the $p-1$ floors of the tower of Figure 4.20. We add the convention $f_0 = e_1$ to account for the case $p = 0$.

In the H-triangulation of Figure 4.21 there are

- 1 common vertex,

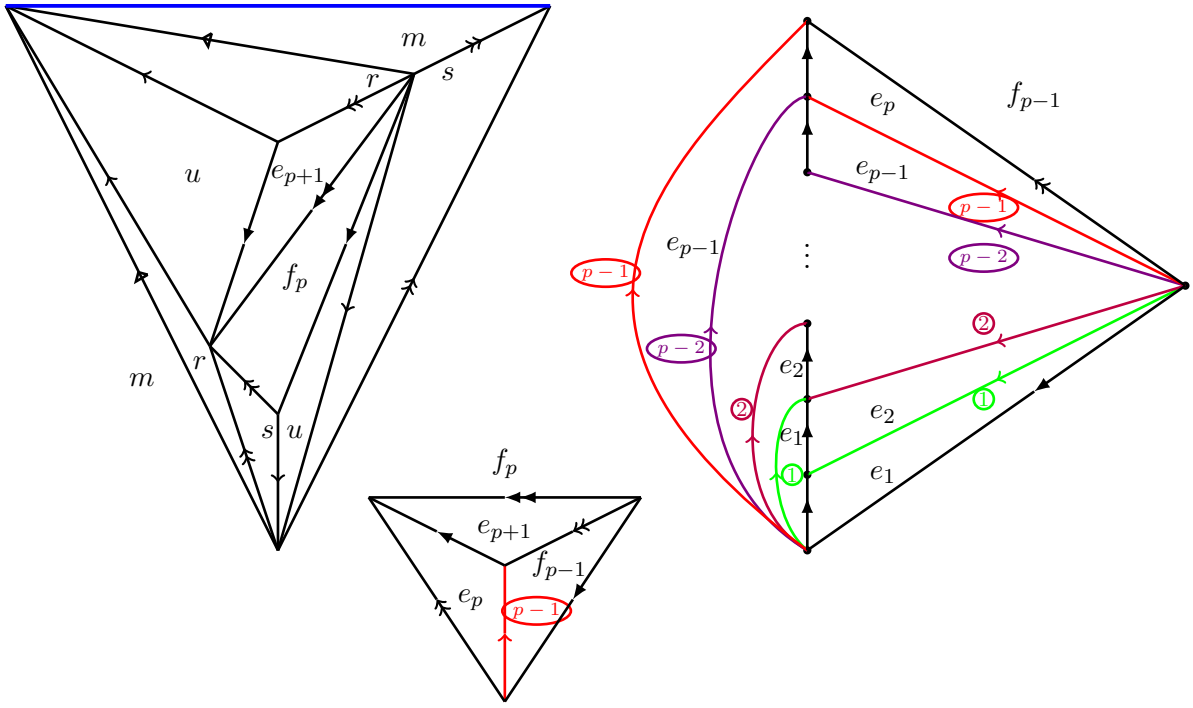

Figure 4.20: A flip move and a tower of tetrahedra.

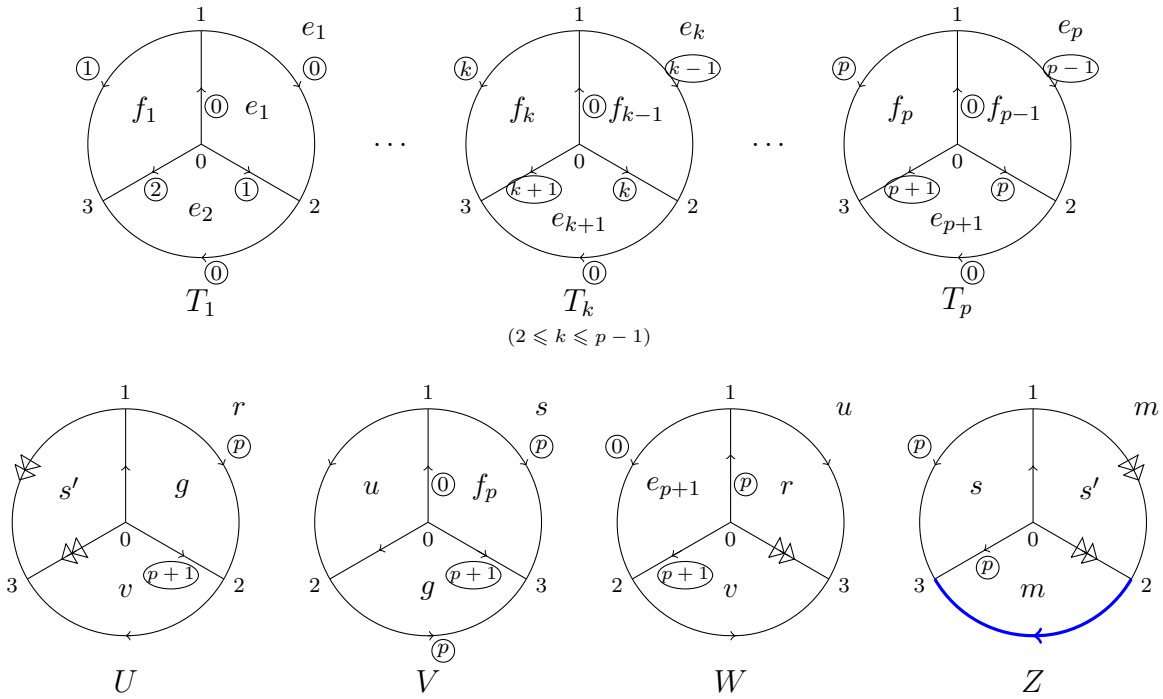

Figure 4.21: An H-triangulation for (S^3, K_n), n even, $n \geqslant 4$, with $p = \frac{n-2}{2}$.

- $p + 5 = \frac{n+8}{2}$ edges (simple arrow $\overrightarrow{e_s}$, double white triangle arrow $\overrightarrow{e_d}$, blue simple arrow $\overrightarrow{K_n}$, and the simple arrows $\overrightarrow{e_0}, \ldots, \overrightarrow{e_{p+1}}$ indexed by $0, \ldots, p+1$ in circles)
- $2p + 8 = n + 6$ faces $(e_1, \ldots, e_{p+1}, f_1, \ldots, f_p, g, m, r, s, s', u, v)$,

- $p+4 = \frac{n+6}{2}$ tetrahedra $(T_1, \dots, T_p, U, V, W, Z)$.

Finally, by collapsing the tetrahedron Z (like in the previous section) we obtain the ideal triangulation of $S^3 \setminus K_n$ described in Figure 4.22. We identified the face s' with s and the white triangle arrow with the arrow circled by p.

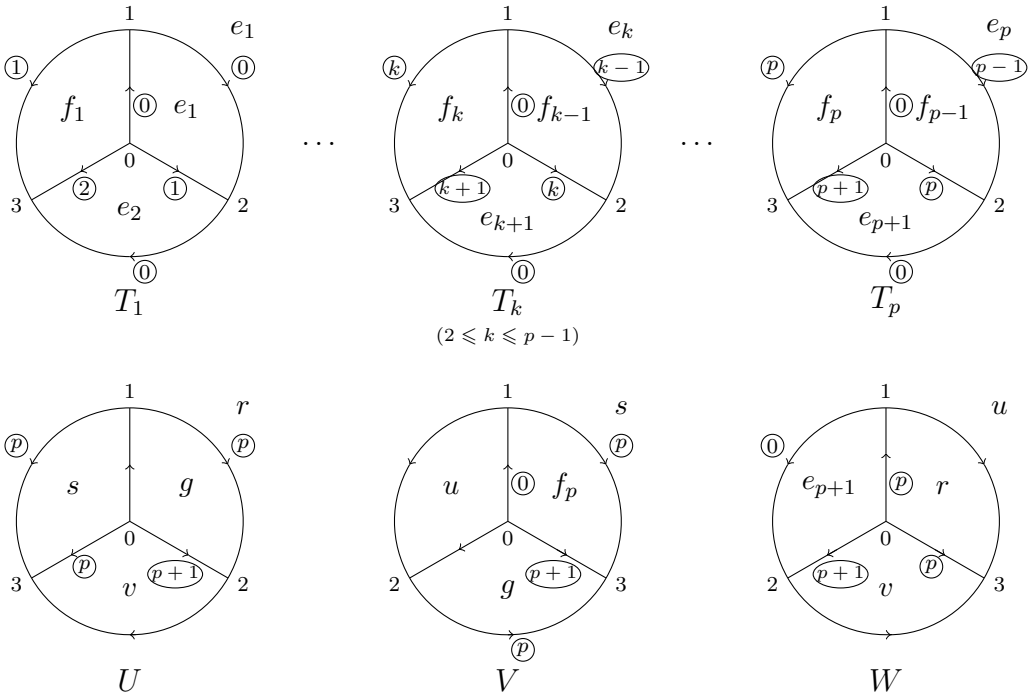

Figure 4.22: An ideal triangulation for $S^3 \setminus K_n$, n even, $n \geqslant 4$, with $p = \frac{n-2}{2}$.

In Figure 4.22 there are

- 1 common vertex,
- $p+3 = \frac{n+4}{2}$ edges (simple arrow $\overrightarrow{e_s}$ and the simple arrows $\overrightarrow{e_0}, \dots, \overrightarrow{e_{p+1}}$ indexed by $0, \dots, p+1$ in circles),
- $2p+6 = n+4$ faces $(e_1, \dots, e_{p+1}, f_1, \dots, f_p, g, r, s, u, v)$,
- $p+3 = \frac{n+4}{2}$ tetrahedra $(T_1, \dots, T_p, U, V, W)$.

Remark 4.40. When $n = 2$, i.e. $p = 0$ here, the triangulations of Figures 4.21 and 4.22 are still correct (with the convention $f_0 = e_1$), one just needs to stop the previous reasoning at Figure 4.19 (b) and collapse the bigon G into a segment.

In this case, the ideal triangulation X_2 of the figure-eight knot complement $S^3 \setminus K_2$ described in Figure 4.22 has three tetrahedra, although it is well-known that this knot complement has Matveev complexity 2 (see Example 2.7). The ideal triangulations of Figures 2.5 and 4.22 are actually related by a Pachner 3-2 move.

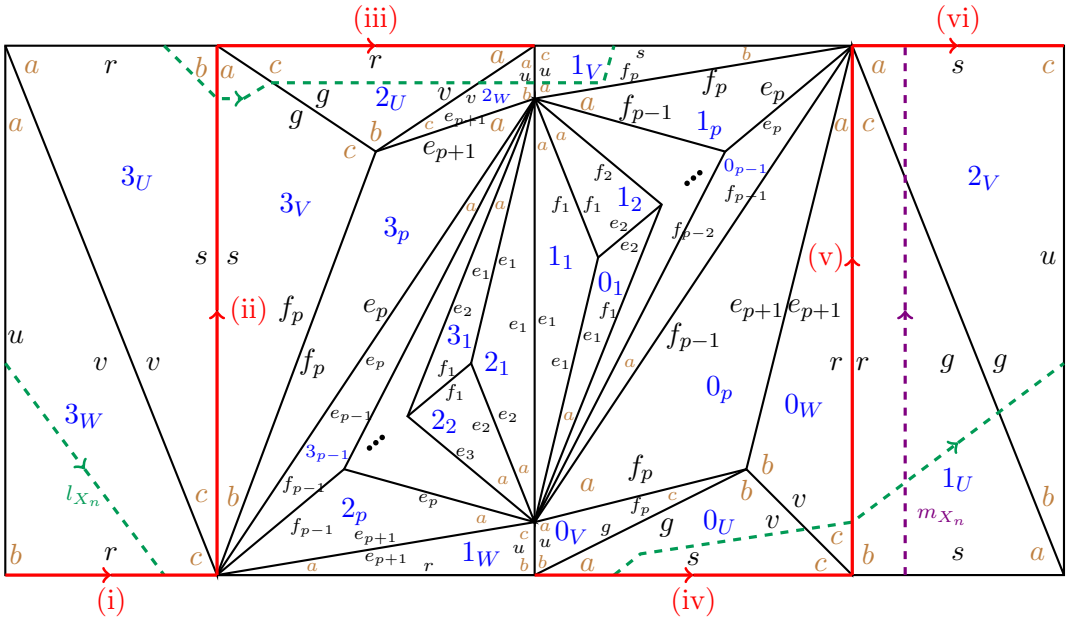

Figure 4.23: Triangulation of the boundary torus for the truncation of X_n, n even, with angles (brown), meridian curve m_{X_n} (violet, dashed), longitude curve l_{X_n} (green, dashed) and preferred longitude curve (i)$\cup\cdots\cup$(vi) (red).

4.7.2 Gluing equations and proving geometricity

As in Section 4.3.3, we constructed in Figure 4.23 a triangulation of the boundary torus $\partial\nu(K_n)$ from the datum in Figure 4.22. Here for the positive tetrahedra $T_1,\dots,T_p$ we only indicated the brown a angles for readability (the b and c follow clockwise). We also drew a meridian curve m_{X_n} in violet and dashed, a longitude curve l_{X_n} in green and dashed, and a preferred longitude curve (i)$\cup\cdots\cup$(vi) in red (one can check it is indeed a preferred longitude in Figure 4.24).

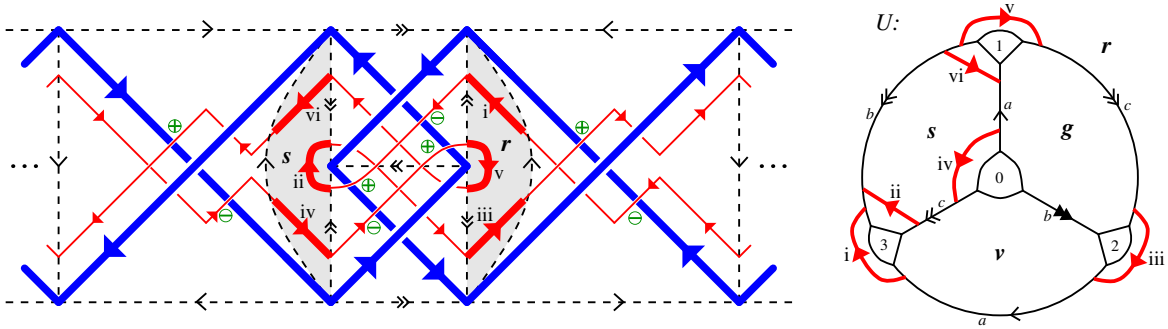

Figure 4.24: A preferred longitude (i) $\cup\cdots\cup$ (vi) (in red) for the even twist knot K_n, seen in $S^3\setminus K_n$ (left) and on the truncated tetrahedron U (right).

Let us now list the angular and complex weight functions associated to edges of X_n. For $\alpha=(a_1,b_1,c_1,\dots,a_p,b_p,c_p,a_U,b_U,c_U,a_V,b_V,c_V,a_W,b_W,c_W)\in\mathcal{S}_{X_n}$ a shape structure on X_n, we compute the weights of each edge:

- $\omega_s(\alpha):=\omega_{X_n,\alpha}(\overrightarrow{e_s})=2a_U+b_V+c_V+a_W+b_W$

- $\omega_0(\alpha) := \omega_{X_n,\alpha}(\overrightarrow{e_0}) = 2a_1 + c_1 + 2a_2 + \cdots + 2a_p + a_V + c_W$
- $\omega_1(\alpha) := \omega_{X_n,\alpha}(\overrightarrow{e_1}) = 2b_1 + c_2$
- $\omega_k(\alpha) := \omega_{X_n,\alpha}(\overrightarrow{e_k}) = c_{k-1} + 2b_k + c_{k+1} \quad (\text{for } 2 \leqslant k \leqslant p-1)$
- $\omega_p(\alpha) := \omega_{X_n,\alpha}(\overrightarrow{e_p}) = c_{p-1} + 2b_p + b_U + 2c_U + a_V + b_V + a_W + c_W$
- $\omega_{p+1}(\alpha) := \omega_{X_n,\alpha}(\overrightarrow{e_{p+1}}) = c_p + b_U + c_V + b_W.$

For a complex shape structure $\widetilde{\mathbf{z}} = (z_1, \ldots, z_p, z_U, z_V, z_W) \in (\mathbb{R} + i\mathbb{R}_{>0})^{p+3}$, its complex weight functions are:

- $\omega_s^{\mathbb{C}}(\widetilde{\mathbf{z}}) := \omega_{X_n,\alpha}^{\mathbb{C}}(\overrightarrow{e_s}) = 2\mathrm{Log}(z_U) + \mathrm{Log}(z'_V) + \mathrm{Log}(z''_V) + \mathrm{Log}(z_W) + \mathrm{Log}(z'_W)$
- $\omega_0^{\mathbb{C}}(\widetilde{\mathbf{z}}) := \omega_{X_n,\alpha}^{\mathbb{C}}(\overrightarrow{e_0}) = 2\mathrm{Log}(z_1) + \mathrm{Log}(z'_1) + 2\mathrm{Log}(z_2) + \cdots + 2\mathrm{Log}(z_p) + \mathrm{Log}(z_V) + \mathrm{Log}(z''_W)$
- $\omega_1^{\mathbb{C}}(\widetilde{\mathbf{z}}) := \omega_{X_n,\alpha}^{\mathbb{C}}(\overrightarrow{e_1}) = 2\mathrm{Log}(z''_1) + \mathrm{Log}(z'_2)$
- $\omega_k^{\mathbb{C}}(\widetilde{\mathbf{z}}) := \omega_{X_n,\alpha}^{\mathbb{C}}(\overrightarrow{e_k}) = \mathrm{Log}(z'_{k-1}) + 2\mathrm{Log}(z''_k) + \mathrm{Log}(z'_{k+1}) \quad (\text{for } 2 \leqslant k \leqslant p-1)$
- $\omega_p^{\mathbb{C}}(\widetilde{\mathbf{z}}) := \omega_{X_n,\alpha}^{\mathbb{C}}(\overrightarrow{e_p}) = \mathrm{Log}(z'_{p-1}) + 2\mathrm{Log}(z''_p) + 2\mathrm{Log}(z'_U) + \mathrm{Log}(z''_U) + \mathrm{Log}(z_V) + \mathrm{Log}(z'_V) + \mathrm{Log}(z_W) + \mathrm{Log}(z''_W)$
- $\omega_{p+1}^{\mathbb{C}}(\widetilde{\mathbf{z}}) := \omega_{X_n,\alpha}^{\mathbb{C}}(\overrightarrow{e_{p+1}}) = \mathrm{Log}(z'_p) + \mathrm{Log}(z''_U) + \mathrm{Log}(z''_V) + \mathrm{Log}(z'_W).$

To the meridian curve m_{X_n} and the longitude curve l_{X_n} are associated angular holonomies

$$m_{X_n}(\alpha) := a_V - a_U, \quad l_{X_n}(\alpha) := 2(a_W - b_V),$$

and one possible completeness equation is once again (from the meridian curve):

$$\mathrm{Log}(z_U) - \mathrm{Log}(z_V) = 0.$$

Furthermore, one can again see in Figure 4.23 that in the homology group of the boundary torus, we have the relation

$$(\mathrm{i}) \cup \cdots \cup (\mathrm{vi}) = l_{X_n} + 2m_{X_n}.$$

Using properties of shape structures, we see that the balancing conditions are equivalent to the following $p+2$ equations:

- $E_s(\alpha):\ 2a_U + b_V + c_V + a_W + b_W = 2\pi$
- $E_1(\alpha):\ 2b_1 + c_2 = 2\pi$
- $E_k(\alpha):\ c_{k-1} + 2b_k + c_{k+1} = 2\pi \quad (\text{for } 2 \leqslant k \leqslant p-1)$

- $E_p(\alpha):\ c_{p-1} + 2b_p + b_U + 2c_U + a_V + b_V + a_W + c_W = 2\pi$
- $E_{p+1}(\alpha):\ c_p + b_U + c_V + b_W = 2\pi.$

The missing $(p+3)$-rd equation, stating that the angles around the vertices of degree $2p+3$ in Figure 4.23 add up to 2π, is redundant: summed with all of the above, it becomes simply that the sum of all angles is $(p+3)\pi$.

Theorem 4.41. *X_n is geometric for $n \geqslant 2$ even.*

Proof. We begin by treating the case of $n \geqslant 6$, i.e. $p \geqslant 2$. First we show that the space of positive angle structures is non-empty. For small enough $\epsilon > 0$, the values

$$\begin{pmatrix} a_j \\ b_j \\ c_j \end{pmatrix} := \begin{pmatrix} \epsilon \\ \pi - \epsilon(j^2+1) \\ \epsilon j^2 \end{pmatrix} \text{ for } 1 \leqslant j \leqslant p-1, \quad \begin{pmatrix} a_p \\ b_p \\ c_p \end{pmatrix} := \begin{pmatrix} 3\pi/4 - \epsilon(p^2+2p-1)/2 \\ \pi/4 - \epsilon(p^2-2p+1)/2 \\ \epsilon p^2 \end{pmatrix},$$

$$\begin{pmatrix} a_U \\ b_U \\ c_U \end{pmatrix} = \begin{pmatrix} a_V \\ c_V \\ b_V \end{pmatrix} = \begin{pmatrix} c_W \\ b_W \\ a_W \end{pmatrix} := \begin{pmatrix} \pi/4 + \epsilon p^2/2 \\ 2\pi/3 - \epsilon p^2/3 \\ \pi/12 - \epsilon p^2/6 \end{pmatrix}$$

give a positive solution to $E_s, E_1, \ldots, E_{p+1}$.

Next, we claim that among the volume maximizers, there is one such that U, V, W have identical angles modulo the permutation used in the formula above. Let F_j denote the constraint $a_j + b_j + c_j = \pi$. The angles of U, V, W appear only in equations E_s, E_p, E_{p+1}. These can be rewritten

$$\begin{array}{r|l} E_{p+1} & c_p + (b_U + c_V + b_W) = 2\pi \\ 3E_p + 2E_s - (3F_U + 2F_V + 2F_W) & 3c_{p-1} + 6b_p + (a_U + a_V + c_W) + 3(c_U + b_V + a_W) = 3\pi \\ E_s - (F_V + F_W) & 2a_U = a_V + c_W. \end{array}$$

The involution $(a_V, b_V, c_V) \leftrightarrow (c_W, a_W, b_W)$ preserves these equations, so by concavity of the volume function, there is a maximizer such that $(a_V, b_V, c_V) = (c_W, a_W, b_W)$. The last of the 3 equations above then gives $a_U = a_V = c_W$. The order-3 substitution of variables

$$(a_U, b_U, c_U) \to (a_V, c_V, b_V) \to (c_W, b_W, a_W) \to (a_U, b_U, c_U)$$

then clearly leaves the other two equations unchanged, so by concavity we may average out and find a maximizer such that $(a_U, b_U, c_U) = (a_V, c_V, b_V) = (c_W, b_W, a_W)$, as desired.

These identifications make E_s redundant. Moreover, dropping the angles of V and W as variables, we may now rewrite the system of constraints as

- $E_1:\ 2b_1 + c_2 = 2\pi$
- $E_k:\ c_{k-1} + 2b_k + c_{k+1} = 2\pi \quad (\text{for } 2 \leqslant k \leqslant p-1)$
- $E'_p:\ c_{p-1} + 2b_p + a_U + 3c_U = \pi \quad (\text{not } 2\pi!)$
- $E'_{p+1}:\ c_p + 3b_U = 2\pi$

Recall from Lemma 4.10 that at a volume maximizer, if $a_j b_j c_j = 0$ then a_j, b_j, c_j are $0, 0, \pi$ up to order.

Lemma 4.42. *At a volume maximizer, if $a_k b_k c_k = 0$ then $k = p$ and $(a_p, b_p, c_p) = (0, 0, \pi)$.*

Proof. First, E'_{p+1} gives $b_U = (2\pi - c_p)/3 \in [\pi/3, 2\pi/3]$ so the tetrahedron U is non-degenerate.

• Let us show by induction on $1 \leqslant k \leqslant p-1$ that $b_k > 0$. By E_1 we have $b_1 = \pi - c_2/2 \geqslant \pi/2$, giving the case $k = 1$. For the induction step, suppose $2 \leqslant k \leqslant p-1$ and $b_{k-1} > 0$. Then $c_{k-1} < \pi$, which by E_k implies that $b_k > 0$.

• Let us now show by *descending* induction on $p-1 \geqslant k \geqslant 1$ that $b_k < \pi$. For the initialization, suppose $(a_{p-1}, b_{p-1}, c_{p-1}) = (0, \pi, 0)$ and aim for a contradiction. Recall that $p \geqslant 2$: by E_{p-1} we have $c_p = 0$, hence $b_U = 2\pi/3$ by E'_{p+1}. But $c_p = 0$ also implies $b_p \in \{0, \pi\}$, hence $b_p = 0$ by E'_p. Together with $c_{p-1} = 0$, by E'_p this yields $a_U + 3c_U = \pi$. But we showed that $b_U = 2\pi/3$, hence $(a_U, b_U, c_U) = (0, 2\pi/3, \pi/3)$, a forbidden configuration. This contradiction shows $b_{p-1} < \pi$.

For the (downward) induction step, suppose $p-2 \geqslant k \geqslant 1$ and $b_{k+1} < \pi$. Actually $0 < b_{k+1} < \pi$ (previous bullet-point), hence $0 < c_{k+1}$: by E_k, this implies $b_k < \pi$.

• It only remains to rule out $c_p = 0$. Note that the non-negative sequence $(0, c_1, \dots, c_p)$ is convex, because E_k can be rewritten $c_{k-1} - 2c_k + c_{k+1} = 2a_k \geqslant 0$ (agreeing that "c_0" stands for 0). But we showed $0 < b_{p-1} < \pi$: hence, $c_{p-1} > 0$ which entails $c_p \geqslant \frac{p}{p-1} c_{p-1} > 0$. □

We can now prove that the volume maximizer has only positive angles. By the above lemma, if not, then we may assume $(a_p, b_p, c_p) = (0, 0, \pi)$ and that all other tetrahedra are non-degenerate. We will exhibit a smooth path of deformations of the angles, along which the derivative of the volume is positive (as a function of the angles, the volume of an ideal tetrahedron is not smooth near the point $(0, 0, \pi)$, but it has a well-defined derivative in the direction of any segment.).

Using E_{p-1}, E'_p, E'_{p+1}, it is straightforward to check that the angles satisfy

$$\begin{pmatrix} a_{p-1} & a_p & a_U \\ b_{p-1} & b_p & b_U \\ c_{p-1} & c_p & c_U \end{pmatrix} = \begin{pmatrix} (\pi + c_{p-2} - 2c_{p-1})/2 & 0 & (\pi + c_{p-1})/2 \\ (\pi - c_{p-2})/2 & 0 & \pi/3 \\ c_{p-1} & \pi & \pi/6 - c_{p-1}/2 \end{pmatrix}. \tag{4.43}$$

For small $t > 0$, the t-deformation given by $(a_k^t, b_k^t, c_k^t) = (a_k, b_k, c_k)$ for $1 \leqslant k \leqslant p-2$ and

$$\begin{pmatrix} a_{p-1}^t & a_p^t & a_U^t \\ b_{p-1}^t & b_p^t & b_U^t \\ c_{p-1}^t & c_p^t & c_U^t \end{pmatrix} = \begin{pmatrix} a_{p-1} & 0 & a_U \\ b_{p-1} & 0 & b_U \\ c_{p-1} & \pi & c_U \end{pmatrix} + t \begin{pmatrix} -1 & 2 & -1 \\ 1 & 0 & 2/3 \\ 0 & -2 & 1/3 \end{pmatrix}$$

is still an angle structure, i.e. satisfies $E_1, \dots, E_{p-1}, E'_p, E'_{p+1}$. By definition of the volume functional $\mathcal{V}$ (Definition 2.49), we have for this deformation

$$\exp\left(\frac{-\partial \mathcal{V}}{\partial t}\right)\Big|_{t=0} = \frac{\sin(b_{p-1})}{\sin(a_{p-1})} \frac{\sin^2(b_U)\sin(c_U)}{\sin^3(a_U)}. \tag{4.44}$$

Each factor $\sin(\theta)$ appears to the power $\partial\theta/\partial t$, but tripled for $\theta = a_U, b_U, c_U$ because there are 3 isometric copies of the tetrahedron U. The p-th tetrahedron stays flat, hence does not contribute volume. The formula for c_U in (4.43) gives $0 \leqslant c_{p-1} \leqslant \pi/3$. We proved in the lemma above that $(0, c_1, \ldots, c_p)$ is convex, hence (4.43) also yields $a_{p-1} \in [\pi/6, \pi/2]$. Therefore,

$$\frac{\sin(b_{p-1})}{\sin(a_{p-1})} \leqslant \frac{1}{\sin(\pi/6)} = 2.$$

On the other hand, still using (4.43),

$$\frac{\sin^2(b_U)\sin(c_U)}{\sin^3(a_U)} = \frac{3}{4}\frac{\sin(\pi/6 - c_{p-1}/2)}{\sin^3(\pi/2 + c_{p-1}/2)} \leqslant \frac{3}{4}\frac{\sin(\pi/6)}{\sin^3(\pi/2)} = \frac{3}{8}$$

by an easy monotonicity argument for c_{p-1} ranging over $[0, \pi/3]$. In conclusion, (4.44) is bounded above by $2 \cdot 3/8 < 1$, hence $(\partial\mathcal{V}/\partial t)_{t=0^+} > 0$ as desired.

Thus, the volume maximizer is interior to the space of angle structures. By Theorem 2.52, this implies Theorem 4.41 for $p \geqslant 2$. It only remains to discuss $p = 0, 1$.

• For $p = 1$ we find the initial gluing equations

$$\begin{array}{rrcl} E_s: & 2a_U + b_V + c_V + a_W + b_W & = & 2\pi \\ E_1: & 2b_1 + b_U + 2c_U + a_V + b_V + a_W + c_W & = & 2\pi \\ E_2: & c_1 + b_U + c_V + b_W & = & 2\pi \end{array}$$

(only the term "c_{p-1}" has disappeared from E_1). Symmetry between U, V, W can be argued as in the $p \geqslant 2$ case, reducing the above to

$$\begin{array}{rrcl} E_1': & 2b_1 + a_U + 3c_U & = & \pi \\ E_2': & c_1 + 3b_U & = & 2\pi. \end{array}$$

The tetrahedron U is not flat, as $b_U = (2\pi - c_1)/3 \in [\pi/3, 2\pi/3]$. If $c_1 = 0$ then $b_1 \in \{0, \pi\}$ must be 0 by E_1', hence $(a_U, b_U, c_U) = (0, 2\pi/3, \pi/3)$ which is prohibited. If $c_1 = \pi$ then

$$\begin{pmatrix} a_1 & a_U \\ b_1 & b_U \\ c_1 & c_U \end{pmatrix} = \begin{pmatrix} 0 & \pi/2 \\ 0 & \pi/3 \\ \pi & \pi/6 \end{pmatrix} \text{ can be perturbed by adding } t \begin{pmatrix} 2 & -1 \\ 0 & 2/3 \\ -2 & 1/3 \end{pmatrix}$$

(where $0 < t \ll 1$) to produce a path of angle structures, yielding as before

$$\exp\left(\frac{-\partial\mathcal{V}}{\partial t}\right)\Big|_{t=0} = \frac{\sin^2(b_U)\sin(c_U)}{\sin^3(a_U)} = \frac{3}{8} < 1.$$

• For $p = 0$ it is straightforward to check that $(a_U, b_U, c_U) = (a_V, c_V, b_V) = (c_W, b_W, a_W) = (\pi/6, 2\pi/3, \pi/6)$ yields the complete hyperbolic metric (this is actually the result of a 2-3 angled Pachner move on the ideal triangulation of the figure-eight knot complement with two regular tetrahedra given in Figure 2.5). Theorem 4.41 is proved. □

4.7.3 Computation of the partition functions

The following theorem is the version of Theorem 4.13 for even n. Note that here $\mu_{X_n}(\alpha) = -m_{X_n}(\alpha)$ and once again $\lambda_{X_n}(\alpha) = l_{X_n}(\alpha) + 2m_{X_n}(\alpha)$ corresponds to a preferred longitude.

Theorem 4.45. *Let n be a positive even integer and $p = \frac{n-2}{2}$. Consider the ideal triangulation X_n of $S^3 \setminus K_n$ described in Figure 4.22. Then for all angle structures $\alpha = (a_1, \dots, c_W) \in \mathcal{A}_{X_n}$ and all $\hbar > 0$, we have:*

$$\mathcal{Z}_\hbar(X_n, \alpha) \stackrel{\star}{=} \int_{\mathbb{R}+i\frac{\mu_{X_n}(\alpha)}{2\pi\sqrt{\hbar}}} J_{X_n}(\hbar, x) e^{\frac{1}{2\sqrt{\hbar}} x \lambda_{X_n}(\alpha)} dx,$$

with

- *the degree one angle polynomial $\mu_{X_n} \colon \alpha \mapsto a_U - a_V$,*
- *the degree one angle polynomial $\lambda_{X_n} \colon \alpha \mapsto 2(a_V - a_U + a_W - b_V)$,*
- *the map*

$$J_{X_n} \colon (\hbar, x) \mapsto \int_{\mathcal{Y}'} d\mathbf{y}' \, e^{2i\pi \mathbf{y}'^T Q_n \mathbf{y}'} e^{2i\pi x(x - y'_U - y'_W)} e^{\frac{1}{\sqrt{\hbar}}(\mathbf{y}'^T \mathcal{W}_n - \pi x)} \frac{\Phi_{\mathsf{b}}(x - y'_U)\, \Phi_{\mathsf{b}}(y'_W)}{\Phi_{\mathsf{b}}(y'_1) \cdots \Phi_{\mathsf{b}}(y'_p)\, \Phi_{\mathsf{b}}(y'_U)},$$

where

$$\mathcal{Y}' := \left(\prod_{k=1,\dots,p,U} \left(\mathbb{R} - \frac{i}{2\pi\sqrt{\hbar}}(\pi - a_k) \right) \right) \times \left(\mathbb{R} + \frac{i}{2\pi\sqrt{\hbar}}(\pi - a_W) \right),$$

$$\mathbf{y}' := \begin{bmatrix} y'_1 \\ \vdots \\ y'_p \\ y'_U \\ y'_W \end{bmatrix}, \quad \mathcal{W}_n := \begin{bmatrix} -2p\pi \\ \vdots \\ -2\pi\left(kp - \frac{k(k-1)}{2}\right) \\ \vdots \\ -p(p+1)\pi \\ -(p^2+p+3)\pi \\ \pi \end{bmatrix} \quad \text{and} \quad Q_n := \begin{bmatrix} 1 & 1 & \cdots & 1 & 1 & 0 \\ 1 & 2 & \cdots & 2 & 2 & 0 \\ \vdots & \vdots & \ddots & \vdots & \vdots & \vdots \\ 1 & 2 & \cdots & p & p & 0 \\ 1 & 2 & \cdots & p & p+1 & -\frac{1}{2} \\ 0 & 0 & \cdots & 0 & -\frac{1}{2} & 0 \end{bmatrix}.$$

Proof. Since the computations are very similar to those of the proof of Theorem 4.13 we will not give all the details. Let $n \geqslant 2$ be an even integer and set $p := \frac{n-2}{2}$. As before, we denote $\widetilde{\mathbf{t}} := (t_1, \dots, t_{p-1}, t_p, t_U, t_V, t_W)^T \in \mathbb{R}^{X^3}$ the vector whose coordinates are associated to the tetrahedra, and $\mathbf{x} := (e_1, \dots, e_p, e_{p+1}, f_1, \dots, f_p, v, r, s, g, u)^T \in \mathbb{R}^{X^2}$ the face variables vector.

Like in Lemma 4.16, we compute $\mathcal{K}_{X_n}\left(\widetilde{\mathbf{t}}\right) = \frac{1}{|\det(A_e)|} e^{2i\pi \widetilde{\mathbf{t}}^T (-R_e A_e^{-1} B) \widetilde{\mathbf{t}}}$, where B is like in the proof of Lemma 4.16, but R_e, A_e (e standing for *even*) are given by

$$R_e := \begin{array}{c} \\ t_1 \\ \vdots \\ t_p \\ \hline t_U \\ t_V \\ t_W \end{array} \left[\begin{array}{cccc|ccc|ccccc} e_1 & \dots & e_p & e_{p+1} & f_1 & \dots & f_p & v & r & s & g & u \\ \hline 1 & & & 0 & & & & & & & & \\ & \ddots & & & & 0 & & & & 0 & & \\ 0 & & 1 & & & & & & & & & \\ \hline & & & & & & & 0 & 1 & 0 & 0 & 0 \\ & 0 & & & & 0 & & 0 & 0 & -1 & 0 & 0 \\ & & & & & & & 0 & 0 & 0 & 0 & -1 \end{array}\right],$$

$$
A_e := \begin{array}{c}
 \\ w_1 \\ \vdots \\ \vdots \\ w_p \\ \hline w_U \\ w_V \\ w_W \\ \hline w_1' \\ \vdots \\ \vdots \\ w_p' \\ \hline w_U' \\ w_V' \\ w_W'
\end{array}
\begin{array}{ccccc|cccc|ccccc}
e_1 & e_2 & \ldots & e_p & e_{p+1} & f_1 & f_2 & \ldots & f_p & v & r & s & g & u \\
1 & -1 & & & & 1 & & & & & & & & \\
 & \ddots & \ddots & 0 & & & \ddots & 0 & & & & 0 & & \\
 & 0 & \ddots & \ddots & & & 0 & \ddots & & & & & & \\
 & & & 1 & -1 & & & & 1 & & & & & \\
\hline
 & & & & & & & & 0 & -1 & 1 & 1 & 0 & 0 \\
 & & 0 & & & & & & 1 & 0 & 0 & 1 & -1 & 0 \\
 & & & & & & & & 0 & -1 & 1 & 0 & 0 & 1 \\
\hline
-1 & & & & & 1 & & & & & & & & \\
 & & & & & -1 & \ddots & 0 & & & & 0 & & \\
 & & & & & & \ddots & \ddots & & & & & & \\
 & & & & & & 0 & -1 & 1 & & & & & \\
\hline
 & & & & 0 & & & & 0 & 0 & 0 & 1 & -1 & 0 \\
 & & & & 0 & & & & 1 & 0 & 0 & 0 & 0 & -1 \\
 & & & & -1 & & & & 0 & 0 & 1 & 0 & 0 & 0
\end{array}.
$$

Careful computation yields that $\det(A_e) = -1$ and that A_e^{-1} is equal to

$$
\begin{array}{c}
 \\ e_1 \\ e_2 \\ \vdots \\ \\ e_p \\ e_{p+1} \\ \hline f_1 \\ f_2 \\ \vdots \\ f_{p-1} \\ f_p \\ \hline v \\ r \\ s \\ g \\ u
\end{array}
\begin{array}{ccccc|ccc|ccccc|ccc}
w_1 & w_2 & \ldots & w_{p-1} & w_p & w_U & w_V & w_W & w_1' & w_2' & \ldots & w_{p-1}' & w_p' & w_U' & w_V' & w_W' \\
0 & & \cdots & & 0 & 0 & 1 & 0 & -1 & -1 & \cdots & & -1 & -1 & 0 & 0 \\
-1 & 0 & & & & 0 & 2 & 0 & -1 & -2 & \cdots & & -2 & -2 & 0 & 0 \\
-1 & -1 & \ddots & & \vdots & & & & & & \ddots & & \vdots & & & \\
\vdots & & \ddots & 0 & 0 & \vdots & \vdots & \vdots & \vdots & \vdots & & 1-p & 1-p & \vdots & \vdots & \vdots \\
 & & & -1 & 0 & & & & & & & 1-p & -p & & & \\
-1 & & \cdots & & -1 & 0 & p+1 & 0 & -1 & -2 & \cdots & 1-p & -p & -p-1 & 0 & 0 \\
\hline
 & & & & & 0 & 1 & 0 & 0 & -1 & \cdots & & -1 & -1 & 0 & 0 \\
 & & & & & & 1 & & 0 & 0 & \ddots & & \vdots & -1 & & \\
 & & 0 & & & \vdots & \vdots & \vdots & \vdots & & \ddots & -1 & -1 & \vdots & \vdots & \vdots \\
 & & & & & & & & 0 & & & 0 & -1 & & & \\
 & & & & & 0 & 1 & 0 & 0 & & \cdots & & 0 & -1 & 0 & 0 \\
\hline
-1 & & \cdots & & -1 & 0 & p+2 & -1 & -1 & -2 & \cdots & & -p & -p-2 & -1 & 1 \\
-1 & & \cdots & & -1 & 0 & p+1 & 0 & -1 & -2 & \cdots & & -p & -p-1 & 0 & 1 \\
 & & & & & 1 & 1 & -1 & & & & & & -1 & -1 & 0 \\
 & & 0 & & & 1 & 1 & -1 & & & 0 & & & -2 & -1 & 0 \\
 & & & & & 0 & 1 & 0 & & & & & & -1 & -1 & 0
\end{array}.
$$

Hence $\mathcal{K}_{X_n}\left(\widetilde{\mathbf{t}}\right) = \exp\left(2i\pi\widetilde{\mathbf{t}}^T\widetilde{Q}_n\widetilde{\mathbf{t}}\right)$, where

$$\widetilde{Q}_n := \frac{(-R_eA_e^{-1}B)+(-R_eA_e^{-1}B)^T}{2} = \begin{array}{c} \\ t_1 \\ t_2 \\ \vdots \\ t_{p-1} \\ t_p \\ \hline t_U \\ t_V \\ t_W \end{array} \left[\begin{array}{ccccc|ccc} t_1 & t_2 & \cdots & t_{p-1} & t_p & t_U & t_V & t_W \\ \hline 1 & 1 & \cdots & 1 & 1 & 1 & 0 & 0 \\ 1 & 2 & \cdots & 2 & 2 & 2 & 0 & 0 \\ \vdots & \vdots & \ddots & \vdots & \vdots & \vdots & \vdots & \vdots \\ 1 & 2 & \cdots & p-1 & p-1 & p-1 & 0 & 0 \\ 1 & 2 & \cdots & p-1 & p & p & 0 & 0 \\ \hline 1 & 2 & \cdots & p-1 & p & p+1 & -1/2 & -1 \\ 0 & 0 & \cdots & 0 & 0 & -1/2 & -1 & -1/2 \\ 0 & 0 & \cdots & 0 & 0 & -1 & -1/2 & 0 \end{array}\right].$$

Now, like in Lemma 4.17, if we denote $\widetilde{C}(\alpha) := (c_1, \dots, c_W)^T$, and $\widetilde{\Gamma}(\alpha) := (a_1-\pi, \dots, a_p-\pi, a_U-\pi, \pi-a_V, \pi-a_W)^T$, then (indexing entries by $k \in \{1, \dots, p+3\}$) we can compute: $2\widetilde{Q}_n\widetilde{\Gamma}(\alpha) + \widetilde{C}(\alpha) =$

$$\begin{array}{c} k=1 \\ \vdots \\ k=p \end{array} \left(\begin{array}{c} \vdots \\ k(\omega_s(\alpha) - 2(p+2)\pi) + \sum_{j=1}^{k} j\omega_{k-j}(\alpha) \\ \vdots \\ \omega_s(\alpha) - \omega_{p+1}(\alpha) + \left(p(\omega_s(\alpha) - 2(p+2)\pi) + \sum_{j=1}^{p} j\omega_{p-j}(\alpha)\right) - 4\pi + \frac{1}{2}\lambda_{X_n}(\alpha) \\ \frac{1}{2}\lambda_{X_n}(\alpha) - \pi \\ 3\pi - \omega_s(\alpha) \end{array}\right),$$

where $\lambda_{X_n}(\alpha) := 2(-a_U+a_V-b_V+a_W)$. Notably we have for all angle structures $\alpha \in \mathcal{A}_{X_n}$:

$$2\widetilde{Q}_n\widetilde{\Gamma}(\alpha) + \widetilde{C}(\alpha) = \begin{array}{c} k=1 \\ \vdots \\ k=p \end{array} \left(\begin{array}{c} \vdots \\ -2\pi\left(kp - \dfrac{k(k-1)}{2}\right) \\ \vdots \\ -(p^2+p+4)\pi + \frac{1}{2}\lambda_{X_n}(\alpha) \\ \frac{1}{2}\lambda_{X_n}(\alpha) - \pi \\ \pi \end{array}\right).$$

The above computations are fairly quick consequences of the similarities between the matrices $\widetilde{Q}_n$ and the weights $\omega_j(\alpha)$ whether n is odd or even.

Denote again $\alpha = (a_1, b_1, c_1, \dots, a_W, b_W, c_W)$ a general vector of dihedral angles in $\mathcal{A}_{X_n}$. Let $\hbar > 0$. Since the tetrahedron T_U is of positive sign here, the dynamical content $\mathcal{D}_{\hbar,X_n}\left(\widetilde{\mathbf{t}}, \alpha\right)$ thus becomes

$$e^{\frac{1}{\sqrt{\hbar}}\widetilde{C}(\alpha)^T\widetilde{\mathbf{t}}} \frac{\Phi_{\mathsf{b}}\left(t_V + \frac{i}{2\pi\sqrt{\hbar}}(\pi - a_V)\right)\Phi_{\mathsf{b}}\left(t_W + \frac{i}{2\pi\sqrt{\hbar}}(\pi - a_W)\right)}{\Phi_{\mathsf{b}}\left(t_1 - \frac{i}{2\pi\sqrt{\hbar}}(\pi - a_1)\right)\cdots\Phi_{\mathsf{b}}\left(t_p - \frac{i}{2\pi\sqrt{\hbar}}(\pi - a_p)\right)\Phi_{\mathsf{b}}\left(t_U - \frac{i}{2\pi\sqrt{\hbar}}(\pi - a_U)\right)}.$$

According to tetrahedra signs, we do the following change of variables:

- $y'_k = t_k - \frac{i}{2\pi\sqrt{\hbar}}(\pi - a_k)$ for $k \in \{1, \dots, p, U\}$,
- $y'_l = t_l + \frac{i}{2\pi\sqrt{\hbar}}(\pi - a_l)$ for $l \in \{V, W\}$,

and we define $\widetilde{\mathbf{y}'} := \left(y'_1, \dots, y'_p, y'_U, y'_V, y'_W\right)^T$. We also denote

$$\widetilde{\mathcal{Y}}'_{\hbar,\alpha} := \prod_{k=1,\dots,p,U} \left(\mathbb{R} - \frac{i}{2\pi\sqrt{\hbar}}(\pi - a_k)\right) \times \prod_{l=V,W} \left(\mathbb{R} + \frac{i}{2\pi\sqrt{\hbar}}(\pi - a_l)\right).$$

After computations similar to the ones in the proof of Theorem 4.13, we obtain:

$$\mathcal{Z}_\hbar(X_n, \alpha) \stackrel{\star}{=} \int_{\widetilde{\mathbf{y}'} \in \widetilde{\mathcal{Y}}'_{\hbar,\alpha}} d\widetilde{\mathbf{y}'} e^{2i\pi \widetilde{\mathbf{y}'}^T \widetilde{Q}_n \widetilde{\mathbf{y}'} + \frac{1}{\sqrt{\hbar}}\left(2\widetilde{Q}_n \widetilde{\Gamma}(\alpha) + \widetilde{C}(\alpha)\right)^T \widetilde{\mathbf{y}'}} \frac{\Phi_{\mathsf{b}}\left(y'_V\right) \Phi_{\mathsf{b}}\left(y'_W\right)}{\Phi_{\mathsf{b}}\left(y'_1\right) \cdots \Phi_{\mathsf{b}}\left(y'_p\right) \Phi_{\mathsf{b}}\left(y'_U\right)},$$

We define a new variable $x := y'_U + y'_V$ living in the set

$$\mathcal{Y}^0_{\hbar,\alpha} := \mathbb{R} + \frac{i}{2\pi\sqrt{\hbar}}(a_U - a_V),$$

and we also define $\mathbf{y}'$ (respectively $\mathcal{Y}'_{\hbar,\alpha}$) exactly like $\widetilde{\mathbf{y}'}$ (respectively $\widetilde{\mathcal{Y}}'_{\hbar,\alpha}$) but with the second-to-last coordinate (corresponding to y_V) taken out. We also define

$$\mathcal{W}_n = \begin{bmatrix} \mathcal{W}_{n,1} \\ \vdots \\ \mathcal{W}_{n,k} \\ \vdots \\ \mathcal{W}_{n,p} \\ \mathcal{W}_{n,U} \\ \mathcal{W}_{n,W} \end{bmatrix} := \begin{bmatrix} -2p\pi \\ \vdots \\ -2\pi\left(kp - \frac{k(k-1)}{2}\right) \\ \vdots \\ -p(p+1)\pi \\ -(p^2+p+3)\pi \\ \pi \end{bmatrix} \quad \text{and} \quad Q_n := \begin{bmatrix} 1 & 1 & \cdots & 1 & 1 & 0 \\ 1 & 2 & \cdots & 2 & 2 & 0 \\ \vdots & \vdots & \ddots & \vdots & \vdots & \vdots \\ 1 & 2 & \cdots & p & p & 0 \\ 1 & 2 & \cdots & p & p+1 & -\frac{1}{2} \\ 0 & 0 & \cdots & 0 & -\frac{1}{2} & 0 \end{bmatrix}.$$

This time, Q_n is obtained from $\widetilde{Q}_n$ by replacing the two rows corresponding to y_U and y_V with their difference (row of y_U minus row of y_V), and by replacing the two columns corresponding to y_U and y_V with their difference. We now use the substitution $y'_V = x - y'_U$ and we compute

$$\begin{aligned} 2i\pi \widetilde{\mathbf{y}'}^T \widetilde{Q}_n \widetilde{\mathbf{y}'} &= 2i\pi \left((\mathbf{y}'^T Q_n \mathbf{y}' - (p+1){y'_U}^2 + y'_U y'_W) + (p+1){y'_U}^2 - y'_U y'_V - 2y'_U y'_W - {y'_V}^2 - y'_V y'_W \right) \\ &= 2i\pi \left(\mathbf{y}'^T Q_n \mathbf{y}' + x y'_U - x y'_W - x^2 \right), \end{aligned}$$

and $\frac{1}{\sqrt{\hbar}} \left(2\widetilde{Q}_n \widetilde{\Gamma}(\alpha) + \widetilde{C}(\alpha)\right)^T \widetilde{\mathbf{y}'} = \frac{1}{\sqrt{\hbar}} \left(\mathcal{W}_n^T \mathbf{y}' + x(\frac{1}{2}\lambda_{X_n}(\alpha) - \pi)\right)$, thus

$$\begin{aligned} \mathcal{Z}_\hbar(X_n, \alpha) &\stackrel{\star}{=} \int_{\widetilde{\mathbf{y}'} \in \widetilde{\mathcal{Y}}'_{\hbar,\alpha}} d\widetilde{\mathbf{y}'}\, e^{2i\pi \widetilde{\mathbf{y}'}^T \widetilde{Q}_n \widetilde{\mathbf{y}'} + \frac{1}{\sqrt{\hbar}}\left(2\widetilde{Q}_n \widetilde{\Gamma}(\alpha) + \widetilde{C}(\alpha)\right)^T \widetilde{\mathbf{y}'}} \frac{\Phi_{\mathsf{b}}\left(y'_V\right) \Phi_{\mathsf{b}}\left(y'_W\right)}{\Phi_{\mathsf{b}}\left(y'_1\right) \cdots \Phi_{\mathsf{b}}\left(y'_p\right) \Phi_{\mathsf{b}}\left(y'_U\right)} \\ &\stackrel{\star}{=} \int dx d\mathbf{y}'\, e^{2i\pi\left(\mathbf{y}'^T Q_n \mathbf{y}' + x(y'_U - y'_W - x)\right) + \frac{1}{\sqrt{\hbar}}\left(\mathcal{W}_n^T \mathbf{y}' + x(\frac{1}{2}\lambda_{X_n}(\alpha) - \pi)\right)} \frac{\Phi_{\mathsf{b}}\left(x - y'_U\right) \Phi_{\mathsf{b}}\left(y'_W\right)}{\Phi_{\mathsf{b}}\left(y'_1\right) \cdots \Phi_{\mathsf{b}}\left(y'_p\right) \Phi_{\mathsf{b}}\left(y'_U\right)}, \end{aligned}$$

where the variables $(\mathbf{y}', x)$ in the last integral lie in $\mathcal{Y}'_{\hbar,\alpha} \times \mathcal{Y}^0_{\hbar,\alpha}$. The theorem follows. □

We now state the counterpart of Corollary 4.19, which is proven in exactly the same way.

Corollary 4.46. *Let n be a positive even integer, $p = \frac{n-2}{2}$ and X_n the ideal triangulation of $S^3 \setminus K_n$ from Figure 4.22. Then for all angle structures $\alpha \in \mathcal{A}_{X_n}$ and all $\hbar > 0$, we have:*

$$\mathcal{Z}_\hbar(X_n, \alpha) \overset{\star}{=} \int_{\mathbb{R}+i\mu_{X_n}(\alpha)} \mathfrak{J}_{X_n}(\hbar, \mathsf{x}) e^{\frac{1}{4\pi\hbar}\mathsf{x}\lambda_{X_n}(\alpha)}\, d\mathsf{x},$$

with the map

$$\mathfrak{J}_{X_n} \colon (\hbar, \mathsf{x}) \mapsto \left(\frac{1}{2\pi\sqrt{\hbar}}\right)^{p+3} \int_{\mathcal{Y}_\alpha} d\mathbf{y}\, e^{\frac{i\mathbf{y}^T Q_n \mathbf{y} + ix(y_U - y_W - \mathsf{x}) + \mathbf{y}^T \mathcal{W}_n - \pi\mathsf{x}}{2\pi\hbar}} \frac{\Phi_{\mathsf{b}}\left(\frac{\mathsf{x}-y_U}{2\pi\sqrt{\hbar}}\right)\Phi_{\mathsf{b}}\left(\frac{y_W}{2\pi\sqrt{\hbar}}\right)}{\Phi_{\mathsf{b}}\left(\frac{y_1}{2\pi\sqrt{\hbar}}\right)\cdots\Phi_{\mathsf{b}}\left(\frac{y_p}{2\pi\sqrt{\hbar}}\right)\Phi_{\mathsf{b}}\left(\frac{y_U}{2\pi\sqrt{\hbar}}\right)},$$

where $\mu_{X_n}, \lambda_{X_n}, \mathcal{W}_n, Q_n$ are the same as in Theorem 4.45, and

$$\mathcal{Y}_\alpha := \left(\prod_{k=1,\dots,p,U} (\mathbb{R} - i(\pi - a_k))\right) \times (\mathbb{R} + i(\pi - a_W))\,.$$

Proof. Exactly similar to the proof of Corollary 4.19. □

We finally come to H-triangulations for even twists knots. Again, before stating Theorem 4.47, we compute the weights on each edge of the H-triangulation Y_n given in Figure 4.21 (for $n \geqslant 3$ even).

We use exactly the same notations as the odd case. We denote $\overrightarrow{e_0}, \dots, \overrightarrow{e_{p+1}}, \overrightarrow{e_s}, \overrightarrow{e_d}, \overrightarrow{K_n} \in Y_n^1$ the $p+5$ edges in Y_n respectively represented in Figure 4.21 by arrows with circled 0, …, circled $p+1$, simple arrow, double arrow and blue simple arrow.

For $\alpha = (a_1, b_1, c_1, \dots, a_p, b_p, c_p, a_U, b_U, c_U, a_V, b_V, c_V, a_W, b_W, c_W, a_Z, b_Z, c_Z) \in \mathcal{S}_{Y_n}$ a shape structure on Y_n, the weights of each edge are given by:

- $\widehat{\omega}_s(\alpha) := \omega_{Y_n,\alpha}(\overrightarrow{e_s}) = 2a_U + b_V + c_V + a_W + b_W + a_Z$
- $\widehat{\omega}_d(\alpha) := \omega_{Y_n,\alpha}(\overrightarrow{e_d}) = b_U + c_U + c_W + b_Z + c_Z$
- $\omega_0(\alpha) := \omega_{Y_n,\alpha}(\overrightarrow{e_0}) = 2a_1 + c_1 + 2a_2 + \dots + 2a_p + a_V + c_W$
- $\omega_1(\alpha) := \omega_{Y_n,\alpha}(\overrightarrow{e_1}) = 2b_1 + c_2$
- $\omega_k(\alpha) := \omega_{Y_n,\alpha}(\overrightarrow{e_k}) = c_{k-1} + 2b_k + c_{k+1}$ (for $2 \leqslant k \leqslant p-1$)
- $\widehat{\omega}_p(\alpha) := \omega_{Y_n,\alpha}(\overrightarrow{e_p}) = c_{p-1} + 2b_p + c_U + a_V + b_V + a_W + b_Z + c_Z$
- $\omega_{p+1}(\alpha) := \omega_{Y_n,\alpha}(\overrightarrow{e_{p+1}}) = c_p + b_U + c_V + b_W$
- $\widehat{\omega}_{\overrightarrow{K_n}}(\alpha) := \omega_{Y_n,\alpha}(\overrightarrow{K_n}) = a_Z$.

We can now compute the partition function for the H-triangulations Y_n (n even), and prove the following theorem. As for the odd case, we will denote $\mathcal{S}_{Y_n \setminus Z}$ the space of shape structures on every tetrahedron of Y_n except for Z.

Theorem 4.47. *Let n be a positive even integer and $p = \frac{n-2}{2}$. Consider the one-vertex H-triangulation Y_n of the pair (S^3, K_n) described in Figure 4.21. Then for every $\hbar > 0$ and for every $\tau \in \mathcal{S}_{Y_n \setminus Z} \times \overline{\mathcal{S}_Z}$ such that $\omega_{Y_n,\tau}$ vanishes on $\overrightarrow{K_n}$ and is equal to 2π on every other edge, one has*

$$\lim_{\substack{\alpha \to \tau \\ \alpha \in \mathcal{S}_{Y_n}}} \Phi_{\mathsf{b}} \left(\frac{\pi - \omega_{Y_n,\alpha}\left(\overrightarrow{K_n}\right)}{2\pi i \sqrt{\hbar}} \right) \mathcal{Z}_\hbar(Y_n, \alpha) \stackrel{\star}{=} J_{X_n}(\hbar, 0),$$

where J_{X_n} is defined in Theorem 4.45.

Proof. Let n be an even integer and $p = \frac{n-2}{2}$. The proof is similar to the odd case and will be separated in three steps: computing the partition function $\mathcal{Z}_\hbar(Y_n, \alpha)$, applying the dominated convergence theorem in $\alpha \to \tau$ and finally retrieving the value $J_{X_n}(\hbar, 0)$ in $\alpha = \tau$.

Step 1. Computing the partition function $\mathcal{Z}_\hbar(Y_n, \alpha)$.

Like in the proof of Theorem 4.45 we start by computing the kinematical kernel. We denote $\widehat{\mathbf{t}} := (t_1, \dots, t_p, t_U, t_V, t_W, t_Z) \in \mathbb{R}^{Y_n^3}$ and $\widehat{\mathbf{x}} := (e_1, \dots, e_p, e_{p+1}, f_1, \dots, f_p, v, r, s, s', g, u, m) \in \mathbb{R}^{Y_n^2}$.

Like in the proof of Theorem 4.20, using Figure 4.21, we compute

$$\mathcal{K}_{Y_n}\left(\widehat{\mathbf{t}}\right) = \int_{\widehat{\mathbf{x}} \in \mathbb{R}^{Y_n^2}} d\widehat{\mathbf{x}} \int_{\widehat{\mathbf{w}} \in \mathbb{R}^{2(p+4)}} d\widehat{\mathbf{w}}\, e^{2i\pi \widehat{\mathbf{t}}^T \widehat{S_e} \widehat{\mathbf{x}}} e^{-2i\pi \widehat{\mathbf{w}}^T \widehat{H_e} \widehat{\mathbf{x}}} e^{-2i\pi \widehat{\mathbf{w}}^T \widehat{D} \widehat{\mathbf{t}}},$$

where $\widehat{D}$ is like in proof of Theorem 4.20, whereas the matrices $\widehat{H_e}$ and $\widehat{S_e}$ are given by:

$\widehat{H_e} :=$

	e_1	e_2	...	e_p	e_{p+1}	f_1	f_2	...	f_p	v	r	s	s'	g	u	m
w_1	1	-1				1										
$\vdots$		$\ddots$	$\ddots$		0		$\ddots$		0							
$\vdots$		0	$\ddots$	$\ddots$			0		$\ddots$				0			
w_p				1	-1				1							
w_U									0	-1	1	0	1	0	0	0
w_V									1	0	0	1	0	-1	0	0
w_W			0						0	-1	1	0	0	0	1	0
w_Z									0	0	0	1	0	0	0	0
w'_1	-1					1										
$\vdots$						-1	$\ddots$		0							
$\vdots$							$\ddots$	$\ddots$					0			
w'_p						0		-1	1							
w'_U					0				0	0	0	0	1	-1	0	0
w'_V					0				1	0	0	0	0	0	-1	0
w'_W					-1				0	0	1	0	0	0	0	0
w'_Z					0				0	0	0	1	-1	0	0	0

$$\widehat{S_e} := \begin{array}{c} \\ t_1 \\ \vdots \\ t_p \\ \hline t_U \\ t_V \\ t_W \\ t_Z \end{array} \begin{array}{c} \begin{array}{cccc|ccc|ccccccc} e_1 & \dots & e_p & e_{p+1} & f_1 & \dots & f_p & v & r & s & s' & g & u & m \end{array} \\ \left[\begin{array}{cccc|ccc|ccccccc} 1 & & & 0 & & & & & & & & & & \\ & \ddots & & & & 0 & & & & & 0 & & & \\ 0 & & 1 & & & & & & & & & & & \\ \hline & & & & & & & 0 & 1 & 0 & 0 & 0 & 0 & 0 \\ & 0 & & & & 0 & & 0 & 0 & -1 & 0 & 0 & 0 & 0 \\ & & & & & & & 0 & 0 & 0 & 0 & 0 & -1 & 0 \\ & & & & & & & 0 & 0 & 0 & 0 & 0 & 0 & 1 \end{array}\right] \end{array}.$$

Like in the odd case, let us define S_e the submatrix of $\widehat{S_e}$ without the m-column, H_e the submatrix of $\widehat{H_e}$ without the m-column and the w_V-row, $R_{e,V}$ this very w_V-row of $\widehat{H_e}$, D the submatrix of $\widehat{D}$ without the w_V-row, $\mathbf{x}$ the subvector of $\widehat{\mathbf{x}}$ without the variable m and $\mathbf{w}$ the subvector of $\widehat{\mathbf{w}}$ without the variable w_V. We remark that H_e is invertible and $\det(H_e) = -1$. Hence, by using multi-dimensional Fourier transform and the integral definition of the Dirac delta function like in the odd case, we compute

$$\mathcal{K}_{Y_n}\left(\widehat{\mathbf{t}}\right) = \delta(-t_Z) e^{2i\pi \widehat{\mathbf{t}}^T(-S_e H_e^{-1} D)\widehat{\mathbf{t}}} \delta\left(-R_{e,V} H_e^{-1} D\widehat{\mathbf{t}}\right).$$

We can now compute $H_e^{-1} =$

$$\begin{array}{c} \\ e_1 \\ e_2 \\ \vdots \\ e_p \\ e_{p+1} \\ \hline f_1 \\ f_2 \\ \vdots \\ f_{p-1} \\ f_p \\ \hline v \\ r \\ s \\ s' \\ g \\ u \end{array} \begin{array}{c} \begin{array}{ccccc|ccc|ccccccc} w_1 & w_2 & \dots & w_{p-1} & w_p & w_U & w_W & w_Z & w'_1 & w'_2 & \dots & w'_{p-1} & w'_p & w'_U & w'_V & w'_W & w'_Z \end{array} \\ \left[\begin{array}{ccccc|ccc|ccccccc} 0 & & \cdots & & 0 & -1 & 1 & 1 & -1 & -1 & & \cdots & -1 & 0 & 1 & 0 & -1 \\ -1 & 0 & & & & -2 & 2 & 2 & -1 & -2 & & \cdots & -2 & 0 & 2 & 0 & -2 \\ -1 & -1 & \ddots & & \vdots & & & & & & \ddots & & \vdots & & & & \\ \vdots & & \ddots & 0 & 0 & \vdots & \vdots & \vdots & \vdots & \vdots & & 1-p & 1-p & \vdots & \vdots & \vdots & \vdots \\ & & & -1 & 0 & & & & & & & 1-p & -p & & & & \\ -1 & & \cdots & & -1 & -p-1 & p+1 & p+1 & -1 & -2 & \cdots & 1-p & -p & 0 & p+1 & 0 & -p-1 \\ \hline & & & & & -1 & 1 & 1 & 0 & -1 & & \cdots & -1 & 0 & 1 & 0 & -1 \\ & & & & & & & & 0 & 0 & \ddots & & \vdots & & & & \\ & & 0 & & & \vdots & \vdots & \vdots & \vdots & & \ddots & -1 & -1 & \vdots & \vdots & \vdots & \vdots \\ & & & & & & & & 0 & & & 0 & -1 & & & & \\ & & & & & -1 & 1 & 1 & 0 & & \cdots & & 0 & 0 & 1 & 0 & -1 \\ \hline -1 & & \cdots & & -1 & -p-2 & p+1 & p+2 & -1 & -2 & & \cdots & -p & 0 & p+1 & 1 & -p-2 \\ -1 & & \cdots & & -1 & -p-1 & p+1 & p+1 & -1 & -2 & & \cdots & -p & 0 & p+1 & 1 & -p-1 \\ & & & & & 0 & 0 & 1 & & & & & & 0 & 0 & 0 & 0 \\ & & & & & 0 & 0 & 1 & & & & & & 0 & 0 & 0 & -1 \\ & & 0 & & & 0 & 0 & 1 & & & 0 & & & -1 & 0 & 0 & -1 \\ & & & & & -1 & 1 & 1 & & & & & & 0 & 0 & 0 & -1 \end{array}\right] \end{array},$$

and thus find that $-R_{e,V}H_e^{-1}D\widehat{\mathbf{t}} = -t_U - t_V$ and

$$-S_eH_e^{-1}D = \begin{array}{c} \\ t_1 \\ t_2 \\ \vdots \\ t_{p-1} \\ t_p \\ \hline t_U \\ t_V \\ t_W \\ t_Z \end{array} \begin{array}{c} \begin{array}{ccccccccc} t_1 & t_2 & \cdots & t_{p-1} & t_p & t_U & t_V & t_W & t_Z \end{array} \\ \left[\begin{array}{ccccc|cccc} 1 & 1 & \cdots & 1 & 1 & 0 & -1 & 0 & 1 \\ 1 & 2 & \cdots & 2 & 2 & 0 & -2 & 0 & 2 \\ \vdots & \vdots & \ddots & \vdots & \vdots & \vdots & \vdots & \vdots & \vdots \\ 1 & 2 & \cdots & p-1 & p-1 & 0 & -(p-1) & 0 & p-1 \\ 1 & 2 & \cdots & p-1 & p & 0 & -p & 0 & p \\ \hline 1 & 2 & \cdots & p-1 & p & 0 & -(p+1) & -1 & p+1 \\ 0 & 0 & \cdots & 0 & 0 & 0 & 0 & 0 & 0 \\ 0 & 0 & \cdots & 0 & 0 & 0 & 0 & 0 & -1 \\ 0 & 0 & \cdots & 0 & 0 & 0 & 0 & 0 & 0 \end{array}\right] \end{array}.$$

Since

$$\widehat{\mathbf{t}}^T(-S_eH_e^{-1}D)\widehat{\mathbf{t}} = \mathbf{t}^TQ_n\mathbf{t} + (-t_U-t_V)(t_1+\cdots+pt_p+(p+1)t_U) + t_Z(t_1+\cdots+pt_p+(p+1)t_U-t_W),$$

where $\mathbf{t} := (t_1, \ldots, t_p, t_U, t_W)$ and Q_n is defined in Theorem 4.45, we conclude that the kinematical kernel can be written as

$$\mathcal{K}_{Y_n}\left(\widehat{\mathbf{t}}\right) = e^{2i\pi\left(\mathbf{t}^TQ_n\mathbf{t} - t_Wt_Z + (t_Z-t_U-t_V)(t_1+\cdots+pt_p+(p+1)t_U)\right)}\delta(t_Z)\delta(-t_U-t_V).$$

We now compute the dynamical content. We denote $\alpha = (a_1, b_1, c_1, \ldots, a_W, b_W, c_W, a_Z, b_Z, c_Z)$ a general vector in $\mathcal{S}_{Y_n}$. Let $\hbar > 0$. The dynamical content $\mathcal{D}_{\hbar,Y_n}\left(\widehat{\mathbf{t}}, \alpha\right)$ is equal to:

$$e^{\frac{1}{\sqrt{\hbar}}\widehat{C}(\alpha)^T\widehat{\mathbf{t}}}\frac{\Phi_{\mathsf{b}}\left(t_V + \frac{i}{2\pi\sqrt{\hbar}}(\pi - a_V)\right)\Phi_{\mathsf{b}}\left(t_W + \frac{i}{2\pi\sqrt{\hbar}}(\pi - a_W)\right)}{\prod_{k=1}^{p}\Phi_{\mathsf{b}}\left(t_k - \frac{i}{2\pi\sqrt{\hbar}}(\pi - a_k)\right)\Phi_{\mathsf{b}}\left(t_U + \frac{i}{2\pi\sqrt{\hbar}}(\pi - a_U)\right)\Phi_{\mathsf{b}}\left(t_Z - \frac{i}{2\pi\sqrt{\hbar}}(\pi - a_Z)\right)},$$

where $\widehat{C}(\alpha) := (c_1, \ldots, c_p, c_U, c_V, c_W, c_Z)^T$.

Let us come back to the computation of the partition function of the Teichmüller TQFT. We begin by integrating over the variables t_V and t_Z, which consists in removing the two Dirac delta functions $\delta(-t_Z)$ and $\delta(-t_U - t_V)$ in the kinematical kernel and replacing t_Z by 0 and t_V by $-t_U$ in the other terms. Therefore, we have

$$\Phi_{\mathsf{b}}\left(\frac{\pi - a_Z}{2\pi i\sqrt{\hbar}}\right)\mathcal{Z}_\hbar(Y_n, \alpha) \overset{\star}{=} \int_{\mathbf{t}\in\mathbb{R}^{p+2}} d\mathbf{t}\, e^{2i\pi\mathbf{t}^TQ_n\mathbf{t}}e^{\frac{1}{\sqrt{\hbar}}(c_1t_1+\cdots+c_pt_p+(c_U-c_V)t_U+c_Wt_W)}\Pi(\mathbf{t}, \alpha, \hbar),$$

and

$$\Pi(\mathbf{t}, \alpha, \hbar) := \frac{\Phi_{\mathsf{b}}\left(-t_U + \frac{i}{2\pi\sqrt{\hbar}}(\pi - a_V)\right)\Phi_{\mathsf{b}}\left(t_W + \frac{i}{2\pi\sqrt{\hbar}}(\pi - a_W)\right)}{\Phi_{\mathsf{b}}\left(t_1 - \frac{i}{2\pi\sqrt{\hbar}}(\pi - a_1)\right)\cdots\Phi_{\mathsf{b}}\left(t_p - \frac{i}{2\pi\sqrt{\hbar}}(\pi - a_p)\right)\Phi_{\mathsf{b}}\left(t_U - \frac{i}{2\pi\sqrt{\hbar}}(\pi - a_U)\right)}.$$

Step 2. Applying the dominated convergence theorem for $\alpha \to \tau$.

This step is exactly as in the proof of Theorem 4.20. As for the odd case, for the rest of the proof, set

$$\tau := (a_1^\tau, b_1^\tau, c_1^\tau, \ldots, a_Z^\tau, b_Z^\tau, c_Z^\tau) \in \mathcal{S}_{Y_n\setminus Z} \times \overline{\mathcal{S}_Z}$$

be such that $\omega_j(\tau) = 2\pi$ for all $j \in \{0, 1, \dots, p-1, p+1\}$, $\widehat{\omega}_j(\tau) = 2\pi$ for all $j \in \{s, d, p\}$ and $\widehat{\omega}_{\overrightarrow{K_n}}(\tau) = a_Z^\tau = 0$.

Step 3. Retrieving the value $J_{X_n}(\hbar, 0)$ in $\alpha = \tau$.

Similarly as in the odd case, we do the following change of variables:

- $y'_k = t_k - \frac{i}{2\pi\sqrt{\hbar}}(\pi - a_k)$ for $k \in \{1, \dots, p, U\}$,
- $y'_W = t_W + \frac{i}{2\pi\sqrt{\hbar}}(\pi - a_W)$,

and we denote $\mathbf{y}' := \left(y'_1, \dots, y'_p, y'_U, y'_W\right)^T$. Again $a_U^\tau - a_V^\tau = (\widehat{\omega}_s(\tau) - 2\pi) + (\widehat{\omega}_d(\tau) - 2\pi) = 0$.

We also denote

$$\widetilde{\mathcal{Y}}'_{\hbar,\tau} := \prod_{k=1,\dots,p,U} \left(\mathbb{R} - \frac{i}{2\pi\sqrt{\hbar}}(\pi - a_k^\tau)\right) \times \left(\mathbb{R} + \frac{i}{2\pi\sqrt{\hbar}}(\pi - a_W^\tau)\right),$$

the subset of $\mathbb{C}^{p+2}$ on which the variables in $\mathbf{y}'$ reside.

By a similar computation as in the proof of Theorem 4.45, we obtain

$$\begin{aligned}
&\int_{\mathbf{t}\in\mathbb{R}^{p+2}} d\mathbf{t}\, e^{2i\pi\mathbf{t}^T Q_n \mathbf{t}} e^{\frac{1}{\sqrt{\hbar}}(c_1^\tau t_1 + \dots + c_p^\tau t_p + (c_U^\tau - c_V^\tau)t_U + c_W^\tau t_W)} \Pi(\mathbf{t}, \tau, \hbar) \\
&\overset{\star}{=} \int_{\mathbf{y}'\in\mathcal{Y}'_{\hbar,\tau}} d\mathbf{y}' e^{2i\pi\mathbf{y}'^T Q_n \mathbf{y}' + \frac{1}{\sqrt{\hbar}}\mathcal{W}(\tau)^T \mathbf{y}'} \frac{\Phi_{\mathsf{b}}\left(-y'_U\right)\Phi_{\mathsf{b}}\left(y'_W\right)}{\Phi_{\mathsf{b}}\left(y'_1\right)\cdots\Phi_{\mathsf{b}}\left(y'_p\right)\Phi_{\mathsf{b}}\left(y'_U\right)},
\end{aligned}$$

where for any $\alpha \in \mathcal{S}_{Y_n \setminus Z}$, $\mathcal{W}(\alpha)$ is defined as

$$\mathcal{W}(\alpha) := 2Q_n\Gamma(\alpha) + C(\alpha) + (0, \dots, 0, -c_V, 0)^T,$$

with $\Gamma(\alpha) := (a_1 - \pi, \dots, a_p - \pi, a_U - \pi, \pi - a_W)^T$ and $C(\alpha) := (c_1, \dots, c_p, c_U, c_W)^T$. Hence, from the value of $J_{X_n}(\hbar, 0)$, it remains only to prove that $\mathcal{W}(\tau) = \mathcal{W}_n$.

Let us denote $\Lambda : (u_1, \dots, u_p, u_U, u_V, u_W) \mapsto (u_1, \dots, u_p, u_U, u_W)$ the process of forgetting the second-to-last coordinate. Then obviously $C(\alpha) = \Lambda(\widetilde{C}(\alpha))$. Recall from the proof of Theorem 4.45 that $\widetilde{\mathcal{W}}(\alpha) = 2\widetilde{Q}_n\widetilde{\Gamma}(\alpha) + \widetilde{C}(\alpha)$ depends almost only on edge weights of the angles in X_n.

Thus, a direct calculation shows that for any $\alpha \in \mathcal{S}_{Y_n \setminus Z}$, we have

$$\mathcal{W}(\alpha) = \Lambda(\widetilde{\mathcal{W}}(\alpha)) + \begin{bmatrix} 0 \\ \vdots \\ 0 \\ -c_V + (\pi - a_V) + (\pi - a_W) \\ a_U - a_V \end{bmatrix}.$$

Now, if we specify $\alpha = \tau$, then the weights $\omega_{X_n,j}(\alpha)$ appearing in $\Lambda(\widetilde{\mathcal{W}}(\alpha))$ all become 2π, since $\omega_s(\tau) = \widehat{\omega}_s(\tau) - \widehat{\omega}_{\overrightarrow{K_n}}(\tau) = 2\pi$ and $\omega_p(\tau) = \widehat{\omega}_d(\tau) + \widehat{\omega}_p(\tau) - 2\left(\pi - \widehat{\omega}_{\overrightarrow{K_n}}(\tau)\right) = 2\pi$.

Hence

$$\mathcal{W}(\tau) = \mathcal{W}_n + \begin{bmatrix} 0 \\ \vdots \\ 0 \\ \frac{1}{2}\lambda_{X_n}(\tau) - \pi - c_V^\tau + (\pi - a_V^\tau) + (\pi - a_W^\tau) \\ a_U^\tau - a_V^\tau \end{bmatrix}.$$

Finally, since $\frac{1}{2}\lambda_{X_n}(\tau) = a_V^\tau - a_U^\tau + a_W^\tau - b_V^\tau$ and $a_U^\tau - a_V^\tau = 0$, we conclude that $\mathcal{W}(\tau) = \mathcal{W}_n$ and the theorem is proven. □

4.7.4 Geometricity implies the volume conjecture

In this section we will prove the following theorem, which can be compared with Theorem 4.22.

Theorem 4.48. *Let n be a positive even integer, and $J_{X_n}, \mathfrak{J}_{X_n}$ the functions defined in Theorem 4.45 and Corollary 4.46. If the ideal triangulation X_n is geometric, then*

$$\lim_{\hbar\to 0^+} 2\pi\hbar \log|J_{X_n}(\hbar, 0)| = \lim_{\hbar\to 0^+} 2\pi\hbar \log|\mathfrak{J}_{X_n}(\hbar, 0)| = -\mathrm{Vol}(S^3 \setminus K_n).$$

The following Corollary 4.49 is an immediate consequence of Theorem 4.48 and Theorem 4.41.

Corollary 4.49. *The Teichmüller TQFT volume conjecture of Andersen–Kashaev is proven for the even twist knots.*

Proof of Theorem 4.48. To prove Theorem 4.48, we will follow exactly the same general path as in Section 4.6. For the sake of brevity, we will thus only state the modifications that are due to the fact that n is even instead of odd. For the remainder of the section, let n be a positive even integer such that X_n is geometric. Let us first list the changes in notations:

- The open "multi-band" is now $\mathcal{U} := \left(\prod_{k=1,\dots,p,U} (\mathbb{R} + i(-\pi, 0))\right) \times (\mathbb{R} + i(0, \pi))$, and the closed one $\mathcal{U}_\delta$ (for $\delta > 0$) is $\mathcal{U}_\delta := \prod_{k=1,\dots,p,U} (\mathbb{R} + i[-\pi + \delta, -\delta]) \times (\mathbb{R} + i[\delta, \pi - \delta])$.
- As said in Corollary 4.46, $\mathcal{Y}_\alpha := \left(\prod_{k=1,\dots,p,U} (\mathbb{R} - i(\pi - a_k))\right) \times (\mathbb{R} + i(\pi - a_W))$.
- The potential function $S\colon \mathcal{U} \to \mathbb{C}$ is now $S := \mathbf{y} \mapsto$

  $$i\mathbf{y}^T Q_n \mathbf{y} + \mathbf{y}^T \mathcal{W}_n + i\mathrm{Li}_2(-e^{y_1}) + \cdots + i\mathrm{Li}_2(-e^{y_p}) + i\mathrm{Li}_2(-e^{y_U}) - i\mathrm{Li}_2\left(-e^{-y_U}\right) - i\mathrm{Li}_2(-e^{y_W}).$$

  The expressions of its quantum deformations S_b and S'_b (for $\mathsf{b} > 0$) should be obvious.
- The vector η, first appearing in Proposition 4.36, is now $\eta := (-1, \dots, -1, -2, 1)$.

We will state and prove several facts, which are variants of statements in Section 4.6.

Before all, let us remark that the non-degeneracy of the holomorphic hessian of S (Lemma 4.24) and the strict concavity of $\Re(S)$ (Lemma 4.26) are obtained immediately by arguments and computations similar with the ones in Section 4.6.

However, relating the vanishing of ∇S to Thurston's gluing equations (Lemma 4.25) needs a little more detail:

Fact 1. The diffeomorphism ψ induces a bijective mapping between $\{\mathbf{y} \in \mathcal{U} \mid \nabla S(\mathbf{y}) = 0\}$ and $\{\mathbf{z} \in (\mathbb{R} + i\mathbb{R}_{>0})^{p+2} \mid \mathcal{E}^{co}_{X_n}(\mathbf{z})\}$.

The system $\mathcal{E}^{co}_{X_n}(\mathbf{z})$ of equations (satisfied by the complete hyperbolic structure) is:

- $\mathcal{E}_{X_n,0}(\mathbf{z})$: $\mathrm{Log}(z'_1) + 2\mathrm{Log}(z_1) + \cdots + 2\mathrm{Log}(z_p) + 2\mathrm{Log}(z_U) = 2i\pi$
- $\mathcal{E}_{X_n,1}(\mathbf{z})$: $2\mathrm{Log}(z''_1) + \mathrm{Log}(z'_2) = 2i\pi$
- $\mathcal{E}_{X_n,k}(\mathbf{z})$: $\mathrm{Log}(z'_{k-1}) + 2\mathrm{Log}(z''_k) + \mathrm{Log}(z'_{k+1}) = 2i\pi$ (for $2 \leqslant k \leqslant p-1$)
- $\mathcal{E}^{co}_{X_n,p+1}(\mathbf{z})$: $\mathrm{Log}(z'_p) + 2\mathrm{Log}(z''_U) + \mathrm{Log}(z_W) = 2i\pi$
- $\mathcal{E}^{co}_{X_n,s}(\mathbf{z})$: $\mathrm{Log}(z''_W) - \mathrm{Log}(z_U) = 0$

To prove Fact 1, let us first compute, for $\mathbf{y} \in \mathcal{U}$:

$$\nabla S(\mathbf{y}) = 2iQ_n\mathbf{y} + \mathcal{W}_n + i\begin{pmatrix} -\mathrm{Log}(1+e^{y_1}) \\ \vdots \\ -\mathrm{Log}(1+e^{y_p}) \\ -\mathrm{Log}(1+e^{y_U}) - \mathrm{Log}(1+e^{-y_U}) \\ \mathrm{Log}(1+e^{y_W}) \end{pmatrix}.$$

Then, we define the matrix $A :=$

$$\begin{array}{c|c} & \begin{array}{ccccccc} y_1 & y_2 & y_3 & \cdots & y_p & y_U & y_W \end{array} \\ \begin{array}{c} y_1 \\ y_2 \\ y_3 \\ \vdots \\ y_p \\ \hline y_U \\ y_W \end{array} & \left[\begin{array}{ccccc|cc} 1 & & & & & & \\ -2 & 1 & & & 0 & & \\ 1 & -2 & 1 & & & & \\ & \ddots & \ddots & \ddots & & & \\ & & 1 & -2 & 1 & 0 & 0 \\ \hline & & & & -1 & 1 & 1 \\ & 0 & & & 0 & 0 & 1 \end{array}\right] \end{array} \in GL_{p+2}(\mathbb{Z}),$$

and we compute $A \cdot \nabla S(\mathbf{y}) =$

$$\begin{pmatrix} 2i(y_1 + \cdots + y_p - y_U) - 2\pi p - i\mathrm{Log}(1+e^{y_1}) \\ -2iy_1 + 2\pi + 2i\mathrm{Log}(1+e^{y_1}) - i\mathrm{Log}(1+e^{y_2}) \\ -2iy_2 + 2\pi - i\mathrm{Log}(1+e^{y_1}) + 2i\mathrm{Log}(1+e^{y_2}) - i\mathrm{Log}(1+e^{y_3}) \\ \vdots \\ -2iy_k + 2\pi - i\mathrm{Log}(1+e^{y_{k-1}}) + 2i\mathrm{Log}(1+e^{y_k}) - i\mathrm{Log}(1+e^{y_{k+1}}) \\ \vdots \\ -2iy_{p-1} + 2\pi - i\mathrm{Log}(1+e^{y_{p-2}}) + 2i\mathrm{Log}(1+e^{y_{p-1}}) - i\mathrm{Log}(1+e^{y_p}) \\ iy_U - iy_W - 2\pi - i\mathrm{Log}(1+e^{y_p}) - i\mathrm{Log}(1+e^{y_U}) - i\mathrm{Log}(1+e^{-y_U}) + i\mathrm{Log}(1+e^{y_W}) \\ -iy_U + i\pi + i\mathrm{Log}(1+e^{y_W}) \end{pmatrix}.$$

Hence we compute, for all $\mathbf{z} \in (\mathbb{R} + i\mathbb{R}_{>0})^{p+2}$,

$$A \cdot (\nabla S)(\psi(\mathbf{z})) = i \begin{pmatrix} \mathrm{Log}(z'_1) + 2\mathrm{Log}(z_1) + \cdots + 2\mathrm{Log}(z_p) + 2\mathrm{Log}(z_U) - 2i\pi \\ 2\mathrm{Log}(z''_1) + \mathrm{Log}(z'_2) - 2i\pi \\ \mathrm{Log}(z'_1) + 2\mathrm{Log}(z''_2) + \mathrm{Log}(z'_3) - 2i\pi \\ \vdots \\ \mathrm{Log}(z'_{k-1}) + 2\mathrm{Log}(z''_k) + \mathrm{Log}(z'_{k+1}) - 2i\pi \\ \vdots \\ \mathrm{Log}(z'_{p-2}) + 2\mathrm{Log}(z''_{p-1}) + \mathrm{Log}(z'_p) - 2i\pi \\ -\mathrm{Log}(z'_p) - 2\mathrm{Log}(z''_U) - \mathrm{Log}(z'_W) + 2i\pi \\ \mathrm{Log}(z''_W) - \mathrm{Log}(z_U) \end{pmatrix},$$

which is zero if and only if the system $\mathcal{E}^{co}_{X_n}(\mathbf{z})$ is satisfied. Fact 1 then follows from the invertibility of A.

The second fact, a variant of Lemma 4.28, is proven similarly, using Proposition 2.41:

Fact 2. The function $S\colon \mathcal{U} \to \mathbb{C}$ can be re-written

$$S(\mathbf{y}) = i\mathrm{Li}_2\left(-e^{y_1}\right) + \cdots + i\mathrm{Li}_2\left(-e^{y_p}\right) + 2i\mathrm{Li}_2\left(-e^{y_U}\right) + i\mathrm{Li}_2\left(-e^{-y_W}\right) + i\mathbf{y}^T Q_n \mathbf{y} + i\frac{y_U^2}{2} + i\frac{y_W^2}{2} + \mathbf{y}^T \mathcal{W}_n + i\frac{\pi^2}{3}.$$

Consequently, the fact that $\Re(S)(\mathbf{y^0}) = -\mathrm{Vol}(S^3 \backslash K_n)$ is proven like in the proof of Lemma 4.29, using the particular form of S stated in Fact 2, and the fact that at the complete angle structure, $-e^{y_U^0} = z_U^0 = z_V^0 = -e^{-y_V^0}$ is the complex shape of both tetrahedra U and V.

The rest of the statements in Section 4.6 (Lemma 4.27 and Proposition 4.30 to Proposition 4.39) are proven in exactly the same way, using the new notations defined at the beginning of this proof.

Notably, we obtain the following asymptotic behaviour for $\mathfrak{J}_{X_n}(\hbar, 0)$:

$$\mathfrak{J}_{X_n}(\hbar, 0) = \left(\frac{1}{2\pi\sqrt{\hbar}}\right)^{p+3} e^{\frac{1}{2\pi\hbar}S(\mathbf{y^0})} \left(\rho' \hbar^{\frac{p+2}{2}} \left(1 + o_{\hbar \to 0^+}(1)\right) + \mathcal{O}_{\hbar \to 0^+}(1)\right).$$

□

❧ Chapter 5 ❧

Calculations for knots in lens spaces

In this chapter, we start by giving a method to construct H-triangulations of pairs (M, L) from specific ideal triangulations of the complement $M \setminus L$. Using this method, we will construct for all $n \geqslant 1$, H-triangulations of pairs $(L(n,1), \mathcal{K}_n)$, where $\mathcal{K}_n$ is obtained by an $(n,1)$-Dehn surgery on one component of the Whitehead link. We then compute the Teichmüller TQFT partition function for this infinite family of hyperbolic fibered knots in $L(n,1)$ and also for some isolated cases of hyperbolic knots in $\mathbb{R}P^3$.

5.1 Construction of exotic hyperbolic H-triangulations

If M is a closed oriented 3-manifold different from the 3-sphere, then one can still easily find an H-triangulation of a pair (M, K), with $K \subset M$ a knot, because any triangulation of M with one vertex is an H-triangulation. However, in this case we absolutely do not have any control on the knot K, in particular on its complement. The aim of this section is to give a very simple way to construct an H-triangulation, called *T-surgery*, only from an ideal triangulation of its complement. We start by some definitions and explaining the assumptions that we need on the ideal triangulation to apply this method.

5.1.1 Split ideal triangulations

We give some new terminologies and technical definitions which will be important to explain our construction.

Definition 5.1. Let Y be an H-triangulation of (M, L). If $L \subset M$ is a hyperbolic link, we say that Y is *hyperbolic*. If $M \neq S^3$, we say that Y is *exotic*.

Definition 5.2. Let $\mathbb{T}$ be the torus. A closed curve $\gamma \subset \mathbb{T}$ is *cylindrical* if $\mathbb{T} \setminus \gamma$ is homeomorphic to $S^1 \times (0,1)$.

Definition 5.3. Let X be an ideal triangulation. We say that $F \in X^2$ is *admissible* if there exist $\widetilde{H} \in \widetilde{\mathfrak{h}}_X$ and $\widetilde{e} \in \widetilde{\mathfrak{s}}_X$ with $\widetilde{e} \subset \widetilde{H}$ such that $p(\widetilde{H}) = \Theta(F)$ and $p(\widetilde{e})$ is a cylindrical curve.

Definition 5.4. Let X be a triangulation. For $F \in X^2$, $e \in X^1$ and $a, b \in X^0$, we say that F is $(e|a,b)$-*conic* if there is $e' \in X^1$ with $e' \neq e$, such that F is one of the forms given in Figure 5.1.

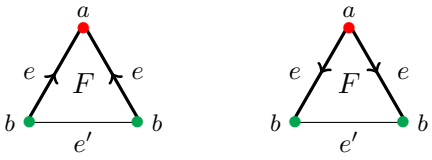

(a) Type U. (b) Type D.

Figure 5.1: The two types of an $(e|a,b)$-conic face.

Definition 5.5. Let X be an ideal triangulation with $X^0 = \{v_1, \dots, v_n\}$. We say that X is *split* if there exist $F_1, \dots, F_n \in X^2$, $e_1, \dots, e_n \in X^1$ with $e_i \neq e_j$ for $i \neq j$ and a permutation $\sigma \in S_n$ such that for $i = 1, \dots, n$,

(i) F_i is admissible,

(ii) F_i is $(e_i|v_i, v_{\sigma(i)})$-conic.

We say that $\{F_1, \dots, F_n\}$ is a *splitting family*. If $n = 1$, we simply say that F_1 is *splitting*.

Example 5.6. The ideal triangulation X of Figure 2.5 is split. In this case, all the faces are splitting. Indeed, if we denote by $*$ the only ideal vertex of X and if we look at Figures 2.25 and 2.26 for cylindrical curves, then

- A is admissible with cylindrical curve j and $(\uparrow|*,*)$-conic of type U;
- B is admissible with cylindrical curve e and $(\Uparrow|*,*)$-conic of type D;
- C is admissible with cylindrical curve a and $(\uparrow|*,*)$-conic of type D;
- D is admissible with cylindrical curve h and $(\Uparrow|*,*)$-conic of type U.

5.1.2 T-surgery

We now have all the necessary tools to state the method of construction.

Proposition 5.7. *Let X be a split ideal triangulation of a 3-manifold with boundary tori with m tetrahedra and n ideal vertices. Then there exists an H-triangulation of a pair (M, L) with $m + n$ tetrahedra such that $M \setminus L$ is homeomorphic to $X \setminus X^0$.*

Proof. Let $\{F_1, \dots, F_n\}$ be a splitting family. Denote the vertices by $v_1, \dots, v_n$ and assume that F_i is $(e_i|v_i, v_{\sigma(i)})$-conic for $i = 1, \dots, n$ with some permutation $\sigma \in S_n$. Fix $k \in \{1, \dots, n\}$ and assume that F_k is of type U. Let $H_k, H_k' \in \widetilde{\mathfrak{h}}_X$ be such that $p(H_k) = p(H_k') = \Theta(F_k)$. We illustrate them in Figure 5.2.

Consider the truncated tetrahedron in Figure 5.3 (a). Denote

$$a := p(e_1), \qquad b := p(e_2) = p(e_3), \qquad c := p(e_4),$$

Figure 5.2: Hexagonal cells H_k and H'_k. After gluing, the red short cells live in $\mathrm{Lk}(v_k)$ and the green short cells in $\mathrm{Lk}(v_{\sigma(k)})$.

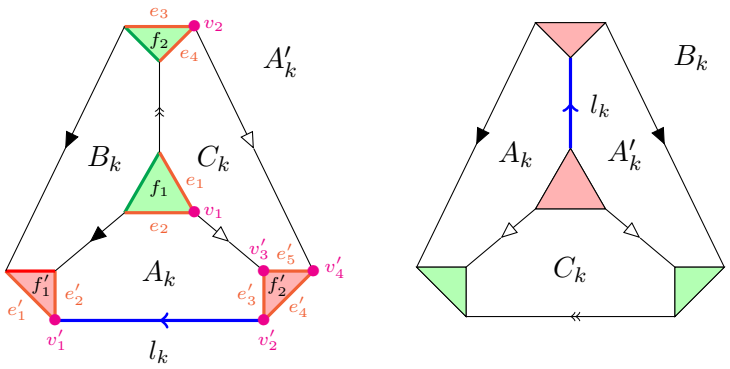

(a) For type U. (b) For type D.

Figure 5.3: Truncated tetrahedra which will be glued. Only the long 1-cells are given with the gluing informations.

$$a' := p(e'_1) = p(e'_2), \qquad b' := p(e'_3) = p(e'_4), \qquad c' := p(e'_5),$$

and

$$u := p(v_1) = p(v_2), \qquad u' := p(v'_1), \qquad v' := p(v'_2), \qquad w' := p(v'_3) = p(v'_4).$$

Construct a new truncated triangulation by identifying A_k to A'_k, B_k to H_k, C_k to H'_k and keeping all the other relations on $\Theta(X)$. Green triangle parts will modify $\mathrm{Lk}(v_{\sigma(k)})$ and red triangle parts will modify $\mathrm{Lk}(v_k)$. Let us denote the respective new vertex links by $\mathrm{Lk}^{\mathrm{new}}(v_{\sigma(k)})$ and $\mathrm{Lk}^{\mathrm{new}}(v_k)$. More precisely, $\mathrm{Lk}^{\mathrm{new}}(v_{\sigma(k)})$ admits one new vertex u, three new short edges a, b, c and two new faces f_1, f_2 (see Figure 5.4). Therefore, the Euler characteristic is unchanged and thus $\mathrm{Lk}^{\mathrm{new}}(v_{\sigma(k)})$ is still a topological torus. For $\mathrm{Lk}^{\mathrm{new}}(v_k)$, it admits three new vertices u', v', w', three new short edges a', b', c' and two new faces f'_1, f'_2 (see Figure 5.5). The Euler characteristic has increased of 2, and thus the result will be a topological 2-sphere. Note that admissibility of F_k has been used to cut $\mathrm{Lk}(v_k)$ along the cylindrical curve to obtain a cylinder in Figure 5.5.

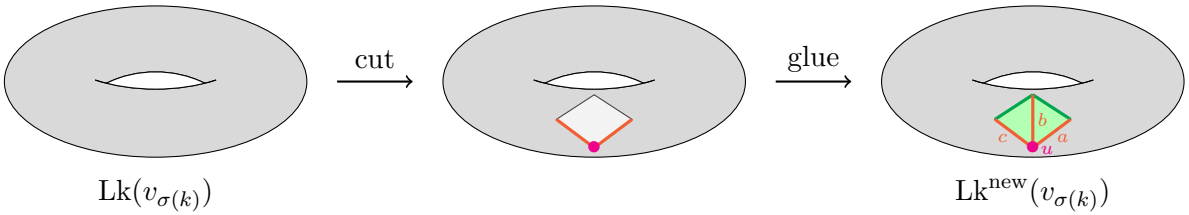

Figure 5.4: Modification of $\mathrm{Lk}(v_{\sigma(k)})$.

If F_k is of type D, we do a similar reasoning with the truncated tetrahedron of Figure 5.3 (b).

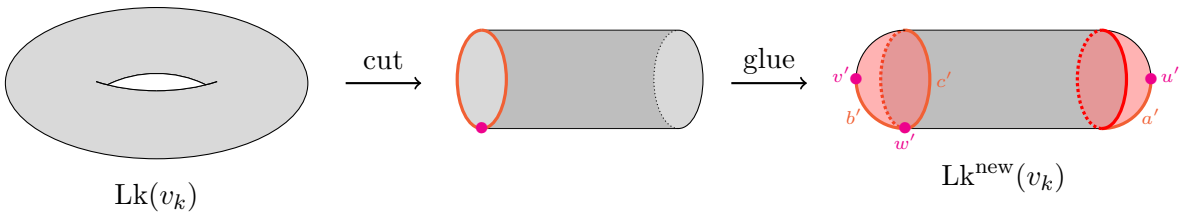

Figure 5.5: Modification of $\mathrm{Lk}(v_k)$.

The resulting truncated triangulation admits $n-1$ boundary tori and one spherical boundary. Applying this method for $k = 1, \ldots, n$, we finish by getting a truncated triangulation Z with n spherical boundaries, thus the underlying space of $\Theta^{-1}(Z)$ becomes a closed 3-manifold. At each step we added a distinguished edge (blue ones in Figures 5.3 (a) and 5.3 (b)) and at the end these edges will form a link with n components.

Finally, if we collapse each of these distinguished edges of $\Theta^{-1}(Z)$, then we get n bigons with different boundary edges, and thus each bigon can again be contracted into one edge. Consequently, one comes back to the original ideal triangulation X. □

Terminology 5.8. The technique of "snatching and adding tetrahedra" on the splitting family $\{F_1, \ldots, F_n\}$ used in the proof of Proposition 5.7 will be called *T-surgery* on $\{F_1, \ldots, F_n\}$ for the rest of the thesis.

Notation 5.9. Let X be a split ideal triangulation with n vertices with a splitting family $\{F_1, \ldots, F_n\}$. Then the resulting H-triangulation from T-surgery on $\{F_1, \ldots, F_n\}$ is denoted by $t_X(F_1, \ldots, F_n)$ and the underlying closed 3-manifold by $\widehat{t}_X(F_1, \ldots, F_n)$.

Example 5.10. Since the face A of the ideal triangulation X given in Example 2.7 is splitting, then Proposition 5.7 allows us to apply T-surgery on the face A, and we obtain the triangulation of Figure 5.6.

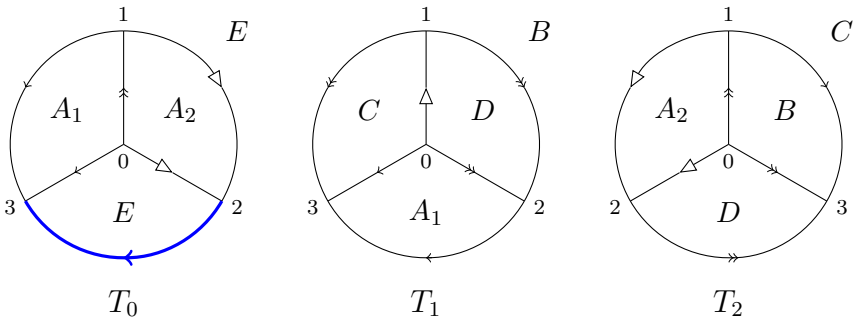

Figure 5.6: The triangulation $t_X(A)$.

We can check that $\widehat{t}_X(A) = S^3$ and the blue bold edge represents a knot in S^3 with complement homeomorphic to $S^3 \setminus 4_1$. Since knots in S^3 are determined by their complements and the figure-eight knot is amphichiral, the blue bold edge is exactly the figure-eight knot. Consequently, $t_X(A)$ is an H-triangulation of $(S^3, 4_1)$. In fact, we remark that $t_X(A)$ is nothing else than the H-triangulation of $(S^3, 4_1)$ that we found in Section 2.1.7.1.

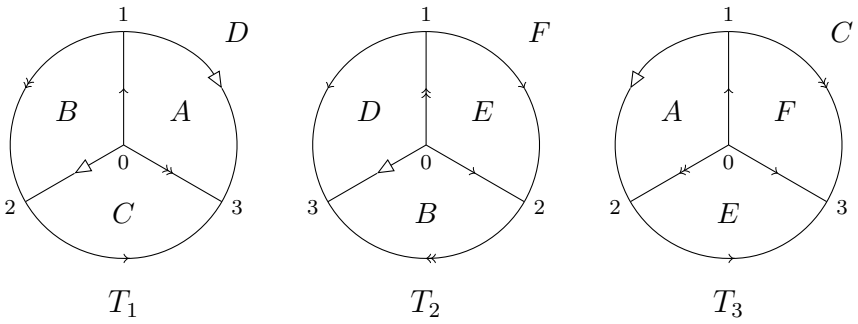

Figure 5.7: An ideal triangulation of $m009$.

5.1.3 Examples of exotic hyperbolic H-triangulations

We now apply Proposition 5.7 to construct some new examples of H-triangulations of pairs (M, K) with $K \subset M$ a hyperbolic knot and $M \neq S^3$. We will compute their partition functions in Section 5.3.

Definition 5.11. Let Y be an H-triangulation of a pair (M, K), where $K \subset M$ is a knot. We say that Y is *null-homologous* if K is null-homologous.

5.1.3.1 Cusped 3-manifold $m009$

It is known that $m009$ (in `SnapPy` census) is a cusped hyperbolic 3-manifold, with volume 2.66674..., obtained by performing a $(2, 1)$-Dehn surgery on one component of the Whitehead link. Since a $(2, 1)$-Dehn surgery on the trivial knot yields the real projective space $\mathbb{R}P^3$ (which is the lens space $L(2, 1)$), we see that $m009$ is the complement of a hyperbolic knot in $\mathbb{R}P^3$. Let us take the ideal triangulation X of $m009$ of Figure 5.7. As in Example 5.10, we can easily check that E is a splitting face, and thus X is split. The graphical representation is given in Figure 5.9 (a), where the face E is marked by a red dot. Performing a T-surgery on the face E, one obtains the H-triangulation illustrated in Figure 5.8.

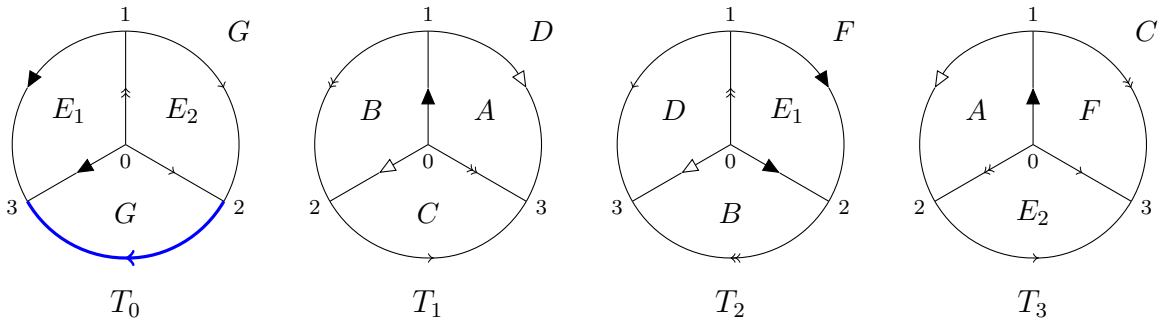

Figure 5.8: H-triangulation obtained from Figure 5.7.

Using this triangulation, we can easily check that $\pi_1(\widehat{t}_X(E)) = \mathbb{Z}/2\mathbb{Z}$, and since $\widehat{t}_X(E)$ is a closed 3-manifold by Proposition 5.7, it implies that $\widehat{t}_X(E) = \mathbb{R}P^3$ (see for example [AFW15]). Thus, the blue bold edge represents a hyperbolic knot in $\mathbb{R}P^3$ with complement homeomorphic to $m009$. Moreover, as an intermediate step, we see that the knot is trivial

in $\pi_1(\widehat{t_X}(E))$, and thus $t_X(E)$ is null-homologous. Graphically, the H-triangulation of Figure 5.8 is represented in Figure 5.9 (b). We will generalize this example in Section 5.2.

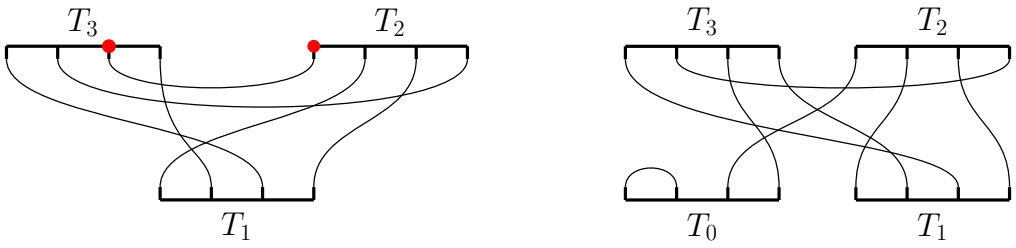

(a) (b)

Figure 5.9: Graphical representations of triangulations of Figures 5.7 (left) and 5.8 (right).

Remark 5.12. In graphical representation, doing a T-surgery is similar to cut the path joining the splitting faces and attach the remaining faces of the tetrahedron that we add. Therefore, we will from now give only a split ideal triangulation of the cusped 3-manifold by specifying the splitting face (with a red dot), and we will denote by M the resulting closed 3-manifold from T-surgery.

5.1.3.2 Cusped 3-manifold $m045$

The cusped 3-manifold $m045$ is hyperbolic with volume 3.27587..., obtained by a $(2,1)$-Dehn surgery on the red component of the link 7_8^2, illustrated in Figure 5.10 (a). A split geometric ideal triangulation of $m045$ is given in Figure 5.10 (b), where all tetrahedra are positive. As before, we see that $\pi_1(M) = \mathbb{Z}/2\mathbb{Z}$, and thus $M = \mathbb{R}P^3$. Moreover, the H-triangulation is null-homologous.

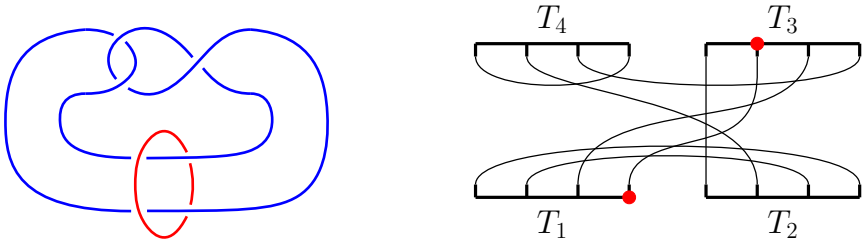

(a) (b)

Figure 5.10: The link 7_8^2 (left) and an ideal triangulation of $m045$ (right).

5.1.3.3 Cusped 3-manifold $m148$

The cusped 3-manifold $m148$ is hyperbolic with volume 3.75884..., obtained by a $(2,1)$-Dehn surgery on one component of the link 6_3^2, illustrated in Figure 5.11 (a). A split geometric ideal triangulation of $m148$ is given in Figure 5.11 (b), where all tetrahedra are positive. Again, we see that $M = \mathbb{R}P^3$ with null-homologous H-triangulation.

5.1.3.4 Cusped 3-manifold $m137$

Our last example is the cusped hyperbolic 3-manifold $m137$ with volume 3.66386..., obtained by a $(0,1)$-Dehn surgery on one component of the link 7_2^2 illustrated in Figure

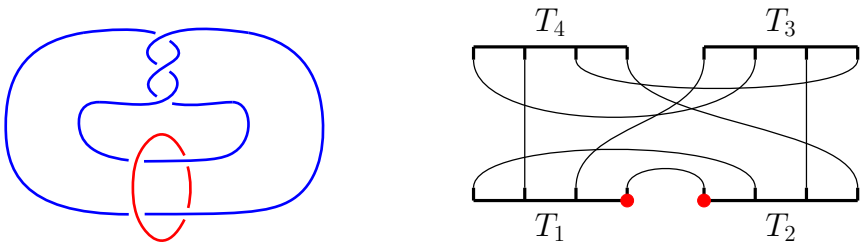

(a) (b)

Figure 5.11: The link 6_3^2 (left) and an ideal triangulation of $m148$ (right).

5.12 (a). Thus $m137$ is the complement of a hyperbolic knot in $S^1 \times S^2$, and a split geometric ideal triangulation is given in Figure 5.12 (b), where the bottom tetrahedra are positive and the top tetrahedra negative. Since $\pi_1(M) = \mathbb{Z}$, one concludes that $M = S^1 \times S^2$.

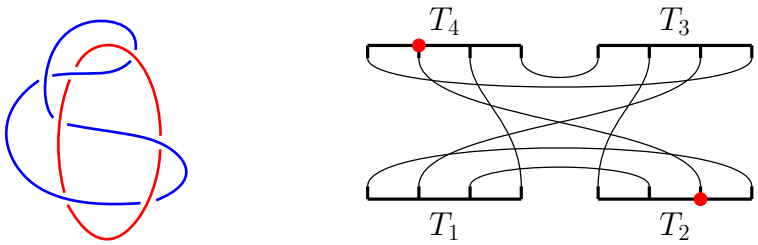

(a) (b)

Figure 5.12: The link 7_2^2 (left) and an ideal triangulation of $m137$ (right).

5.1.4 Links in lens spaces

Before stating computations, let us do a quick overview about knot theory in lens spaces.

We recall that a knot K in an oriented 3-manifold M is *determined by its complement* if the existence of a homeomorphism between $M \setminus K$ and $M \setminus K'$ for some knot $K' \subset M$, implies the existence of homeomorphism (not necessarily orientation preserving) between the pair (M, K) and (M, K'). Gordon and Luecke [GL89] proved that knots in S^3 are determined by their complements, and a similar result has been proved by Gabai [Gab87] for knots in $S^1 \times S^2$. Later, Matignon [Mat10] showed that non-hyperbolic knots in lens spaces are determined by their complements, except the axes in $L(p, q)$ when $q^2 \equiv \pm 1 \pmod{p}$. The situation seems more mysterious for hyperbolic knots. Indeed, an example of a hyperbolic knot in $L(49, 18)$ which is not determined by its complement has been found [BHW99], and Matignon [Mat17] gave a general explanation of this phenomenon using H-knots.

Drobotukhina gave a classification of knots in $\mathbb{R}P^3$ up to 6 crossings [Dro94] generalizing the Jones polynomial for knots in $\mathbb{R}P^3$ [Dro91]. There are different ways to represent a link in a lens space and a method to shift between them is explained in [GM18]. We will easily explain this method and use it to find an explicit diagram for the knots constructed in Section 5.1.3.

For p and q coprime integers satisfying $0 < q < p$, since $L(p, q)$ can be seen as the 3-ball B^3 with the upper hemisphere identified with the lower hemisphere with a rotation of angle $2\pi q/p$, one way to represent a link in $L(p, q)$ is the *disk diagram*. This consists in projecting

the link onto the equatorial disk of B^3, with the resolution of double points with overpasses and underpasses. To avoid confusion, we label the endpoints of the projection of the link coming from the upper hemisphere by $+1, \dots, +t$, and with $-1, \dots, -t$ the endpoints coming from the lower hemisphere, respecting the rule $+i \sim -i$ for all $i = 1, \dots, t$. We illustrate an example in Figure 5.13.

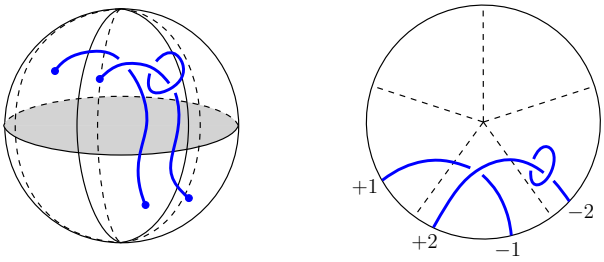

Figure 5.13: A link in $L(5,1)$ (left) and its disk diagram (right).

Recall that $L(p,q)$ can also be constructed by a (p,q)-Dehn surgery over the unknot $U \subset S^3$. This implies that a link $L \subset L(p,q)$ can be represented by a link $L' \cup U \subset S^3$, and since the complement of the unknot in S^3 is a solid torus, we conclude that a link in $L(p,q)$ can be represented by a link in the solid torus, and its "regular" projection onto a rectangle (see [GM18] for more details) is called the *band diagram*. An example is given in Figure 5.14.

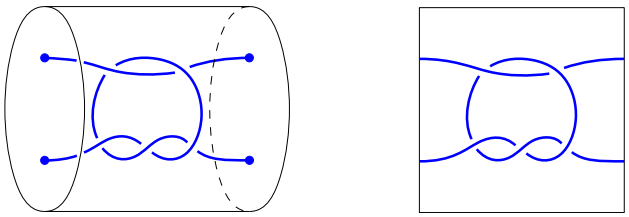

Figure 5.14: A link in the solid torus (left) and its corresponding band diagram (right).

Remark 5.13. Note that we only consider (p,q)-Dehn surgeries with p and q positive, because $L(p,q)$ and $L(p,-q)$ (or $L(-p,q)$) are homeomorphic (via an orientation reversing homeomorphism). Consequently, if we denote by $(L')^* \cup U$ the link $L' \cup U$ that we changed all the crossings on L', the link $L \subset L(p,q)$ can also be constructed doing a $(p,-q)$-Dehn surgery (or $(-p,q)$-Dehn surgery) on U.

A natural question is to understand how to pass from the band diagram to the disk diagram, and conversely. The answer is given by the following result.

Proposition 5.14 ([GM18, Proposition 2])**.** *Let L be a link in $L(p,q)$ assigned via a band diagram B_L. A disk diagram D_L representing L can be obtained by the transformation in Figure 5.15, where Δ is the Garside element in the braid group B_t (see Figure 5.16).*

Recall that an *L-space* (originally introduced in [OS05]) is a rational homology sphere Y with "smallest" Heegaard Floer homology, in the sense that $\operatorname{rank}(\widehat{HF}(Y)) = |H_1(Y,\mathbb{Z})|$.

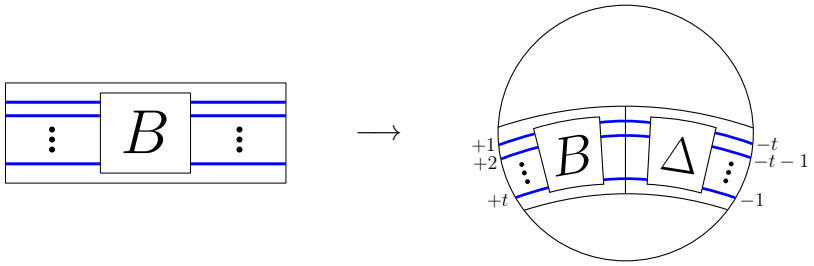

Figure 5.15: From band diagram B_L to disk diagram D_L.

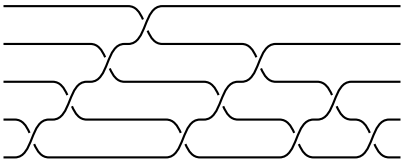

Figure 5.16: The Garside element Δ in B_5.

Gainullin states the following result as a consequence of the surgery characterization of the unknot for null-homologous knot in L-spaces. For the proof, see [Gai18, Theorem 8.2].

Theorem 5.15 (Gainullin [Gai18])**.** *Null-homologous knots in L-spaces are determined by their complements.*

We immediately obtain the following consequence.

Corollary 5.16. *Let M be an L-space and $K_1 \subset M$ a null-homologous knot. Let X be a split ideal triangulation of $M \setminus K_1$ with splitting face F. If $t_X(F)$ is a null-homologous H-triangulation of a pair (M, K_2) such that $M \setminus K_1$ is homeomorphic to $M \setminus K_2$, then K_1 and K_2 are ambient isotopic (up to mirror imaging).*

Let us now try to find out the disk diagrams for the knots constructed in Sections 5.1.3.1, 5.1.3.2 and 5.1.3.3. For the example of Section 5.1.3.1, since $m009$ is obtain by a $(2, 1)$-Dehn surgery on a component of the Whitehead link complement, the band diagram of the corresponding knot in $\mathbb{R}P^3$, with complement $m009$, is given in Figure 5.17. Using Proposition 5.14, we see that its corresponding disk diagram is given in Figure 5.18 (a). According to Drobotukhina's notation [Dro94], let us denote this knot by 3_1. We also know that lens spaces are L-spaces (see [OS05]). To show that the knot 3_1 (or its mirror image) is ambient isotopic to the knot in the H-triangulation of Figure 5.8 constructed from T-surgery, it remains to show that the knot 3_1 is null-homologous in $\mathbb{R}P^3$. For that, let us explain the general method of [CMM13].

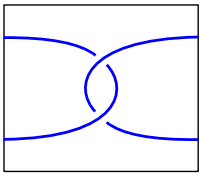

Figure 5.17: Band diagram of the knot in $\mathbb{R}P^3$ coming from surgery on the Whitehead link.

Assume that K is a knot in $L(p,q)$ represented with a disk diagram, and we fix an orientation for K. Label by $+1,\dots,+t$ the endpoints of K on the upper hemisphere. For $i=1,\dots,t$, define

$$\epsilon_i := \begin{cases} +1 & \text{if } K \text{ starts from the point } +i \text{ (according to the orientation on } K), \\ -1 & \text{otherwise.} \end{cases}$$

Then, define two numbers by

$$n_1 := |\{\epsilon_i \mid \epsilon_i = +1,\ i=1,\dots,t\}| \qquad \text{and} \qquad n_2 := |\{\epsilon_i \mid \epsilon_i = -1,\ i=1,\dots,t\}|.$$

Finally, we define the element $\delta_K := [q(n_2-n_1)] \in \mathbb{Z}/p\mathbb{Z}$ and we state the following useful lemma.

Lemma 5.17 ([CMM13, Lemma 4])**.** *If $K \subset L(p,q)$ is an oriented knot and $[K]$ is the homology class of K in $H_1(L(p,q),\mathbb{Z}) \cong \mathbb{Z}/p\mathbb{Z}$, then $[K] = \delta_K$.*

Let us come back to our problem. From Lemma 5.17, one can directly see that the knot 3_1 is null-homologous in $\mathbb{R}P^3$. Consequently, we can apply Corollary 5.16 and conclude that the knot in the H-triangulation of Figure 5.8 is ambient isotopic to the knot 3_1 (or to its mirror image). By a similar reasoning, we can show that the disk diagrams of the knots constructed in Sections 5.1.3.2 and 5.1.3.3 are respectively given in Figures 5.18 (b) and 5.18 (c), and we denote them respectively by 4_1 and 4_2.

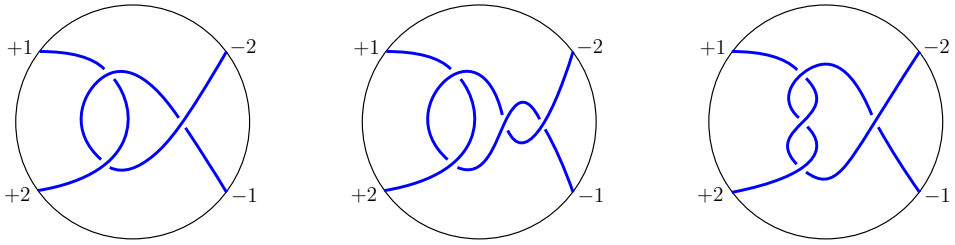

(a) 3_1 in $\mathbb{R}P^3$. (b) 4_1 in $\mathbb{R}P^3$. (c) 4_2 in $\mathbb{R}P^3$.

Figure 5.18: Knots constructed in Sections 5.1.3.1, 5.1.3.2 and 5.1.3.3.

5.2 Calculations for the family $(L(n,1),\mathcal{K}_n)$ with $n \geqslant 1$

Let $K \cup U$ be the Whitehead link described in Figure 4.3 and $n \in \mathbb{Z}$. If $\mathcal{K}_n$ denotes the knot corresponding to K obtained by $(n,1)$-Dehn surgery on U, then $\mathcal{K}_n$ becomes a knot in the lens space $L(n,1)$, and we will denote $WL(n,1) := L(n,1) \setminus \mathcal{K}_n$. We recall the following well-known result [HMW92, Proposition 3].

Proposition 5.18. *The cusped 3-manifold $WL(n,1)$ is homeomorphic to the once-punctured torus bundle over the circle with monodromy*

$$\begin{bmatrix} n+2 & 1 \\ -1 & 0 \end{bmatrix}. \tag{5.19}$$

Moreover, the matrix (5.19) is conjugate to the canonical form RL^n (where R and L are defined in (1.17)) when $n \geqslant 0$ and to $-RL^m$ when $n = -4-m \leqslant -4$.

Using Theorem 1.16, we immediately see that $WL(n,1)$ is hyperbolic if and only if $n \neq 0,\dots,-4$. Some examples are illustrated in Figure 5.19. Note that $m004$ is nothing else than the complement of the figure-eight knot and $m003$ its sister.

n	`SnapPy` census	Dehn Surgery coefficient from the Whitehead link	Hyperbolic volume
-6	$m010$	$(-6,1)$	2.66674478...
-5	$m003$	$(-5,1)$	2.02988321...
1	$m004$	$(1,1)$	2.02988321...
2	$m009$	$(2,1)$	2.66674478...
3	$m023$	$(3,1)$	2.98912028...
4	$m039$	$(4,1)$	3.17729327...
5	$s000$	$(5,1)$	3.29690241...
6	$v0000$	$(6,1)$	3.37759740...

Figure 5.19: Examples of $WL(n,1)$.

Theorem 5.20. *For all $n \geqslant 1$, Conjecture 3.68 holds for the pair $(L(n,1),\mathcal{K}_n)$.*

Remark 5.21. The reason that we could not check Conjecture 3.68 for $n \leqslant -5$ is that the monodromy triangulation of $WL(n,1)$ admits cycles for $n \leqslant -5$ (see Remark 2.23 (a)). If we eliminate cycles by increasing the number of tetrahedra, the new ideal triangulation is no more geometric (which is crucial for the third point of Conjecture 3.68) and not split, and thus we cannot directly construct H-triangulations using Proposition 5.7, as we will do for the case $n \geqslant 1$.

In a similar way as Chapter 4, we separate the proof of Theorem 5.20 into three parts (Theorems 5.22, 5.42 and 5.58). Since the computations are quite similar, we will give less explanations.

5.2.1 Monodromy triangulation of $WL(n,1)$ for $n \geqslant 1$

Let $n \geqslant 1$ be an integer. Taking the convention to give the positive sign to the first tetrahedron, the monodromy triangulation of $WL(n,1)$, for which the monodromy is conjugate to the element RL^n in $SL_2(\mathbb{Z})$ (Proposition 5.18), will be denoted X_n. The triangulation is given in Figure 5.20 and its graphical representation in Figure 5.21. The elements of X_n^1 are $\overrightarrow{a},\overrightarrow{e_0},\dots,\overrightarrow{e_{n-1}}$ with the convention that $\overrightarrow{e_0}=\overrightarrow{e_n}$, and we do not put overarrows on the edges on the figure (all represented by a simple arrow). The face D (represented by a red dot in Figure 5.21) is a splitting face and thus X_n is split. We added a blue dot for the crossing points of the lines in Figure 5.21 which means in this case that the two tetrahedra involved in this gluing part admit different signs. Finally, we added either an "R" or an "L" next to each tetrahedron in Figure 5.21 to show explicitly which tetrahedron represents either a right or a left flip.

For $\alpha=(a_1,b_1,c_1,\dots,a_{n+1},b_{n+1},c_{n+1}) \in \mathcal{S}_{X_n}$ a shape structure on X_n, we compute the weights of each edge:

- $\omega_a(\alpha) := \omega_{X_n,\alpha}(\overrightarrow{a}) = 2b_1+c_1+2a_2+\dots+2a_{n+1}+c_{n+1}$
- $\omega_0(\alpha) := \omega_{X_n,\alpha}(\overrightarrow{e_0}) = 2a_1+c_2+c_n+2b_{n+1}$

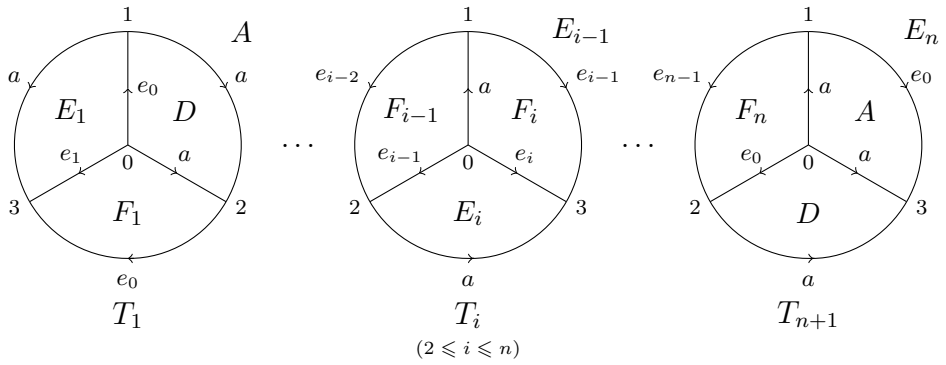

Figure 5.20: Monodromy triangulation X_n of $WL(n,1)$.

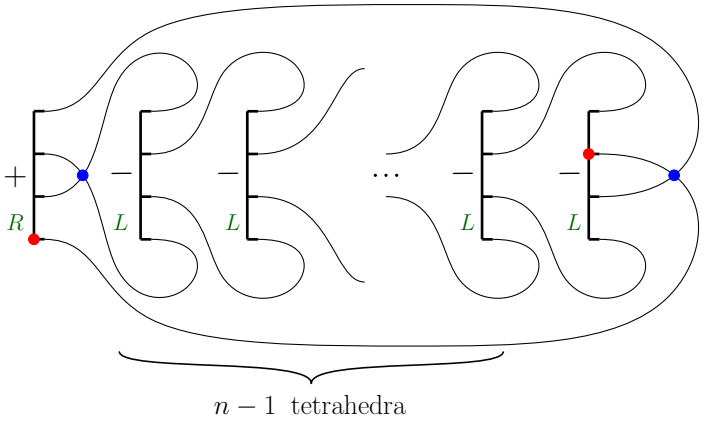

Figure 5.21: Graphical representation of Figure 5.20.

- $\omega_k(\alpha) := \omega_{X_n,\alpha}(\overrightarrow{e_k}) = c_k + 2b_{k+1} + c_{k+2}$ (for $1 \leqslant k \leqslant n-1$).

Theorem 5.22. *Let $n \geqslant 1$ be an integer. Consider the monodromy triangulation X_n of Figure 5.20. Then for all angle structures $\alpha = (a_1, \ldots, c_{n+1}) \in \mathcal{A}_{X_n}$ and all $\hbar > 0$, we have:*

$$\mathcal{Z}_\hbar(X_n, \alpha) \stackrel{\star}{=} \int_{\mathbb{R}+i\frac{\mu_{X_n}(\alpha)}{2\pi\sqrt{\hbar}}} J_{X_n}(\hbar, x) e^{\frac{1}{2\sqrt{\hbar}} x \lambda_{X_n}(\alpha)}\, dx,$$

with

- *the degree one angle polynomial $\mu_{X_n} : \alpha \mapsto a_1 - a_2 - \cdots - a_{n+1}$,*
- *the degree one angle polynomial*

$$\lambda_{X_n} : \alpha \mapsto 2(2-n)a_1 + 2(1-n)a_2 + 4\sum_{j=3}^{n}(j-n-1)a_j - 2nb_1 + 2(n-1)b_2,$$

- *the map $(\hbar, x) \mapsto J_{X_n}(\hbar, x)$*

$$:= \int_{\mathcal{Y}'} d\mathbf{y}'\, e^{2i\pi\left(\mathbf{y}'^T Q_n \mathbf{y}' + x(\eta_n x + \kappa_n)\right)} e^{\frac{1}{\sqrt{\hbar}}\left(\mathbf{y}'^T \mathcal{W}_n + \sigma_n x\right)} \frac{\Phi_{\mathsf{b}}\left(-y'_1 - \cdots - y'_n + \theta_n\right)}{\Phi_{\mathsf{b}}\left(y'_1\right)} \prod_{j=2}^{n} \Phi_{\mathsf{b}}\left(y'_j\right),$$

where

$$\mathcal{Y}' := \left(\mathbb{R} - \frac{i}{2\pi\sqrt{\hbar}}(\pi - a_1)\right) \times \prod_{k=2}^{n}\left(\mathbb{R} + \frac{i}{2\pi\sqrt{\hbar}}(\pi - a_k)\right),$$

$$\mathbf{y}' := (y'_1,\dots,y'_n)^T, \quad \theta_n := \frac{i}{\sqrt{\hbar}}\left(\frac{n-1}{2}\right), \quad \kappa_n(\mathbf{y}') := 2\left(ny'_1 + (n-1)y'_2 + \cdots + y'_n\right),$$

$$\eta_n := \frac{n(-3n-1)+2}{2}, \quad \sigma_n := \frac{\pi}{n}(n(4-3n)-2) + 2\pi(2n-1)(n-1).$$

Moreover the k-th row of the vector $\mathcal{W}_n$ is defined by

$$(\mathcal{W}_n)_k := \pi(-1+k-n)(-1+k)$$

and the matrix Q_n is defined by (the element in i-th row and j-th column)

$$(Q_n)_{i,j} := \frac{1}{n}\left((i-1)(j-1) - n(\min(i,j)-1)\right).$$

To prove Theorem 5.22, we give some intermediate results.

Lemma 5.23. *Let $n \geqslant 1$ be an integer. Consider the monodromy triangulation X_n of Figure 5.20. The kinematical kernel of X_n is given by $\mathcal{K}_{X_n}\left(\widetilde{\mathbf{t}}\right) = \exp\left(2i\pi\widetilde{\mathbf{t}}^T\widetilde{Q}_n\widetilde{\mathbf{t}}\right)$, where $\widetilde{\mathbf{t}} := (t_1,\dots,t_{n+1})^T$ and the matrix $\widetilde{Q}_n$ is defined by (the element in i-th row and j-th column)*

$$(\widetilde{Q}_n)_{i,j} := \frac{1}{n}((i-2)(j-2) - n(\min(i,j)-1)).$$

Proof. Let $n \geqslant 1$ be an integer. We denote the generic vector in $\mathbb{R}^{X_n^2}$ which corresponds to face variables by

$$\mathbf{x} := (e_1,\dots,e_{n+1},f_1,\dots,f_{n+1})^T \in \mathbb{R}^{X_n^2},$$

where e_{n+1} is the face variable on D, f_{n+1} is the face variable on A and e_i (resp. f_i) is the face variable on E_i (resp. F_i) for $i = 1,\dots,n$. The kinematical kernel is given by

$$\mathcal{K}_{X_n}\left(\widetilde{\mathbf{t}}\right) = \int_{\mathbf{x}\in\mathbb{R}^{X_n^2}} d\mathbf{x}\, e^{2i\pi(f_{n+1}t_1 - \sum_{i=1}^n e_i t_{i+1})}\delta_{f_{n+1}-f_1+e_1}\delta_{e_1-e_{n+1}+t_1}\prod_{i=1}^{n}\delta_{e_i-e_{i+1}+f_{i+1}}\delta_{f_{i+1}-f_i+t_{i+1}}.$$

We thus need to solve the following linear system with variables t_i $(i = 1,\dots,n+1)$:

$$f_{n+1} - f_1 + e_1 = 0, \tag{5.24}$$

$$e_1 - e_{n+1} + t_1 = 0, \tag{5.25}$$

$$e_i - e_{i+1} + f_{i+1} = 0 \quad (i = 1,\dots,n), \tag{5.26}$$

$$f_{i+1} - f_i + t_{i+1} = 0 \quad (i = 1,\dots,n). \tag{5.27}$$

By (5.27), we get that

$$f_i = -\sum_{j=2}^{i} t_j + f_1 \tag{5.28}$$

for $i = 2,\dots,n+1$. Substituting (5.28) in (5.26), one gets

$$e_i = e_1 + \sum_{j=2}^{i} f_j = e_1 + (i-1)f_1 - \sum_{j=2}^{i}\sum_{k=2}^{j} t_k = e_1 + (i-1)f_1 - (i-k+1)\sum_{k=2}^{i} t_k \tag{5.29}$$

for $i = 2, \dots, n+1$. Taking the case $i = n+1$ in (5.28) and substituting it in (5.24), one gets $e_1 = \sum_{k=2}^{n+1} t_k$.

Similarly, taking the case $i = n+1$ in (5.29) and substituting it in (5.25), we get $f_1 = \frac{1}{n}\left(t_1 + \sum_{k=2}^{n+1}(n-k+2)t_k\right)$. Therefore, we obtain that

$$f_i = \frac{1}{n}\left(t_1 - \sum_{k=2}^{i}(k-2)t_k + \sum_{k=i+1}^{n+1}(n-k+2)t_k\right)$$
$$e_i = \frac{i-1}{n}t_1 + \sum_{k=2}^{i}\left(k-1-\frac{(i-1)(k-2)}{n}\right)t_k + \sum_{k=i+1}^{n+1}\left(i-\frac{(i-1)(k-2)}{n}t_k\right)$$

for any $i = 1, \dots, n+1$. Let us set $\Lambda_{X_n} = f_{n+1}t_1 - \sum_{i=1}^{n} e_i t_{i+1}$. Then we have

$$\begin{aligned}
\Lambda_{X_n} &= \frac{1}{n}\left(t_1 - \sum_{k=2}^{n+1}(k-2)t_k\right)t_1 - \sum_{i=1}^{n}\left[\frac{i-1}{n}t_1 + \sum_{k=2}^{i}\left(k-1-\frac{(i-1)(k-2)}{n}\right)t_k\right. \\
&\quad \left. + \sum_{k=i+1}^{n+1}\left(i-\frac{(i-1)(k-2)}{n}\right)t_k\right]t_{i+1} \\
&= \frac{1}{n}t_1^2 - \sum_{j=2}^{n+1}\frac{j-2}{n}t_1t_j - \sum_{i=2}^{n+1}\frac{i-2}{n}t_it_1 - \sum_{i=2}^{n+1}\sum_{j=2}^{i-1}\left(j-1-\frac{(i-2)(j-2)}{n}\right)t_it_j \\
&\quad - \sum_{i=2}^{n+1}\sum_{j=i}^{n+1}\left(i-1-\frac{(i-2)(j-2)}{n}\right)t_it_j \\
&= \frac{1}{n}\left(t_1^2 - 2\sum_{j=2}^{n+1}(j-2)t_1t_j - \sum_{i=2}^{n+1}\sum_{j=2}^{n+1}\left(n(\min(i,j)-1) - (i-2)(j-2)\right)t_it_j\right) \\
&= \frac{1}{n}\sum_{i=1}^{n+1}\sum_{j=1}^{n+1}\left((i-2)(j-2) - n(\min(i,j)-1)\right)t_it_j.
\end{aligned}$$

□

Lemma 5.30. *Let $n \geqslant 1$ be an integer and $\alpha = (a_1, \dots, c_{n+1}) \in \mathcal{S}_{X_n}$ a shape structure. Denote by $\widetilde{Q}_n$ the symmetric matrix given in Lemma 5.23, $\widetilde{C}(\alpha) := (c_1, \dots, c_{n+1})^T$, $\widetilde{\Gamma}(\alpha) := (a_1 - \pi, \pi - a_2, \dots, \pi - a_{n+1})^T$ and $\widetilde{\mathcal{W}}(\alpha) := 2\widetilde{Q}_n\widetilde{\Gamma}(\alpha) + \widetilde{C}(\alpha)$. Then we have*

$$AB\widetilde{\mathcal{W}}(\alpha) = D(\alpha) \tag{5.31}$$

where $D(\alpha) := \left(\omega_0(\alpha) - 2\pi, \omega_1(\alpha), \dots, \omega_{n-1}(\alpha), \widetilde{\mathcal{W}}_{n+1}(\alpha)\right)^T$,

$$A := \begin{bmatrix} 0 & 1 & 0 & \cdots & 0 & 1 & 0 \\ 1 & -2 & 1 & 0 & \cdots & \cdots & 0 \\ 0 & 1 & -2 & 1 & 0 & \cdots & 0 \\ \vdots & \ddots & \ddots & \ddots & \ddots & \ddots & \vdots \\ 0 & \cdots & 0 & 1 & -2 & 1 & 0 \\ 0 & \cdots & \cdots & 0 & 1 & -2 & 0 \\ 0 & \cdots & \cdots & \cdots & \cdots & 0 & 1 \end{bmatrix} \quad \textit{and} \quad B := \begin{bmatrix} 1 & 0 & \cdots & \cdots & 0 & -1 \\ 0 & 1 & 0 & \cdots & 0 & -1 \\ \vdots & \ddots & \ddots & \ddots & \vdots & \vdots \\ 0 & \cdots & 0 & 1 & 0 & -1 \\ 0 & \cdots & \cdots & 0 & 1 & -1 \\ 0 & \cdots & \cdots & \cdots & 0 & 1 \end{bmatrix},$$

where $\widetilde{\mathcal{W}}_k(\alpha)$ denotes the k-th component of $\widetilde{\mathcal{W}}(\alpha)$. In particular, if $\alpha \in \mathcal{A}_{X_n}$ is an angle structure, then we have

$$\widetilde{\mathcal{W}}_k(\alpha) - \widetilde{\mathcal{W}}_{n+1}(\alpha) = \frac{\pi}{n}(-1+k-n)(2+(-3+k)n) \tag{5.32}$$

for $k = 1, \dots, n+1$.

Proof. Relation (5.31) is proved from direct calculations.

To prove relation (5.32), we multiply both sides of (5.31) by the inverse matrix A^{-1}. By an easy calculation, we see that for $k = 1, \dots, n$, the k-th row of the identity $B\widetilde{\mathcal{W}}(\alpha) = A^{-1}D(\alpha)$ is

$$\begin{aligned}\widetilde{\mathcal{W}}_k(\alpha) - \widetilde{\mathcal{W}}_{n+1}(\alpha) = \left(\frac{n-(k-1)}{n}\right)(\omega_0(\alpha) - 2\pi) + \sum_{j=2}^{k-1}\Bigg(\frac{n+(j-1)(j-n-2)}{n} \\ + \frac{(k-j)(j-2)}{n}\Bigg)\omega_j(\alpha) + \sum_{j=k}^{n-1}\left(\frac{n+(k-1)(j-n-2)}{n}\right)\omega_j(\alpha).\end{aligned}$$

If α is an angle structure, we have $\omega_j(\alpha) = 2\pi$ for all $j = a, 0, \dots, n-1$, and the above relation becomes

$$\widetilde{\mathcal{W}}_k(\alpha) - \widetilde{\mathcal{W}}_{n+1}(\alpha) = \frac{\pi}{n}(-1+k-n)(2+(-3+k)n).$$

For $k = n+1$, this relation is trivially satisfied. Therefore relation (5.32) is verified. □

Remark 5.33. Note that relation (5.32) could have been proved by computing explicitly the value of $\widetilde{\mathcal{W}}_k(\alpha)$ for $1 \leqslant k \leqslant n+1$ and $\alpha \in \mathcal{A}_{X_n}$ an angle structure. In this case, the idea is to write all the angles in terms of $a_1, \dots, a_n, b_1, b_2$, and after some calculations we obtain that

$$\widetilde{\mathcal{W}}_k(\alpha) = \xi(k,n) + \frac{1}{2}\lambda_{X_n}(\alpha), \tag{5.34}$$

with

$$\xi(k,n) := \frac{\pi}{n}\left(-4+5n-k(-2+n(4-k+n))\right) \tag{5.35}$$

and $\lambda_{X_n}(\alpha)$ given as in Theorem 5.22. The reason that we proved relation (5.32) using matrices A and B is that this will help us to guess the matrix F defined in (5.64), which is exactly the matrix AB deleting the last row and the last column.

Proof of Theorem 5.22. Let $n \geqslant 1$ be an integer. Let us compute the partition function of the monodromy triangulation X_n and let us show that it is of the required form. We already know the kinematical kernel from Lemma 5.23. Moreover, for $\alpha = (a_1, \dots, c_{n+1}) \in \mathcal{A}_{X_n}$, $\hbar > 0$ and $\widetilde{\mathbf{t}} := (t_1, \dots, t_{n+1})^T \in \mathbb{R}^{X_n^3}$, the dynamical content is given by

$$\mathcal{D}_{\hbar,X_n}\left(\widetilde{\mathbf{t}},\alpha\right) = e^{\frac{1}{\sqrt{\hbar}}\widetilde{C}(\alpha)^T\widetilde{\mathbf{t}}}\frac{\Phi_{\mathsf{b}}\left(t_2 + \frac{i}{2\pi\sqrt{\hbar}}(\pi - a_2)\right)\cdots\Phi_{\mathsf{b}}\left(t_{n+1} + \frac{i}{2\pi\sqrt{\hbar}}(\pi - a_{n+1})\right)}{\Phi_{\mathsf{b}}\left(t_1 - \frac{i}{2\pi\sqrt{\hbar}}(\pi - a_1)\right)},$$

where $\widetilde{C}(\alpha) := (c_1, \dots, c_{n+1})^T$ as in the statement of Lemma 5.30.

We start by performing the following change of variables:

- $y'_1 = t_1 - \frac{i}{2\pi\sqrt{\hbar}}(\pi - a_1)$,
- $y'_k = t_k + \frac{i}{2\pi\sqrt{\hbar}}(\pi - a_k) \quad (\text{for } 2 \leqslant k \leqslant n+1)$,

and we denote $\widetilde{\mathbf{y}}' := (y'_1, \cdots, y'_{n+1})^T$. We also denote

$$\widetilde{\mathcal{Y}}'_{\hbar,\alpha} := \left(\mathbb{R} - \frac{i}{2\pi\sqrt{\hbar}}(\pi - a_1)\right) \times \prod_{k=2}^{n+1}\left(\mathbb{R} + \frac{i}{2\pi\sqrt{\hbar}}(\pi - a_k)\right) \subset \mathbb{C}^{n+1}$$

and we see that $\widetilde{\mathbf{y}}' \in \widetilde{\mathcal{Y}}'_{\hbar,\alpha}$. Finally, we denote

$$\widetilde{\Gamma}(\alpha) := \frac{2\pi\sqrt{\hbar}}{i}(\widetilde{\mathbf{y}}' - \widetilde{\mathbf{t}}) = (a_1 - \pi, \pi - a_2, \ldots, \pi - a_{n+1})^T,$$

as in Lemma 5.30.

We now compute the partition function

$$\begin{aligned}
\mathcal{Z}_\hbar(X_n, \alpha) &= \int_{\widetilde{\mathbf{t}} \in \mathbb{R}^{X_n^3}} d\widetilde{\mathbf{t}}\, \mathcal{K}_{X_n}\left(\widetilde{\mathbf{t}}\right) \mathcal{D}_{\hbar,X_n}\left(\widetilde{\mathbf{t}}, \alpha\right) \\
&= \int_{\widetilde{\mathbf{y}}' \in \widetilde{\mathcal{Y}}'_{\hbar,\alpha}} d\widetilde{\mathbf{y}}'\, \mathcal{K}_{X_n}\left(\widetilde{\mathbf{y}}' - \frac{i}{2\pi\sqrt{\hbar}}\widetilde{\Gamma}(\alpha)\right) \mathcal{D}_{\hbar,X_n}\left(\widetilde{\mathbf{y}}' - \frac{i}{2\pi\sqrt{\hbar}}\widetilde{\Gamma}(\alpha), \alpha\right) \\
&\overset{\star}{=} \int_{\widetilde{\mathbf{y}}' \in \widetilde{\mathcal{Y}}'_{\hbar,\alpha}} d\widetilde{\mathbf{y}}'\, e^{2i\pi\widetilde{\mathbf{y}}'^T\widetilde{Q}_n\widetilde{\mathbf{y}}' + \frac{2}{\sqrt{\hbar}}\widetilde{\Gamma}(\alpha)^T\widetilde{Q}_n\widetilde{\mathbf{y}}' + \frac{1}{\sqrt{\hbar}}\widetilde{C}(\alpha)^T\widetilde{\mathbf{y}}'} \frac{\Phi_{\mathsf{b}}\left(y'_2\right)\cdots\Phi_{\mathsf{b}}\left(y'_{n+1}\right)}{\Phi_{\mathsf{b}}\left(y'_1\right)} \\
&= \int_{\widetilde{\mathbf{y}}' \in \widetilde{\mathcal{Y}}'_{\hbar,\alpha}} d\widetilde{\mathbf{y}}' e^{2i\pi\widetilde{\mathbf{y}}'^T\widetilde{Q}_n\widetilde{\mathbf{y}}' + \frac{1}{\sqrt{\hbar}}\widetilde{\mathcal{W}}(\alpha)^T\widetilde{\mathbf{y}}'} \frac{\Phi_{\mathsf{b}}\left(y'_2\right)\cdots\Phi_{\mathsf{b}}\left(y'_{n+1}\right)}{\Phi_{\mathsf{b}}\left(y'_1\right)},
\end{aligned}$$

where $\widetilde{\mathcal{W}}(\alpha) := 2\widetilde{Q}_n\widetilde{\Gamma}(\alpha) + \widetilde{C}(\alpha)$ as in the statement of Lemma 5.30.

We define a new variable $x := y'_1 + \cdots + y'_{n+1} - \frac{i}{\sqrt{\hbar}}\left(\frac{n-1}{2}\right)$ which lives in the set

$$\mathcal{Y}^0_{\hbar,\alpha} := \mathbb{R} + \frac{i}{2\pi\sqrt{\hbar}}(a_1 - a_2 - \cdots - a_{n+1}).$$

Moreover, we define $\mathbf{y}'$ (respectively $\mathcal{Y}'_{\hbar,\alpha}$) exactly like $\widetilde{\mathbf{y}}'$ (respectively $\widetilde{\mathcal{Y}}'_{\hbar,\alpha}$) but with the last row deleted. Finally, we also define a vector $\mathcal{W}_n$ (of size n) and a symmetric matrix Q_n (of size $n \times n$) as follows. The k-th row of $\mathcal{W}_n$ is

$$(\mathcal{W}_n)_k := \pi(-1 + k - n)(-1 + k) \tag{5.36}$$

and the element in the i-th row and j-th column of Q_n by

$$(Q_n)_{i,j} := \frac{1}{n}\left((i-1)(j-1) - n(\min(i,j) - 1)\right).$$

Using relation (5.32), we notice that

$$(\mathcal{W}_n)_k = \widetilde{\mathcal{W}}_k(\alpha) - \widetilde{\mathcal{W}}_{n+1}(\alpha) + \frac{2\pi}{n}(n-1)(-1+k-n). \tag{5.37}$$

Using the substitution $y'_{n+1} = x - y'_1 - \cdots - y'_n + \frac{i}{\sqrt{\hbar}}\left(\frac{n-1}{2}\right)$, we compute the following quantities:

$$2i\pi\widetilde{\mathbf{y}}'^T\widetilde{Q}_n\widetilde{\mathbf{y}}' = 2i\pi\left[\mathbf{y}'^T Q_n \mathbf{y}' + \frac{i}{\sqrt{\hbar}}\left(\frac{n-1}{n}\right)\sum_{k=1}^{n}(n-k+1)y'_k + x^2\left(\frac{n(-3n-1)+2}{2}\right)\right.$$
$$\left. +2x\left(ny'_1 + (n-1)y'_2 + \cdots + y_n + (-2n+1)\frac{i}{\sqrt{\hbar}}\left(\frac{n-1}{2}\right)\right)\right],$$

and using formula (5.34), we compute

$$\begin{aligned}\frac{1}{\sqrt{\hbar}}\widetilde{\mathcal{W}}(\alpha)^T\widetilde{\mathbf{y}}' &= \frac{1}{\sqrt{\hbar}}\sum_{k=1}^{n}\left(\widetilde{\mathcal{W}}_k(\alpha) - \widetilde{\mathcal{W}}_{n+1}(\alpha)\right)y'_k + \frac{1}{\sqrt{\hbar}}\widetilde{\mathcal{W}}_{n+1}(\alpha)x \\ &= \frac{1}{\sqrt{\hbar}}\sum_{k=1}^{n}\left(\widetilde{\mathcal{W}}_k(\alpha) - \widetilde{\mathcal{W}}_{n+1}(\alpha)\right)y'_k + \frac{1}{\sqrt{\hbar}}\left(\xi(n+1,n) + \frac{1}{2}\lambda_{X_n}(\alpha)\right)x,\end{aligned}$$

where $\xi(n+1,n)$ is given by formula (5.35).

Finally, let us define

$$\theta_n := \frac{i}{\sqrt{\hbar}}\left(\frac{n-1}{2}\right), \quad \kappa_n(\mathbf{y}') := 2\left(ny'_1 + (n-1)y'_2 + \cdots + y'_n\right), \quad \eta_n := \frac{n(-3n-1)+2}{2},$$

$$\sigma_n := \xi(n+1,n) + 2\pi(2n-1)(n-1) = \frac{\pi}{n}\left(n(4-3n)-2\right) + 2\pi(2n-1)(n-1).$$

Then using formula (5.37), the partition function becomes

$$\mathcal{Z}_\hbar(X_n,\alpha) \overset{\star}{=} \int_{\mathbb{R}+i\frac{\mu_{X_n}(\alpha)}{2\pi\sqrt{\hbar}}} J_{X_n}(\hbar,x)e^{\frac{1}{2\sqrt{\hbar}}x\lambda_{X_n}(\alpha)}\,dx,$$

where

$$J_{X_n}(\hbar,x) := \int_{\mathcal{Y}'} d\mathbf{y}'\, e^{2i\pi\left(\mathbf{y}'^T Q_n\mathbf{y}' + x(\eta_n x + \kappa_n(\mathbf{y}'))\right)}e^{\frac{1}{\sqrt{\hbar}}\left(\mathbf{y}'^T\mathcal{W}_n + \sigma_n x\right)}\frac{\Phi_{\mathsf{b}}\left(x - y'_1 - \cdots - y'_n + \theta_n\right)}{\Phi_{\mathsf{b}}\left(y'_1\right)}\prod_{j=2}^{n}\Phi_{\mathsf{b}}\left(y'_j\right)$$

$\mathcal{Y}' := \mathcal{Y}'_{\hbar,\alpha}$, and $\mu_{X_n}(\alpha) := a_1 - a_2 - \cdots - a_{n+1}$. This concludes the proof. □

As for twist knots, it will be important to work with a form of the partition function such that the integration multi-contour is independent of the quantum parameter $\hbar$ in order to apply the saddle point method in Section 5.2.3.

Corollary 5.38. *Let $n \geqslant 1$ be an integer. Consider the monodromy triangulation X_n of Figure 5.20. Then for all angle structures $\alpha = (a_1,\ldots,c_{n+1}) \in \mathcal{A}_{X_n}$ and all $\hbar > 0$, we have:*

$$\mathcal{Z}_\hbar(X_n,\alpha) \overset{\star}{=} \int_{\mathbb{R}+i\mu_{X_n}(\alpha)} \mathfrak{J}_{X_n}(\hbar,\mathsf{x})e^{\frac{1}{4\pi\hbar}\mathsf{x}\lambda_{X_n}(\alpha)}\,d\mathsf{x},$$

with $\mathfrak{J}_{X_n} : \mathbb{R}_{>0}\times\mathbb{C}\to\mathbb{C}$ defined by

$$\mathfrak{J}_{X_n}(\hbar,\mathsf{x}) := \left(\frac{1}{2\pi\sqrt{\hbar}}\right)^{n+1}\int_{\mathcal{Y}_\alpha} d\mathbf{y}\, e^{\frac{i\mathbf{y}^T Q_n\mathbf{y} + i\mathsf{x}(\eta_n\mathsf{x} + \kappa_n(\mathbf{y})) + \mathbf{y}^T\mathcal{W}_n + \sigma_n\mathsf{x}}{2\pi\hbar}}\frac{\Phi_{\mathsf{b}}\left(\frac{\mathsf{x}-y_1-\cdots-y_n}{2\pi\sqrt{\hbar}} + \theta_n\right)}{\Phi_{\mathsf{b}}\left(\frac{y_1}{2\pi\sqrt{\hbar}}\right)}\prod_{j=2}^{n}\Phi_{\mathsf{b}}\left(\frac{y_j}{2\pi\sqrt{\hbar}}\right),$$

where $\mu_{X_n}, \lambda_{X_n}, \theta_n, \kappa_n(\mathbf{y}), \eta_n, \sigma_n, \mathcal{W}_n, Q_n$ *are the same as in Theorem 5.22, and*

$$\mathcal{Y}_\alpha := (\mathbb{R} - i\,(\pi - a_1)) \times \prod_{k=2}^{n} (\mathbb{R} + i\,(\pi - a_k))\,.$$

Proof. Starting again from the expressions in Theorem 5.22 and for a fixed $\hbar > 0$, we do the change of variables $y_j = (2\pi\sqrt{\hbar})y'_j$ and $\mathsf{x} = (2\pi\sqrt{\hbar})x$. □

5.2.2 H-triangulation of $(L(n,1), K_n)$ for $n \geqslant 1$

Let $n \geqslant 1$ be an integer. As already said at the beginning of Section 5.2.1, the monodromy triangulation of $WL(n,1)$ given in Figure 5.20 is split (with splitting face D). We can thus apply Proposition 5.7 to perform a T-surgery on D and we obtain an H-triangulation Y_n of a pair (M_n, K_n) such that $M_n \setminus K_n$ is homeomorphic to $WL(n,1)$. We denote the elements of Y_n^1 by $\overrightarrow{a}$, $\overrightarrow{b}$, $\overrightarrow{e_0}, \ldots, \overrightarrow{e_{n-1}}, \overrightarrow{K_n}$ with the convention that $\overrightarrow{e_0} = \overrightarrow{e_n}$, and we do not put overarrows on the edges on the figure (all represented by a simple arrow) as for the monodromy triangulation. This H-triangulation is illustrated in Figure 5.22. Before calculating the partition function for Y_n, we start by detecting the 3-manifold M_n and the knot K_n.

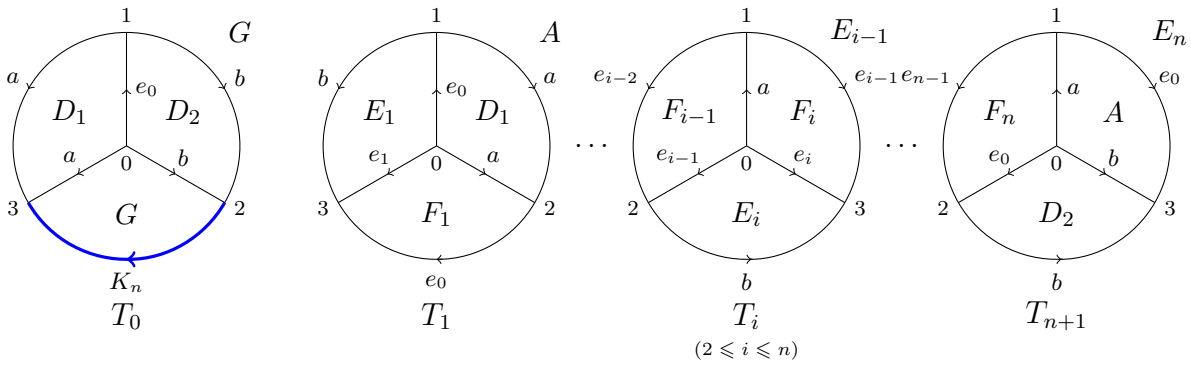

Figure 5.22: H-triangulation Y_n of (M_n, K_n).

Proposition 5.39. *Let $n \geqslant 1$ be an integer. Consider the one-vertex H-triangulation Y_n of the pair (M_n, K_n) described in Figure 5.22. Then we have $M_n = L(n,1)$. As a consequence, K_n is ambient isotopic (up to mirror imaging) to $\mathcal{K}_n$ (constructed at the beginning of Section 5.2).*

Proof. Let Y_n be the one-vertex H-triangulation of (M_n, K_n) given in Figure 5.22. Using this triangulation, we can check that $\pi := \pi_1(M_n) = \{\mathsf{a} \mid \mathsf{a}^n = 1\} \cong \mathbb{Z}/n\mathbb{Z}$. More precisely, we obtain the following relations for the edges in the fundamental group:

$$a = b = \mathsf{a}, \qquad K_n = 1, \qquad e_i = \mathsf{a}^i \quad (0 \leqslant i \leqslant n-1). \tag{5.40}$$

Since M_n is oriented and closed, M_n is the lens space $L(n,k)$ for some $k \in \{1, \ldots, n-1\}$. Let us show that $k = 1$ computing the Reidemeister torsion $\tau_\varphi(Y_n)$ for some ring homomorphism $\varphi : \mathbb{Z}[\pi] \to \mathbb{C}$.

Consider the lifting of Y_n to the universal cover S^3 represented in Figure 5.23 and we denote it by $\widehat{Y}_n$. We also put a hat $\widehat{\ }$ on some lifted i-cells for $0 \leqslant i \leqslant 3$ and we deduce all

the cells using the action of $\pi_1(M_n)$ on the universal cover. Moreover, we fix orientations on i-cells for $1 \leqslant i \leqslant 3$, induced by the numbering on vertices. We say that a tetrahedron has positive orientation if the tetrahedron is positive (in the sense explained in Section 2.1.2). A face has positive orientation if the numbering on vertices are counterclockwise. Finally, an edge has positive orientation if the edge is directed from smaller to bigger vertex.

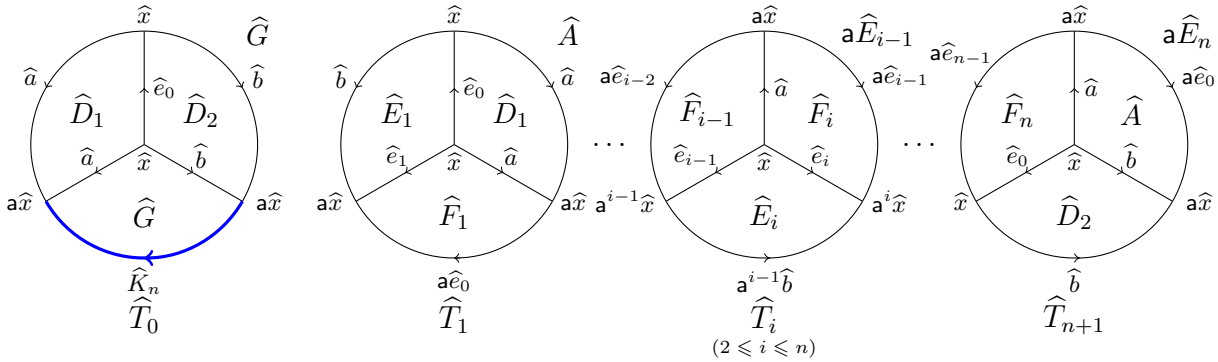

Figure 5.23: Lifting of Y_n to the universal cover.

We take the ring homomorphism

$$\begin{aligned} \varphi : \mathbb{Z}[\pi] &\to \mathbb{C} \\ \mathsf{a} &\mapsto \zeta := e^{\frac{2\pi i}{n}}, \end{aligned}$$

which induces a $\mathbb{Z}[\pi]$-module structure on $\mathbb{C}$. Defining $C_i^{\varphi}(\widehat{Y}_n) := \mathbb{C} \otimes_{\varphi} C_i(\widehat{Y}_n)$ and $\partial_i : C_i^{\varphi}(\widehat{Y}_n) \to C_{i-1}^{\varphi}(\widehat{Y}_n)$ as the boundary map for $i = 0, 1, 2, 3$, one obtains an acyclic chain complex of $\mathbb{C}$-vector spaces:

$$0 \longrightarrow C_3^{\varphi}(\widehat{Y}_n) \xrightarrow{\partial_3} C_2^{\varphi}(\widehat{Y}_n) \xrightarrow{\partial_2} C_1^{\varphi}(\widehat{Y}_n) \xrightarrow{\partial_1} C_0^{\varphi}(\widehat{Y}_n) \longrightarrow 0.$$

Denote by $\mathcal{B}_i$ the basis of $C_i^{\varphi}(\widehat{Y}_n)$ given as follows for $i = 0, 1, 2, 3$:

$$\begin{aligned} \mathcal{B}_0 &= \{\widehat{x}\}, \\ \mathcal{B}_1 &= \{\widehat{a}, \widehat{b}, \widehat{e}_0, \widehat{e}_1, \ldots, \widehat{e}_{n-1}, \widehat{K}_n\}, \\ \mathcal{B}_2 &= \{\widehat{A}, \widehat{D}_1, \widehat{D}_2, \widehat{E}_1, \widehat{F}_1, \widehat{E}_2, \widehat{F}_2, \ldots, \widehat{E}_n, \widehat{F}_n, \widehat{G}\}, \\ \mathcal{B}_3 &= \{\widehat{T}_0, \ldots, \widehat{T}_{n+1}\}. \end{aligned}$$

According to these bases, the boundary maps ∂_i (for $1 \leqslant i \leqslant 3$) are defined as follows.

On 1-cells:

$$\partial_1(\widehat{a}) = (\zeta - 1)\widehat{x}, \quad \partial_1(\widehat{b}) = (\zeta - 1)\widehat{x}, \quad \partial_1(\widehat{e}_i) = (\zeta^i - 1)\widehat{x} \quad (0 \leqslant i \leqslant n-1), \quad \partial_1(\widehat{K}_n) = 0.$$

On 2-cells:

$$\partial_2(\widehat{A}) = \widehat{a} + \zeta\widehat{e}_0 - \widehat{b}, \quad \partial_2(\widehat{D}_1) = \widehat{e}_0, \quad \partial_2(\widehat{D}_2) = \widehat{e}_0, \quad \partial_2(\widehat{G}) = \widehat{b} + \widehat{K}_n - \widehat{a},$$

$$\partial_2(\widehat{E}_i) = \widehat{e}_{i-1} + \zeta^{i-1}\widehat{b} - \widehat{e}_i, \quad \partial_2(\widehat{F}_i) = \widehat{a} + \zeta\widehat{e}_{i-1} - \widehat{e}_i \quad (1 \leqslant i \leqslant n).$$

On 3-cells:

$$\partial_3(\widehat{T}_0) = \widehat{D}_1 - \widehat{D}_2, \quad \partial_3(\widehat{T}_1) = \widehat{A} - \widehat{F}_1 + \widehat{E}_1 - \widehat{D}_1,$$
$$\partial_3(\widehat{T}_i) = -\zeta\widehat{E}_{i-1} + \widehat{E}_i - \widehat{F}_i + \widehat{F}_{i-1} \quad (2 \leqslant i \leqslant n), \quad \partial_3(\widehat{T}_{n+1}) = -\zeta\widehat{E}_n + \widehat{D}_2 - \widehat{A} + \widehat{F}_n.$$

Consider the following subbases $\mathcal{C}_i \subset \mathcal{B}_i$ for $i = 0, \ldots, 3$:

$$\begin{aligned}
\mathcal{C}_0 &= \{\widehat{x}\},\\
\mathcal{C}_1 &= \{\widehat{b}, \widehat{e}_0, \widehat{e}_1, \ldots, \widehat{e}_{n-1}, \widehat{K}_n\},\\
\mathcal{C}_2 &= \{\widehat{A}, \widehat{D}_1, \widehat{E}_1, \widehat{F}_1, \widehat{F}_2, \ldots, \widehat{F}_{n-1}\},\\
\mathcal{C}_3 &= \varnothing,
\end{aligned}$$

and the projection maps $\pi_i : C_i^{\varphi}(\widehat{Y}_n) \to \mathrm{Span}(\mathcal{C}_i)$ for $i = 0, 1, 2$. Moreover, for $i = 1, 2, 3$, we write $\widehat{\partial}_i := \partial_i|_{\mathrm{Span}(\mathcal{B}_i \setminus \mathcal{C}_i)}$ and $S_i := [\pi_{i-1} \circ \widehat{\partial}_i]_{\mathcal{C}_{i-1}, \mathcal{B}_i \setminus \mathcal{C}_i}$, where $[\pi_{i-1} \circ \widehat{\partial}_i]_{\mathcal{C}_{i-1}, \mathcal{B}_i \setminus \mathcal{C}_i}$ is the matrix representation of $\pi_{i-1} \circ \widehat{\partial}_i$ according to bases $\mathcal{B}_i \setminus \mathcal{C}_i$ and $\mathcal{C}_{i-1}$. Then the square matrices S_i are given by

$$S_1 = \begin{array}{c} \\ \widehat{x} \end{array} \begin{array}{c} \begin{array}{c} \widehat{a} \end{array} \\ \left[\begin{array}{c} \zeta - 1 \end{array}\right] \end{array},$$

$$S_2 = \begin{array}{c} \\ \widehat{b} \\ \widehat{e}_0 \\ \widehat{e}_1 \\ \widehat{e}_2 \\ \vdots \\ \widehat{e}_{n-2} \\ \widehat{e}_{n-1} \\ \widehat{K}_n \end{array} \begin{array}{c} \begin{array}{cccccccc} \widehat{D}_2 & \widehat{E}_2 & \widehat{E}_3 & \cdots & \widehat{E}_{n-1} & \widehat{E}_n & \widehat{F}_n & \widehat{G} \end{array} \\ \left[\begin{array}{cccccccc} 0 & \zeta & \zeta^2 & \cdots & \zeta^{n-2} & \zeta^{n-1} & 0 & 1 \\ 1 & 0 & 0 & \cdots & 0 & -1 & -1 & 0 \\ 0 & 1 & 0 & \cdots & \cdots & 0 & 0 & 0 \\ 0 & -1 & 1 & 0 & \cdots & 0 & 0 & 0 \\ \vdots & \ddots & \ddots & \ddots & \ddots & \vdots & \vdots & \vdots \\ 0 & \cdots & 0 & -1 & 1 & 0 & 0 & 0 \\ 0 & \cdots & \cdots & 0 & -1 & 1 & \zeta & 0 \\ 0 & \cdots & \cdots & \cdots & 0 & 0 & 0 & 1 \end{array}\right] \end{array},$$

$$S_3 = \begin{array}{c} \\ \widehat{A} \\ \widehat{D}_1 \\ \widehat{E}_1 \\ \widehat{F}_1 \\ \widehat{F}_2 \\ \vdots \\ \widehat{F}_{n-1} \end{array} \begin{array}{c} \begin{array}{ccccccc} \widehat{T}_0 & \widehat{T}_1 & \widehat{T}_2 & \widehat{T}_3 & \cdots & \widehat{T}_n & \widehat{T}_{n+1} \end{array} \\ \left[\begin{array}{ccccccc} 0 & 1 & 0 & 0 & \cdots & 0 & -1 \\ 1 & -1 & 0 & 0 & \cdots & \cdots & 0 \\ 0 & 1 & -\zeta & 0 & \cdots & \cdots & 0 \\ 0 & -1 & 1 & 0 & \cdots & \cdots & 0 \\ 0 & 0 & -1 & 1 & 0 & \cdots & 0 \\ \vdots & \vdots & \ddots & \ddots & \ddots & \ddots & \vdots \\ 0 & 0 & \cdots & 0 & -1 & 1 & 0 \end{array}\right] \end{array}.$$

By elementary computations, we obtain that

$$\det(S_1) = \zeta - 1, \qquad \det(S_2) = (-1)^{n+1}\zeta^n, \qquad \det(S_3) = (-1)^{n+1}(\zeta - 1).$$

The Reidemeister torsion is defined in $\mathbb{C}^*/\{\pm\zeta\}$ and the value for Y_n is given by

$$\tau_{\varphi}(Y_n) = \frac{\det(S_2)}{\det(S_3)\det(S_1)} = \frac{(-1)^{n+1}\zeta^n}{(-1)^{n+1}(\zeta - 1)^2} = \frac{1}{(\zeta - 1)^2}. \tag{5.41}$$

We remark that the value (5.41) coincide with the one of $L(n, 1)$ (see for example [Nic03] or [Tur00]). Since Reidemeister torsion detects all the lens spaces, we thus conclude that $k = 1$.

The second part of the statement follows from the fact that Y_n is a null-homologous H-triangulation (see (5.40)) and also that $\mathcal{K}_n$ is null-homologous. Indeed, the disk diagram of $\mathcal{K}_n$ is the same as the one of Figure 5.18 (a) with the underlying space replaced by $L(n,1)$. One concludes by Corollary 5.16. □

We can now start computations. For $\alpha = (a_0, b_0, c_0, \dots, a_{n+1}, b_{n+1}, c_{n+1}) \in \mathcal{S}_{Y_n}$ a shape structure on Y_n, the weight of each edge are given by:

- $\widehat{\omega}_a(\alpha) := \omega_{Y_n,\alpha}(\overrightarrow{a}) = b_0 + c_0 + b_1 + c_1 + a_2 + \cdots + a_{n+1}$
- $\widehat{\omega}_b(\alpha) := \omega_{Y_n,\alpha}(\overrightarrow{b}) = b_0 + c_0 + b_1 + a_2 + \cdots + a_{n+1} + c_{n+1}$
- $\widehat{\omega}_0(\alpha) := \omega_{Y_n,\alpha}(\overrightarrow{e_0}) = a_0 + 2a_1 + c_2 + c_n + 2b_{n+1}$
- $\omega_k(\alpha) := \omega_{Y_n,\alpha}(\overrightarrow{e_k}) = c_k + 2b_{k+1} + c_{k+2} \quad$ (for $1 \leqslant k \leqslant n-1$)
- $\widehat{\omega}_{K_n}(\alpha) := \omega_{Y_n,\alpha}(\overrightarrow{K_n}) = a_0$.

Similarly to Chapter 4, some of these weights have the same value as the ones for X_n listed in Section 5.2.1 (and are thus also denoted $\omega_j(\alpha)$), and some are specific to Y_n (and are written with a hat). Moreover, we will denote $\mathcal{S}_{Y_n \setminus T_0}$ the space of shape structures on every tetrahedron of Y_n except for T_0.

Theorem 5.42. *Let $n \geqslant 1$ be an integer. Consider the one-vertex H-triangulation Y_n of the pair $(L(n,1),K_n)$ described in Figure 5.22. Then for every $\hbar > 0$ and for every $\tau \in \overline{\mathcal{S}_{T_0}} \times \mathcal{S}_{Y_n \setminus T_0}$ such that $\omega_{Y_n,\tau}$ vanishes on $\overrightarrow{K_n}$ and is equal to 2π on every other edge, one has*

$$\lim_{\substack{\alpha \to \tau \\ \alpha \in \mathcal{S}_{Y_n}}} \Phi_{\mathsf{b}}\left(\frac{\pi - \omega_{Y_n,\alpha}\left(\overrightarrow{K_n}\right)}{2\pi i\sqrt{\hbar}}\right) \mathcal{Z}_\hbar(Y_n,\alpha) \stackrel{\star}{=} J_{X_n}(\hbar,0),$$

where J_{X_n} is defined in Theorem 5.22.

As in Section 5.2.1, we separate the proof of Theorem 5.42 into several lemmas.

Lemma 5.43. *Let $n \geqslant 1$ be an integer. Consider the one-vertex H-triangulation Y_n of the pair $(L(n,1),K_n)$ described in Figure 5.22. The kinematical kernel of Y_n is given by*

$$\mathcal{K}_{Y_n}\left(\widehat{\mathbf{t}}\right) = e^{2i\pi \mathbf{t}^T Q_n \mathbf{t}} \delta(t_0)\delta(t_1 + \cdots + t_{n+1}), \tag{5.44}$$

where $\widehat{\mathbf{t}} := (t_0, t_1, \dots, t_{n+1})^T$, $\mathbf{t} := (t_1, \dots, t_n)^T$ and the matrix Q_n is the same as in Theorem 5.22.

Proof. Let $n \geqslant 1$ be an integer. We denote the generic vector in $\mathbb{R}^{Y_n^2}$ which corresponds to face variables by

$$\widehat{\mathbf{x}} := (e_1, \dots, e_{n+1}, f_1, \dots, f_{n+1}, g, s)^T \in \mathbb{R}^{Y_n^2},$$

where g is the face variable for G, s for D_1, e_{n+1} for D_2, f_{n+1} for A and e_i (resp. f_i) is the face variable for E_i (resp. F_i) for $i = 1, \dots, n$. The kinematical kernel is thus given by

$$\mathcal{K}_{Y_n}\left(\widehat{\mathbf{t}}\right) = \int_{\widehat{\mathbf{x}} \in \mathbb{R}^{Y_n^2}} d\widehat{\mathbf{x}}\, e^{2i\pi(gt_0 + f_{n+1}t_1 - \sum_{i=1}^n e_i t_{i+1})} \Delta(\widehat{\mathbf{x}}, \widehat{\mathbf{t}}), \tag{5.45}$$

where

$$\Delta(\widehat{\mathbf{x}},\widehat{\mathbf{t}}) := \delta_s\delta_{s-e_{n+1}+t_0}\delta_{f_{n+1}-f_1+e_1}\delta_{e_1-s+t_1}\prod_{i=1}^{n}\delta_{e_i-e_{i+1}+f_{i+1}}\delta_{f_{i+1}-f_i+t_{i+1}}.$$

Since there is no Dirac distribution term with variable g in (5.45), one can eliminate the term $e^{2i\pi gt_0}$ by integrating over the variable g and replacing by δ_{t_0}. Since there are $2n+1$ integration variables and $2n+2$ delta functions, we need to keep one well-chosen delta aside. If we choose $\delta_{f_{n+1}-f_n+t_{n+1}}$, then the following linear system becomes non-degenerate and we will see that it admits a unique solution (written in terms of t_i with $i=0,\dots,n+1$):

$$s = 0, \tag{5.46}$$
$$e_i - e_{i+1} + f_{i+1} = 0 \quad (i=1,\dots,n), \tag{5.47}$$
$$f_{i+1} - f_i + t_{i+1} = 0 \quad (i=1,\dots,n-1), \tag{5.48}$$
$$s - e_{n+1} + t_0 = 0, \tag{5.49}$$
$$f_{n+1} - f_1 + e_1 = 0, \tag{5.50}$$
$$e_1 - s + t_1 = 0. \tag{5.51}$$

From (5.46), (5.49) and (5.51), we already see that $e_{n+1} = t_0$ and $e_1 = -t_1$. Then, (5.48) implies that

$$f_i = -\sum_{k=2}^{i} t_k + f_1 \tag{5.52}$$

for $i=2,\dots,n$. Combining (5.52) and (5.47), one gets

$$e_i = \sum_{j=2}^{i} f_j + e_1 = e_1 + (i-1)f_1 - \sum_{j=2}^{i}\sum_{k=2}^{j} t_k = e_1 + (i-1)f_1 - \sum_{k=2}^{i}(i-k+1)t_k \tag{5.53}$$

for $i=2,\dots,n$. Taking the case $i=n$ in (5.47), and combining with (5.50) leads to

$$e_n = t_0 - t_1 - f_1. \tag{5.54}$$

Considering the case $i=n$ in (5.53) and using (5.54), we get

$$-t_1 + (n-1)f_1 - \sum_{k=2}^{n}(n-k+1)t_k = e_n = t_0 - t_1 - f_1,$$

and therefore

$$f_1 = \frac{1}{n}\left(t_0 + \sum_{k=2}^{n}(n-k+1)t_k\right). \tag{5.55}$$

Substituting (5.55) in (5.50), (5.52) and (5.53), one obtains

$$f_{n+1} = f_1 - e_1 = \frac{1}{n}t_0 + t_1 + \frac{1}{n}\sum_{k=2}^{n}(n-k+1)t_k,$$

$$f_i = -\sum_{k=2}^{i} t_k + f_1 = \frac{1}{n}t_0 + \frac{1}{n}\sum_{k=2}^{i}(1-k)t_k + \sum_{k=i+1}^{n}(n-k+1)t_k$$

for all $i = 2, \ldots, n$, and

$$\begin{aligned} e_i &= e_1 + (i-1)f_1 - \sum_{k=2}^{i}(i-k+1)t_k \\ &= \left(\frac{i-1}{n}\right)t_0 - t_1 + \left(\frac{i-1}{n}\right)\sum_{k=2}^{n}(n-k+1)t_k - \sum_{k=2}^{i}(i-k+1)t_k \\ &= \left(\frac{i-1}{n}\right)t_0 - t_1 + \sum_{k=2}^{i}\left(\frac{(n-k+1)(i-1)}{n} - i + k - 1\right)t_k + \left(\frac{i-1}{n}\right)\sum_{k=i+1}^{n}(n-k+1)t_k \end{aligned}$$

for all $i = 2, \ldots, n$.

Finally, the remaining delta $\delta(f_{n+1} - f_n + t_{n+1})$ becomes

$$\delta(f_{n+1} - f_n + t_{n+1}) = \delta\left(f_{n+1} + \sum_{k=2}^{n+1}t_k - f_1\right) = \delta\left(\sum_{k=2}^{n+1}t_k - e_1\right) = \delta\left(\sum_{k=1}^{n+1}t_k\right).$$

Let us set $\Lambda_{Y_n} := f_{n+1}t_1 - \sum_{i=1}^{n} e_i t_{i+1}$. Then we have

$$\begin{aligned} \Lambda_{Y_n} &= t_1^2 + \frac{1}{n}\sum_{j=2}^{n+1}(n-j+1)t_1t_j + \sum_{i=2}^{n+1}t_1t_i - \sum_{i=2}^{n+1}\sum_{j=2}^{i-1}\left(\frac{(n-j+1)(i-2)}{n} - i + j\right)t_jt_i \\ &\quad - \sum_{i=2}^{n+1}\sum_{j=i}^{n+1}\frac{(n-j+1)(i-2)}{n}t_jt_i \\ &= t_1^2 + \frac{1}{n}\sum_{j=2}^{n+1}((n-j+1)+n)t_1t_j - \sum_{i=2}^{n+1}\sum_{j=2}^{i-1}\left(\frac{(n-j+1)(i-2)}{n} + (\min(i,j)-i)\right)t_jt_i \\ &= \frac{1}{n}\left(nt_1^2 + \sum_{j=2}^{n+1}(2n-j+1)t_1t_j + \sum_{i=2}^{n+1}\sum_{j=2}^{n+1}\left[(n-j+1)(2-i) + (i-\min(i,j))n\right]t_it_j\right). \end{aligned}$$

Define

$$a_{i,j} := (n-j+1)(2-i) + (i-\min(i,j))n$$

for $i, j \in \{1, \ldots, n+1\}$. Remark that $a_{1,1} = n$ and

$$a_{i,1} + a_{1,j} = n(2-i) + (i-1)n + n - j + 1 = 2n - j + 1$$

for $i, j \in \{1, \ldots, n+1\}$. This allows to say that

$$\begin{aligned} \Lambda_{Y_n} &= \frac{1}{2n}\sum_{i=1}^{n+1}\sum_{j=1}^{n+1}(a_{i,j} + a_{j,i})t_it_j \\ &= \frac{1}{n}\sum_{i=1}^{n+1}\sum_{j=1}^{n+1}\left(\left(i-\frac{3}{2}\right)\left(j-\frac{3}{2}\right) - n(\min(i,j)-2) - \frac{1}{4}\right)t_it_j. \end{aligned}$$

Finally, if we define $\widetilde{\mathbf{t}} := (t_1, \ldots, t_n, -t_1 - \cdots - t_n)^T$, $\mathbf{t} := (t_1, \ldots, t_n)^T$ and the symmetric matrix P_n (of size $(n+1) \times (n+1)$) by (the element in i-th row and j-th column)

$$(P_n)_{i,j} := \frac{1}{n}\left(\left(i-\frac{3}{2}\right)\left(j-\frac{3}{2}\right) - n(\min(i,j)-2) - \frac{1}{4}\right),$$

then we have to show that $\widetilde{\mathbf{t}}^T P_n \widetilde{\mathbf{t}} = \mathbf{t}^T Q_n \mathbf{t}$. By direct calculations, we get

$$\begin{aligned}
\widetilde{\mathbf{t}}^T P_n \widetilde{\mathbf{t}} &= \frac{1}{n}\sum_{k=1}^{n}\sum_{j=1}^{n}\left(\left(k-\frac{3}{2}\right)\left(j-\frac{3}{2}\right) - n(\min(k,j)-2) - \frac{1}{4}\right) t_k t_j \\
&\quad + \frac{1}{n}\sum_{l=1}^{n}(n-l+1)\, t_l\,(-t_1-\cdots-t_n) \\
&= \frac{1}{n}\sum_{k=1}^{n}\sum_{j=1}^{n}\left((k-1)\,(j-1) - \frac{k}{2} - \frac{j}{2} + 1 - n(\min(k,j)-1) + n\right) t_k t_j \\
&\quad + \frac{1}{n}\sum_{k=1}^{n}\sum_{j=1}^{n}\left(-\frac{1}{2}\,(n-k+1) - \frac{1}{2}\,(n-j+1)\right) t_k t_j \\
&= \mathbf{t}^T Q_n \mathbf{t}.
\end{aligned}$$

□

Remark 5.56. For $n \geqslant 1$ an integer, Lemma 5.43 shows that $Q_n = A^T P_n A$, where A is the $((n+1)\times n)$-matrix defined by

$$A = \begin{bmatrix} 1 & 0 & \cdots & \cdots & 0 \\ 0 & 1 & 0 & \cdots & 0 \\ \vdots & \ddots & \ddots & \ddots & \vdots \\ 0 & \cdots & 0 & 1 & 0 \\ 0 & \cdots & \cdots & 0 & 1 \\ -1 & \cdots & \cdots & \cdots & -1 \end{bmatrix}.$$

Lemma 5.57. *Let $n \geqslant 1$ be an integer and $\alpha = (a_0, \ldots, c_{n+1}) \in \overline{\mathcal{S}_{Y_n}}$ an extended shape structure. Denote by Q_n the symmetric matrix given in Theorem 5.22, $C(\alpha) := (c_1, \ldots, c_n)^T$, $\Gamma(\alpha) := (a_1 - \pi, \pi - a_2, \ldots, \pi - a_n)^T$, $\nu_n(\alpha) := (-c_{n+1}, \ldots, -c_{n+1})^T$ and $\mathcal{W}(\alpha) := 2Q_n\Gamma(\alpha) + C(\alpha) + \nu_n(\alpha)$. If $\tau \in \overline{\mathcal{S}_{T_0}} \times \mathcal{S}_{Y_n \setminus T_0}$ is such that $\omega_{Y_n,\tau}$ vanishes on $\overrightarrow{K_n}$ and is equal to 2π on every other edge, then we have $\mathcal{W}(\tau) = \mathcal{W}_n$, where $\mathcal{W}_n$ is given as in the statement of Theorem 5.22.*

Proof. Direct calculations. □

Proof of Theorem 5.42. Let $n \geqslant 1$ be an integer and $\alpha = (a_0, \ldots, c_{n+1}) \in \mathcal{S}_{Y_n}$. For $\hbar > 0$ and $\widehat{\mathbf{t}} := (t_0, \ldots, t_{n+1})^T$, the dynamical content is given by

$$\mathcal{D}_{\hbar,Y_n}\left(\widehat{\mathbf{t}}, \alpha\right) = e^{\frac{1}{\sqrt{\hbar}}\widehat{C}(\alpha)^T\widehat{\mathbf{t}}} \frac{\Phi_{\mathsf{b}}\left(t_2 + \frac{i}{2\pi\sqrt{\hbar}}\,(\pi - a_2)\right)\cdots\Phi_{\mathsf{b}}\left(t_{n+1} + \frac{i}{2\pi\sqrt{\hbar}}\,(\pi - a_{n+1})\right)}{\Phi_{\mathsf{b}}\left(t_0 - \frac{i}{2\pi\sqrt{\hbar}}\,(\pi - a_0)\right)\Phi_{\mathsf{b}}\left(t_1 - \frac{i}{2\pi\sqrt{\hbar}}\,(\pi - a_1)\right)},$$

where $\widehat{C}(\alpha) := (c_0, \ldots, c_{n+1})^T$.

Let us come back to the calculation of the partition function. We have

$$\mathcal{Z}_\hbar(Y_n, \alpha) = \int_{\widehat{\mathbf{t}} \in \mathbb{R}^{Y_n^3}} d\widehat{\mathbf{t}}\, \mathcal{K}_{Y_n}\left(\widehat{\mathbf{t}}\right) \mathcal{D}_{\hbar,Y_n}\left(\widehat{\mathbf{t}}, \alpha\right)$$

where $\mathcal{K}_{Y_n}\left(\widehat{\mathbf{t}}\right)$ is the kinematical kernel given in (5.44). Integrating over the variables t_0 and t_{n+1}, we remove the two Dirac distributions $\delta(t_0)$ and $\delta(t_1+\cdots+t_{n+1})$ in the kinematical kernel and we replace t_0 by 0 and t_{n+1} by $-t_1-\cdots-t_n$. We thus get

$$\Phi_{\mathsf{b}}\left(\frac{\pi-a_0}{2\pi i\sqrt{\hbar}}\right)\mathcal{Z}_\hbar(Y_n,\alpha)=\int_{\mathbf{t}\in\mathbb{R}^n}d\mathbf{t}\,e^{2i\pi\mathbf{t}^TQ_n\mathbf{t}}e^{\frac{1}{\sqrt{\hbar}}(c_1-c_{n+1})t_1+\cdots+(c_n-c_{n+1})t_n}\Pi(\mathbf{t},\alpha,\hbar),$$

where $\mathbf{t}:=(t_1,\ldots,t_n)^T$ and

$$\Pi(\mathbf{t},\alpha,\hbar):=\frac{\Phi_{\mathsf{b}}\left(t_2+\frac{i}{2\pi\sqrt{\hbar}}(\pi-a_2)\right)\cdots\Phi_{\mathsf{b}}\left(-t_1-\cdots-t_n+\frac{i}{2\pi\sqrt{\hbar}}(\pi-a_{n+1})\right)}{\Phi_{\mathsf{b}}\left(t_1-\frac{i}{2\pi\sqrt{\hbar}}(\pi-a_1)\right)}.$$

Let $\tau:=(a_0^\tau,b_0^\tau,c_0^\tau,\ldots,a_{n+1}^\tau,b_{n+1}^\tau,c_{n+1}^\tau)\in\overline{\mathcal{S}_{T_0}}\times\mathcal{S}_{Y_n\setminus T_0}$ be such that $\omega_k(\tau)=2\pi$ for all $k=1,\ldots,n-1$, $\widehat{\omega}_k(\tau)=2\pi$ for all $k=0,a,b$ and $\widehat{\omega}_{K_n}(\tau)=a_0^\tau=0$. Using the same argument as in Chapter 4, we conclude by the dominated convergence theorem that

$$\lim_{\alpha\to\tau}\Phi_{\mathsf{b}}\left(\frac{\pi-a_0}{2\pi i\sqrt{\hbar}}\right)\mathcal{Z}_\hbar(Y_n,\alpha)=\int_{\mathbf{t}\in\mathbb{R}^n}d\mathbf{t}\,e^{2i\pi\mathbf{t}^TQ_n\mathbf{t}}e^{\frac{1}{\sqrt{\hbar}}(c_1^\tau-c_{n+1}^\tau)t_1+\cdots+(c_n^\tau-c_{n+1}^\tau)t_n}\Pi(\mathbf{t},\tau,\hbar).$$

It remains to prove that

$$\int_{\mathbf{t}\in\mathbb{R}^n}d\mathbf{t}\,e^{2i\pi\mathbf{t}^TQ_n\mathbf{t}}e^{\frac{1}{\sqrt{\hbar}}(c_1^\tau-c_{n+1}^\tau)t_1+\cdots+(c_n^\tau-c_{n+1}^\tau)t_n}\Pi(\mathbf{t},\tau,\hbar)=J_{X_n}(\hbar,0).$$

We do the following change of variables:

- $y_1'=t_1-\frac{i}{2\pi\sqrt{\hbar}}(\pi-a_1^\tau)$,
- $y_k'=t_k+\frac{i}{2\pi\sqrt{\hbar}}(\pi-a_k^\tau)$ for $k=2,\ldots,n$,

and we denote $\mathbf{y}':=(y_1',\ldots,y_n')^T$. The term $\Phi_{\mathsf{b}}\left(-t_1-\cdots-t_n+\frac{i}{2\pi\sqrt{\hbar}}\left(\pi-a_{n+1}^\tau\right)\right)$ will become $\Phi_{\mathsf{b}}\left(-y_1'-\cdots-y_n'+\frac{i}{\sqrt{\hbar}}\left(\frac{n-1}{2}\right)\right)$ since we have the relation $a_1^\tau-a_2^\tau-\ldots-a_{n+1}^\tau=0$.

We also denote

$$\mathcal{Y}_{\hbar,\tau}':=\left(\mathbb{R}-\frac{i}{2\pi\sqrt{\hbar}}(\pi-a_1^\tau)\right)\times\prod_{k=2}^n\left(\mathbb{R}+\frac{i}{2\pi\sqrt{\hbar}}(\pi-a_k^\tau)\right),$$

the subset of $\mathbb{C}^n$ where the generic vector $\mathbf{y}'$ lives. By a similar computation as in the proof of Theorem 5.22, one obtains

$$\begin{aligned}&\int_{\mathbf{t}\in\mathbb{R}^n}d\mathbf{t}\,e^{2i\pi\mathbf{t}^TQ_n\mathbf{t}}e^{\frac{1}{\sqrt{\hbar}}(c_1^\tau-c_{n+1}^\tau)t_1+\cdots+(c_n^\tau-c_{n+1}^\tau)t_n}\Pi(\mathbf{t},\tau,\hbar)\\&\overset{\star}{=}\int_{\mathbf{y}'\in\mathcal{Y}_{\hbar,\tau}'}d\mathbf{y}'\,e^{2i\pi\mathbf{y}'^TQ_n\mathbf{y}'+\frac{1}{\sqrt{\hbar}}\mathbf{y}'^T\mathcal{W}(\tau)}\frac{\Phi_{\mathsf{b}}(y_2')\cdots\Phi_{\mathsf{b}}(y_n')\,\Phi_{\mathsf{b}}\left(-y_1'-\cdots-y_n'+\frac{i}{\sqrt{\hbar}}\left(\frac{n-1}{2}\right)\right)}{\Phi_{\mathsf{b}}(y_1')},\end{aligned}$$

where $\mathcal{W}(\tau)$ is given as in the statement of Lemma 5.57. Since $\mathcal{W}(\tau)=\mathcal{W}_n$ by Lemma 5.57, this finishes the proof of the theorem. □

5.2.3 Asymptotic behavior

Theorem 5.58. *Let $n \geqslant 1$ be an integer, and $J_{X_n}, \mathfrak{J}_{X_n}$ the functions defined in Theorem 5.22 and Corollary 5.38. Then we have*

$$\lim_{\hbar \to 0^+} 2\pi\hbar \log |J_{X_n}(\hbar, 0)| = \lim_{\hbar \to 0^+} 2\pi\hbar \log |\mathfrak{J}_{X_n}(\hbar, 0)| = -\mathrm{Vol}(WL(n,1)).$$

Let us start by listing the hyperbolicity and completeness equations for X_n. For a vector of complex shape parameters $\mathbf{z} = (z_1, \ldots, z_{n+1}) \in (\mathbb{R} + i\mathbb{R}_{>0})^{n+1}$, its complex weight functions are:

- $\omega_a^{\mathbb{C}}(\mathbf{z}) := \omega_{X_n,\alpha}^{\mathbb{C}}(\overrightarrow{a}) = \mathrm{Log}(z_1') + 2\mathrm{Log}(z_1'') + 2\mathrm{Log}(z_2) + \cdots + 2\mathrm{Log}(z_{n+1}) + \mathrm{Log}(z_{n+1}'')$
- $\omega_0^{\mathbb{C}}(\mathbf{z}) := \omega_{X_n,\alpha}^{\mathbb{C}}(\overrightarrow{e_0}) = 2\mathrm{Log}(z_1) + \mathrm{Log}(z_2'') + \mathrm{Log}(z_n'') + 2\mathrm{Log}(z_{n+1}')$
- $\omega_1^{\mathbb{C}}(\mathbf{z}) := \omega_{X_n,\alpha}^{\mathbb{C}}(\overrightarrow{e_1}) = \mathrm{Log}(z_1') + 2\mathrm{Log}(z_2') + \mathrm{Log}(z_3'')$
- $\omega_k^{\mathbb{C}}(\mathbf{z}) := \omega_{X_n,\alpha}^{\mathbb{C}}(\overrightarrow{e_k}) = \mathrm{Log}(z_k'') + 2\mathrm{Log}(z_{k+1}') + \mathrm{Log}(z_{k+2}'')$ (for $2 \leqslant k \leqslant n-1$).

The hyperbolicity equations are given by

$$\omega_a^{\mathbb{C}}(\mathbf{z}) = \omega_0^{\mathbb{C}}(\mathbf{z}) = \ldots = \omega_{n+1}^{\mathbb{C}}(\mathbf{z}) = 2i\pi$$

as well as the completeness equation by

$$\mathrm{Log}(z_1) - \mathrm{Log}(z_2) - \cdots - \mathrm{Log}(z_{n+1}) = 0$$

coming from the curve m_{X_n} represented in Figure 5.24. Keeping the same notations as in Chapter 4, we put all the angles for the tetrahedron T_1 and only on the $\overrightarrow{01}$ edges for the remaining tetrahedra (as the angles b and c follow counterclockwise).

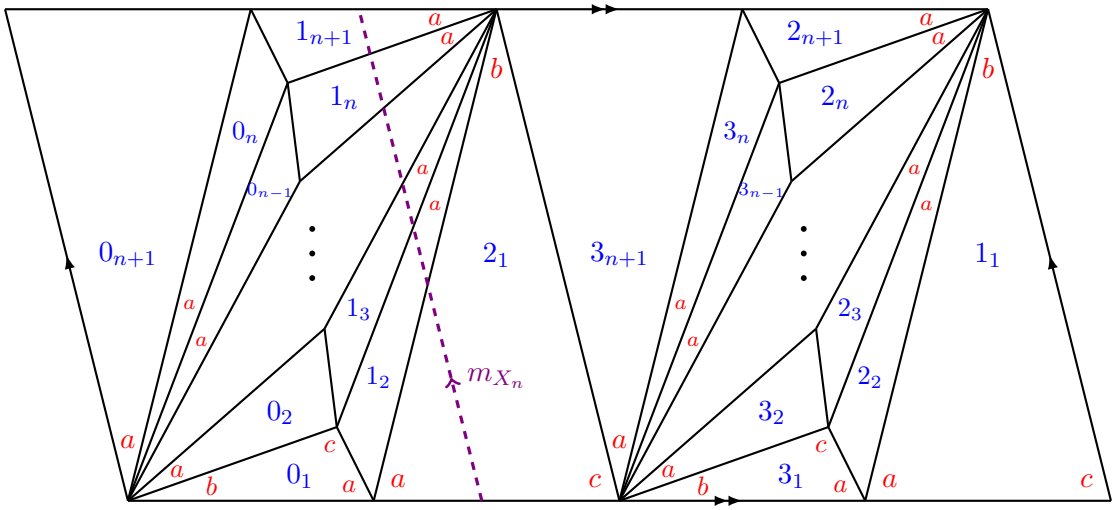

Figure 5.24: Triangulation of the boundary torus for the truncation of X_n, with angles (red), the curve m_{X_n} (violet, dashed).

These equations are equivalent to the following system of equations on $\mathbf{z}$:

- $\mathcal{E}^{co}_{X_n,0}(\mathbf{z})$: $2\mathrm{Log}(z_2)+\cdots+2\mathrm{Log}(z_n)+\mathrm{Log}(z_2'')+\mathrm{Log}(z_n'')-2\mathrm{Log}(z_{n+1}'')=0$
- $\mathcal{E}_{X_n,1}(\mathbf{z})$: $-\mathrm{Log}(z_1)-\mathrm{Log}(z_1'')-2\mathrm{Log}(z_2)-2\mathrm{Log}(z_2'')+\mathrm{Log}(z_3'')+i\pi=0$
- $\mathcal{E}_{X_n,k}(\mathbf{z})$: $\mathrm{Log}(z_k'')-2\mathrm{Log}(z_{k+1})-2\mathrm{Log}(z_{k+1}'')+\mathrm{Log}(z_{k+2}'')=0 \quad (\text{for } 2\leqslant k\leqslant n-1)$
- $\mathcal{E}_{X_n,co}(\mathbf{z})$: $\mathrm{Log}(z_1)-\mathrm{Log}(z_2)-\cdots-\mathrm{Log}(z_{n+1})=0$.

We define the domain $\mathcal{U}\subset\mathbb{C}^n$ by

$$\mathcal{U}:=(\mathbb{R}+i(-\pi,0))\times\prod_{k=2}^{n}(\mathbb{R}+i(0,\pi))$$

and the potential function $S:\mathcal{U}\to\mathbb{C}$ by

$$S(\mathbf{y}):=i\mathrm{Li}_2(-e^{y_1})-i\sum_{k=2}^{n}\mathrm{Li}_2(-e^{y_k})-i\mathrm{Li}_2\left((-1)^n e^{-\sum_{k=1}^n y_k}\right)+i\mathbf{y}^T Q_n\mathbf{y}+\mathbf{y}^T\mathcal{W}_n.$$

Let us start by explaining how to relate the vanishing of ∇S to gluing equations.

Lemma 5.59. *Let us consider the diffeomorphism*

$$\psi:=\left(\prod_{T\in\{T_1,\dots,T_n\}}\psi_T\right):(\mathbb{R}+i\mathbb{R}_{>0})^n\to\mathcal{U}, \tag{5.60}$$

where ψ_T was defined in Section 2.2.1. Then ψ induces an injection from $\mathcal{S}_T$ to $\mathcal{S}_P$, where

$$\mathcal{S}_T:=\{\mathbf{z}\in(\mathbb{R}+i\mathbb{R}_{>0})^{n+1}\mid\mathcal{E}^{co}_{X_n,0}(\mathbf{z})\wedge\cdots\wedge\mathcal{E}_{X_n,n-1}(\mathbf{z})\wedge\mathcal{E}_{X_n,co}(\mathbf{z})\}$$

and

$$\mathcal{S}_P:=\{\mathbf{y}\in\mathcal{U}\mid\nabla S(\mathbf{y})=0\}.$$

In particular, S admits a critical point $\mathbf{y}^0\in\mathcal{U}$ coming from the complete hyperbolic structure $\mathbf{z}^0\in(\mathbb{R}+i\mathbb{R}_{>0})^{n+1}$ on the geometric ideal triangulation X_n.

Proof. We start by computing $\nabla S(\mathbf{y})$ for $\mathbf{y}\in\mathcal{U}$:

$$\nabla S(\mathbf{y})=2iQ_n\mathbf{y}+\mathcal{W}_n+i\begin{pmatrix}-\mathrm{Log}(1+e^{y_1})\\ \mathrm{Log}(1+e^{y_2})\\ \vdots\\ \mathrm{Log}(1+e^{y_n})\end{pmatrix}-i\begin{pmatrix}\vdots\\ \mathrm{Log}\left(1+(-1)^{n+1}e^{-\sum_{k=1}^n y_k}\right)\\ \vdots\end{pmatrix}.$$

Define the variable $y_{n+1}:=\psi_{T_{n+1}}(z_{n+1})=-\mathrm{Log}(z_{n+1})+i\pi$. Then the completeness equation $\mathcal{E}_{X_n,co}(\mathbf{z})$ implies that

$$\begin{aligned}y_{n+1}&=-\mathrm{Log}(z_1)+\mathrm{Log}(z_2)+\cdots+\mathrm{Log}(z_n)+i\pi\\&=(-\psi_{T_1}(z_1)-i\pi)+(-\psi_{T_2}(z_2)+i\pi)+\cdots+(-\psi_{T_n}(z_n)+i\pi)+i\pi\\&=-y_1-\cdots-y_n+i(n-1)\pi.\end{aligned} \tag{5.61}$$

Each component of the last vector can thus be written as

$$\mathrm{Log}\left(1+(-1)^{n+1}e^{-\sum_{k=1}^{n}y_k}\right)=\mathrm{Log}(1+e^{y_{n+1}})=\mathrm{Log}(z''_{n+1}). \tag{5.62}$$

Using the diffeomorphism (5.60), the equality (5.62) and the fact that

$$(\mathcal{W}_n)_k=2\pi\sum_{j=1}^{n}(Q_n)_{k,j}\quad\forall k=1,\dots,n, \tag{5.63}$$

which is easily checked, we get that

$$\nabla S(\psi(\mathbf{z}))=2iQ_n\begin{pmatrix}\mathrm{Log}(z_1)\\-\mathrm{Log}(z_2)\\\vdots\\-\mathrm{Log}(z_n)\end{pmatrix}+i\begin{pmatrix}i\pi-\mathrm{Log}(z_1)-\mathrm{Log}(z''_1)\\\mathrm{Log}(z''_2)\\\vdots\\\mathrm{Log}(z''_n)\end{pmatrix}-i\begin{pmatrix}\vdots\\\mathrm{Log}(z''_{n+1})\\\vdots\end{pmatrix}.$$

We now multiply $\nabla S(\psi(\mathbf{z}))$ by the following invertible matrix

$$F:=\begin{bmatrix}0&1&0&\cdots&\cdots&0&1\\1&-2&1&0&\cdots&\cdots&0\\0&1&-2&1&0&\cdots&0\\\vdots&\ddots&\ddots&\ddots&\ddots&\ddots&\vdots\\0&\cdots&0&1&-2&1&0\\0&\cdots&\cdots&0&1&-2&1\\0&\cdots&\cdots&\cdots&0&1&-2\end{bmatrix}\in GL_n(\mathbb{R}). \tag{5.64}$$

An elementary calculation shows that

$$FQ_n=\begin{bmatrix}0&-1&\cdots&-1&-1\\0&1&0&\cdots&0\\\vdots&\ddots&\ddots&\ddots&\vdots\\0&\cdots&0&1&0\\0&\cdots&\cdots&0&1\end{bmatrix}, \tag{5.65}$$

and thus we obtain

$$F\cdot\nabla S(\psi(\mathbf{z}))=i\begin{pmatrix}2\mathrm{Log}(z_2)+\cdots+2\mathrm{Log}(z_n)+\mathrm{Log}(z''_2)+\mathrm{Log}(z''_n)-2\mathrm{Log}(z''_{n+1})\\-2\mathrm{Log}(z_2)+i\pi-\mathrm{Log}(z_1)-\mathrm{Log}(z''_1)-2\mathrm{Log}(z''_2)+\mathrm{Log}(z''_3)\\-2\mathrm{Log}(z_3)+\mathrm{Log}(z''_2)-2\mathrm{Log}(z''_3)+\mathrm{Log}(z''_4)\\\vdots\\-2\mathrm{Log}(z_n)+\mathrm{Log}(z''_{n-1})-2\mathrm{Log}(z''_n)+\mathrm{Log}(z''_{n+1})\end{pmatrix}.$$

Consequently, since F is invertible, we have that

$$\nabla S(\psi(\mathbf{z}))=0\iff\mathcal{E}^{co}_{X_n,0}(\mathbf{z})\wedge\mathcal{E}_{X_n,1}(\mathbf{z})\wedge\cdots\wedge\mathcal{E}_{X_n,n-1}(\mathbf{z}).$$

□

Remark 5.66 (Cases $n=1,2$)**.** Note that the notation (5.64) makes sense only for $n\geqslant 3$. For $n=1$, the matrix F is simply the scalar 2 and we get $FQ_1=0$. For $n=2$, we have that

$$F=\begin{bmatrix}0&2\\1&-2\end{bmatrix}$$

and the formula (5.65) is satisfied.

Consider the multi-contour

$$\mathcal{Y}^0 := \mathcal{Y}_{\alpha^0} = \big(\mathbb{R} - i(\pi - a_1^0)\big) \times \prod_{k=2}^{n} \big(\mathbb{R} + i(\pi - a_k^0)\big) \subset \mathcal{U},$$

where $\alpha^0 = (a_1^0, \dots, c_{n+1}^0) \in \mathcal{A}_{X_n}$ denotes the angle structure corresponding to the complete structure $\mathbf{z}^0$. We see that $\mathbf{y}^0 \in \mathcal{Y}^0$ and we parametrize $\mathbf{y} \in \mathcal{Y}^0$ as

$$\mathbf{y} = \begin{pmatrix} y_1 \\ \vdots \\ y_n \end{pmatrix} = \begin{pmatrix} x_1 + id_1^0 \\ \vdots \\ x_n + id_n^0 \end{pmatrix} = \mathbf{x} + i\mathbf{d}^0,$$

where $d_1^0 := -(\pi - a_1^0) < 0$ and $d_k^0 := \pi - a_k^0 > 0$ for $k = 2, \dots, n$.

Note that considering the imaginary parts of equations $\mathcal{E}^{co}_{X_n,0}(\mathbf{z}), \mathcal{E}_{X_n,1}(\mathbf{z}), \dots, \mathcal{E}_{X_n,n-1}(\mathbf{z})$ and $\mathcal{E}_{X_n,co}(\mathbf{z})$, one gets the following relations on angles:

$$2a_2^0 + \cdots + 2a_n^0 + c_2^0 + c_n^0 - 2c_{n+1}^0 = 0, \tag{5.67}$$

$$c_k^0 - 2a_{k+1}^0 - 2c_{k+1}^0 + c_{k+2}^0 = 0 \quad (\text{for } 1 \leqslant k \leqslant n-1), \tag{5.68}$$

$$a_1^0 - a_2^0 - \cdots - a_{n+1}^0 = 0. \tag{5.69}$$

The holomorphic hessian is no more diagonal as in the case of twist knots, but its non-degeneracy is still preserved on the contour $\mathcal{Y}^0$. Before, we recall a basic result of linear algebra.

Lemma 5.70. *Let $m \geqslant 1$ be an integer and $S, T \in M_m(\mathbb{R})$ such that S is diagonal with positive values and T with all same positive values. Then the matrix $S + T$ is positive definite.*

Proof. Assume that the diagonal values of S are $s_1, \dots, s_n$ and all the values in T are t. Let $\mathbf{v} = (v_1, \dots, v_m)^T \in \mathbb{C}^m$ be a non-trivial vector. Then we have

$$\langle \mathbf{v} | (S+T)\mathbf{v} \rangle = \langle \mathbf{v} | S\mathbf{v} \rangle + \langle \mathbf{v} | T\mathbf{v} \rangle = \sum_{k=1}^{m} s_k |v_k|^2 + t \sum_{i,j=1}^{m} \overline{v_i} v_j = \sum_{k=1}^{m} s_k |v_k|^2 + t \left| \sum_{k=1}^{m} v_k \right|^2 > 0.$$

□

Lemma 5.71. *The holomorphic hessian* $\mathrm{Hess}(S)(\mathbf{y})$ *of S has non-zero determinant for every $\mathbf{y} \in \mathcal{Y}^0$.*

Proof. For $\mathbf{y} \in \mathcal{U}$, a direct calculation shows that the holomorphic hessian is given by

$$\mathrm{Hess}(S)(\mathbf{y}) = 2iQ_n + i \begin{pmatrix} \frac{-1}{1+e^{-y_1}} + d & d & \cdots & \cdots & d \\ d & \frac{1}{1+e^{-y_2}} + d & d & \cdots & d \\ \vdots & d & \ddots & \ddots & \vdots \\ \vdots & \vdots & \ddots & \ddots & d \\ d & d & \cdots & d & \frac{1}{1+e^{-y_n}} + d \end{pmatrix},$$

where

$$d := \frac{(-1)^{n+1} e^{-\sum_{k=1}^{n} y_k}}{1 + (-1)^{n+1} e^{-\sum_{k=1}^{n} y_k}}.$$

We clearly see that $\Im(\mathrm{Hess}(S)(\mathbf{y}))$ is symmetric. Assume that $\mathbf{y} \in \mathcal{Y}^0$ and denote $\eta := -y_1 - \cdots - y_n + i(n-1)\pi$. Then, $d = \frac{1}{1+e^{-\eta}}$ and $\eta \in \mathbb{R} + i(\pi - a^0_{n+1})$ using relation (5.69). Moreover, since $\Im(y_1) \in (-\pi, 0)$ and $\Im(\eta), \Im(y_k) \in (0, \pi)$ for $k = 2, \ldots, n$, we have that $-\Im\left(\frac{-1}{1+e^{-y_1}}\right) < 0$ and $-\Im\left(\frac{1}{1+e^{-\eta}}\right), -\Im\left(\frac{1}{1+e^{-y_k}}\right) < 0$ for $k = 2, \ldots, n$. Consequently, $\Re(\mathrm{Hess}(S)(\mathbf{y}))$ is negative definite by Lemma 5.70, and it follows again from Lemma 4.23 that $\mathrm{Hess}(S)(\mathbf{y})$ is invertible. □

Lemma 5.72. *The function $\Re(S) : \mathcal{Y}^0 \to \mathbb{R}$ admits a unique strict global maximum on $\mathbf{y}^0 \in \mathcal{Y}^0$.*

Proof. Since the holomorphic gradient of $S : \mathcal{U} \to \mathbb{C}$ vanishes on $\mathbf{y}^0 \in \mathcal{Y}^0$ by Lemma 5.59, the gradient of $\Re(S)$ also vanishes on $\mathbf{y}^0$, and thus $\mathbf{y}^0$ is a critical point of $\Re(S)|_{\mathcal{Y}^0}$. Finally, the proof of Lemma 5.71 shows that $\Re(S)|_{\mathcal{Y}^0}$ is strictly concave, thus $\mathbf{y}^0$ is the unique global maximum of $\Re(S)|_{\mathcal{Y}^0}$. □

Lemma 5.73. *We have*

$$\Re(S)(\mathbf{y}^0) = -\mathrm{Vol}(WL(n,1)).$$

Proof. We start by rewriting the potential function $S : \mathcal{U} \to \mathbb{C}$ as

$$\begin{aligned} S(\mathbf{y}) = i\mathrm{Li}_2(-e^{y_1}) + i\sum_{k=2}^{n} \mathrm{Li}_2(-e^{-y_k}) + i\mathrm{Li}_2\left((-1)^n e^{\sum_{k=1}^{n} y_k}\right) \\ + i\mathbf{y}^T Q_n \mathbf{y} + \frac{i}{2}\sum_{k=2}^{n} y_k^2 + \frac{i}{2}\mathrm{Log}\left((-1)^{n+1} e^{\sum_{k=1}^{n} y_k}\right)^2 + \mathbf{y}^T \mathcal{W}_n + in\frac{\pi^2}{6}, \end{aligned}$$

using Proposition 2.41 (1). We thus have

$$\begin{aligned} \Re(S)(\mathbf{y}) = &- \Im\left(\mathrm{Li}_2(-e^{y_1})\right) - \sum_{k=2}^{n} \Im\left(\mathrm{Li}_2(-e^{-y_k})\right) - \Im\left(\mathrm{Li}_2\left((-1)^n e^{\sum_{k=1}^{n} y_k}\right)\right) \\ &- \Im\left(\mathbf{y}^T Q_n \mathbf{y} + \frac{1}{2}\sum_{k=2}^{n} y_k^2 + \frac{1}{2}\mathrm{Log}\left((-1)^{n+1} e^{\sum_{k=1}^{n} y_k}\right)^2\right) + \Re\left(\mathbf{y}^T \mathcal{W}_n\right) \end{aligned}$$

If $\mathbf{z}^0 := (z_1^0, \ldots, z_{n+1}^0)$ is the complete hyperbolic structure of X_n and if we denote $y_{n+1}^0 := \psi_{T_{n+1}}(z_{n+1}^0) = x_{n+1}^0 + id_{n+1}^0$, then relation (5.61) implies that $(-1)^n e^{\sum_{k=1}^{n} y_k^0} = -e^{-y_{n+1}^0}$, and we have

$$\Re(S)(\mathbf{y}^0) = -\sum_{k=1}^{n+1} D(z_k^0) - c_1^0 x_1^0 + \sum_{k=2}^{n+1} b_k^0 x_k^0 - 2(\mathbf{x}^0)^T Q_n \mathbf{d}^0 - \sum_{k=2}^{n+1} x_k^0 d_k^0 + (\mathbf{x}^0)^T \mathcal{W}_n, \quad (5.74)$$

where D is the Bloch–Wigner function and $\mathbf{x}^0 := \Im(\mathbf{y}^0)$. Replacing x_{n+1}^0 by $-x_1^0 - \cdots - x_n^0$ (again by relation (5.61)) in (5.74), we get

$$\Re(S)(\mathbf{y}^0) = -\mathrm{Vol}(WL(n,1)) + (\mathbf{x}^0)^T \mathcal{T},$$

where

$$\mathcal{T} := \begin{pmatrix} -c_1^0 - b_{n+1}^0 \\ b_2^0 - b_{n+1}^0 \\ \vdots \\ b_n^0 - b_{n+1}^0 \end{pmatrix} + \mathcal{W}_n - 2Q_n\mathbf{d}^0 + \begin{pmatrix} d_{n+1}^0 \\ -d_2^0 + d_{n+1}^0 \\ \vdots \\ -d_n^0 + d_{n+1}^0 \end{pmatrix}.$$

Let us show that $\mathcal{T} = 0$. Since $d_l^0 = \pi - a_l^0 = b_l^0 + c_l^0$ for $l = 2, \dots, n+1$, then using relation (5.63), we see that

$$\mathcal{T} = 2Q_n \begin{pmatrix} a_1^0 \\ -a_2^0 \\ \vdots \\ -a_n^0 \end{pmatrix} + \begin{pmatrix} c_1^0 - c_{n+1}^0 \\ \vdots \\ c_n^0 - c_{n+1}^0 \end{pmatrix}.$$

Multiplying $\mathcal{T}$ by the invertible matrix F (defined in (5.64)) and using relation (5.65), one gets

$$F\mathcal{T} = \begin{pmatrix} 2a_2^0 + \cdots + 2a_n^0 + c_2^0 + c_n^0 - 2c_{n+1}^0 \\ -2a_2^0 + c_1^0 - 2c_2^0 + c_3^0 \\ \vdots \\ -2a_n^0 + c_{n-1}^0 - 2c_n^0 + c_{n+1}^0 \end{pmatrix},$$

which is the zero vector by relations (5.67) and (5.68). □

Finally, the remaining arguments are proven in exactly the same way as in Chapter 4 (Sections 4.6.4 to 4.6.6) and we obtain the following asymptotic behavior for $\mathfrak{J}_{X_n}(\hbar, 0)$:

$$\mathfrak{J}_{X_n}(\hbar, 0) = \left(\frac{1}{2\pi\sqrt{\hbar}}\right)^{n+1} e^{\frac{1}{2\pi\hbar}S(\mathbf{y}^0)} \left(\rho' \hbar^{\frac{n}{2}} (1 + o_{\hbar\to 0^+}(1)) + \mathcal{O}_{\hbar\to 0^+}(1)\right).$$

This concludes the proof of Theorem 5.58.

Remark 5.75. In this section, we studied the family $(L(n,1), \mathcal{K}_n)$ where the complement $L(n,1)\setminus\mathcal{K}_n$ is the once-punctured torus bundle over the circle with monodromy conjugate to RL^n for all $n \geqslant 1$. It should not be difficult to generalize all the calculations of Section 5.2.1 to the case where the monodromy is conjugate to $R^{a_1}L^{b_1}\cdots R^{a_m}L^{b_m}$ (with a_i, b_i positive integers and $m \geqslant 1$) and prove the part (3) of Conjecture 3.68. Unfortunately, the monodromy triangulation is no more split in this case, and thus one cannot apply a T-surgery to get an H-triangulation.

5.3 Calculations for other knots in $\mathbb{R}P^3$

To finish this chapter, we compute the partition functions for the knots constructed in Sections 5.1.3.2 and 5.1.3.3 (represented respectively in Figures 5.18 (b) and 5.18 (c)) and we will check numerically the third part of Conjecture 3.68. The reason that we cannot present the computations for the example of Section 5.1.3.4 is that, if Y is a triangulation of $S^1 \times S^2$ with one vertex, then $H_2(Y \setminus Y^0, \mathbb{Z}) \neq 0$ (see Theorem 3.52). As explained in Remark 3.54 (b), the computation becomes possible with the new formulation [AK13], but more technical, due to the appearance of infinite series.

Notations 5.76. To improve readability, we introduce the following notations only for this Section 5.3:

$$\langle x\rangle := e^{\pi i x^2} \qquad \text{and} \qquad \langle x,y\rangle := e^{2\pi i xy}$$

for $x, y \in \mathbb{R}$.

5.3.1 The pair $(\mathbb{R}P^3, 4_1)$

For ideal triangulation of $\mathbb{R}P^3 \setminus 4_1$

Let us use the ideal triangulation X of $\mathbb{R}P^3 \setminus 4_1 = m045$ represented in Figure 5.10 (b). Moreover, we denote $\mathbf{t} := (t_1, t_2, t_3, t_4)^T$ and $\mathbf{x} := (a, b, c, e, f, g, h, j)^T$. The kinematical kernel of X is

$$\begin{aligned}\mathcal{K}_X(\mathbf{t}) &= \int_{\mathbb{R}^8} \langle a, t_1\rangle\langle f, t_2\rangle\langle h, t_3\rangle\langle j, t_4\rangle \delta_{a-b+c}\delta_{c-e+t_1}\delta_{f-g+b}\delta_{b-a+t_2}\delta_{h-c+e}\delta_{e-f+t_3}\delta_{j-h+g}\delta_{g-j+t_4}\, d\mathbf{x} \\ &= \langle -3t_1 + 4t_2 - 2t_3 - t_4, t_1\rangle^{\frac{1}{2}} \langle t_1 - t_2 + t_3, t_2\rangle \langle t_1, t_3\rangle^{-1} \langle -t_1 + t_4, t_4\rangle^{\frac{1}{2}} \\ &= \langle t_1, t_2\rangle^3 \langle t_1, t_3\rangle^{-2} \langle t_1, t_4\rangle^{-1} \langle t_2, t_3\rangle \langle t_1\rangle^{-3} \langle t_2\rangle^{-2} \langle t_4\rangle.\end{aligned}$$

Let $\alpha = (a_1, \dots, c_4) \in \mathcal{S}_X$ be a shape structure. The balancing conditions are

$$\begin{aligned} b_1 + 2c_1 + a_2 + c_2 + b_3 + c_3 + c_4 &= 2\pi, \\ 2a_1 + b_2 + c_2 + a_3 + b_3 &= 2\pi, \\ b_1 + b_2 + a_3 + 2a_4 + c_4 &= 2\pi, \\ a_2 + c_3 + 2b_4 &= 2\pi, \end{aligned}$$

which imply the following relations on angles:

$$c_3 = 2a_1 - a_2, \tag{5.77}$$

$$a_4 - b_3 = a_1 - b_1 + c_2, \tag{5.78}$$

$$b_4 = \pi - a_1. \tag{5.79}$$

Using formulas (3.44), (3.45) and (3.46), the partition function becomes

$$\begin{aligned}\mathcal{Z}_\hbar(X, \alpha) &\overset{\star}{=} \int_{\mathbb{R}^4} \langle t_1, t_2\rangle^3 \langle t_1, t_4\rangle^{-1} \langle t_3, -2t_1 + t_2\rangle \langle t_1\rangle^{-3} \langle t_2\rangle^{-2} \langle t_4\rangle \psi_{c_1,b_1}(t_1)\psi_{c_2,b_2}(t_2)\psi_{c_3,b_3}(t_3)\psi_{c_4,b_4}(t_4)\, d\mathbf{t} \\ &= \int_{\mathbb{R}^3} \langle t_1, t_2\rangle^3 \langle t_1, t_4\rangle^{-1} \langle t_1\rangle^{-3} \langle t_2\rangle^{-2} \langle t_4\rangle \psi_{c_1,b_1}(t_1)\psi_{c_2,b_2}(t_2)\widetilde{\psi}_{c_3,b_3}(2t_1 - t_2)\psi_{c_4,b_4}(t_4)\, dt_1 dt_2 dt_4 \\ &\overset{\star}{=} \int_{\mathbb{R}^3} \langle t_1, t_2\rangle \langle t_1, t_4\rangle^{-1} \langle t_1\rangle \langle t_2\rangle^{-1} \langle t_4\rangle \psi_{c_1,b_1}(t_1)\psi_{c_2,b_2}(t_2)\psi_{b_3,a_3}(2t_1 - t_2)\psi_{c_4,b_4}(t_4)\, dt_1 dt_2 dt_4.\end{aligned}$$

Let us do the following change of variables:

$$t_1 = -x + \tfrac{i}{2\pi\sqrt{\hbar}}(\pi - a_1), \qquad t_2 = -x + y + \tfrac{i}{2\pi\sqrt{\hbar}}(\pi - a_2), \qquad t_4 = -z + \tfrac{i}{2\pi\sqrt{\hbar}}(\pi - a_4).$$

To simplify computations, we move a bit the integration domain. Since $a_1, a_2, a_4 \in (0, \pi)$, using Cauchy theorem we can suppose that $x, z \in \mathbb{R} + i0$ and also $y \in \mathbb{R}$, because we

can still find an angle structure with the condition $a_1 = a_2$ (for example the complete structure). Moreover, we also have that

$$\begin{aligned} 2t_1 - t_2 - \tfrac{i}{2\pi\sqrt{\hbar}}(\pi - c_3) &= -2x + 2\tfrac{i}{2\pi\sqrt{\hbar}}(\pi - a_1) + x - y - \tfrac{i}{2\pi\sqrt{\hbar}}(\pi - a_2) - \tfrac{i}{2\pi\sqrt{\hbar}}(\pi - c_3) \\ &= -x - y + \tfrac{i}{2\pi\sqrt{\hbar}}(-2a_1 + a_2 + c_3) \\ &= -x + y, \end{aligned}$$

where we used relation (5.77) in the last equality. We thus get

$$\psi_{c_1,b_1}(t_1) \overset{\star}{=} \frac{e^{-\frac{1}{\sqrt{\hbar}}c_1 x}}{\Phi_{\mathsf{b}}(-x)}, \qquad \psi_{c_2,b_2}(t_2) \overset{\star}{=} \frac{e^{-\frac{1}{\sqrt{\hbar}}c_2(x-y)}}{\Phi_{\mathsf{b}}(y-x)},$$
$$\psi_{b_3,a_3}(2t_1 - t_2) \overset{\star}{=} \frac{e^{-\frac{1}{\sqrt{\hbar}}b_3(x+y)}}{\Phi_{\mathsf{b}}(-x-y)}, \qquad \psi_{c_4,b_4}(t_4) \overset{\star}{=} \frac{e^{-\frac{1}{\sqrt{\hbar}}c_4 z}}{\Phi_{\mathsf{b}}(-z)}.$$

Coming back to calculation of partition function, we have that

$$\begin{aligned} \mathcal{Z}_\hbar(X,\alpha) \overset{\star}{=} \int_{(\mathbb{R}+i0)^2} dxdz \int_{\mathbb{R}} dy \frac{e^{-\frac{1}{\sqrt{\hbar}}(c_1 x + c_2(x-y) + b_3(x+y) + c_4 z)}}{\Phi_{\mathsf{b}}(-x)\Phi_{\mathsf{b}}(y-x)\Phi_{\mathsf{b}}(-x-y)\Phi_{\mathsf{b}}(-z)} \\ \times \langle x\rangle^2 \langle x,y\rangle^{-1} e^{\frac{1}{\sqrt{\hbar}}(\pi - a_2)x} e^{-\frac{1}{\sqrt{\hbar}}(\pi-a_1)(y-x)} \langle x,z\rangle^{-1} e^{-\frac{1}{\sqrt{\hbar}}(\pi-a_4)x} e^{-\frac{1}{\sqrt{\hbar}}(\pi-a_1)z} \\ \times \langle x\rangle e^{\frac{1}{\sqrt{\hbar}}(\pi-a_1)x} \langle y-x\rangle^{-1} e^{-\frac{1}{\sqrt{\hbar}}(\pi-a_2)(x-y)} \langle z\rangle e^{\frac{1}{\sqrt{\hbar}}(\pi-a_4)z}. \end{aligned}$$

Using relation (5.78), the exponential term with x and $\frac{1}{\sqrt{\hbar}}$ becomes

$$e^{\frac{1}{\sqrt{\hbar}}(\pi - c_1 - c_2 - b_3 - 2a_1 + a_4)x} = 1.$$

Using relation (5.79), the exponential term with z and $\frac{1}{\sqrt{\hbar}}$ becomes

$$e^{\frac{1}{\sqrt{\hbar}}(-\pi + b_4 + a_1)z} = 1.$$

The exponential term with y and $\frac{1}{\sqrt{\hbar}}$ is

$$e^{\frac{1}{\sqrt{\hbar}}(c_2 - b_3 + a_1 - a_2)y} = e^{\frac{1}{2\sqrt{\hbar}}\lambda_X(\alpha)y},$$

where we defined $\lambda_X(\alpha) := 2a_1 - 2a_2 + 2c_2 - 2b_3$.

Finally, the remaining terms are

$$\langle x\rangle^2 \langle x,y\rangle^{-1} \langle x,z\rangle^{-1} \langle x\rangle \langle y-x\rangle^{-1} \langle z\rangle = \langle x,z\rangle^{-1} \langle x\rangle^2 \langle y\rangle^{-1} \langle z\rangle.$$

Consequently, the partition function becomes

$$\begin{aligned} \mathcal{Z}_\hbar(X,\alpha) &\overset{\star}{=} \int_{(\mathbb{R}+i0)^2} dxdz \int_{\mathbb{R}} dy \frac{\langle x,z\rangle^{-1} \langle x\rangle^2 \langle y\rangle^{-1} \langle z\rangle e^{\frac{1}{2\sqrt{\hbar}}\lambda_X(\alpha)y}}{\Phi_{\mathsf{b}}(-x)\Phi_{\mathsf{b}}(y-x)\Phi_{\mathsf{b}}(-x-y)\Phi_{\mathsf{b}}(-z)} \\ &\overset{\star}{=} \int_{\mathbb{R}} dy \left(\int_{(\mathbb{R}+i0)^2} dxdz \frac{\Phi_{\mathsf{b}}(x)\Phi_{\mathsf{b}}(z)\langle x,z\rangle^{-1} \langle x\rangle \langle y\rangle^{-1}}{\Phi_{\mathsf{b}}(y-x)\Phi_{\mathsf{b}}(-x-y)} \right) e^{\frac{1}{2\sqrt{\hbar}}\lambda_X(\alpha)y}, \end{aligned}$$

where we used relation (3.37) for the second equality. Defining $J_X : \mathbb{R}_{>0} \times \mathbb{C} \to \mathbb{C}$ by

$$J_X(\hbar, y) := \int_{(\mathbb{R}+i0)^2} dxdz \frac{\Phi_{\mathsf{b}}(x)\Phi_{\mathsf{b}}(z)\langle x, z\rangle^{-1}\langle x\rangle\langle y\rangle^{-1}}{\Phi_{\mathsf{b}}(y-x)\Phi_{\mathsf{b}}(-x-y)},$$

part (1) of Conjecture 3.68 is satisfied.

For H-triangulation of $(\mathbb{R}P^3, 4_1)$

Since the ideal triangulation represented in Figure 5.10 (b) is split (with the splitting face marked with a red dot), we can do a T-surgery and obtain the H-triangulation Y given in Figure 5.25.

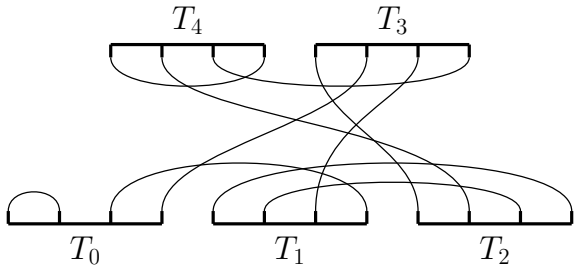

Figure 5.25: H-triangulation constructed from the ideal triangulation of Figure 5.10 (b).

Denote $\mathbf{t} := (t_0, t_1, t_2, t_3, t_4)^T$ and $\mathbf{x} := (q, r, s, t, u, v, w, x, y, z)^T$. The kinematical kernel of Y is

$$\begin{aligned}
\mathcal{K}_Y(\mathbf{t}) &= \int_{\mathbb{R}^{10}} \langle r, t_0\rangle\langle t, t_1\rangle\langle w, t_2\rangle\langle y, t_3\rangle\langle z, t_4\rangle\delta_q\delta_{q-s+t_0}\delta_{t-u+v}\delta_{v-q+t_1}\delta_{w-x+u}\delta_{u-t+t_2}\delta_{y-v+s} \\
&\qquad \delta_{s-w+t_3}\delta_{z-y+x}\delta_{x-z+t_4}\, d\mathbf{x} \\
&= \int_{\mathbb{R}} \langle r, t_0\rangle\langle \tfrac{t_0+t_1-t_4}{2} - 2t_0 - t_3, t_1\rangle\langle t_0 + t_3, t_2\rangle\langle -t_0 - t_1, t_3\rangle\langle \tfrac{-t_0-t_1+t_4}{2}, t_4\rangle\delta_{t_2-t_1}\, dr \\
&= \langle t_0 + t_1 - t_4, t_1\rangle^{\frac{1}{2}}\langle -2t_0 - t_3, t_1\rangle\langle t_0 + t_3, t_2\rangle\langle -t_0 - t_1, t_3\rangle\langle -t_0 - t_1 + t_4, t_4\rangle^{\frac{1}{2}}\delta_{t_0}\delta_{t_2-t_1} \\
&= \langle t_1, t_4\rangle^{-1}\langle t_1, t_3\rangle^{-1}\langle t_1\rangle\langle t_4\rangle\delta_{t_0}\delta_{t_2-t_1}.
\end{aligned}$$

Let $\alpha = (a_0, b_0, c_0, \ldots, a_4, b_4, c_4) \in \mathcal{S}_Y$ and $\tau = (a_0^\tau, b_0^\tau, c_0^\tau, \ldots, a_4^\tau, b_4^\tau, c_4^\tau) \in \overline{\mathcal{S}_{T_0}} \times \mathcal{S}_{Y\setminus T_0}$ be such that the weights around each edge is 2π except around the knot which is 0. We get the following relations:

$$a_2^\tau = a_1^\tau, \tag{5.80}$$
$$c_3^\tau = a_1^\tau, \tag{5.81}$$
$$a_4^\tau - b_3^\tau = \pi - b_1^\tau - b_2^\tau, \tag{5.82}$$
$$b_4^\tau = \pi - a_1^\tau. \tag{5.83}$$

The partition function of Y for α is

$$\begin{aligned}\mathcal{Z}_\hbar(Y,\alpha) &\stackrel{\star}{=} \psi_{c_0,b_0}(0)\int_{\mathbb{R}^3}\langle t_1,t_4\rangle^{-1}\langle t_1,t_3\rangle^{-1}\langle t_1\rangle\langle t_4\rangle\psi_{c_1,b_1}(t_1)\psi_{c_2,b_2}(t_1)\psi_{c_3,b_3}(t_3)\psi_{c_4,b_4}(t_4)\,dt_1dt_3dt_4\\ &= \psi_{c_0,b_0}(0)\int_{\mathbb{R}^2}\langle t_1,t_4\rangle^{-1}\langle t_1\rangle\langle t_4\rangle\psi_{c_1,b_1}(t_1)\psi_{c_2,b_2}(t_1)\widetilde{\psi}_{c_3,b_3}(t_1)\psi_{c_4,b_4}(t_4)\,dt_1dt_4\\ &\stackrel{\star}{=} \psi_{c_0,b_0}(0)\int_{\mathbb{R}^2}\langle t_1,t_4\rangle^{-1}\langle t_1\rangle^2\langle t_4\rangle\psi_{c_1,b_1}(t_1)\psi_{c_2,b_2}(t_1)\psi_{b_3,a_3}(t_1)\psi_{c_4,b_4}(t_4)\,dt_1dt_4.\end{aligned}$$

Let us do the following change of variables:

$$t_1 = -x + \tfrac{i}{2\pi\sqrt{\hbar}}(\pi - a_1), \qquad t_4 = -z + \tfrac{i}{2\pi\sqrt{\hbar}}(\pi - a_4).$$

Since $a_1, a_4 \in (0,\pi)$, using Cauchy theorem, as in the case of the ideal triangulation, we can assume that $x, z \in \mathbb{R} + i0$. We get

$$\psi_{c_1,b_1}(t_1) \stackrel{\star}{=} \frac{e^{-\frac{1}{\sqrt{\hbar}}c_1x}}{\Phi_{\mathsf{b}}(-x)}, \qquad \psi_{c_2,b_2}(t_1) \stackrel{\star}{=} \frac{e^{-\frac{1}{\sqrt{\hbar}}c_2x}}{\Phi_{\mathsf{b}}\left(-x-\frac{i}{2\pi\sqrt{\hbar}}(a_1-a_2)\right)},$$

$$\psi_{b_3,a_3}(t_1) \stackrel{\star}{=} \frac{e^{-\frac{1}{\sqrt{\hbar}}b_3x}}{\Phi_{\mathsf{b}}\left(-x-\frac{i}{2\pi\sqrt{\hbar}}(a_1-c_3)\right)}, \qquad \psi_{c_4,b_4}(t_4) \stackrel{\star}{=} \frac{e^{-\frac{1}{\sqrt{\hbar}}c_4z}}{\Phi_{\mathsf{b}}(-z)}.$$

Using dominated convergence theorem and relations (5.80) and (5.81), we have that

$$\begin{aligned}\lim_{\alpha\to\tau}\Phi_{\mathsf{b}}\left(\frac{\pi-a_0}{2\pi i\sqrt{\hbar}}\right)\mathcal{Z}_\hbar(Y,\alpha) \stackrel{\star}{=} \int_{(\mathbb{R}+i0)^2} dxdz\frac{e^{-\frac{1}{\sqrt{\hbar}}(c_1^\tau x+c_2^\tau x+b_3^\tau x+c_4^\tau z)}}{\Phi_{\mathsf{b}}(-x)^3\Phi_{\mathsf{b}}(-z)}\\ \times\langle x,z\rangle^{-1}e^{-\frac{1}{\sqrt{\hbar}}(\pi-a_4^\tau)x}e^{-\frac{1}{\sqrt{\hbar}}(\pi-a_1^\tau)z}\langle x\rangle^2e^{\frac{1}{\sqrt{\hbar}}(2\pi-2a_1^\tau)x}\langle z\rangle e^{\frac{1}{\sqrt{\hbar}}(\pi-a_4^\tau)z}.\end{aligned}$$

Using relations (5.80) and (5.82), the exponential term with x and $\frac{1}{\sqrt{\hbar}}$ becomes

$$e^{\frac{1}{\sqrt{\hbar}}(\pi+a_4^\tau-2a_1^\tau-c_1^\tau-c_2^\tau-b_3^\tau)x} = e^{\frac{1}{\sqrt{\hbar}}(2\pi-b_1^\tau-b_2^\tau-a_1^\tau-a_2^\tau-c_1^\tau-c_2^\tau)x} = 1.$$

Using relation (5.83), the exponential term with z and $\frac{1}{\sqrt{\hbar}}$ becomes

$$e^{\frac{1}{\sqrt{\hbar}}(a_1^\tau-a_4^\tau-c_4^\tau)z} = 1.$$

Consequently, we have that

$$\begin{aligned}\lim_{\alpha\to\tau}\Phi_{\mathsf{b}}\left(\frac{\pi-a_0}{2\pi i\sqrt{\hbar}}\right)\mathcal{Z}_\hbar(Y,\alpha) &\stackrel{\star}{=} \int_{(\mathbb{R}+i0)^2} dxdz\frac{\langle x\rangle^2\langle z\rangle\langle x,z\rangle^{-1}}{\Phi_{\mathsf{b}}(-x)^3\Phi_{\mathsf{b}}(-z)}\\ &\stackrel{\star}{=} \int_{(\mathbb{R}+i0)^2} dxdz\frac{\Phi_{\mathsf{b}}(x)\Phi_{\mathsf{b}}(z)\langle x\rangle\langle x,z\rangle^{-1}}{\Phi_{\mathsf{b}}(-x)^2}\\ &= J_X(\hbar,0),\end{aligned}$$

and this proves the part (2) of Conjecture 3.68.

Numerical evidence of asymptotic behavior

We will no more prove rigorously, but we will only show numerically and with many details left out that the asymptotic behavior of $2\pi\hbar \log|J_X(\hbar,0)|$ when $\hbar \to 0^+$ retrieves the hyperbolic volume of $m045$. The potential function is given by

$$S(x,z) := -2i\mathrm{Li}_2(-e^x) + i\mathrm{Li}_2(-e^{-x}) - i\mathrm{Li}_2(-e^z) - ixz.$$

Using Mathematica, we find that the critical point which contribute to the integral is the pair

$$(x_0, z_0) \approx (0.628028 + 2.04616i, 0.914429 + 2.41048i),$$

and by substituting in S, we get

$$\Re(S(x_0,z_0)) \approx -3.2758716439439341528 \approx -\mathrm{Vol}(m045).$$

Therefore, point (3) of Conjecture 3.68 is checked numerically.

5.3.2 The pair $(\mathbb{R}P^3, 4_2)$

For ideal triangulation of $\mathbb{R}P^3 \setminus 4_2$

Let us use the ideal triangulation X of $\mathbb{R}P^3 \setminus 4_2 = m148$ represented in Figure 5.11 (b). We denote $\mathbf{t} := (t_1,t_2,t_3,t_4)^T$ and $\mathbf{x} := (a,b,c,e,f,g,h,j)^T$. The kinematical kernel of X is

$$\begin{aligned}\mathcal{K}_X(\mathbf{t}) &= \int_{\mathbb{R}^8} \langle a,t_1\rangle\langle e,t_2\rangle\langle h,t_3\rangle\langle g,t_4\rangle \delta_{a-b+c}\delta_{c-e+t_1}\delta_{e-a+f}\delta_{f-g+t_2}\delta_{h-f+j}\delta_{j-c+t_3}\delta_{g-h+b}\delta_{b-j+t_4}\, d\mathbf{x} \\ &= \langle -t_3-t_4, t_1\rangle\langle 2t_1 - t_2 + 2t_3 + t_4, t_2\rangle^{\frac{1}{2}}\langle -t_1+t_2-2t_3-2t_4, t_3\rangle\langle -2t_1+3t_2-4t_3-3t_4, t_4\rangle^{\frac{1}{2}} \\ &= \langle t_1, t_2-2t_3-2t_4\rangle\langle t_2,t_3\rangle^2\langle t_2,t_4\rangle^2\langle t_3,t_4\rangle^{-4}\langle t_2\rangle^{-1}\langle t_3\rangle^{-4}\langle t_4\rangle^{-3}.\end{aligned}$$

Let $\alpha = (a_1,\dots,c_4) \in \mathcal{S}_X$ be a shape structure. The balancing conditions are

$$\begin{aligned} a_1+b_1+b_2+c_2+2a_3+2a_4 &= 2\pi, \\ c_1+a_2+2b_3+2c_4 &= 2\pi, \\ a_1+c_1+a_2+b_2+b_4 &= 2\pi, \\ b_1+c_2+2c_3+b_4 &= 2\pi. \end{aligned}$$

Using angle relations, we get the following equalities:

$$c_3 + b_1 = a_2 + b_2, \tag{5.84}$$
$$2(a_3+a_4) = c_1 + a_2, \tag{5.85}$$
$$2(b_1+c_4) = c_1 + a_2 + 2b_2 + 2a_3. \tag{5.86}$$

The partition function is

$$\begin{aligned}\mathcal{Z}_\hbar(X,\alpha) &\overset{\star}{=} \int_{\mathbb{R}^4} \langle t_1, t_2-2t_3-2t_4\rangle \langle t_2,t_3\rangle^2 \langle t_2,t_4\rangle^2 \langle t_3,t_4\rangle^{-4} \langle t_2\rangle^{-1} \langle t_3\rangle^{-4} \langle t_4\rangle^{-3} \\ &\qquad \psi_{c_1,b_1}(t_1)\psi_{c_2,b_2}(t_2)\psi_{c_3,b_3}(t_3)\psi_{c_4,b_4}(t_4)\, d\mathbf{t} \\ &= \int_{\mathbb{R}^3} \langle t_2,t_3\rangle^2 \langle t_2,t_4\rangle^2 \langle t_3,t_4\rangle^{-4} \langle t_2\rangle^{-1} \langle t_3\rangle^{-4} \langle t_4\rangle^{-3} \widetilde{\psi}_{c_1,b_1}(2t_3+2t_4-t_2) \\ &\qquad \psi_{c_2,b_2}(t_2)\psi_{c_3,b_3}(t_3)\psi_{c_4,b_4}(t_4)\, dt_2dt_3dt_4 \\ &\overset{\star}{=} \int_{\mathbb{R}^3} \langle t_4\rangle \psi_{b_1,a_1}(2t_3+2t_4-t_2)\psi_{c_2,b_2}(t_2)\psi_{c_3,b_3}(t_3)\psi_{c_4,b_4}(t_4)\, dt_2dt_3dt_4.\end{aligned}$$

Let us do the following change of variables:

$$t_3 = x + \tfrac{i}{2\pi\sqrt{\hbar}}(\pi - a_3), \qquad t_4 = z + \tfrac{i}{2\pi\sqrt{\hbar}}(\pi - a_4), \qquad t_2 = x+y+z+\tfrac{i}{2\pi\sqrt{\hbar}}(2\pi - a_2).$$

Since $a_2, a_3, a_4 \in (0,\pi)$, using Cauchy theorem we can suppose that $x, z \in \mathbb{R} - i0$ and also $y \in \mathbb{R}$, because we can still find an angle structure with the condition $a_2 = a_3 + a_4$ (for example the complete structure). Moreover, we also have that

$$\begin{aligned}2t_3+2t_4-t_2-\tfrac{i}{2\pi\sqrt{\hbar}}(\pi-c_1) &= x-y+z+\tfrac{i}{2\pi\sqrt{\hbar}}(\pi-2a_3-2a_4+a_2+c_1) \\ &= x-y+z+\tfrac{i}{2\sqrt{\hbar}},\end{aligned}$$

where we used relation (5.85) in the last equality. We thus get

$$\psi_{b_1,a_1}(2t_3+2t_4-t_2) \overset{\star}{=} \frac{e^{-\frac{1}{\sqrt{\hbar}}b_1(-x+y-z)}}{\Phi_{\mathsf{b}}\left(x-y+z+\frac{i}{2\sqrt{\hbar}}\right)}, \quad \psi_{c_2,b_2}(t_2) \overset{\star}{=} \frac{e^{\frac{1}{\sqrt{\hbar}}c_2(x+y+z)}}{\Phi_{\mathsf{b}}\left(x+y+z+\frac{i}{2\sqrt{\hbar}}\right)},$$

$$\psi_{c_3,b_3}(t_3) \overset{\star}{=} \frac{e^{\frac{1}{\sqrt{\hbar}}c_3x}}{\Phi_{\mathsf{b}}(x)}, \qquad \psi_{c_4,b_4}(t_4) \overset{\star}{=} \frac{e^{\frac{1}{\sqrt{\hbar}}c_4z}}{\Phi_{\mathsf{b}}(z)}.$$

Coming back to calculation of partition function, we have that

$$\mathcal{Z}_\hbar(X,\alpha) \overset{\star}{=} \int_{(\mathbb{R}-i0)^2} dxdz \int_{\mathbb{R}} dy \frac{e^{-\frac{1}{\sqrt{\hbar}}(b_1(-x+y-z)-c_2(x+y+z)-c_3x-c_4z)}\langle z\rangle e^{-\frac{1}{\sqrt{\hbar}}(\pi-a_4)z}}{\Phi_{\mathsf{b}}\left(x-y+z+\frac{i}{2\sqrt{\hbar}}\right)\Phi_{\mathsf{b}}\left(x+y+z+\frac{i}{2\sqrt{\hbar}}\right)\Phi_{\mathsf{b}}(x)\Phi_{\mathsf{b}}(z)}.$$

Using relation (5.84), the exponential term with x and $\frac{1}{\sqrt{\hbar}}$ becomes

$$e^{\frac{1}{\sqrt{\hbar}}(b_1+c_2+c_3)x} = e^{\frac{1}{\sqrt{\hbar}}(b_1+c_2+a_2-b_1+b_2)x} = e^{\frac{1}{\sqrt{\hbar}}\pi x}.$$

Using relations (5.85) and (5.86), the exponential term with z and $\frac{1}{\sqrt{\hbar}}$ becomes

$$e^{\frac{1}{\sqrt{\hbar}}(b_1+c_2+c_4-\pi+a_4)z} = e^{\frac{1}{\sqrt{\hbar}}(-\pi+b_1+c_2+c_4-\frac{c_1}{2}+\frac{a_2}{2}-a_3)z} = e^{\frac{1}{\sqrt{\hbar}}(-\pi+c_2+a_2+b_2)z} = 1.$$

The exponential term with y and $\frac{1}{\sqrt{\hbar}}$ is

$$e^{\frac{1}{\sqrt{\hbar}}(-b_1+c_2)y} = e^{\frac{1}{2\sqrt{\hbar}}\lambda_X(\alpha)y},$$

where we defined $\lambda_X(\alpha) := -2b_1 + 2c_2$.

Finally, since the only remaining term is $\langle z \rangle$, the partition function becomes

$$\begin{aligned}\mathcal{Z}_\hbar(X,\alpha) &\overset{\star}{=} \int_{(\mathbb{R}-i0)^2} dxdz \int_{\mathbb{R}} dy \frac{\langle z\rangle e^{\frac{1}{\sqrt{\hbar}}\pi x} e^{\frac{1}{2\sqrt{\hbar}}\lambda_X(\alpha)y}}{\Phi_{\mathsf{b}}\left(x-y+z+\frac{i}{2\sqrt{\hbar}}\right)\Phi_{\mathsf{b}}\left(x+y+z+\frac{i}{2\sqrt{\hbar}}\right)\Phi_{\mathsf{b}}(x)\Phi_{\mathsf{b}}(z)} \\ &\overset{\star}{=} \int_{\mathbb{R}} dy \left(\int_{(\mathbb{R}-i0)^2} dxdz \frac{\Phi_{\mathsf{b}}(-z) e^{\frac{1}{\sqrt{\hbar}}\pi x}}{\Phi_{\mathsf{b}}\left(x-y+z+\frac{i}{2\sqrt{\hbar}}\right)\Phi_{\mathsf{b}}\left(x+y+z+\frac{i}{2\sqrt{\hbar}}\right)\Phi_{\mathsf{b}}(x)} \right) e^{\frac{1}{2\sqrt{\hbar}}\lambda_X(\alpha)y}.\end{aligned}$$

Defining the function $J_X : \mathbb{R}_{>0} \times \mathbb{C} \to \mathbb{C}$ by

$$J_X(\hbar, y) := \int_{(\mathbb{R}-i0)^2} dxdz \frac{\Phi_{\mathsf{b}}(-z) e^{\frac{1}{\sqrt{\hbar}}\pi x}}{\Phi_{\mathsf{b}}\left(x-y+z+\frac{i}{2\sqrt{\hbar}}\right)\Phi_{\mathsf{b}}\left(x+y+z+\frac{i}{2\sqrt{\hbar}}\right)\Phi_{\mathsf{b}}(x)},$$

part (1) of Conjecture 3.68 is satisfied.

For H-triangulation of $(\mathbb{R}P^3, 4_2)$

The ideal triangulation represented in Figure 5.11 (b) is split (with the splitting face marked with a red dot), thus one can perform a T-surgery and obtain the H-triangulation Y given in Figure 5.26.

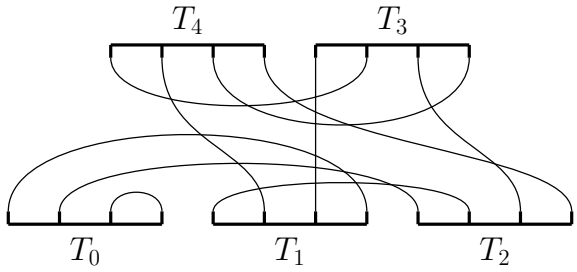

Figure 5.26: H-triangulation constructed from the ideal triangulation of Figure 5.11 (b).

Denote $\mathbf{t} := (t_0, t_1, t_2, t_3, t_4)^T$ and $\mathbf{x} := (q, r, s, t, u, v, w, x, y, z)^T$. The kinematical kernel of Y is

$$\begin{aligned}\mathcal{K}_Y(\mathbf{t}) &= \int_{\mathbb{R}^{10}} \langle q, t_0\rangle\langle t, t_1\rangle\langle s, t_2\rangle\langle y, t_3\rangle\langle x, t_4\rangle \delta_{q-s+r}\delta_{t_0}\delta_{t-u+v}\delta_{v-q+t_1}\delta_{s-t+w}\delta_{w-x+t_2}\delta_{y-w+z} \\ &\qquad \delta_{z-v+t_3}\delta_{x-y+u}\delta_{u-z+t_4}\, d\mathbf{x} \\ &= \int_{\mathbb{R}} \langle r, t_2-t_3-t_4\rangle\langle -t_3-t_4, t_1\rangle\langle 2t_1-t_2+2t_3+t_4, t_2\rangle^{\frac{1}{2}}\langle -t_1+t_2-2t_3-2t_4, t_3\rangle \\ &\qquad \langle -2t_1+3t_2-4t_3-3t_4, t_4\rangle^{\frac{1}{2}}\delta_{t_0}\, dr \\ &= \langle t_1, t_3+t_4\rangle^{-1}\langle t_3, t_4\rangle^{-1}\langle t_3\rangle^{-1}\delta_{t_0}\delta_{t_2-t_3-t_4}.\end{aligned}$$

Let $\alpha = (a_0, b_0, c_0, \ldots, a_4, b_4, c_4) \in \mathcal{S}_Y$ and $\tau = (a_0^\tau, b_0^\tau, c_0^\tau, \ldots, a_4^\tau, b_4^\tau, c_4^\tau) \in \overline{\mathcal{S}_{T_0}} \times \mathcal{S}_{Y\setminus T_0}$ be such that the weights around each edge is 2π except around the knot which is 0. We get

the following relations:

$$a_2^\tau = c_1^\tau, \tag{5.87}$$
$$c_2^\tau + c_3^\tau = a_1^\tau + c_1^\tau, \tag{5.88}$$
$$a_4^\tau = c_1^\tau - a_3^\tau, \tag{5.89}$$
$$c_2^\tau + c_4^\tau = a_1^\tau + a_3^\tau. \tag{5.90}$$

The partition function of Y for α is

$$\begin{aligned}\mathcal{Z}_\hbar(Y,\alpha) &\stackrel{\star}{=} \psi_{c_0,b_0}(0)\int_{\mathbb{R}^3}\langle t_1, t_3+t_4\rangle^{-1}\langle t_3,t_4\rangle^{-1}\langle t_3\rangle^{-1}\psi_{c_1,b_1}(t_1)\psi_{c_2,b_2}(t_3+t_4)\psi_{c_3,b_3}(t_3)\psi_{c_4,b_4}(t_4)\,dt_1dt_3dt_4\\ &= \psi_{c_0,b_0}(0)\int_{\mathbb{R}^2}\langle t_3,t_4\rangle^{-1}\langle t_3\rangle^{-1}\widetilde{\psi}_{c_1,b_1}(t_3+t_4)\psi_{c_2,b_2}(t_3+t_4)\psi_{c_3,b_3}(t_3)\psi_{c_4,b_4}(t_4)\,dt_3dt_4\\ &\stackrel{\star}{=} \psi_{c_0,b_0}(0)\int_{\mathbb{R}^2}\langle t_4\rangle\psi_{b_1,a_1}(t_3+t_4)\psi_{c_2,b_2}(t_3+t_4)\psi_{c_3,b_3}(t_3)\psi_{c_4,b_4}(t_4)\,dt_3dt_4.\end{aligned}$$

Let us do the following change of variables:

$$t_3 = x + \tfrac{i}{2\pi\sqrt{\hbar}}(\pi - a_3), \qquad t_4 = z + \tfrac{i}{2\pi\sqrt{\hbar}}(\pi - a_4).$$

Since $a_3, a_4 \in (0,\pi)$, using Cauchy theorem, we can assume that $x, z \in \mathbb{R} - i0$. We get

$$\psi_{b_1,a_1}(t_3+t_4) \stackrel{\star}{=} \frac{e^{\frac{1}{\sqrt{\hbar}}b_1(x+z)}}{\Phi_{\mathsf{b}}\left(x+z+\frac{i}{2\pi\sqrt{\hbar}}(\pi-a_3-a_4+c_1)\right)}, \qquad \psi_{c_3,b_3}(t_3) \stackrel{\star}{=} \frac{e^{\frac{1}{\sqrt{\hbar}}c_3x}}{\Phi_{\mathsf{b}}(x)},$$
$$\psi_{c_2,b_2}(t_3+t_4) \stackrel{\star}{=} \frac{e^{\frac{1}{\sqrt{\hbar}}c_2(x+z)}}{\Phi_{\mathsf{b}}\left(x+z+\frac{i}{2\pi\sqrt{\hbar}}(\pi-a_3-a_4+a_2)\right)}, \qquad \psi_{c_4,b_4}(t_4) \stackrel{\star}{=} \frac{e^{\frac{1}{\sqrt{\hbar}}c_4z}}{\Phi_{\mathsf{b}}(z)}.$$

Using dominated convergence theorem and relations (5.87) and (5.89), we have that

$$\lim_{\alpha\to\tau}\Phi_{\mathsf{b}}\left(\frac{\pi-a_0}{2\pi i\sqrt{\hbar}}\right)\mathcal{Z}_\hbar(Y,\alpha) \stackrel{\star}{=} \int_{(\mathbb{R}-i0)^2} dxdz\,\frac{e^{\frac{1}{\sqrt{\hbar}}((b_1^\tau+c_2^\tau+c_3^\tau)x+(b_1^\tau+c_2^\tau+c_4^\tau)z)}\langle z\rangle e^{-\frac{1}{\sqrt{\hbar}}(\pi-a_4^\tau)z}}{\Phi_{\mathsf{b}}\left(x+z+\frac{i}{2\sqrt{\hbar}}\right)^2\Phi_{\mathsf{b}}(x)\Phi_{\mathsf{b}}(z)}.$$

Using relation (5.88), the exponential term with x and $\frac{1}{\sqrt{\hbar}}$ becomes

$$e^{\frac{1}{\sqrt{\hbar}}(b_1^\tau+c_2^\tau+c_3^\tau)x} = e^{\frac{1}{\sqrt{\hbar}}(b_1^\tau+a_1^\tau+c_1^\tau)x} = e^{\frac{1}{\sqrt{\hbar}}\pi x}.$$

Using relations (5.89) and (5.90), the exponential term with z and $\frac{1}{\sqrt{\hbar}}$ becomes

$$e^{\frac{1}{\sqrt{\hbar}}(b_1^\tau+c_2^\tau+c_4^\tau-\pi+a_4^\tau)z} = e^{\frac{1}{\sqrt{\hbar}}(b_1^\tau+a_1^\tau-\pi+c_1^\tau)z} = 1.$$

Consequently, we have that

$$\begin{aligned}\lim_{\alpha\to\tau}\Phi_{\mathsf{b}}\left(\frac{\pi-a_0}{2\pi i\sqrt{\hbar}}\right)\mathcal{Z}_\hbar(Y,\alpha) &\overset{\star}{=} \int_{(\mathbb{R}-i0)^2} dxdz \frac{\langle z\rangle e^{\frac{1}{\sqrt{\hbar}}\pi x}}{\Phi_{\mathsf{b}}\left(x+z+\frac{i}{2\sqrt{\hbar}}\right)^2\Phi_{\mathsf{b}}(x)\Phi_{\mathsf{b}}(z)}\\ &\overset{\star}{=} \int_{(\mathbb{R}-i0)^2} dxdz \frac{\Phi_{\mathsf{b}}(-z)e^{\frac{1}{\sqrt{\hbar}}\pi x}}{\Phi_{\mathsf{b}}\left(x+z+\frac{i}{2\sqrt{\hbar}}\right)^2\Phi_{\mathsf{b}}(x)}\\ &= J_X(\hbar,0),\end{aligned}$$

and this proves the part (2) of Conjecture 3.68.

Numerical evidence of asymptotic behavior

As in the previous example, we will only study numerically the asymptotic behavior of $2\pi\hbar\log|J_X(\hbar,0)|$ when $\hbar\to 0^+$. The potential function is given by

$$S(x,z) := -i\mathrm{Li}_2(-e^{-z}) + i\mathrm{Li}_2(-e^{x}) + 2i\mathrm{Li}_2(e^{x+z}) + \pi x.$$

Mathematica tells us that the critical point which contribute to the integral is the pair

$$(x_0,z_0)\approx(0.167023-2.44832i,-0.282853-2.53611i),$$

and by substituting in S, we get

$$\Re(S(x_0,z_0))\approx -3.7588449482372849886\approx -\mathrm{Vol}(m148).$$

Consequently, point (3) of Conjecture 3.68 is checked numerically.

❧ Chapter 6 ❧

Characters in quantum Teichmüller theory

In this chapter, we at first define the notion of *extended trace*, originally proposed in [Kas17a]. This will potentially allow to generalize the usual definition of the trace for a larger family of operators in $L^2(\mathbb{R}^n)$. Then we will compute the extended trace of operators coming from the unitary representations of mapping class group of the once-punctured torus in quantum Teichmüller theory. This value will be related to the Teichmüller TQFT for the underlying mapping torus through new technical terms.

6.1 Extended trace

In this section we define the extended trace and we give an example of computation with the figure-eight knot complement.

6.1.1 Definition

Let us start by some results which can be used to propose a generalized definition of the trace in a natural way. Another merit of this definition is that calculations become feasible.

Lemma 6.1. *Let A be an operator on $L^2(\mathbb{R})$ such that its integral kernel is a tempered distribution. Then there exists a unique tempered distribution f_A such that*

$$A = \int_{\mathbb{R}^2} f_A(x,y) e^{2\pi i x \mathsf{q}} e^{2\pi i y \mathsf{p}} \, dxdy. \tag{6.2}$$

Proof. Since

$$\langle u | e^{2\pi i x \mathsf{q}} e^{2\pi i y \mathsf{p}} | v \rangle = e^{2\pi i u x} \langle u | e^{2\pi i y \mathsf{p}} | v \rangle = e^{2\pi i u x} \langle u + y | v \rangle = e^{2\pi i u x} \delta(u + y - v),$$

equality (6.2) means that

$$\langle u | A | v \rangle = \int_{\mathbb{R}} f_A(x, v-u) e^{2\pi i u x} \, dx.$$

By a change of variables, we get

$$\langle u|A|v+u\rangle = \int_{\mathbb{R}} f_A(x,v)e^{2\pi iux}\,dx.$$

Finally, applying inverse Fourier transform, we obtain

$$f_A(x,v) = \int_{\mathbb{R}} \langle u|A|v+u\rangle e^{-2\pi iux}\,du.$$

□

Corollary 6.3. *Assume that $A \in \mathcal{T}_1(L^2(\mathbb{R}))$ with integral kernel $K_A \in L^2(\mathbb{R}^2)$. If K_A is continuous almost everywhere on the diagonal, then we have that*

$$\mathrm{Tr}(A) = f_A(0,0).$$

Proof. Straightforward from Lemma 6.1 and Theorem 1.63. □

Remark 6.4. For simplicity, Lemma 6.1 and Corollary 6.3 are stated only for the one-dimensional case, but they can naturally be generalized for higher dimensions.

Corollary 6.3 motivates the following definition.

Definition 6.5. Let A be an operator on $L^2(\mathbb{R}^n)$ such that its integral kernel is a tempered distribution. If there is a neighborhood V of $(0,0) \in \mathbb{R}^n \times \mathbb{R}^n$ such that $f_A \in C^0(V,\mathbb{C})$, then we say that A is *extended trace class* and we define the *extended trace* of A by $\mathrm{Tr}_E(A) := f_A(0,0)$.

Remark 6.6. Assume that $A \in \mathcal{T}_1(L^2(\mathbb{R}^n))$ and satisfies the same assumptions as Corollary 6.3. If A is also extended trace class, then we have that $\mathrm{Tr}_E(A) = \mathrm{Tr}(A)$.

Example 6.7. Consider the operator $\mathsf{R} = \zeta e^{3\pi i\mathsf{q}^2}e^{\pi i(\mathsf{p}+\mathsf{q})^2}$ defined in Theorem 3.25. Then since R is unitary, all its eigenvalues live on the unit circle, and thus R cannot be trace class. Nevertheless it is extended trace class. Indeed, using formulas (1.49), (1.73) and (1.74) we obtain

$$\begin{aligned}
\langle u|e^{3\pi i\mathsf{q}^2}e^{\pi i(\mathsf{p}+\mathsf{q})^2}|v\rangle &= \langle u|e^{2\pi i\mathsf{q}^2}e^{\pi i\mathsf{p}^2}e^{\pi i\mathsf{q}^2}|v\rangle \\
&= \int_{\mathbb{R}^2} \langle u|e^{2\pi i\mathsf{q}^2}|t\rangle\langle t|e^{\pi i\mathsf{p}^2}|s\rangle\langle s|e^{\pi i\mathsf{q}^2}|v\rangle\,dtds \\
&= \int_{\mathbb{R}^2} e^{2\pi iu^2}\delta_{u-t}e^{-\pi i(t-s)^2+\frac{\pi i}{4}}e^{\pi is^2}\delta_{s-v}\,dtds \\
&= e^{\frac{\pi i}{4}}e^{\pi iu^2}e^{2\pi iuv}.
\end{aligned}$$

Using formula (1.72), we get that

$$f_{\mathsf{R}}(x,v) = \int_{\mathbb{R}} \langle u|\mathsf{R}|v+u\rangle e^{-2\pi iux}\,du = e^{\frac{\pi i}{4}}\zeta\int_{\mathbb{R}} e^{\pi iu^2}e^{2\pi iu(v+u)}e^{-2\pi iux}\,du = \frac{i\zeta}{\sqrt{3}}e^{-\frac{i\pi(x-v)^2}{3}}.$$

Therefore, R is extended trace class, and we get that

$$\mathrm{Tr}_E(\mathsf{R}) = f_{\mathsf{R}}(0,0) = \frac{i\zeta}{\sqrt{3}}.$$

We now give an example of an operator which is not extended trace class.

Example 6.8. The position operator q is not extended trace class. Indeed, we have

$$\begin{aligned} f_{\mathsf{q}}(x,v) &= \int_{\mathbb{R}} \langle u|\mathsf{q}|v+u\rangle e^{-2\pi i u x}\, du \\ &= \int_{\mathbb{R}} u\delta_v e^{-2\pi i u x}\, du \\ &= \delta_v \int_{\mathbb{R}} \left(\frac{i}{2\pi}\frac{\partial}{\partial x}\right) e^{-2\pi i u x}\, du \\ &= \frac{i}{2\pi}\delta_v \delta'_x, \end{aligned}$$

and thus f_{q} is not a continuous function in a neighborhood of $(0,0)$.

6.1.2 Example with the figure-eight knot complement

Recall that if Σ is a punctured surface with negative Euler characteristic, then Remark 3.43 tells that we have unitary projective representations $F_{\mathsf{b}} : \mathrm{MCG}(\Sigma) \to \mathcal{U}(L^2(\mathbb{R}^n))$, where n is the number of ideal triangles in any ideal triangulation of Σ. If $\varphi \in \mathrm{MCG}(\Sigma)$, then $F_{\mathsf{b}}(\varphi)$ can be expressed with R, P and $\mathsf{T} = \mathsf{W}^{-1}$, where their integral kernels are given by

$$\langle x|\mathsf{R}|y\rangle = \zeta e^{\frac{\pi i}{4}} e^{\pi i x^2} e^{2\pi i x y}, \qquad \langle x_1, x_2|\mathsf{P}|y_1, y_2\rangle = \delta_{x_1 - y_2}\delta_{x_2 - y_1}$$

and

$$\langle x_1, x_2|\mathsf{T}|y_1, y_2\rangle \overset{\star}{=} \delta_{x_1 - y_1 + x_2} e^{2\pi i x_1 (y_2 - x_2)} \psi_{0,\pi}(y_2 - x_2) = \int_{\mathbb{R}} Q^{x_1,x_2,z}_{y_1,y_2} \psi_{0,\pi}(z)\, dz,$$

with $Q^{x_1,x_2,z}_{y_1,y_2} := e^{2\pi i x_1 z}\delta_{x_1 - y_1 + x_2}\delta_{x_2 - y_2 + z}$.

We will now focus on the case $\Sigma = \Sigma_{1,1}$ with monodromy $\varphi_{4_1} = RL$ (recall Example 2.25) and let us take $\tau \in \Delta_\Sigma$ as:

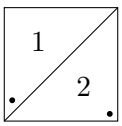

Figure 6.1: The decorated ideal triangulation τ.

The action of R and L on τ are described in Figures 6.2 and 6.3 respectively.

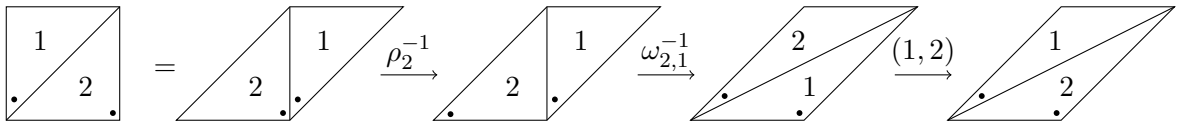

Figure 6.2: The action of R on τ.

We thus have that

$$R = \rho_2^{-1}\omega_{2,1}^{-1}(1,2) \qquad \text{and} \qquad L = \omega_{1,2}^{-1}. \tag{6.9}$$

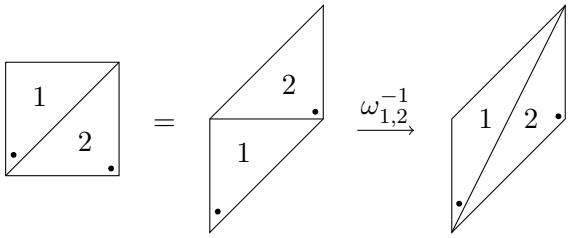

Figure 6.3: The action of L on τ.

Therefore,

$$F_{\mathsf{b}}(\varphi_{4_1}) = F_{\mathsf{b}}(R)F_{\mathsf{b}}(L) = \mathsf{R}_2^{-1}\mathsf{T}_{2,1}\mathsf{P}\mathsf{T}_{1,2} = \mathsf{R}_2^{-1}\mathsf{T}_{2,1}^2\mathsf{P}.$$

We now *assume* that $F_{\mathsf{b}}(\varphi_{4_1})$ is extended trace class. Let us compute the extended trace of $F_{\mathsf{b}}(\varphi_{4_1})$. We define the variable $\mathbf{t} := (a, b, s, t, u, v)^T$. The integral kernel of $F_{\mathsf{b}}(\varphi_{4_1})$ is

$$\begin{aligned}\langle x, y|\mathsf{R}_2^{-1}\mathsf{T}_{2,1}^2\mathsf{P}|w, z\rangle &= \int_{\mathbb{R}^6} \overline{\langle a, b|\mathsf{R}_2|x, y\rangle}\langle a, b|\mathsf{T}_{2,1}|s, t\rangle\langle s, t|\mathsf{T}_{2,1}|u, v\rangle\langle u, v|\mathsf{P}|w, z\rangle\, d\mathbf{t} \\ &\overset{\star}{=} \int_{\mathbb{R}^8} d\mathbf{t}dy_1dy_2\, e^{-\pi i a^2}e^{-2\pi i a x}\delta_{b-y}Q_{s,t}^{a,b,y_1}\psi_{0,\pi}(y_1)Q_{u,v}^{s,t,y_2}\psi_{0,\pi}(y_2)\delta_{u-z}\delta_{v-w}.\end{aligned}$$

Then we define

$$K(y_1, y_2) := \int_{\mathbb{R}^8} e^{-\pi i a^2}e^{-2\pi i a x}Q_{s,t}^{a,b,y_1}Q_{u,v}^{s,t,y_2}\delta_{b-y}\delta_{u-y}\delta_{v-x}\, d\mathbf{t}dxdy,$$

which can be simplified by elementary calculations:

$$\begin{aligned}K(y_1, y_2) &= \int_{\mathbb{R}^8} e^{-\pi i a^2}e^{-2\pi i a x}e^{2\pi i a y_1}e^{2\pi i s y_2}\delta_{a-s+b}\delta_{b-t+y_1}\delta_{s-u+t}\delta_{t-v+y_2}\delta_{b-y}\delta_{u-y}\delta_{v-x}\, d\mathbf{t}dxdy \\ &= e^{-2\pi i y_1 y_2}\int_{\mathbb{R}} e^{\pi i a^2}e^{2\pi i a(y_1-y_2)}\, da \\ &\overset{\star}{=} e^{-2\pi i y_1 y_2}e^{-\pi i(y_1-y_2)^2} \\ &= e^{-\pi i(y_1^2+y_2^2)}.\end{aligned}$$

Finally, we conclude that

$$\mathrm{Tr}_E(F_{\mathsf{b}}(\varphi_{4_1})) \overset{\star}{=} \int_{\mathbb{R}^2} e^{-\pi i(y_1^2+y_2^2)}\psi_{0,\pi}(y_1)\psi_{0,\pi}(y_2)\, dy_1dy_2.$$

On the other hand, if we compute the partition function for the ideal triangulation X of $S^3 \setminus 4_1$ given in Example 2.7 with shape structure $\alpha = (a_1, b_1, c_1, a_2, b_2, c_2) \in \mathcal{S}_X$, we get (see [AK14c] or Chapter 4)

$$\mathcal{Z}_\hbar(X, \alpha) = \int_{\mathbb{R}^2} e^{2\pi i(x^2-y^2)}\psi_{c_1,b_1}(x)\overline{\psi_{c_2,b_2}(y)}\, dxdy.$$

Recall (see Example 2.20) that there is only one linearly independent gauge transformation $h : \mathcal{GS}_X \times \mathbb{R} \to \mathcal{GS}_X$ defined by

$$h(\alpha, \varepsilon) := (a_1 - \varepsilon, b_1 - \varepsilon, c_1 + 2\varepsilon, a_2 - \varepsilon, b_2 - \varepsilon, c_2 + 2\varepsilon). \tag{6.10}$$

If α^0 denotes the complete structure of X (all the angles are $\frac{\pi}{3}$) and if we take $\varepsilon = \frac{\pi}{3}$, then we have

$$h\left(\alpha^0, \frac{\pi}{3}\right) = (0, 0, \pi, 0, 0, \pi) =: \tau,$$

and thus α^0 and τ are gauge equivalent. This is consistent with Theorem 2.59, because τ is the veering structure of X. By Theorem 3.52 and relation (3.47), we get

$$\mathcal{Z}_\hbar(X, \alpha^0) \overset{\star}{=} \int_{\mathbb{R}^2} e^{2\pi i(x^2-y^2)} \psi_{\pi,0}(x)\overline{\psi_{\pi,0}(y)}\, dxdy \overset{\star}{=} \int_{\mathbb{R}^2} e^{\pi i(x^2-y^2)} \overline{\psi_{0,\pi}(x)}\psi_{0,\pi}(y)\, dxdy.$$

Consequently, we have that

$$|\mathrm{Tr}_E(F_{\mathsf{b}}(\varphi_{4_1}))| = |\mathcal{Z}_\hbar(X, \alpha^0)|.$$

The aim of this chapter is to generalize this example to all the family of mapping tori with once-punctured torus fiber and pseudo-Anosov monodromy.

6.2 Quantum monodromy triangulations

We saw in Example 2.26 that the monodromy triangulation of the figure-eight knot sister admits cycles and thus one cannot compute the partition function. To solve this problem, we will give a construction of a new ideal triangulation X_φ without cycles, called *quantum monodromy triangulation*, which contains the information of the monodromy triangulation.

6.2.1 Quasi-geometric ideal triangulations

Before explaining the construction, let us define a notion which generalizes geometric ideal triangulations. Then we will state our main result of this chapter. Moreover, we advise the reader to become familiar with the definitions of Section 3.4.3.

Definition 6.11. Let X be an ideal triangulation. We say that X is

- *nice* if X does not contain bigon suspension;
- *improvable* if one can obtain a nice ideal triangulation, denoted $\check{X}$, applying only 2-0 moves;
- *quasi-geometric* if X is improvable and $\check{X}$ is geometric.

If X is an improvable ideal triangulation and $\alpha \in \mathcal{GA}_X$ is sharpened, then one gets naturally an induced structure $\check{\alpha} \in \mathcal{GA}_{\check{X}}$. This fact yields the next definition.

Definition 6.12. Let X be an improvable ideal triangulation and $\alpha \in \mathcal{GA}_X$. We say that α is

- *quasi-taut* if α is sharpened and $\check{\alpha}$ is a taut structure of $\check{X}$;
- *quasi-complete* if α is sharpened and $\check{\alpha}$ is the complete structure of $\check{X}$.

Remark 6.13. A geometric ideal triangulation is quasi-geometric since a geometric ideal triangulation cannot contain bigon suspensions. Moreover, a quasi-complete structure is, in general, not unique.

Definition 6.14. Let X be a triangulation. The *conic representation* of X, denoted X_C, is the cell-decomposition constructed from X by looking all the friendly pairs as bigon suspensions. A tetrahedron which is not friendly with any other tetrahedron is *lone*.

Notation 6.15. If X is a triangulation, then we denote by $\widetilde{X}^1_C$, the set of 1-cells in X_C "before gluing", in a similar way as for triangulations (see Notations 2.2).

Let us give two examples to illustrate the previous definitions.

Example 6.16. In Figure 6.4 (a), we give an ideal triangulation X of $S^3 \setminus 3_1$ and we give its conic representation X_C in Figure 6.4 (b) (see Section 2.1.7.2). The ideal triangulation X is not nice and also not improvable since one cannot apply a 2-0 move in this case. In this example, $\widetilde{X}^1_C$ admits 6 elements.

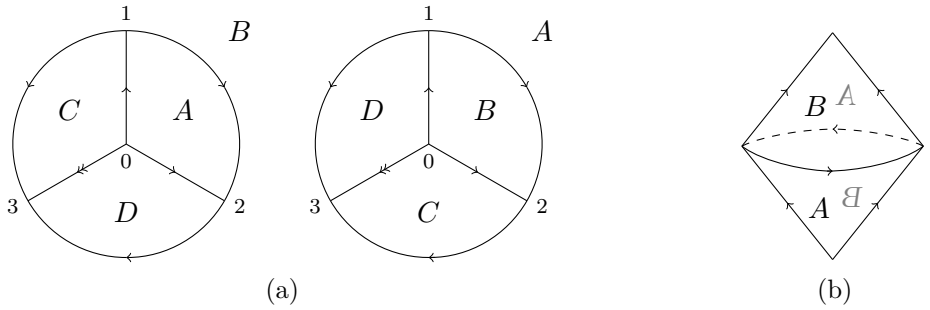

Figure 6.4: An ideal triangulation of $S^3 \setminus 3_1$ (left) and its conic representation (right).

Example 6.17. The ideal triangulation X of $S^3 \setminus 4_1$ given, in conic representation, in Figure 6.5 is quasi-geometric. We see that if we apply a 2-0 move on the bigon suspension S, then the lone tetrahedra T_1 and T_2 will become the two tetrahedra of the geometric ideal triangulation of Figure 2.5.

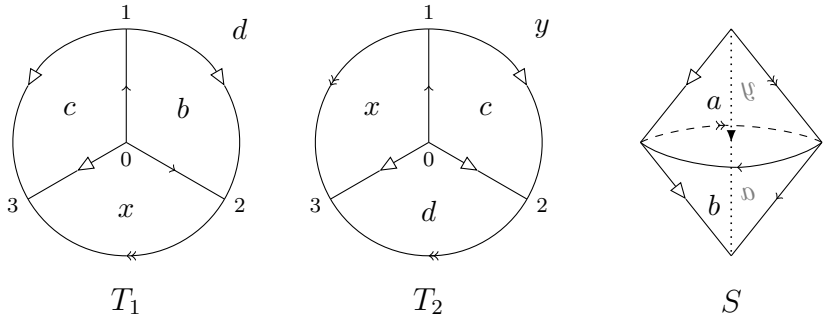

Figure 6.5: The conic representation of a quasi-geometric ideal triangulation of $S^3 \setminus 4_1$.

The elements

$$\tau = (0, \pi, 0 \,|\, 0, \pi, 0 \,|\, 0, 0, \pi \,|\, 0, 0, \pi) \qquad \text{and} \qquad \alpha = (\tfrac{\pi}{3}, \tfrac{\pi}{3}, \tfrac{\pi}{3} \,|\, \tfrac{\pi}{3}, \tfrac{\pi}{3}, \tfrac{\pi}{3} \,|\, 0, 0, \pi \,|\, 0, 0, \pi)$$

are respectively a quasi-taut and a quasi-complete structure of X. We notice that in this case, τ is a taut structure.

We now state the main result of this chapter.

Theorem 6.18. *Let $\varphi \in \mathrm{MCG}(\Sigma_{1,1})$ pseudo-Anosov and M_φ the mapping torus of φ. Then there exist an ordered well-oriented quasi-geometric ideal triangulation X_φ of M_φ and a quasi-complete structure $\alpha \in \mathcal{GA}_{X_\varphi}$, such that if $F_{\mathsf{b}}(\varphi)$ is extended trace class, then*

$$|\mathrm{Tr}_E(F_{\mathsf{b}}(\varphi))| = |\mathcal{Z}_\hbar(X_\varphi, \alpha)|,$$

and $\check{X}_\varphi$ is the monodromy triangulation of M_φ.

Definition 6.19. The ideal triangulation X_φ of Theorem 6.18 is called *quantum monodromy triangulation.*

6.2.2 The construction

The idea of the construction of the quantum monodromy triangulation is very similar to the one of monodromy triangulation. The main difference is that we will not add only tetrahedra, but also *pairs of cones* that will become bigon suspensions. We will treat separately the case where the trace of the monodromy φ is positive and negative.

6.2.2.1 Case 1: $\mathrm{Tr}(\varphi) > 2$

Let $\varphi \in \mathrm{MCG}(\Sigma_{1,1})$ be a pseudo-Anosov monodromy with positive trace, thus φ is expressed as a product of R and L with positive sign (where R and L are defined in (1.17)). As we did in Section 6.1.2, we start by the decorated ideal triangulation $\tau \in \Delta_{\Sigma_{1,1}}$ of Figure 6.1. We put an orientation on the edges of τ with the rule that we turn in the counter-clockwise direction around the marked corner of each ideal triangle and the orientation of the last edge is chosen so that we do not create cycle (Figure 6.6). We see that there is no ambiguity on the diagonal edge with τ.

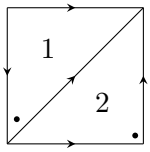

Figure 6.6: Orientating the edges of τ.

Replace all the R and L in φ by the formulas (6.9) and, for simplicity, we bring all the permutations at the end (right). For the R move, since all the rotations ρ_i^{-1} come from this move, we at first translate the left triangle to the right side (Figure 6.2), then we apply ρ_i^{-1}. This allows to keep the orientation on the edges for the new triangulation without ambiguity. Then we apply $\omega_{i,j}^{-1}$ coming from R and this still maintains a consistent orientation on the edges of the resulting triangulation. For the L move, we translate the right triangle above (Figure 6.3), then we can apply $\omega_{i,j}^{-1}$, and the ensuring triangulation admits a consistent orientation on the edges.

We now associate cells to each elementary movement as for the monodromy triangulation, but this time we also add cones and the orientation on the edges are known in advance. For ρ_i^{-1}, we add one cone of type B_-, then we overlay with one cone of type A_+ (Figure 6.7). For $\omega_{i,j}^{-1}$, we simply add one positive tetrahedron (Figure 6.8). For the permutation $(1, 2)$, we do not need to associate a cell, since it only gives the gluing information for the last tetrahedron.

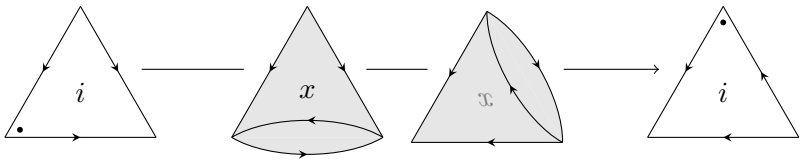

Figure 6.7: The two cones associated to ρ_i^{-1}.

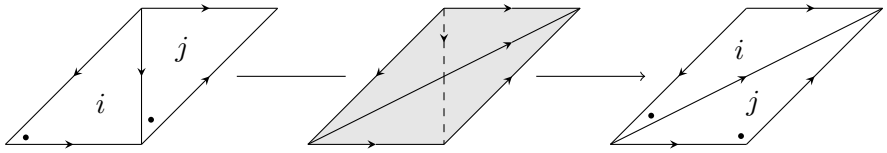

Figure 6.8: The tetrahedron associated to $\omega_{i,j}^{-1}$.

Finally, we glue up all these cells as in the case of the monodromy triangulation. However, in this case, we need to find the identifications on the bigons to create bigon suspensions. To achieve this, we start by finding the equivalence class of each edge of all the bigons. Let us denote all the rotations in order by $\rho_+^{(0)}, \dots, \rho_+^{(n-1)}$ (with coefficients in $\mathbb{Z}/n\mathbb{Z}$) and the cones associated to $\rho_+^{(k)}$ by $\rho_+^{(k)}(A_+)$ and $\rho_+^{(k)}(B_-)$ for all $k \in \mathbb{Z}/n\mathbb{Z}$. Moreover, let us write $C_1 \sim C_2$ if the bigon of C_1 is identified to the bigon of C_2. Then we conclude that the only choice is given by $\rho_+^{(k)}(A_+) \sim \rho_+^{(k+1)}(B_-)$ for all $k \in \mathbb{Z}/n\mathbb{Z}$.

We illustrate this construction in Example 6.20.

Example 6.20. Let us see the construction of the quantum monodromy triangulation of the figure-eight knot complement which has monodromy $\varphi_{4_1} = RL$. The sequence of elementary movements is described in Figure 6.9.

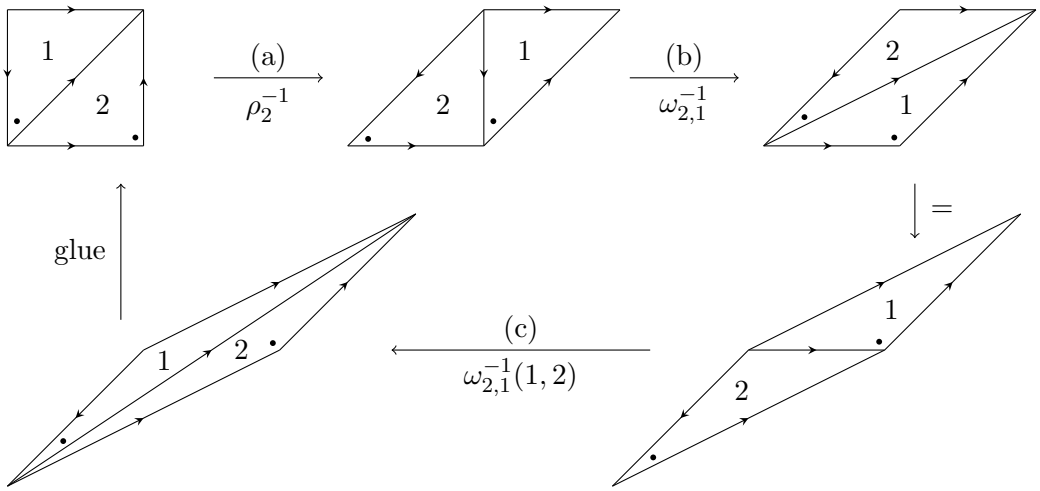

Figure 6.9: Decomposition of φ_{4_1} into elementary movements.

After finding the cells (Figure 6.10), we find the equivalence classes of the edges on the bigons and we finally glue all the cells. We realize that it is exactly the ideal triangulation of Figure 6.5.

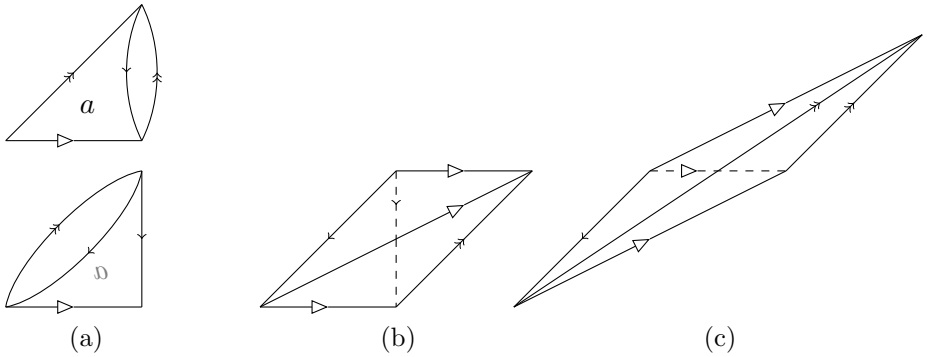

Figure 6.10: Cells that we glue in step (a),(b) and (c) in Figure 6.9.

6.2.2.2 Case 2: $\mathrm{Tr}(\varphi) < -2$

Let $\varphi \in \mathrm{MCG}(\Sigma_{1,1})$ be a pseudo-Anosov monodromy, but this time φ is expressed as a product of R and L with a minus sign. In other words, $\varphi = -\psi$ with $\psi \in \mathrm{MCG}(\Sigma_{1,1})$ pseudo-Anosov and $\mathrm{Tr}(\psi) > 2$. Therefore, the only difference compare to the previous case is that we need to apply $-\mathrm{id}$ at the end. The action of $-\mathrm{id}$ on τ can be expressed by $\rho_1^{-1}\rho_2(1,2)$.

As before, we write ψ with elementary movements and we compose after by $\rho_1^{-1}\rho_2(1,2)$. Then we also bring all the permutations at the end. We find the cells that we associate to each elementary movement, but this time we also associate cones to ρ_i (coming from the $-\mathrm{id}$) that are one cone of type A_- and we overlay with one cone of type B_+ (Figure 6.11).

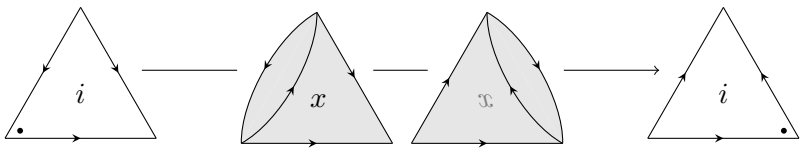

Figure 6.11: The two cones associated to ρ_i.

Although the situation looks very similar to the previous case, the choice of gluing on bigons is no more unique as before. We keep the same notations as the previous case for ψ and we denote the two last rotations (coming from the $-\mathrm{id}$) in order by $\rho_-^{(0)}, \rho_-^{(1)}$ and their respective cones by $\rho_-^{(0)}(A_+), \rho_-^{(0)}(B_-), \rho_-^{(1)}(A_-)$ and $\rho_-^{(1)}(B_+)$. Then, the two possibilities are:

(A) $\rho_-^{(0)}(A_+) \sim \rho_-^{(1)}(A_-)$, $\rho_-^{(0)}(B_-) \sim \rho_-^{(1)}(B_+)$, $\rho_+^{(k)}(A_+) \sim \rho_+^{(k+1)}(B_-)$. $(k \in \mathbb{Z}/n\mathbb{Z})$

(B) $\rho_-^{(0)}(A_+) \sim \rho_-^{(1)}(A_-)$, $\rho_+^{(1)}(B_-) \sim \rho_-^{(1)}(B_+)$, $\rho_+^{(0)}(A_+) \sim \rho_-^{(0)}(B_-)$, $\rho_+^{(0)}(B_-) \sim \rho_+^{(n-1)}(A_+)$, $(n \geqslant 2)$ $\rho_+^{(k)}(A_+) \sim \rho_+^{(k+1)}(B_-)$ $(k = 1, \dots, n-2$ with $n \geqslant 3)$.

Since the choice (A) is more natural (as we keep the gluings for the ψ part), we define the quantum monodromy triangulation as the case (A). We will describe this phenomenon in Example 6.21.

Example 6.21. We illustrate the construction with the example of the figure-eight knot sister which has monodromy $\varphi_{\text{sister}} = -\varphi_{4_1}$. The situation is described in Figure 6.12, and the cells are given in Figure 6.13 with the face identifications (but not for edges).

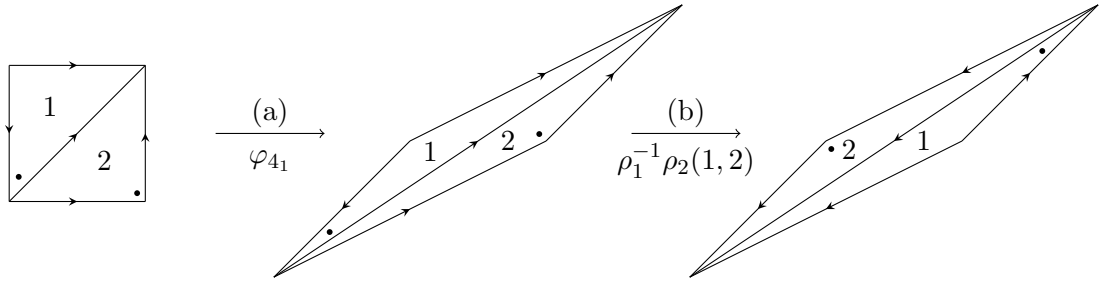

Figure 6.12: Decomposition of φ_{sister} into φ_{4_1} and elementary movements.

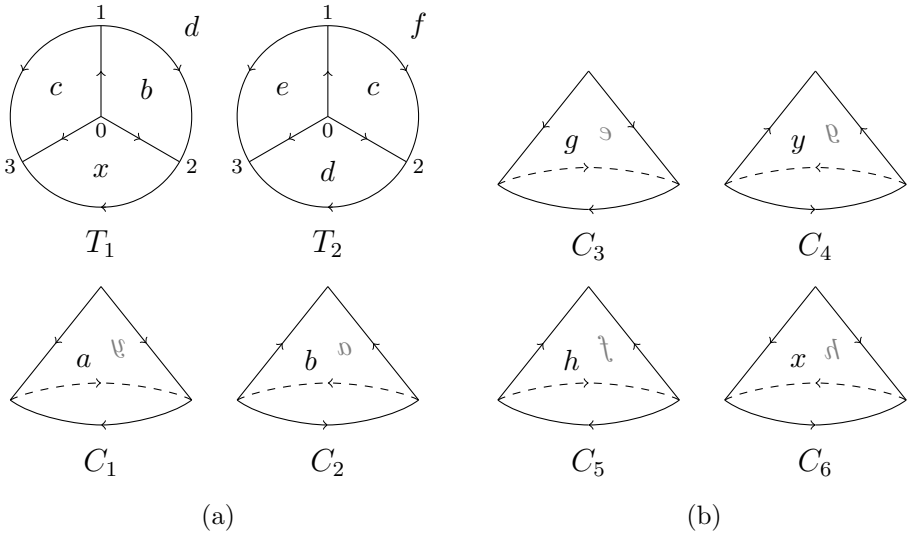

Figure 6.13: Cells that we glue in step (a) and (b) in Figure 6.12.

With the choice (A), one gets the identifications $C_1 \sim C_2, C_3 \sim C_6, C_4 \sim C_5$, and for (B) we have $C_1 \sim C_6, C_2 \sim C_3, C_4 \sim C_5$. The ideal triangulations (in conic representation) corresponding to the choice (A) and (B) are respectively described in Figure 6.14 and 6.15. If we decompose each bigon suspension S_i into two tetrahedra T_{2i+1} (the front one) and T_{2i+2} (the back one) for $i = 1, 2, 3$, and if we denote the angles on the tetrahedra T_k by $T_k(a_k, b_k, c_k)$ for $k = 1, \ldots, 8$, then a quasi-taut and a quasi-complete structure for the choice (A) are respectively given by

$$\begin{array}{llll} T_1(0,\pi,0), & T_2(0,\pi,0), & T_3(0,\pi,0), & T_4(-\pi,0,2\pi), \\ T_5(\pi,0,0), & T_6(\pi,0,0), & T_7(\pi,0,0), & T_8(\pi,0,0) \end{array}$$

and

$$\begin{array}{llll} T_1(\frac{\pi}{3},\frac{\pi}{3},\frac{\pi}{3}), & T_2(\frac{\pi}{3},\frac{\pi}{3},\frac{\pi}{3}), & T_3(0,\frac{\pi}{3},\frac{2\pi}{3}), & T_4(-\frac{\pi}{3},0,\frac{4\pi}{3}), \\ T_5(\frac{\pi}{3},0,\frac{2\pi}{3}), & T_6(\frac{5\pi}{3},-\frac{2\pi}{3},0), & T_7(\pi,0,0), & T_8(\pi,0,0). \end{array}$$

Similarly, for the choice (B), such examples are given by

$$T_1(0,\pi,0),\quad T_2(0,\pi,0),\quad T_3(\pi,0,0),\quad T_4(\pi,0,0),$$
$$T_5(0,\pi,0),\quad T_6(-\pi,0,2\pi),\quad T_7(\pi,0,0),\quad T_8(\pi,0,0)$$

and

$$T_1(\tfrac{\pi}{3},\tfrac{\pi}{3},\tfrac{\pi}{3}),\quad T_2(\tfrac{\pi}{3},\tfrac{\pi}{3},\tfrac{\pi}{3}),\quad T_3(\pi,0,0),\quad T_4(\pi,0,0),$$
$$T_5(0,\pi,0),\quad T_6(-\pi,0,2\pi),\quad T_7(\pi,0,0),\quad T_8(\pi,0,0).$$

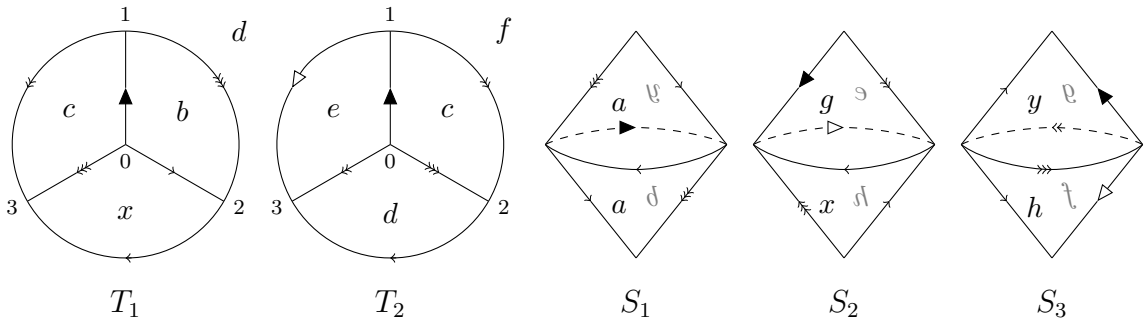

Figure 6.14: Conic representation of the ideal triangulation of figure-eight knot sister with choice (A).

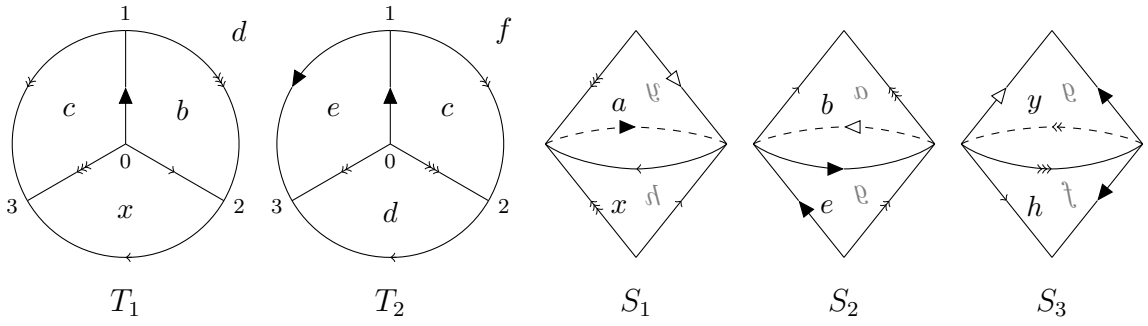

Figure 6.15: Conic representation of the ideal triangulation of figure-eight knot sister with choice (B).

In the both ideal triangulations, if we collapse the bigon suspensions S_1, S_2, S_3, then T_1 and T_2 will become the two tetrahedra of the geometric ideal triangulation of Figure 2.12.

6.2.3 Proof of Theorem 6.18

We start by a result which gives a decomposition of the integral kernel of R in terms of the distributions associated to the cones (formulas (3.62) and (3.63)).

Lemma 6.22. *The following identities are satisfied:*

$$\langle x|\mathsf{R}|y\rangle \overset{\star}{=} \int_{\mathbb{R}} \langle x, s|B_+\rangle\langle A_-|s, y\rangle\, ds, \qquad \langle y|\mathsf{R}^{-1}|x\rangle \overset{\star}{=} \int_{\mathbb{R}} \langle y, s|A_+\rangle\langle B_-|s, x\rangle\, ds.$$

Proof. We get by direct calculation

$$\int_{\mathbb{R}} \langle x, s|B_+\rangle\langle A_-|s, y\rangle\, ds = \int_{\mathbb{R}} e^{\pi i(x-s)^2}\delta_{s+y}e^{-\pi i y^2}\, ds = e^{\pi i x^2}e^{2\pi i xy} \overset{\star}{=} \langle x|\mathsf{R}|y\rangle.$$

The second formula can be proven in a similar way using the fact that $\langle y|\mathsf{R}^{-1}|x\rangle = \overline{\langle x|\mathsf{R}|y\rangle}$. □

Definition 6.23. Let X be a triangulation and S a bigon suspension of X. An element $e \in \widetilde{X}^1_C$ is an *equatorial edge of* S if e lies on the bigon part of S, and $p(e) \in X^1$ is the *class of* e. The remaining 1-cells of S are called *side edges of* S. Moreover, if s is a side edge of S and if (T_1, T_2) is the friendly pair that forms S, then the two 1-simplices of T_1 and T_2 (elements in $\widetilde{X}^1$) which are glued together to form s are called *subside edges of* s. See Figure 6.16.

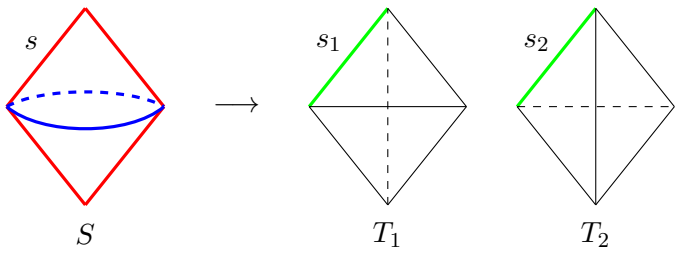

Figure 6.16: The two equatorial edges in blue, the four side edges in red, and s_1, s_2 (in green) are the two subside edges of s.

Lemma 6.24. *The quantum monodromy triangulation is an ordered well-oriented quasi-geometric ideal triangulation and comes with a canonical quasi-taut structure.*

Proof. Let us denote the quantum monodromy triangulation by X_φ, with monodromy φ. By construction, X_φ is ordered and well-oriented. Moreover, since $\check{X}_\varphi$ is exactly the monodromy triangulation, which is geometric (Remark 2.35 (b)), X_φ is quasi-geometric. We also know that $\check{X}_\varphi$ comes with a canonical taut structure $\beta \in \mathcal{TA}_{\check{X}_\varphi}$, which is also a veering structure by Theorem 2.57.

If $\mathrm{Tr}(\varphi) > 2$, then any two different bigon suspensions have all distinct equatorial edges classes by construction. Moreover, each of these equatorial edges classes appears exactly once in a lone tetrahedron with the value π. This implies that β can naturally be extended to a taut structure $\widehat{\beta} \in \mathcal{TA}_{X_\varphi}$, which is exactly β on the lone tetrahedra, and we assign the angle π to the equatorial edges and 0 to the side edges of each bigon suspension, which in turn is decomposed into two taut tetrahedra (see Figure 6.17).

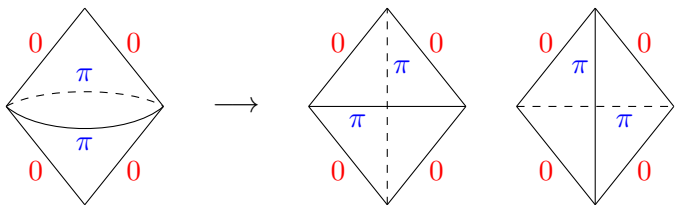

Figure 6.17: Decomposition of a bigon suspension into two taut tetrahedra.

For the case $\mathrm{Tr}(\varphi) < -2$, let us keep the same notations as in the construction of Section 6.2.2.2. Define S_+ and S_- to be the bigon suspensions corresponding respectively to the identifications $\rho_+^{(0)}(B_-) \sim \rho_+^{(n-1)}(A_+)$ and $\rho_-^{(0)}(B_-) \sim \rho_-^{(1)}(B_+)$. Then there are equatorial edges e_+^1 of S_+ and e_-^1 of S_- which have the same class e, and (S_+, S_-) is the only distinct pair of bigon suspensions that have a common equatorial edge class. Then the class of the other equatorial edge of S_+ (say e_+^2) does not appear in any of the lone tetrahedra with angle π. All the other equatorial edges classes appear exactly once in an edge of a lone tetrahedron with angle π. We can now define a generalized angle structure $\widehat{\beta} \in \mathcal{GA}_{X_\varphi}$ as follows. For the part with lone tetrahedra we attribute β as in the previous case. On the bigon suspensions, we assign the value 2π to e_+^2, 0 to e_+^1, π to all the remaining equatorial edges and 0 to all the side edges. Finally, decomposing S_+ as in Figure 6.18 and the other bigon suspensions as in Figure 6.17, this shows that $\widehat{\beta}$ is a quasi-taut structure.

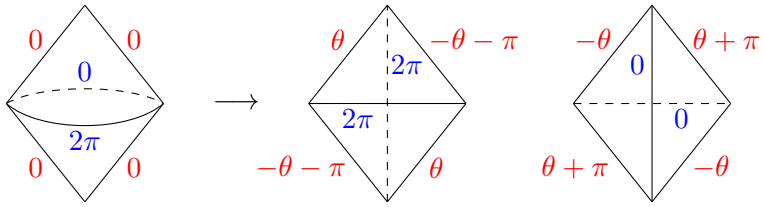

Figure 6.18: Decomposition of S_+ for any fixed angle $\theta \in \mathbb{R}$.

□

Lemma 6.25. *The quantum monodromy triangulation admits a quasi-complete structure which is gauge equivalent to the canonical quasi-taut structure.*

Proof. Let us say that

$$X_\varphi^1 = \{e_1, \dots, e_n\} \qquad \text{and} \qquad \check{X}_\varphi^1 = \{g_1, \dots, g_m\}.$$

Then there is a natural surjective map $\pi : X_\varphi^1 \to \check{X}_\varphi^1$. Let $\alpha^0 \in \mathcal{A}_{\check{X}_\varphi}$ be the complete structure and $\beta \in \mathcal{TA}_{\check{X}_\varphi}$ the canonical veering structure. We recall that β is transformed to α^0 by gauge transformations (Theorem 2.59) with fixed parameters $\varepsilon_1^0, \dots, \varepsilon_m^0$, which correspond respectively to the edges $g_1, \dots, g_m$. We also denote by η_j the parameter of the gauge transformation associated to the edge e_j for all $j = 1, \dots, n$. Let us write the canonical quasi-taut structure on X_φ (Lemma 6.24) by $\widehat{\beta} := (\beta, \gamma)$, where γ is the vector of angles coming from the bigon suspensions part. For $k \in \{1, \dots, m\}$, if $\pi^{-1}(g_k) = \{e_{i_1}, \dots, e_{i_l}\}$, then we fix $\eta_{i_s} = \varepsilon_k^0$ for all $s = 1, \dots, l$. With this choice of parameters, $\widehat{\beta}$ is transformed to $\widehat{\alpha^0} := (\alpha^0, \gamma') \in \mathcal{GA}_{X_\varphi}$ for some γ'.

It remains to prove that $\widehat{\alpha^0}$ is a quasi-complete structure. For that, take a bigon suspension S and e a side edge of S. If e_1 and e_2 are the subside edges of e, then we know that if the angle on e_1 is changed by $+\lambda$ with a gauge transformation for some $\lambda \in \mathbb{R}$, then the angle on e_2 will be changed by $-\lambda$ with the same transformation (see Remark 3.66). This concludes that $\widehat{\alpha^0}$ is sharpened and thus $\widehat{\alpha^0}$ is a quasi-complete structure. □

Using all these lemmas, one can finally prove Theorem 6.18.

Proof of Theorem 6.18. Let $\varphi \in \mathrm{MCG}(\Sigma_{1,1})$ be a pseudo-Anosov monodromy. Let X_φ be the quantum monodromy triangulation and $\widehat{\beta} \in \mathcal{GA}_{X_\varphi}$ the canonical quasi-taut structure which comes from Lemma 6.24. We start by writing φ, as we did in Section 6.2.2, with the three movements $(1,2), \rho_i^{\pm 1}$ and $\omega_{j,k}^{-1}$, then $F_{\mathsf{b}}(\varphi)$ with the respective operators $\mathsf{P}, \mathsf{R}_i^{\pm 1}$ and $\mathsf{T}_{j,k}$. For the rest of the proof, all the equalities will be up to a phase factor. Consider the integral kernel $\langle x, y | F_{\mathsf{b}}(\varphi) | w, z \rangle$ and write it with the kernels of $\mathsf{R}^{\pm 1}$ and $\mathsf{T} = \mathsf{T}(0,0)$ using the decomposition (1.57). Then replace all the kernels of $\mathsf{R}^{\pm 1}$ with the distributions associated to the cones using Lemma 6.22. Finally, according to the construction of Section 6.2.2, match up the corresponding distributions of the cones, which in turn will become one integral kernel of $\mathsf{T}(a_i, c_i)$ and one of $\mathsf{T}(a_{i+1}, c_{i+1})$, where $a_i, c_i, a_{i+1}, c_{i+1}$ are the angles of $\widehat{\beta}$ on the corresponding friendly pair of X_φ.

Replace now the variables w, z by x, y respectively and integrate in the variables x, y. This quantity is exactly $\mathcal{Z}_\hbar(X_\varphi, \widehat{\beta})$, which also coincide with $\mathrm{Tr}_E(F_{\mathsf{b}}(\varphi))$. Let $\widehat{\alpha^0} \in \mathcal{GA}_{X_\varphi}$ be the quasi-complete structure given by Lemma 6.25. By Theorem 3.52, we conclude that $\mathcal{Z}_\hbar(X_\varphi, \widehat{\beta}) \overset{\star}{=} \mathcal{Z}_\hbar(X_\varphi, \widehat{\alpha^0})$. □

Theorem 6.18 tells that the quantity $\mathrm{Tr}_E(F_{\mathsf{b}}(\varphi))$ is strongly related to the complete hyperbolic structure. This gives a reason to expect the following conjecture, inspired by Conjecture 3.68 (3), which was already predicted by Kashaev.

Conjecture 6.26. *Let $\varphi \in \mathrm{MCG}(\Sigma_{1,1})$ pseudo-Anosov. Then we have*

$$\lim_{\mathsf{b} \to 0^+} 2\pi \mathsf{b}^2 \log |\mathrm{Tr}_E(F_{\mathsf{b}}(\varphi))| = -\mathrm{Vol}(M_\varphi).$$

❧ Chapter 7 ❧

Open questions and future perspectives

The problems treated in this dissertation have given rise to new questions for further study. This last chapter lists these questions with some insights.

On the Matveev complexity

We can ask the same question as Question 4.7, mentioned for twist knots, but this time for the knots $\mathcal{K}_n \subset L(n,1)$ in the Section 5.2.

Question. Let $n \geqslant 1$ be an integer. Do we have

$$\mathfrak{c}\left(L(n,1), \mathcal{K}_n\right) = \mathfrak{c}\left(WL(n,1)\right) + 1 \ \ ?$$

More generally, it can be interesting, but probably far from easy, to understand for which kind of knots we have the above equality.

Dehn surgery and T-surgery

A natural question is to understand if one can realize any Dehn surgery by a T-surgery. If the answer to this question is positive, then it means that for any knot K in any oriented closed 3-manifold M, we can always find an ideal triangulation of $M \setminus K$ and an one-vertex H-triangulation of the pair (M, K) which admits one more tetrahedron. However, this seems to be too much expected, even if no counterexample has been found at the time of writing this thesis. We should perhaps start by finding solutions to the following questions:

Question. Find a split ideal triangulation of the figure-eight knot sister. More generally, is it possible to find a split ideal triangulation for any cusped hyperbolic 3-manifold ?

Question. Find two one-vertex H-triangulations of pairs $(M, K), (M', K')$ with $M \neq M'$, K and K' represented by an edge in a single tetrahedron, such that $M \setminus K$ is homeomorphic to $M' \setminus K'$.

On exotic H-triangulations

The method that we used to find H-triangulations and ideal triangulations (explained in Section 2.1.7) works so far only for knots in S^3. It can be interesting to understand how to generalize this method to knots in lens spaces for example. For that, we can start by solving the following more concrete question.

Question. How to find the H-triangulations of Chapter 5 only from knot diagrams ?

Generalization of Chapter 6

All the theory in the Chapter 6 is for once-punctured torus bundles over the circle. Then the following question arises naturally.

Question. How to generalize Theorem 6.18 for higher genus punctured surfaces ?

One possibility is to use Agol's triangulations, which generalize monodromy triangulations (see Remark 2.23 (b)). However, Agol's triangulations are not geometric in general, so we need to find an analogous notion of quasi-geometric ideal triangulations. Nevertheless, since they are veering (Remark 2.58 (a)), one can maybe use the triviality of the angular holonomy [FG13, Lemma 6.5].

Comparison with the new formulation

As already mentioned in Remark 3.54 (b), the initial formulation [AK14c] (used in this thesis) and the new formulation [AK13] coincide for H-triangulations on homology spheres and do not coincide in general on rational homology spheres.

Question. What is the relation between these two formulations for the examples of H-triangulations of Chapter 5 ?

State integrals for $\mathsf{b} = 1$

Using the quasi-periodicity of Faddeev's quantum dilogarithm and results of complex analysis, Garoufalidis and Kashaev [GK14] found a very simplified formula for Φ_1, that is

$$\Phi_1(x) = \exp\left(\frac{i}{2\pi}\left(\mathrm{Li}_2(e^{2\pi x}) + 2\pi x \log(1 - e^{2\pi x})\right)\right).$$

As a consequence, they confirmed the following state integral formula, which was already predicted by Garoufalidis and Zagier [GZ13] through a numerical computation:

$$\int_{\mathbb{R}+i\varepsilon} \Phi_1(x)^2 e^{-i\pi x^2}\, dx = \frac{e^{\frac{i\pi}{6}}}{\sqrt{3}}\left(e^{\frac{V}{2\pi}} - e^{-\frac{V}{2\pi}}\right), \tag{7.1}$$

where $V = 2\Im(\mathrm{Li}_2(e^{\frac{i\pi}{3}})) = 2.02988...$ is the hyperbolic volume of $S^3\backslash 4_1$. We at first remark that the LHS of (7.1) is exactly the value of the partition function for the H-triangulation of $(S^3, 4_1)$. Moreover, the RHS of (7.1) is a mysterious value which is a mixture of the volume of the geometric representation of 4_1, its Galois conjugate, some phase factor and $\sqrt{3}$ which is actually a torsion.

Question. What are the explicit values of the partition functions for the examples of H-triangulations in this thesis for $\mathsf{b} = 1$?

Neumann–Zagier datum from kinematical kernel

Let X be an ideal triangulation of a cusped hyperbolic 3-manifold M. Garoufalidis conjectured [Gar15] that one can obtain the Neumann–Zagier datum of X (see for example [DG13]) only from the kinematical kernel of X.

Question. Does this conjecture hold for the infinite families of Chapters 4 and 5 ?

Moreover, using these Neumann–Zagier data, Dimofte and Garoufalidis [DG13] constructed a formal power series with coefficients in the trace field of M which should agree with the asymptotic expansion of the Kashaev invariant to all orders. The n-th subleading term of this formal power series is called the *n-loop invariant* (for $n \geqslant 1$ integer). They proved the topological invariance of the 1-loop invariant and conjectured that it coincide (up to a sign) with the non-abelian Reidemeister torsion of M with respect to the meridian defined in [Dub06, Por97]. This fact is verified numerically up to 1000 digits for all 59924 hyperbolic knots with at most 14 crossings.

AJ-conjecture for twist knots

The AJ-conjecture was originally proposed by Garoufalidis in [Gar04], which gives, roughly speaking, a relation between the colored Jones polynomial and the A-polynomial of a knot [CCG$^+$94]. Andersen and Malusà formulated in [AM17] a similar conjecture for the Teichmüller TQFT using the function $J_X : \mathbb{R}_{>0} \times \mathbb{C} \to \mathbb{C}$ in the Conjecture 3.68, and proved it for 4_1 and 5_2. Since we have the function J_X for all the twist knots (Theorems 4.13 and 4.45), we can try to solve the next question:

Question. How to generalize their proofs for 4_1 and 5_2 to all the family of twist knots ?

This is already a work in progress which is a joint work with F. Ben Aribi and A. Malusà.

Back to the original volume conjecture

Originally, Kashaev defined an invariant of triangulated links, denoted $\langle L \rangle_{M,N}$, for any link L in an oriented closed 3-manifold M [Kas94, Kas95a]. Then he gave an R-matrix formulation of his invariant in the case $M = S^3$ (and usually denoted $\langle \cdot \rangle_N$) [Kas95b]. He conjectured in [Kas97] that the following equality holds for any hyperbolic knot $K \subset S^3$:

$$\lim_{N \to \infty} \frac{2\pi}{N} \log |\langle K \rangle_N| = \mathrm{Vol}(S^3 \setminus K). \tag{7.2}$$

Let M be an oriented closed 3-manifold. Since $\langle \cdot \rangle_{M,N}$ is a natural extension of $\langle \cdot \rangle_N$, we can even expect that for any hyperbolic knot $K \subset M$, we have:

$$\lim_{N \to \infty} \frac{2\pi}{N} \log |\langle K \rangle_{M,N}| = \mathrm{Vol}(M \setminus K). \tag{7.3}$$

So far, equality (7.2) is proven only for some knots and links (see for example [MY18]), but equality (7.3) has never been checked for any knots in $M \neq S^3$. The reason is that all the proofs used the R-matrix formulation, which makes the computations much easier, but is only available for knots in the 3-sphere. Moreover, Kashaev mentioned in [Kas18] that, using the original formulation [Kas94, Kas95a] in the case of 3-manifolds different from the 3-sphere, the volume conjecture (equality (7.3)) has not been tested yet because of technical difficulties that are:

(a) Finding an H-triangulation of the pair (M, K) which satisfies the necessary assumptions to compute $\langle K \rangle_{M,N}$ (see [Kas94, Kas95a] for details).

(b) Simplifying the calculations.

Using the H-triangulation of Figure 5.22, Kashaev and the author of this thesis found recently an H-triangulation of the pair $(\mathbb{R}P^3, K_2)$ (given in the Section 5.2.2) with 14 tetrahedra which satisfies the necessary assumptions enabling to compute $\langle K_2 \rangle_{\mathbb{R}P^3,N}$. Improvements of computations are still in progress, but the calculations done in Section 5.2.2 give us an intuition that the final form should contain only three quantum dilogarithms.

Finally, note that J. Murakami found knot invariants in 3-manifolds which give back the Kashaev invariant $\langle \cdot \rangle_N$ in the case of the 3-sphere, and he observed numerically some relations with the hyperbolic volume for some knots in lens spaces [Mur17]. Moreover, the volume conjecture (Part (3) of Conjecture 3.68) has been proven for a family of hyperbolic knots in infinitely many different lens spaces for the Teichmüller TQFT (Theorem 5.58), which is an infinite dimensional analogue of the Kashaev invariant. Hence there is great hope that the original volume conjecture is also true for knots in lens spaces.

Bibliography

[Abi80] W. Abikoff. *The Real Analytic Theory of Teichmüller Space*. Lecture Notes in Mathematics. Springer-Verlag, Berlin, 1980.

[AFW15] M. Aschenbrenner, S. Friedl, and H. Wilton. *3-manifold groups*, volume 20. European Mathematical Society Zürich, 2015.

[Ago11] I. Agol. Ideal triangulations of pseudo-Anosov mapping tori. *Contemporary Mathematics, Geometry and Topology in Dimension three*, 560:1–17, 2011.

[Ago13] I. Agol. The Virtual Haken Conjecture. Appendix by I. Agol, D. Groves, and J. Manning. *Documenta Mathematica*, 18:1045–1087, 2013.

[AH06] J.E Andersen and S.K. Hansen. Asymptotics of the quantum invariants for surgeries on the figure 8 knot. *Journal of Knot Theory and its Ramifications*, 15(04):479–548, 2006.

[AK13] J.E. Andersen and R. Kashaev. A new formulation of the Teichmüller TQFT. *arXiv preprint arXiv:1305.4291*, 2013.

[AK14a] J.E. Andersen and R. Kashaev. Complex Quantum Chern–Simons. *arXiv preprint arXiv:1409.1208*, 2014.

[AK14b] J.E. Andersen and R. Kashaev. Quantum Teichmüller theory and TQFT. In *XVIIth International Congress on Mathematical Physics*, pages 684–692, 2014.

[AK14c] J.E. Andersen and R. Kashaev. A TQFT from Quantum Teichmüller Theory. *Communications in Mathematical Physics*, 330(3):887–934, 2014.

[AK15] J.E. Andersen and R. Kashaev. Faddeev's quantum dilogarithm and state-integrals on shaped triangulations. In D. Calaque and T. Strobl, editors, *Mathematical Aspects of Quantum Field Theories*, pages 133–152. Springer International Publishing, 2015.

[AK18] J.E. Andersen and R. Kashaev. The Teichmüller TQFT. In *Proceedings of the International Congress of Mathematicians*, volume 3, pages 2559–2584, Rio de Janeiro, 2018.

[Aki99] H. Akiyoshi. On the Ford domains of once-punctured torus groups. 数理解析研究所講究録 , 1140:109–121, 1999.

[AM17] J.E. Andersen and A. Malusà. The AJ-conjecture for the Teichmüller TQFT. *arXiv preprint arXiv:1711.11522*, 2017.

[Ame05] G. Amendola. A calculus for ideal triangulations of three-manifolds with embedded arcs. *Mathematische Nachrichten*, 278(9):975–994, 2005.

[AN17] J.E. Andersen and J-J.K. Nissen. Asymptotic aspects of the Teichmüller TQFT. *Travaux mathématiques*, 25:41–95, 2017.

[Ati88] M.F. Atiyah. Topological quantum field theory. *Publications Mathématiques de l'IHÉS*, 68:175–186, 1988.

[Ati10] M. Atiyah. Geometry in 2, 3 and 4 Dimensions. Clay Research Conference, 2010.

[BAGPN20] F. Ben Aribi, F. Guéritaud, and E. Piguet-Nakazawa. Geometric triangulations and the Teichmüller TQFT volume conjecture for twist knots. *arXiv preprint arXiv:1903.09480v3*, 2020.

[BAPN19] F. Ben Aribi and E. Piguet-Nakazawa. The Teichmüller TQFT volume conjecture for twist knots. *Comptes Rendus Mathematique*, 357(3):299–305, 2019.

[Bax72] R.J. Baxter. Partition function of the Eight-Vertex lattice model. *Annals of Physics*, 70(1):193–228, 1972.

[Bax16] R.J. Baxter. *Exactly Solved Models in Statistical Mechanics*. Elsevier, 2016.

[BB04] S. Baseilhac and R. Benedetti. Quantum hyperbolic invariants of 3-manifolds with $PSL(2,\mathbb{C})$-characters. *Topology*, 43(6):1373–1423, 2004.

[BF04] M. Banagl and G. Friedman. Triangulations of 3-dimensional pseudomanifolds with an application to state-sum invariants. *Algebraic and Geometric Topology*, 4(1):521–542, 2004.

[BHMV92] C. Blanchet, N. Habegger, G. Masbaum, and P. Vogel. Three-manifold invariants derived from the Kauffman bracket. *Topology*, 31(4):685–699, 1992.

[BHMV95] C. Blanchet, N. Habegger, G. Masbaum, and P. Vogel. Topological quantum field theories derived from the Kauffman bracket. *Topology*, 34(4):883–928, 1995.

[BHW99] S.A. Bleiler, C.D. Hodgson, and J.R. Weeks. Cosmetic Surgery on Knots. *Geometry and Topology Monographs*, 2:23–34, 1999.

[BMS07] V.V. Bazhanov, V.V. Mangazeev, and S.M. Sergeev. Faddeev–Volkov solution of the Yang–Baxter equation and discrete conformal symmetry. *Nuclear Physics B*, 784(3):234–258, 2007.

[BMS08] V.V. Bazhanov, V.V. Mangazeev, and S.M. Sergeev. Quantum geometry of three-dimensional lattices. *Journal of Statistical Mechanics: Theory and Experiment*, 2008(07):P07004, 2008.

[Bon09] F. Bonahon. *Low-dimensional geometry: From Euclidean surfaces to hyperbolic knots*, volume 49. American Mathematical Society, 2009.

[BP92] R. Benedetti and C. Petronio. *Lectures on Hyperbolic Geometry*. Universitext. Springer, 1992.

[Bri91] C.M. Brislawn. Traceable integral kernels on countably generated measure spaces. *Pacific Journal of Mathematics*, 150(2):229–240, 1991.

[Bur13] B.A. Burton. Computational topology with Regina: Algorithms, heuristics and implementations. *Geometry and topology down under*, 597:195–224, 2013.

[BZH13] G. Burde, H. Zieschang, and M. Heusener. *Knots*, volume 5. De Gruyter, third edition, 2013.

[CCG+94] D. Cooper, M. Culler, H. Gillet, D.D. Long, and P.B. Shalen. Plane curves associated to character varieties of 3-manifolds. *Inventiones mathematicae*, 118(1):47–84, 1994.

[CF99] L. Chekhov and V.V. Fock. A quantum Teichmüller space (in Russian). *Teoreticheskaya i Matematicheskaya Fizika*, 120(3):511–528, 1999.

[CHW99] P.J. Callahan, M.V. Hildebrand, and J.R. Weeks. A census of cusped hyperbolic 3-manifolds. *Mathematics of Computation*, 68(225):321–332, 1999.

[CJR82] M. Culler, W. Jaco, and H. Rubinstein. Incompressible Surfaces in Once-Punctured Torus Bundles. *Proceedings of the London Mathematical Society*, 3(3):385–419, 1982.

[CMM13] A. Cattabriga, E. Manfredi, and M. Mulazzani. On knots and links in lens spaces. *Topology and its Applications*, 160(2):430–442, 2013.

[CMY09] J. Cho, J. Murakami, and Y. Yokota. The complex volumes of twist knots. *Proceedings of the American Mathematical Society*, 137(10):3533–3541, 2009.

[Cos07] F. Costantino. Coloured Jones invariants of links and the volume conjecture. *Journal of the London Mathematical Society*, 76(1):1–15, 2007.

[CY18] Q. Chen and T. Yang. Volume conjectures for the Reshetikhin–Turaev and the Turaev–Viro invariants. *Quantum Topology*, 9(3):419–460, 2018.

[Deh38] M. Dehn. Die Gruppe der Abbildungsklassen: Das arithmetische Feld auf Flächen. *Acta Mathematica*, 69:135–206, 1938.

[DG13] T. Dimofte and S. Garoufalidis. The quantum content of the gluing equations. *Geometry and Topology*, 17(3):1253–1315, 2013.

[Dir39] P.A.M. Dirac. A new notation for quantum mechanics. *Mathematical Proceedings of the Cambridge Philosophical Society*, 35(3):416–418, 1939.

[Do13] N. Do. Moduli spaces of hyperbolic surfaces and their Weil–Petersson volumes. 2013.

[Dri85] V.G. Drinfeld. Hopf algebras and the quantum Yang–Baxter equation. In *Doklady Akademii Nauk SSSR*, volume 32, pages 254–258, 1985.

[Dro91] Y.V. Drobotukhina. An analogue of the Jones polynomial for links in $\mathbb{R}P^3$ and a generalization of the Kauffman–Murasugi theorem. *Leningrad Mathematical Journal*, 2(3):613–630, 1991.

[Dro94] Y.V. Drobotukhina. Classification of Links in $\mathbb{R}P^3$ with at Most Six Crossings. *Advances in Soviet Mathematics*, 18:87–121, 1994.

[Dub06] J. Dubois. Non Abelian Twisted Reidemeister Torsion for Fibered Knots. *Canadian Mathematical Bulletin*, 49(1):55–71, 2006.

[Duf72] M. Duflo. Généralités sur les représentations induites, Représentations des Groupes de Lie Résolubles. *Monographies de la Société Mathématique de France*, 4:93–119, 1972.

[Fad94] L.D. Faddeev. Current-Like Variables in Massive and Massless Integrable Models. *arXiv preprint hep-th/9408041*, 1994.

[Fad95] L.D. Faddeev. Discrete Heisenberg–Weyl Group and modular group. *Letters in Mathematical Physics*, 34(3):249–254, 1995.

[Fed77] M.V. Fedoryuk. *The saddle-point method (in Russian).* Izdat. "Nauka", Moscow, 1977.

[Fed89] M.V. Fedoryuk. Asymptotic Methods in Analysis. In *Analysis I*, pages 83–191. Springer, 1989.

[FG11] D. Futer and F. Guéritaud. From angled triangulations to hyperbolic structures. *Contemporary Mathematics, Interactions Between Hyperbolic Geometry, Quantum Topology, and Number Theory*, 541:159–182, 2011.

[FG13] D. Futer and F. Guéritaud. Explicit angle structures for veering triangulations. *Algebraic and Geometric Topology*, 13(1):205–235, 2013.

[FH82] W. Floyd and A. Hatcher. Incompressible surfaces in punctured-torus bundles. *Topology and its Applications*, 13(3):225–336, 1982.

[FK94] L.D. Faddeev and R.M. Kashaev. Quantum dilogarithm. *Modern Physics Letters A*, 9(5):427–434, 1994.

[FKP10] D. Futer, E. Kalfagianni, and J.S. Purcell. Cusp areas of Farey manifolds and applications to knot theory. *International Mathematics Research Notices*, 2010(23):4434–4497, 2010.

[FKV01] L.D. Faddeev, R.M. Kashaev, and A.Y. Volkov. Strongly Coupled Quantum Discrete Liouville Theory. I: Algebraic Approach and Duality. *Communications in Mathematical Physics*, 219(1):199–219, 2001.

[FM12] B. Farb and D. Margalit. *A Primer on Mapping Class Groups.* Princeton University Press, Princeton and Oxford, 2012.

[FTW18] D. Futer, E.J. Taylor, and W. Worden. Random veering triangulations are not geometric. *arXiv preprint arXiv:1808.05586*, 2018.

[FY09] L.D. Faddeev and O.A. Yakubovskii. *Lectures on Quantum Mechanics for Mathematics Students*, volume 47 of *Student Mathematical Library*. American Mathematical Society, 2009.

[Gab87] D. Gabai. Foliations and the topology of 3-manifolds, II. *Journal of the American Mathematical Society*, 26:461–478, 1987.

[Gai18] F. Gainullin. Heegaard Floer homology and knots determined by their complements. *Algebraic and Geometric Topology*, 18(1):69–109, 2018.

[Gar04] S. Garoufalidis. On the characteristic and deformation varieties of a knot. *Geometry and Topology Monograph*, 7:291–309, 2004.

[Gar15] S. Garoufalidis. Evaluation of state integrals via Grothendieck residues. Conference: New developments in TQFT, 2015.

[Gel50] I.M. Gelfand. Eigenfunction expansions for an equation with periodic coefficients (in Russian). In *Dokl. Akad. Nauk SSSR*, volume 73, pages 1117–1120, 1950.

[GK14] S. Garoufalidis and R. Kashaev. Evaluation of state integrals at rational points. *arXiv preprint arXiv:1411.6062*, 2014.

[GKT12] N. Geer, R. Kashaev, and V. Turaev. Tetrahedral forms in monoidal categories and 3-manifold invariants. *Journal für die reine und angewandte Mathematik (Crelles Journal)*, 2012(673):69–123, 2012.

[GL89] McA.C. Gordon and J. Luecke. Knots are determined by their complements. *Journal of the American Mathematical Society*, 2(2):371–415, 1989.

[GM18] B. Gabrovšek and E. Manfredi. On the KBSM of links in lens spaces. *Journal of Knot Theory and Its Ramifications*, 27(01):1850006, 2018.

[GRS12] S.N. Gurbatov, O.V. Rudenko, and A.I. Saichev. *Waves and Structures in Nonlinear Nondispersive Media: General Theory and Applications to Nonlinear Acoustics*. Springer, 2012.

[Gué06] F. Guéritaud. On canonical triangulations of once-punctured torus bundles and two-bridge link complements. Appendix by D. Futer. *Geometry and Topology*, 10(3):1239–1284, 2006.

[GW99] C. Gasquet and P. Witomski. *Fourier Analysis and Applications*. Texts in Applied Mathematics 30. Springer, 1999.

[GZ13] S. Garoufalidis and D. Zagier. Empirical relations between q-series and Kashaev's invariant of knots. *Preprint*, 2013.

[Hal13] B.C. Hall. *Quantum Theory for Mathematicians*, volume 267 of *Graduate Texts in Mathematics*. Springer, 2013.

[Hal15] B. Hall. *Lie groups, Lie algebras, and Representations: An Elementary Introduction*, volume 222 of *Graduate Texts in Mathematics*. Springer, second edition, 2015.

[HIS16] C.D. Hodgson, A. Issa, and H. Segerman. Non-geometric veering triangulations. *Experimental Mathematics*, 25(1):17–45, 2016.

[HMW92] C.D. Hodgson, G.R. Meyerhoff, and J.R. Weeks. Surgeries on the Whitehead Link Yield Geometrically Similar Manifolds. In B. Apanasov, W.D. Neumann, A.W. Reid, and L. Siebenmann, editors, *Topology'90*, pages 195–206. Walter de Gruyter, 1992.

[HRS12] C.D. Hodgson, J.H. Rubinstein, and H. Segerman. Triangulations of hyperbolic 3-manifolds admitting strict angle structures. *Journal of Topology*, 5 (4):887–908, 2012.

[HRST11] C.D. Hodgson, J.H. Rubinstein, H. Segerman, and S. Tillmann. Veering triangulations admit strict angle structures. *Geometry and Topology*, 15(4): 2073–2089, 2011.

[Hub06] J.H. Hubbard. *Teichmüller Theory and Applications to Geometry, Topology, and Dynamics*, volume 1. Matrix Editions, Ithaca, NY, 2006.

[IN16] M. Ishikawa and K. Nemoto. Construction of spines of two-bridge link complements and upper bounds of their Matveev complexities. *Hiroshima Mathematical Journal*, 46(2):149–162, 2016.

[Jim85] M. Jimbo. A q-difference analogue of $U(\mathfrak{g})$ and the Yang–Baxter equation. *Letters in Mathematical Physics*, 10(1):63–69, 1985.

[Jim86] M. Jimbo. A q-analogue of $U(\mathfrak{gl}(N+1))$, Hecke algebra, and the Yang–Baxter equation. *Letters in Mathematical Physics*, 11(3):247–252, 1986.

[Jon85] V.F.R. Jones. A polynomial invariant for knots via von Neumann algebras. *Bulletin (New Series) of the American Mathematical Society*, 12(1):103–111, 1985.

[Kan98] R.P. Kanwal. *Generalized functions: theory and technique.* Birkhäuser, second edition, 1998.

[Kas94] R.M. Kashaev. Quantum dilogarithm as a 6j-symbol. *Modern Physics Letters A*, 9(40):3757–3768, 1994.

[Kas95a] R.M. Kashaev. An invariant of triangulated links from the quantum dilogarithm (in Russian). *Zapiski Nauchnykh Seminarov POMI*, 224:208–214, 1995. Translation in: *Journal of Mathematical Sciences*, 88(2):244–248, 1998.

[Kas95b] R.M. Kashaev. A link invariant from quantum dilogarithm. *Modern Physics Letters A*, 10(19):1409–1418, 1995.

[Kas97] R.M. Kashaev. The hyperbolic volume of knots from the quantum dilogarithm. *Letters in Mathematical Physics*, 39(3):269–275, 1997.

[Kas98] R. M. Kashaev. Quantization of Teichmüller Spaces and the Quantum Dilogarithm. *Letters in Mathematical Physics*, 43(2):105–115, 1998.

[Kas01] R.M. Kashaev. On the spectrum of Dehn twists in quantum Teichmüller theory. In A.N. Kirillov and N. Liskova, editors, *Physics and Combinatorics*, pages 63–81. World Scientific Publishing, 2001.

[Kas14] R. Kashaev. Lecture notes: Aspects mathématiques de la théorie quantique, Université de Genève, 2014.

[Kas16] R. Kashaev. Combinatorics of the Teichmüller TQFT. *Winter Braids Lecture Notes*, 3:1–16, 2016.

[Kas17a] R. Kashaev. Lecture notes: Introduction to quantum topology II, Université de Genève, 2017.

[Kas17b] R. Kashaev. Lectures on quantum Teichmüller theory, School on quantum topology and geometry, 2017.

[Kas18] R. Kashaev. The Volume conjecture for knots in arbitrary 3-manifolds. Conference: Volume Conjecture in Tokyo, 2018.

[Kim16] H.K. Kim. Ratio coordinates for higher Teichmüller spaces. *Mathematische Zeitschrift*, 283(1):469–513, 2016.

[Kir95] A.N. Kirillov. Dilogarithm Identities. *Progress of Theoretical Physics Supplement*, 118:61–142, 1995.

[KLV16] R. Kashaev, F. Luo, and G. Vartanov. A TQFT of Turaev–Viro Type on Shaped Triangulations. *Annales Henri Poincaré*, 17(5):1109–1143, 2016.

[Kra01] S.G. Krantz. *Function Theory of Several Complex Variables*, volume 340. American Mathematical Society, second edition, 2001.

[KZ84] V.G. Knizhnik and A.B. Zamolodchikov. Current algebra and Wess–Zumino model in two dimensions. *Nuclear Physics B*, 247(1):83–103, 1984.

[Lac00] M. Lackenby. Taut ideal triangulations of 3-manifolds. *Geometry and Topology*, 4:369–395, 2000.

[Lac03] M. Lackenby. The canonical decomposition of once-punctured torus bundles. *Commentarii Mathematici Helvetici*, 78(2):363–384, 2003.

[Lic64] W.B.R. Lickorish. A finite set of generators for the homeotopy group of a 2-manifold. *Mathematical Proceedings of the Cambridge Philosophical Society*, 60(4):769–778, 1964.

[Lic66] W.B.R. Lickorish. On the homeotopy group of a 2-manifold (Corrigendum). *Mathematical Proceedings of the Cambridge Philosophical Society*, 62:679–681, 1966.

[LT08] F. Luo and S. Tillmann. Angle structures and normal surfaces. *Transactions of the American Mathematical Society*, 360(6):2849–2866, 2008.

[Mar16] B. Martelli. An introduction to geometric topology. *arXiv preprint arXiv:1610.02592*, 2016.

[Mat07a] S. Matveev. *Algorithmic topology and classification of 3-manifolds*, volume 9. Springer, 2007.

[Mat07b] S. Matveev. Transformations of special spines and the Zeeman conjecture. *Mathematics of the USSR-Izvestiya*, 31:423–434, 2007.

[Mat10] D. Matignon. On the knot complement problem for non-hyperbolic knots. *Topology and its Applications*, 157:1900–1925, 2010.

[Mat17] D. Matignon. Hyperbolic H-knots in non-trivial lens spaces are not determined by their complement. *Topology and its Applications*, 228:391–432, 2017.

[Men83] W. Menasco. Polyhedral representation of link complements. *AMS Contemporary Mathematics*, 20:305–325, 1983.

[Mik18] V. Mikhaylov. Teichmüller TQFT vs. Chern–Simons theory. *Journal of High Energy Physics*, 2018(4):85, 2018.

[Mil82] J.W. Milnor. Hyperbolic geometry: the first 150 years. *Bulletin (New Series) of the American Mathematical Society*, 6(1):9–24, 1982.

[MM01] H. Murakami and J. Murakami. The colored Jones polynomials and the simplicial volume of a knot. *Acta Mathematica*, 186(1):85–104, 2001.

[Moi52] E.E. Moise. Affine structures in 3-manifolds: V. The triangulation theorem and Hauptvermutung. *Annals of mathematics*, pages 96–114, 1952.

[Mos73] G.D. Mostow. *Strong Rigidity of Locally Symmetric Spaces*, volume 78 of *Annals of Mathematics Studies*. Princeton University Press, Princeton, N.J., 1973.

[Mur00] J. Murakami. “結び目と量子群” *(Knots and quantum groups), in Japanese.* 朝倉書店, 2000.

[Mur11] H. Murakami. An introduction to the volume conjecture. *Interactions between hyperbolic geometry, quantum topology and number theory*, 541:1–40, 2011.

[Mur17] J. Murakami. Generalized Kashaev invariants for knots in three manifolds. *Quantum Topology*, 8(1):35–73, 2017.

[MY18] H. Murakami and Y. Yokota. *Volume conjecture for knots*, volume 30. Springer, 2018.

[Nic03] L.I. Nicolaescu. *The Reidemeister Torsion of 3-Manifolds*. Walter de Gruyter, 2003.

[NZ85] W.D. Neumann and D. Zagier. Volumes of hyperbolic three-manifolds. *Topology*, 24(3):307–332, 1985.

[Oht99] T. Ohtsuki. “量子不変量：3 次元トポロジーと数理物理の遭遇” *(Quantum Invariants: Encounter between 3-dimensional topology and mathematical physics), in Japanese.* 日本評論社, 1999.

[Oht02] T. Ohtsuki. *Quantum Invariants: A Study of Knots, 3-Manifolds, and Their Sets*, volume 29. World Scientific, 2002.

[Oht15] T. Ohtsuki. “結び目の不変量” *(Invariants of knots), in Japanese.* 共立出版, 2015.

[Oht18] T. Ohtsuki. On the asymptotic expansion of the quantum $SU(2)$ invariant at $q = \exp(4\pi\sqrt{-1}/N)$ for closed hyperbolic 3-manifolds obtained by integral surgery along the figure-eight knot. *Algebraic and Geometric Topology*, 18 (7):4187–4274, 2018.

[OS05] P. Ozsváth and Z. Szabó. On knot Floer homology and lens space surgeries. *Topology*, 44(6):1281–1300, 2005.

[Pen87] R.C. Penner. The decorated Teichmüller space of punctured surfaces. *Communications in Mathematical Physics*, 113(2):299–339, 1987.

[Pen12] R.C. Penner. *Decorated Teichmüller Theory*. European Mathematical Society, Aarhus, 2012.

[Per02] G. Perelman. The entropy formula for the Ricci flow and its geometric applications. *arXiv preprint math/0211159*, 2002.

[Per03a] G. Perelman. Finite extinction time for the solutions to the Ricci flow on certain three-manifolds. *arXiv preprint math/0307245*, 2003.

[Per03b] G. Perelman. Ricci flow with surgery on three-manifolds. *arXiv preprint math/0303109*, 2003.

[Pie88] R. Piergallini. Standard moves for standard polyhedra and spines. *Rendiconti del Circolo Matemàtico di Palermo, suppl. 18*, 37:391–414, 1988.

[Por97] J. Porti. Torsion de Reidemeister pour les variétés hyperboliques. *Memoirs of the American Mathematical Society*, 128(612), 1997.

[PP99] C. Petronio and J. Porti. Negatively Oriented Ideal Triangulations and a Proof of Thurston's Hyperbolic Dehn Filling Theorem. *arXiv preprint math/9901045*, 1999.

[PP09] E. Pervova and C. Petronio. Complexity of links in 3-manifolds. *Journal of Knot Theory and Its Ramifications*, 18(10):1439–1458, 2009.

[Pra73] G.E. Prasad. Strong rigidity of $\mathbb{Q}$-rank 1 lattices. *Inventiones mathematicae*, 21:255–286, 1973.

[Pur20] J.S. Purcell. Hyperbolic Knot Theory. *arXiv preprint arXiv:2002.12652*, 2020.

[Rat06] J.G. Ratcliffe. *Foundations of Hyperbolic Manifolds*. Springer, New York, second edition, 2006.

[Riv94] I. Rivin. Euclidean Structures on Simplicial Surfaces and Hyperbolic Volume. *Annals of Mathematics*, 139(3):553–580, 1994.

[RS12] M. Reed and B. Simon. *Methods of modern mathematical physics: Functional analysis*. Elsevier, 2012.

[RST18] H. Rubinstein, H. Segerman, and S. Tillmann. Traversing three-manifold triangulations and spines. *arXiv preprint arXiv:1812.02806*, 2018.

[RT90] N.Y. Reshetikhin and V.G. Turaev. Ribbon Graphs and Their Invariants Derived from Quantum Groups. *Communications in Mathematical Physics*, 127(1):1–26, 1990.

[RT91] N. Reshetikhin and V.G. Turaev. Invariants of 3-manifolds via link polynomials and quantum groups. *Inventiones mathematicae*, 103(1):547–597, 1991.

[Rub87] D. Ruberman. Mutation and volumes of knots in S^3. *Inventiones Mathematicae*, 90(1):189–215, 1987.

[Seg88] G.B. Segal. The definition of conformal field theory. In *Differential geometrical methods in theoretical physics*, pages 165–171. Springer, 1988.

[SS07] E.M. Stein and R. Shakarchi. *Fourier Analysis: An Introduction*. Princeton University Press, Princeton and Oxford, 2007.

[ST80] H. Seifert and W. Threlfall. *A Textbook of Topology*, volume 89 of *Pure and Applied Mathematics*. Academic Press Inc., 1980.

[Tak08] L.A. Takhtajan. *Quantum Mechanics for Mathematicians*, volume 95 of *Graduate Studies in Mathematics*. American Mathematical Society, 2008.

[Tes01] J. Teschner. Liouville theory revisited. *Classical Quantum Gravity*, 18:R153–R222, 2001.

[Tes07] J. Teschner. From Liouville theory to the quantum geometry of Riemann surfaces. *Contemporary Mathematics*, 437:231–246, 2007.

[Thu78] W.P. Thurston. The Geometry and Topology of Three-Manifolds. Princeton lecture notes, 1978.

[Thu82] W.P. Thurston. Three dimensional manifolds, Kleinian groups and hyperbolic geometry. *Bulletin (New Series) of the American Mathematical Society*, 6(3):357–381, 1982.

[Thu88] W.P. Thurston. On the geometry and dynamics of diffeomorphisms of surfaces. *Bulletin of the American Mathematical Society*, 19(2):417–431, 1988.

[Thu98] W.P. Thurston. Hyperbolic structures on 3-manifolds, II: Surface groups and 3-manifolds which fiber over the circle. *arXiv preprint math/9801045*, 1998.

[Tur00] V. Turaev. *Introduction to Combinatorial Torsions*. Birkhäuser Verlag, 2000.

[Tur10] V.G. Turaev. *Quantum Invariants of Knots and 3-Manifolds*. De Gruyter, Berlin, Boston, third edition, 2010.

[TV92] V.G. Turaev and O.Y. Viro. State sum invariants of 3-manifolds and quantum $6j$-symbols. *Topology*, 31(4):865–902, 1992.

[vdV08] R. van der Veen. Proof of the volume conjecture for Whitehead chains. *Acta Mathematica Vietnamica*, 33(3):421–431, 2008.

[Wei51] A. Weil. *L'intégration dans les groupes topologiques et ses applications*. Hermann, Paris, 1951.

[Wie81] N.J. Wielenberg. Hyperbolic 3-manifolds which share a fundamental polyhedron. *Annals of Mathematics Studies*, (97):505–513, 1981.

[Wit88] E. Witten. Topological quantum field theory. *Communications in Mathematical Physics*, 117(3):353–386, 1988.

[Wit89] E. Witten. Quantum field theory and the Jones polynomial. *Communications in Mathematical Physics*, 121(3):351–399, 1989.

[Won01] R. Wong. *Asymptotic Approximations of Integrals*, volume 34. SIAM, 2001.

[Wor00] S.L. Woronowicz. Quantum Exponential Function. *Reviews in Mathematical Physics*, 12:873–920, 2000.

[Wor20] W. Worden. Experimental statistics of veering triangulations. *Experimental Mathematics*, 29(1):101–122, 2020.

[Yan67] C.N. Yang. Some exact results for the many-body problem in one dimension with repulsive delta-function interaction. *Physical Review Letters*, 19(23): 1312–1315, 1967.

[Zag06] D. Zagier. The dilogarithm function. In P.E. Cartier, B. Julia, P. Moussa, and P. Vanhove, editors, *Frontiers in Number Theory, Physics and Geometry II*, pages 3–65. Springer-Verlag, 2006.

[Zak67] J. Zak. Finite translations in solid state physics. *Physical Review Letters*, 19 (24):1385–1397, 1967.